31st IUGG
Conference on Mathematical Geophysics

6-10 June 2016

Paris, France

http://cmg2016.sciencesconf.org/

Table of contents

Invited speakers

Maria T. Zuber
Massachusetts Institute of Technology
Vice President for Research , E.A. Griswold Professor of Geophysics
http://www-geodyn.mit.edu/zubersite/vitae.html

Tuesday, June 7th, 14 :00-15 :00

Chris Paola
Department of Earth Sciences Interim Director,
St Anthony Falls Laboratory,
University of Minnesota,
Minneapolis MN 55414 USA
http://www.safl.umn.edu/researchgroup/chris-paola

Thursday, June 9th, 14 :00-15 :00

INVITED TALK,

Maria T. Zuber
Department of Earth, Atmospheric and Planetary Sciences
Massachusetts Institute of Technology
USA

Tuesday, June 7th, 14 :00-15 :00

TITLE:

Advances in Planetary Gravity Mapping

ABSTRACT:

Remote observation of the gravity fields of solid planetary bodies provides a plethora of information relevant to structure and evolution. This talk will review results from gravity mapping investigations from three planets – Mercury, Mars and the Moon. The results for Mercury will emphasize core composition and state and their relevance to the planet's evolution. Results for Mars will focus on atmospheric structure and the detection and quantitative characterization of the annual cycle of CO2 exchange between the cryosphere and atmosphere. Results for the Moon will focus on understanding the history of impact bombardment and volcanism. Implications for other solid planetary bodies will be addressed as will opportunities for future advances.

INVITED TALK,
Chris Paola
Department of Earth Sciences Interim Director,
St Anthony Falls Laboratory,
University of Minnesota,
Minneapolis,USA
Thursday, June 9th, 14 :00-15 :00

TITLE:

Using unscaled and partially scaled experiments in geophysics

ABSTRACT:

There are numerous instances in surface processes, and elsewhere in geophysics. where strict scaling of experiments is impossible. Yet in many such cases, experiments can still provide insight. We will explore examples of unscaled and partially scaled experiments, and how behavior for limiting cases of governing nondimensional numbers (e.g. Re, Fr) can help us understand when such experiments are and are not useful.

Ocean

Size matters: another reason why the Atlantic is saltier than the Pacific

C S Jones and Paola Cessi

Idealized numerical experiments are performed with an ocean-only circulation forced by wind-stress, surface temperature and freshwater flux, all independent of longitude, in a domain consisting of two basins, differing only in their widths, which are connected by a circumpolar channel at the south and. These experiments show that a spontaneous asymmetry in the latitudinal distribution of surface salinity develops, which favors salinification of the narrow basin over the wide basin. This salinification induces a stable pole-to-pole overturning in the narrow basin, maintained by the salt-advection feedback. Pole-to-pole overturning in the wide basin does not occur for zonally-symmetric forcing, but can be induced by reducing the precipitation over the northern end of the wide basin. The preference for sinking at the northern end of the narrow basin over sinking in the wide basin is due to two compounding processes: a larger overturning velocity associated with narrow-basin sinking, and a smaller gyral velocity, which is always found in the narrow basin compared to the wide basin. Together, these differences in salt advection favor sinking in the narrow basin.

REFRACTION OF SWELL BY SURFACE CURRENTS

Basile Gallet[1], W.R. Young[2]
[1]*Service de Physique de l'État Condensé, CEA Saclay, 91191 Gif–Sur–Yvette, France*
[2]*Scripps Institution of Oceanography, University of California at San Diego, La Jolla CA92093, USA*

Key words surface gravity wave, swell, geometric optics, spherical ray tracing

Using recordings of swell from pitch-and-roll buoys, we have reproduced the classic observations of long-range surface gravity wave propagation between the Southern Ocean and California (Munk et al., 1963). In the modern data, the direction of the incoming swell fluctuates by about $\pm 10^\circ$ on a time scale of one hour. But if the incoming direction is averaged over the duration of an event then, in contrast with the observations by Munk et al. (1963), the sources inferred by great-circle backtracking are most often in good agreement with the location of large storms on weather maps of the Southern Ocean. However there are a few puzzling failures of great-circle backtracking e.g., in one case, the direct great-circle route is blocked by the Tuamoto Islands and the inferred source falls on New Zealand. Mirages like this occur more frequently in the earlier observations of Munk et al. (1963), where several inferred sources fell on the Antarctic continent.

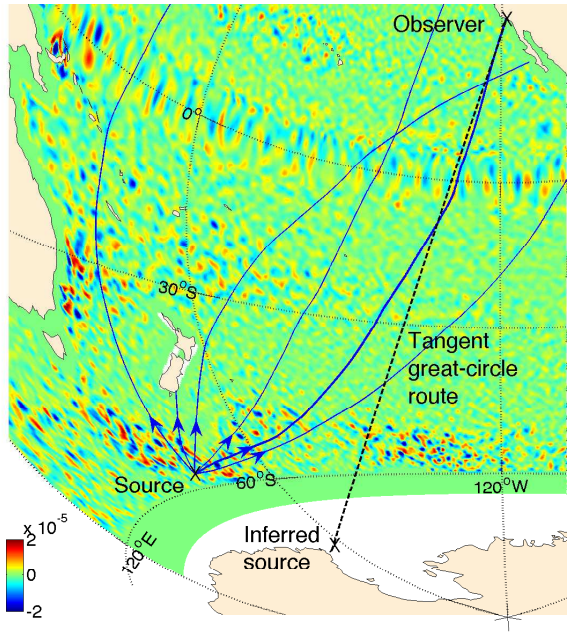

Figure 1. This map uses azimuthal projection centered on a Californian observer at $\times$; great circles passing through the observer are straight lines. The color scale is sea-surface vorticity (s^{-1}) inferred from satellite altimetry and vector wind data by the Ocean Surface Current Analysis in Real-time (OSCAR) dataset (Bonjean & Lagerloef, 2002). A point source in the Southern Ocean emits six rays all of which show significant refraction by ocean currents. The thick ray connects the point source to the receiver; because of ocean surface currents this ray does not follow a great circle. Great-circle backtracking (the dashed great circle) thus infers a source under the ice. Rays are bent from great circles only where there is strong surface vorticity in localized current systems such as the Antarctic Circumpolar Current, the subtropical frontal zone and the equatorial current system. The thick ray undergoes strong refraction when crossing these three features, and then travels more-or-less on great circles in between. For example, after leaving the Southern Ocean the thick ray is on a great circle headed away from the receiver. But refraction by a large equatorial eddy then bends the ray onto a great circle passing through the receiver.

With spherical ray tracing we investigate the hypothesis that the refraction of surface gravity waves by ocean currents produces the mirages. The group velocity of surface waves is much greater than the typical speed of ocean currents, and in this limit the curvature of a ray is nearly equal to the vertical vorticity of the surface currents divided by the group velocity (Landau & Lifshitz 1987). Thus the vertical vorticity of surface currents is the key environmental variable controlling the departure of rays from great circles. Using observed surface currents we show that mesoscale vorticity is strong enough to produce significant deflections, so that the source and receiver are connected by a bundle of many rays, none of which precisely follow a great circle. The $\pm 10^\circ$ directional fluctuations at the receiver result from the arrival of wave packets that have travelled along the different rays within this multipath. The occasional failure of great-circle backtracking, and the associated mirages, probably results from partial topographic obstruction of the multipath, which biases the directional average at the receiver.

References

[1] W. H. MUNK, G. R. MILLER, F.E. SNODGRASS AND N.F. BARBER. *Directional recording of swell from distant storms*. Philosophical Transactions of the Royal Society of London, series A, **255**, 1062, 505-584 (1963).
[2] L.D. LANDAU AND E.M. LIFSHITZ, *Fluid Mechanics*, (1987)
[3] F. BONJEAN AND G.S.E. LAGERLOEF, *Diagnostic model and analysis of the surface currents in the tropical Pacific Ocean.* Journal of Physical Oceanography, **32** (2002).

cmg2016 - - Monday, June 6, 2016 - 11:00/11:15 (15min)

THE INHERENT STABILIZING EFFECT OF NON-BOUSSINESQ BAROCLINIC TORQUE ON INTERNAL GRAVITY WAVES

E. Heifetz[1], J. Mak[2]
[1]*Tel-Aviv University, Israel*
[2]*University of Edinburgh, UK*

Key words interacting vorticity waves, shear instability, sharp density gradients

An approximation that is often made when studying the dynamics of oceanic stratified flows is the Boussinesq approximation. However, in regions of strong vertical density gradients this approximation may not be valid and the baroclinic torque, resulted from such sharp density gradients, can play an important role in altering the propagation and the instability mechanism of internal gravity waves. Here we investigate this phenomena with a special focus on the associated consequences for the mechanistic interpretation of stably stratified shear instability arising from the interaction between vorticity-propagating waves. To illustrate and elucidate the physical effects we consider three examples of increasing complexity: wave propagation supported by a uniform background flow; wave propagation supported on a piecewise-linear shear flow possessing one density jump; and an instability problem of a piecewise-linear shear flow possessing two jumps, which supports the possibility of shear instability. We find that the non-Boussinesq effects introduce a preference for the direction of wave propagation that depends on the sign of the shear in the region where waves are supported. This in turn defects the phase-locking between the waves that is crucial for the wave resonance, and consequently has an inherent tendency for stabilization [1].

References

[1] E. Heifetz and J. Mak, *Stratified shear flow instabilities in the non-Boussinesq regime*, Phys. Fluids **27**, 086601 (2015); doi: 10.1063/1.4928738

cmg2016 - - Monday, June 6, 2016 - 9:30/10:00 (30min)

SUBMESOSCALE WRINKLES IN THE ANTARCTIC CIRCUMPOLAR CURRENT

J.R. Taylor[1], P. Hosegood [2], J.-B. Sallee [3], K. Adams[2], S. Bachman[1], & M. Stamper[1]
[1]*Department of Applied Mathematics and Theoretical Physics, University of Cambridge, UK*
[2]*School of Marine Science and Engineering, Plymouth University, UK*
[3]*University Pierre and Marie Curie, Paris VI, Paris, France*

Key words Southern Ocean, Physical Oceanography, Submesoscale Dynamics

The Southern Ocean is home to the Antarctic Circumpolar Current (ACC), one of the earth's major current systems, flowing around the globe from west to east. The ACC plays a central role in the global ocean overturning circulation by providing a pathway by which water can move from the ocean interior to the surface along surfaces of constant density. The Southern Ocean is also known to have hotspots of mesoscale eddy activity. On smaller scales, submesoscale eddies and fronts with scales between 1-10km are associated with enhanced vertical velocity that aids the exchange of water between the mixed layer and thermocline. Despite their importance in other regions, very little is known about the role of submesoscale features in the ACC.

Here, we will present new observations and high-resolution numerical simulations of submesoscale features in the ACC. Observations were made as part of the SMILES project from April-May 2015 east of Drake Passage in the Scotia Sea. During the cruise, a large northward meander of the ACC was sampled at high resolution using towed bodies, surface drifters, microstructure, and dye release. Satellite imagery indicated the presence of submesoscale 'wrinkles' along the sharp temperature gradient associated with the ACC. Observations using a moving vessel profiler (MVP) will be shown which reveal rich three-dimensional structure associated with these features. Numerical simulations, initialized with an idealized version of the observed front qualitatively reproduce these features. The numerical simulations allow us to quantify the vertical velocity associated with the submesoscale features, and their interaction with the strong barotropic flow associated with the ACC.

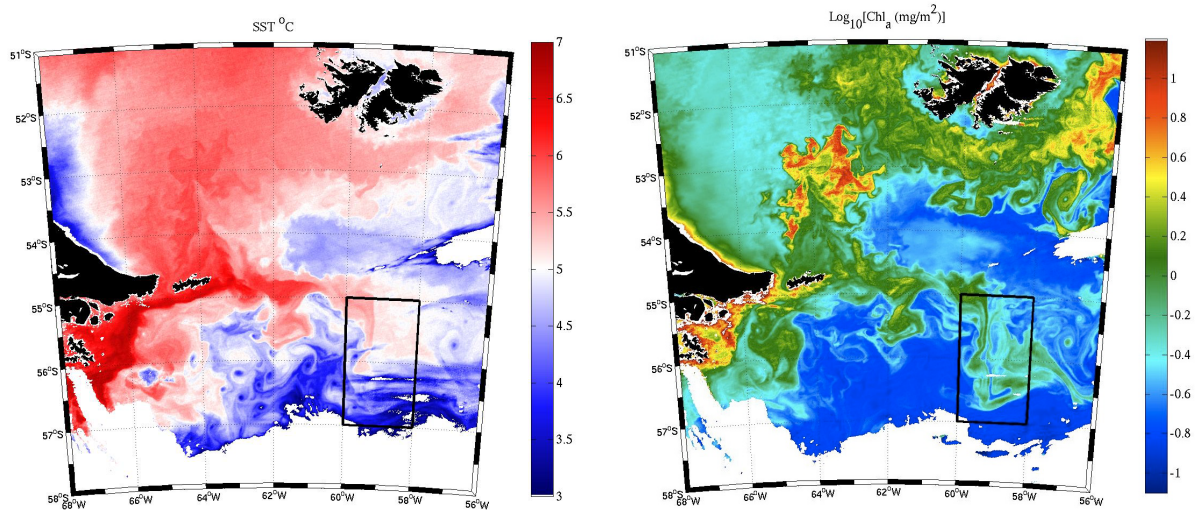

Figure 1. Sea surface temperature (left) and near surface Chlorophyll (right) from the NASA MODIS satellite

cmg2016 - - Monday, June 6, 2016 - 11:15/11:30 (15min)

NONLINEAR INTERACTIONS AMONG OCEAN INTERNAL WAVES IN THE WAKE OF A MOVING CYCLONE.

A. N. Meroni[1], M. Miller[2], E. Tziperman[2,3] & C. Pasquero[1]
[1]*Department of Earth and Environmental Sciences, University of Milan-Bicocca, Milan, Italy*
[2]*Department of Earth and Planetary Sciences, Harvard University, Cambridge, Massachusetts*
[3]*School of Engineering and Applied Sciences, Harvard University, Cambridge, Massachusetts*

Key words Nonlinear interactions, internal normal modes, response of the ocean to a tropical cyclone, internal waves.

The nonlinear dynamics leading to the generation of superinertial internal waves in the ocean, in the wake of a cyclonic storm, is investigated by means of theoretical arguments and of numerical integration of the hydrostatic Boussinesq equations in a simplified realistic open-ocean setting. The velocity fields are first decomposed into internal baroclinic modes and then the energy transfer across modes and at different frequencies is computed. The well known triangle condition for (k_z', k_z'', k_z''') triad interactions in vertical wavenumber space, $|k_z' \pm k_z''| = k_z'''$, in the case of realistic (i.e. non constant) stratification can be transposed to a condition on the interacting triads in baroclinic mode-number space. This confirms that the (n, m, l) triad of modes interacts when $|n \pm m| = l$ and highlights that other mode-number triads can be resonant and that even the interaction of a mode with itself becomes possible. The energy transfer across modes is dominated by the advection of high mode (m) waves by the second mode wave $(n = 2)$, which is the most energetic, and this results in the excitation of the $l = m - 2$ mode wave at the double inertial frequency. The analyzed nonlinear interactions lead to a transfer of energy from the near-inertial waves, directly excited by the storm, to the superinertial waves, which typically propagate faster and further than their lower frequency parents and can lead to internal mixing even at large distances from the region of the large air-sea momentum fluxes.

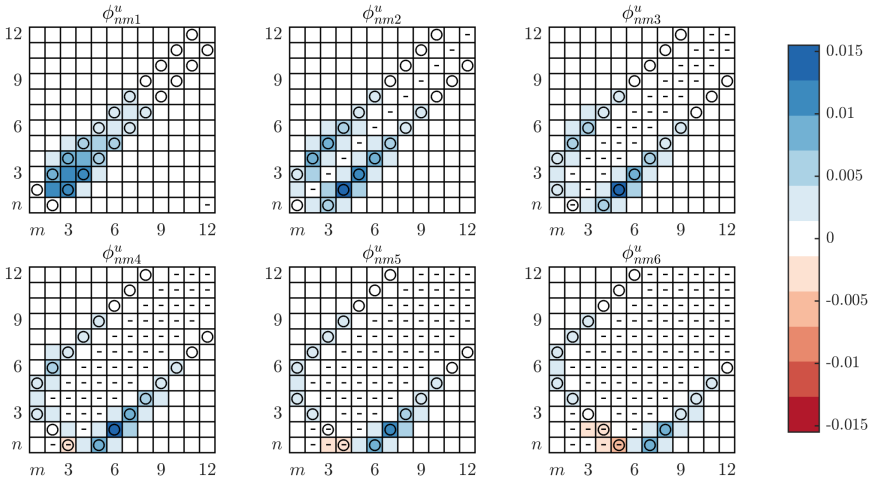

Figure 1. The analytical coefficients ϕ^u_{nml} represent the energy transferred from the inertial range of the (n, m)-th modes waves to the double inertial energy range of the power spectrum of the l-th mode waves. The strongest interaction is the one involving the $n = 2$ and $m = l + 2$ mode waves. The circles denote the lines where the strict triangle condition $|n \pm m| = l$ applies and it is clear that weaker interactions take place also in the neighborhood of these lines. The minus highlights the negative interactions.

References

[1] Danioux E. and P. Klein, *A resonance mechanism leading to wind-forced motions with a 2f frequency*, J. Phys. Oceanogr. **38**, 2322-2329 (2008).
[2] Nilsson J., *Energy flux from traveling hurricanes to the oceanic internal wave field*, J. Phys. Oceanogr. **25**, 558-573 (1995).
[3] Niwa Y. and T. Hibiya, *Nonlinear processes of energy transfer from traveling hurricanes to the deep ocean internal wave field*, J. Geophys. Res. **102**, 12469-12477 (1997).
[4] Ripa P., *On the theory of nonlinear wave-wave interactions among geophysical waves*, J. Fluid Mech. **103**, 87-115 (1981).
[5] Zedler S. E., *Simulations of the ocean response to a hurricane: nonlinear processes*, J. Phys. Oceanogr. **39**, 2618-2634 (2009).

Midlatitude-equatorial dynamics of a grounded deep western boundary current

Gordon E. Swaters
Department of Mathematical and Statistical Sciences, and
Institute for Geophysical Research
University of Alberta, Canada

A theoretical study of the nonlinear hemispheric-scale midlatitude and cross-equatorial steady-state dynamics of a grounded deep western boundary current (DWBC) is described. The domain considered is an idealized differentially rotating meridionally aligned basin with zonally varying parabolic bottom topography so that the model ocean shallows on the western and eastern sides of the basin. Away from the equator, the equatorward flow is governed by nonlinear planetary-geostrophic dynamics on sloping topography in which the potential vorticity equation can be explicitly solved. As the flow enters the equatorial region, it speeds up and becomes increasingly nonlinear and passes through two distinguished inertial layers referred to as the “intermediate” and “inner” inertial equatorial boundary layers, respectively. The flow in the intermediate equatorial region is shown to acceleration and turn eastward forming a narrow equatorial jet. The large-scale structure of the flow within the inner equatorial region corresponds to a zonally aligned nonlinear stationary planetary wave pattern that meanders about the equator in which the flow exits the equatorial region on the eastern side of the basin. If the DWBC exits the equatorial region into the opposite hemisphere from its source hemisphere, the characteristics of the flow must necessarily intersect within the inner equatorial region. It is in the regions of intersecting characteristics that dissipation makes a leading order contribution to the dynamics and induces the requisite potential vorticity adjustment permitting the cross-equatorial flow of a DWBC that is in planetary-geostrophic dynamical balance in mid-latitudes.

Uncertainty of Linear Trend in Global SST Due to Multi-Scale Internal Variation

Tao Lian * [1]

[1] State Key Lab of Satellite Ocean Environment Dynamics, Second Institute of Oceanography – China

In most parts of the global ocean, the amplitude of multi-scale internal variation of local sea surface temperature (SST) is much larger than that of its long-term linear trend. One can thus use the record of a specified period to arbitrarily determine the value and the sign of the long-term linear trend in regional SST, and further leading to controversial conclusions on how global SST responds to global warming in the recent history. In this study, we first investigate the theoretical expression of the coefficient derived by the ordinary least-square method when the residual term in the linear regression model is regarded as a set of oscillations. It is found that the sign of the resulting linear trend will not depend on the phase of the oscillations only when its magnitude is greater than a theoretical threshold. An improved smoothed least-square method is proposed to decrease the theoretical threshold. When applying these two methods to a global reconstruction from 1881 to 2013, we find that in most of global oceanic regions including the Pacific, southern Indian Ocean and North Atlantic, it is impossible to exclude the influence of multi-scale internal variation on the sign of the long-term linear trend in local SST. Therefore, the resulting linear trend can not be fully attributed to the long-term changing SST in these regions.

*Speaker

cmg2016 - - Monday, June 6, 2016 - 11:45/12:30 (45min)

OCEANIC MODELS UNDER UNCERTAINTY

V. Resseguier[1,2], E. Mémin[1] & B. Chapron[2]
[1]*INRIA Bretagne Atlantique, Rennes, France*
[2]*IFREMER, Brest, France*

Key words Random simulation, ensemble forecasting, subgrid parametrization, oceanic models, mesoscale, asymmetry cyclone/anticyclone.

Stochastic models can be developed to perform ensemble forecasts of geophysical fluid dynamical systems to more efficiently handle subgrid parametrizations. As numerical simulations do not usually resolve all temporal scales, solutions can be found by decomposing the velocity $\boldsymbol{u}$ into a smooth resolved component, $\boldsymbol{w}$, and an unresolved one, $\boldsymbol{\sigma}\dot{\boldsymbol{B}}$, uncorrelated in time and inhomogeneous in space. In turn, this new point of view changes the usual interpretation of transport and fundamental conservation laws (mass, momentum and 1^{st} principle). Indeed, following a stochastic version of the Reynolds transport theorem ([3]), three terms naturally emerge: a multiplicative noise, an anisotropic and inhomogeneous diffusion, and a drift correction. For instance, neglecting diabatic effects implies the conservation of the temperature T along the flow as : $\frac{DT}{Dt} = 0$, with the material derivative $\frac{D}{Dt}$, now understood in the stochastic sense:

$$\frac{DT}{Dt}\mathrm{d}t = D_tT = \mathrm{d}_tT + (\boldsymbol{w}^*\mathrm{d}t + \boldsymbol{\sigma}\mathrm{d}\boldsymbol{B}_t)\cdot\boldsymbol{\nabla}T - \boldsymbol{\nabla}\cdot\left(\frac{\boldsymbol{a}}{2}\boldsymbol{\nabla}T\right)\mathrm{d}t, \text{ with } \boldsymbol{a} = \boldsymbol{\sigma}\boldsymbol{\sigma}^T \text{ and } \boldsymbol{w}^* = \boldsymbol{w} - \frac{1}{2}\left(\boldsymbol{\nabla}\cdot\boldsymbol{a}\right)^T. \quad (1)$$

As such, the rigorous derivation of this model relates the random forcing to the subgrid parametrization. This further ensures important properties such as energy conservation $\left(\frac{\mathrm{d}}{\mathrm{d}t}\int_{\mathbb{R}^d} T^2 = 0\right)$ and also simplifies the derivation of ensemble forecasts in defining a clear mathematical framework.

Using this new framework, stochastic versions of geophysical models have been derived, namely: Navier-Stokes equations in a rotating frame, the Boussinesq approximation, Quasi-Geostrophy (QG) and Surface Quasi-Geostrophy (SQG). Depending on the amount of randomness, the QG approximation ($Ro \ll 1$ and $Ro \ll Bu$) can lead to two different models. With moderate uncertainty, the horizontal transport of the Potential Vorticity (PV), Q, in the interior of the fluid, has 3 sources terms. For homogeneous turbulence, two of them, disappear. The remaining term, a noise uncorrelated in time, encodes the interactions between the resolved and the unresolved velocity gradient tensors. The ensuing SQG model is then derived assuming a zero PV in the interior, as in the deterministic case ([1]). Yet, the buoyancy transport at the surface of the fluid has to be understood in the stochastic sense (1). Increasing to strong uncertainty, the QG approximation further leads to a vanishing PV in the interior. As such, a classical SQG relationship remains. However, for that case, an ageostrophic component appears, contributing to intensify asymmetries between cyclones and anticyclones, as in the SQG+ model ([2]). Frontogenesis occurs on the cold side of fronts, on uncertain locations, and frontolysis smooths the warm side of fronts.

Figure 1 shows the simulation of an initially symmetric flow with the deterministic SQG model and our stochastic version. As obtained, the flow topology is changed by the noise and the divergent component, and the symmetry breaks more rapidly. Larger the uncertainty, faster the symmetry is broken. Simulating an ensemble of realizations then enables to track the different possible topologies and all the bifurcations of the system.

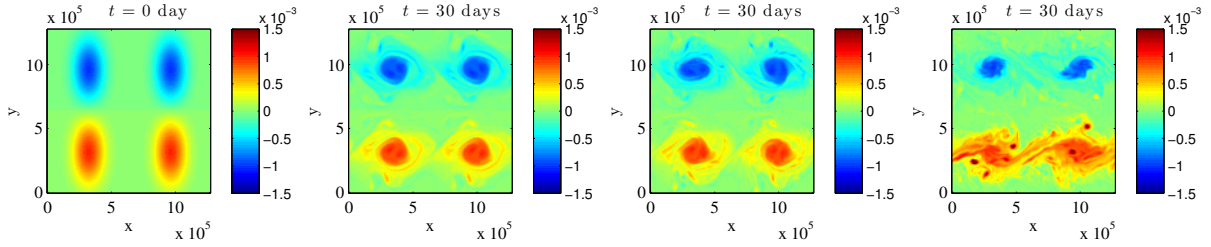

Figure 1. Buoyancy ($m.s^{-2}$) at the initial state and after 30 days of advection for (from left to right) the classical SQG model, the SQG model with moderate uncertainty and with strong uncertainty. The turbulence is assumed to be homogeneous. Its energy is specified by the diffusion coefficient $\frac{a_H}{2} = 9\ m^2.s^{-1}$ for moderate uncertainty and $\frac{a_H}{2} = 103\ m^2.s^{-1}$ for strong uncertainty. The size of the domain is 128×128 and the boundaries are doubly periodic.

References

[1] I. Held, R. Pierrehumbert, S. Garner, & K. Swanson, *Surface quasi-geostrophic dynamics*, Journal of Fluid Mechanics, **282**, 1-20, (1995).
[2] G. Hakim, C. Snyder, & D. Muraki, *A new surface model for cyclone-anticyclone asymmetry*, Journal of the atmospheric sciences, **59**, 16, 2405–2420, (2002).
[3] E. Mémin, *Fluid flow dynamics under location uncertainty*, Geophysical & Astrophysical Fluid Dynamics, **108**, 2, 119–146, (2014).

cmg2016 - - Monday, June 6, 2016 - 11:45/12:30 (45min)

ANALYSIS AND MODELLING OF SCALING PROCESSES IN THE OCEAN SCIENCES

F. G. Schmitt[1], Y. Huang[2]
[1]*CNRS, Laboratoire d'Oceanologie et de Geosciences, Wimereux, France*
[2]*Xiamen University, State Key Lab. of Marine Environmental Science, Xiamen, China*

Key words Scaling; turbulence; Oceanography; Stochastic modelling; Empirical mode decomposition; Multifractals.

In the geosciences, many fields and processes are highly fluctuating over large range of time and space scales. At smaller scales, the variability is often related to turbulent forcing, inducing scaling properties and possible intermittent fluctuations. We work here in such framework and consider time series in oceanographic sciences, recorded at high frequency.
Often such time series possess scaling fluctuations, superposed to deterministic forcing associated with tidal, daily or annual scales. We discuss how to analyse and model fluctuations in such situations. We especially present an analysis approach of intermittency, based on Empirical Mode Decomposition (EMD), a decomposition method developed in the late 1990s to represent a nonlinear time series into a sum of modes, each having a characteristic frequency. Based on EMD, we have developed a method called arbitrary order Hilbert spectral analysis: such method is able to extract intermittency scaling exponents from time series possessing strong deterministic forcing [1, 2].
Here we present this method and we illustrate it using several examples from the field of oceanic sciences [3]:

- Coastal marine velocity turbulence, recorded in the surf zone using an Acoustic Doppler Velocimeter (ADV);
- Oceanic temperature compared to atmospheric simultaneous values, dissolved oxygen, as well as fluorescence measurements, each recorded every 20 minutes in the coastal waters of the English Channel (Boulogne-sur-mer);
- Hourly water level series, modelled and measured, in the ports of Boulogne-sur-mer, Calais and Dunkerque (Eastern English Channel).

We finally discuss scaling stochastic processes able to generate series possessing such scaling and intermittent properties.

References

[1] Huang Y., F. G. Schmitt, Z. Lu, Y. Liu, *An amplitude-frequency study of turbulent scaling intermittency using Hilbert spectral analysis*, EPL **84**, 40010 (2008).
[2] Huang, Y., F.G. Schmitt, J.-P. Hermand, Y. Gagne, Z. M. Lu, Y.L. Liu, *Arbitrary order Hilbert spectral analysis for time series possessing scaling statistics: a comparison study with detrended fluctuation analysis and wavelet leaders*, Physical Review E **84**, 016208 (2011).
[3] F.G. Schmitt and Y. Huang, *Stochastic analysis of scaling time series; from turbulence theory to applications*, Cambridge University Press (2016).

cmg2016 - - Monday, June 6, 2016 - 11:45/12:30 (45min)

EXPERIMENTAL STUDY OF VORTEX DISTORTION BY THE CRAIK-LEIBOVICH FORCE

T. Humbert, B. Gallet & S. Aumaître
SPEC, CEA, CNRS, Université Paris-Saclay, CEA Saclay, 91191 Gif-sur-Yvette, France

Key words Wave-vortex interaction, surface waves, Craik-Leibovich force.

In a seminal paper aimed at providing a realistic theoretical model of Langmuir circulations [1], A. Craik and S. Leibovich introduced the mean force that a surface wave field exerts on the underlying flow. We report an experimental study on the influence of such a wave field on a single vortex: how is the wave field refracted by the vortex, and more importantly, how are the vortex structure and intensity affected by the waves?

We drive a steady circular vortex by running electrical current in an electrically conducting fluid, in the presence of magnetic field. A paddle generates waves propagating towards the vortex, with controlled amplitude and frequency. The surface velocity field is measured through Particle Tracking Velocimetry.

Coherent averaging of the surface velocity at the wave frequency allows us to extract the surface wave field, while long-time average leads to the vortex structure. In the top panels of figure 1, we show the base flow without waves, and the pure surface waves in absence of the vortex. The interaction between the two leads to the bottom panels of figure 1, that clearly display wave refraction, together with vortex recoil. A simple analytical model describing the balance between the driving force, the Craik-Leibovich one and turbulent viscosity leads to scaling laws that are verified experimentally.

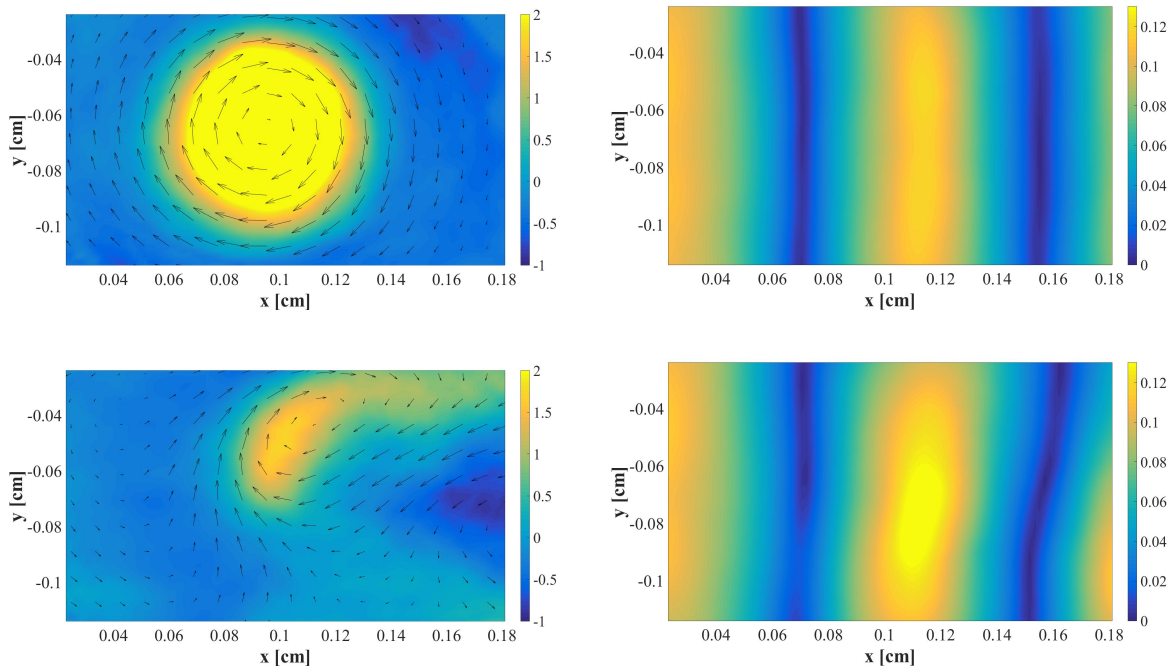

Figure 1. Top-left: vorticity map of the steady vortex without waves, in inverse seconds. Top-right: surface waves in the absence of the vortex (color codes for the magnitude of velocity, in m/s). The interaction between these two ingredients leads to refracted wavefronts (bottom-right panel) and vortex recoil (bottom-left panel).

References

[1] A. D. D. Craik, S. Leibovich, *A rational model for Langmuir circulations.* J. Fluid Mech. **73(3)**, 401-426 (1976).
[2] O. Bühler, *Waves and mean flows.* Cambridge University press (2009).
[3] O. Bühler, M.E. McIntyre, *Remote recoil: a new wave-mean interaction effect.* Journal of Fluid Mechanics, **492**, 207-230 (2003).

cmg2016 - - Monday, June 6, 2016 - 11:45/12:30 (45min)

EARTH-SYSTEM STABILITY THROUGH GEOLOGIC TIME

Daniel H. Rothman[1] and Samuel A. Bowring[1]

[1]*Lorenz Center, Department of Earth, Atmospheric, and Planetary Sciences, Massachusetts Institute of Technology, Cambridge, MA 02139 USA*

Key words Carbon cycle, mass extinctions, Earth system, stability

The five great mass extinctions of the last 500 million years are each associated with significant perturbations of Earth's carbon cycle. But there are also many such environmental events not associated with mass extinction. What makes them different? We show that natural perturbations of the carbon cycle exhibit a critical rate of change resulting from a transient balance between the photosynthetic uptake and respiratory return of CO_2. The critical rate is also the fastest rate at which the resulting excess CO_2 can be produced in a sustained steady state. We identify the critical rate with marginal stability, and find that four of the five great mass extinctions occur on the fast, unstable side of the stability boundary. Moreover, many severe yet relatively benign events occur close to the boundary. These results suggest that major environmental change is characterized by common mechanisms of Earth-system instability. The most rapid instabilities result in mass extinction.

PHYSICAL PROCESSES IN TITAN'S HYDROCARBON SEAS

R.D.Lorenz[1]
[1]*JHU Applied Physics Laboratory, Laurel, MD, USA.*

Key words Titan, Hydrocarbons, Oceanography, Waves, Tides.

Titan's hydrocarbon seas present a new laboratory for geophysical studies : oceanography is no longer just an Earth science. Air-sea exchange of heat, matter and momentum may take place under quite different conditions from Earth, challenging many empirical parameterizations of these processes which are critical in hurricane intensification, wave generation and erosion, climate evolution and so on. On a world at 94K with gravity similar to our Moon, but with a nitrogen atmosphere 4x denser than ours, methane takes the role of water. Ethane is likely present (although its apparent low abundance is a mystery) and acts somewhat analogously to salt on Earth, a relatively involatile tracer. Nitrogen dissolves significantly in methane, so the seas are principally a ternary mixture. It is possible that a latitude gradient in the amount of methane rainfall 'flushes' Ligeia Mare much like the Baltic or Black Seas on Earth, concentrating solutes in Kraken Mare. The extent to which this occurs depends on the tidal mixing between the seas. Analytic and numerical models have been applied to this problem. Remote sensing by the Cassini spacecraft has provided some constraints on sea-surface roughness, and on composition. Titan's seas are an attractive target for future exploration, e.g. by a floating capsule like the Titan Mare Explorer (TiME) Discovery Phase A study, or even by a submarine, a concept being explored by the NASA Innovative Advanced Concepts (NIAC) program. The interaction of such vehicles with their environment (e.g. the response of a capsule to waves, or the thermodynamic exsolution of nitrogen associated with heat rejection from a radioisotope heat source) poses new and interesting challenges to engineers.

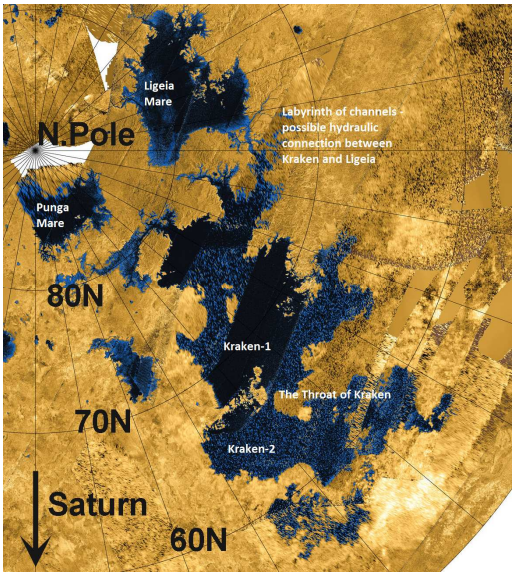

Figure 1. Radar Map of Titan's Seas. Ligeia Mare is about 350km across and is linked to Kraken by a narrow channel, Trevize Fretum. Interesting tidal dynamics are also expected at Seddon Fretum (aka, The Throat of Kraken)

References

[1] Lorenz, R. and J. Mann, 2015. Seakeeping on Ligeia Mare : Dynamic Response of a Floating Capsule to Waves on the Hydrocarbon Seas of Saturn's Moon Titan, Johns Hopkins/APL Technical Digest,33(2), 82-94

Atmosphere and Climate

cmg2016 - - Monday, June 6, 2016 - 15:00/15:15 (15min)

SUBGRID-SCALE PARAMETERIZATION AND LOW-FREQUENCY VARIABILITY - A RESPONSE THEORY APPROACH

J. Demaeyer and S. Vannitsem
Institut Royal Météorologique de Belgique, Avenue Circulaire, 3, 1180 Brussels, Belgium

Key words Subgrid parameterization; Response theory; Low-frequency variability; Ocean–atmosphere coupled model; Multi-scale systems

Weather and climate models are limited in the possible range of resolved spatial and temporal scales. However, due to the huge space- and time-scale ranges involved in the Earth System dynamics, the effects of many sub-grid processes should be parameterized. These parameterizations have an impact on the forecasts or projections. In particular, it could affect the low-frequency variability present in the system (such as the one associated to ENSO or NAO). An important question is therefore to know what is the impact of stochastic parameterizations on the Low-Frequency Variability generated by the system and its model representation.

In this context, we consider a stochastic subgrid-scale parameterization based on the Ruelle's response theory and proposed in Ref. [1]. We test this approach in the context of a low-order coupled ocean-atmosphere model, detailed in Ref. [2], for which a part of the atmospheric modes is considered as unresolved. A natural separation of the phase-space into a slow invariant set and its fast complement allows for an analytical derivation of the different terms involved in the parameterization, namely the average, the fluctuation and the long memory terms.

The stochastic parameterization is then applied for two cases: a weak and a strong (natural) coupling between the resolved and unresolved components. For the weak coupling, the method accurately corrects the low-frequency variability along the invariant subset. For the strong coupling, the low-frequency variability in the ocean is still very well corrected while a less important, but still impressive, correction is found within the atmosphere. This new approach of scale separation opens new avenues of subgrid-scale parameterizations in multiscale systems used for climate forecasts.

References

[1] Wouters J, Lucarini V. 2012. Disentangling multi-level systems: averaging, correlations and memory. *Journal of Statistical Mechanics: Theory and Experiment* **2012**(03): P03 003.

[2] Vannitsem S, Demaeyer J, De Cruz L, Ghil M. 2015. Low-frequency variability and heat transport in a low-order nonlinear coupled ocean–atmosphere model. *Physica D: Nonlinear Phenomena* **309**: 71–85.

cmg2016 - - Monday, June 6, 2016 - 14:45/15:00 (15min)

SIMULATION OF HEAT WAVES IN CLIMATE MODELS USING LARGE DEVIATION ALGORITHMS

F. Ragone[1], F. Bouchet[1,2] & J. Wouters[3,4]
[1]*Ecole Normale Supérieure, Lyon, France*
[2]*CNRS, Lyon, France*
[3]*School of Mathematics and Statistics, University of Sydney, Australia*
[4]*Meteorologisches Institut, University of Hamburg, Germany*

Key words Large deviations, extremes, general circulation models, heat waves.

One of the goals of climate science is to characterize the statistics of extreme, potentially dangerous events (e.g. exceptionally intense precipitations, wind gusts, heat waves) in the present and future climate. The study of extremes is however hindered by both a lack of past observational data for events with a return time larger than decades or centuries, and by the large computational cost required to perform a proper sampling of extreme statistics with state of the art climate models. The study of the dynamics leading to extreme events is especially difficult as it requires hundreds or thousands of realizations of the dynamical paths leading to similar extremes.

We will discuss here a new numerical algorithm, based on large deviation theory, that allows to efficiently sample very rare events in complex climate models. A large ensemble of realizations are run in parallel, and selection and cloning procedures are applied in order to oversample the trajectories leading to the extremes of interest. The statistics and characteristic dynamics of the extremes can then be computed on a much larger sample of events. This kind of importance sampling method belongs to a class of genetic algorithms that have been successfully applied in other scientific fields (statistical mechanics, complex biomolecular dynamics), allowing to decrease by orders of magnitude the numerical cost required to sample extremes with respect to standard direct numerical sampling.

We study the applicability of this method to the computation of the statistics of European surface temperatures with the Planet Simulator (Plasim), an intermediate complexity general circulation model of the atmosphere. We demonstrate the efficiency of the method by comparing its performances against standard approaches. Dynamical paths leading to heat waves are studied, enlightening the relation of Plasim heat waves with blocking events, and the dynamics leading to these events. We then discuss the feasibility of this method for applications with state of the art climate models, and we explain why this new approach could represent a change of paradigm for the study of extreme events, allowing to study their dynamics extensively at a reasonable computational cost.

cmg2016 - - Monday, June 6, 2016 - 14:30/14:45 (15min)

MONTE CARLO SIMULATION OF THREE-DIMENSIONAL SOLAR RADIATIVE TRANSFER OVER COMPLEX TERRAIN

T.V. Russkova, P.N. Zenkova, T.B. Zhuravleva
V.E. Zuev Institute of Atmospheric Optics, Tomsk, Russian Federation

Key words Radiative transfer equation, numerical simulation, complex terrain, Monte Carlo method.

Large parts of the land surface are characterized by complex terrain. The structure and reflective properties of the surface have an influence on remote sensing results and ground-based observations as well. Consequently, the topography effects can lead to errors in the retrieval of aerosol and cloud characteristics and other atmospheric constituents. To model accurately the radiative signal received, for instance, at aircraft or satellite level, the spatial variability of the underlying surface properties must be taken into account.

The focus of this study is an algorithm, based on the Monte Carlo method, developed to solve the radiative transfer equation over rugged terrain and included in a constantly updating program package MATHART (Monte Carlo codes for Three-Dimensional Radiative Transfer). While the 3D Monte Carlo simulation is very time consuming technique for radiative calculations under complex atmospheric conditions (highly structured terrain, cumulus broken cloudiness, etc.), it remains the best approach for the intricate radiative transfer modeling in vertically and horizontally inhomogeneous media.

The present Monte Carlo code is realized for a plane-parallel, aerosol-molecular model of the cloudless atmosphere. The approach of photon tracing simulation in any irregular and inhomogeneous space is considered. To investigate the three-dimensional topography effect on the upward and downward solar radiation, both simplified and the real digital elevation models are used.

The study was supported by the Russian Ministry of Education and Science under the Grant of the President of the Russian Federation MK-5381.2016.5 and partially supported by the Russian Foundation for Basic Research (Grant No. 16-01-00617 a).

cmg2016 - - Monday, June 6, 2016 - 14:00/14:30 (30min)

THE SELF-ORGANIZATION OF TROPICAL CONVECTION

C. Muller[1], S. Bony[2], J.Y. Grandpeix[2] & A. Lahellec[2]
[1]*LMD, Ecole Normale Supérieure, Paris, France*
[2]*LMD, Université Pierre et Marie Curie, Paris, France*

Key words Tropical convection, convective organization, self-aggregation, radiative feedbacks.

The organization of tropical convection is ubiquitous, but its physical understanding remains limited. One particular type of organization is the spatial self-aggregation of convection (figure), taking the form of cloud clusters, or tropical cyclones in the presence of rotation.

We show that several physical processes can give rise to self-aggregation, and highlight the key features responsible for it using idealized simulations. Longwave radiative feedbacks yield a “radiative aggregation". In that case, sufficient spatial variability of radiative cooling rates yields a low-level circulation, which induces the up-gradient energy transport and radiative-convective instability. Not only do vertically-integrated radiative budgets matter, but the vertical profile of cooling is also crucial.

Convective aggregation is facilitated when downdrafts below clouds are weak (“moisture-memory aggregation"). Interestingly, this is sufficient to trigger aggregation in the absence of longwave radiative feedbacks. These results shed some light on the sensitivity of self-aggregation to various parameters, including resolution or domain size.

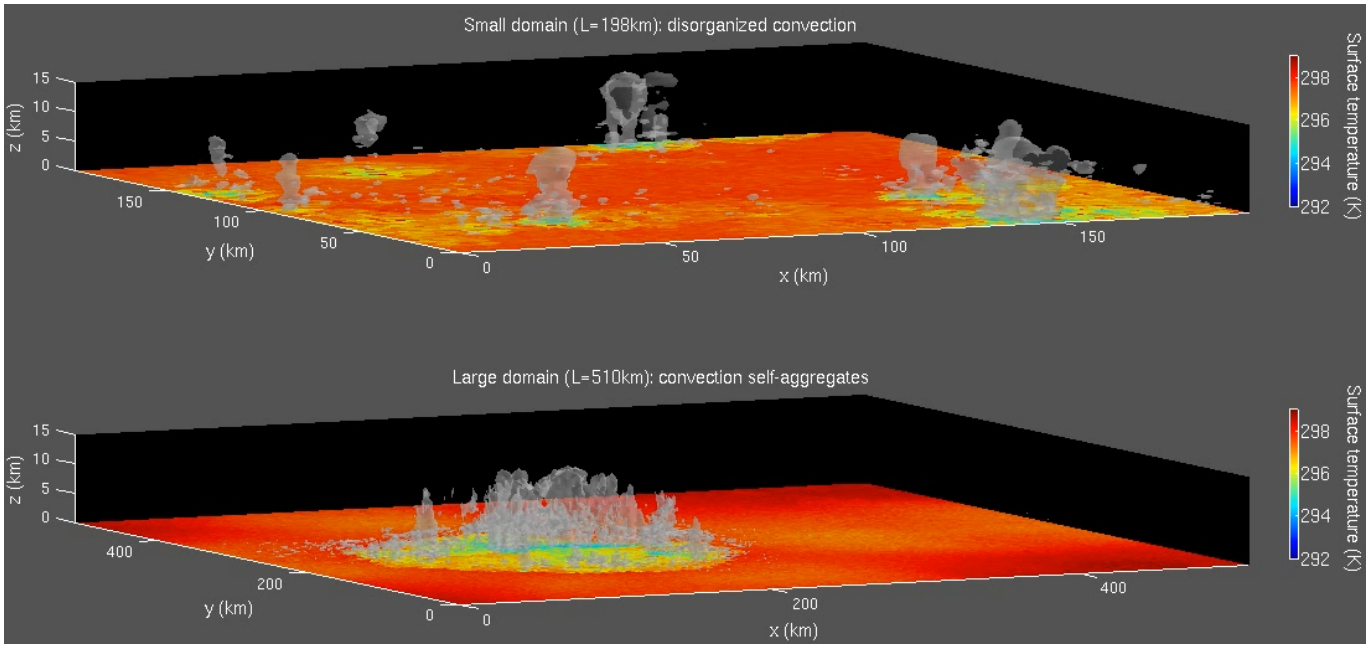

Figure. *Clouds (gray surfaces) and near-surface temperatures (colors) in two simulations in radiative-convective equilibrium. The simulations only differ by their domain size. In the large-domain simulation (bottom panel), the convection spontaneously self-aggregates in space.*

cmg2016 - - Monday, June 6, 2016 - 15:15/15:30 (15min)

DATA-DRIVEN STOCHASTIC MODELING AND PREDICTION OF ARCTIC SEA ICE

D. Kondrashov[1], M.D. Chekroun[1], & M. Ghil[1,2]
[1] *University of California, Los Angeles, USA*
[2] *Ecole Normale Supérieure, Paris, France*

Key words stochastic modeling, data-adaptive, Arctic sea ice, prediction

We present results of data-driven predictive analyses of sea ice over the main Arctic regions. Our approach relies on the Multilayer Stochastic Modeling (MSM) framework of [1] and it leads to probabilistic prognostic models of sea ice concentration (SIC) anomalies on seasonal time scales. This approach is applied to monthly time series of state-of-the-art data-adaptive decompositions of SIC and selected climate variables over the Arctic.

We evaluate the predictive skill of MSM models by performing retrospective forecasts with "no-look ahead" for up to 6-months ahead. It will be shown in particular that the memory effects included intrinsically in the formulation of our non-Markovian MSM models allow for improvements of the prediction skill of large-amplitude SIC anomalies in certain Arctic regions on the one hand, and of September Sea Ice Extent, on the other.

Further improvements allowed by the MSM framework will adopt a nonlinear formulation and explore next-generation data-adaptive decompositions, namely extension of Principal Oscillation Patterns (POP) and rotated Multichannel Singular Spectrum Analysis (M-SSA).

References

[1] Kondrashov, D., M. Chekroun, and M. Ghil, 2015: *Data-driven non-Markovian closure models*. **Physica D.**, **297**, 33–55.

Evidence of a strange nonchaotic attractor in the El Niño dynamics from re-analyses versus CMIP5 models

Serykh Ilya, Sonechkin Dmitry
P.P.Shirshov Institute of Oceanology, Russian Academy of Sciences, Moscow
iserykh@ocean.ru

Based on a mathematical idea about the so-called strange nonchaotic attractor (SNA) in the quasi-periodically forced dynamical systems, the currently available re-analyses data are considered. It is found that the El Niño - Southern Oscillation (ENSO) is driven not only by the seasonal heating, but also by three more external periodicities (incommensurate to the annual period) associated with the ~18.6-year lunar-solar nutation of the Earth rotation axis, ~11-year sunspot activity cycle and the ~14-month Chandler wobble in the Earth's pole motion. Because of the incommensurability of their periods all four forces affect the system in inappropriate time moments. As a result, the ENSO time series look to be very complex (strange in mathematical terms) but nonchaotic.

The power spectra of ENSO indices reveal numerous peaks located at the periods that are multiples of the above periodicities as well as at their sub- and super-harmonic. In spite of the above ENSO complexity, a mutual order seems to be inherent to the ENSO time series and their spectra. This order reveals itself in the existence of a scaling of the power spectrum peaks and respective rhythms in the ENSO dynamics that look like the power spectrum and dynamics of the SNA. It means there are no limits to forecast ENSO, in principle. In practice, it opens a possibility to forecast ENSO for several years ahead.

Global spatial structures of anomalies during El Niño and power spectra of ENSO indices from re-analyses are compared with the respective output quantities in the CMIP5 climate models (the Historical experiment). It is found that the models reproduce global spatial structures of the near surface temperature and sea level pressure anomalies during El Niño very similar to these fields in the re-analyses considered. But the power spectra of the ENSO indices from the CMIP5 models show no peaks at the same periods as the re-analyses power spectra. We suppose that it is possible to improve modeled rhythms if the afore-mentioned external periodicities are taken in an explicit consideration in the models.

cmg2016 - - Monday, June 6, 2016 - 11:45/12:30 (45min)

USING CONTINUOUS WAVELET TRANSFORM TO ANALYSE SYNOPTIC-SCALE PROCESSES

V. Khokhlov[1], N. Yermolenko[1]
[1]*Odessa State Environmental University, Odessa, Ukraine*

Key words Weather systems, Continuous wavelet transform, North Atlantic Oscillation, Droughts.

Wavelets are fundamental building block functions, analogous to the trigonometric sine and cosine functions. Wavelet transform expands time series into time-frequency space and can therefore find localized intermittent periodicities. The continuous wavelet transform is commonly used to extract details from time series, and the cross-wavelet transform (XWT) of two time series allows revealing their common features in time-frequency space. Here, we used the wavelet analysis (i) to determine a possible linkage between the North Atlantic Oscillation (NAO) and processes over Ukraine at synoptic time scale, and (ii) to examine an impact of the NAO on drought's conditions in Ukraine. The first task seems to be tempted as the NAO-induced changes of hydrometeorological parameters and weather phenomena in Ukraine appear to be not very considerable as its territory is remote relative to the centres of action related to the NAO. The second task is interesting owing to the impact of climate change on characteristics of droughts.

One can be noted that the synoptic conditions in North Atlantic can be connected with changes of weather patterns over Ukraine. However it must be taken into account the fact that this connection occurred only during a few days or 2–3 weeks within cold season [1]. The change of synoptic situation is the process with low noise-to-signal ratio. That the wavelet analysis may reveal some significant variability, the synoptic processes must be active as, for example, the blocking or the evolution of intensive cyclone. Then the changes of these processes would stand out against a background of common synoptic conditions.

Then we used the multiscalar drought index – standardized precipitation evapotranspiration index, SPEI12 – to investigate spatiotemporal droughts variability caused by the climate change. The cross-wavelet transform was applied to reveal a connection between the droughts in Ukraine and teleconnection patterns in the North Atlantics. The analysis showed that the North Atlantic Oscillation (NAO) has a maximal effect on the droughts in Ukraine. The anti-phase relation is registered for the joint fluctuations with the periods 2-3 years and is most prominent in the Southern Ukraine (Fig. 1). On the contrary, the NAO has a small impact on the Northern Ukraine. This fact can be explained by the orientation of main storm tracks for positive and negative phases of the NAO.

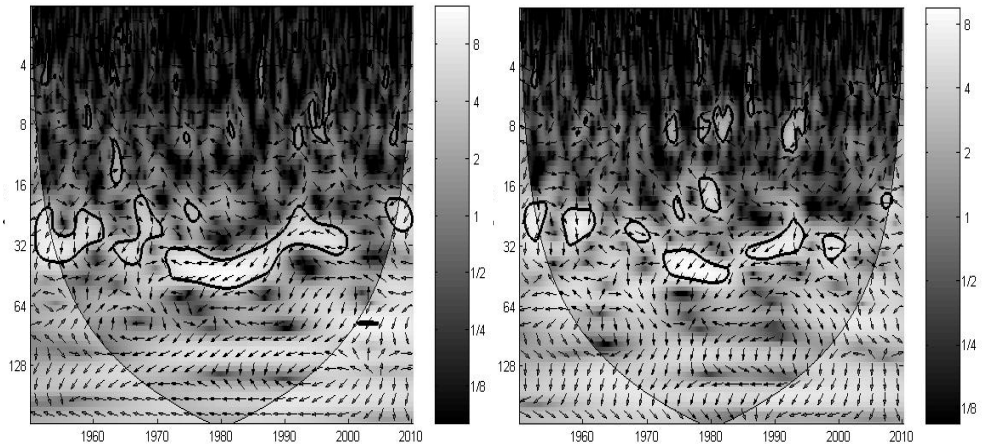

Figure 1. Cross-wavelet transform of NAO indices and SPEI12 for southern (left panel) and northern part of Ukraine; *x*-axis – years, *y*-axis – period (months).

Our results showed that wavelet transform is the best method to detect possible peculiarities from various non-stationary hydrometeorological time series.

References

[1] V. Khokhlov and A. Romanova, *Joint principal component – wavelet analysis of atmospheric teleconnection: the North Atlantic Oscillation case*, Stoch. Environ. Res. Risk Assess., **28**, 369-381 (2014).

Co-existence of Chaos and Order in Weather and Climate Dynamics

Dmitry M. Sonechkin

P.P. Shirshov Oceanology Institute, Russian Academy of Sciences, Moscow, Russia
E-mail: dsonech@yandex.ru

Abstract: It is widely accepted to believe that the atmospheric dynamics is chaotic, and so unpredictable for more or less distant future. It is because all solutions of the hydrothermodynamical equations governing the dynamics are unstable to small disturbances of their initial data. The aim of this report is to demonstrate that it is not fatal as seen because some orderings always co-exist with the chaos induced by these instabilities. Taking different ordering elements into account it is possible to exclude from further consideration certain of the above-mentioned instabilities. In particular, the processes within the timescales of 10**4 – 10**5 years (like the glacial cycles of climate) are affected by many insolation oscillations with incommensurate periods. By this reason, the attractor of these processes modeling turns out to be similar to the so-called strange but nonchaotic attractors (SNA) well-known in the dynamical system theory. The history of these processes evolution seen in paleoclimatic records can be depicted as a sequence of the period multiplying bifurcations from a simple limit cycle attractor during the Pliocene to a SNA-like attractor during the late Pleistocene including the main period-doubling bifurcation at the moment of the famous mid-Pleistocene transition. The processes of the interannual atmospheric variations (like El-Nino – Southern Oscillation) are governed not only by the annual periodic heating of the climate system but also luni-solar nutations of the Earth's rotation axis and the Chandler wobble in the Earth's pole motion. By these reasons, these processes reveal another SNA-like climatic attractor. Consideration of the ENSO-processes with details will be given in a report of my young colleague I.V. Serykh.
These facts open the door for hyper- and super-long term climatic predictions.

Keywords: Weather chaos, Strange nonchaotic climatic variations.

cmg2016 - - Monday, June 6, 2016 - 11:45/12:30 (45min)

A MATHEMATICAL MODEL OF NEAR RESONANCE WAVE PERTURBATIONS IN THE ATMOSPHERE

O. Savina[1] & P. Bespalov[2]
[1]*National Research University Higher School of Economics, Nizhny Novgorod, Russia*.
[2]*Institute of Applied Physics, Russian Academy of Sciences, Nizhny Novgorod ,Russia.*

Key words Atmosphere, Wave propagation, Lamb wave.

An original model of acoustic-gravity wave propagation in the Earth's atmosphere with a realistic model high-altitude temperature profile is analyzed. We carry out an analysis of acoustic-gravity wave behavior near the resonance level, at which the condition of equality of horizontal phase wave velocity is equal to the local value of the sound velocity. Shaping of a narrow domain with elevated pressure in the resonance region where the horizontal phase wave velocity is equal to the sound velocity is examined theoretically within the framework of the linearized equations. In this study generalized Lamb waves in a nonisothermal atmosphere have been examined theoretically. Our results suggest that the pressure component of the Lamb wave decreases exponentially upwards near the layer with an extremum of sound speed. Numerical simulations for the model profiles of atmospheric temperature and viscosity confirm analytical result for the special feature of wave fields.

References

[1] P.A. Bespalov, O.N.Savina. *Exponential and local Lamb waves in the nonisothermal atmosphere as an obstacle to the acoustic-gravity disturbance propagation up to the ionosphere* , J. Atm. Solar-Terr. Phys. **123**, 2015 (137).

cmg2016 - - Monday, June 6, 2016 - 11:45/12:30 (45min)

INTERNAL WAVE EXCITATION BY TURBULENT CONVECTION

D. Lecoanet[1], M. Le Bars[2,3], K. J. Burns[4], E. Quataert[1], G. M. Vasil[5], B. P. Brown[6] & J. S. Oishi[7]
[1]*University of California, Berkeley, USA*
[2]*IRPHE, Marseille, France*
[3]*University of California, Los Angeles, USA*
[4]*MIT, Cambridge, USA*
[5]*University of Sydney, Sydney, Australia*
[6]*University of Colorado, Boulder, USA*
[7]*Farmingdale State College, Farmingdale, USA*

Key words Convection; internal waves.

Convection near a stably stratified region can excite internal gravity waves. This occurs in a wide range of geophysical settings, including the Earth's atmosphere and core, as well as in astrophysical systems like some gas giants like Saturn, and most stars including the sun. Internal waves excited by convection are thought to play an important role in the atmosphere, for instance, driving the quasi-biennial oscillation. Water's density maximum at 4°C makes it well suited to study this problem: an increasing temperature profile is unstable to convection below 4°C, but stably stratified above 4°C. We present numerical simulations of a water-like fluid near its density maximum in a two dimensional domain (Fig. 1, [1]), inspired by the experimental study of [2]. The simulation is run using the flexible, open-source pseudo-spectral code Dedalus [3].

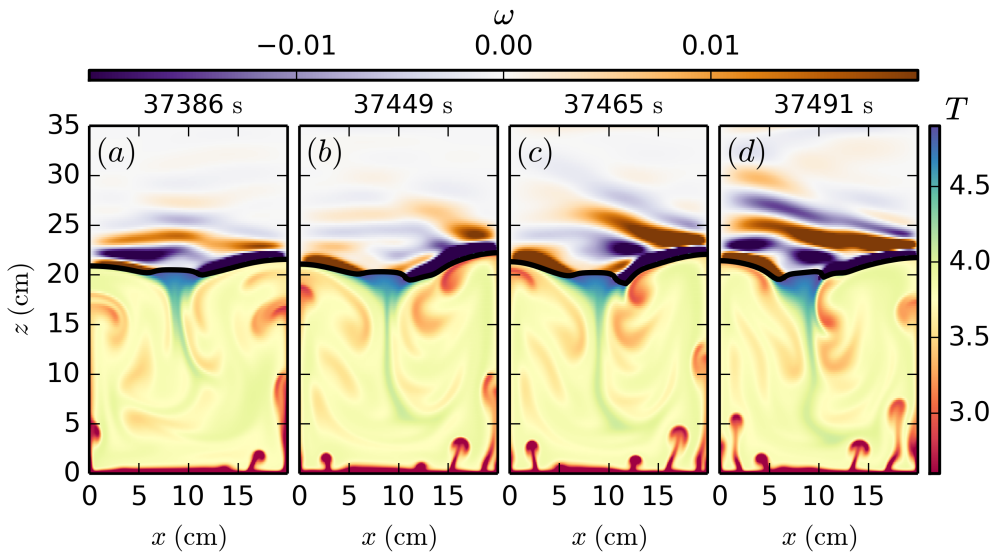

Figure 1. Four simulation snapshots. The bottom part of the domain (below the thick black line) shows the temperature field. Recall that below 4°C, cold water (red) is less dense than hot water (blue). The thick black line is the 5°C isotherm and shows the boundary between the convective region (below) and the stably stratified region (above). The top part of the domain (above the thick black line) shows the vorticity field associated with internal gravity waves.

To isolate the physical mechanism exciting internal waves, we use data from the full simulation as source terms in two simplified models of internal-wave excitation by convection: bulk excitation by convective Reynolds stresses, and interface forcing via the mechanical oscillator effect. We find excellent agreement between the waves generated in the full simulation and the simplified simulation implementing the bulk excitation mechanism.

References

[1] D. Lecoanet, M. Le Bars, K. J. Burns, G. M. Vasil, B. P. Brown, E. Quataert, J. S. Oishi, Phys. Rev. E **91**, 063016 (2015).
[2] M. L. Bars, D. Lecoanet, S. Perrard, A. Ribeiro, L. Rodet, J. M. Aurnou, and P. L. Gal, Fluid Dyn. Res. **47**, 045502 (2015).
[3] The code is available at `dedalus-project.org`.

cmg2016 - - Monday, June 6, 2016 - 11:45/12:30 (45min)

EXPERIMENTAL RESULTS ON INERTIA GRAVITY WAVE EMISSION FROM BAROCLINIC JETS

Costanza Rodda[1], Ion D. Borcia[1], & Uwe Harlander[1]
[1]*Brandenburg University of Technology (BTU) Cottbus-Senftenberg, Aerodynamics and Fluid Mechanics, Cottbus, Germany (haruwe@tu-cottbus.de)*

Key words inertia-gravity waves, rotating annulus experiment, spontaneous imbalance

Large-scale balanced flows can spontaneously radiate meso-scale inertia-gravity waves (IGWs) and are thus in fact unbalanced. While flow-dependent parameterizations for the radiation of IGWs from orographic and convective sources do exist, the situation is less developed for spontaneously emitted IGWs. Observations identify increased IGW activity in the vicinity of jet exit regions. A direct interpretation of those based on geostrophic adjustment might be tempting. However, directly applying this concept to the parameterization of spontaneous imbalance is difficult since the dynamics itself is continuously re-establishing an unbalanced flow which then sheds imbalances by GW radiation. Examining spontaneous IGW emission in the atmosphere and validating parameterization schemes confronts the scientist with particular challenges. Due to its extreme complexity, GW emission will always be embedded in the interaction of a multitude of interdependent processes, many of which are hardly detectable from analysis or campaign data. The benefits of repeated and more detailed measurements, while representing the only source of information about the real atmosphere, are limited by the non-repeatability of an atmospheric situation. The same event never occurs twice. This argues for complementary laboratory experiments, which can provide a more focused dialogue between experiment and theory. Indeed, life cycles are also examined in rotating-annulus laboratory experiments. Thus, these experiments might form a useful empirical benchmark for theoretical and modeling work that is also independent of any sort of subgrid model. In addition, the more direct correspondence between experimental and model data and the data reproducibility makes lab experiments a powerful testbed for parameterizations. Here we show first results from a small rotating annulus experiments and we will further present our new experimental facility to study wave emission from jets and fronts.

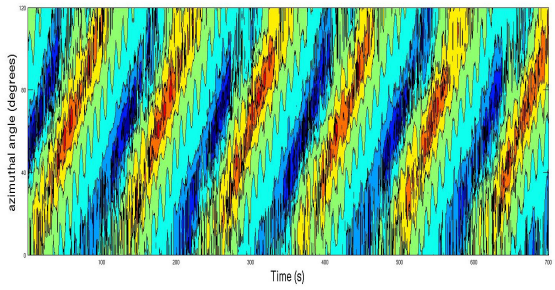

Figure 1. Hovmöller (time-space) plot of the radial velocity at a constant radial distance from the rotation axis. The data are measured in the rotating annulus experiment using the Particle Image Velocimetry (PIV) measurement technique.

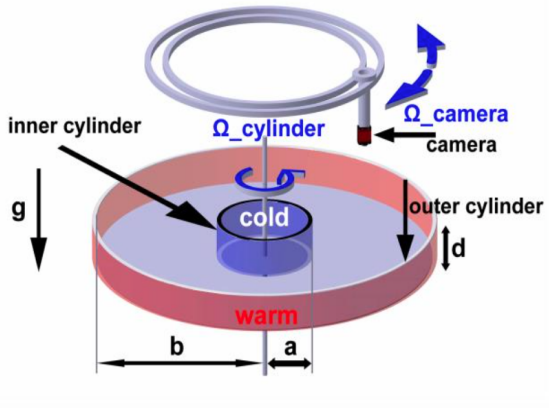

Figure 2. Sketch of the new experimental apparatus. The radius a (b) of the inner (outer) cylinder is 12cm (70cm), d=30cm. Also visible is the feature tracking system that consists of a camera that can follow flow features due to the fact that the camera can rotate with a different angular velocity than the confinement. This setup is ideal to follow a baroclinic jet that usually rotates somewhat faster than the annulus.

cmg2016 - - Monday, June 6, 2016 - 11:45/12:30 (45min)

Response of El Niño Events to Higher CO_2 Forcing: Role of Nonlinearity

De-Zheng Sun[1], Shao Sun[2], & Jin Liang[3]
[1]*University of Colorado, Colorado, USA*
[2] *China Meteorological Administration, Beijing, China*
[3]*Nanjing University, Nanjing, China*

Key words Climate Change, El Niño, Nonlinearity, CMIP5 Climate Models

As El Nino—Southern Oscillation (ENSO) affects climate worldwide, how ENSO events respond to higher CO2 forcing is a critical question in the science of climate change. Theory based on a nonlinear, analytical model predicts an increase in the level of ENSO activity in response to higher CO2 forcing even when the level of activity is gauged by the traditional measure—the variance of Nino3 SST. This contrasts the average results from the state-of-the art climate models collected by CMIP5 that suggest a largely muted response. However, we find that that CMIP5 models have a common deficiency in simulating ENSO—an underestimate of the asymmetry between the two phases of ENSO. The nonlinear model that the theoretical prediction is based on, in contrast, does simulate this fundamental aspect of the observed ENSO. We further find that the number of models that project a consistent positive response of ENSO (i.e., an increase in the level of ENSO activity) to higher CO2 forcing under two different rates of CO2 increases is comparable to the number of models that give a consistent muted response of ENSO activity of CO2. More importantly, ENSO simulated in the historical runs of the models that predict a consistent positive response in the level of ENSO activity are found to be more comparable to the observations in amplitude and asymmetry than ENSO in the runs that project a muted response. These findings suggest a critical role of nonlinear dynamics in the response of ENSO events to higher CO2 forcing. The results also suggest that the theoretical prediction from a nonlinear, analytical model is not necessarily in consistent with projections by the state-of-the-art climate models.

cmg2016 - - Monday, June 6, 2016 - 11:45/12:30 (45min)

OCEAN CONTROL OF TYPHOON PEAK INTENSITY

W. Mei[1], C. Pasquero[2], S.-P. Xie[1], F. Primeau[3] & J.C. McWilliams[4]
[1]*Scripps Institution of Oceanography, University of California, San Diego, USA*
[2]*University of Milan-Bicocca, Italy*
[3]*University of California, Irvine, USA*
[4]*University of California, Los Angeles, USA*

Key words: Typhoons, air-sea interactions, Bayesian approach

Dominant climatic factors controlling the lifetime peak intensity of typhoons are determined from six decades of Pacific typhoon data, using a Bayesian uncertainty analysis to confirm robustness of the results. None of the climatic metrics related to the atmosphere that were tested (including vertical shear of horizontal winds, low-level vorticity, mid-level vertical velocity and moisture, and seal-level pressure) present a significant correlation with the seasonally averaged lifetime peak intensity of typhoons. We find that upper ocean temperatures in the low-latitude northwestern Pacific (LLNWP) and sea surface temperatures in the central equatorial Pacific control the seasonal average lifetime peak intensity by setting the rate and duration of typhoon intensification, respectively. An anomalously strong LLNWP upper ocean warming has favored increased intensification rates and led to unprecedentedly high average typhoon intensity during the recent global warming hiatus period, despite a reduction in intensification duration tied to the central equatorial Pacific surface cooling. Continued LLNWP upper ocean warming as predicted under a moderate [that is, Representative Concentration Pathway (RCP) 4.5] climate change scenario is expected to further increase the average typhoon intensity by an additional 14% by 2100.

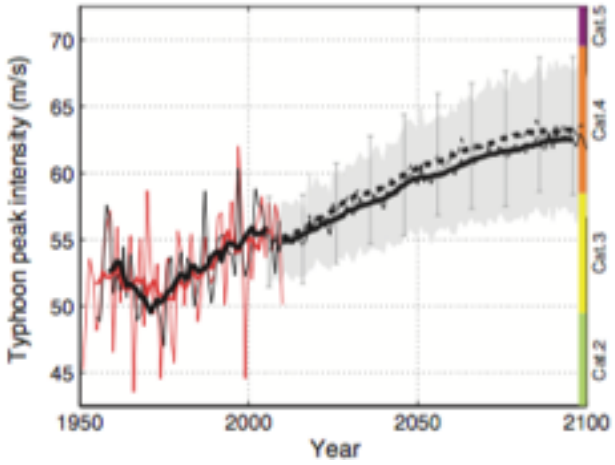

Figure 1. Observed and projected typhoon lifetime peak intensity. Observed (thin red), predicted (1950-2009, thin black), and projected (2006-2100, thin black) seasonal mean typhoon lifetime peak intensity (m/s) and their 9-year running mean (thick curves). Two projections are given: one (solid) considers both changes in SST and subsurface stratification with continuous gray shading showing error bars, and the other (dashed) ignores changes in subsurface stratification with error bars shown discretely for years 2006, 2016, …, and 2096. The colors on the right y axis denote the range of typhoon intensity from category 2 up to category 5 based on the Saffir-Simpson hurricane scale.

Planetary Geophysics

cmg2016 - - Tuesday, June 7, 2016 - 15:45/16:00 (15min)

FRAGMENTATION AND EXCHANGES DURING PLANETARY CORE FORMATION

J.-B. Wacheul[1], M. Le Bars[1]
[1]*CNRS, Aix-Marseille University, ECM, IRPHE UMR 7342, Marseille cedex 13, France*

Key words Fragmentation, turbulent exchanges, core formation.

Telluric planet formation involved the settling of large amounts of liquid iron coming from impactors into an ambient viscous magma ocean [1]. Planetary initial state was largely determined by diffusive exchanges of heat and elements during this iron rain. Current models often assume that the metal rapidly equilibrated as drops of single capillary size settling at the Stokes velocity. But the dynamics is more complex, and influenced by the large viscosity ratio between the metal and ambient fluid. We study this two-phase flow using a model experiment, where a balloon of heated liquid metal is popped at the top of a tank filled with viscous liquid (see figure 1). We explore the relevant planetary regimes, including the whole range of viscosity ratios. High-speed videos allow determining the statistics of drop sizes, shapes, and velocities. Measures of the temperature decrease during settling allow defining a global turbulent diffusion coefficient, confronted to current analytical models.

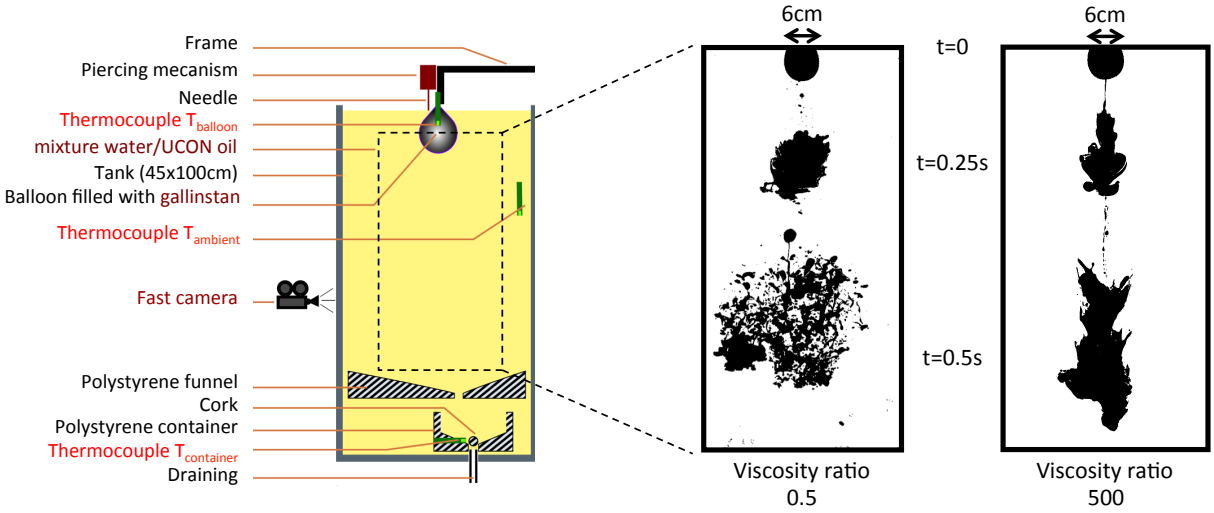

Figure 1. Sketch of the experimental set-up (left) and two examples of the observed sedimentation and fragmentation processes for identical initial metal blobs (right). Only the viscosity of the ambient fluid is changed between the two experiments, with pure water on the left and a mixture of water and Ucon oil on the right, leading to a viscosity ratio of 0.5 and 500 respectively. Each picture shows the liquid metal blob at two times following the balloon piercing at $t = 0$.

Our first conclusion is directly visible in the pictures of figure 1: while the mean settling of a metal blob does not depend on the ambient viscosity (i.e. our study is indeed in the Newtonion regime), the fragmentation dynamics strongly depends on the ratio between the ambient and internal viscosities. A low viscosity ratio leads to the standard formation of an "iron rain", with a Gamma distribution of drop sizes [2]. But a large viscosity ratio leads to the overall stabilisation of large blobs with a significantly distorded surface. It is then expected that these different behaviors lead to different equilibration scalings. The classical approach of equilibration consists in quantifying temperature exchanges by considering diffusion across a turbulent boundary layer scaling as the square root of the Péclet number (e.g. [3]). To assess this model, we systematically measure the temperature decrease of the metal blob during settling in our tank. Using systematic experiments, we propose new scalings laws regarding the evolution of the turbulent diffusion coefficient as a function of the Reynolds number and viscosity ratio. Building upon a better understanding of the sedimentation and fragmentation processes provided by our fluid mechanics approach, more relevant models of planet formation based on a reliable dynamical ground will be developed.

References

[1] D. J. Stevenson, *Fluid dynamics of core formation*, Origin of the Earth **1**, 231-249 (1990).
[2] J. B. Wacheul et al., *Laboratory experiments on the breakup of liquid metal diapirs*, Earth Planet. Sci. Lett. **403**, 236-245 (2014).
[3] H. Samuel, *A re-evaluation of metal diapir breakup and equilibration in terrestrial magma oceans*, Earth Planet. Sci. Lett. **313**, 105-114 (2012).

cmg2016 - - Tuesday, June 7, 2016 - 11:00/11:30 (30min)

NEW CHALLENGES IN PLANETARY DUNES

Clément Narteau[1]
[1]*Institut de Physique du Globe de Paris, Sorbonne Paris Cité,*
Univ Paris Diderot, UMR 7154 CNRS, 1 rue Jussieu, 75238 Paris, Cedex 05, France.

Key words Dunes, sand flow path, sediment availability, wind regimes, grain-size segregation, Mars, Titan.

Dune fields have been extensively studied in the domain of physical geography, where there is still much work to be done, for example regarding the impact of climate change on desertification. However, the center of mass of this domain of research progressively shifts to mathematical geophysics thanks to new experimental, numerical and theoretical methods as well as new observations using satellite data on Earth, Mars and Titan (the Saturn's largest moon). Recent studies have established scaling laws (Claudin et al., 2006) and distinguished between two dune growth mechanisms in multidirectional regimes (Courrech du Pont et al., 2014), especially where there is a change in sediment availability. Here we show how these results could be used to revisit the description of planetary dune fields and test new conjectures on their present and past dynamics. Using Earth analogs, we pay a particular attention to dune fields on Mars and Titan to bring new quantitative constrains on General Circulation Models (Fig. 1). Then, we discuss the role of grain-size segregation in controlling sediment availability as well as the systematic changes in dune shape and orientation along sand flow paths.

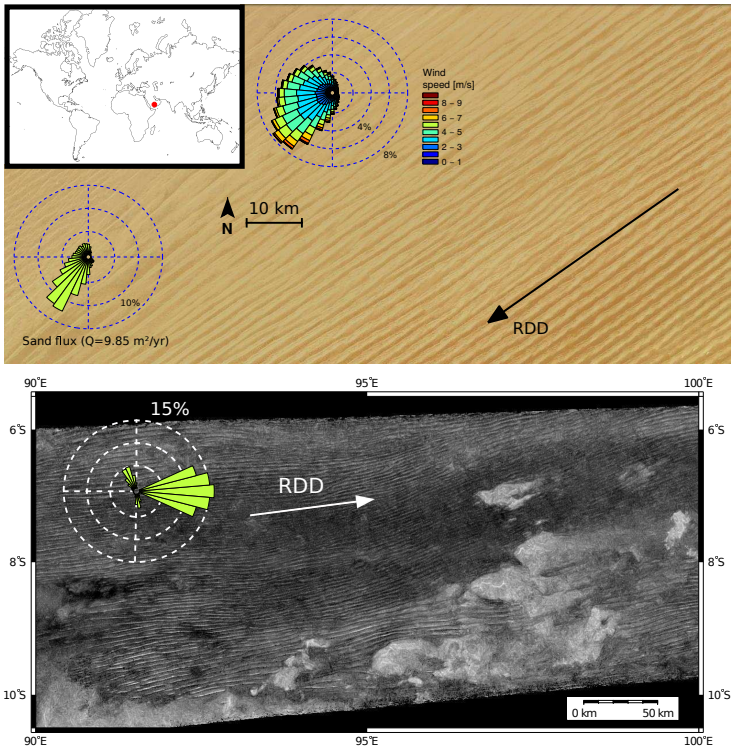

Figure 1. Analogy between linear dunes on Earth (top) and Titan (bottom). In presence of multidirectional wind regimes, dunes align along the resultant sand flux direction in both cases. For the terrestrial case, in the Rub al-Khali desert, inset show the wind and sand flux roses extracted from the ERA-Interim-project from the 1/1/1979 to the 31/12/2012. For Titan, the inset shows the sand flux rose calculated at 7.5° considering storms and averaging the effect of Saturn's eccentricity (Charnay et al., 2015).

References

[1] Charnay, B., Barth, E., Narteau C., Lebonnois S., Rodriguez S., Courrech du Pont, S. and Lucas A. *Methane storms as a driver of Titan's dune orientation*, Nature Geoscience, **8**, 362-366 (2015).
[2] Claudin P., and Andreotti B. *A scaling law for aeolian dunes on Mars, Venus, Earth, and for subaqueous ripples*, Earth Plan. Sci. Lett., **252**, 30-44 (2006).
[3] Courrech du Pont S., Narteau C. and Gao X. *T*wo modes for dune orientation, Geology, **42**, 743-746 (2014).

cmg2016 - - Tuesday, June 7, 2016 - 15:00/15:15 (15min)

THE TURBULENT RESPONSE OF PLANETARY FLUID INTERIORS TO TIDAL AND LIBRATIONAL FORCING

A. M. Grannan[1], B. Favier[2], M. Le Bars[2] & J. M. Aurnou[1]

[1]*Department of Earth, Planetary, and Space Sciences, University of California - Los Angeles, Los Angeles, CA, USA*

[2]*Aix-Marseille Université, CNRS, École Centrale Marseille, IRPHE UMR 7342, Marseille, France*

Key words Librational Forcing, Tidal Forcing, Elliptical Instability, Turbulence

The turbulence generated in the electrically conductive liquid metal cores and subsurface oceans of planetary bodies may be due to the role of boundary forcing through such geophysically relevant mechanisms of precession/nutation, libration, tidal forcing, and collisions. Here, we combine laboratory equatorial velocity measurements with selected high-resolution numerical simulations to show, for the first time, the generation of bulk filling turbulence driven by tidal forcing. The transition to saturated turbulence is characterized by an elliptical instability that first establishes an ellipsoidal base flow, excites primary and secondary inertial modes of the system, and finally generates small-scale turbulence. This progression is shown in three snapshots of a laboratory experiment and numerical simulation in Figure 1.a and 1.b, respectively. The amplitude of the tidally forced saturated turbulence scales with the body's elliptical distortion, β.

The results of the current tidal studies are compared with recent laboratory experiments and numerical simulations of the libration-driven turbulent flows, illustrated in Figure 1.c and 1.d, from [1] and [2], respectively. These separate analog models, tides and libration, correspond to two end-member types of geophysical mechanical forcing. In tidal forcing, non-synchronous satellites possess elastically deformable boundaries such that shape of the distortion has a non-zero mean motion. For librational forcing, the core-mantle boundary possesses an inherently rigid, frozen-in ellipsoidal shape such that the oscillatory motion of the elliptically deformed boundary has zero mean motion. We find striking similarities between tidal and librational forcing through both the transition to bulk turbulence and the enhanced zonal flow. Such similarities hint at a generic fluid response independent of the forcing mechanism.

The saturated turbulence scaling, found in the current work, is extrapolated for several orbiting bodies to argue that tidal forcing is sufficient for generating a magnetic field in the past and present-day core of the Earth and early Moon, while librational forcing could drive a core dynamo in Io, Europa, and Super-Earths *55CnC e*, *CoRoT-7b*, and *GJ 1214b*. In the context of subsurface oceans, the turbulence induced by mechanical forcing can homogenize the density stratification in these layers, providing a bound for the strength of the stratification that may exist in these fluid layers.

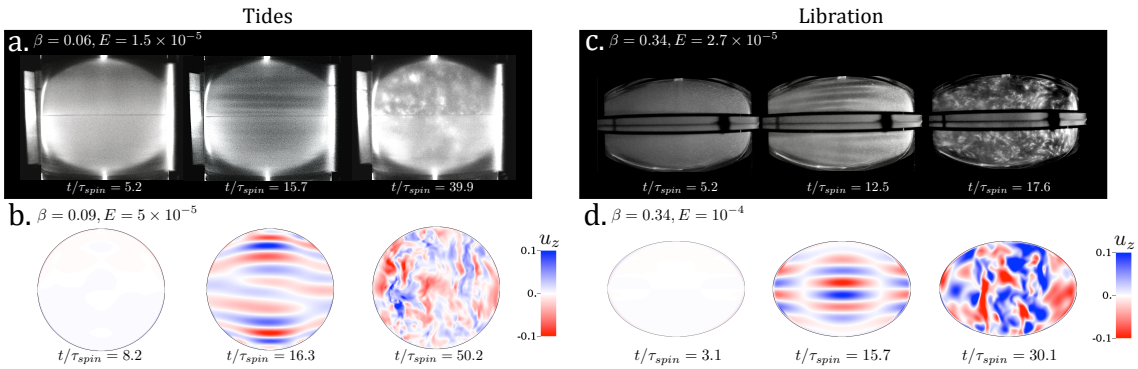

Figure 1. Sideview visualizations showing the onset of mechanically forced turbulence. Tidally forced flow as seen, **a)**, experimentally using flow tracers and, **b)**, in numerical simulation using the vertical velocity. The same visualizations taken from, **c)**, laboratory experiments and, **d)**, numerical simulation of libration driven flows.

References

[1] A. M. Grannan, B. Favier, M. LeBars, J. M. Aurnou, *Experimental study of global-scale turbulence in a librating ellipsoid*, Phys. Fluids. **26**, 126601 (2014).

[2] B. Favier, A. M. Grannan, M. LeBars, J. M. Aurnou, *Generation and maintenance of bulk turbulence by libration-driven elliptical instability*, Phys. Fluids. **27**, 066601 (2015).

cmg2016 - - Tuesday, June 7, 2016 - 15:15/15:30 (15min)

THERMO-CHEMICAL-TECTONIC EVOLUTION OF TERRESTRIAL PLANETS: THE KEY INFLUENCE OF MAGMATISM

P. J. Tackley[1], T. Nakagawa[2], D. Lourenco[1] & A. Rozel[1]
[1]*ETH Zurich, Zurich, Switzerland*
[2]*JAMSTEC, Yokohama, Japan.*

Key words Mantle convection, plate tectonics, Mars, Venus, stagnant lid.

Convection of the rocky mantle is the key process that drives the evolution of Earth's interior: it causes plate tectonics, controls heat loss from the metallic core (which generates the magnetic field) and drives long-term volatile cycling between the atmosphere/ocean and interior. It is now possible to numerically model the evolution of a terrestrial planet from the magma ocean stage to the present day using a 2D or 3D model of the mantle-lithosphere system couped to a parameterized model of the core (and sometimes, atmosphere), including the effects of magmatism and variations in tectonic mode. Previous works have identified stagnant lid, episodic overturn and mobile lid (plate tectonics) as possible tectonic modes, depending on the effective strength of the lithosphere and convective parameters. Simple scalings [1] as well as more complex models [2] indicate that plate tectonics should be easier on larger planets (super-Earths), other things being equal. Our recent models find that melting has several key effects on planetary evolution. Firstly, it produces compositional heterogeneity in the lithosphere, including continental cratons [3] and basaltic crust [4], which facilitate plate tectonics by focussing or producing stresses, making it 'easier' for the lid to break. Thus, scaling laws that are based on purely thermal convection cannot be literally applied to planetary evolution. Secondly, magmatism acts as a thermostat on mantle temperature, losing large amounts of heat when the mantle is hot, when internal heat production is high such as early in a planet's evolution [5] or in a stagnant-lid mode – [6] showed that in a stagnant-lid Venus-like planet most of the heat loss is accommodated by magmatic heat pipe volcanism. Thirdly, it can produce compositional stratification in the deep mantle, which modules heat flux from the core, determining geodynamo evolution [7]. Additionally crust may be substantially weaker, and regional models that take this weakness into account find that significant crustal deformation or even internal convection may take place under Venus-like conditions [8], which would mean that Venus-like planets do not have a real stagnant lid but rather a "squishy-lid" tectonic mode.

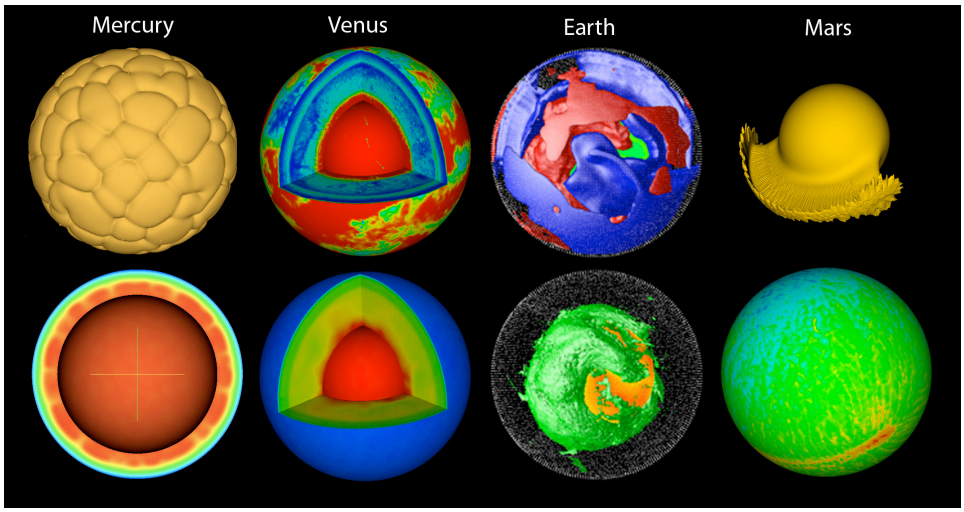

Figure 1. Simulations of the terrestrial planets as labelled.

References

[1] H. van Heck and P.J. Tackley, Earth Planet. Sci. Lett. 310, 252-261 (2011).
[2] P.J. Tackley, M. Ammann, J.P. Brodholt, D.P. Dobson & D. Valencia, Icarus 225, 50-61 (2013).
[3] T. Rolf & P.J. Tackley, Geophys. Res. Lett. 38, doi:10.1029/2011GL048677 (2011).
[4] D. Lourenco, A. Rozel & P. J. Tackley, Earth Planet. Sci. Lett., in press. (2016).
[5] T. Nakagawa & P.J. Tackley, Earth Planet. Sci. Lett. 329-330, 1-10 (2012).
[6] M. Armann & P.J. Tackley, J. Geophys. Res. 117, doi:10.1029/2012JE004231 (2012).
[7] T. Nakagawa & P.J. Tackley, Geophys. Geochem. Geosyst. 11, doi:10.1029/2010GC003031 (2010).
[8] Gerya T. V., Earth Planet. Sci. Lett. 391, 183-192 (2014).

cmg2016 - - Tuesday, June 7, 2016 - 11:30/11:45 (15min)

AN EXPLANATION FOR THE BEDFORMS ON COMET 67P/CHURYUMOV-GERASIMENKO

P. Jia, B. Andreotti & P. Claudin
Laboratoire de Physique et Mécanique des Milieux Hétérogènes, PMMH UMR 7636 ESPCI – CNRS – UPD – UPMC, 10 rue Vauquelin, 75005, Paris, France.

Key words Comet. Sedimentary pattern.

The recent approach of comet 67P/Churyumov-Gerasimenko by the European Space Agency spacecraft Rosetta has revealed the presence of geomorphologic features at its surface. In particular, surface patterns resembling aeolian ripples or dunes as well as 'wind tails' have been observed, especially in the 'neck' region. Erosion/deposition processes are unexpected on a comet because of the absence of an atmosphere, that would generate a wind to transport the grains at the surface. However, it is well known that comets experience outgassing when approaching the sun: the solar heat flux induces ice sublimation, generating dust/gas jets, which is at the origin of the comet's coma. Combining a description of sediment transport and hydrodynamics with a thermal model of the comet's surface and outgassing, we show that, albeit generated by a rarefied atmosphere, these bedforms are paradoxically analogous to ripplemarks emerging on granular beds submitted to viscous shear flows.

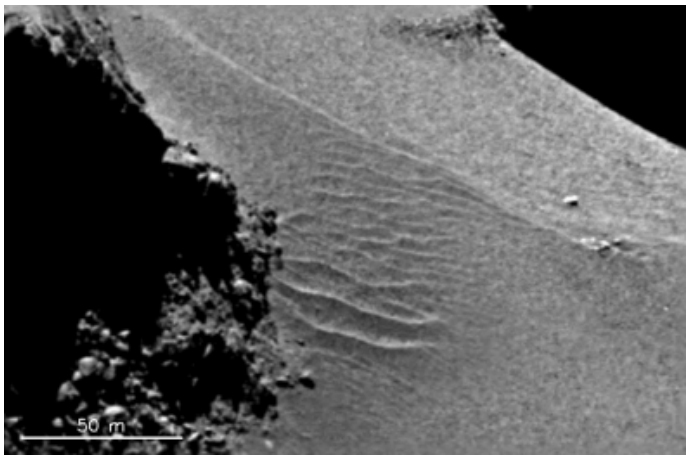

Figure 1. Ripplemarks on comet 67P/Churyumov-Gerasimenko in the neck 'Hapi' region. Photo credit: ESA/Rosetta/MPS for OSIRIS Team.

cmg2016 - - Tuesday, June 7, 2016 - 16:00/16:15 (15min)

MAGNETIC FIELD GAIN IN A LABORATORY MODEL OF THE EARTH'S OUTER CORE

D.P. Lathrop[1]
[1]*Department of Physics, Department of Geology, University of Maryland, College Park, MD, USA*

Geomagnetism, planetary magnetism, rotating fluid flow

Strongly nonlinear fluid flows germane to the planetary cores are possible in laboratory settings. Both measures of nonlinearity, Reynolds and magnetic Reynolds number, can be matched between the earth and experiments in rapidly rotating liquid sodium flows. The resulting observables, magnetic field gain, power dissipation, hydrodynamic states, were not predicted and are a challenge to simulate. There is much open territory for scientific discovery by the comparison of advanced modeling and laboratory experiments. The University of Maryland Three Meter Experiment is a world-unique spherical Couette experiment filled with liquid sodium and geometrically similar to the Earth's core[1]. It allows us to study hydrodynamic and hydromagnetic phenomena in rapidly rotating turbulence. An external coil applies an external magnetic field, while an array of 31 external Hall sensors measures the Gauss coefficients of the resulting magnetic field. We use this configuration to explore hydromagnetic effects relevant to the Earth's outer core, such as dynamo gain. The flow state is strongly dependent on the Rossby number, $Ro=(\Omega_I-\Omega_O)/\Omega_O$, where Ω_I and Ω_O are the inner and outer sphere rotation frequencies, respectively. We report on magnetic field gain in both dipole and quadupole magnetic fields. We also have progress in measuring the zonal flows[2], using modal acoustic velocemitry, that are responsible for our sizable azimuthal magnetic fields due to the Ω-effect of toroidal shear flows. This project is supported by the U.S. National Science Foundation grant EAR-1417148.

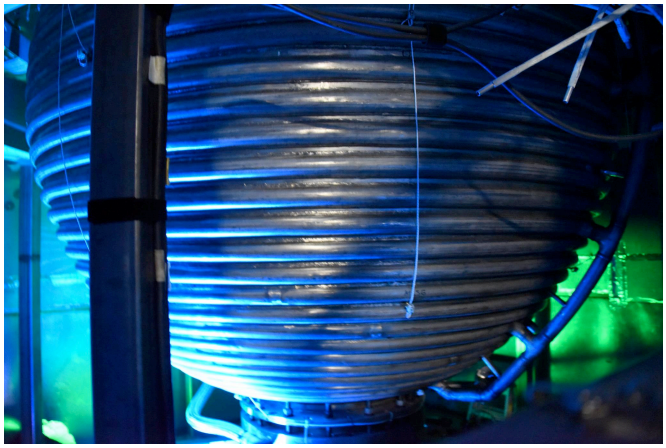

Figure 1. Image of the three meter liquid sodium system .

References

[1] D.S. Zimmerman, S.A. Triana, H.-C. Nataf, and D.P. Lathrop "A turbulent, high magnetic Reynolds number experimental model of Earth's core," J. of Geophysical Res.: Solid Earth, 119, 4538 (2014).
[2] S.A. Triana, D.S. Zimmerman, H.-C. Nataf, A. Thorette, V. Lekic, and D.P. Lathrop, "Helioseismology in a bottle: modal acoustic velocimetry," New J. of Phys. 16, 113005 (2014).

Thermal Evolution of Earth's Core during Accretion: A Primordial Solid Inner Core

Jafar Arkani-Hamed

Department of Physics, University of Toronto, Toronto, Canada

The formation of solid inner core has conventionally been explained in terms of secular core cooling. Accordingly, a solid inner core is initiated as the Earth cools and the temperature at the center of the core reduces below the melting temperature. A solid inner core may also form if the pressure in the core of a growing proto-Earth exceeds a threshold value and the existing core temperature becomes lower than the pressure-dependent melting temperature of core. Assuming a Mars-type initial proto-Earth, the lithostatic pressure at the center increases from ~60 GPa to ~300 GPa during the accretion, implying a high probability of an inner core growth. The formation of an inner core during the accretion of Earth is investigated assuming that Earth is formed by accreting a total of 25 or 50 Moon to Mars size planetary embryos, creating self-gravitating and compressible Earth models. The impact of an embryo heats the proto-Earth's interior differentially, more directly blow the impact site than elsewhere. The rotating low-viscosity impact-heated core stably stratifies shortly after each impact, with a spherically symmetric and radially increasing temperature distribution. Merging of an embryo to an existing proto-Earth increases the lithostatic pressure, hence the pressure-dependent melting temperature of core, resulting in core solidification. A total of 13 thermal evolution models of the proto-Earth's core are calculated to investigate effects of major physical parameters, such as the total number of impacting embryos, the partition coefficient of gravitational energy released during the descent of an embryo's iron core in the interior of existing proto-Earth model, thermal conductivity of the core and overlying silicate mantle, effects of core impunity on the solidus and liquidus of the core. No solidification is taken into account in the first 9 models. At the end of accretion, temperatures in the upper ~1000 km of the core are significantly different among the models. However, temperatures in the deeper part of the core of the models are very similar and well below the melting temperature of the core, indicating a possible solid inner core during accretion. The core solidification is considered in the remaining 4 models, which drastically changes the temperature distribution in the deeper parts of the core. All of the latter models show a large solid inner core of ~1600 km radius by the end of accretion.

THE SURFACE-BOUNDED EXOSPHERES OF CERES AND THE MOON

N. Schorghofer
Institute for Astronomy, University of Hawaii, Honolulu, Hawaii, USA

Key words Ceres, continuum approximations, diffusion, exosphere, ice, Moon, random walk

Sufficiently large airless bodies, such as dwarf planet Ceres or the Earth's Moon, can hold on to a tenuous exosphere of thermalized molecules that hop along ballistic trajectories [1]. Various molecular species have been detected in the lunar exosphere, but it is the water exosphere that is significant for transporting molecules to cold traps. Thanks to the Dawn spacecraft, asteroid Ceres is the newest example of an exosphere under study [2]. Although the number of investigations and questions is growing, a general mathematical description of this type of exosphere is in its infancy [3, 4].

Surface-bounded exospheres are collisionless, and although three-dimensional in nature, they can be fully described in terms of a two-dimensional random walk or as a two-dimensional partial (or integro-partial) differential equation, derived from the probability distribution of thermal ballistic hops. As a step toward a general mathematical description, a continuum equation is derived and used to calculate the steady state distribution of the surface concentration of volatile water molecules. This leads, for example, to a determination of the mass- and the length-scale of the pile-up of water molecules near the morning terminator.

In the specific case of Ceres, the water exosphere is expected to seasonally condense around the winter pole. Recent discoveries from the Dawn mission and relevant questions about Ceres and its exosphere will be presented.

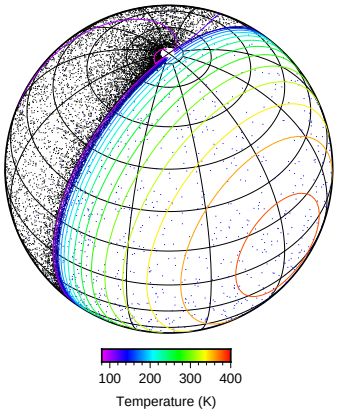

Figure 1. Monte-Carlo model calculation for the lunar water exosphere, where black dots correspond to molecules resident on the surface and blue dots to molecules in-flight [4].

References

[1] R. M. Killen and W.-H. Ip. The surface-bounded atmospheres of Mercury and the Moon. *Rev. Geophys.* **37**, 361–406 (1999).
[2] L. Tu, W.-H. Ip, and Y.-C. Wang. A sublimation driven exospheric model of Ceres. *Planet. Space Sci.* **104**, 157–162 (2014).
[3] R. R. Hodges. Applicability of a diffusion model to lateral transport in the terrestrial and lunar exospheres. *Planet. Space Sci.* **20**, 103–115 (1972).
[4] N. Schorghofer. Two-dimensional description of surface-bounded exospheres with application to the migration of water molecules on the Moon. *Phys. Rev. E* **91**, 052154 (2015).

cmg2016 - - Tuesday, June 7, 2016 - 11:45/12:30 (45min)

INTERACTING INERTIAL MODES AND THEIR INSTABILITY IN A DIFFERENTIALLY ROTATING SPHERICAL GAP FLOW

M. Hoff[1], U. Harlander[1], S. A. Triana[2] & C. Egbers[1]
[1]*Department of Aerodynamics and Fluid Mechanics, Brandenburg University of Technology Cottbus - Senftenberg, Germany*
[2]*Royal Observatory, Brussels, Belgium*

Key words geophysical and astrophysical flows, waves in rotating fluids, instability, wave-turbulence interaction

Inertial modes are Coriolis-restored linear wave modes, often arise in rapidly-rotating fluids (e.g. in the Earth's liquid outer core [1]). Recent experimental works showed that inertial modes exist in differentially rotating spherical shells. A set of particular inertial modes, characterized by $(l, m, \hat{\omega})$, where l, m is the polar and azimuthal wavenumber and $\hat{\omega} = \omega/\Omega_{out}$ the dimensionless frequency [2], has been found [4, 6]. It is an open issue why only a few modes develop and how they get enhanced.

We present an experimental study of inertial modes, based on Particle-Image-Velocimetry (PIV) data, in a spherical gap flow ($\eta = r_i/r_o = 1/3$) where the inner sphere is subrotating/ counter-rotating at Ω_{in} with respect to the outer shell at Ω_{out}, characterized by the Rossby number $Ro = (\Omega_{in} - \Omega_{out}/\Omega_{out})$. Based on a frequency-Rossby number spectrogram (figure 1), we can partly confirm previous considerations with respect to the onset of inertial modes [4, 6]. In contrast, the behavior of the modes in the counter-rotation regime is different. We found a triad interaction between three dominant inertial modes, where one is a slow axisymmetric Rossby mode [3]. We show that the amplitude of the most dominant mode $(l = 3, m = 2)$ is increasing with increasing $|Ro|$ until a critical Rossby number Ro_{crit} (left red line). At the particular Ro_{crit}, the flow breaks down into small-scale disorder [5], together with a strong increase of the zonal mean flow which significantly expands outside the tangent cylinder at η. We found that the critical Rossby number scales approximately with $E^{1/5}$.

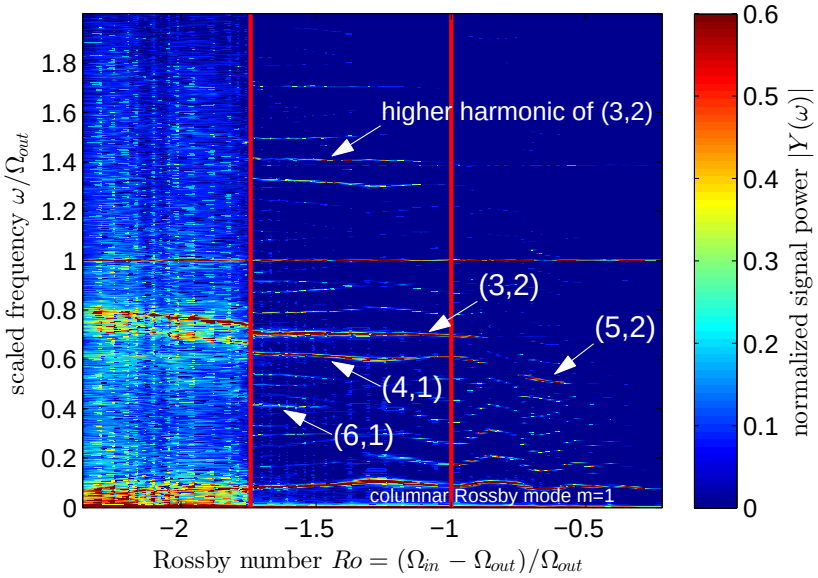

Figure 1. Azimthal velocity spectrogram for $\Omega_o \approx 64$rpm ($E \approx 1.35 \times 10^{-5}$). The inner sphere rotation Ω_i was variable.

References

[1] K. D. Aldridge,L. I. Lumb, *Inertial waves identified in the Earth's fluid outer core*, Nature **325**, 421–423 (1987).
[2] H. P. Greenspan, *The theory of rotating fluids*, Cambridge University Press, London (1968).
[3] M. Hoff, U. Harlander, C. Egbers, *Experimental survey of linear and nonlinear inertial waves and wave instabilities in a spherical shell*, J. Fluid Mech., **789**, 589–616 (2016).
[4] D. H. Kelley, S. A. Triana, D. S. Zimmerman, D. P. Lathrop, *Selection of inertial modes in spherical Couette flow*, Phys. Rev. E, **81**, 026311 (2010).
[5] R. R. Kerswell, *Secondary instabilities in rapidly rotating fluids: inertial wave breakdown*, J. Fluid Mech., **382**, 283–306 (1999).
[6] M. Rieutord, S. A. Triana, D. S. Zimmerman, D. P. Lathrop, *Excitation of inertial modes in an experimental spherical Couette flow*, Phys. Rev. E, **86**, 2, 026304 (2010).

cmg2016 - - Tuesday, June 7, 2016 - 11:45/12:30 (45min)

ROTATION OF A VISCOELASTIC, SYNCHRONOUS CRUST

B. Noyelles
NaXys, University of Namur, Rempart de la Vierge 8, B-5000 Namur, Belgium

Key words Icy satellites – Tides – Rotational dynamics

The space missions Galileo and Cassini have revealed the presence of several subsurfacic ocean for mid-sized icy moons, like Europa, Ganymede, Enceladus, or Titan. The viscoelastic deformations of the icy crusts coating the oceans can strongly affect the rotational response to the tidal torque of the parent body [1], in particular they lower the amplitude of the physical librations [6, 5]. The goal of this study is to give a comprehensive overview of the rotational response of a viscoelastic crust to the tidal forcing of its parent planet. I stress in particular how the librations and the obliquity will be affected, in considering the frequency-dependent rheology.

I use both the analytical and the numerical tools. From the analytical study I propose a new way to see the librations and the obliquity, based on the geometry of the tidal torque. The numerical study consists to model the 3 rotational degrees of freedom simultaneously, i.e. the longitude, latitude, and polar motion, in propagating the relevant equations. They include a complete modeling of the position of the parent planet, from orbital ephemerides [3]. These ephemerides stress the influence of different frequencies present in the dynamics, because of the gravitational perturbations of the other satellites. Two tidal models are considered, i.e. the classical Maxwell model, and the Andrade one that is more relevant for high-frequency excitations [2]. A digital filtering, based on frequency analysis [4], is used to model the time variations of the tensor of inertia. The Maxwell time τ_M plays a critical role, as a limit between the elastic and the anelastic behaviours (Fig. 1). The results are tested in modeling the rotation and the deformations of the Jovian satellite Europa.

I get a numerical modeling of the 3 degrees-of-freedom rotation of a viscoelastic, synchronous crust. It combines the rotational response with the tidal deformation of the body. It not only confirms the influence of the elasticity on the amplitude and phase of the longitudinal and latitudinal librations, but also provides clues on the future possibilities to validate or discard some tidal models from observations of the rotation.

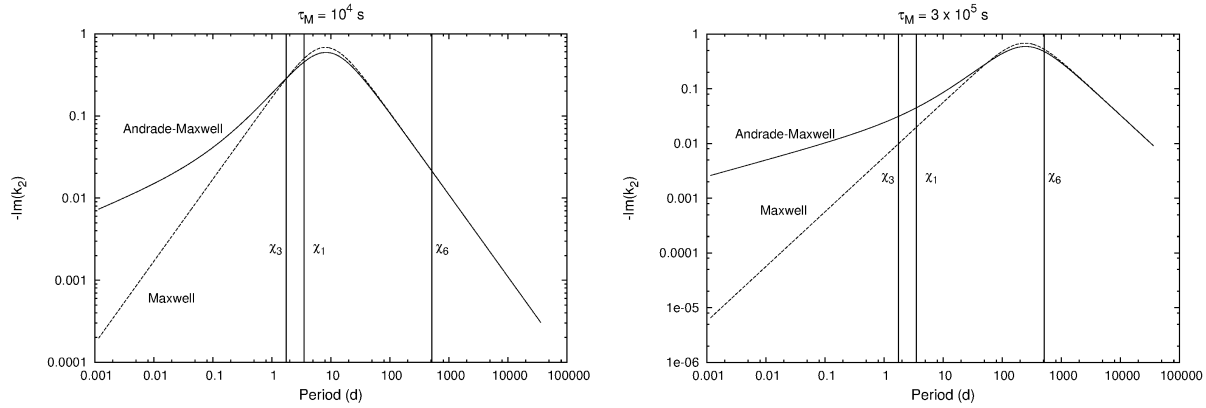

Figure 1. Dependency of the imaginary part of the tidal Love number k_2^* with respect to the tidal frequency. The 3 vertical lines locate the frequencies χ_1, χ_3 and χ_6, present in the forced rotational dynamics of Europa. They correspond to the periods 3.52546, 1.76273 and 509.26890 days, respectively. τ_M is the Maxwell time.

Acknowledgements This work benefited from the financial support of the contract Prodex CR90253 from the Belgian Science Policy Office (BELSPO).

References

[1] P.M. Goldreich & J.L. Mitchell, *Elastic ice shells of synchronous moons: Implications for cracks on Europa and non-synchronous rotation of Titan*, Icarus, **209**, 631 (2010)
[2] S.-I. Karato, *Deformation of Earth materials*, Cambridge University Press, Cambridge (2008)
[3] V. Lainey, L. Duriez & A. Vienne, *Synthetic representation of the Galilean satellites' orbital motions from L1 ephemerides*, Astronomy and Astrophysics, **456**, 783 (2006)
[4] J. Laskar, *Introduction to frequency analysis*, In: Proceedings of 3DHAM95 NATO Advanced Institute, S'Agaro, *553*, 134 (1999)
[5] A. Richard, N. Rambaux & B.Charnay, *Librational response of a deformed 3-layer Titan perturbed by non-Keplerian orbit and atmospheric couplings*, Planetary and Space Science, **93-94**, 22 (2014)
[6] T. Van Hoolst, R.-M. Baland & A. Trinh, *On the librations and tides of large icy satellites*, Icarus, **226**, 299 (2013)

Statistical scaling properties of planetary topographic fields

Francois Landais * [1], Frédéric Schmidt [1], Shaun Lovejoy [2]

[1] GEOPS – Université Paris XI - Paris Sud – Univ. Paris-Sud, CNRS, Université Paris-Saclay, Rue du Belvédère, Bât. 504-509, 91405 Orsay, France, France
[2] McGill – Physics, McGill University, Montreal, Quebec, Canada

*Speaker

cmg2016 - - Tuesday, June 7, 2016 - 11:45/12:30 (45min)

QUANTITATIVELY TESTING NUMERICAL MODELS OF CONTINENTAL BREAK-UP

J.J. Armitage[1], S. Goes[2], & J.O.S. Hammond[3]
[1]*Institut de Physique du Globe, Paris, France*
[2]*Department of Earth Science and Engineering, Imperial College London, London, UK*
[3]*Department of Earth and Planetary Science, Birkbeck, University of London, London, UK*

Key words numerical modelling, geochemistry, seismology, synthetic tomography

With increasing computational power the complexity of numerical models of continental break-up is ever increasing. High resolution two and three dimensional models show a rich set of behaviours in terms of rift architecture and asthenosphere to lithosphere interaction. Historically these models tend to be compared qualitatively with geological evidence from passive margins. However, to understand how continental break-up occurs we would argue that it is necessary to test plausible dynamic scenarios against a wide range of observations. For example, the structure of the upper mantle below Afar, at the northern end of the largest active rift zone on the planet, is uncertain. Based on geochemical and seismic data, there is ongoing debate as to the existence, or not, of a large thermal plume, and if the region is currently rifting or has achieved break-up [1, 2]. The likelihood of each argument can be assessed through quantitative comparisons between physically plausible forward models and observational constraints.

We have developed a relatively simple 2-D geodynamic model of decompression melting during extension that incorporates melt retention and dehydration. This model can explain the seismic structure below the East Pacific Rise as imaged by surface waves, including a double low velocity zone, with triangular anomaly above 50-60 km depth due to dry melting and low velocity layer between 60 and 200km depth mainly resulting from solid-state anelasticity in hydrated mantle [3]. When the same simple 2-D numerical model of extension is tested against the rock geochemistry and seismic structure of the upper mantle below Afar in the northern East African Rift, we find that extension above a $1450\,^{\circ}\mathrm{C}$ hot upper mantle matches the timing and composition of the Pleistocene lavas. Furthermore, recent S and P-wave tomographic models of the region show a complex strucutre, with zones of fast and slow anomalies within the upper mantle [4]. By converting a simple 3-D numerical model of the growth of Rayleigh Taylor instabilities to synthetic tomographic images, we find that the tomographic models inverted from the true observation can be explained simply by the growth of small plumes at a wavelength of roughly 500 km. These plumes form due to an increase in temperature from $1350\,^{\circ}\mathrm{C}$ to $1450\,^{\circ}\mathrm{C}$ at the base of the model domain (at a depth of 700 km).

By comparing the predicted melt chemistry and seismic structure from forward numerical models against the observations, we therefore find that that it is most likely that the Afar region is still in a state of continental extension and that the upper mantle below Afar contains small-scale convective instabilities. These instabilities rise from the below the 660 km discontinuity, most probably due to the ponding of a deeper larger plume-like structure. These idealised forward numerical models therefore suggest a more complex interaction between rifting and deep mantle plumes, and they demonstrate that simple geodynamic structures can appear complex due to the resolution of seismic studies.

References

[1] C.A. Rychert et al., *Volcanism in the Afar Rift sustained by decompression melting with minimal plume influence*, Nature Geoscience **5**, 406-409 (2012).
[2] D.J. Ferguson et al., *Melting during late-stage rifting in Afar is hot and deep* Nature **499**, 70-73 (2013)
[3] S. Goes et al., *Low seismic velocities below mid-ocean ridges: Attenuation versus melt retention* J. Geophys. Res. **117**, B12403 (2012)
[4] C. Civiero et al., *Multiple mantle upwellings in the transition zone beneath the northern East-African Rift system from relative P-wave travel-time tomography* Geochem. Geophys. Geosys. **16**, 2949-2968 (2012)

cmg2016 - - Tuesday, June 7, 2016 - 11:45/12:30 (45min)

SIZE AND TEMPERATURE DISTRIBUTION OF PLANETESIMALS

Y. Ricard[1], D. Bercovici[2], F. Albarède[1]
[1]*Laboratoire de Géologie, Ecole Normale Supérieure, Lyon, France*
[2]*Department of Geology & Geophysics, Yale University, New Haven, USA*

Key words Planetesimals, Planetary formation, Thermal histories, Accretion, Asteroid vesta

Although the mass distribution of planetesimals during the early stages of planetary formation has been discussed in various studies, this is not the case for their temperature distribution. Mass and temperature distributions are closely linked, since the ability of planetesimals to dissipate the heat produced by both radioactive decay and impacts is related to their size and hence mass. Here, we propose a simple model of the evolution of the joint mass-temperature distribution through a formalism that encompass the classical statistical approach of [1]. We will present the mathematical formalism and how it has been numerically implemented. We will show the connection of our formalism with that of von Smoluchowski [2]. We then compute the statistical distribution of planetesimals by using simple rules for aggregation. We show the possible thermal evolutions of a swarm of planetesimal under various possible conditions. Although melting temperatures can be easily reached, the formation of molten planetary embryos requires that they be formed in only a few 100 kyrs. Our aggregation model, which even ignores fragmentation during collision, predicts that planetesimals with radii less than approximately 20 km will not melt during their formation.

References

[1] Wetherill, G., 1990. Comparison of analytical and physical modeling of planetesimal accumulation, *Icarus*, **88**(2), 336–354.
[2] von Smoluchowski, M., 1917. Experiments on a mathematical theory of kinetic coagulation of coloid solutions., *Z. Fur Physikalische Chemie–stochiometrie Und Verwandtschaftslehre*, **92**, 129–168.

cmg2016 - - Tuesday, June 7, 2016 - 11:45/12:30 (45min)

EARLY PHYSICAL PROCESSES IN THE MANTLE OF TERRESTRIAL PLANETS

S. Padovan[1], N. Tosi[1,2], & A.-C. Plesa[1]
[1]*Department of Planetary Physics, German Aerospace Center (DLR), Berlin, Germany*
[2]*Department of Astronomy and Astrophysics, Technische Universität Berlin, Berlin, Germany*

Key words Convection, Impacts, Tides, Mercury

The early phases of the evolution of the terrestrial bodies of the Solar System correspond to a period when vigorous convection dominate the energy transport across the mantle, an effect of the high interior temperature and the large amount of energy available from radioactive decays. During about the first billion of years, large number of bodies would hit the surfaces of the recently formed planets, in events that can affect the dynamics of the underlying mantle by inducing large thermal perturbations in the subsurface. In addition, depending on the orbital geometry, tidal dissipation may also contribute significantly to a body's energy budget, as was the case for the young Moon and is still the case for Jupiter's natural satellite Io. In order to model all these processes and consistently estimate their effects on a body's thermal evolution, we are creating a numerical tool that combines the finite-volume convection code Gaia [1] with a code that can estimate the tidal dissipation in the interior. We treat impacts as instantaneous thermal perturbations in the interior by employing scaling laws (e.g., [5]). Convection and tides are characterized by extremely different timescales. Thus, to consistently model the rheological response of mantle materials for these two processes it is necessary to employ a timescale-dependent rheology. We adopt the Andrade pseudo-period model [2, 4] which includes the rheological effects of temperature, pressure, grain size, and forcing period. The model parameters are obtained by fitting torsional oscillation data for olivine at forcing periods no longer than 1000 s [2]. We extrapolated the model to longer periods to test its applicability to convection and tidal problems. Figure 1 shows the dynamic viscosity as a function of the period. At very large forcing periods, corresponding to convective timescales, and for a reasonable range of parameters, the viscosity compares favorably with the reference viscosities commonly adopted in convection studies (e.g., [6]). At timescales relevant to the post glacial rebound process, the viscosity also matches the value inferred from geodetic observations (e.g., [3]). These findings indicate that the Andrade pseudo-period model is appropriate to consistently evaluate the rheological response of the mantle for convective and tidal processes.

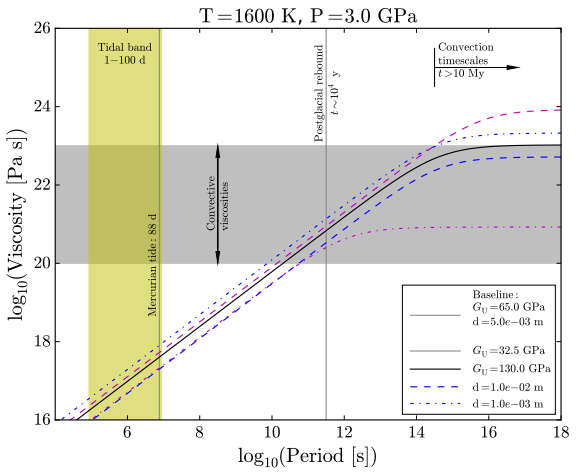

Figure 1. Viscosity as a function of the forcing period for the Andrade rheological model at T = 1600 K and P = 3 GPa. The baseline model has an unrelaxed shear modulus G_U = 65 GPa and a grain size d = 5 mm. The other models are obtained by varying a single parameter as indicated by the legend. Additional parameters correspond to melt-free olivine (for additional details see [2] and [4]).

We present the initial results that we obtain when applying the code to the case of the early evolution of the planet Mercury.

References

[1] Hüttig, C., Tosi, N. and Moore, W. B. (2013), An improved formulation of the incompressible Navier-Stokes equations with variable viscosity, *Phys. Earth Planet. Inter.*, *220*, 11–18, doi:10.1016/j.pepi.2013.04.002.
[2] Jackson, I., U. H. Faul, D. Suetsugu, C. Bina, T. Inoue, and M. Jellinek (2010), Grainsize-sensitive viscoelastic relaxation in olivine: Towards a robust laboratory-based model for seismological application, *Phys. Earth Planet. Inter.*, *183*, 151–163, doi:10.1016/j.pepi.2010.09.005.
[3] Kaufmann, G. and Lambeck, K. (2000), Mantle dynamics, postglacial rebound and the radial viscosity profile, *Phys. Earth Planet. Inert.*, *121*, 301–324, doi:10.1016/S0031-9201(00)00174-6.
[4] Padovan, S., J.-L. Margot, S. A. Hauck II, W. B. Moore, and S. C. Solomon (2014), The tides of Mercury and possible implications for its interior structure, *J. Geophys. Res. Planets*, *119*, 850–866, doi:10.1002/2013JE004459.
[5] Roberts, J. H., and O. S. Barnouin (2012), The effect of the Caloris impact on the mantle dynamics and volcanism of Mercury, *J. Geophys. Res. Planets*, *117*, E02007, doi:10.1029/2011JE003876.
[6] Tosi, N., M. Grott, A.-C. Plesa, and D. Breuer (2013), Thermochemical evolution of Mercury's interior, *J. Geophys. Res. Planets*, *118*, 2474–2487, doi:10.1002/jgre.20168.

cmg2016 - - Tuesday, June 7, 2016 - 11:45/12:30 (45min)

CHALLENGES IN MODELLING MAGMA OCEAN EVOLUTION USING A 1-D ATMOSPHERE-INTERIOR COUPLED MODEL FOR THE EARLY EARTH

A. Nikolaou[1,2] & N. Tosi[1,2]
[1]*German Aerospace Center DLR, Berlin, Germany*
[2]*Technische Universität Berlin, Germany*

Key words Planetary science, magma ocean, thermal convection, Hadean.

The early phases of the evolution of the Earth and terrestrial planets have been likely characterised by one or multiple vigorously convecting magma oceans. Even super earths at a close distance to their host star can presently be in a similar condition. Understanding magma ocean evolution can serve to better characterise the evolution of the Earth and of terrestrial bodies that experienced a magma ocean state in their early history.

The evolution of a vigorously convecting magma ocean is poorly known due to the paucity of constraints from the geological record and to the difficulty of assessing the mechanical and thermal properties of molten and partially molten materials at the extreme conditions of a magma ocean. The evolution of the potential temperature dictates the rate of mantle crystallization of the interior, which likely proceeds from the bottom upwards because of the steeper slope of the mantle adiabat compared to the solidus. A challenging factor is the extreme parameter range of the regime of thermal convection. The dynamic viscosity of silicate liquids is expected to be of the order of $10^{-3} Pa\,s$, which implies Rayleigh and Prandtl numbers of $\sim 10^{30}$ and ~ 1, respectively. This makes it presently impossible to tackle the problem with direct numerical simulations and thus requires the use of parametrised models. The intense delivery of volatiles with greenhouse potential from the interior to the atmosphere adds another level of complexity to the overall energy balance. The resulting atmosphere could be deviating from the radiative two-stream approximation that is widely used in the earth system modelling, by possibly activating more atmospheric windows in the optical range of the spectra, and by being in the supercritical regime of water vapour.

Using a simple 1-D model we simulate the evolution of a primitive magma ocean coupled with a grey atmosphere, based on the work of Lebrun et al. (2013) [1]. Comparing cases with and without atmospheric coupling, we show that the atmosphere generated by magma ocean degassing, which is rich in greenhouse gases, can strongly retard the cooling and solidification time of the interior by up to a few million years.

In order to monitor the planetary cooling rate during the lifetime of the magma ocean and its co-evolving atmosphere, there is room for improvement in the coupling of the two systems. This approach could benefit from a close interaction between the interior dynamics and climate modelling communities and from the contribution of novel experimental data covering a broader range of parameters.

References

[1] T. Lebrun, H. Massol, E. Chassefière, A. Davaille, E. Marcq, P. Sarda, F. Leblanc and G. Brandeis, *Thermal evolution of an early magma ocean in interaction with the atmosphere*, J. Geoph. Res. and Planets **118**, 6 (2013).

Geomorphology

cmg2016 - - Thursday, June 9, 2016 - 9:45/10:00 (15min)

EQUILIBRIUM, QUASI-EQUILIBRIUM, AND TRANSIENT RIVER LONGITUDINAL PROFILES

A. Blom[1], E. Viparelli[2] & V. Chavarrías[1]
[1]*Delft University of Technology, Delft, Netherlands*
[2]*University of South Carolina at Columbia, Columbia, USA*

Key words river profile concavity, downstream fining, equilibrium, transient, alluvial rivers

There has long been a debate on the relative importance of particle abrasion and grain size selective transport regarding downstream fining and river profile concavity. Here we analytically solve the problem and show that in the equilibrium or graded state profile concavity and downstream fining in an alluvial river are mild, whereas in the transient state grain size selective transport can lead to large spatial gradients in grain size and slope. Figure 1 illustrates how predicted data on equilibrium profile concavity and downstream fining nicely fall within the envelope of measured data for natural streams collected by Morris and Williams (1999). The predicted data do not cover those field data that are governed by large concavity and downstream fining values, as (1) part of the field data is governed by transient conditions and associated stronger concavity and downstream fining, and (2) the predicted data do not include the effect of tributaries. We show how the gravel-sand transition generally is a characteristic of a transient or ungraded river profile and results from a progradational gravel wedge. The migration speed of the wedge front is very small and, under conditions of base level rise, subsidence or delta progradation, potentially zero or negative. The large time scale of front migration generally allows us to assume a state of quasi-equilibrium in the gravel-bed and the sand-bed reach and apply the formulations of a graded river to both reaches.

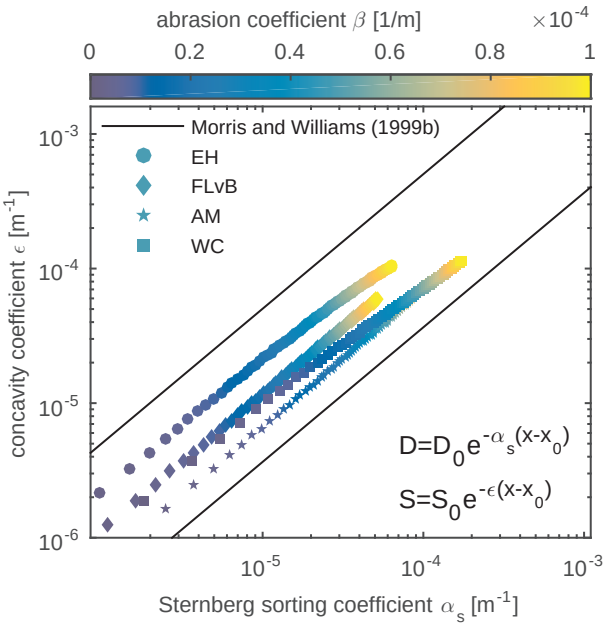

Figure 1: Predicted equilibrium values of the downstream fining coefficient α_s versus the profile concavity coefficient ϵ, for a varying abrasion coefficient, for a base case. The black lines indicate the envelope of field data for natural streams collected by [1]. We applied four sediment transport relations: [2] (EH), [3] (FLvB), [4] (AM), and [5] (WC).

References

[1] P. H. Morris and D. J. Williams, Worldwide correlations for subaerial aqueous flows with exponential longitudinal profiles, *Earth Surf. Process. Landf.*, *24*(10), 867–879, doi:10.1002/(SICI)1096-9837(199909)24:10<867::AID-ESP16>3.0.CO;2-L (1999).
[2] F. Engelund and E. Hansen, Monograph on sediment transport in alluvial streams, *Tech. Rep.*, Hydraul. Lab., Tech. Univ. of Denmark, Copenhagen, Denmark (1967).
[3] R. Fernandez-Luque and R. Van Beek, Erosion and transport of bed-load sediment, *Journal of Hydraulic Research*, *14*(2), 127–144, doi:10.1080/00221687609499677 (1976).
[4] K. Ashida and M. Michiue, Study on hydraulic resistance and bed-load transport rate in alluvial streams, *J. Civil Eng., Jpn. Soc. Civil Eng.*, *206*, 59–69 (1972).
[5] P. R. Wilcock and J. C. Crowe, Surface-based transport model for mixed-size sediment, *J. Hydr. Eng.*, *129*(2), 120–128, doi:10.1061/(ASCE)0733-9429(2003)129:2(120) (2003).

cmg2016 - - Thursday, June 9, 2016 - 11:15/11:30 (15min)

EROSION PATTERNS ON DISSOLVING BLOCKS

C. Cohen, M. Berhanu, J. Derr & S. Courrech du Pont
Lab. Matière et Systèmes complexes, Université Paris Diderot, Paris, France

Key words Dissolution, Buoyancy driven flow, Iceberg, Rayleigh-Bénard instability

Patterns in nature are shaped under water flows and wind action, and the understanding of their morphodynamics goes through the identification of the physical mechanisms at play. When a dissoluble body is exposed to a water flow, typical patterns with scallop-like shapes may appear [1, 2]. These shapes are observed on the walls of underground rivers or icebergs.

We experimentally study the erosion of dissolving bodies made of salt, caramel or ice into water solutions without external flow. The dissolving mixture, which is created at the solid/liquid interface, undergoes a buoyancy-driven instability comparable to a Rayleigh-Bénard instability so that the dissolving front destabilizes into filaments. This mechanism yields to spatial variations of solute concentration and to differential dissolution of the dissolving block. We first observe longitudinal stripes with a well defined wavelength, which evolve towards chevrons and scallops that interact and move again the dissolving current.

Thanks to a careful analysis of the competing physical mechanisms, we propose scaling laws, which account for the characteristic lengths and times of the early regime in experiments. The long-term evolution of patterns is understood qualitatively.

A close related mechanism has been proposed to explain structures observed on the basal boundary of ice cover on brakish lakes [3] and we suggest that our experiments are analogous and explain the scallop-like patterns on iceberg walls.

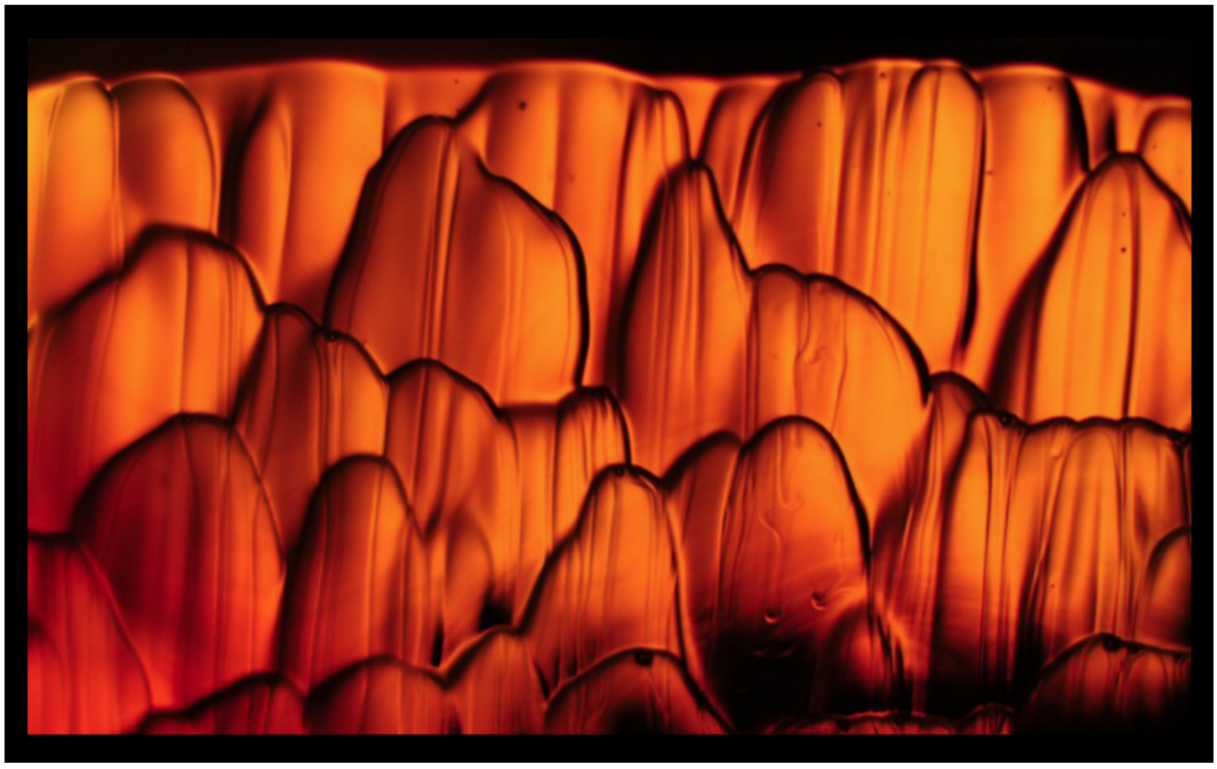

Figure 1. Centimeter scale patterns on a caramel block dissolving into water.

References

[1] P. Meakin and B. Jamtveit, *Geological pattern formation by growth and dissolution in aqueous systems,* Proc. R. Soc. A **466**, 659–694 (2010).
[2] P.N. Blumberg and R.L. Curl, *Experimental and theoretical studies of dissolution roughness,* J. Fluid Mech. **65**, 735–751 (1974).
[3] L. Solari and G. Parker, *Morphodynamic modelling of the basal boundary of ice cover on brakish lakes,* J.G.R. **118**, 1432–1442 (2013).

cmg2016 - - Thursday, June 9, 2016 - 11:00/11:15 (15min)

GENERATION OF TOPOGRAPHIC WAVES AT AN ICE-AIR INTERFACE BY SUBLIMATION IN A TURBULENT STEADY FLOW

S. Carpy[1], C. Blanchard[1], L. Perret[2], H. Mathis[1], C. Herny[1], O. Bourgeois[1] & S. Rodriguez[3]
[1] *Laboratoire de Planétologie et Géodynamique de Nantes, Nantes, France*
[2]*Laboratoire de recherche en Hydrodynamique, Energétique et Environnement Atmosphérique, Nantes, France*
[3]*CEA-Saclay, DSM/IRFU/Service d'Astrophysique, Gif/Yvette, France.*

Key words Turbulent flow, sublimation, ice waves, linear stability analysis.

The surface shape of glaciers is controlled by various processes, which include ice accumulation, ice ablation and ice deformation. In specific environments, where the partial pressure of water in the atmosphere is low, sublimation significantly contributes to ablation and, as such, takes a part in the development of surface landforms on glaciers. For example, complex interactions between sublimation-related mass transfers and turbulent flow in the lower-atmosphere lead to the development of stunning spiral-shaped topographic waves at the surface of the North Polar cap of Mars. Interpretations of topographic data, optical images, spectroscopic data and stratigraphic radar soundings reveal that periodic spatial variations in sublimation-related ablation rates are responsible for the development of these topographic waves [1, 2]. To explore the role of sublimation in the development of such wavy patterns, we have conducted experiments in an atmospheric wind-tunnel using dry ice as a sublimating material. The growth of a small-amplitude wave into a ripple pattern has been observed experimentally under terrestrial conditions. In the present work, in order to identify the relevant dynamical mechanisms controlling the mass and energy balance, we apply a linear stability analysis on the coupled ice-airflow interface under turbulent flow conditions. We first solve the flow dynamics in response to rippled ice surface using numerical techniques analogous to those used in sand-wave models [3]: because the topographic evolution is slow compared to the relevant time-scales of the atmospheric turbulent flow, we can use the Reynolds-averaged Navier-Stokes equations (RANS) with a Prandtl-like closure in addition to the continuity equation of flow. We employ an exponential damping of the Prandtl mixing length described by the Van Driest formula in the vicinity of a smooth surface. We then use the transport/diffusion equation of vapor and the surface energy balance. An analogy between momentum and mass transfer is explored as a means for evaluating the turbulent diffusion terms. Wave induced variations of the normal convective flow combined with the properties of turbulence induces a periodic variation of the transfer. We evaluate the phase of the spatial variation of the sublimation rate to determine the evolution of the ice surface and the amplification or damping of the initial ice-ripple perturbation.

Acknowledgements

This work benefited from financial supports from the "Programme National de Planétologie" (PNP) and from the "Agence Nationale de la Recherche" (Project ANR-12-BS05-001 EXODUNES)

References

[1] Herny, C., Massé, M, Bourgeois, O, Carpy, S., Le Mouélic, S., Appéré, T., Smith, I.B., Spiga, A., and Rodriguez, S.: *Sedimentation waves on the Martian North Polar Cap: Analogy with megadunes in Antarctica*, Earth and Planetary Sciences Letters, **Vol 403**, pp. 56-66, (2014).

[2] Smith, I.B., Holt, J.W., Spiga, A., Howard, A.D., and Parker, G.: *The spiral troughs of Mars as cyclic steps*, Journal of Geophysical Research (Planets), **118 (9),** pp. 1835-1857 (2013).

[3] Charru F., Andreotti B. and Claudin P.: *Sand Ripples and Dunes,* Annu. Rew. Fluid Mech., **45,** pp. 469-493 (2013).

cmg2016 - - Thursday, June 9, 2016 - 9:00/9:30 (30min)

ON THE PHYSICS BEHIND COASTAL MORPHODYNAMIC PATTERNS

F. Ribas[1], A. Falqués[1], H. E. de Swart[2], N. Dodd[3], R. Garnier[4] & D. Calvete[1]
[1]*Department of Physics, Universitat Politècnica de Catalunya, Barcelona, Spain*
[2]*Institute for Marine and Atmospheric research Utrecht, Utrecht University, Utrecht, the Netherlands*
[3]*Faculty of Engineering, University of Nottingham, Nottingham, UK*
[4]*Instituto de Hidráulica Ambiental Cantabria, Universidad de Cantabria, Santander, Spain*

Key words coastal morphodynamic patterns, nearshore sand bars, beach cusps, sand ridges, sediment transport, self-organization

The focus of this contribution is to understand the physical processes behind the development of a number of coastal morphodynamic features that have an alongshore rhythmic pattern: beach cusps, surf zone transverse and crescentic bars, and shoreface-connected sand ridges. We will present a formulation and methodology, based on the knowledge of the depth-averaged currents and the depth-averaged sediment concentration (DASC, which equals the sediment load divided by the water depth), that has been successfully used to understand the characteristics of these features ([1] and references therein). These sand bodies, relevant for coastal engineering and other disciplines, are located in different parts of the coastal zone and are characterized by different spatial and temporal scales (Figure 1) but the same technique can be used to understand them. Since they occur in the presence of depth-averaged currents, the sediment transport approximately equals a sediment load times the current. Moreover, it is assumed that waves essentially mobilize the sediment, and the current increases this mobilization and advects the sediment. In such conditions, knowing the spatial distribution of the DASC and the depth-averaged currents induced by the forcing (waves, wind, and pressure gradients) over the patterns allows inferring the convergence/divergence of sediment transport. Deposition (erosion) occurs where the current flows from areas of high to low (low to high) values of DASC. The formulation and methodology are especially useful to understand the positive feedback mechanisms between flow and morphology leading to the formation of those morphological features, but the physical mechanisms for their migration, their finite-amplitude behavior and their decay can also be explored.

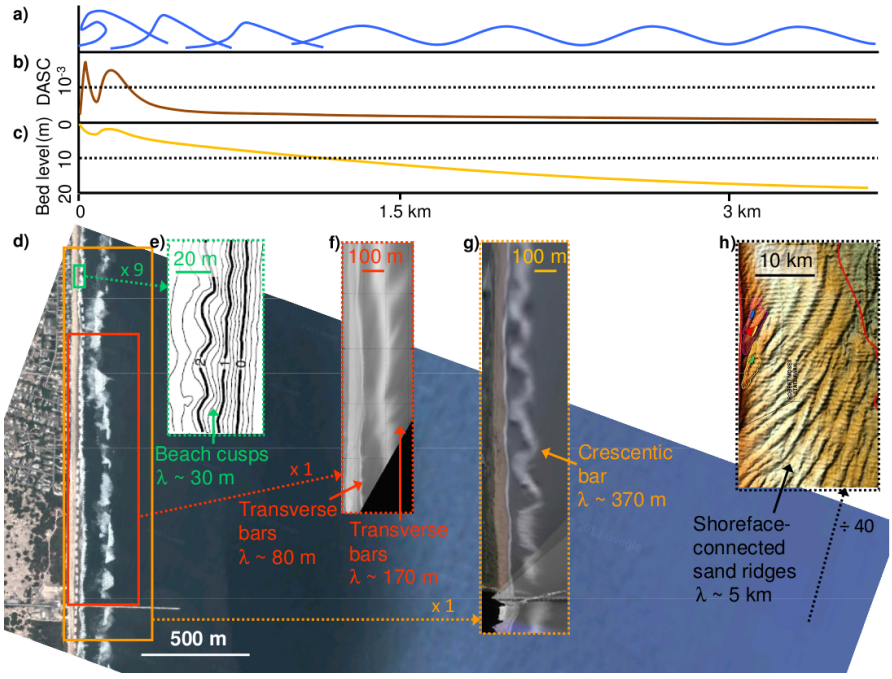

Figure 1. Illustration of the (a) incoming waves, (b) depth-averaged sediment concentration profile (DASC), and (c) bed level on the coastal zone. (d) Satellite image of the coastal zone in front of Duck, North Carolina, USA. Superimposed to it, examples of (e) beach cusps, (f) surf zone transverse and (g) crescentic bars, and (h) shoreface-connected sand ridges. Figure from [1].

References

[1] Ribas, F., A. Falqués, H. E. de Swart, N. Dodd, R. Garnier & D. Calvete (2015), *Understanding coastal morphodynamic patterns from depth-averaged sediment concentration*, Rev. Geophys. **53**, 362–410, doi:10.1002/2014RG000457.

LANDSCAPE EVOLUTION AND RE-ORGANIZATION UNDER STEADY AND TRANSIENT STATES: RESULTS FROM AN EXPERIMENTAL INVESTIGATION

A. Singh[1], A. Tejedor[2], C. Keylock[3], I. Zaliapin[4] & E. Foufoula-Georgiou[2]
[1]*University of Central Florida, Orlando, USA*
[2]*University of Minnesota, Minneapolis, USA.*
[3]*University of Sheffield, Sheffield, UK.*
[4]*University of Nevada, Reno, USA.*

Key words Landscape evolution; Drainage network dynamics; Extreme events; Transport regimes

Understanding and quantifying landscapes dynamics under steady and transient states in terms of their geomorphic and topologic re-organization across a range of scales is an issue of timely interest in view of recent climatic trends in many regions of the world. Although several studies have addressed the large-scale response, studies that focus on the smaller-scale drainage pattern re-organization and quantification of landscape vulnerability to the timing, magnitude, and frequency of the changing forcing are lacking. The reason is the absence of data for such an analysis. To that goal, a series of controlled laboratory experiments were conducted at the St. Anthony Falls laboratory of the University of Minnesota to study the effect of space-time variable and changing precipitation patterns on landscape evolution at the short and long-time scales. High resolution digital elevation (DEM) both in space and time were measured for a range of rainfall patterns and uplift rates. These experiments were designed to create an evolving and self-organized drainage network by growth and propagation of erosional instabilities in response to external forcing, such as, tectonic uplift and rainfall dynamics. Results from our study show distinct signatures of extreme climatic fluctuations on the statistics and geometry of topographical features which are evident in widening and deepening of channels and valleys, change in drainage patterns within a basin and change in the probabilistic structure of “hot-spots” of change contributing to mass-wasting events, such as, landslides and debris flows. These results suggest a regime shift, during the onset of the transient state, in the transport processes on the fluvial regime of the landscape, i.e., from supply-limited to transport-limited. We also analyze landscape features, extracted via an innovative curvelet-based decomposition approach, to understand and quantify landscape reorganization in terms of the evolution in the energy distribution across scales and directions.

cmg2016 - - Thursday, June 9, 2016 - 10:45/11:00 (15min)

THE RIPPLING INSTABILITY OF ICICLES

Jake Wells[1], Alina Barnett[2], Josh Calafato[1], Ken Liao[1],
Antony Szu-Han Chen[3], John Ladan[1], & Stephen W. Morris[1]
[1]*Dept. of Physics, University of Toronto, Toronto ON Canada M5S 1A7.*
[2]*Dept. of Physics, McMaster University of Toronto, Hamilton ON Canada L8S 4M1.*
[3]*Southern Alberta Institute of Technology, Calgary AB Canada T2M 0L4.*

Key words ice, solidification, instability, hydrodynamics, geomorphology.

Icicles are a common ice formation, familiar to anyone who lives in a cold climate. The shape of an icicle emerges from a delicate dance between solidification, hydrodynamics and heat transport. Many, but not all, natural icicles are observed to be decorated around their circumference by ribs or ripples [1]. These features are presumed to be the result of a morphological instability in the growth process of the ice. The sides of an icicle are covered by a thin supercooled water film which flows down their nearly vertical surface. The wavelength of the ripples, which is always found to be near 1 cm, is surprisingly constant, even under diverse growing conditions. A recent detailed study in which hundreds of icicles were grown in controlled laboratory experiments [2] revealed that trace amounts of impurities are required for the formation of the ripples. Icicles grown from distilled water have no ripples. Ripples appear at a remarkably low concentration of impurity, becoming measurable above a concentration of just 10^{-3} weight % of salt. Thereafter, they grow at a rate which is roughly logarithmic in the concentration of the impurity. These effects are not explained by linear stability theory [3 - 7], which does not account for impurities.

In this paper, we will discuss our recent experiments in which the concentration and molecular species of the impurity were varied, as well as our progress toward a generalized linear stability analysis of the growing ice surface, which includes the effects of impurities.

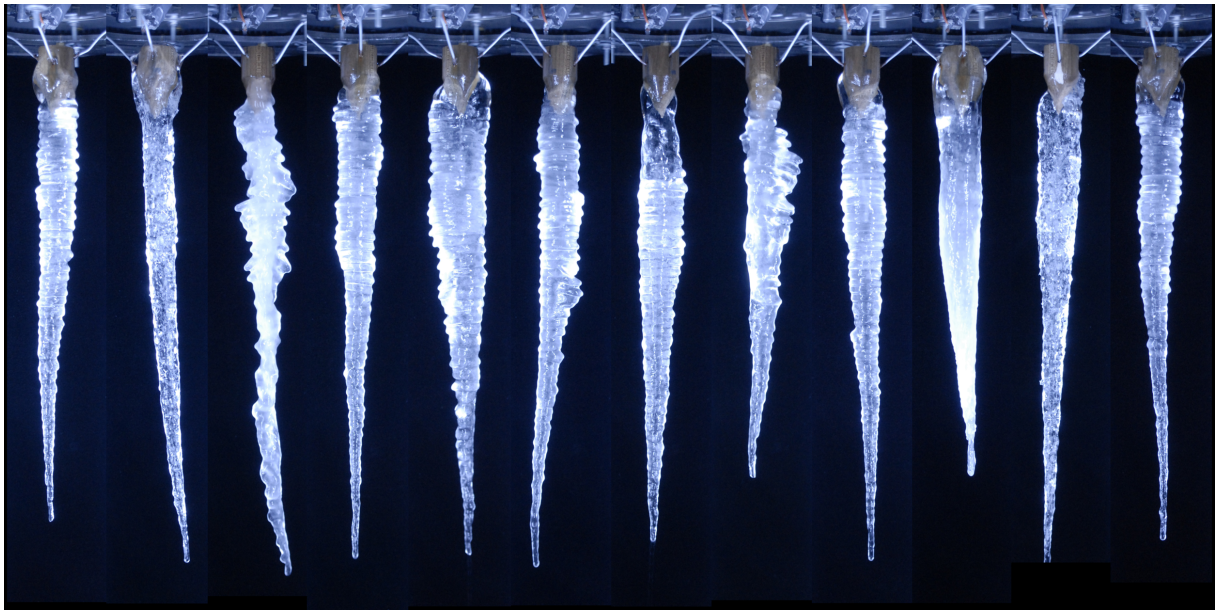

Figure 1. A selection of laboratory grown icicles with various morphologies. All of the data from this experiment is available online in the **Icicle Atlas**, *http://www.physics.utoronto.ca/Icicle_Atlas*.

References

[1] T. Terada, *"Stripe patterns in Nature"*, essay in Japanese, (1933).
[2] Antony Szu-Han Chen & Stephen W. Morris, *New Journal of Physics*, **15**, 103012 (2013).
[3] N. Ogawa and Y. Furukawa, *Phys. Rev. E* **66**, 041202 (2002).
[4] K. Ueno, *Phys. Rev. E*, **68**, 021603 (2003); *Phys. Rev. E*, **69**, 051604 (2004); *Phys. Fluids*, **19**, 093602 (2007).
[5] K. Ueno and M. Farzaneh, *Phys. Fluids*, **22**, 017102 (2010).
[6] K. Ueno, M. Farzaneh, S. Yamaguchi, and H. Tsuji, *Fluid Dyn. Res.* **42**, 025508 (2010).

[7] K. Ueno and M. Farzaneh, *Phys. Fluids*, **23**, 042103 (2011).

cmg2016 - - Thursday, June 9, 2016 - 9:30/9:45 (15min)

THE MORPHOLOGY OF RIVER BIFURCATIONS

R. Yi[1], O. Devauchelle[2], Y. Cohen[1], H. Seybold[3] & D. Rothman[1]
[1]*Massachusetts Institute of Technology, Cambridge, Massachusetts*
[2]*Institut de Physique du Globe, Paris, France*
[3]*ETH Zürich, Zürich, Switzerland*

Key words Seepage, bifurcation, river, groundwater, migration

Recent work has demonstrated, both theoretically and empirically, that river networks fed by subsurface flow form bifurcations on average at an angle of $2\pi/5$ [1]. Yet, a network-wide averaging of several thousand such channel bifurcations on the Florida panhandle reveals a departure from this angle near the point of bifurcation (Fig. 1). On average, these bifurcations initially open at a wide angle, greater than $2\pi/5$, only to return to angle narrower than $2\pi/5$ after a few meters. We suggest that these two shapes are suggestive of a competition between two processes in our system: channel migration, and growth in the direction of the groundwater field. While erosion due to groundwater reemergence plays a predominant role in directing channel growth as a valley initially forms, rivers may migrate in response to asymmetric fluxes to the valley sidewalls, ultimately leading to adjustments on the valley scale. We therefore study how these processes might reconcile, and extract the shapes of our channels as they lengthen to present empirical evidence supporting our findings.

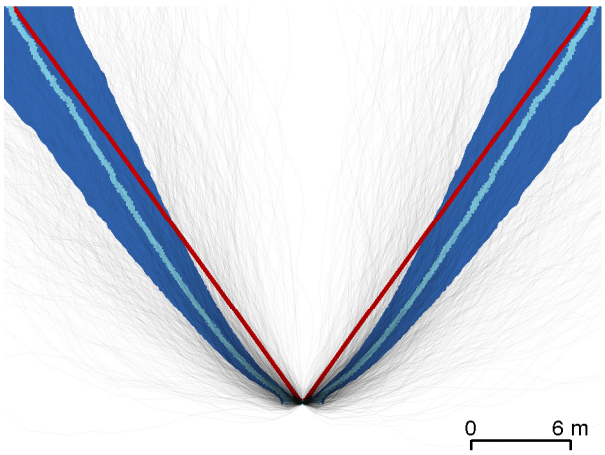

Figure 1. Average shape of 1225 first-order bifurcations (light blue), against a $2\pi/5$ bifurcation (red). The individual channels are superimposed in grey. (x, y) coordinates were binned radially according to distance from bifurcation.

References

[1] O. Devauchelle, A.P. Petroff, H.F. Seybold, and D.H. Rothman. Ramification of stream networks. 2012:2–6.

cmg2016 - - Thursday, June 9, 2016 - 10:30/10:45 (15min)

SHAPES AND GROWTH VELOCITIES OF SOLUTION PIPES

Piotr Szymczak[1], Filip Dutka[1], Virat Upadhyay[2] & Anthony J.C. Ladd[2]
[1]*Faculty of Physics, University of Warsaw, Warsaw, Poland*
[2]*Chemical Engineering Department, University of Florida, Gainesville, FL, USA*

Key words solution pipes, reactive flow, reactive-infiltration instability, karst formation

Cylindrical, vertical structures called solution pipes are a characteristic feature of epikarst, encountered in different parts of the world, both in relatively cold areas such as England and Poland (where their formation is linked to glacial processes) [1] and in coastal areas in tropical or subtropical climate (Bermuda, Australia, South Africa, Caribbean, Mediterranean) [2, 3]. They are invariably associated with weakly cemented, porous limestones and relatively high groundwater fluxes. Many of them develop under the colluvial sandy cover and contain the fill of clayey silt. Although it is accepted that they are solutional in origin, the exact mechanism by which the flow becomes focused is still under debate. The hypotheses include the concentration of acidified water around stems and roots of plants, or the presence of pre-existing fractures, which would determine the points of entry for the focused groundwater flows. However, there are field sites where neither of this mechanisms was apparently at play and yet the pipes are formed in large quantities [1]. In this communication we show that the systems of solution pipes can develop spontaneously in nearly uniform matrix due to the reactive-infiltration instability: a homogeneous porous matrix is unstable with respect to small variations in local permeability; regions of high permeability dissolve faster because of enhanced transport of reactants, which leads to increased rippling of the front. This leads to the formation of a system of solution pipes which then advance into the matrix. We study this process numerically, by a combination of 2d- and 3d-simulations, solving the coupled flow and transport equations at the Darcy scale. We quantify the factors which control the pipe diameters as well as their growth rates.

The most interesting result is the existence of two morphological phase transition in the finger shapes as the Peclet number is changed. At high Pe, well-separated, cyllindrical shafts are formed, of a nearly uniform diameter all along their lengths. They advance quickly into the matrix, with velocities several times larger than that of a unperturbed, planar dissolution front. Interestingly, this regime is analytically tractable, which allows us to derive the dependence of the pipe advancement velocity on the flow and reaction rate On the other and, for small flow rates, the pipes are funnel-shaped with parabolic tips and their advancement velocity is of the same order as that of a planar front. The transition between the two forms is abrupt, with no intermediate forms observed. The simulation results are compared with field evidence from limestone quarries in Smerdyna, Poland, where several hundred of solution pipes have been exposed. Interestingly, both forms (shaft-like and tunnel-like) are found in the field, sometimes in close proximity to each other.

Figure 1. Parabolic (left) and linear (right) solution pipes in the limestone quarry at Smerdyna (Poland). Photo on the right is courtesy of dr Łukasz Uzarowicz (Warsaw University of Life Sciences - SGGW, Poland).

References

[1] P. Walsh and I. Morawiecka-Zacharz, A dissolution pipe palaeokarst of mid-Pleistocene age preserved in Miocene limestones near Staszow, Poland, Palaeogeogr. Palaeoclimatol. Palaeoecol., 174 (2001), pp. 327-350.
[2] K. G. Grimes, Solution pipes and pinnacles in syngenetic karst. In: Gines A., Knez M., Slabe T., Dreybrodt W. (Eds.), Karst Rock Features: Karren Sculpturing. Ljubljana, ZRC Publishing, (2009), pp. 513-523.
[3] J. De Waele, S. E. Lauritzen and M. Parise On the formation of dissolution pipes in Quaternary coastal calcareous arenites in Mediterranean settings. Earth. Surf. Proc. Land" 36, (2011), pp. 143-157.

cmg2016 - - Thursday, June 9, 2016 - 11:45/12:30 (45min)

Stressed deserts: A new vegetation/sediment-transport model for dryland environments

J. Mayaud[1], R. Bailey[1], G. Wiggs[1]
[1]*School of Geography and the Environment, University of Oxford, UK*

Key words cellular automata, self-organisation, sediment transport, dunes, wind erosion

In many drylands, vegetation is patchy and dynamic through time and space, with complex ecohydrological feedbacks and plant-plant interactions leading to the emergence of characteristic vegetation patterning. There is increasing evidence that information from the patterns themselves can be used as indicators of a dryland system's proximity to collapse. However, current models simulating the evolution of these vegetation patterns do not account for their effects on wind flow and on the entrainment, transport and redistribution of wind-blown material. Significant uncertainty therefore remains about how these vulnerable landscapes will react to increasing climate forcing and land-use pressure over the 21st century.

We present the coupled Vegetation and Sediment TrAnsport model (ViSTA), a new, multi-scale cellular automaton model designed to simulate transport in vegetated dryland contexts. The model is parameterised using empirical data collected during a field campaign in Namibia that sought to investigate the impact of desert vegetation on wind speed and turbulence at the surface. A new turbulence-based model for aeolian transport is also used to drive the movement of sediment within ViSTA. We show that this coupled approach allows for realistic simulations of dynamics at both the bedform and landscape scale, and present applications of the model to various environmental issues pertinent to drylands.

It is especially important to understand the geomorphological responses of vegetated semi-arid landscapes to a variety of simulated stresses, since these regions are often heavily used for pastoralism, agriculture and habitation. In characterising possible transition scenarios between patterned and desert states, the ViSTA model therefore represents a powerful tool that has direct relevance to land management policies in highly vulnerable environments.

cmg2016 - - Thursday, June 9, 2016 - 11:45/12:30 (45min)

A NUMERICAL IMPLEMENTATION OF LANDSCAPE EVOLUTION MODELS

M. Lebrun[1], J. Darbon[2] & J.M. Morel[2]
[1]*CNES - CNRS, France*
[2]*Ecole Normale Supérieure, Cachan, France*

Key words Landscape evolution model, Partial differential equations, River networks, Conservation laws, Detachment-limited and transport-limited erosion.

In this communication our goal is to propose a simple and efficient numerical solution for the solution of a system of three partial differential equations arising in the modeling of landscape evolution. Indeed, as remarked by several authors, the main physical laws that have been proposed in landscape evolution models (LEMs) can be converted into a minimal system of three partial differential equations. The first one is a transport equation that governs the water run-off. It is the simplest interpretation of Saint-Venant shallow water equations. A second equation, of Hamilton-Jacobi type with a dissipative term, governs the terrain evolution by detachment-limited erosion, creep and sedimentation. A third equation is necessary to describe the sediment transport in water. This equation governs the transport of the suspended sediment load in water. The challenge that we address is to simulate in reasonable time such a system of equations on a large enough digital elevation model, generally acquired by satellite or aerial imaging. We compare our proposed solution with existing implementations and explain how each equation can be reformulated as a discrete scheme on a raster, that is still conservative as the continuous equations. Furthermore we show that the systematic introduction of a multiscale procedure leads to extremely fast simulations. This permits to simulate water run-off on fixed landscapes, and to explore and compare in reasonable time several models and their parameters. Last but not least, we address the problem of an efficient visualisation of a three phases results : the elevation, the water height and the sediment load.
Fig. 1 shows a typical result for the Island “La Réunion” with 15% lands off.

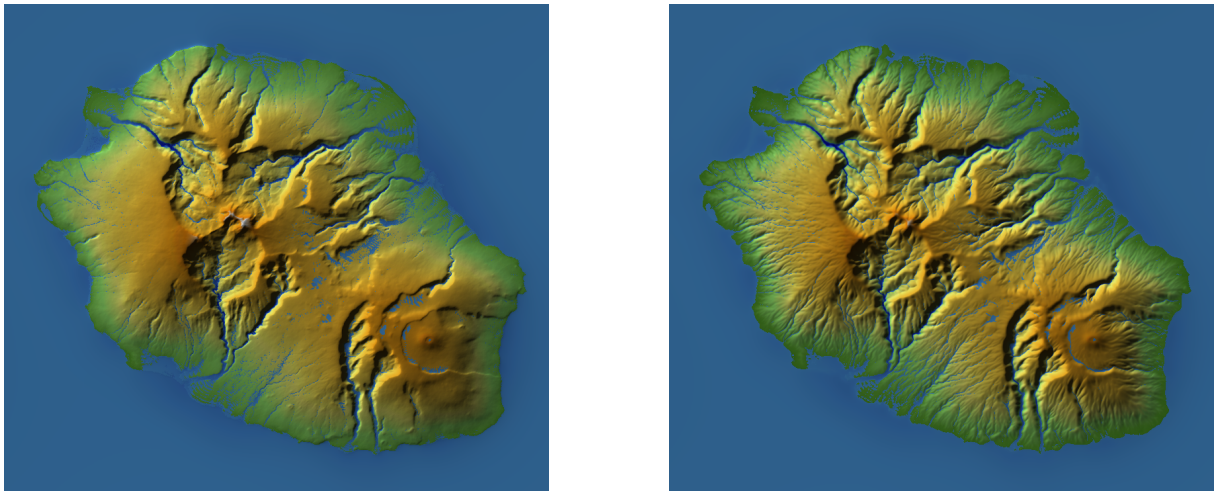

Figure 1. Simulated evolution of “La Réunion”, emergence of the fine river network.

A demo (usr:demo, pwd:demo) can be tested on line at the adress

`http://dev.ipol.im/~ibal/ipol_demo/LEM/`

References

[1] A. Chen, J. Darbon, J.M. Morel, *Landscape evolution models: A review of their fundamental equations*, Geomorphology **219**, 68–86 (2014).
[2] T.J. Coulthard, J.C. Neal, P.D. Bates, J. Ramirez, G.A. Almeida, G.R. Hancock, *Integrating the LISFLOOD-FP 2D hydrodynamic model with the CAESAR model: implications for modelling landscape evolution*, Earth Surface Processes and Landforms **38(15)**, 1897–1906 (2013)
[3] T.J. Coulthard, *Landscape evolution models: a software review.*, Hydrological processes **15(1)**, 165–173 (2001)

cmg2016 - - Thursday, June 9, 2016 - 11:45/12:30 (45min)

AN OVERVIEW OF TIMESTACK IMAGE APPLICATIONS FOR NEARSHORE STUDIES

U. Andriolo[1]
[1]*IDL, University of Lisbon, Faculty of Science, Department of Geology, Lisbon, Portugal*

Key words Coastal videomonitoring, littoral hydrodynamics, surf zone morphodynamics

In the littoral zone, video monitoring technique has been providing crucial information to coastal engineers and scientists for the last three decades. The video remote sensing proved to be an economic and efficient way to collect high-resolution and continuos data, which allow the analysis of beach morphological behaviour and hydrodynamic phenomena in the nearshore zone.
The methodology consists in placing optical devides, such as Internet Protocol cameras, acquiring images of the coast (Fig.1, a) from an elevated position. The technique is based on the use of specific images (e.g. Time-Exposure, Sigma-variance and Timestacks). In particular, timestack images (Fig.1, c) are optical products generated by sampling cross-shore pixel intensity time series over georectified video frames (Fig.1, b). The image intensity variation along the selected cross-shore transects visually depicts wave carachteristics in the nearshore zone and swash motion on the beach face.

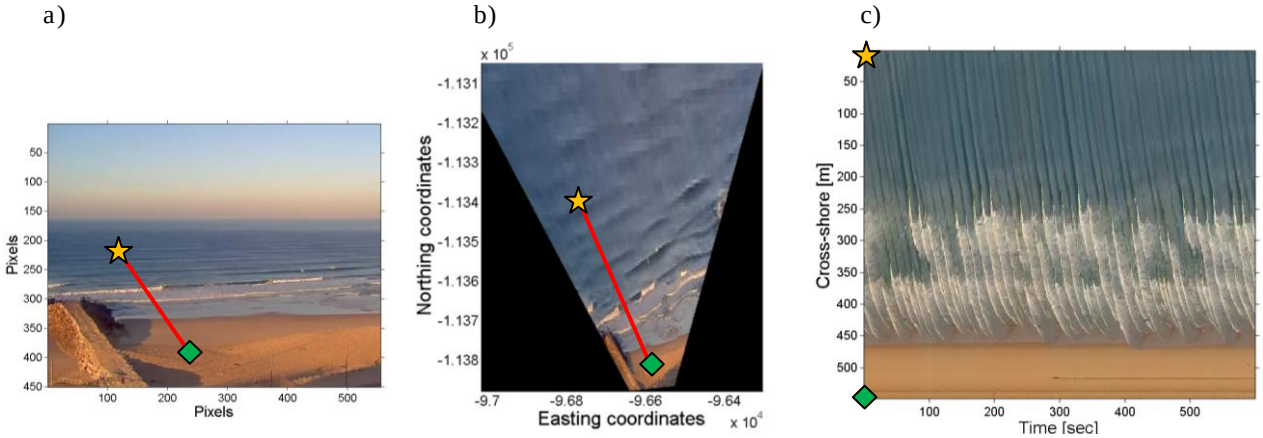

Figure 1 Procedure for timestack production. a) single frame acquired by the camera; b) geo.rectified image; c) timestack image obtained over 10 minutes images sequence (1 Hz acquisition frequency). Red line represents chosen profile for timestack production. Yellow star and green diamond indicate offshore and onshore profile limits, respectively.

This communication will report the state-of-art of timestack images applications for nearshore hydrodynamic characterization, which is a key element for improving storm-related risk assessment and designing coastal protection structures. Examples will show how the utilization of timestack images allowed the monitoring and evaluation of high-frequency hydrodynamic parameters such as wave run-up run up elevation [2,5] and incident wave carachteristics [1,4].Such essential factors can support the development of algortithms for nearshore bathymetry estimation [3,4]. Discussion will introduce a novel methodology to distinguish coastal areas based on the timestack image statistical behaviour. Such new practice will support a stand-alone algorithm for deriving bathymetry over shallow water and intertidal zone, along with an automatic detection of wave run-up elevation on the beach face.

References

[1] Almar, R., Cienfuegos, R., Catalán, P.A., Michallet, H., Castelle, B. Bonneton, P., Marieu, V. 2012. *A new breaking wave height direct estimator from video imagery*. Coastal Engineering, 61, pp. 42-48
[2] Andriolo, U., Herminio, J., Ribeiro, M., Taborda, R., 2015. *Insights on run-up processes through high resolution video measurements*. VIII International Symposium on the Iberian Atlantic Margin (MIA15), Malaga, Spain
[3] Stockdon H.F., Holman R.A., 2000. *Estimation of Wave Phase Speed and Nearshore Bathymetry from Video Imagery*. Journal of Geophysical Research, 105, pp 22,015-22,033
[4] Yoo, J. *Nonlinear Bathymetry Inversion Based on Wave Property Estimation from Nearshore Video Imagery*. PhD report of the Georgia Institute of Technology. 2007
[5] Vousdoukas, M. I., Wziatek, D., Almeida, L. P., 2012. *Coastal vulnerability assessment based on video wave run-up observations at a meso-tidal, reflective beach*. Ocean Dynamics, 62 (1), pp. 123–137

cmg2016 - - Thursday, June 9, 2016 - 11:45/12:30 (45min)

MORPHODYNAMIC MODELLING OF A COMPLETE ACCRETIONARY BEACH SEQUENCE

B. Dubarbier[1], B. Castelle[2], V. Marieu[2] & B.G. Ruessink[3]
UMR EPOC, [1]Université Bordeaux, [2]CNRS, France
[3]Department of Physical Geography, Faculty of Geosciences, Utrecht University, The Netherlands

Key words Sandbar morphodynamics, downstate sequence, cross-shore processes, process-based modelling.

Wave-dominated sandy beaches are one of the most dynamic and vulnerable coastal environments. Most of sandy beaches exhibit underwater ridges of sand, referred to as surf-zone sandbars, that act as a natural protection against storm-driven hinterland flooding and erosion by dissipating wave energy offshore through depth-induced breaking. Following [1], sequential erosive (upstate) and accretive downstate sequences characterize the dynamics of intermediate beaches, which are ubiquitous worldwide. Despite these sequences have been observed through field surveys and video monitoring for decades, to date there is no morphodynamic model able to simulate these sequences entirely. As hypothesized by [4], we advocate that the main reason is that these morphodynamic models do not account for state-of-the-art parametrizations of cross-shore sediment transport driven by the respective contribution of wave nonlinearities and undertow. In this study, we focus on the full downstate sequence that describes the transition through four beach states under accretionary wave conditions. The cross-shore sediment transport processes described in detail in [3] are implemented in a coupled wave-current-sediment transport model [2]. Simulations start from a nature-like concave alongshore-uniform single-barred beach bathymetry, with constant wave and water-level conditions. Fig.1 shows, to our knowledge, the first complete modelled downstate sandbar sequence, with: (1) the evolution from an initial alongshore-uniform longshore bar-trough state to a rhythmic sandbar state characterized by a crescentic sandbar (fig.1a-b), (2) the attachment of the sandbar horns to the shore give rise a transverse bar and rip state (fig.1b-c) and finally (3) the complete welding of the sandbar to the shore with the formation of a terrace cut by shallower rip channels (fig.1c-d). This full down-state beach sequence modelling offers a unique opportunity to address the respective contributions of the different sediment transport modes to the different sequences. These respective contributions as well as additional simulations showing the influence of the main offshore wave characteristics, namely wave height, period and direction, will be presented.

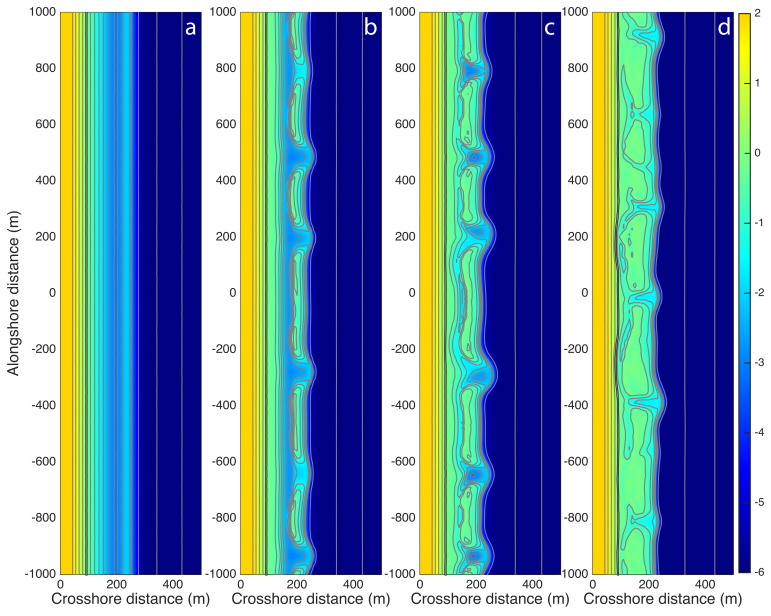

Figure 1. Simulation of a complete downstate beach evolution showing the sequential transition (a) LBT state - (b) RBB state - (c) TBR state - (d) LTT state. Colours indicate water depth, the black line shows the still water shoreline and the isocontours of the bathymetry are contoured in the background.

References

[1] L. D. Wright and A. D. Short, *Morphodynamic variability of surf zones and beaches: A synthesis*, Marine Geology. **56**, 93-118 (1984).
[2] B. Castelle and B. G. Ruessink, *Modeling formation and subsequent nonlinear evolution of rip channels: time-varying versus time-invariant wave forcing*, Journal of Geophysical Research. **116**, (2011).
[3] B. Dubarbier and B. Castelle and V. Marieu and B. G. Ruessink, *Process-based modelling of beach profile behavior*, Coastal Engineering. **95**, 35-50 (2015).
[4] H. Michallet and B. Castelle and E. Barthélemy and C. Berni and P. Bonneton, *Physical modeling of three-dimensional intermediate beach morphodynamics*, Journal of Geophysical Research. **118**, 1-15 (2013).

cmg2016 - - Thursday, June 9, 2016 - 11:45/12:30 (45min)

INSTABILITY OF AN INFILTRATION-DRIVEN DISSOLUTION-PRECIPITATION FRONT

P. Kondratiuk, F. Dutka & P. Szymczak
Faculty of Physics, University of Warsaw, Warsaw, Poland

Key words Instability, dissolution, precipitation, porous media, reaction front

Infiltration of a rock by an external fluid very often drives it out of chemical equilibrium. As a result, alteration of the rock mineral composition occurs. It does not however proceed in the whole rock volume uniformly. Instead, there form one or more reaction fronts, i.e., zones of increased chemical activity, separating the altered (product) rock from the yet unaltered (primary) one. One of the simplest examples of such an alteration is the dissolution of some of the minerals building the primary rock. For instance, calcium carbonate minerals can be dissolved by infiltrating acidic fluids. In such a case the product rock has higher porosity and permeability than the primary one. Due to positive feedbacks between the reactant transport, fluid flow, and porosity generation, the reaction fronts in dissolution systems are inherently unstable. An arbitrarily small protrusion of the front gets magnified and develops into a highly porous channel. This feature of dissolution fronts, dubbed the "reactive-infiltration instability" [1], is responsible for the formation of a number of geological patterns, such as solution pipes. It is also of practical importance, since spontaneous development of localized highly porous flow paths is favourable by petroleum engineers, who apply acidization to oil-bearing reservoirs in order to increase their permeability.

However, dissolution might not be the only reaction in an infiltration-driven system. For instance, the products of dissolution might react with other species and reprecipitate [2]. The dissolution and precipitation fronts develop and start to propagate with equal velocities, forming a single replacement front. The porosity profile is not monotonic as in the case of pure dissolution, but it typically has a minimum in the vicinity of the front. Additionally, the porosity difference between the primary rock far-downstream and the fully developed secondary rock far-upstream can be either negative or positive, which either destabilizes or stabilizes the front.

We propose a theoretical model of a simple infiltration-driven dissolution-precipitation system. By performing linear stability analysis of the planar reaction front we show that the front can be unstable for a wide range of control parameters (the Péclet and Damköhler numbers, the ratio of molar volumes of the primary and the secondary mineral), even if the porosity of the secondary rock is lower than the porosity of the primary rock. Next, by numerical simulations of the complete dynamics we present the long-term evolution of the system. The nonlinear couplings between the flow, transport and the chemical reactions cause the development of an intricate pattern in the secondary phase (Fig. 1).

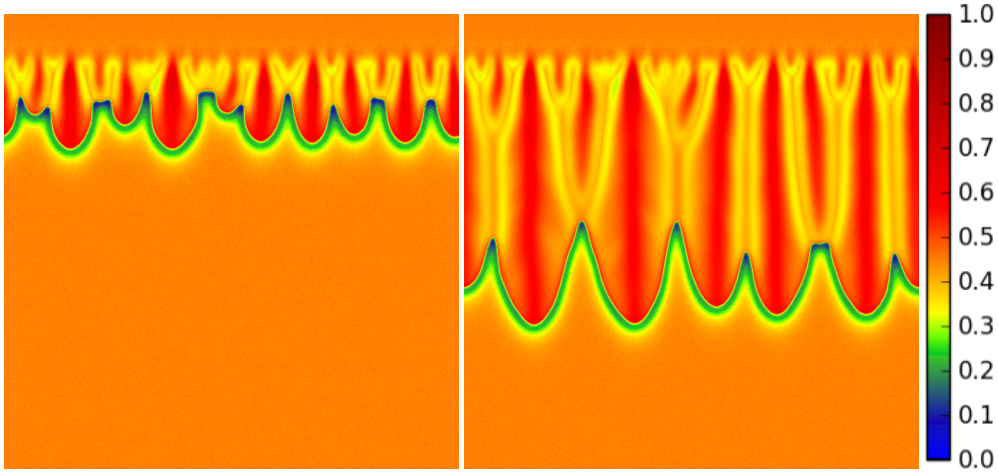

Figure 1. Development of a striped pattern in the secondary mineral phase during the infiltration-driven replacement process. The fluid flow and the reaction front propagation is from the top to the bottom. The colors correspond to different values of porosity.

References

[1] J. Chadam, D. Hoff, E. Merino, P. Ortoleva, and A. Sen, *Reactive infiltration instabilities*, J. Appl. Math. **36**, pp. 207–221, 1986.
[2] A. Putnis, *Mineral Replacement Reactions*, Rev. Mineral. Geochemistry **70**, no. 1, pp. 87–124, 2009.

cmg2016 - - Thursday, June 9, 2016 - 11:45/12:30 (45min)

ILL-POSEDNESS OF THE SAINT-VENANT-HIRANO MODEL

V. Chavarrías[1], A. Blom[1] & G. Stecca[2]
[1]*Delft University of Technology, Delft, The Netherlands*
[2]*National Institute of Water and Atmospheric Research, Christchurch, New Zealand.*

Key words River morphodynamics, mixed size sediment, ellipticity.

The morphodynamic evolution of a river is generally modelled using a set of conservation equations for water mass and momentum and sediment mass. For unisize sediment this set of conservation equations comprises the Shallow Water Equations and the Exner equation. For modelling processes associated with mixed-size sediment (e.g. armoring, downstream fining) it is necessary to introduce a conservation equation for each grain size fraction. The first and most widely applied model is that of Hirano [1], i.e. the active layer model. A necessary condition for the model to be representative of physical processes is that the set of partial differential equations is well-posed. In the case of a time-evolving problem the system of equations must be of the hyperbolic (or parabolic) type, which is ensured by real eigenvalues, i.e. the information must propagate at a real celerity. Yet, using the Hirano model the system's character may become elliptic [2], which happens when an eigenvalue becomes complex. We have conducted an analysis of the system of equations to gain insight into its well-posedness. To that end we assume quasi-steady one-dimensional flow over a bi-modal sediment mixture. We then obtain analytical expressions of the eigenvalues (λ) which can be written as a combination of two celerities: the De Vries celerity (of disturbances that arise due to spatial gradients in the bed load transport rate that are unrelated to mixed sediment) and the Ribberink celerity (of those disturbances that originate from the presence of mixed sediment). When these two celerities are similar (Figure 1a), the discriminant of the eigenvalues (Δ) may become negative (Figure 1b) and the system loses its hyperbolic character. To study the consequences of the elliptic behavior we conduct a perturbation analysis and we run numerical simulations. A solution of a river degrading into a fine substrate (Simulation 1, Figure 1c) is elliptic for certain values of active layer thickness (Simulation 2, Figure 1d), which result in oscillations that are not related to physical mechanisms. If mixed-size sediment simulations suffer from ellipticity the results are not only unreallistic but also largely affected by the domain discretization. Paradoxically, a more detailed discretization of the domain, which leads to more accurate results, increases the velocity at which oscillations grow. Also, the absence or presence of oscillations is no guarantee of elliptic or hyperbolic character and the representativeness of the results can only be assured by a specified mathematical assessment of the system's character.

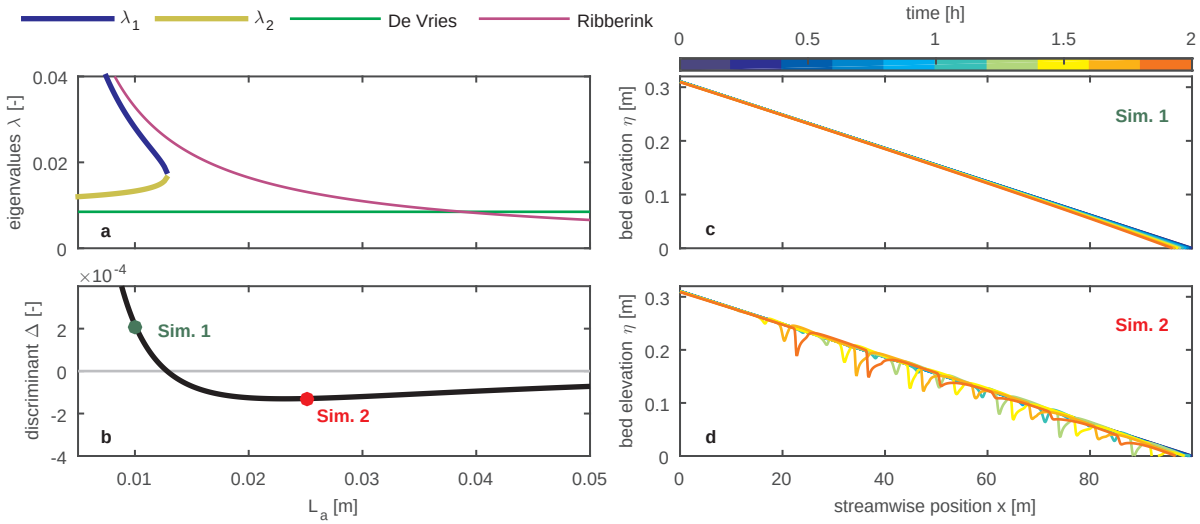

Figure 1: Eigenvalues (**a**), and discriminant (**b**) for a varying active layer thickness. Numerical results of a hyperbolic run (Simulation 1, **c**) and elliptic run (Simulation 2, **d**).

References

[1] Hirano, M. (1971), River bed degradation with armouring, *Trans. Jpn. Soc. Civ. Eng*, *3*(2), 194–195.
[2] Ribberink, J. S. (1987), Mathematical modelling of one-dimensional morphological changes in rivers with non-uniform sediment, Ph.D. thesis, Delft University of Technology, The Netherlands.

cmg2016 - - Thursday, June 9, 2016 - 11:45/12:30 (45min)

SIMPLIFIED TREATMENT OF THE FLOW AND THE USE OF A MORPHODYNAMIC FACTOR IN LONG-TERM MORPHODYNAMIC COMPUTATIONS

L. Arkesteijn[1], A. Blom[1] & R.J. Labeur[1]

[1]*Delft University of Technology, Faculty of Civil Engineering and Geociences, Department of Hydraulic Engineering, Delft, The Netherlands*

Key words river morphodynamics, morphodynamic factor, time-scales, simplified flow treatment

A complicating factor in long term morphodynamic computations is the presence of multiple time scales for the propagation of disturbances in the water surface elevation (fast) and bed elevation changes (slow). The general consequence for a numerical model is a combination of a long simulation time with a small time step to capture all the effects to a particular disturbance. For a large scale computation in a two dimensional domain, however, the computational effort becomes too large, and artificial 'tricks' become necessary. Common techniques are a simplified treatment of the flow that eliminates the small scale effects, such as the steady state backwater curve or normal flow approximation, or the use of a morphodynamic acceleration factor. In the latter, the computed sediment transport rate is multiplied by the morphodynamic factor such that the resulting bed elevation change represents the change that occurs during a larger time step. In other words, the morphodynamic change is accelerated and the total simulation time is divided by the morphodynamic factor. Here we study the impact of these techniques on long-term morphodynamic runs. Numerical simulations have been performed to assess these effects and make a comparison between the techniques. Figure 1 shows an example in which we study the response of the river bed to a yearly cycled hydrograph with one yearly peak for (1) an unsteady treatment of the flow (i.e. the Saint-Venant equations), (2) a steady state treatment of the flow (i.e. a backwater curve), and (3) an unsteady treatment of the flow accelerated by various values of the morphodynamic factor (10, 20, 40, 80). The runs start from a constant bed slope and normal flow conditions. At the upstream end, the equilibrium sediment transport rate and the yearly cycled hydrograph are prescribed, and at the downstream end the water surface elevation is fixed at the initial normal flow depth of the dominant water discharge. This results in an M1-backwater effect during base flow, and an M2-backwater effect during peak flow, the effect of which on the bed elevation, balance each other (i.e. in a dynamic equilibrium). Figure 1 shows the situation after 100 years. While the output of the steady simulation resembles the unsteady simulation quite well, the simulation result with the morphodynamic acceleration factor reduces with increasing morphodynamic factor. This can be explained by the damping of the peak discharge before it reaches the downstream end of the domain, such that there are M1 curves during both base and peak flow.

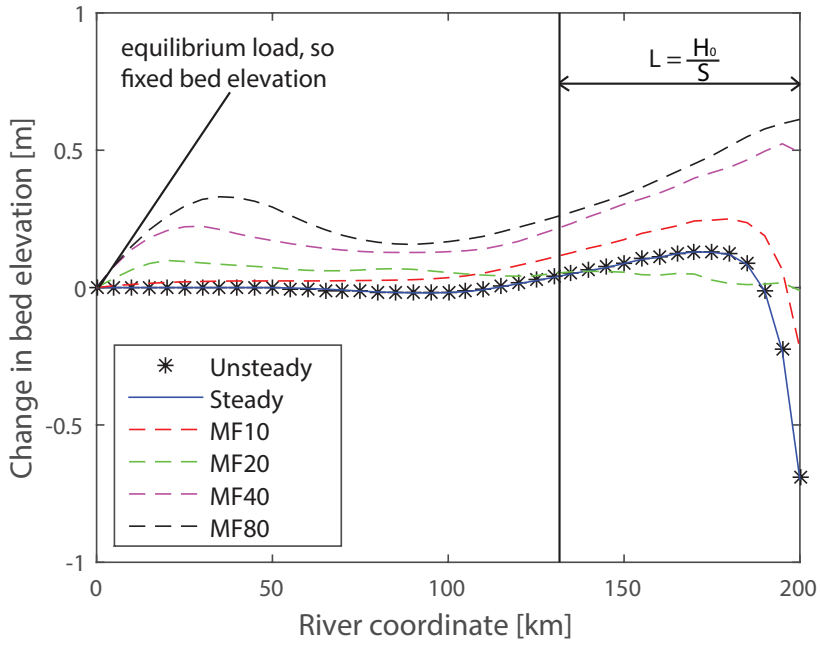

Figure 1. Change in bed elevation (relative to the initial state) after a 100 year run, under a cyclic (1 year period) hydrograph. L indicates a characteristic backwater length, H_0 is a characteristic flow depth, and S is the channel bed slope.

cmg2016 - - Thursday, June 9, 2016 - 11:45/12:30 (45min)

Suspended sediment prediction in Kebir watershed, northeast of Algeria

K. Khanchoul[1], A. Amamara[2]

[1] *Department of Geology, Badji Mokhtar University-Annaba, P.O. Box 12, 23000 Annaba, Algeria.*

[2] *Soils and Sustainable Development Laboratory, Department of Biology, Badji Mokhtar University-Annaba, P.O. Box 12, 23000 Annaba, Algeria.*

Key words geomorphology, ANN, regression, prediction, suspended sediment modeling.

The objective of this research was to identify potential equivalences between artificial neural networks and statistical regression and to verify these equivalences when applied to modeling sediment loads in the Kebir river, located in the northeast of Algeria. The watershed (681 Km²) has shown a construction of two reservoirs, Mexa (Algeria) and Barbara (Tunisia) in 1999 (Figure 1).

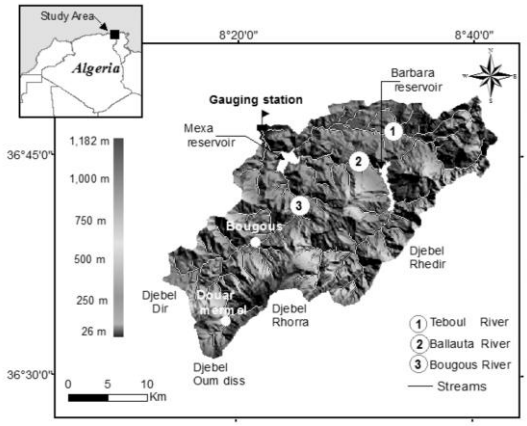

Figure 1. Location map of the Kebir watershed.

Basically, the river discharge (Q) and suspended sediment concentration (C) data were based on daily measurements. In this regard 129 daily data sets have been collected over 20 years (1979 to 1999). First, the sediment rating curve (SRC) was used as a power function of the form [1]: C or $Qs = aQ^b$; Qs is the sediment discharge (product of Q and C).

In designing MLP and Lm, the input combinations were covering the geomorphological parameters and the target layer was consisting of the unique sediment load data and the expression could be written in the mathematical form for ANN model given by following equation: $Qs = fcn\ (Q^{\sqrt{Dd}}, Q^{\sqrt{Sf}}, Q^{\sqrt{S}}, Q^{\sqrt{Li}}, Q^{\sqrt{Fi}})$; where Dd is the drainage density, Sf is the shape factor of the basin, S is the mean basin slope, Li is the lithologic index, and Fi is the forest cover. Before training, the data sets have been normalized and then divided into three parts as: training, testing and validation [2]. *RMSE* (root mean squared error) was noted for each analysis and cross validation was also performed to estimate R^2 values. The model efficiency factor *EF* of observed and predicted values were also estimated for different predictions on validation datasets.

Based on the measured paired values of Q and Qs data from the training subset, SRC model has given $R^2 = 0.89$. The developed regression underestimated the true sediment load by – 14.90% and had a model efficiency (*EF*) of 0.88. The normalized *RMSE* value found equal to 0.069 was in acceptable range. The MLP and Lm methods provided better performance in sediment estimation compared to SRC. Values of R in the training phases were higher with coefficients of correlation equal to 0.96 and 0.97, *RMSE* ranged from 0.040 to 0.054 and *EF* varied between 0.91 and 0.94. The Lm best network for the testing period was provided by the nine neuron model in the hidden layer, with a slight underestimation of only -0.48. As a conclusion, we can say that the use of the three-layered ANN structure with the number of neurons in hidden layer via Levenberg-Marquardt algorithm (Lm) has improved the simulation results and the performance of the developed models for prediction of sediment load found very satisfactory on the basis of statistical indices.

References

[1] Asselman N.E.M. 2000. Fitting and interpretation of sediment rating curves. J. Hydrol., 234: 228–48.

[2] Boukhrissa Z.A., Khanchoul K., Le Bissonnais Y., Tourki M. (2013): Prediction of sediment load by sediment rating curve and neural network (ANN) in El Kebir catchment, Algeria. J. Earth Syst Sci., 122(5): 1303–1312.

cmg2016 - - Thursday, June 9, 2016 - 11:45/12:30 (45min)

SHORELINE DYNAMICS: EXPLICIT FORMULATIONS FROM THE NON-LINEAR PELNARD-CONSIDÈRE EQUATION

F. Bouchette[1], M. Manna[2]
[1]*Géosciences-Montpellier, Université de Montpellier/CNRS, Montpellier*
[2]*Laboratoire Charles Coulomb, Université de Montpellier/CNRS, Montpellier*

Key words Pelnard-Considère, non-linear diffusion, anti-diffusion, shoreline features, erosion, cuspate, spits.

We tentatively contribute to a better understanding of shoreline dynamics starting from a non-linear Pelnard-Considère equation [3]. In the following, we define the shoreline as being a curve moving in plan view, averaging the location of the interface between land and sea over time scales of the order of days or weeks at least.

Many works analyze how natural or human-controlled shoreline features – such as sand spits, cuspates, flying spits, tombolos – may develop through time [6]. In the past, research activities on this topic strictly developed from a diffusion equation [8], with severe restrictions on the physics embedded. More recent works introduced non-linear effects and successfully modeled the growth of single instabilities or repetitive patterns [1, 4, 2, 5, 7]. Non-linearity is crucial to tackle problems such as 1) the cyclic distribution of geomorphic features alongshore, 2) the spontaneous nucleation of single features, 3) the migration of morphologies, 4) the interactions between shoreline instabilities. Amongst these works, Ashton & Murray [2] suggested that the following equation (S being the plan viewed shoreline position):

$$\frac{\partial S}{\partial t} = \kappa \frac{\partial^2 S}{\partial x^2} \tag{1}$$

where some kind of diffusivity κ depends upon wave breaking angle, was a good expression to model shoreline instabilities. More specifically, they develop a numerical tool solving this equation for the growth of sand spits. From the analysis of the numerical results, they suggest the existence of relationships between the dimensions of geomorphic features and their age.

In this work, we write the following local diffusive/ anti-diffusive shoreline equation:

$$\frac{\partial S}{\partial t} = G_0 \cos 2\delta_0 \frac{\partial^2 S}{\partial x^2} + 2G_0 \sin 2\delta_0 \frac{\partial S}{\partial x}\frac{\partial^2 S}{\partial x^2} \tag{2}$$

where G_0 a longshore diffusivity, δ_0 the deep-water incident wave angle. Obviously, the linearization of this equation leads to the so-called linear diffusion equation of Pelnard-Considère [8].

First, we show that Eqs 1 and 2 are strongly connected although they show important discrepancies, especially the fact that Eq. 2 embeds non-linearity but does not require any information relative to the wave angle at wave breaking, where non-linear effects may develop. We also deeply explore the effects of anti-diffusive effects in the Eq. 2. Then, although Eq. 2 does not offer any trivial general solution, we successfully derive peculiar explicit solutions for the growth of cuspate spits, and we give a formal proof of the existence of an alternative relationship between the dimensions of a cuspate, its age and the surrounding longshore diffusivity; we also provide a solution for the growth of tombolos.

Finally, we present the on-going developments to solve numerically the non-linear Pelnard-Considère equation.

References

[1] A. Asthon, B. Murray, O. Arnault, *Formation of coastline features by large-scale instabilities induced by high-angle waves*, Nature, **414**, 296–299 (2001).
[2] A. Asthon, B. Murray, *High-angle wave instability and emergent shoreline shapes: 1) modeling of sand waves, flying spits and capes*, Journal of Geophysical Research, **111**, F04011 (2006).
[3] F. Bouchette, M. Manna, P. Montalvo, A. Nutz, M. Schuster, J.-F. Ghienne, *Growth of cuspate spits*, J. of Coastal Research, **SI69** (2014).
[4] D. Calvete, H. E. de Swart, A. , Falquès, *Effect of depth-dependent wave stirring on the final amplitude of shoreface-connected sand ridges*, Continental Shelf Research, **22**(18-19), 2763-2776 (2002).
[5] G. Coco, B. Murray, *Patterns in the sand: From forcing templates to self-organization*, Geomorphology, **91**(3-4), 271–290 (2007).
[6] J. Dronkers, *Dynamics of coastal systems*, World Scientific, **25**, 255p (2005).
[7] A. Falquès, N. Dodd, R. Garnier, F. Ribas, L. MacHardy, P. Larroudé, D. Calvete, F. Sancho, *Rhythmic surf zone bars and morphodynamic self-organization*, Coastal Engineering, **55**(7-8), 622–641 (2008).
[8] R. Pelnard-Considère, *Essai de théorie de l'évolution des formes de rivages en plages de sable et de galets*, La Houille Blanche (1956).
[9] V. P., Zenkovitch, *On the genesis of cuspate spits along lagoon shores*, The Journal of Geology, **67**, 269–277 (1959).

cmg2016 - - Thursday, June 9, 2016 - 11:45/12:30 (45min)

PHYSICAL PROCESSES CAUSING THE FORMATION OF PENITENTES

P. Claudin[♯], H. Jarry[♯], G. Vignoles[♠], M. Plapp[❄] & B. Andreotti[♯]
[♯]*Laboratoire de Physique et Mécanique des Milieux Hétérogènes,*
PMMH UMR 7636 ESPCI – CNRS – UPD – UPMC, 10 rue Vauquelin, 75005, Paris, France.
[♠]*Laboratoire des Composites ThermoStructuraux,*
LCTS UMR 5801 CNRS – UB1 – CEA – Safran, 3 allée La Boetie, 33600 Pessac, France.
[❄]*Condensed Matter Physics, Ecole Polytechnique, CNRS, 91128 Palaiseau, France.*

Key words Penitentes. Sublimation patterns

Penitentes are natural patterns made of compact snow or ice (Fig. 1). They are typically found in mountains at high altitudes where humidity and temperature are low and solar radiation is intense. In these conditions, solid water sublimates when heated, and tall thin spikes oriented toward the main direction of the sun emerge by differential ablation. They have been reproduced at a centimeter scale in laboratory experiments [1].

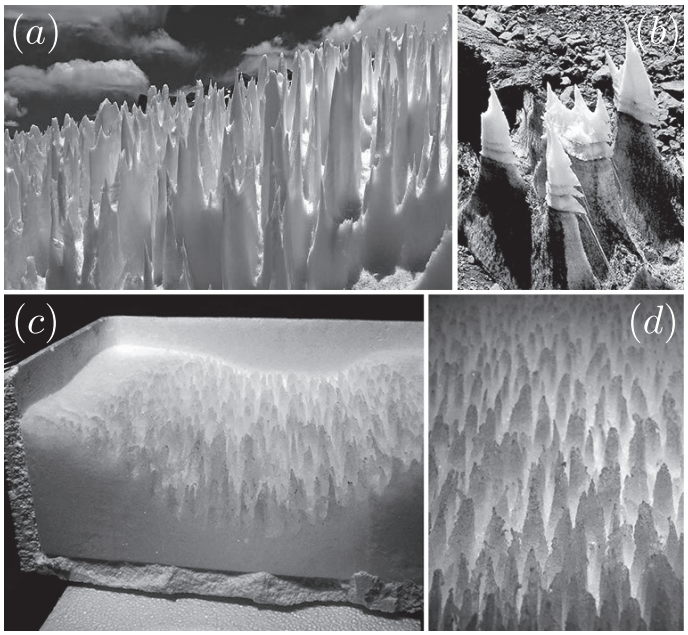

Figure 1. (a,b) Photographs of natural penitentes on the Aconcagua mountain (Argentina). Peak separation: a few tens of cm. (c,d) Micropenitentes in the laboratory, from Ref. [1]. Peak separation $\simeq$ 1 cm.

We have investigated the physical processes at the initial stage of penitente growth and performed the linear stability analysis of a flat surface submitted to the solar heat flux. We have shown that these patterns do not simply result from the self-illumination of the surface –a scale-free process– but are primarily controlled by vapor diffusion and heat conduction. The wavelength at which snow penitentes emerge is derived and discussed. We found that it is controlled by aerodynamic mixing of vapor above the ice surface [2].

References

[1] V. Bergeron, C. Berger and M.D. Betterton, *Controlled irradiative formation of penitentes*, Phys. Rev. Lett. **96**, 098502 (2006).
[2] P. Claudin, H. Jarry, G. Vignoles, M. Plapp and B. Andreotti, *Physical processes causing the formation of penitentes*, Phys. Rev. E **92**, 033015 (2015).

cmg2016 - - Thursday, June 9, 2016 - 11:45/12:30 (45min)

DIRECT NUMERICAL SIMULATIONS OF AEOLIAN SAND RIPPLES

O. Durán[✿,✺], B. Andreotti[✿] & P. Claudin[✿]
✿ *Laboratoire de Physique et Mécanique des Milieux Hétérogènes, PMMH UMR 7636 ESPCI – CNRS – UPD – UPMC, 10 rue Vauquelin, 75005, Paris, France.*
✺ *MARUM – Center for Marine Environmental Research, Bremen University, Germany.*

Key words Aeolian transport. Wind ripples. Resonance

Aeolian ripples form regular patterns at the surface of sand sheets and dunes, both on Earth and Mars. Their emergence at a wavelength much larger than the grain size was unexplained. Here we report direct numerical simulations of grains interacting with a wind flow that are able to reproduce the spontaneous growth of ripples with an initial wavelength and a propagation velocity linearly increasing with the wind speed. The instability turns out to be driven by resonant grain trajectories, whose length is close to a ripple wavelength and whose splash leads to a mass displacement towards the ripple crests. The pattern selection results from a compromise between this destabilizing mechanism and a diffusive downslope transport which stabilizes small wavelengths.

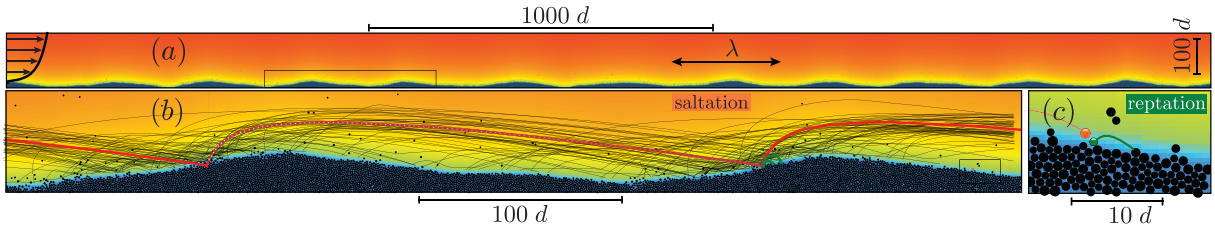

Figure 1. Ripples emerging from a flat bed in a simulation ($u_*/u_{th} = 3$). (a) Large-scale view of the system composed of 45000 grains in a quasi two-dimensional xyz box of respective dimensions $3400\,d \times 1\,d \times 1000\,d$). Periodic boundary conditions are used in the x (wind) direction. The results presented here are obtained for a density ratio $\rho_p/\rho_f = 500$, a grain Reynolds number $\mathcal{R} = d/\nu\sqrt{(\rho_p/\rho_f - 1)gd} = 22$ (ν is the air kinematic viscosity) and shear velocities in the range $u_*/u_{\rm th} = 1$–5. The colored background codes for the wind velocity, see wind profile (left). (b) Close-up view at the scale of the ripple wavelength, featuring saltation trajectories, with hop-height between 15 and $30d$. The average resonant trajectory is shown in red. (c) Zoom at the level of the interfacial. A collision between a salton (orange) and a repton (green) is sketched.

References

[1] O. Durán, P. Claudin, B. Andreotti, *Direct numerical simulations of aeolian sand ripples*, Proc. Natl. Acad. Sci. USA **111**, 15665–15668 (2014).

cmg2016 - - Thursday, June 9, 2016 - 11:45/12:30 (45min)

Attractor Reconstruction of Spatiotemporal Interpsike Intervals with Application to a Coupled Human-Natural System

D. E. McNamara[1], N. Cortale[1], S. Armstrong[2], E. Lazarus[2] & K. Ells[3]
[1]*Department of Physics and Physical Oceanography, UNC Wilmington, USA*
[2]*School of Earth and Ocean Sciences, Cardiff University, UK.*
[3]*Center for Marine Science, UNC Wilmington, USA .*

Key words Nonlinear Time Series Forecasting, Coupled Human-Natural Systems.

Highly populated coastlines in many locations around the world represent some of the most glaring examples of geophysical systems with strong human interactions. Most commonly, these interactions take the form of altering the plan view position of the coastline through engineered placement of sand on the beach to counteract coastal erosion and enhance property value [1,2]. This process of beach nourishment makes human-occupied coastlines tightly coupled dynamical systems dominated by an array of feedbacks, thresholds, and emergent behaviors characteristic of complex systems [3-5]. While tools developed in nonlinear data analysis such as time series embedding for attractor reconstruction and forecasting [6,7] are becoming more prominent in the analysis of natural systems [8-10], they have yet to be used to analyze coupled human-natural systems. A primary difficulty in applying such data analysis techniques is the lack of data for variables that appropriately capture the long term dynamics of coupled human-natural systems. Furthermore, most embedding techniques tend to be focused on time series; aside from a few examples [11-13], they have not been adjusted for systems that evolve in both time and space. Here, we expand the attractor reconstruction and nonlinear forecasting technique for interspike intervals [14] to account for systems with integrate-and-fire dynamics that are linked in space, and apply this new technique to spatiotemporal data for beach nourishment. Because beach nourishment is often driven by a temporal integration of total net economic benefits for a given town, with a dependence on coastline position [2], we have collected the time between nourishment events in a range of towns that span a large portion of the U.S. East Coast as a data set representative of integrate-and-fire dynamics for a coupled human-coastal system. As an initial demonstration of the efficacy of applying attractor reconstruction to interpsike intervals in space and time, we apply the technique to generic integrate-and-fire data generated from a chaotic spatiotemporal map. We then show results illustrating the degree of nonlinear determinism in beach nourishment practices for different states along the U.S. East Coast as found from attractor reconstruction and forecasting of interspike intervals between nourishment episodes. We also explore using the attractor reconstruction of beach nourishment intervals to measure dynamical stability of the coupled human-coastal system. The implications of this analysis for large-scale management and prediction of human-occupied coastal systems will be discussed.

References

[1] G. Galilei, *E pur si muove !*, J. Planet. Sci. **1**, 007 (1633).

[1] Dean, R. G, *Beach nourishment*. World Scientific (2002).

[2] Smith, M. D., et al. *Beach nourishment as a dynamic capital accumulation problem*. Journal of Environmental Economics and Management **58** (2009).

[3] McNamara, D. E., & B. T. Werner. *Coupled barrier island–resort model: 1. Emergent instabilities induced by strong human-landscape interactions*. Journal of Geophysical Research: Earth Surface **113.F1** (2008).

[4] Werner, B. T., & D. E. McNamara. *Dynamics of coupled human-landscape systems*. Geomorphology **91.3** (2007).

[5] Lazarus, E. D., et al. *Emergent behavior in a coupled economic and coastline model for beach nourishment*. Nonlinear Processes in Geophysics **18(6)** (2011).

[6] Abarbanel, H. *Analysis of observed chaotic data*. Springer Science & Business Media (2012).

[7] Kantz, H. & Schreiber. T. *Nonlinear time series analysis*. Vol. 7. Cambridge university press (2004).

[8] Sugihara, G., et al. *Distinguishing Error from Chaos in Ecological Time Series*. Philosophical Transactions of the Royal Society B: Biological Sciences **330.1257** (1990).

[9] Sugihara, G., et al. *Nonlinear control of heart rate variability in human infants*. Proceedings of the National Academy of Sciences **93.6** (1996).

[10] Schreiber, T. *Interdisciplinary application of nonlinear time series methods*. Physics reports **308.1** (1999).

[11] Rubin, D. M. *Use of forecasting signatures to help distinguish periodicity, randomness, and chaos in ripples and other spatial patterns.* Chaos: An Interdisciplinary Journal of Nonlinear Science **2.4** (1992).

[12] Parlitz, U., & Merkwirth, C. *Prediction of spatiotemporal time series based on reconstructed local states*. Physical Review Letters **84.9** (2000).

[13] Grimes, D. J., et al. *Nonlinear forecasting of intertidal shoreface evolution*. Chaos: An Interdisciplinary Journal of Nonlinear Science **25.10** (2015).

[14] Sauer, T. *Interspike interval embedding of chaotic signals*. Chaos: An Interdisciplinary Journal of Nonlinear Science **5.1** (1995).

cmg2016 - - Thursday, June 9, 2016 - 11:45/12:30 (45min)

COASTLINE SHAPES : LARGE-SCALE MORPHODYNAMICS AND RESPONSES TO CLIMATES AND HUMANS

A.Brad Murray[1], A. Ashton[2], A. Barkwith[3], M. Ellis[3], K. Ells[4], M. Jones[5], M. Hurst[3], D. McNamara[4], L. Moore[5], C. Thomas[3], & J. Wood[1]

[1]*Nicholas School of the Environment ; Center for Nonlinear and Complex Systems, Duke University., Durham, NC, USA.*
[2]*Woods Hole Oceanographic Institution, Woods Hole, MA, USA.*
[3]*British Geological Survey, Keyworth and Edinborough, UK.*
[4]*Univeristy of North Carolina, Willmington, NC, USA.*
[5]*Univeristy of North Carolina, Chapel Hill, NC, USA.*

Key words Landscape evolution ; coastline morphodynamics ; climate change responses ; coupled human/natural system.

The flux toward shore of alongshore momentum, which drives alongshore sediment flux, varies with local coastline orientation, and with local degree of exposure to waves. Coastline shape therefore influences the alongshore patterns of alongshore sediment flux. Gradients in this flux, in turn, alter coastline shape—a morphodynamic feedback. Modeling studies show that such feedbacks lead ultimately to dynamic-equilibrium coastline shapes, including sandwaves, capes, and spits [1]; crenulate bays [2] and pocket beaches on rocky coastlines; and convex, spit-bounded coastlines. One conclusion arises in each of these studies: Coastline shape depends sensitively on the wave climate, defined as the angular distribution of wave influences on alongshore sediment transport.

Given this sensitive dependence, shifts in wave climate, as can be expected from shifts in storm statistics, will tend to alter coastline shape—involving decadal-scale changes in the location and intensity of coastal erosion zones. Such changes, likely related to changing influence from hurricane-generated waves, have been detected along undeveloped large-scale cuspate capes [3]. On a developed cape nearby, shoreline stabilization through beach nourishment has prevented an equivalent change in erosion rates. Combined observations and modelling indicate that the signal of wave climate change can be detected in the human component of the system, in the form of increased nourishment rates on one flank of the cape (Johnson et al., 2015). Finally, these recent works involved the implicit assumption that coastline response to changing forcing occurs in a quasi-equilibrium manner. However, new modeling shows that in some cases coastline responses can exhibit long-term memory and path dependence, complicating potential detection and forecasting of climate change signals in some human/coastline systems.

Because shoreline stabilization decisions, made in response to coastline changes, affect large-scale coastline change, the present and future evolution of developed coastlines results from coupled physical and human dynamics. Case studies from the Carolina and Virginia coasts, USA, provide examples.

References

[1] A. Ashton and A.B. Murray. High-angle wave instability and emergent shoreline shapes: 1. Modeling of capes, flying spits and sandwaves, J. Geophys. Res. 111, F04011, doi:10.1029/2005JF000422 (2006).
[2] M. Hurst, et al. *Exploring the sensitivities of crenulate bay shorelines to wave climates using a new vector-based one-line model*, J. Geophys. Res. Earth Surf., 120, 2586–2608, *doi:*10.1002/2015JF003704 (2015).
[3] L. Moore, et al. *Observed changes in hurricane-driven waves explain the dynamics of modern cuspate shorelines*, Geophys. Research Lett., 40, 5867–5871, doi:10.1002/2013GL057311 (2013).
[4] J. Johnson, et al. *Recent Shifts in Coastline Change and Shoreline Stabilization Linked to Storm Climate Change*, Earth Surface Processes and Landforms. DOI: 10.1002/esp.3650 (2015).

ON THE ORIGIN OF SELF-ORGANIZED KM-SCALE SANDY SHORELINE UNDULATIONS

A. Falqués[1], D. Idier[2], F. Ribas[1], M. Garcin[2], J. Rohmer[2]
[1]*Department of Physics, Universitat Politècnica de Catalunya, Barcelona, Catalonia, Spain*
[2] *BRGM, Orleans, France*

Key words coastal morphodynamic patterns, sediment transport, self-organization, ocean waves

Sandy shorelines often exhibit undulations in planview with an alongshore wavelength in the range $1-15$ km that are linked to similar undulations in the bathymetry and that are also known as shoreline sand waves. *Ashton et al.* (2001) showed that they can emerge from self-organization through a positive morphodynamic feedback between the morphology and the wave field if the wave incidence angle (between wave fronts and shoreline) is large enough. We here review the physics behind the feedback mechanisms providing new insight into it and we test the self-organization hypothesis against global data analysis.

Waves propagating onshore with an angle experience refraction and shoaling and eventually break. They drive an alongshore current carrying sediments and the sediment flux is an increasing function of wave height and wave angle at breaking relative to the local shoreline. The undulating bathymetry causes alongshore gradients in wave energy and wave angle and thereby in sediment flux. If sediment flux converges near the undulation crest, sediment deposition occurs there so that the undulation grows. We identify four feedback sources: 1) more wave refraction at the downdrift flank of the sand wave (wave-angle mechanism), 2) more refractive wave energy spreading at the downdrift flank (wave-energy mechanism), 3) changes in relative wave angle due to changes in shoreline orientation (undulation shape mechanism) and 4) wave energy focusing by the capes (wave-focusing mechanism). The undulation shape and the wave-focusing mechanisms provide a negative feedback mechanism while the wave-angle wave-energy mechanism mechanisms induces positive feedback. According to a linear stability model (*Falqués and Calvete*, 2005), which mechanism is dominant and whether sand waves form or not depend on wave characteristics, on the cross-shore bathymetric profile and on the closure depth, D_c (maximum offshore reach of the bathymetric undulations). A total length of 8800 km of sandy (also gravel) coastal stretches has been analyzed to find shoreline undulations in the range $1-15$ km wavelength and to test model results. We find a 61% of shoreline stretches exhibiting undulations. Data analysis also reveals that undulations are more frequent for steep surf zone slopes, large incidence angles, large D_c and shallow shorefaces. Although large angles tend to favour sand wave development, both data and modeling show there is not a single critical angle θ_c above which shoreline undulations develop. The parameter having the largest influence on θ_c is the mean surf zone slope. The present work tends to confirm that the four feedback mechanisms described above hold in nature and govern shoreline undulation dynamics at such length scales.

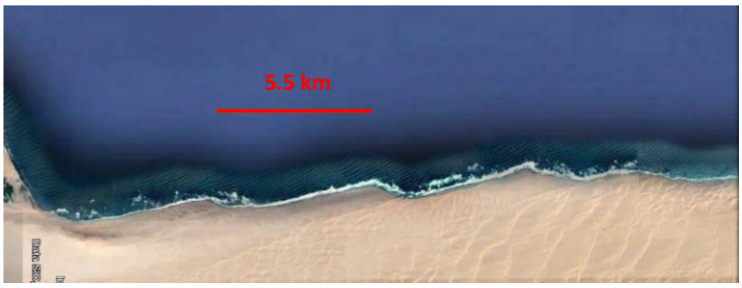

Figure 1. km-scale shoreline sand waves at Namibia coast (from Google Earth).

References

Ashton, A., A. B. Murray, and O. Arnault (2001), Formation of coastline features by large-scale instabilities induced by high-angle waves, *Nature*, *414*, 296–300.

Falqués, A., and D. Calvete (2005), Large scale dynamics of sandy coastlines. Diffusivity and instability, *J. Geophys. Res.*, *110*(C03007), doi:10.1029/2004JC002587.

cmg2016 - - Thursday, June 9, 2016 - 11:45/12:30 (45min)

SCALE SELECTION IN COLUMNAR JOINTING: INSIGHTS FROM STEARIC ACID EXPERIMENTS AND NUMERICAL SIMULATIONS

A. Christensen[1], C. Raufaste[2], M. Misztal[1], F. Celestini[2], M. Guidi[1], C. Ellegaard[1] & J. Mathiesen[1]
[1]*The Niels Bohr Institute, University of Copenhagen, Denmark*
[2]*CNRS, Université Nice Sophia Antipolis, France*

Key words Columnar jointing. Pattern formation. Fracture. Scale selection. Geomorphology. Model systems.

Many natural fracture systems are characterized by a single length scale, which is the distance between neighboring fractures. Examples are mudcracks and columnar joints. In columnar jointing the origin of this scale has been a long-standing issue. Here we show that the diameter of columnar joints is a non-trivial function of the elastic and thermal parameters of the system. From a model of fracture propagation in a thermally contracting elastic material, we determine the shape of this function analytically and show that it is in agreement with numerical simulations, field data and experiments on a new model system for columnar jointing: stearic acid. As opposed to the widely studied corn starch model system, columnar jointing in stearic acid is driven by thermal contraction and not by dessication. If better experimental control of the temperature evolution is gained, we suggest that the stearic acid experiments can be used as a model system for igneous columnar jointing in order to gain insight into the effect of an initial surface crack pattern, entablature formation and scale selection.

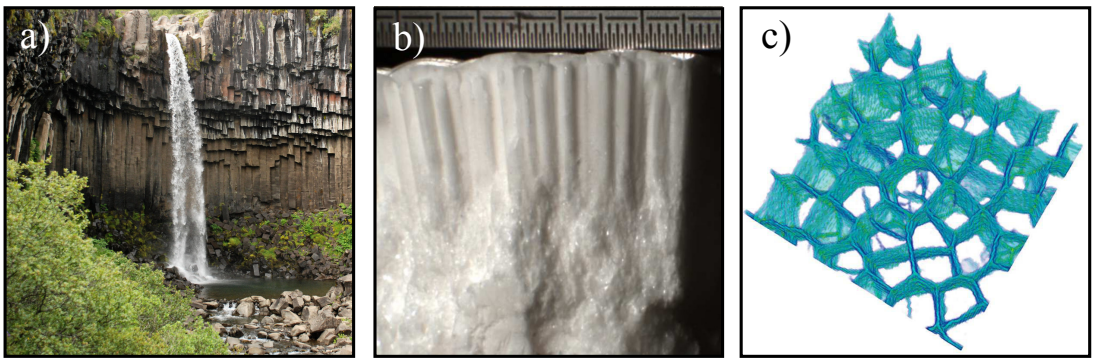

Figure 1. *a)* Exposed columnar joint formation at Svartifoss, Iceland. *b)* Columnar joint formation in stearic acid. The columnar joints are formed when the initally hot and fluid stearic acid cools and solidifies. *c)* Discrete element simulation of columnar jointing.

cmg2016 - - Thursday, June 9, 2016 - 11:45/12:30 (45min)

INTERNAL STRUCTURE OF MOBILE BARCHAN SAND DUNES

N.M. Vriend[1], M.I. Arran[1], M.Y. Louge[2], A.G. Hay[3] & A. Valance[4]
[1]*University of Cambridge, Department of Applied Mathematics and Theoretical Physics (DAMTP), Cambridge, United Kingdom*
[2]*Cornell University, Sibley School of Mechanical and Aerospace Engineering, Ithaca, United States of America*
[3]*Cornell University, Microbiology, Ithaca, United States of America*
[4]*Université de Rennes 1, Institut de Physique de Rennes, CNRS UMR 6251, Rennes, France*

Key words Internal dune structure, desert dune migration, granular avalanches, segregation.

In this work, we visualize the internal structure of mobile barchan desert dunes at the avalanche scale. We reveal an intriguing history of dune building using a novel combination of local sand sampling and advanced geophysical techniques resulting in high resolution measurements of individual avalanche events.
We present scientific data on the structure obtained from two mobile barchan dunes during recent desert field campaigns (2014, 2015) in Qatar. The area at 25.01°N, 51.34°E in the Al Wakrah municipality in the Umm Said desert near Doha, Qatar, has been equipped with a weather station and has been regularly visited by a multidisciplinary research team in recent years (e.g. [1]). The two barchan dunes have distinct dimensions, the larger dune rises to $h \sim 28 \pm 2m$ while the smaller dune reaches $h \sim 5.0 \pm 0.5m$; mass conservation [2] ensures the dunes move at different migration speeds, $V \sim 5.1 \pm 0.3m$ versus $V \sim 18.4 \pm 0.1m$ respectively.
Due to progressive rebuilding and erosional and depositional processes, these marching barchan dunes are reworked every few years and a characteristic zebra-pattern, orientated parallel to the slipface, is apparent at regular intervals as illustrated in figure 1a.

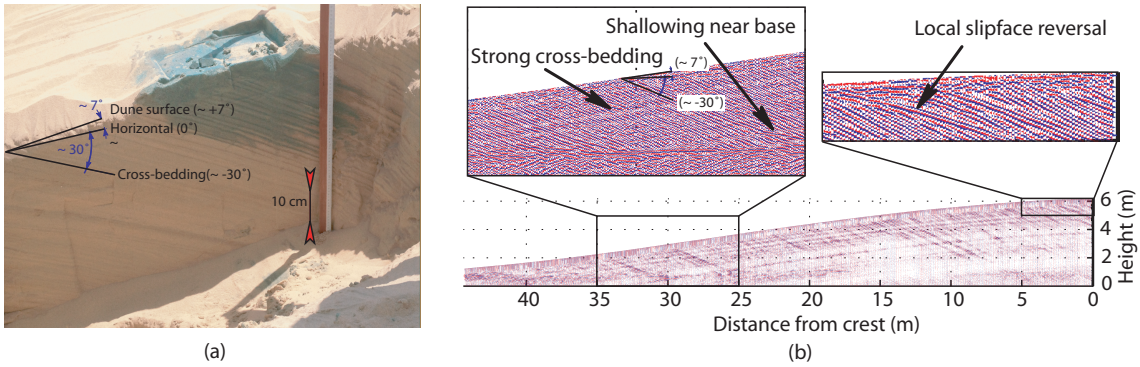

Figure 1. (a) Characteristic zebra-pattern on a midline cross-section of a mobile barchan dune, (b) typical continuous Ground Penetrating Radar profile across the midline.

The dune stratigraphy, exposed by a few sandpits, reveals regular cross-bedding inclined at the angle of repose ($\sim 30°$). By applying high-frequency (1200 MHz) ground penetrating radar (GPR) transects across the midline, as illustrated in figure 1b, we map the continuous evolution of this cross-bedding deep within the dune. The GPR also reveals a slope reduction of the slipface near the base of the dune; evidence of irregular wind reversals; and the presence of a harder aeolian cap around the crest and extending to the brink. The data is supplemented with granulometry from layers stabilized by dyed water injection and uncovered by excavating vertical walls perpendicular to old buried avalanches. We attribute visible differences in water penetration between adjacent layers to fine particle segregation processes in granular avalanches.
This work was made possible by the support of NPRP grant 6-059-2-023 from the Qatar National Research Fund.

References

[1] Louge, M. Y., A. Valance, A. Ould el-Moctar, J. Xu, A. G. Hay, and R. Richer, *Temperature and humidity within a mobile barchan sand dune, implications for microbial survival*, J. Geophys. Res. **118**, doi:10.1002/2013JF002839 (2013).
[2] Bagnold, R. A., *The Physics of Blown Sand and Desert Dunes*, Methuen, London (1941).

cmg2016 - - Thursday, June 9, 2016 - 11:45/12:30 (45min)

FROM VISCOUS FINGERS TO WORMHOLES - INTERACTIONS BETWEEN EMERGENT FINGERS IN UNSTABLE GROWTH

A. Budek[1,2], K. Kwiatkowski [2] & P. Szymczak[2]
[1]*Institute of Geophysics, Polish Academy of Sciences, Poland*
[2]*Institute of Theoretical Physics, University of Warsaw, Poland*

Dissolution of porous and fractured rock can lead to instabilities, where long finger-like channels or "wormholes" are spontaneously formed, focusing the majority of the flow. Formation of those structures leads to a significant increase in permeability of the system, and is thus important in many engineering applications, e.g. in acidization during oil and gas recovery stimulation. In this communication, we analyse this process using two different numerical models (a network model and a Darcy scale one). We show that wormhole patterns depend strongly on the amount of soluble material in the system, as quantified by the permeability contrast κ between the dissolved and undissolved medium. For small and intermediate values of κ, a large number of relatively thin and strongly interacting channels are formed. The longer channels attract shorter ones, with loops being formed as a result. However, for large values of κ the pattern gets sparse with individual wormholes repelling each other.

Interestingly, a similar succession of patterns can be observed in viscous fingering simulations, with fingers growing in a rectangular network of channels. In such a system, anisotropy of the network promotes the growth of long and thin fingers which behave similarly to wormholes. The attraction rate between growing fingers depends strongly on the viscosity ratio and the distance between the fingers. To explain this behaviour, we have created a simple analytical model of interacting fingers, allowing us to quantify their mutual interaction as a function of finger lengths, distances between them and – most importantly – relative permeabilities. The theoretical predictions are in a good agreement with simulation data for both dissolution and viscous fingering processes.

cmg2016 - - Thursday, June 9, 2016 - 11:45/12:30 (45min)

A graph-theoretic approach to infer process from patterns in deltaic systems.

Alejandro Tejedor[1], Anthony Longjas[1], Ilya Zaliapin[2], and Efi Foufoula-Georgiou[1]

[1]*Saint Anthony Falls Laboratory, University of Minnesota, Minneapolis, USA*
[2]*Department of Mathematics and Statistics, University of Nevada, Reno, USA*

.

Key words Deltas, Graph Theory, Complexity, Galloway.

River deltas are drained by channel networks that self-organize to a variety of stunning and complex patterns. Although these patterns are expected to encode to a large degree the signature of their forming processes, e.g., climate, tide and wave influence, sediment cohesion, vegetation, etc., no formal framework exists to test this hypothesis and quantitatively relate process and form. Here we present a quantitative framework based on spectral graph theory within which a systematic study of the topology and transport dynamics of river deltas can be performed. Specifically, this framework which conceptualizes a delta channel network as a directed graph where channels are modeled by edges and junctions as vertices (Figure 1), allows us, from algebraic computations, to depict structural features of the delta system such as sub-networks (from apex to shoreline outlets), and contributing and nourishing areas within any point in the network. Using this framework we also introduce metrics of topologic and dynamic complexity and define a multidimensional complexity space where each delta projects. By analyzing field, numerical and experimental deltas we present encouraging results towards a quantitative classification of deltas to replace the qualitative approach still in use today [*Galloway*, 1975; *Orton and Reading*, 1993]. We also show that the framework offers the potential to quantify the heterogeneity of spatial patterns within a given delta and provide a formalism for interrogating system vulnerability in response to perturbations. Using simulated deltas, for which the explicit spatial-temporal structure is available over the full history of the delta, the question of what can be learned about the past from a frozen spatial image of a delta is also addressed.

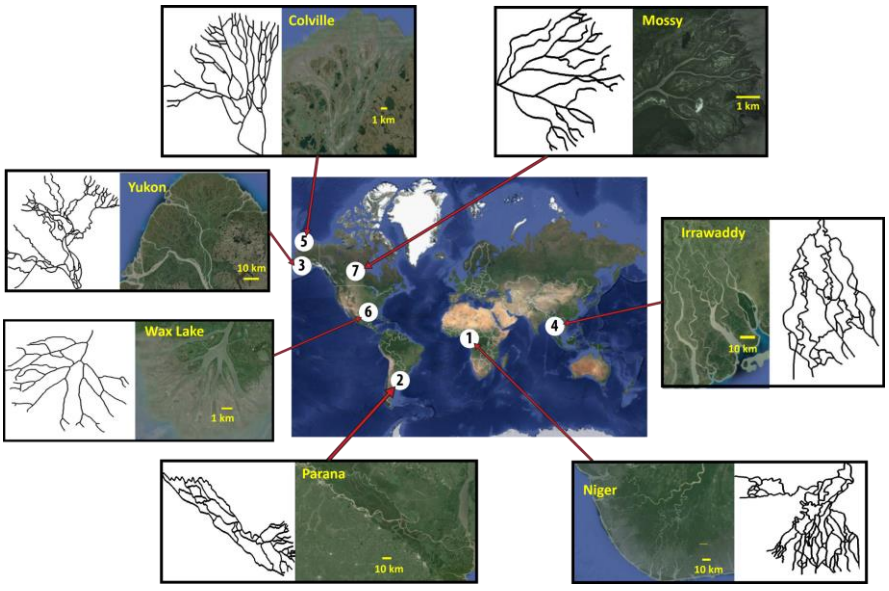

Figure 1. Seven deltas and their corresponding channel networks numbered according to size (largest to smallest area)

Gravitational flows

cmg2016 - - Thursday, June 9, 2016 - 15:30/15:45 (15min)

A TWO-PHASE SOLID/FLUID MODEL FOR DENSE GRANULAR FLOWS INCLUDING DILATANCY EFFECTS

A. Mangeney[1,2], F. Bouchut[3], E. D. Fernandez-Nieto[4], E. Koné[1], G. Narbona-Reina[4]
[1]*Institut de Physique du Globe & Université Paris-Diderot, Sorbonne Paris Cité, France*
[2]*ANGE Team, CEREMA, Inria, Lab. J.-L. Lions, CNRS, France*
[3]*CNRS & Université Paris-Est, France*
[4]*University of Sevilla, Applied Mathematics, Sevilla, Spain*

Key words debris flows, two-phase granular flows, dilatancy

Describing grain/fluid interaction in debris flows models is still an open and challenging issue with key impact on hazard assessment [1, 2]. We present here a two-phase two-thin-layer model for fluidized debris flows that takes into account dilatancy effects. It describes the velocity of both the solid and the fluid phases, the compression/dilatation of the granular media and its interaction with the pore fluid pressure [3].

The model is derived from a 3D two-phase model proposed by Jackson [4] based on the 4 equations of mass and momentum conservation within the two phases. This system has 5 unknowns: the solid and fluid velocities, the solid and fluid pressures and the solid volume fraction. As a result, an additional equation inside the mixture is necessary to close the system. Surprisingly, this issue is inadequately accounted for in the models that have been developed on the basis of the work of Jackson [5]. In particular, Pitman and Le [6] replaced this closure simply by imposing an extra boundary condition at the surface of the flow. When making a shallow expansion, this condition can be considered as a closure condition. However, the corresponding model cannot account for a dissipative energy balance.

We propose here an approach to correctly deal with the thermodynamics of the model of Jackson by closing the mixture equations by a weak compressibility relation following Roux and Radjai [7]. This relation implies that the occurrence of dilation or contraction of the granular material in the model depends on whether the solid volume fraction is respectively higher or lower than a critical value. When dilation occurs, the fluid is sucked into the granular material, the pore pressure decreases and the friction force on the granular phase increases. On the contrary, in the case of contraction, the fluid is expelled from the mixture, the pore pressure increases and the friction force diminishes. To account for this transfer of fluid into and out of the mixture, a two-layer model is proposed with a fluid layer on top of the two-phase mixture layer. Mass and momentum conservation are satisfied for the two phases, and mass and momentum are transferred between the two layers. A thin-layer approximation is used to derive average equations. Special attention is paid to the drag friction terms that are responsible for the transfer of momentum between the two phases and for the appearance of an excess pore pressure with respect to the hydrostatic pressure.

We present several numerical tests of two-phase granular flows over sloping topography that are compared to the results of the model proposed by [6]. In particular, we quantify the role of the fluid and compression/dilatation processes on granular flow velocity field and runout distance.

References

[1] R.M. Iverson, M. Logan, R.G. LaHusen, M. Berti, *The perfect debris flow? Aggregated results from 28 large-scale experiments*, J. Geophys. Res. **115**, F03005 (2010).
[2] R. Delannay, A. Valance, A. Mangeney, O. Roche, P. Richard, *Granular and particle-laden flows: from laboratory experiments to field observations*, J. Phys. D: Appl. Phys., submitted (2016).
[3] F. Bouchut, E. D. Fernández-Nieto, A. Mangeney, G. Narbona-Reina, *A two-phase two-layer model for fluidized granular flows with dilatancy effects*, J. Fluid Mech., submitted (2016).
[4] R. Jackson, *The Dynamics of Fluidized Particles*, Cambridges Monographs on Mechanics (2000).
[5] F. Bouchut, E.D. Fernández-Nieto, A. Mangeney, G. Narbona-Reina, *A two-phase shallow debris flow model with energy balance*, ESAIM: Math. Modelling Num. Anal., **49**, 101-140 (2015).
[6] E.B. Pitman, L. Le, *A two-fluid model for avalanche and debris flows*, Phil.Trans. R. Soc. A, **363**, 1573-1601 (2005).
[7] S. Roux, F. Radjai, *Texture-dependent rigid plastic behaviour*, Proceedings: Physics of Dry Granular Media, September 1997. (eds. H. J. Herrmann et al.). Kluwer. Cargése, France, 305-311 (1998).

cmg2016 - - Thursday, June 9, 2016 - 15:45/16:00 (15min)

Multi-Stage Release Gravity Currents

V.L. Ho[1], R.M. Dorrell[1], G.M. Keevil[1], A.D. Burns[2], W.D. McCaffrey[1].
[1] *School of Earth and Environment, University of Leeds, Leeds UK.*
[2] *School of Chemical and Process Engineering, University of Leeds, Leeds UK.*

Key words Gravity Currents, Intrusions.

Recent research, postulating that seafloor density driven flow (turbidity current) deposits may provide a long-term geological record of seismic event frequency and aftershock history [Goldfinger, 2012], has motivated a series of novel experiments looking at the dynamics of multi-stage release gravity current experiments. The experiments have investigated the effect of multi-stage delays in the release of a denser than ambient saline fluid, generating pulsed flows to mimic sequential seafloor slope failure. To relate the experimental flow to real-world scales, the effect of key dimensionless parameters have been considered, including: initial release geometries; dimensionless delay times; ratios of motive to viscous forces. The experiments show that (turbulent) multi-stage release gravity currents merge, i.e. the front position of the second release overtakes that of the first (Figure 1a). That the gravity currents merge is of significant interest in determining how far from source pulsed flow signals may persist and where paleoseismic reconstruction from turbidity current deposits may be conducted.

Density driven flows are subject to frictional drag at their upper and lower boundary, generating a flow with an internal velocity maximum. This vertical variation in velocity means that flow near the centre of the flow is advected towards the head of the gravity current, implying that closely spaced multi-stage flows merge. However, the merging of all multi-stage flows is significantly enhanced by the dynamics of primary and secondary flow release. The initial collapse of primary generates significant entrainment of ambient fluid; this generates a vertically stratified flow whose density tends to that of the surrounding ambient. The secondary flow then forms an intrusion at a neutrally buoyant level within the primary flow, above the flow bed and beneath ambient fluid interface (Figure 1a). As the secondary flow is removed from frictional boundaries it experiences less drag and thus travels faster than the primary flow, enabling flow merging.

Interestingly, it is observed that as the delay time flows is increased, the front position of the primary flow begins to lag behind that of a single stage flow of equivalent volume and density (Figure 1b). This may be explained, as the initial volume of release from the multi-stage flow is smaller than the single stage flow, implying the flow exits the slumping phase of gravity current propagation sooner. Counter-intuitively however, it is later observed that multi-stage flows travel faster than a comparable single stage flow (Figure 1b). This is attributed to the protection that secondary flow intrusions are afforded by reduced basal and interface shear. Thus, in the multi-stage flows the intrusion suffers reduced turbulent mixing and ambient fluid entrainment. This enables multi-stage flows to transport higher solute concentrations, with associated greater velocities, over longer distances in comparison to otherwise equivalent single stage gravity currents.

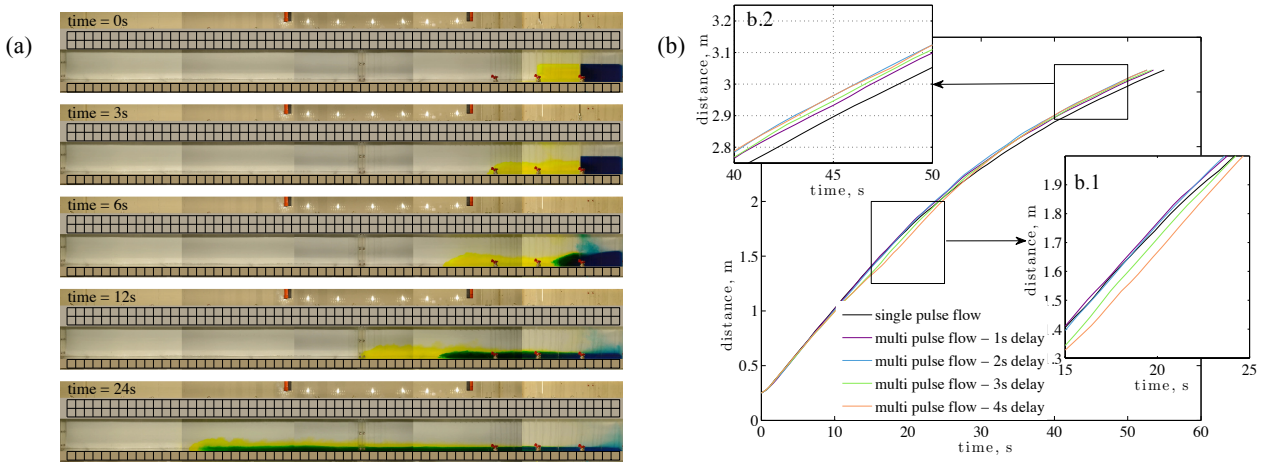

Figure 1. Evolution of a multi-stage gravity current (a), showing: initial flow division (t=0s); collapse of the primary (t=3s) and secondary (t=6s) flow releases; intrusion of the secondary release within the primary flow (t=12s); merging of primary and secondary flows Evolution of the front position (primary flow release) in space and time, as a function of delay time between primary and secondary release. Highlighted is the increasing initial lag of flow, compared with single release flow, with increasing delay time (insert b.1) and the long term increased velocity of the multi-release flows in comparison to the single release flow (insert b.2).

References

[1] Goldfinger, C. (2011). Submarine paleoseismology based on turbidite records. *Annual Review of Marine Science*, 3, 35-66.

cmg2016 - - Thursday, June 9, 2016 - 15:00/15:30 (30min)

DEBRIS FLOWS: MECHANISMS FOR DRY SNOUT FORMATION

B. Turnbull
Faculty of Engineering, University of Nottingham, Nottingham, GB

Key words Debris flows and debris avalanches are complex, gravity-driven currents of rock, water and sediments that can be highly mobile. This combination of component materials leads to a rich morphology and unusual dynamics, exhibiting features of both granular materials and viscous gravity currents, even at a single instance within a single flow. For example, a dry 'snout' with collisional granular behaviour often forms ahead of a wet, viscous tail. This works explores the range of mechanisms that in theory could control the formation and extent of the dry snout, and to understand when each can play a part in a debris flow.

Fig. 1 i shows an experimental model of a debris flow, comprising a marble-water mixture flowing down a rough incline. This flow is unsteady and intermittent, which leads to difficulty in its characterisation. To separate the unsteadiness of the mean flow from the rapid fluctuations images were captured at a high frame rate, such that an ensemble average over 14 frames (≈0.02 s) reliably provided mean flow characteristics. Deviation from these local ensemble averages effectively discriminates between plug-like regions with low intermittency and collisional regions with high intermittency. Fig. 1 ii shows these regions in light and dark grey respectively, together with local ensemble averaged velocity profiles through the flow depth at two positions for mono- and polydisperse flows of particles.

This method allows us to explore how a dry granular snout can form from and co-exist with a plug-like viscous flow. One of the most striking features of the Fig. 1 ii velocity maps, is that this dilute, collisional regime, where the stresses are all supported by binary particle collisions occurs even for monodisperse flows so it does not require segregation to occur. This is somewhat surprising since the formation of a dry snout is usually attributed to particle size segregation and the role of fine sediments [2]. The formation of snout architecture in monodisperse flows with relatively high particle Reynold?s numbers, suggests that there are alternative fluid-particle processes at play.

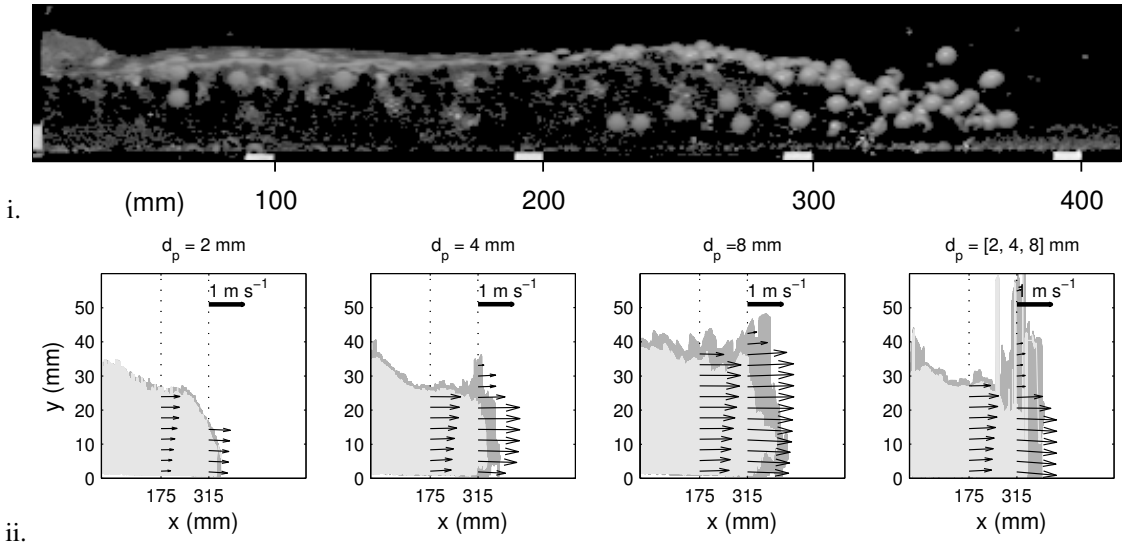

Figure 1. i. Side view of 1 litre glass bead-water mixture, with solid volume fraction 0.4, released from behind a lock gate to flow down a 27° chute, $\mathrm{Re_p} \approx 10^4$. The beads have diameters 8 mm (coloured white), 4 mm (coloured black) and 2 mm (colourless), and the chute has 8 mm diameter beads fixed to the surface to generate roughness. ii, Debris flows of $d_p = [2, 4, 8]$ mm diameter glass beads and a mixture of those sizes in water over a rough surface formed of 4 mm diameter beads. The flow front is at 9 times the length of the release volume down the slope. Quivers show the magnitudes of the velocities at 10% and 50% of the flow length from the head averaged over 14 video frames. Pale grey indicates regions with low standard deviation from this mean, and dark grey regions are those with high standard deviations from the mean.[1]

References

[1] B. Turnbull, E. T. Bowman & J. N. McElwaine, *Debris flows: Experiments and modelling*, Comptes Rendus Phisique **16**, 86–96 (2015).
[2] J. M. N. T. Gray & A. R. Thornton. *A theory for particle size segregation in shallow granular free-surface flows*, Proceedings of the Royal Society of London A **461**, 2057 (2005).

cmg2016 - - Thursday, June 9, 2016 - 16:00/16:15 (15min)

ON THE FRONT OF A GRANULAR FLOW DOWN A ROUGH INCLINE

G. Saingier[1,2], S. Deboeuf[1] & P.-Y. Lagrée[1]
[1]*Institut d'Alembert (UPMC/CNRS UMR 7190), Paris, France*
[2]*Surface du Verre et Interface (Saint-Gobain/CNRS UMR 125), Aubervilliers, France*

Key words granular flow; inclined plane; front; morphology; dynamics; frictional rheology $\mu(I)$; St-Venant, shallow water, depth-averaged equations; velocity profile; Bagnold-like profile

Granular material flowing on complex topographies are ubiquitous in industrial and geophysical situations: civil engineering, food-processing industry, rock avalanches, pyroclastic flows, ... Even simpler controlled granular flows are difficult to understand and predict. To date, the frictional rheology $\mu(I)$ allows unifying different configurations of granular flows: plane shear flow, inclined plane flow, ... [1, 2, 3]. However, the rheology $\mu(I)$ does not succeed in describing some transient flows or some phenomenologies: creep flow, deposit height, ... Is it attributable to the rheology, to non-local effects, to the choice of the function $\mu(I)$, ...? Also, it is not obvious to solve the general equations of movements for a granular flow or to impose the right boundary conditions in order to predict the response of a granular fluid of $\mu(I)$ rheology to a complex sollicitation. To study these questions, our general approach is to compare experimental results, numerical simulations and analytical solutions when possible. Here, we study the small-scale model of a granular layer flowing on a rough incline and we focus on the front of the flow by using both experimental and analytical computational approaches [4]. Our experimental data of front profiles are quantitatively compared with analytical solutions obtained from some generalization of mass and momentum equations [5, 6, 7] incorporating the frictional rheology $\mu(I)$. These equations are depth-averaged equations (shallow water or St-Venant equations), usually used for classical liquids, snow avalanches or granular flows. However, some assumptions made to write these equations for granular flows still need to be clarified. Unlike previous studies where a plug flow is assumed in the depth, we consider the case of a general vertical velocity profile by introducing a shape factor to determine the solution of the front profile of a steady flow on an incline. Such a way, we put in evidence an effect on the front profile of inertia through the Froude number and the shape factor. The analytical predictions are compared with previous experimental results [6] and with our new experimental data obtained at higher Froude numbers. A good agreement between theory and experiments is found when assuming a Bagnold-like velocity profile. However some discrepancies appear at the head of the front where the height vanishes, suggesting that here the velocity profile is different.

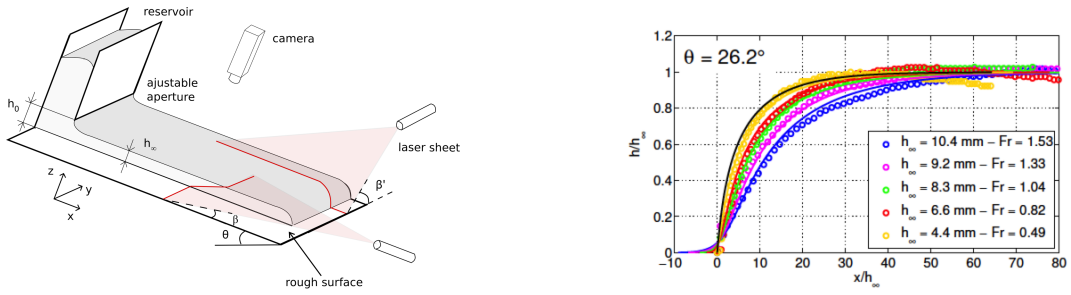

Figure 1. Inclined plane. Superposition of front profiles of granular flows from experiments and analytical solutions.

References

[1] GDR MiDi, *On dense granular flows*, Eur. Phys. J. E., **14**, 341-365 (2004).
[2] F. da Cruz, S. Emam, M. Prochnow, J.-N. Roux & F. Chevoir, *Rheophysics of dense granular flows: discrete simulation of plane shear flows*, Phys. Rev. E, **72**, 021309 (2005).
[3] P. Jop, Y. Forterre & O. Pouliquen, *A constitutive relation for dense granular flows*, Nature, **44**, 727-730 (2006).
[4] G. Saingier, S. Deboeuf & P.-Y. Lagrée, *On the front shape of an inertial granular flow down a rough incline*, arxiv (2016).
[5] S. B. Savage & K. Hutter, *The motion of a finite mass of granulat material down a rough incline*, J. Fluid Mech., **199**, 177-215 (1989).
[6] O. Pouliquen, *On the shape of granular fronts down rough inclined planes*, Phys. Fluids, **11**, 7, 1956-1958 (1999).
[7] J. M. N. T. Gray & C. Ancey, *Segregation, recirculation and deposition of coarse particles near two-dimensional avalanche fronts*, J. Fluid Mech., **629**, 387-423 (2009).

cmg2016 - - Thursday, June 9, 2016 - 11:45/12:30 (45min)

A HYDROSTATIC MULTILAYER MODEL WITH THE $\mu(I)$-RHEOLOGY FOR DRY GRANULAR FLOWS

E.D. Fernández-Nieto[1], J. Garres-Díaz[2], A. Mangeney[3] & G. Narbona-Reina[1]
[1]*Dpto. Matemática Aplicada I. ETS Arquitectura - Universidad de Sevilla, Seville, Spain*
[2]*IMUS & Dpto. Matemática Aplicada I. Universidad de Sevilla, Seville, Spain*
[3]*Institut de Physique du Globe de Paris, Equipe Sismologie, University Paris-Diderot, Paris, France*

Key words Multilayer approach, dry granular flows, $\mu(I)$-rheology, shallow model, splitting finite volume method.

Granular flows have been widely studied in recent years because of their importance in industrial processes and geophysical flows such as avalanches, debris or rock avalanches, landslides, etc. The behaviour of real geophysical flows is very complex due to topography effects, heterogeneity of the material involved, etc. Hence it becomes a major challenge to develop a mathematical model able to reproduce correctly the dynamic of such flows. One of the issues recently analyzed by some authors (see [7, 3]) on granular collapse is the different behaviour of the runout distance in the presence or not of an erodible bed. They showed experimentally a significant increase of the runout distance and flow duration with increasing thickness of the erodible bed. The question remains as to whether this behaviour can be reproduced by granular flow models.

Due to the high computational cost of solving the full 3D Navier-Stokes equations, granular flows have often been simulated using depth-averaged shallow models. But, as it is well known, with this kind of approximation one lose the vertical nature of these flows. Indeed, the introduction of the multilayer models is aimed at resolving this lack inherent to the simple one-layer shallow models, because they take into account the change of the velocity field in the normal direction to the topography.

On the other hand, the rheology of granular flows has been usually described by viscoplastic laws and namely by the so-called $\mu(I)$ rheology [1, 4, 6]. The $\mu(I)$-rheology, introduced by Jop et al. [5], considers a Drucker-Prager plasticity criterion and the shear stress tensor is assumed proportional to the normal one, where the variable coefficient $\mu(I)$ depends on the inertial number I.

Following [2], in this work we present a multilayer approach of the $\mu(I)$-rheology model with hydrostatic pressure. The multilayer approach allows us to recover the vertical profile of the velocity for these flows, and to improve the approximation of the vertical diffusion term in the model.

Several comparisons of the numerical results with different Bagnold flows and with laboratory data will be presented. By comparing with the laboratory data for a granular collapse experiment (see [7]) we show that our model well reproduces the influence of the erodible bed on the flow dynamics and deposit.

References

[1] J. Chauchat and M. Médale. A three-dimensional numerical model for dense granular flows based on the μ(I)-rheology. *Journal of Computational Physics*, 256(0):696 – 712, 2014.
[2] E.D. Fernández-Nieto, E.H. Koné, and T. Chacón Rebollo. A Multilayer Method for the Hydrostatic Navier-Stokes Equations: A Particular Weak Solution. *Journal of Scientific Computing*, 60(2):408–437, 2014.
[3] M. Farin, A. Mangeney, O. Roche. *Fundamental changes of granular flow dynamics, deposition, and erosion processes at high slope angles: Insights from laboratory experiments*. Journal of Geophysical Research: Earth Surface, **119(3)**, 504–532, (2014).
[4] J. M. N. T. Gray and A. N. Edwards. A depth-averaged μ(I)-rheology for shallow granular free-surface flows. *Journal of Fluid Mechanics*, 755:503–534, 2014.
[5] P. Jop, Y. Forterre, and O. Pouliquen. A constitutive law for dense granular flows. *Nature*, 441(7094):727–730, 2006.
[6] P.-Y. Lagrée, L. Staron, and S. Popinet. The granular column collapse as a continuum: validity of a two-dimensional Navier-Stokes with a μ(I)-rheology. *Journal of Fluid Mechanics*, 686:378–408, 2011.
[7] A. Mangeney, O. Roche, O. Hungr, N. Mangold, G. Faccanoni and A. Lucas. Erosion and mobility in granular collapse over sloping beds. *Journal of Geophysical Research: Earth Surface (2003–2012)*, 115(F3), 2010.

cmg2016 - - Thursday, June 9, 2016 - 11:45/12:30 (45min)

USING SEISMIC DATA AND MODELLING TO BETTER CONSTRAIN THE DYNAMICS OF ROCKFALLS IN THE DOLOMIEU CRATER, PITON DE LA FOURNAISE, LA REUNION

V. Durand[1], P. Le Bouteiller[2], A. Mangeney[1], E.H Kone[1], A. Protin[1], P. Kowalski[3], F. Lauret[3], C. Brunet[3], K. Wegner[4], F. Haas[4] & A. Delorme[1]

[1]*Institut de Physique du Globe, Paris, France*

[2]*IFP Energies Nouvelles, Paris, France*

[3]*Observatoire Volcanologique du Piton de la Fournaise, La Reunion*

[4]*Katholische Universitat Eichstatt-Ingolstadt, Ingolstadt, Germany*

Key words Rockfalls, numerical simulations, seismic signals

The seismic and photogrammetric networks of the Piton de la Fournaise volcano (La Reunion Island), maintained by the OVPF, are well appropriate for the study of seismic signals generated by rockfalls occurring in the Dolomieu crater. In particular it makes it possible to relate the rockfall dynamics recorded by the cameras with the time change of the seismic energy [1, 2]. Furthermore, the availability of the videos enables us to better constrain our numerical models by fixing the starting location and the path taken by the rockfalls. The aims of this study are to better extract the information contained in the seismic signals, and to better constrain the physical characteristics of rockfalls. Simulations of rockfalls on 2D and 3D topographies obtained by laser-scanner survey of the crater are performed using the thin layer depth-averaged code SHALTOP developed within a collaboration between IPGP and LAMA, Marne-la-Vallée [3]. On one hand, a detailed comparison of the simulated dynamics with the movies of several rockfalls (Fig. 1) makes it possible to identify the different phases of the flow (initial collapse, impacts and interaction with the topography, stopping phase) and to relate them to the observed seismic signal. On the other hand, comparing the work rate, potential and kinematic energy changes calculated using the numerical models of rockfalls with the generated seismic power during the rockfall propagation down the slope of the Dolomieu crater (Fig. 1) gives information on physical parameters. In particular we test the effect of the friction law (constant friction and volume or velocity weakening friction) on the simulated force and work rate to investigate if the signature of the friction law may be identified on seismic records.

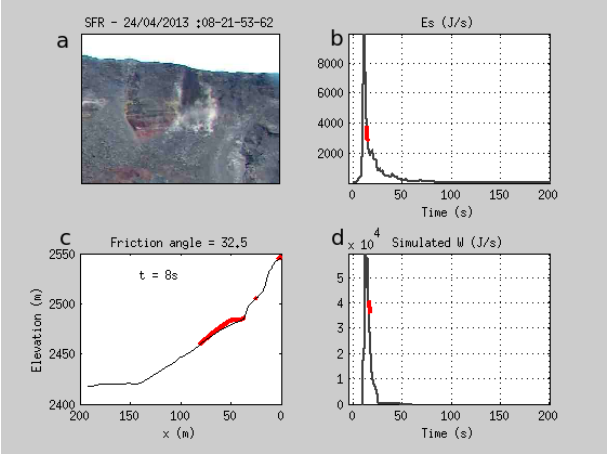

Figure 1. Comparison between the video, the seismic energy and the numerical simulation results. a) Picture of a rockfall occurring inside the Dolomieu crater. b) Observed seismic energy. c) Position of granular mass at time t=8s of the simulation. d) Computed power loss from the simulation.

References

[1] Hibert, C., A. Mangeney, G. Grandjean, and N. M. Shapiro, *Slope instabilities in Dolomieu crater, Reunion Island: From seismic signals to rockfall characteristics*, J. Geophys. Res. **116**, F04032 (2011).

[2] Hibert, C., A. Mangeney, G. Grandjean, C. Baillard, D. Rivet, N. M. Shapiro, C. Satriano, A. Maggi, P. Boissier, V. Ferrazzini, and W. Crawford, *Automated identification, location, and volume estimation of rockfalls at Piton de la Fournaise volcano*, J. Geophys. Res. Earth Surf. **119** (2014).

[3] Mangeney, A., F. Bouchut, N. Thomas, J.P. Vilotte, and M.O. Bristeau, *Numerical modeling of self-channeling granular flows and of their levee-channel deposits*, J. Geophys. Res. **112**, F02017 (2007).

cmg2016 - - Thursday, June 9, 2016 - 11:45/12:30 (45min)

Anthropogenic turbidity flows in La Fonera Submarine Canyon

M. Payo-Payo[1,2], R. S. Jacinto[2], G. Lastras[3], M. Rabineau[1], P. Puig[4], J. Martín[4,5] & M. Canals[3]
[1] *IUEM, Université Bretagne Occidentale, Plouzané, France*
[2] *IFREMER, Plouzané, France.*
[3] *CRG Marine Geosciences, Facultat de Geologia, Universitat de Barcelona, Spain*
[4] *Institut de Ciències del Mar-CSIC, Barcelona, Spain*
[5] *Centro Austral de Investigaciones Científicas(CADIC-CONICET), Ushuaia, Argentina*

Key words Turbidity currents, numerical modelling, inverse analysis, trawling, anthropogenic impact.

Bottom trawling is a non-selective fishing technique involving the towing of a heavy collecting device to harvest living resources. Recent studies have shown bottom trawling is a driver of seabed evolution[1] and sediment transfer in canyons[2]. Present knowledge on trawling-induced resuspension and transport is based on seldom and geographically localized observations and *a posteriori* interpretations. Our aim is to assess trawling impact on sediments dynamics in La Fonera submarine canyon (NW Mediterranean Sea) and improve the understanding of its sedimentary functioning. Our methodology combines inverse analysis and the implementation of a process-based numerical model (Nixes-TC). Model results are compared to data at the Montgrí valley mooring station deployed at 980m depth (41°52.49'N; 3°20.66'E). Nixes-TC follows the principles of the models developed by Parker[3] and Bradford and Katopodes[4,5], solving depth-averaged conservation equations for fluid momentum, fluid continuity and suspended sediment mass. Fishing grounds are defined on both flanks of the canyon on the basis of satellite-based navigation tracks from the Vessel Monitoring System. Model responses obtained at the mooring site for different initial conditions over the fishing grounds allow the decomposition of the modelled signal into two functions: a transfer function and an amplitude function. The former contains the processes between the remobilisation over the canyon flanks and the arrival of the event at the mooring point whilst the latter is related to the external forcing. We consider the signal obtained at the mooring station as linear superposition of n different instantaneous remobilisation events over the fishing grounds. The modelled instantaneous sediment transport at the mooring site is given by the convolution of the transfer function and the different amplitudes. We consider these amplitudes as a function of the part of the measured signal due to the external forcing that we isolate through application of the Autoregressive-Moving Average (ARMA) model. By linearizing and discretizing the problem, we are able to relate the discrete data measurements at the mooring site to the discrete inverse model parameters (i.e. unknown amplitude of the different events). This comparison (i.e. measurements vs inverse model results)(Fig.1B) allows us to infer the amplitude time series of the different events and to deduce the key variable in trawling impact, which is the remobilisation over the fishing grounds causing turbidity events comparable to those measured at the mooring station (Fig.1A). The inferred resuspension over the fishing grounds is integrated in Nixes-TC in terms of instantaneous sediment flux over the area affected by trawling, allowing us to take into account the non-linearity inherent to turbidity currents. Based on the good agreement found between modelled transport and measurements at the mooring site (Fig1B), we identify the propagation patterns of the resuspended sediment towards the canyon axis and beyond. Our results are in agreement with previous studies in La Fonera submarine canyon: trawling impacts extend substantially deeper than the fishing grounds and lead to the development of trawl-driven depocentres[6], and confirm the value of numerical models to complete and enlarge our understanding of the sediment transfer from shallower to deeper areas in the ocean.

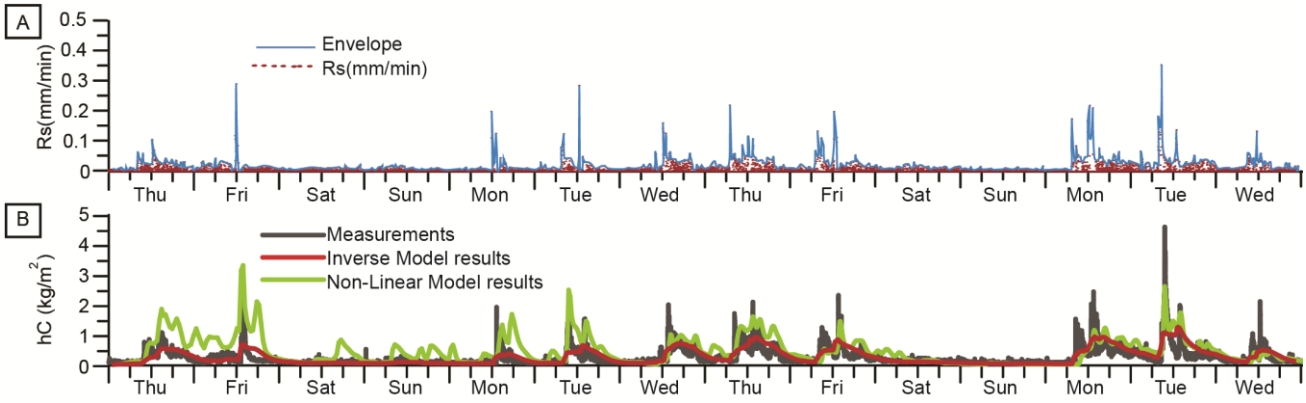

Figure 1. A) Time series of remobilisation events over the LFC fishing grounds obtained through inverse modelling (red dots) and its envelope (blue line). This remobilisation corresponds to the activity of 16-21 fishing vessels operating in the area in agreement with the actual fishing fleet in the investigated fishing grounds. B) Values of instantaneous sediment transport at the mooring site for the inverse model (red), the non-linear model (green) and the in situ measurements (grey).

References

1. Puig, P. *et al.* Ploughing the deep sea floor. *Nature* **489,** 286–289 (2012).
2. Martín, J., Puig, P., Palanques, A. & Ribó, M. Trawling-induced daily sediment resuspension in the flank of a Mediterranean submarine canyon. *Deep Sea Res. Part II Top. Stud. Oceanogr.* **104,** 174–183 (2014).
3. Parker, G., Fukushima, Y. & Pantin, H. M. Self-accelerating turbidity currents. *J. Fluid Mech.* **171,** 145–181 (1986).
4. Bradford, S. F. & Katopodes, N. D. Hydrodynamics of turbid underflows. I: Formulation and numerical analysis. *J. Hydraul. Eng.-Asce* **125,** 1006–1015 (1999).
5. Bradford, S. F. & Katopodes, N. D. Hydrodynamics of turbid underflows. II: Aggradation, avulsion, and channelization. *J. Hydraul. Eng.-Asce* **125,** 1016–1028 (1999).
6. Puig, P., Martín, J., Masqué, P. & Palanques, A. Increasing sediment accumulation rates in La Fonera (Palamós) submarine canyon axis and their relationship with bottom trawling activities: Trawling Effects on Sedimentation Rates. *Geophys. Res. Lett.* **42,** 8106–8113 (2015).

cmg2016 - - Thursday, June 9, 2016 - 11:45/12:30 (45min)

Reprocessing and Reanalysis of the steady state chute-flow experiments

H. K. TRUONG [1,2], C.J. KEYLOCK [1], N. ECKERT[2 3]
[1] Sheffield University, Department of Civil and Structural Engineering, Sir Frederick Mappin Building, Mappin Street, Sheffield, UK.
[2] Irstea, UR ETGR, centre de Grenoble, 2 rue de la Papeterie-BP 76, F-38402 St-Martin-d'Hères, France.
[3] Université Grenoble Alpes, F-38041 Grenoble, France.

Key words : *Snow, Avalanche, Maximum cross correlation, wavelet transform, probability distribution function, Velocity profile*

Snow avalanches affect the livelihoods and economies of alpine communities and effective modelling of the dynamics is needed for mitigation against avalanche hazards. However, there is no precise understanding of the rheology of flowing snow to underpin such modelling, which means that basic experiments are still required. Seventy-five small-scale in-situ flow experiments were performed in an inclined snow chute under various slopes, temperatures and flow depths, in order to determine the velocity structure in the flow, infer shear rates and thus, rheology. However, to determine velocity fluctuations from such sensors (to estimate quantities like granular temperature) is rather complex. A velocity sensor is made up of a pair of optical sensors; right and left phototransistors are arranged in parallel on the channel wall, separated by a known, small distance. The raw data consists of pairs of voltage time series signals, which are classically converted into a velocity series using the lag to maximum cross-correlation (MCC) between the pairs, and the displacement between sensors [1]. Previously work has shown that the mean velocity profiles could be considered as a bilinear function of height [2]. The bilinear model can be interpreted as a consequence of a shear-induced evolution of snow microstructure: a sheared basal layer made of single snow grains and a less sheared upper layer made of large aggregates [2]. This work goes into the data processing in greater depth to attempt to provide greater physical insight into the dynamics of these flows for a steady and uniform chute flow.

The results from the MCC method depend on the window size adopted for undertaking the correlation of the voltage series: A big window size tends to over-smooth velocity series; a small window tends to estimate more aberrant values. The optimal value for our data (acquired at 10 kHz) is around 150 points. In this paper we demonstrate the advantage of adopting a wavelet transform, more specifically, the Maximal Overlap Discrete Wavelet Transform (MODWT) for extracting velocity series that are more informative and consistent, reflecting an implementation that is more continuous in nature than the windowing operator used to apply the MCC.

The reanalysis shows there are up to five shapes of mean velocity profiles. The environmental conditions at the time of the experiment (snow type, temperature) seem to explain these different shapes. In addition, we are able to extract profiles of the velocity distributions, which evolve from an unimodal distribution to a multimodal distribution, according to the height. Multimodality can be interpreted as a reflection of the degree of mixture of the different physics involved.

References

[1] Bouchet, A., Naam, M., Bellot, H., Ousset, F., 2004. Experimental Study of Dense Snow Avalanches : Velocity Profiles in Steady and Fully Developed Flows *Annals of Glaciology* 49, 30–34.

[2] Rognon, P., Chevoir, F., Bellot, H., Ousset, F., Naaim, M., Coussot, P., 2008. Rheology of dense snow flows: Inferences from steady state chute-flow experiments. *Journal of Rheology* 52, 729–748

cmg2016 - - Thursday, June 9, 2016 - 11:45/12:30 (45min)

A LABORATORY AND THEORETICAL STUDY OF FLUIDISED GRANULAR FLOWS, AND IMPLICATIONS FOR PYROCLASTIC FLOW DYNAMICS

D. E. Jessop[1,2], A. J. Hogg[3] & M. A. Gilbertson[3]
[1]*Laboratoire Magmas et Volcans, Clermont-Ferrand, France*
[2]*University of British Columbia, Vancouver, Canada*
[3]*University of Bristol, UK*

Key words A few key words.

Fluidisation transforms frictionally-dominated granular materials into highly mobile, dense, gravity-driven flows. Fluidised granular currents are able to propagate over very shallow and even horizontal surfaces upon which "dry" (i.e. non-fluidised) granular materials would form quasi-static piles [2]. Field evidence suggests that fluidisation could be responsable for the high mobility of pyroclastic flows (e.g. [1]). Fluidisation is also widely exploited in industrial applications where powders have to be transported over long distances. However, despite all these applications, a theoretical model that comprehensively describes the dynamics of such flows is severely lacking.

Laboratory experiments using fluidised granular flows are analagous to the dense, basal portion of pyroclastic flows. Accordingly we perform experiments where a monodisperse granular material is released at a constant flux, q, into a 1 m long apparatus which can be inclined to some angle θ. The base of the apparatus is porous to gas and allows the flow to be fully fluidised along their entire length. We make detailed measurements of the height along the current, velocity profiles with respect to current depth, and the front position of flows, x_f, as a function of time for a range of q and θ. In parallel, we develop a theoretical model which assumes that the particle phase can be considered as a continuum and that particulate collisions are the dominant mode of momentum transfer. The model and experimental results are in good agreement and show, notably, that there is a non-zero velocity in the particle phase at the base of the flow, that a "freeboard" region exists at the top of the flow where the velocity and volume fraction of particles is greatly reduced (see Fig. 1), that whilst flows along horizontal surfaces decelerate and show a scaling with time of $x_f \sim t^{6/7}$, flows on slopes as shallow as 3° rapidly evolve into a steady state. The existance of a freeboard at the top of such flows is of significance when understanding how a dilute flow can by sustained above the dense basal layer in pyroclastic flows as, here, particles have balistic trajectories and may therefore be more entrained more easily into the overlying dilute particle cloud.

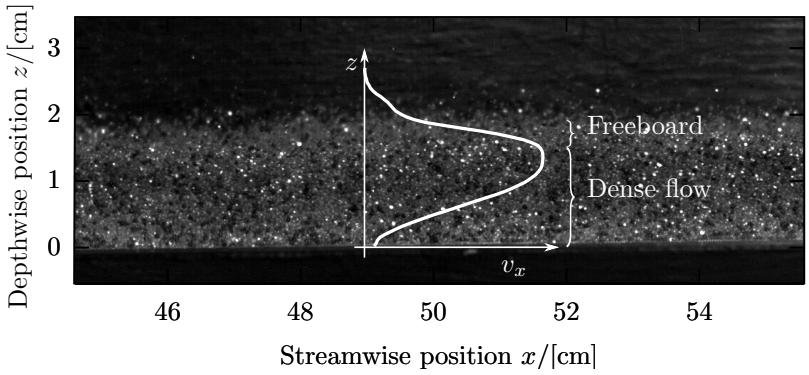

Figure 1. An image of a fluidised granular current overlain by a velocity profile with respect to flow depth.

References

[1] R. S. J. Sparks. Gas release rates from pyroclastic flows: an assesssment of the role of fluidisation in their emplacement. *Bull. Volcanol.*, 41(1):1–9, 1978.

[2] I. Eames and M. A. Gilbertson. The flow of aerated particles over a horizontal rigid surface. *J. Fluid Mech.*, 424:169–195, 2000.

cmg2016 - - Thursday, June 9, 2016 - 11:45/12:30 (45min)

SLIP VELOCITY DURING A GRANULAR MASS FLOW

L. Staron & P.-Y. Lagrée & S. Popinet
Institut Jean le Rond d'Alembert, CNRS-Université Paris VI,
4 place Jussieu, Paris 75252 Cedex 5, France

Key words Mass flow mobility, Slip velocity, Robin-Navier condition, Discrete and continuum simulations

Catastrophic granular mass flows form an important natural hazard. In particular, their ability to travel long distances away from the release point remain a challenge to understanding and modelling. The mobility of granular flows is commonly characterised through the definition of rheological properties and effective friction, namely bulk properties. Yet, the flow boundary conditions and the slip velocity they induce may also play a significant role in the overall flow behaviour [1]. Their correct description is crucial in the perspective of continuum modelling.
In this contribution, we aim at disentangling the effect of bulk properties and boundary conditions on the spreading of a granular mass. Applying discrete simulations, we induce increasing slip velocities in different flow configurations. This is achieved by changing the roughness of the substrate over which flow occurs. We first consider a chute flow configuration. Changing the substrate roughness induces changes in the bottom velocity without affecting the flow profile, namely without affecting the bulk properties. The results are interpreted in terms of a Robin-Navier slip condition [2] (see figure 1). A second flow configuration is the column collapse. By changing the substrate roughness, we change the spreading length and dynamics. We reproduce both using a continuum Navier-Stokes solver (Gerris, [3]) in which we have implemented the Robin-Navier condition. In general, our results show that omitting the description of boundary conditions may leads to misinterpretation of granular flow properties.

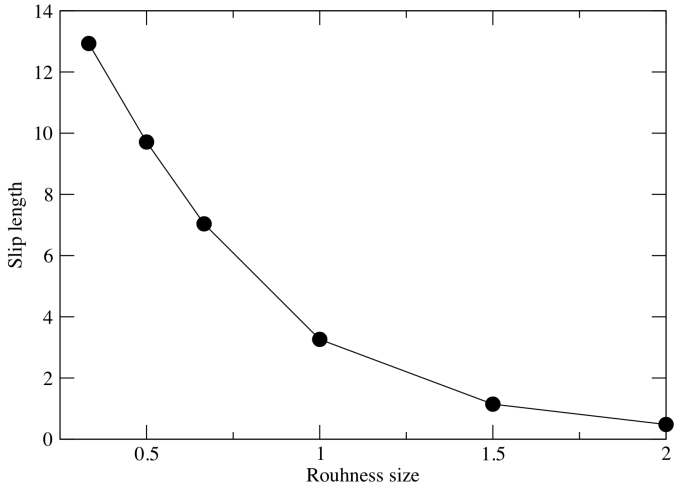

Figure 1. Robin-Navier slip condition: Slip length vs roughness (normalised by the grain size diameter) for chute flows.

References

[1] A. Lucas, A. Mangeney and J.-P. Ampuero, *Frictional velocity-weakening in landslides on Earth and on other planetary bodies* Nature com. **5**, 34-17 (2014).
[2] R. Artoni and Andrea Santomaso, *Effective wall slip in chutes and channels: experiments and discrete element simulations* Granular Matter **16**, 377-382 (2014).
[3] P.-Y. Lagrée, L. Staron and S. Popinet, *The granular column collapse as a continuum: validity of a two-dimensional Navier-Stokes model with the mu(I) rheology*, J. Fluid Mech. **686**, 378-408 (2011).

Granular flows and sediment transport

cmg2016 - - Monday, June 6, 2016 - 17:15/17:30 (15min)

A MODEL FOR THE EROSION ONSET OF BEDLOAD TRANSPORT

Le Yan[1], Antoine Barizien [2], M. Wyart[3]
[1]*Kavli Institute for Theoretical Physics, University of California, Santa Barbara, CA 93106, USA*
[2]*École Polytechnique Université, Paris-Saclay, France*
[3]*Institute of Theoretical Physics, EPFL, CH-1015 Lausanne, Switzerland*

Key words bedload transport, erosion, plastic depinning, spatial organization.

Erosion is central to geomorphology, and takes place when fluid shearing forces overcome the gravitational forces acting on sediments. Although many systems, like gravel rivers, lie close to the erosion threshold where these forces balance, the microscopic description of this transition is debated. We introduce a novel model where interacting particles are channelled by disorder, which predicts the spatial erosion pattern to be organized in a fractal manner with novel exponents. It justifies the linear relation between the erosion flux and the excess shear stress near threshold, and leads to analogies with plastic depinning in superconductors. More generally, it indicates that the spatial organization of the erosion flux can be used to distinguish competing theories.

In particular, we study theoretically the erosion threshold of a granular bed forced by a viscous fluid. We first introduce a novel model of interacting particles driven on a rough substrate. It predicts a continuous transition at some threshold forcing θ_c, beyond which the particle current grows linearly $J \sim \theta - \theta_c$. The stationary state is reached after a transient time $t_{\rm conv}$ which diverges near the transition as $t_{\rm conv} \sim |\theta - \theta_c|^{-z}$ with $z \approx 2.5$. Both features agree with experiments. The model also makes quantitative testable predictions for the drainage pattern: the distribution $P(\sigma)$ of local current is found to be extremely broad with $P(\sigma) \sim J/\sigma$, spatial correlations for the current are negligible in the direction transverse to forcing, but long-range parallel to it. We explain some of these features using a scaling argument and a mean-field approximation that builds an analogy with q-models. We discuss the relationship between our erosion model and models for the plastic depinning transition of vortex lattices in dirty superconductors, where our results may also apply [1].

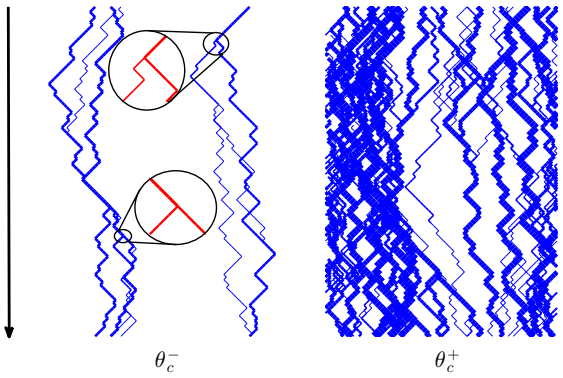

Figure 1. Examples of drainage pattern just below θ_c (Left) and above (Right). The black arrow shows the downhill direction. The thickness of the lines represents $\sigma_{i\to j}$ in logarithmic scale. A few examples showing splitting events are magnified on the left. Here $W = 45$ and $L = 128$, and $J > 0$ even below θ_c due to finite size effects.

References

References

[1] Le Yan, Antoine Barizien, and Matthieu Wyart. A model for the erosion onset of a granular bed sheared by a viscous fluid. *arXiv preprint arXiv:1505.03029*, 2015.

cmg2016 - - Monday, June 6, 2016 - 17:30/17:45 (15min)

THE CESSATION THRESHOLD OF SEDIMENT TRANSPORT IN NEWTONIAN FLUID

Thomas Pähtz[1] & Orencio Durán[2]
[1]*Institute of Physical Oceanography, Ocean College, Zhejiang University, China*
[2]*MARUM-Center for Marine Environmental Sciences, University of Bremen, Germany*

Key words threshold of motion, incipient motion, saltation threshold, aeolian surface features, low-air-density planetary bodies.

One of the classical problems in sediment transport science is to predict the threshold fluid shear stress below which a bed of loose sediment particles sheared by a homogeneous flow of Newtonian fluid ceases to move. Here, we investigate this problem using simulations with the coupled DEM/RANS numerical model of sediment transport in Newtonian fluid by Duran et al. [1]. We simulate conditions with particle-fluid-density ratios ($s = \rho_p/\rho_f$) within the range $s \in [1.2, 2000]$ and particle Reynolds numbers ($\mathrm{Re} = \nu^{-1}\sqrt{(s-1)gd^3}$) within the range $\mathrm{Re} \in [0.1, 100]$. We find that sediment transport is at least partially sustained through impacts of already transported particles onto the sediment bed for all simulated conditions, except viscous bedload (i.e., sufficiently small Re depending on s). This has been well known for turbulent sediment transport in light air, such as on Earth and Mars. However, turbulent sediment transport in liquids, such as water, and heavy air, such as on Venus and Titan, were previously thought to be solely sustained through fluid entrainment (with the notable exception of the recent study by Clark et al. [2]). From our simulations, we further find that sediment transport does not vanish at the cessation threshold. Based on these numerical findings, we propose a physical, analytical model predicting the cessation threshold of sediment transport in Newtonian fluid, which can be applied to arbitrary s and Re. Each equation of this model and the cessation-threshold predictions are consistent with numerical data within the entire range of simulated conditions. Moreover, the cessation-threshold predictions are consistent with measurements in water (Shields diagram), Earth's air, and with an observational estimate on Mars. When applied to conditions on Triton, Pluto, and the comet 67P/Churyumov-Gerasimenko, which all have very thin atmospheres, it predicts much smaller threshold wind shear velocities (u_t) than previous models. In particular, it predicts $u_t \approx 1$m/s for particles with size $d \approx 2$mm on Triton and Pluto, which is a wind shear velocity often reached during storms on Earth and Mars, and thresholds consistent with estimates of wind shear velocities on 67P/Churyumov-Gerasimenko (e.g., $u_t \approx 45$m/s for $d \approx 1$cm). We thus conclude that the surface features, including what appear to be ripples and dunes, photographed on these planetary bodies during space missions are, indeed, of aeolian origin.

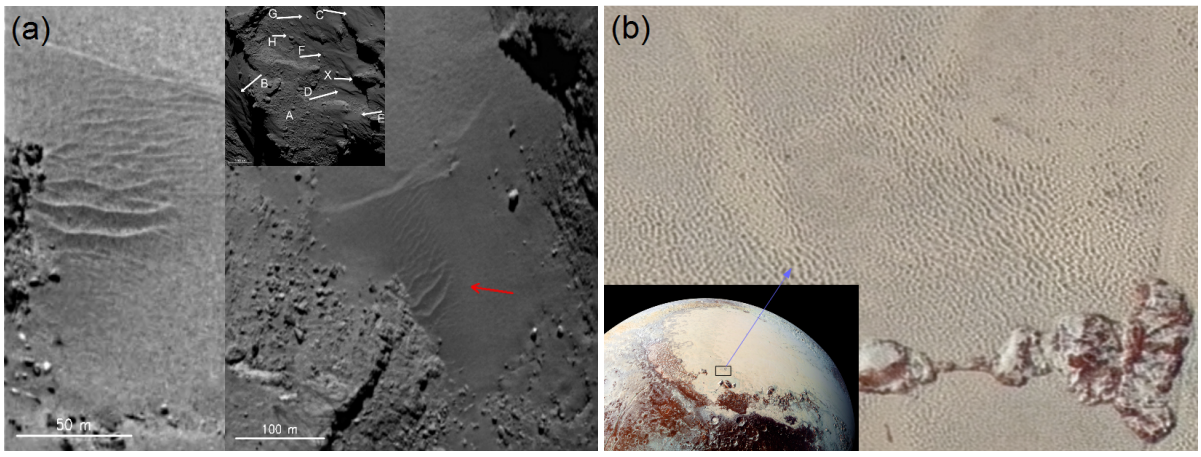

Figure 1. Images of possible ripples and dunes on (a) the comet 67P/Churyumov-Gerasimenko from Thomas et al. [3] and (b) Pluto from Stern et al. [4].

References

[1] O. Durán, P. Claudin, B. Andreotti *Numerical simulation of turbulent sediment transport, from bed load to saltation*, Physics of Fluids **24**, 103306 (2012).
[2] A. H. Clark, M. D. Shattuck, N. T. Ouellette, C. S. O'Hern *Onset and cessation of motion in hydrodynamically sheared granular beds*, Physical Review E **92**, 042202 (2015). A. H. Clark, M. D. Shattuck, N. T. Ouellette, C. S. O'Hern
[3] *Redistribution of particles across the nucleus of comet 67P/Churyumov-Gerasimenko*, Astronomy & Astrophysics **583**, A17 (2015).
[4] S. A. Stern *et al.*, *The Pluto system: Initial results from its exploration by New Horizons*, Science **350**, aad1815 (2015).

cmg2016 - - Monday, June 6, 2016 - 15:30/15:45 (15min)

ON THE ROLE OF VORTICES IN THE THERMAL AND MECHANICAL PROPERTIES OF SHEARED GRANULAR FLOWS.

P. Rognon [1], D. Griffani , P. Kharel & I. Einav
[1]*Particles and Grains Laboratory, School of Civil Engineering, The University of Sydney, Sydney, NSW 2006, Australia.*

Key words Granular flows, rheology, heat transfer, modelling.

Earthquakes and landslides often involve large deformation of granular soils and fragmented rocks. Predicting their dynamics of such events requires the knowledge of constitutive models describing the mechanical properties of this type of material.

We present here a range of experimental and numerical results aiming to better understand the flow properties of granular materials and enrich existing constitutive models. In particular, we discuss (i) the existence of granular clusters -or granular vortices- within granular flows and (ii) their effects on the material viscosity and on the material ability to transfer the heat produced by mechanical dissipation. This discussion synthesises research results published in [1, 2, 3, 4, 5]

Experiments are based on an original Stadium Shear Device producing steady and continuous shear of a layer of plastic cylinders (1.5 cm in diameter) lying on a glass panel, and that allows us to track the trajectory of individual grains within the flow (figure 1). These results evidence the formation of non-laminar kinematic patterns within the flow: transient clusters of grains form, translate and rotate as a rigid body for a short period of time, and then break appart. Discrete Element Method simulation of granular flow in the plane shear geometry compliment these experimental data, including heat transfer between grains.

The analysis of these results reveals clear scaling laws between the granular vortex size and the granular viscosity on one hand, and between the vortex size and the granular Nusselt number quantifying the heat transfer across the sheared layer on the other hand.

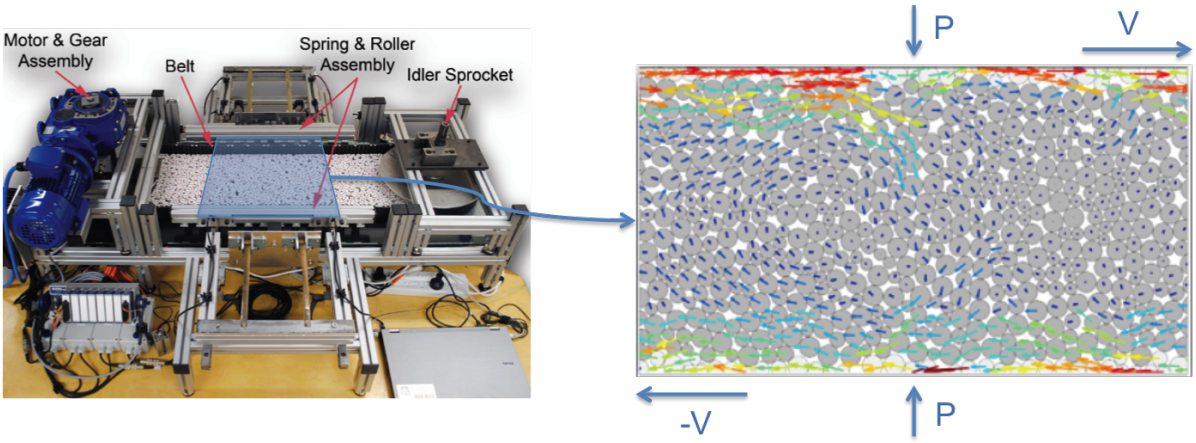

Figure 1. Granular vortices in experimental sheared granular flows. (1) Stadium Shear Device (SSD) where 2D grains are sheared within a belt; (2) Snapshot of the velocity of individual grains in the central section of the SSD showing the formation of granular vortices (V is the belt velocity and P the applied normal stress).

References

[1] P. Rognon and I. Einav, " Thermal transients and convection in dense granular materials," *Phys. Rev. Lett.*, vol. 105, p. 218301, 2010.
[2] T. Miller, P. Rognon, B. Metzger, and I. Einav, "Eddy viscosity in dense granular flows," *Phys. Rev. Lett.*, vol. 111, no. 5, p. 058002, 2013.
[3] D. Griffani, P. Rognon, B. Metzger, and I. Einav, "How rotational vortices enhance transfers," *Phys. Fluids*, vol. 25, no. 9, p. 093301, 2013.
[4] P. G. Rognon, T. Miller, B. Metzger, and I. Einav, "Long-range wall perturbations in dense granular flows," *Journal of Fluid Mechanics*, vol. 764, pp. 171–192, 2015.
[5] P. Rognon, T. Miller, and I. Einav, "A circulation-based method for detecting vortices in granular materials," *Granular Matter*, vol. 17, no. 2, pp. 177–188, 2015.

cmg2016 - - Monday, June 6, 2016 - 17:45/18:00 (15min)

SALTATION ON EARTH AND EXTRATERRESTRIAL ATMOSPHERES

A Valance[1], D. Berzi[2] & J.T. Jenkins[3]

[1] *Institut de Physique de Rennes, CNRS UMR 5261, Université de Rennes 1, Paris, France*

[2] *Department of Civil and Environmental Engineering, Politecnico di Milano, 20133 Milan, Italy*

[3] *School of Civil and Environmental Engineering, Cornell University, Ithaca, NY 14850, USA*

Key words Geophysical flows, granular materials, mixing, multiphase and particle-laden flows, particle/fluid flow, sediment transport

We present an approximate analytical analysis of particle periodic motion over hydrodynamically rough beds [1]. The analysis is based on the calculation of approximate solutions for average periodic trajectories of particles that are accelerated by the turbulent shearing of a fluid, between collisions with the bed (see Fig. 1). We focus on the case in which the mean fluid motion is strong enough to sustain the saltation of the particles, as continuing rather than intermittent, as often seen in weak bedload transport of particles in water.

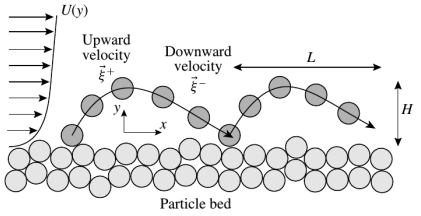

Figure 1. Sketch of the periodic trajectory

From these solutions, we determine the relations between the horizontal particle flux, the strength of the shearing flow and the particle take-off velocity over a range of the grain-to-fluid mass density ratios that vary between those for sand in air and sand in water, in saltation over rigid bumpy and erodible beds. We focus on large values of the Stokes number, where collisions with the bed are not influenced by the fluid.

For saltation over rigid bumpy beds, we predict that there is range of particle flux that the fluid can sustain at a given Shields parameter, irrespective of the density ratio and the Stokes number. That range presents a maximum, which corresponds to the maximum transport capacity of the flow, before particles begin to be deposited and an erodible bed develops. To our knowledge, these findings have been previously demonstrated in the case of aeolian transport only. We also find that the particle trajectory and the fluid shear stress at the bed are essentially independent of the Shields parameter, unlike the particle shear stress and concentration.

For saltation over erodible beds, there is only one horizontal particle flux associated with a given Shields parameter. The analytical solution indicates that this flux scales linearly with the Shields parameter in aeolian transport, while it is roughly proportional to the Shields number to the power of $3/2$ near aquatic transport. These predictions are in agreement with the scaling laws drawn from sand transport experiments in air and water. We also highlight that saltation regimes in air and water are different in nature: aeolian saltation is limited by the splash, while the aquatic saltation is not. In the latter case, the impact velocity of the saltating particles is actually too weak to trigger the splash and, as a consequence, the particle flux is limited by the maximum transport capacity of the system. Interestingly, for intermediate values of the density ratio σ (typically between 30 and a few hundred), we find a crossover regime: the particle flux is proportional to $S^{3/2}$ close to the threshold and linear in S at larger values of the Shields parameter. In other words, for these intermediate values of σ, we observe a transition from an unlimited saltation regime at small Shields parameters to a splash-limited saltation regime at larger Shields parameters. This crossover regime is expected to be relevant for sediment transport in extraterrestrial atmospheres such as on Venus and Titan, where the density ratios are approximately 40 and 200, respectively.

References

[1] D. Berzi, J..T Jenkins and A. Valance, *Periodic saltation over hydrodynamically rough beds: aeolian to aquatic* Journal for Fluid Mechanics **786, 190- 209 (2016).**

cmg2016 - - Monday, June 6, 2016 - 16:00/16:15 (15min)

GRANULAR RHEOLOGY IN BEDLOAD TRANSPORT

R. Maurin[1,2], J. Chauchat[3,4] & P. Frey[1,2]

[1] *Irstea, Grenoble, UR ETGR, 2 rue de la papeterie, BP 76, 38402 Saint-Martin-d'Hères, France*

[2] *Univ. Grenoble Alpes, Irstea, F-38000 Grenoble, France*

[3] *Univ. Grenoble Alpes, LEGI, F-38000 Grenoble, France*

[4] *CNRS, UMR 5519, LEGI, F-38000 Grenoble, France*

Key words Sediment transport, Bedload, granular flow, two-phase flow, granular rheology.

Considering a granular bed submitted to a surface fluid flow, bedload transport is classically defined by opposition to suspension as the part of the load in contact with the granular bed, i.e. in rolling, sliding or small jumping motions. The granular rheology in bedload transport is characteristic of the granular bed response to the fluid shear stress, and is therefore fundamental both in term of transport rate and for upscaling in the framework of two-phase continuous modelling. Using a validated coupled fluid-Discrete Element Model for bedload transport [1], the granular rheology is characterized by computing locally the granular stress tensor as a function of the depth for a serie of simulation varying the Shields number, the particle diameter and the specific density. The obtained results are analyzed in the framework of the $\mu(I)$ rheology and show a collapse of the data for a wide range of inertial numbers. The effect of the interstitial fluid on the granular rheology is shown negligible, supporting recent work [2] suggesting the absence of a clear transition between the free-fall and the turbulent regime. In the low inertial numbers limit, signatures of non-local granular behavior are observed. Meanwhile, the collapse as a function of the inertial number for both the solid volume fraction and the shear to normal stress ratio is observed up to unexpectedly high inertial numbers ($I \sim 3$) in regions showing an important dependency on the restitution coefficient. At higher inertial number, a transition to a granular gas behavior is suggested by the results and is seen to depend on the parameters of the configuration sampled. These results, on the one hand show the relevancy in modelling the granular phase in bedload transport using the $\mu(I)$ framework, and on the other hand challenge the existing conceptions and parametrizations of the $\mu(I)$ rheology. By pragmatically fitting the expression of the latter with the results obtained, a parametrization of the $\mu(I)$ rheology is proposed for bedload transport, and tested using a 1D two-phase continuous model [3, 4]. The latter is shown to reproduce accurately the granular depth profiles, and the classical behavior in terms of dimensionless sediment transport rate as a function of the Shields number. The proposed rheology therefore represents an important step for upscaling in the framework of two-phase continuous modelling of bedload transport.

References

[1] Maurin, R. and Chauchat, J. and Chareyre, B. and Frey, P., A minimal coupled fluid-discrete element model for bedload transport,*Physics of Fluids*, **27** 113302. (2015)

[2] Izard E. and Bonometti T. and Lacaze L., Simulation of an Avalanche in a Fluid with a Soft-sphere/Immersed Boundary Method Including a Lubrication Force,*The Journal of Computational Multiphase Flows*, **6**:391-406. (2014)

[3] Chauchat, J., A comprehensive one-dimensional two-phase flow model for steady uniform sheet-flow based on dense granular flow rheology,*submitted to Journal of Hydraulic Research*

[4] Revil-Baudard, T. and Chauchat, J., A two-phase model for sheet flow regime based on dense granular flow rheology,*Journal of Geophysical Research: Oceans*, **118**:619–634. (2013)

cmg2016 - - Monday, June 6, 2016 - 15:45/16:00 (15min)

DYNAMICS OF SHEARED FLUID-PARTICLE FLOWS : NUMERICAL SIMULATION AT THE GRAIN SCALE

J. Bouteloup, L. Lacaze, T. Bonometti & F. Charru
Institut de Mécanique des Fluides de Toulouse (IMFT) - Université de Toulouse, CNRS-INPT-UPS, Toulouse FRANCE

Key words sediment transport, direct numerical simulation, ripple formation, particle-laden flows

The process of sediment transport by a viscous shear flow over a flat granular bed implies complex mechanisms at different time and spatial scales. In order to describe the evolution of such flows, a better understanding of the influence of local fluid-particle and particle-particle interactions on large scale structures (ripples, dunes[1]) is necessary. For this purpose, local numerical simulations of laminar shear flow eroding a bed of particles were performed. The numerical method used is an Euler-Lagrange model[2], based on the resolution of the Navier-Stokes equations, averaged over cells containing several particles, and Newton's equations for the solid phase using the discrete element method (DEM)[3]. The averaging procedure brings out a solid volume fraction term ε for the fluid phase[4], which mimics the porosity of the effective medium. A fluid-particle interaction term enables a two-way coupling. This method allows us to perform simulations with a large number of particles ($O(10^6)$).

A first set of simulations was performed on relatively small domain ($20d_p \times 20d_p \times 10d_p$) with d_p being the mean diameter of the grains. This size domain allows to reach a steady state, avoiding ripple instabilities. In the present case, the particle Reynolds number $Re_p = 0.48$ and density ratio $\rho_p/\rho_f = 4$ are set constant while the dimensionless shear stress, the Shields number θ, lies in the range [0.1, 0.5]. As observed in Figure 1(a), the variation with θ of the saturated granular flow rate q_{sat}, as obtained from the simulation, is in reasonable agreement with available experimental[5] and numerical[6] data[5, 6], especially for the threshold Shields number $\theta_t \approx 0.12$, which delineates static and moving bed. A second set of simulations was performed on a larger domain ($1000d_p \times 20d_p \times 10d_p$), in order to capture the formation of ripples. Figure 1(b) displays the spatio-temporal evolution of the relative bed height. Ripples clearly grow on the initially flat bed, with a well-defined wavelength. On larger time scales, they tend to merge together, corresponding to the coarsening phenomena observed in the experiments.

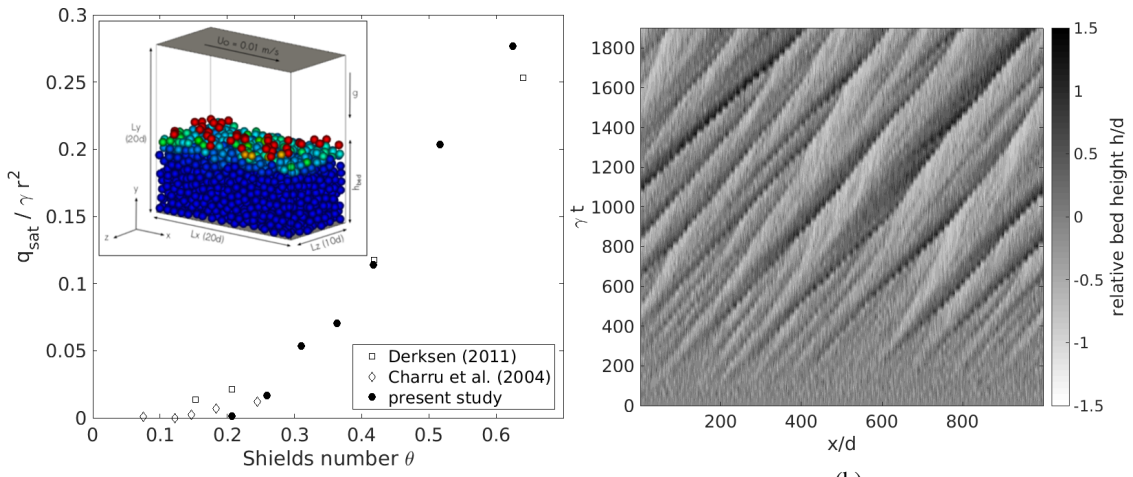

(a) (b)

Figure 1: (a) Dimensionless particle flow rate versus the Shields number θ (inset) computational domain (b) Spatio-temporal evolution of the relative bed height

References

[1] F. Charru, B. Andreotti, and P. Claudin. Sand ripples and dunes. *Annual Review of Fluid Mechanics*, vol. 45(1):469–493, 2013.
[2] J. Capecelatro and O. Desjardins. An euler-lagrange strategy for simulating particle-laden flows. *Journal of Computational Physics*, vol. 238(0):1–31, 2013.
[3] F. Radjaï and F. Dubois. *Discrete-element modeling of granular materials*. Oxford : ISTE, 2011.
[4] R. Jackson. *The Dynamics of Fluidized Particles*. Cambridge Monographs on Mechanics. Cambridge University Press, 2000.
[5] F. Charru, H. Mouilleron, and O. Eiff. Erosion and deposition of particles on a bed sheared by a viscous flow. *Journal of Fluid Mechanics*, vol. 519:55–80, 2004.
[6] J. J. Derksen. Simulations of granular bed erosion due to laminar shear flow near the critical shields number. *Physics of Fluids*, vol. 23(11):1–12, 2011.

cmg2016 - - Monday, June 6, 2016 - 16:45/17:15 (30min)

CREEPY LANDSCAPES: THE ORIGINS AND CONSEQUENCES OF SUB-THRESHOLD TRANSPORT

C. Ortiz[1,2], B. Ferdowsi[1], M. Houssais[3], D.J. Durian[2] & D. Jerolmack[1]
[1]*Dept. Earth and Environmental Science, University of Pennsylvania, Philadelphia, USA*
[2]*Dept. Physics and Astronomy, University of Pennsylvania, Philadelphia, USA*
[3]*Levich Institute, City University of New York, USA*

Key words Creep, hillslopes, rivers, sorting, jamming

Determining the threshold of motion is the zeroth-order problem in geomorphology: under what conditions does transport begin? Recent experiments by our group and others, examining fluid-driven granular transport typical of rivers, have revealed glassy dynamics. In particular: (1) as fluid stress is decreased, the dynamics of particle motion become progressively slower and more heterogeneous indicating a continuous (glass) transition from flowing to jammed; and (2) particles exhibit localized but persistent motion at fluid stresses far below the apparent yield condition, which is characteristic of creep in disordered solids [1]. While a generalized version of a local granular rheology model captures well the flow behavior for particles in bed load and suspension, such models predict a transition to a completely jammed state at a finite yield stress — in contradiction to observed creep dynamics [2]. We present new experimental results that demonstrate two important consequences of sub-threshold creep: (1) it contributes to long timescale changes in the rigidity of the pack through the development of a granular fabric; and (2) it drives vertical segregation of grains throughout the pack, which may be an overlooked but dominant factor in river-bed armoring. We perform Discrete Element Model (DEM) simulations that reveal that observed creep dynamics are insensitive to the presence of the fluid, suggesting a direct link between creep on hillslopes and in river beds. Soil creep on hillslopes is most often described using a heuristic nonlinear flux law relating transport rate to slope, and these dynamics have not been linked to the underlying granular motion. Our DEM simulations demonstrate that creep may occur for slopes significantly below the angle of repose, even in the absence of perturbations. They also show that the nonlinear flux law represents a transition from sub-threshold creep to a dense granular flow that is identical to that observed in our river experiments. The emerging view is that sub-threshold creep is the ubiquitous landscape process, and that the onset of both bed-load transport and landslides/debris flows represents a sharp but continuous transition from creeping to dense granular flow.

References

[1] Houssias, M., Ortiz, C., Durian, D.J., and Jerolmack, D.J., 2015, Onset of sediment transport is a continuous transition driven by fluid shear and granular creep: Nature Communications, doi: 10.1038/ncomms7527.
[2] Houssias, M., Ortiz, C., Durian, D.J., and Jerolmack, D.J., Rheology of sediment transported by a laminar flow: arXiv:1509.08395.

cmg2016 - - Monday, June 6, 2016 - 11:45/12:30 (45min)

BURSTS IN DISCONTINUOUS AEOLIAN SALTATION

M. V. Carneiro[1], K. R. Rasmussen[2] & H. J. Herrmann[1,2]

[1]*Computational Physics, IfB, ETH Zürich, Wolfgang-Pauli-Strasse 27, 8093 Zürich, Switzerland*

[2]*Department of Geoscience, Aarhus University, Hoegh Guldbergsgade 2, 8000 Aarhus C, Denmark*

[3]*Departamento de Física, Universidade Federal do Ceará, 60451-970 Fortaleza, Ceará, Brazil*

Key words Aeolian sand transport, sediment transport, Discrete Element Methods, turbulence.

We find in wind tunnel experiments a regime of discontinuous flux characterized by sand bursts close to the onset of Aeolian saltation. Scaling laws are observed in the time delay between each burst and in the measurements of the wind fluctuations at the fluid threshold Shields number θ_c. The time delay between each burst decreases on average with the increase of the Shields number until sand flux becomes continuous. A numerical model for saltation using discrete element methods consists of a poly-disperse 3D quiescent packing of hard spheres subjected to a logarithmic wind velocity profile imposed in horizontal direction (x-direction). A tracer attached to every particle generates stochastic turbulent perturbations that mimics the wind pick of sand grains and reproduce the sand bursts.

References

[1] M. V. Carneiro, K. R. Rasmussen, and H. J. Herrmann, *Bursts in discontinuous Aeolian saltation*, Scientific Reports **5** 11109 (2015).

cmg2016 - - Monday, June 6, 2016 - 11:45/12:30 (45min)

DYNAMIC BEHAVIOUR OF THE STATIC/FLOWING INTERFACE IN VISCOPLASTIC GRANULAR FLOWS: ANALYTIC, NUMERICAL AND EXPERIMENTAL STUDIES

F. Bouchut[1], A. Mangeney[2], I.R. Ionescu[3], C. Lusso[4], A. Ern[4], M. Farin[5], & O. Roche[6]
[1]*CNRS & Université Paris-Est, France*
[2]*Institut de Physique du Globe & Université Paris-Diderot, Paris, France*
[3]*Université Paris 13, Villetaneuse, France*
[4]*Ecole des Ponts ParisTech, Champs-sur-Marne, France*
[5]*Institut de Physique du Globe, Paris, France*
[6]*Université Blaise Pascal, Clermont-Ferrand, France*

Key words Viscoplastic granular flows, static/flowing interface, granular collapse

Observed avalanche flows of dense granular material have the property to present two possible behaviours: static (solid) or flowing (fluid). In such situation, an important challenge is to describe by differential equations the evolution of the physical interface between the two phases. Defining an equation for this interface in thin-layer models has been done based on phenomenological models or on strong assumptions such as a specified velocity profile or reducing the flow to a sliding block for example in [1, 2]. A review on static/flowing models can be found in [3].

In this talk we would like to describe the evolution of the static/flowing interface via a set of equations derived analytically via an asymptotic expansion starting from a viscoplastic model with Drucker-Prager yield stress, analogous to the $\mu(I)$ rheology of [4]. A set of equations has been derived in [5], and assumes a thin-layer regime. The model takes the form of a formally overdetermined initial-boundary problem in the variable normal to the topography (that does not disappear even with the thin-layer assumption), set in the flowing region only. The extra boundary condition at the static/flowing interface involves a third order derivative of the velocity in the normal direction, and contains the information on how to evolve the static/flowing interface, but in a non explicit manner. It comes out from the continuity of the velocity and shear stress across the interface. The model handles arbitrary velocity profiles, and is therefore more general than classical depth-averaged models. Explicit solutions can be built [6] and show different possible behaviours such as progressive stopping or sudden start of a part of the material. We have performed several studies [7, 8] to numerically resolve our set of equations and compare the results to data from laboratory experiments of granular collapse from [9] and to two-dimensional simulations as those in [10].

References

[1] I.S. Aranson, L.S. Tsimring, *Continuum theory of partially fluidized granular flows*, Phys. Rev. E **65**, 061303 (2002).
[2] D.V. Khakhar, A.V. Orpe, P. Andresen, J.M. Ottino, *Surface flow of granular materials: model and experiments in heap formation*, J. Fluid Mech. **441**, 225-264 (2001).
[3] R.M. Iverson, C. Ouyang, *Entrainment of bed material by Earth-surface mass flows: review and reformulation of depth-integrated theory*, Rev. Geophys. **53**, doi:10.1002/2013RG000447 (2015).
[4] P. Jop, Y. Forterre, O. Pouliquen, *A constitutive law for dense granular flows*, Nature **441**, 727-730 (2006).
[5] F. Bouchut, I.R. Ionescu, A. Mangeney, *An analytic approach for the evolution of the static/flowing interface in viscoplastic granular flows*, submitted, 2015.
[6] C. Lusso, F. Bouchut, A. Ern, A. Mangeney, *Explicit solutions to a free boundary model for the static/flowing transition in granular flows*, submitted, 2015.
[7] C. Lusso, F. Bouchut, A. Ern, A. Mangeney, *A simplified model for static/flowing dynamics in thin-layer flows of granular materials with yield*, submitted, 2015.
[8] C. Lusso, A. Ern, F. Bouchut, A. Mangeney, M. Farin, O. Roche, *Two-dimensional simulation by regularization of free surface viscoplastic flows with Drucker-Prager yield stress and application to granular collapse*, submitted, 2015.
[9] M. Farin, A. Mangeney, O. Roche, *Fundamental changes of granular flow dynamics, deposition, and erosion processes at high slope angles: Insights from laboratory experiments*, J. Geophys. Res. Earth Surf. **119**, 504-532 (2014).
[10] I.R. Ionescu, A. Mangeney, F. Bouchut, O. Roche, *Viscoplastic modeling of granular column collapse with pressure-dependent rheology*, J. Non-Newtonian Fluid Mech. **219**, 1-18 (2015).

cmg2016 - - Monday, June 6, 2016 - 11:45/12:30 (45min)

WHAT CAUSES FRICTIONAL BEHAVIOR IN FLUID-MEDIATED SEDIMENT TRANSPORT?

Thomas Pähtz[1] & Orencio Durán[2]
[1]*Institute of Physical Oceanography, Ocean College, Zhejiang University, China*
[2]*MARUM-Center for Marine Environmental Sciences, University of Bremen, Germany*

Key words sediment transport, friction, rheology, bedload, saltation, particle-bed impacts.

Bagnoldian analytical models of sediment transport in Newtonian fluid (e.g., air or water) are based on Bagnold's assumption of a constant friction coefficient (particle-shear-pressure ratio, μ) at the interface ($z = z_b$) between sediment bed and transport layer. In fact, this assumption is the main reason why these models predict the sediment load (which is the ratio between sediment transport rate and average particle velocity) to be proportional to the excess shear stress ($\tau - \tau_t$), a scaling that has been confirmed in many wind-tunnel and flume experiments. Here, using numerical simulations with the coupled DEM/RANS model of sediment transport in Newtonian fluid by Duran et al. [1], we investigate the physical reasons for this frictional behavior. In the case of subaqueous transport, we find that a local rheology $\mu(I)$, where I is the viscous number, can explain most of the simulation data. However, this rheology breaks down for aeolian transport. In an attempt to unify these transport regimes, we propose a novel characterization of frictional behavior through the dimensionless parameter $\zeta = \langle F_x^c v_x - F_z^c v_z \rangle / \langle F_z^c v_x - F_x^c v_z \rangle$, where $\mathbf{F}^c$ is the contact force, $\mathbf{v}$ the particle velocity, and $\langle \cdot \rangle$ a local ensemble average. We analytically derive $\zeta \approx \sqrt{3} - 1$ for locations within the transport layer and slightly within the particle bed, where each derivation step and the final result are consistent with our numerical simulations throughout all simulated conditions. Our derivation is mainly based on the assumption that the conversion of horizontal kinetic particle energy into vertical kinetic particle energy in low-angle particle-bed impacts is the predominant collisional energy transformation process occurring in sediment transport. We then show that $\zeta(z_s) \approx \mu(z_s)$, where z_s is the location at which the local production rate of particle fluctuation energy is maximal, and thus $\mu(z_s) \approx \sqrt{3} - 1$. This final result, which explains the success of Bagnold's assumption in analytical models of subaqueous and aeolian sediment transport, is consistent with our numerical simulations throughout all simulated conditions. Interestingly, the location z_s can deviate from the bed top (z_b) by up to two particle diameters depending on the simulated conditions.

References

[1] O. Durán, P. Claudin, B. Andreotti *Numerical simulation of turbulent sediment transport, from bed load to saltation*, Physics of Fluids **24**, 103306 (2012).

cmg2016 - - Monday, June 6, 2016 - 11:45/12:30 (45min)

INTEGRATION OF SEDIMENTS TRANSPORT MECHANISMS UNDER RAINFALL IN A GLOBAL WATER EROSION MODEL

A. Nouhou Bako[1,2], F. Darboux[1], F. James[2] & C. Lucas[2]
[1]*Inra, UR0272, UR Science du sol, Centre de recherche Val de Loire, CS 40001, F-45075 Orléans Cedex 2, France*
[2]*MAPMO, UMR CNRS 7349, Fédération Denis Poisson, FR CNRS 2964, Université d'Orléans, F-45067 Orléans cedex 02, France*

Key words Water erosion, raindrops, sediment transport, models.

Hillslope erosion by water is damaging for environment and agricultural soils. The modeling of the problem helps to understand and limit the phenomenon. Current models include the different processes involved in water erosion: detachment, transport and deposition of sediments. In particular, the transport and deposition processes are taken into account through the settling velocities of sediments. However, for rainfall erosion, the influence of rain on this parameter is unknown. We have carried out experimental studies to understand the effect of rainfall on the travel distance of particles. These experiments allow to separate detachment by raindrops from the agitation of the flow by the drops. Different particle sizes and rainfall kinetic energies are investigated. The results assess the exact role of rainfall on sediment transport.

The experiment results are used to calibrate a single and unified model of transfer equations which encompasses the previous models of Gao et al. (2004) [1], Hairsine and Rose (1992, 1991) [2, 3] and Lajeunesse et al. (2013) [4]. This model describes the spatial and temporal variation of the amount of soil loss in both interrill and rill erosion. The dynamic of the granular-flow is described by an exchange between the granular-fluid mixture flow and the layer of deposited sediments (crusts). This exchange can account for multi-class particle transport and is able to simulate both linear and non-linear behaviors.

References

[1] Gao, B., Walter, M. T., Steenhuis, T. S., Hogarth, W. L. and Parlange, J.-Y. *Rainfall Induced Chemical Transport from Soil to Runoff: Theory And Experiments*, Journal of Hydrology **295**, 291-304 (2004).

[2] Hairsine, P. B. and Rose, C. W. *Modeling Water Erosion Due To Overland Flow Using Physical Principals — 1. Sheet Flow*, Water Resources Research **28**, 237-243 (1992).

[3] Hairsine, P. B. and Rose, C. W. *Rainfall Detachment and Deposition: Sediment Transport in the Absence of Flow-driven Processes*, Soil Science Society of America Journal **55**, 320-424 (1991).

[4] Lajeunesse, E., Devauchelle, O., Houssais, M. and Seizilles, G. *Tracer Dispersion in Bedload Transport*, Advances in Geosciences **37**, 1-6 (2013).

cmg2016 - - Monday, June 6, 2016 - 11:45/12:30 (45min)

TURBULENCE LOCALITY AND GRANULAR-LIKE FLUID SHEAR VISCOSITY IN COLLISIONAL SUSPENSIONS

D. Berzi[1] & L. Fraccarollo[2]
[1]*Politecnico di Milano, Milano, Italy*
[2]*Università di Trento, Trento, Italy.*

Key words Sediment transport, kinetic theory, granular flows.

We re-analyse previous experimental measurements [1] of solid volume fraction, mean velocity and velocity fluctuations in collisional suspensions of plastic cylinders and water flowing over inclined, erodible beds. We show that the particle pressure scales with the granular temperature as predicted by kinetic theory of granular gases [2]. Assuming that also the particle shear stress is well predicted by kinetic theory permits the determination of the fluid shear stress and the effective fluid viscosity from the experiments. We suggest that the effective fluid viscosity in collisional suspensions has two components: one associated with the turbulence generated near the surface of the particles and one associated with the transfer of momentum of the fluid mass in conjugate motion with the fluctuating particles (Fig. 1). We model the first contribution using a mixing length approach, and show that the mixing length is local, as it does not scale with distances from boundaries. The mixing length is less than one diameter and decreases with increase in the solid volume fraction. We introduce a granular-like viscosity to model the second contribution to the effective fluid viscosity, by replacing the particle mass density with the density of the added mass of the fluid in the expression of the granular viscosity of the particles of kinetic theory. Finally, we also show how the granular temperature scales in the turbulent and granular limits of the effective fluid viscosity.

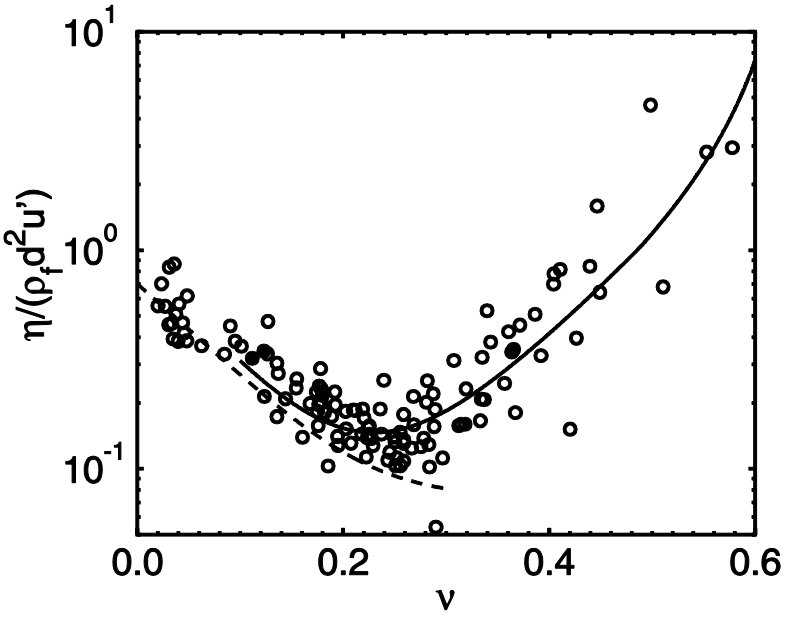

Figure 1. Measured (circles) and theoretical (lines) effective fluid visocsity scaled with the shear rate. At solid volume fractions less and greater than 0.2, the effective fluid viscosity has mainly a turbulent and a granular-like origin, respectively.

References

[1] H. Capart & L. Fraccarollo, *Transport layer structure in intense bed-load*, Geophys. Res. Lett. **38**, L20402 (2011).
[2] V. Garzò & J.W. Dufty, *Dense fluid transport for inelastic hard spheres*, Phys. Rev. E **59**, 5895 (1999).

cmg2016 - - Monday, June 6, 2016 - 11:45/12:30 (45min)

ON A TWO-LAYERS / TWO-PHASES / EXNER MODEL FOR SEDIMENT TRANSPORT WITH EROSION AND DEPOSITION EFFECTS

L. Bonaventura[1], E.D. Fernández-Nieto[2] & G. Narbona-Reina[2]
[1]*MOX – Politecnico di Milano, Milano, Italy*
[2]*Departamento Matemática Aplicada I, Sevilla, Spain*

Key words Sediment transport, suspended load, bed load, erosion rate, deposition rate, two phase, two layer.

In this work we deal with the geophysical problem of sediment transport in river. Our objective is to propose a complete model that describes both suspended and bed load sediment transport, as well as the interactions between them.

The whole physical system includes particles moving as bed load, suspended load and wash load, which is seen indeed as a subset of the suspended load. In the literature on this topic, several proposals to tackle the modelling of the sediment transport have been advanced. In general, the basis are the two-layer and two-phase models. The two-layer models are based on the fact that the different sediment transport types can be seen as separate layers with some kind of interactions among them. The two-phase models keep the property of one fluid formed up of two different components that interacts intrinsically, water and sediment, so the total column is seen as a mixture. Of course, both kind of models are not incompatible and the suitability of each one depends on the physical situations that one would like to focus on.
Furthermore, in this type of geophysical problems, the derivation of depth-integrated models −under the assumption of shallow flows− are extendedly accepted in order to get models mathematically and numerically manageable together with a good review in results that captures the essential effects.

In this work, we present the derivation of a two-layer sediment transport model for both suspended-load and bed-load phenomena, that includes the interaction between the different sediment loads. For this goal we use some established developments in order to obtain a new model that is as complete as possible. We consider the fluid-solid mixture model proposed by Jackson [4] as a basis and we follow different derivations to obtain the dynamics for the two layers. The top layer is defined as a suspension layer made up of water and grains, so we derive a two-phase model based on [3, 2]. For the layer below, we follow the derivation developed in [1] to obtain an Exner type model for arbitrary sloping beds. Erosion, suspension and deposition are considered in the whole system through appropriate boundary conditions. In order to well define the exchange of mass between sediment layers, mass and momentum conservation at the interface are imposed. The rate of erosion/deposition/suspension are defined following [5]. Thus, this model can be seen as a generalization of the existing models. Finally, several numerical tests will be presented.

References

[1] E.D. Fernández-Nieto, T. Morales de Luna, G. Narbona-Reina, J.D. Zabsonré. *Formal deduction of the Saint-Venant-Exner model including arbitrarily sloping sediment beds and associated energy*, submitted to M2AN, (2015).
[2] G. Garegnani, G. Rosatti, L. Bonaventura. *Free surface flows over mobile bed: mathematical analysis and numerical modeling of coupled and decoupled approaches*, Communications In Applied And Industrial Mathematics, **2(1)**, (2011).
[3] G. Garegnani , G. Rosatti, L. Bonaventura. *On the range of validity of the Exner-based models for mobile-bed river flow simulations*, Journal of Hydraulic Research, **51:4**, 380-391, (2013).
[4] R. Jackson, *The Dynamics of Fluidized Particles*, Cambridge University Press, Cambridge, (2000).
[5] Y. Zech, S. Soares-Frazão, B. Spinewine, C. Savary, L. Goutière. *Inertia effects in bed-load transport models*, Can.J.Civ.Eng. **36**, 1587–1597, (2009).

cmg2016 - - Monday, June 6, 2016 - 11:45/12:30 (45min)

ACOUSTIC PROBING OF A SINKING BALL IN SHAKEN GRANULAR SEDIMENTS

S. van den Wildenberg, J. Léopoldès, A. Trabattoni, J.-L. Gennisson, A. Tourin, and X. Jia

ESPCI Paris, PSL Research University, CNRS, Institut Langevin, Paris, France

Key words: sinking ball experiment, dense granular suspension, acoustic monitoring, frictional rheology

A convenient method to determine the viscosity of a fluid is to drop a high density ball in it. As the ball is dropped into the fluid, it accelerates as a result of the gravitational field until it reaches a terminal velocity. In the laminar flow regime, the terminal velocity of the ball is inversely related to the viscosity of the fluid via Stokes' law. Instead, in a yield stress fluid such as foams, emulsions and granular suspensions, the ball will stop sinking at a certain depth due to solid-like friction between the particles, which depends on the sinking velocity of the ball and the normal pressure. The jamming phase diagram provides a general framework to explain such a transition from a liquid-like flowing state to a solid-like jammed state as a function of the density of randomly packed particles and the applied shear.

Understanding an intruder sinking in quicksand remains a conceptual and practical challenge: there are very few direct experimental investigations inside realistic 3D opaque dense granular suspensions. Here, we use acoustic probing to investigate the sinking dynamics of a ball in a vibrated granular sediment saturated by water (Figure 1a). In the absence of vibrations, the ball placed on the surface of the granular sediment will remain still, i.e. the undriven granular suspension exhibits a yield stress. But when the sediment is vibrated its behavior changes dramatically and a ball placed on the surface will immediately begin to slowly sink (Figure 1b).

We investigate the difference between horizontal and vertical vibrations on the preparation of the sediment and on the sinking dynamics of the ball (as an effective temperature). We observe that the two types of vibrations yield suspensions with different packing densities which in turn results in very distinct sinking dynamics. Additionally, we investigate the influence of the intensities of the vibrations on the flow of the sediment and the motion of the ball. Our experimental results are consistent with the frictional rheology revealed in dense granular media [1]. Moreover, we find that the vibrations primarily affect the yield stress (i.e., static friction coefficient) and consequently control the depth of sinking (Figure 1c). This acoustic monitoring should allow a better understanding of the mechanical properties of dense granular suspensions and ocean sediments as well as landsliding.

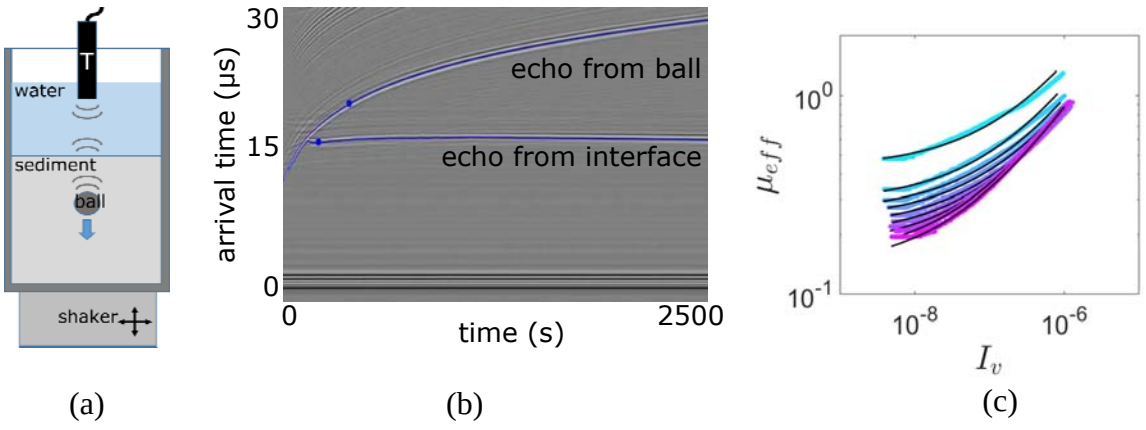

Figure 1. (a) Schematic of ultrasonic monitoring of a sinking ball in dense granular suspension, using a piezoelectric transducer (T). (b) Stack of waveforms showing the reflection of the sinking ball and of the interface. (c) Effective friction coefficient as a function of a viscous number I_v [2] for different vibrational intensities. The black lines represent a fit of the frictional rheology model.

References

[1] GDR MiDi, *On dense granular flows*, Eur. Phys. J. E **14**, 341–365 (2004)
[2] Fall et al, *Rheology of sedimenting particle pastes*, J. Rheol. **57**, 1237 (2013)

cmg2016 - - Monday, June 6, 2016 - 11:45/12:30 (45min)

A PHASE DIAGRAM FOR FLUID-SHEARED GRANULAR BEDS

A. H. Clark[1], M. D. Shattuck[2], N. T. Ouellette[3] & C. S. O'Hern[1]
[1]*Yale University, New Haven, Connecticut, USA*
[2]*The City College of New York, New York, New York, USA*
[3]*Stanford University, Stanford, California, USA*

Key words Sediment transport, granular flow, weakest link statistics

Fluid flowing laterally over a granular bed exerts a shear stress on the grains, and a sufficiently fast flow can transport grains with the fluid, a process that shapes much of the natural world. The nature of the boundary between systems with and without grain motion has been studied for many decades but is still not clearly understood, as it involves nontrivial coupling between several complex physical processes: turbulent fluid flow above the bed, Darcy flow inside the bed, and the yield stress of granular materials of varying shape and size. This large, complex parameter space represents a significant challenge for the field, both to connect the results from the literature (experimental, computational, or field data) into a unified description, as well as to identify the primary physical processes that are responsible for controlling various aspects of sediment transport (and related problems).
Surprisingly, the onset of grain motion in these systems is fairly well captured by two dimensionless numbers. The Shields number Θ is the ratio of the shear stress exerted by the fluid at the bed surface to the downward gravitational stress acting on these grains. The particle Reynolds number Re_p gives the ratio between grain inertia and viscous damping from the fluid. Several recent reviews have shown collections of data, as shown in Fig. 1(a), from experiments and field studies, where the critical Shields number $\Theta = \Theta_c$ required for grains to move is plotted versus Re_p; this data clusters around a curve with plateaus Θ_c^l and Θ_c^h at low and high Re_p, where $\Theta_c^l > \Theta_c^h$, and there is a transitional region between these two limits near $\mathrm{Re}_p \approx 1$. At present, the dominant mechanisms in shaping this curve and the relative importance of each—e.g., friction, turbulence, grain shape, grain size—are not well understood.

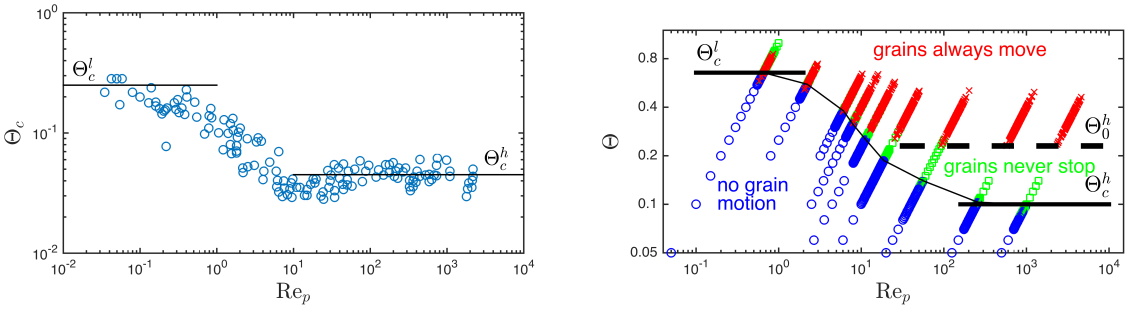

Figure 1. (left panel) A collection of experimental and field data from [1] showing how the critical Shields number Θ_c varies with Re_p; plateaus Θ_c^l and Θ_c^h are marked, representing behavior at low and high Re_p. (right panel) Typical result from simplified two-dimensional DEM simulations [2] with a model fluid that exerts a shear force on a granular bed. Blue circles and green squares represent mobile systems that did and did not stop, respectively. Red crosses show the value of Θ where a static system becomes mobilized. The solid line connecting Θ_c^l and Θ_c^h is $\Theta_c(\mathrm{Re}_p)$, which marks the minimum Θ that can maintain grain motion indefinitely at varying Re_p. The dashed line shows Θ_0^h, the minimum value of Θ at which static systems can become mobilized at high Re_p. As system size grows, all beds at high Re_p will mobilize at $\Theta = \Theta_0$.

Here, I will describe a continuing line of research, where we seek to identify the basic physical mechanisms that govern sediment transport (and related problems) by performing numerical simulations (DEM) of a system with only the most crucial elements. We study granular beds with a free boundary at the surface, as opposed to constant pressure or volume, and the surface grains are thus most susceptible to motion. Instead of constant force or velocity, we apply forcing through a variable fluid flow profile that depends on the state of the grains (relatively large above the bed with a smooth transition to a very small fluid velocity within the bed). The force felt by a grain depends on the difference between the local fluid velocity and the grain velocity, and the strength of the coupling between the fluid flow profile and the grain velocity gives Re_p. The force felt by a static grain at the bed surface gives Θ. We can vary the details of the fluid profile and the grain-grain interactions, but we find a surprisingly robust form for the phase boundaries in our system, as shown in Fig. 1(b), which shows qualitative agreement with the field and experimental data in Fig. 1(a). These boundaries are insensitive to the details of the fluid flow we apply and the grain-scale properties such as shape, friction, and dissipation from intergrain collisions. We find critical-like

behavior near these boundaries (e.g., diverging transient time scales), and we find that the transition from static-to-mobile beds is governed by Weibullian weakest link statistics, where global failure is caused by the failure of the weakest region. These results suggest that the details of the granular structure, a factor that has often been neglected in previous descriptions, plays an important role in determining the onset of grain motion in fluid-driven beds.

References

[1] S. Dey, Sediment Threshold, in *Fluvial Hydrodynamics* Springer Berlin Heidelberg (2014).
[2] A. H. Clark, M. D. Shattuck, N. T. Ouellette, C. S. O'Hern. Onset and cessation of motion in hydrodynamically sheared granular beds, *Phys. Rev. E* **92**, 042202 (2015).

cmg2016 - - Monday, June 6, 2016 - 11:45/12:30 (45min)

SLOPE INFLUENCE ON BEDLOAD TRANSPORT

R. Maurin[1,2], J. Chauchat[3,4] & P. Frey[1,2]

[1] *Irstea, Grenoble, UR ETGR, 2 rue de la papeterie, BP 76, 38402 Saint-Martin-d'Hères, France*

[2] *Univ. Grenoble Alpes, Irstea, F-38000 Grenoble, France*

[3] *Univ. Grenoble Alpes, LEGI, F-38000 Grenoble, France*

[4] *CNRS, UMR 5519, LEGI, F-38000 Grenoble, France*

Key words Sediment transport, two-phase flow, bedload transport, debris flow, slope.

Considering a granular bed submitted to a surface fluid flow, bedload transport is classically defined by opposition to suspension as the part of the load in contact with the granular bed, i.e. in rolling, sliding or small jumping motions. The slope influence on bedload transport is classically considered as resulting from the modification of the gravity contribution on both the granular media and the surface fluid flow. This effect is studied simulating idealized turbulent bedload transport configurations with a validated coupled fluid-Discrete Element Model [1]. Varying the channel inclination angle and the specific density, it is evidenced that these two parameters effect are coupled and not well taken into account by the classical picture. Analyzing analytically the continuous two-phase flow equations, it is shown that the impact of the slope variation on the fluid flow inside the granular bed cannot be neglected and should be taken into account. The latter is responsible for the transition from bedload to debris flow-like behavior, for which the whole granular layer is mobilized. The critical angle of debris flow predicted by Takahashi [2] is recovered from the equations and observed in the simulations. In addition, a rescaling of the Shields number is proposed from the equations and is shown to make all the data collapse onto a master curve when considering the dimensionless sediment transport rate as a function of the modified Shields number. Therefore, the latter characterizes well the slope influence on bedload transport and opens perspectives for a better understanding of the field observations. Further work is required to determine if it should be taken into account in the Shields number formulation or if it can be included in the critical Shields number.

References

[1] Maurin, R. and Chauchat, J. and Chareyre, B. and Frey, P., A minimal coupled fluid-discrete element model for bedload transport,*Physics of Fluids*, **27** 113302. (2015)

[2] Takahashi T., Mechanical characteristics of debris flow,*Journal of the Hydraulics Division*, **104**:1153-1169. (1978)

cmg2016 - - Monday, June 6, 2016 - 11:45/12:30 (45min)

STREAK INSTABILITY INDUCED BY BEDLOAD DIFFUSION

A. Abramian[1], O. Devauchelle[1] & E. Lajeunesse[1]
[1]*Institut de Physique du Globe, Paris, France*

Key words Geomorphology, granular material, instability, sediment transport.

An alluvial river forms its bed with the sediment it transports, either in the bulk of the flow (suspended load) or in a thin layer near the bed surface (bedload). The channel bounds the flow, which in turns deforms it by erosion and sedimentation. This coupling between flow and bedload transport spontaneously selects the shape and size of the river.

Gravity pulls the moving grains towards the center of the channel, thus eroding the banks continually [1]. However, laboratory observations show that, due to the roughness of the bed, the trajectory of a moving grain fluctuates in the transverse direction [2]. The bedload layer is therefore a collection of random walkers which diffuse towards the less active areas of the bed. In a river at equilibrium, bedload diffusion counteracts gravity to maintain the banks.

If an initially flat bed of sediment is perturbed with longitudinal streaks, the flow-induced shear stress is weaker where the flow is shallower. Therefore, we expect bedload diffusion to induce a flux of sediment towards the crests of the perturbation. This positive feedback induces an instability which can generate new channels. We suggest that this mechanism could explain the transition from single-thread rivers to braided ones.

References

[1] G. Parker, *Self-formed straight rivers with equilibrium banks and mobile bed.*, Journal of Fluid Mechanics **89**, 127-146 (1978).
[2] G. Seizilles et. al, *Cross-stream diffusion in bedload transport*, Physique of Fluids **26**, 013302 (2014).

cmg2016 - - Monday, June 6, 2016 - 11:45/12:30 (45min)

LABORATORY ALLUVIAL FAN BUILT BY A SINGLE CHANNEL

P. Delorme[1], O. Devauchelle[1], L. Barrier[1] & F. Métivier[1]
[1]*Institut de Physique du Globe de Paris, Paris, France*

Key words Alluvial fan, analog experiments, single channel river

When a river leaves a mountain range to enter a flat plain, the abrupt change in slope causes it to deposit its load into an alluvial fan. To understand this process, we develop a laboratory experiment where a single channel deposits corundum sand (0.3 mm) into a conical fan. We record the fan progradation with top-view images, and mesure its shape using the deformation of a Moiré pattern. The fan remains virtually self-affine as it grows, with a nearly constant slope. Assuming that the river is close to the threshold for sediment transport, we can relate the the fan morphology to the fluid and sediment discharges [1, 2]. At first order, the water discharge controls the longitudinal slope of the fan, in accordance with our laboratory observations. However, due to the downstream decrease of the sediment load, we expect this slope to get shallower towards the fan's toe. This suggests that the curvature of an alluvial fan could inform us about its growth velocity.

References

[1] Guerit. L, Métivier. F, Devauchelle. O, Lajeunesse. E and Barrier, L *Laboratory alluvial fans in one dimension*, Physical Review E (2014).
[2] Seizilles. G, Devauchelle. O, Lajeunesse. E and Metivier, F *Width of laminar laboratory rivers* Physical Review E (2013)

cmg2016 - - Monday, June 6, 2016 - 11:45/12:30 (45min)

Dynamic suspensions by air injection

C. Picard[1], V. Vidal[1] & S. Joubaud[1]
[1]*Laboratoire de Physique, Université de Lyon, École Normale Supérieure de Lyon - CNRS 46 Allée d Italie, 69364 Lyon cedex 07, France*

Key words Suspension ; Granular matter ; Triphasic flow.

Triphasic flows (grains-liquid-gas) has applications in a wide range of systems. In geophysics, the understanding of the sequestration of gas in oceanic sediments is crucial; in particular, their subsequent release may entail huge cracks [1]. In the industy (petrochemistry, food industry), catalytic gas-fluidized bed reactors have been widely investigated. The objective is to optimize the flow in order to increase the contact surface and mass transfer between gas and liquid phases [2].

Contrary to diphasic flows liquid-grains or gas-grains [3], triphasic cases are less understood due to the complex dynamic of gas through the immersed granular matter [4]. In fact, fundamentally, the three phases and their interaction s play a role on the dynamics of such flow. Different time and length scales will therefore be involved: grains/grains interactions, hydrodynamic coupling between liquid, gas and particles movement, etc. In the particular case where particles are slightly heavier than the liquid, competition between settling and transport is important.

We study experimentally the behavior of an immersed granular layer in a Hele-Shaw cell, when air is injected at the bottom center of the granular bed. The gas initially percolates through the grains (Fig. 1a), then forms bubbles which rise and transport particles in the above liquid (Fig. 1b-1c). The particles settle back on the edges of the cell, deposit and avalanche on the crater formed at the granular bed free surface, and are further entrained by the continuous bubbling at the center (Fig. 1d-1e). We therefore create a dynamic suspension.

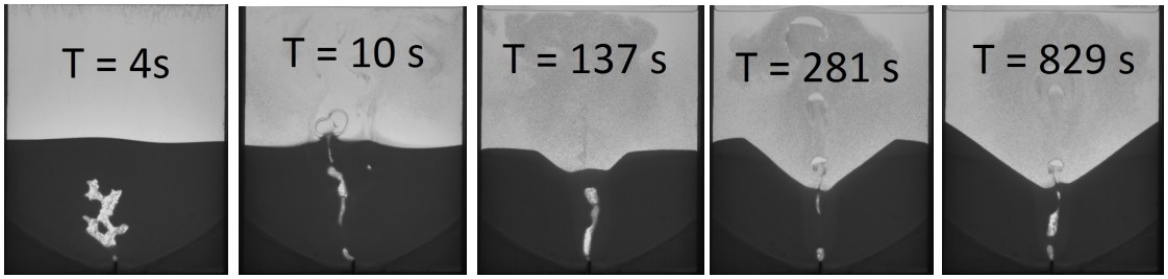

Figure 1 : Temporal evolution of the studied triphasic flow

The study focuses on particles slightly heavier than the surrounding fluid. First, we report the existence of a steady-state, resulting from the balance between particle transport and settling. We quantify so the size of a « dead zone », a part of the granular bed which is not affected by the air flow. A detailed study of the influence of the different parameters (air flow-rate, particle density, cell width…), points out that the bubbles, and especially their characteristic size, are the controlling parameter of this triphasic flow.

References

[1] Q. Kang, I. Tsimpanogiannis, D. Zhang, P. Lichtner, *Numerical simulation of porescale phenomena during CO2 sequestration in oceanic sediments,* Fuel Process. Technol. **86**, 1647-1665 (2005).
[2] M. Dudukovic, F. Larachi, P .Mills, *Multiphase catalytic reactors : A perspective on current knowledge and future trends,* Catal. Rev. Sci. Eng. **44(1)**, 123-246 (2002).
[3] F. Zoueshtiagh, A. Merlen, *Effect of a vertically flowing water jet underneath a granular bed,* Phys. Rev. **E75**, 056313 (2007).
[4] C. Chevalier, A. Linder, M. Leroux, *Morphodynamics during air injection into a confined granular suspension,* J. Non-Newtonian Fluid Mech. **158**, 63 (2009).

cmg2016 - - Monday, June 6, 2016 - 11:45/12:30 (45min)

NUMERICAL SIMULATION OF THE DYNAMICS OF SEDIMENTARY RIVER BEDS WITH A STOCHASTIC EXNER EQUATION,

E. Audusse[1], S. Boyaval[2], N. Goutal[2,3], M. Jodeau[3] & P. Ung[3,4]
[1]*LAGA, Université Paris 13, Villetaneuse, France*
[2]*Lab. Saint-Venant, Chatou, France*
[3]*EDF-LNHE, Chatou, France*
[4]*MAPMO, Univ. Orléans, Orléans, France*

Key words Sediment transport, Exner equation, Uncertainties quantification

At the scale of a river reach, the dynamics of the river bed is typically modelled in industrial softwares by Exner equation (conservation of the solid mass) with an empirical solid flux of transported sediments, which is a simple deterministic algebraic formula function of i) the sediment physical characteristics (size and mass) and of ii) the averaged hydrodynamical description of the ambient water flow computed through the solution of a Saint-Venant type model. This model has proved useful, in particular through numerical simulations, for hydraulic engineering purposes (like estimating the mass of sediments that is drained through an open dam). Though, the model is also coarse. And its applicability at various space and time scales remains a question of considerable interest for engineers and researcher in sediment transport. In particular, physical experiments from the grain scale to the laboratory scale reveal important fluctuations of the solid flux in given hydrodynamical conditions [1, 2] . This work is a preliminary study of the coupling of a stochastic Exner equation with a Saint-Venant type hydrodynamical model for large scales. Stochastic models with a probabilistic solid flux are currently being investigated by various team, but most often from the viewpoint of theoretical physics at the grain scale [3, 4]. It seems to us that there is still a need for computer experiments in order to investigate how the stochastic approach can be used by engineers that are involved in applied hydraulics studies. In this talk we propose first to study a stochastic Saint-Venant model with perturbed bottom using numerical simulations in an appropriate test case. We exhibit a necessary relation between the bottom fluctuations and the friction coefficient to ensure equilibrium, see Fig. 1 on the left. We also show the convergence toward a steady state and analyze in details the sensibility of this steady state to the input perturbations, with particular attention to hydrodynamic variance and covariance results, see Fig. 1 on the right. In a second step, we introduce a stochastic Saint-Venant–Exner model with a perturbed sediment flux and present some results in this more complex framework. A first part of this work was published in [5].

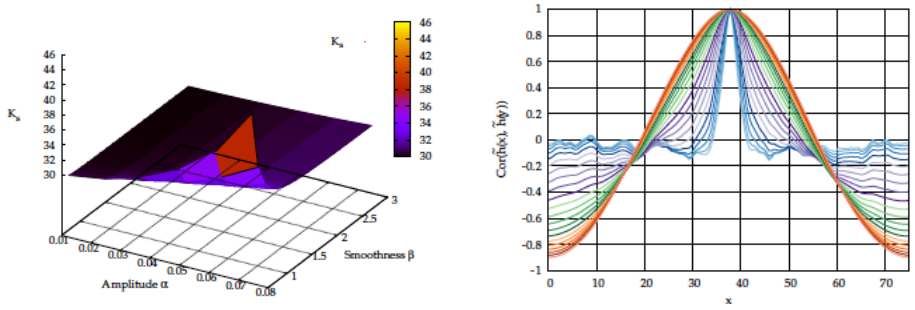

Figure 1. On the left : Evolution of the friction coefficient as a function of the parameters describing the perturbed bottom - On the right : Correlation of the water height as a function of the smoothness parameter of the perturbed bottom.

References

[1] E. Lajeunesse, L. Malverti, and F. Charru. Bed load transport in turbulent flow at the grain scale: Experiments and modeling, *Journal of Geophysical Research*, Vol. 115, 2010.
[2] Recking, A and Frey P. and Paquier, A. and Belleudy, P. and Champagne, J.Y. Bed-Load Transport Flume Experiments on Steep Slopes, *Journal of hydraulic Engineering* , Vol. 134-9, 2008
[3] C. Ancey, Stochastic modeling in sediment dynamics: Exner equation for planar bed incipient bed load transport conditions, *Journal of Geophysical Research*, Vol. 115, 2010.
[4] D.J. Furbish, M.W. Schmeeckle, Probabilistic Formulation of the Exner Sediment Continuity Equation and the Bedload Flux for the Case of Uniform Sediment
[5] E. Audusse, S. Boyaval, N. Goutal and M. Jodeau, P. Ung, Numerical simulation of the dynamics of sedimentary river beds with a stochastic Exner equation, *Esaim: Proceedings and Surveys*, Vol. 48, 2015.

cmg2016 - - Monday, June 6, 2016 - 11:45/12:30 (45min)

INFLUENCE OF MECHANICAL VIBRATIONS ON GRANULAR FRICTION

H. Lastakowski[1], J.-C. Géminard[1] & V. Vidal[1]
[1]*Laboratoire de Physique, École Normale Supérieure de Lyon, Université de Lyon, CNRS, France*

Key words Granular friction, stick-slip motion, vibrations, dynamic earthquake triggering.

Triggering large-scale motion by imposing vibrations to a system can be encountered in many situations, from daily-life shaking of saltcellar to silo unclogging or dynamic earthquakes triggering [1, 2, 3]. In the well-known situation of solid or granular friction, the acceleration of imposed vibrations has often been proposed as the governing parameter for the transition between stick-slip motion and continuous sliding [4]. The threshold acceleration for the onset of continuous slip motion or system unjamming is usually found of the order of the gravitational acceleration [4, 5]. These conclusions are mostly drawn from numerical studies.

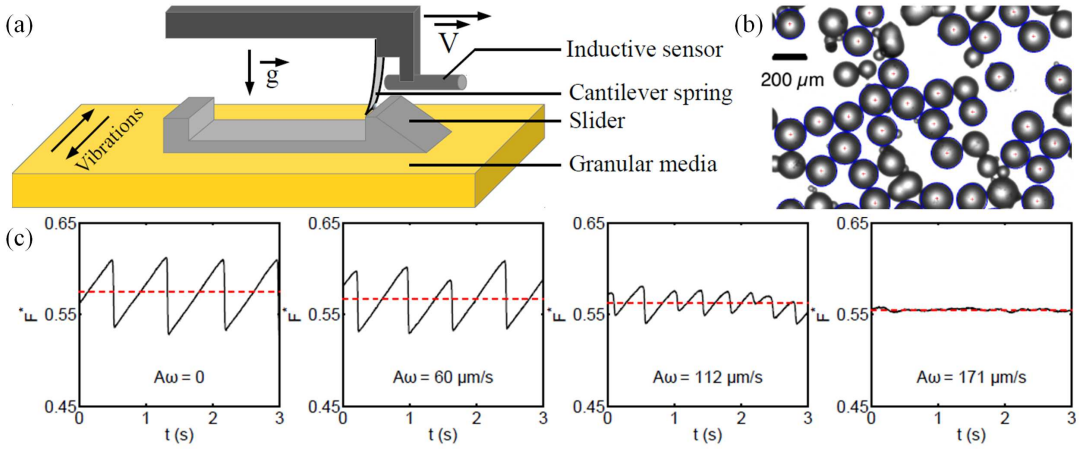

Figure 1. (a) Experimental setup. A slider (mass m) is pulled at constant velocity V, via a cantilever blade, on a granular layer. (b) Typical grains used in the experiments (polydisperse spherical glass beads). (c) Effect of the mechanical vibrations (amplitude A, frequency ω) on the stick-slip motion. F^*=F/mg indicates the normalized force applied on the slider. The stick-slip amplitude (initially without vibration, left panel) decreases (middle panels) until the system undergoes a continuous slip motion.

We investigate, in the laboratory, granular friction by shearing a layer of grains subjected to horizontal vibrations (Fig. 1a,b). When increasing either the amplitude A or frequency ω of the vibrations, the amplitude of the stick-slip motion decreases, until the system exhibits a transition to a continuous slip motion (Fig. 1c). Therefore, under mechanical vibrations, both the static and dynamic friction coefficients decrease. We show that, in contrast to previous results, the quantity that controls the frictional properties is the characteristic velocity $A\omega$, and not the acceleration $A\omega^2$, of the imposed mechanical vibrations [6]. The critical velocity at which the system undergoes the transition to a continuous slip motion is very small, of the order of 100 μm/s. Thus, when the system is statically loaded, the typical acceleration of the vibrations which trigger large slip events is much smaller than the gravitational acceleration. These results may be relevant to understand dynamic earthquake triggering by small ground perturbations [3].

References

[1] A. Janda, D. Maza, A. Garcimartín, E. Kolb, J. Lanuza & E. Clément, *Unjamming a granular hopper by vibration*, Europhysics Lett. **87**, 24002 (2009).
[2] P.A. Johnson & X. Jia, *Nonlinear dynamics, granular media and dynamic earthquake triggering*, Nature **437**, 871–874 (2005).
[3] J. Gomberg, P. Reasenberg, P. Bodin & R. Harris, *Earthquake triggering by seismic waves following the Landers and Hector Mine earthquakes*, Nature **411**, 462–466 (2001).
[4] A.L. Sellerio, D. Mari, G. Gremaud & G. D'Anna, *Glass transition associated with the jamming of vibrated granular matter*, Phys. Rev. E **83**, 021301 (2011).
[5] M. Pica Ciamarra, A. Coniglio, D. De Martino & M. Nicodemi, *Shear-and vibration-induced order-disorder transitions in granular media*, Eur. Phys. J. E **24**, 411–415 (2007).
[6] H. Lastakowski, J.-C. Géminard & V. Vidal, *Granular friction: Triggering large events with small vibrations*, Sci. Rep. **5**, 13455 (2015).

cmg2016 - - Monday, June 6, 2016 - 11:45/12:30 (45min)

THE UNDERESTIMATED ROLE OF PARTICLE-BED IMPACTS FOR SEDIMENT TRANSPORT IN A NEWTONIAN FLUID

Thomas Pähtz[1] & Orencio Durán[2]

[1]*Institute of Physical Oceanography, Ocean College, Zhejiang University, China*

[2]*Department of Physical Sciences, Virginia Institute of Marine Sciences, College of William and Mary, USA*

Key words sediment transport, bedload, saltation, particle-bed impacts, sediment entrainment

Particle-bed impacts have long been thought to play a predominant role in sustaining aeolian sediment transport, but a negligible role in sustaining subaqueous sediment transport. Here, using numerical simulations with the coupled DEM/RANS model of sediment transport in a Newtonian fluid by Duran et al. [1], we present threefold evidence for the hypothesis that the transition between fluid-sustained and impact-sustained transport occurs at a critical impact number ($\mathrm{Im} = \Theta \mathrm{Re}\sqrt{s} \approx 3$), where Θ is the Shields number, Re the particle Reynolds number, and s the particle-fluid-density ratio. First, we show that the effective particle slip velocity gradient in natural units becomes a universal constant when $\mathrm{Im} \gtrapprox 3$. A constant slip velocity has always been recognized as one of the main implications of the fact that particle-bed impacts ("splash") sustain aeolian saltation [1]. Second, we show that the threshold of sediment-transport cessation for fully viscous transport with sufficiently large transport layers obeys $\Theta_t \approx 3(\mathrm{Re}\sqrt{s})^{-1}$, which indicates that Θ_t is just large enough to achieve the necessary slip velocity gradient required for impact-sustained transport. Third, we show that the efficiency of particle-bed impacts in dissipating fluctuation energy reaches a maximal value when $\mathrm{Im} \gtrapprox 3$, which suggests a strong connection between impact entrainment and fluctuation-energy dissipation. Our results imply that only a few relevant sediment-transport regimes (e.g., transport of quartz in water with boundary Reynolds numbers $\mathrm{Re}_b = \mathrm{Re}\sqrt{\Theta_t} \lessapprox 6$) are sustained through direct fluid entrainment, while the vast majority of regimes are sustained through impact entrainment. Our movies, however, indicate that impact entrainment does not necessarily refer to the ejection of bed particles like for aeolian saltation. In the case of bedload, impacting particles rather tend to drag bed particles in front of them.

References

[1] O. Durán, P. Claudin, B. Andreotti *Numerical simulation of turbulent sediment transport, from bed load to saltation*, Physics of Fluids **24**, 103306 (2012).

cmg2016 - - Monday, June 6, 2016 - 11:45/12:30 (45min)

THE ROLE OF THE HYPORHEIC FLOW ON THE STABILITY OF AN ERODIBLE BED: A LABORATORY APPROACH USING PARTICLE IMAGE VELOCIMETRY

G. Rousseau[1], D. Papa[1] & C. Ancey[1]
[1]*Ecole Polytechnique Fédérale de Lausanne (EPFL), Switzerland*

The study of river dynamics usually assumes a turbulent stream on a simplified impermeable bed. However, it is known that up to one third of the total discharge can occur through the erodible bed and especially in mountain rivers context. This hyporheic flow must play an active role on the stability of the erodible bed. The question then arises: How does the hyporheic flow affect the stability of the bed and therefore the bedload transport? Part of the reason of this lack of understanding lies in the difficulty to actually measure the hyporheic flow in natural situations. Laboratory conditions and new measuring techniques bring new perspectives to shed light to this problem. Using PIV-LIF method (Particle Image Velocimetry âĂŞ Laser Induced Fluorescence) we investigate this phenomenon on an erodible bed.

The experiment is conducted in a 2-m-long and 3.4-cm-width flume with 4-mm-diameter glass beads in turbulent stream conditions. Thanks to a gate we are able to force or not the hyporheic flow in the granular bed.

Interestingly, the presence of hyporheic flow affects the bed load transport in a way that less shear stress is needed to initiate the movement of particles. The PIV-LIF results show us that the presence of a hyporheic flow modify the velocity profile and the turbulence. With the hyporheic flow the velocity becomes higher around the grains that are on the bed and facilitate the movement. Experiments are under way to determine the effect of the bed slope on the exchange between the hyporheic and the surface flow. This measurements also shows the important role of the outlet boundary condition in classical flumes since the usual impermeable wall changes the hydraulics conditions upstream.

Hot flows

cmg2016 - - Tuesday, June 7, 2016 - 10:30/10:45 (15min)

STRETCHING THE TRUTH: HOW DO PARTICLES AND EDDIES INTERACT TO MODIFY TURBULENT ENTRAINMENT INTO VOLCANIC JETS?

D. E. Jessop[1,2], A. M. Jellinek[2], J. Dufek[3]
[1]*Laboratoire Magmas et Volcans, Clermont-Ferrand, France*
[2]*University of British Columbia, Vancouver, Canada*
[3]*Georgia Institute of Technology, USA*

Key words Turbulent entrainment; volcanic jets; Stokes number effects

Volcanic jets are highly turbulent mixtures of gas and ash, containing a wide range of particle sizes that are formed during powerful explosive eruptions. Turbulent entrainment is arguably the most important factor in determining the stability of volcanic jets as it allows for the initially negatively buoyant jet to undergo a buoyancy reversal through the entrainment and mixing of ambient air. To physically entrainment fluid into a jet requires the eddies that form its edges to do work in overturning and mixing the density interface between the jet and the ambient air. The ability of a jet to do this mixing is characterised through the Richardson number, $\mathrm{Ri} = g'b/u^2$. These eddies overturn the fluid and the mixing is done by smaller eddies which results in an energy cascade from large to small structures. The energy contained by the eddies at the various scales is therefore strongly affected by the particle-fluid coupling as this alters the eddy size and energy. A useful metric for the particle-fluid stress coupling is the Stokes number, St: when St is small, particles follow fluid pathlines exactly whereas at large St particles have important inertia and are unaffected by accelerations in the flow field. However when $St \sim 1$, particle accelerations influence the flow and flow accelerations influence particle trajectories. These inertial particles thus influence the angular momentum, shape and entraining properties of eddies.

Recent experimental work has shown that entrainment into particle-laden jets varies significantly from particle-free jets [1, 2]. These works also showed that whether enmathrmtrainment is increased (promoting the formation of stable plumes) or decreased (promoting unstable collapsing fountains and the formation of pyroclastic mathrmflows) depends strongly on the geometry of the vent. Accordingly, we perform novel laboratory experiments and numerical calculations containing $\mathrm{St} \sim 1$ particles and measure the energy spectra in jets where the particle concentration (ϕ) and Ri are varied (see Fig. 1). We find that an anisotropy is induced in the turbulent structure of particle-laden jets, which is greatest when Ri is large and note that the same anisotropy is not present in particle-free jets at similar Ri. We interpret these results in terms of how eddies are stretched by the critical coupling with $\mathrm{St} \sim 1$ particles and the ability of these stretched eddies to entrain ambient fluid through the overturning and mixing of the density interface.

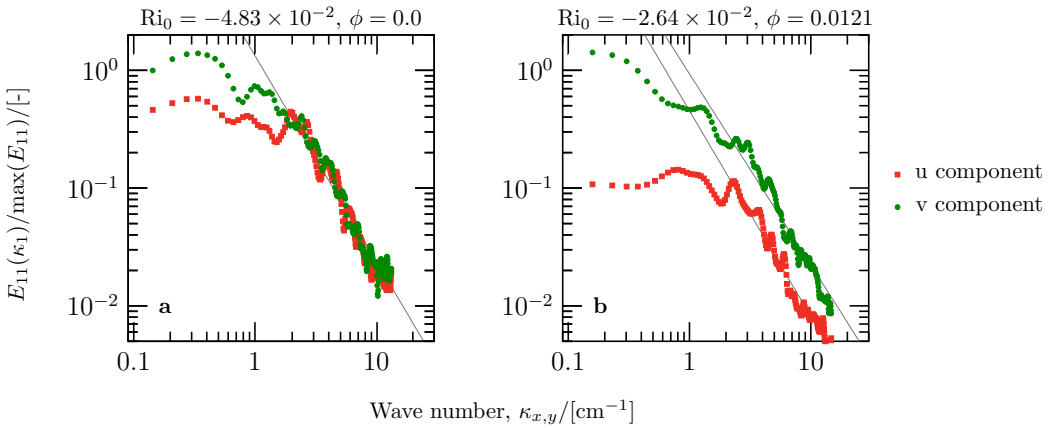

Figure 1. Energy spectra for two jets with equivalent Ri but different particle concentration. The separation of the spectra for the u and v velocity components in the right-hand plot suggests anisotropic turbulence induced by the presence of particles. The lines fitted to the data show approximately -5/3 slopes.

References

[1] D. E. Jessop and A. M. Jellinek. Effects of particle mixtures and nozzle geometry on entrainment into volcanic jets. *Geophys. Res. Lett.*, 41:1–6, 2014.

[2] D. E. Jessop, J. Gilchrist, A. M. Jellinek, and O. Roche. The effect of inertial particles, linear and annular vents on entrainment into volcanic jets. *Earth Planet. Sc. Let.*, in review.

cmg2016 - - Tuesday, June 7, 2016 - 9:30/9:45 (15min)

BOUNDARY CONDITION OPTIMAL CONTROL PROBLEM IN LAVA FLOW MODELLING

A. Ismail-Zadeh[1 2 3], A. Korotkii[1 4 5], D. Kovtunov[1], O. Melnik[1 6] & I. Tsepelev[1 5]

[1] *Karlsruhe Institute of Technology, Institute of Applied Geosciences, Karlsruhe, Germany*
[2] *Russian Academy of Sciences, Inst. of Earthquake Prediction Theory and Math. Geophysics, Moscow, Russia*
[3] *Institut de Physique du Globe, Paris, France*
[4] *Institute of Mathematics and Computer Sciences, Ural Federal University, Yekaterinburg, Russia*
[5] *Institute of Mathematics and Mechanics, Russian Academy of Sciences, Yekaterinburg, Russia*
[6] *Institute of Mechanics, Lomonosov Moscow State University, Moscow, Russia*

Key words inverse theory, adjoint method, numerical solutions

Rapid development of ground based thermal cameras, drones and satellite data allows getting repeated thermal images of the surface of the lava flow. Available instrumentation allows getting a large amount of data during a single lava flow eruption. These data require development of appropriate quantitative techniques to link subsurface dynamics with observations. We present a new approach to assimilation of thermal measurements at lava's surface to the bottom of the lava flow to determine lava's thermal and dynamic characteristics.

We study a problem of steady-state fluid flow with known thermal conditions (e.g., measured temperature and the heat flux at the surface of lava flow) at upper segment of the model boundary and unknown conditions at its lower segment. This problem belongs to a class of boundary condition optimal control problems and can be solved by assimilation of the data from the upper to lower boundary using direct and adjoint models. We derive analytically the adjoint model and test the cost function and its gradient, which minimize the misfit between the known thermal condition and its model counterpart. Using optimization algorithms, we iterate between the direct and adjoint problems and determine the missing boundary condition as well as thermal and dynamic characteristics of the fluid flow. The efficiency of optimization algorithms – Polak-Ribiere conjugate gradient and the limited-memory Broyden-Fletcher-Goldfarb-Shanno algorithms – have been tested with the aim to get a rapid convergence to the solution of this inverse ill-posed problem.

Numerical results show that in the case of smooth input data lava temperature and velocity can be determined with a high accuracy. A noise imposed on the smooth input data results in a less accurate solution, but still acceptable below some noise level. The proposed approach to assimilate measured data brings an opportunity to estimate thermal budget of the lava flow.

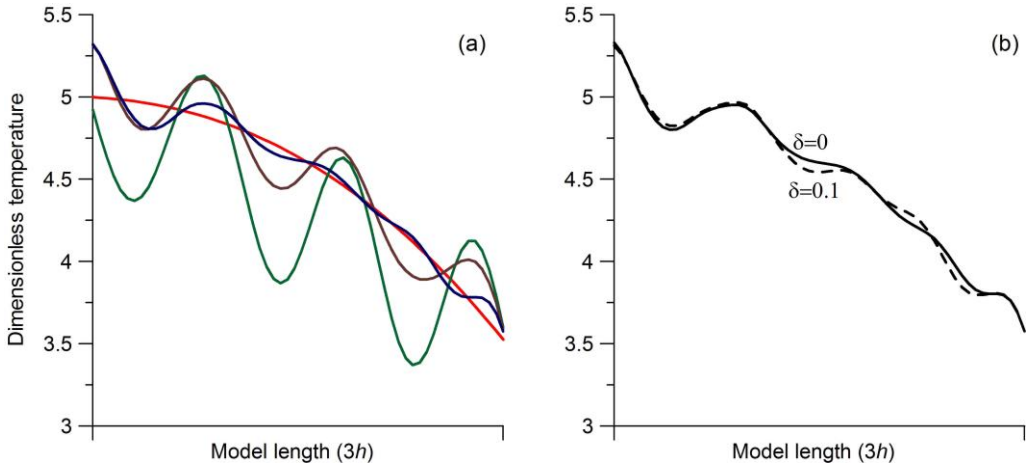

Figure 1. Reconstruction of the temperature at the lower segment of the model boundary (*a*). The red curve corresponds to the target temperature, the green curve to the guess temperature, the brown curve to the temperature after 5 iterations, and the blue curve to the temperature after the 10 iterations. The reconstructed temperature after 10 iterations (*b*) in the case of no noise in the heat flow at the upper segment of the model boundary (solid line; the blue curve in *a*) and in the case of noise in the heat flow (dashed line).

cmg2016 - - Tuesday, June 7, 2016 - 10:45/11:00 (15min)

GRAVITATIONAL INSTABILITIES IN VOLCANIC ASH DEPOSITION : THEIR ROLE AND THEIR DYNAMICS

I. Manzella[1], C. Bonadonna[1], S. Scollo[2], J. C. Phillips[3] & H. Monnard[1]
[1]*Department of Earth Sciences, University of Geneva, Switzerland.*
[2]*Istituto Nazionale di Geofisica e Vulcanologia, Osservatorio Etneo, Sezione di Catania, Italy.*
[3]*School of Earth Sciences, University of Bristol, United Kingdom.*

Key words Gravitational and convective instabilities, fingers, tephra dispersal, fine ash deposition, aggregation, 2010 Eyjafjallajökull eruption

Volcanic ash is a significant hazard for areas close to volcanoes and for aviation. Gravitational instabilities forming at the bottom of spreading volcanic clouds have been observed in many explosive eruptions. For the first time here, we characterize the dynamics of gravitational instabilities from analysis of video imagery from the 2010 eruption of Eyjafjallajökull (Iceland) and field observations of the associated tephra accumulation (Bonadonna et al. [1]) in combination with insights from dedicated laboratory analogue experiments. We analyzed the propagation of fingers recorded using high-resolution video (see Fig. 1) taken on 4th May 2010 (12:49:21 GMT) at a position 7.7 km south of the vent (0568182E, 7047683N). Gravitational instabilities initially took the form of downward-propagating fingers that formed continuously at the base of the cloud, and appeared to be advected passively at the crosswind speed. Measurements of finger propagation are consistent with initial conditions inferred from previous studies of ash cloud dynamics. Our observations challenge the view that aggregation is the primary explanation of proximal fine ash sedimentation, and give direct support for the role of gravitational instabilities in providing regions of high particle concentration that can promote aggregation.

We also developed dedicated laboratory analogue experiments similar to that of Hoyal et al. [4] with an aqueous suspension of particle-laden fluid initially overlying a higher density sugar solution. Two main experimental campaigns have ben carried out, the first one to investigate the evolution of particle concentration in the mixing region that results from propagation of gravitational instabilities and the second one to study the effect of particle size, composition and concentration on finger dynamics and generation. The experimental set-up consisted of a Plexiglas tank of 50 x 30.3 x 7.5 cm equipped with a removable banner for the partition of the two separate layers. In the first series of experiments we used Glass Beads of a diameter range of 45-63 μm, in the second one we used particles of different composition: i.e. Glass Beads with three different diameter range '< 32 μm', '45-63 μm', and '63-90 μm' and Andesitic, Rhyolitic, and Basaltic Volcanic Ash with diameter range of '< 32 μm', '45-63 μm', '63-90 μm', '90-125 μm', '125-180 μm' and '> 180 μm'. Three initial particle concentrations in the upper layer were employed: 3 g/l, 4 g/l and 5 g/l. Results show that finger downward propagation significantly exceeded the settling speed of individual particles, demonstrating that gravitational instabilities provide a possible mechanism for enhanced sedimentation of fine ash and confirming what also suggested by Carazzo and Jellinek [2, 3]. In addition analysis of the finger dynamics show that the number and the speed of fingers increase with particle concentration and the speed increases with particles size while it is independent on particle composition.

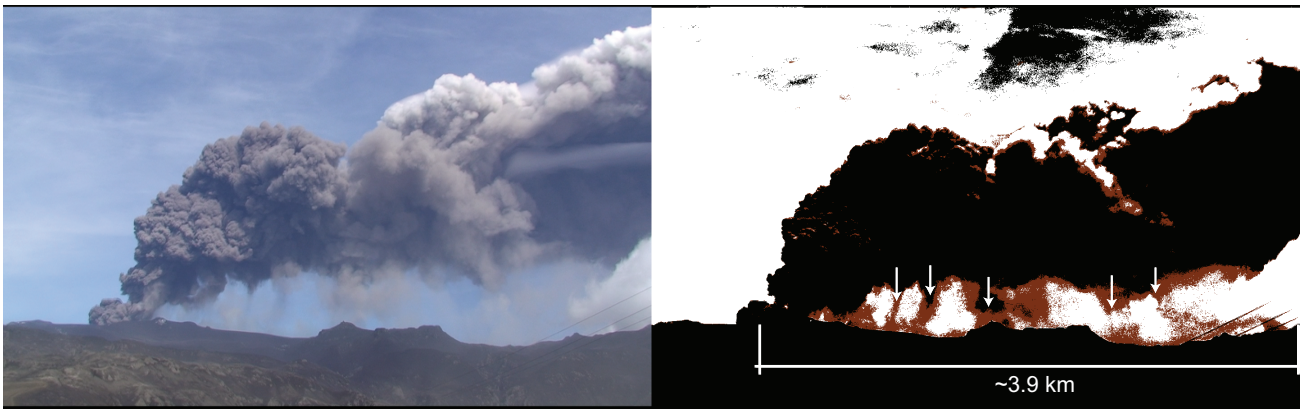

Figure 1. Original and processed snapshot of the video of the Eyafjallajökull plume as observed on 4th May 2010. Finger position is indicated with white arrows (from Manzella et al [5]).

cmg2016 - - Tuesday, June 7, 2016 - 10:45/11:00 (15min)

References

[1] C. Bonadonna, R. Genco, M. Gouhier, M. Pistolesi, R. Cioni, F. Alfano, A. Hoskuldsson, M. Ripepe, *Tephra sedimentation during the 2010 Eyjafjallajökull eruption (Iceland) from deposit, radar, and satellite observations*, Journal of Geophysical Research. Solid Earth **116**, no. B12 (2011)
[2] G. Carazzo, A.M. Jellinek, *A new view of the dynamics, stability and longevity of volcanic clouds*, Earth and Planetary Science Letters **325–326**, 39–51 (2012)
[3] G. Carazzo, A.M. Jellinek, *Particle sedimentation and diffusive convection in volcanic ash-clouds*, Journal of Geophysical Research. Solid Earth, **118, no. 4** 1420–1437 (2013)
[4] D. C. J. D Hoyal, M. I. Bursik, J.F. Atkinson, *Settling-driven convection: A mechanism of sedimentation from stratified fluids*, Journal of Geophysical Research-Oceans **104, no. C4**, 7953-7966 (1999)
[5] I. Manzella, C. Bonadonna, J.C. Phillips, H. Monnard, *The role of gravitational instabilities in deposition of volcanic ash*, Geology **43**, 211–214 (2015)

cmg2016 - - Tuesday, June 7, 2016 - 9:45/10:00 (15min)

EXPERIMENTS ON ENTRAINMENT OF A GRANULAR SUBSTRATE BY PYROCLASTIC FLOWS AND IMPLICATIONS FOR THE PEACH SPRING TUFF SUPER-ERUPTION (USA)

O. Roche[1], D. Buesch[2], G. Valentine[3]
[1]*Laboratoire Magmas et Volcans, Université Blaise Pascal-CNRS-IRD, OPGC, F-63038 Clermont-Ferrand, France.*
[2]*U.S. Geological Survey, 345 Middlefield Road, MS 973, Menlo Park, CA 94025, USA.*
[3]*Department of Geology and Center for Geohazards Studies, University at Buffalo, Buffalo, NY 14260, USA.*

Key words Pyroclastic flows, explosive volcanism, super-eruption, substrate entrainment, discharge rate.

Pyroclastic flows are ground hugging gas-particle mixtures generated during volcanic eruptions. The most voluminous flows are produced by super-eruptions associated with caldera collapse. They are characterized by long run-out distances >100 km on relatively horizontal topographies and form deposits of volume typically >500-1000 km^3. Such pyroclastic flows often entrain large blocks of size of 0.5-1 m from the underlying substrate, which is likely to give insights into the flow dynamics. The entrainment mechanisms of these blocks are poorly understood. We studied the emplacement mechanisms of pyroclastic flows on a granular substrate through laboratory experiments of dense gas-particle flows generated by sudden (dam-break) release of a granular material fluidized in a reservoir and that propagated over a horizontal granular layer of particles in a channel (Fig. 1). The particles were fine glass beads of diameter d=80 µm, which conferred a hydraulic permeability of ~10^{-11} m^2 to the mixture. The low permeability permitted slow diffusion of the interstitial pore-fluid pressure during flow so that the dense mixture propagated in a fluid-like state. The granular substrate consisted of a horizontal layer of coarse steel beads of size d=1500-1590 µm. Experiments filmed at 500-1000 frames/s showed how the large beads were entrained from the granular substrate by the dense gas-particle flow (Fig. 1). Most of the uppermost substrate beads were first surrounded by the fine flow particles, extracted from the substrate, and then dragged slowly at flow base. Many of the dragged beads were uplifted into the flow at a critical velocity [1], to a height up to ~6-8 mm, and were transported downstream. These beads finally settled at flow base and stopped moving at the same time as the granular flow, at height up to ~4-5 mm above the original top of the substrate. We combined our experimental results with the model of [1] to investigate the mechanisms of the pyroclastic flows that formed the >1300 km^3 Peach Spring Tuff (western USA) during the ~18.8 Ma Silver Creek caldera super-eruption, which travelled as far as ~175 km from the eruptive center [2-3]. The Peach Spring Tuff contains substrate-derived blocks up to ~70-90 cm that were entrained along the flow paths by the pyroclastic flows over distances of tens to a several hundreds of meters. Application of the model of [1] suggests that the basal part of the pyroclastic flows had high particle concentrations and that entrainment of the largest substrate blocks required a relatively uniform and modest speed of ~5-20 m/s, which corresponds to a maximum discharge rate of ~10^7-10^8 m^3/s (or ~10^{10}-10^{11} kg/s) for a minimum of 2-8 hours. These rates are two to three orders of magnitude higher than those of the 1991 Mount Pinatubo and the AD 79 Vesuvius eruptions, but are similar to those of other caldera-forming eruptions such as Tambora (~75 ka) and Taupo (~1.8 ka). These results provide new insights into the emplacement dynamics of pyroclastic flows produced by super-eruptions.

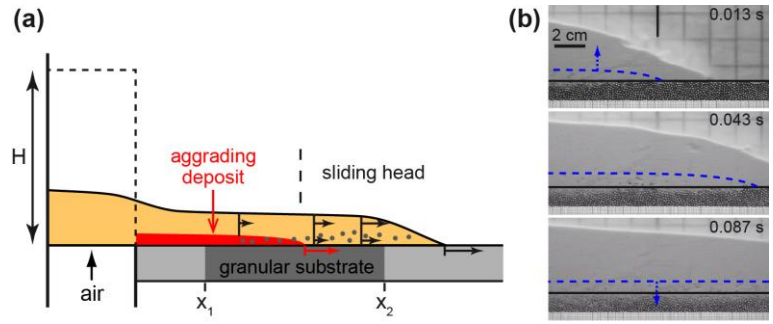

Figure 1. (a) Experimental device. (b) Entrainment of the substrate particles by the gas-particle flow.

References

[1] Roche O. , Y. Niño, A. Mangeney, B. Brand, N. Pollock, G. Valentine, *Dynamic pore pressure variations induce substrate erosion by pyroclastic flows*, Geology **41**, 1107-1110 (2013).
[2] G.A. Valentine, D.C. Buesch, R.V. Fisher, *Basal layered deposits of the Peach Springs Tuff, northwestern Arizona, USA*, Bull. Volcanol. **51**, 395-414 (1989).
[3] D.C. Buesch, *Incorporation and redistribution of locally derived lithic fragments within a pyroclastic flow*, Geol. Soc. Am. Bull. **104**, 1178-1193 (1992).

cmg2016 - - Tuesday, June 7, 2016 - 9:00/9:30 (30min)

SLUGS AND PLUGS – BIG EXPERIMENTS IN VOLCANO PHYSICS

EW Llewellin[1], E Del Bello[2], SA Mathias[1], SJ Lane[3], MR James[3], J Taddeucci[2], A Capponi[3], P Scarlato[2]
[1]*Dept. Earth Sciences, Durham University, Durham, UK*
[2]*INGV Rome, Italy*
[3]*Lancaster Environment Centre, Lancaster University, Lancaster, UK*

Key words Strombolian eruption; analogue experiments; volcanic conduits; gas slugs.

Strombolian activity is characterized by quasi-periodic, short-lived explosions, which vary greatly in magnitude. The explosions are understood to be driven by the bursting of large, overpressured 'slugs' of magmatic gas, which have ascended the conduit. We report analogue experiments[1,2], which model the fluid dynamics of slug-driven basaltic eruptions. Experiments were conducted in liquid-filled vertical pipes at a range of scales, from 0.02 to 0.25 m in diameter, and 2 to 13 m in height, allowing us to investigate Reynolds numbers $10^{-3} < Re < 10^{5}$, encompassing the natural range for volcanoes. The dynamics of both discrete gas slugs (Taylor bubbles) and continuous sluggy flow were quantified. A significant novelty of this study is that we explore the role played by the boundary conditions at the top and bottom of the conduit, which may be either blocked, plugged with a viscous liquid, or held at constant pressure, allowing us to mimic a range of natural conditions.

The presence of a viscous plug at the top of the conduit has been inferred from recent studies of strombolian pyroclasts, which indicate that degassed, crystal-rich magma, and gas-rich, crystal-poor magma co-exist and mingle in the shallow part of the volcanic conduit. We investigate the impact of the plug on eruptive behaviour experimentally, and find that the presence of a viscous plug enhances explosivity by increasing the overpressure within the ascending gas slug. We also find that the plug is prone to fluid-dynamic instability as the gas slug passes through it, causing the low and high viscosity magma analogues to intermingle, explaining the origin of the mingled pyroclasts observed in nature. The instabilities can also cause the slug to break into smaller pockets of gas, providing an explanation for pulsations in strombolian explosions, recently revealed by high-speed videography.

Separate analogue experiments, and numerical modelling, are used to investigate slug ascent under contrasting lower boundary conditions: zero-flux; and constant-pressure. Analogue conduit experiments typically use a zero-flux lower boundary (i.e. the base of the pipe is sealed). We show that a more-realistic constant-pressure boundary condition dramatically changes slug ascent velocity and the development of overpressure. Together these two studies constitute a new framework for understanding the role of the boundary conditions in shaping strombolian explosive activity.

Figure 1. Left) The Large Analogue Volcano Apparatus (LAVA); middle) analogue eruption of LAVA; right) eruption of Stromboli, Italy (from Stromboli online).

References

[1] Del Bello et al. 2015. Viscous plugging can enhance and modulate explosivity of strombolian eruptions. *Earth Planet. Sci. Lett.*, **423**, 210-218.
[2] Del Bello et al. 2012. An analytical model for gas overpressure in slug-driven explosions: insights into strombolian volcanic eruptions. *J. Geophys. Res.*, **117**, B02206

cmg2016 - - Tuesday, June 7, 2016 - 11:45/12:30 (45min)

The effects of solidification on sill propagation dynamics and morphology

L. Chanceaux[1] & T. Menand[1]
[1]*Laboratoire Magmas et Volcans, Université Blaise Pascal - CNRS - IRD, OPGC, Clermont-Ferrand, France*

Key words sill propagation, sill dynamics, solidification, pluton growth, sill morphology, analogue modelling

Sills are an integral part of the formation and development of larger plutons and magma reservoirs. Thus sills are essential for both the transport and the storage of magma in the Earth's crust. However, although cooling and solidification are central to magmatism, their effects on sills have been so far poorly studied. Here, the effects of magma cooling and solidification on sill propagation dynamics and morphology are studied by means of analogue laboratory experiments. Hot fluid vegetable oil (a magma analogue), that solidifies during its propagation, is injected as a sill in a colder layered gelatine solid (an elastic host rock analogue). The injection flux and temperature are maintained constant during an experiment. In order to vary the importance of solidification and quantify its effect on sill propagation, the injection flux and temperature are systematically varied between each experiment. The results are analysed using dimensionless analysis, allowing to extend the results to sill intrusion in nature.
Two extreme behaviours for sill propagation dynamics and morphology are observed. When solidification effects are small (high injection temperatures and fluxes), the propagation is continuous and the sill has a regular and smooth surface. Inversely, when solidification effects are important (low injection temperatures and fluxes), sill propagation is discontinuous and occurs by steps. After each propagation step, the sill stalls, thickens progressively by storing hot fluid vegetable oil beneath the partially solidified intrusion, without growing neither in length nor in breadth, and after a pause, the propagation initiates again, soon followed by a new episode of momentary arrest. The morphology of these sills displays ropy structures on their surface, and lobes with imprints of the leading fronts that correspond to each step of surface creation. These experiments show that for a given, constant injected volume, as solidification effects increase, the surface of the sills decreases, their thickness increases, and the number of propagation steps increases. In the same way lower solidification effects promote larger sill surfaces, lower thicknesses, and a lower number of propagation steps.

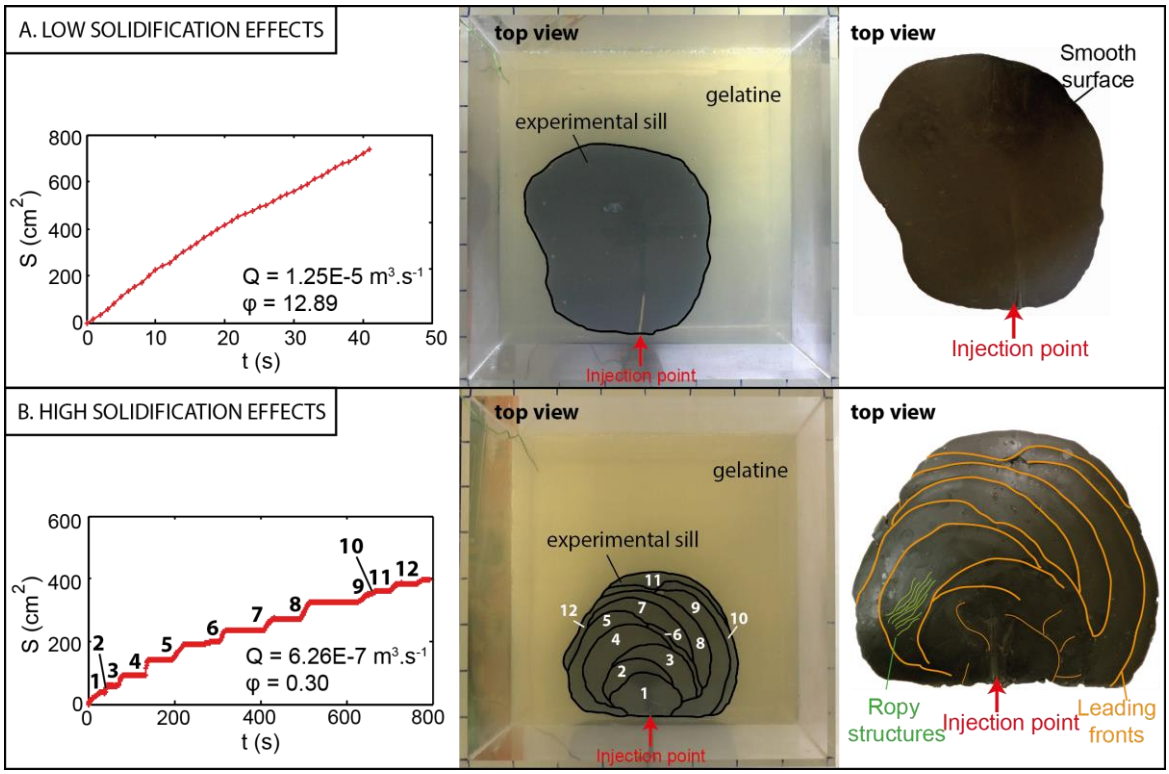

Figure 1: Presentation of the two end-members observed for the effects of solidification on sill intrusion.
(A) Example of an experiment with low solidification effects (high flux Q and dimensionless flux φ; φ is a Peclet number). Evolution of the area S with time t: continuous area creation and simple morphology (smooth surface).
(B) Example of an experiment with high solidification effects (low flux Q and dimensionless flux φ). Evolution of the area S with time t: 12 steps of area creation and complex morphology (ropy structures, imprints of the leading fronts).

These results have various geological and geophysical implications. Regarding the morphology of sills, 3D seismic studies in sedimentary basins reveal sills with lobate structures similar to those of lava flows. Our experiments show how these lobate structures could reflect the effect of magma solidification during their emplacement. Our experiments show also that a non-continuous morphology observed in the field may not necessarily imply multiple sill injections but could instead reflect a continuous, yet complex morphology induced by solidification effects during sill emplacement. Also, as for dykes, important solidification effects in sills will promote a discontinuous propagation associated with bursts of seismic activity, in agreement with the observed seismic activity that preceded the 2010 Eyjafjallajökull eruption. Finally, in restricting the lateral extent of sills, magma cooling and solidification are likely to impact directly the size of plutons constructed incrementally by amalgamated sills.

cmg2016 - - Tuesday, June 7, 2016 - 11:45/12:30 (45min)

NEW INSIGHTS ON MODELING VOLCANIC ASH AGGREGATION: A THEORETICAL VIEW

E.Rossi[1], C.Bonadonna[1]
[1]*Univerity of Geneva, Geneva, Switzerland*

Key words Volcanic ash, Aggregation, Smoluchowski, Sectional methods

Particle aggregation is considered as a key process that may affect dispersal and sedimentation of volcanic ash, with significant implications for the associated hazards. For instance it is well known that aggregation has a major role in particle sedimentation affecting the residence time of volcanic ash in the atmosphere. So far the theoretical description of volcanic ash aggregation is commonly related to the solution of the Smoluchowski Coagulation Equations (SCE), a set of Ordinary Differential Equations (ODEs) which basically describe the change in time of an initial grain-size distribution due to the interaction of "single" particles. The complete solution of SCE is conditioned by our general knowledge of the physics of interaction between classes of particles (kernels) and our capability to solve a set of equations which is theoretically infinite. One of the possible approaches to the solution of SCE is to reduce the continuous particle distribution to a finite number of classes [1]. This perspective is particularly close to our initial field data in volcanology, the so called Total Grain Size Distribution (TGSD). We propose two different sectional methods [2][3] applied to SCE coupled inside a 1-D steady-state volcanic plume model. These methods have been improved in order to take into account new insights from field observations. In particular, we focused on the problem of different features between single particles and aggregates. This algorithm has been applied to observed volcanic eruptions (i.e. Eyjafjallajokull 2010, Sakurajima 2013 and Mt. Saint Helens 1980) to investigate the sensitiveness of our model with respect to the input parameters (total grain-size distribution, collision kernels, sticking efficiencies). Constrains on these parameters come from field observations and laboratory experiments.

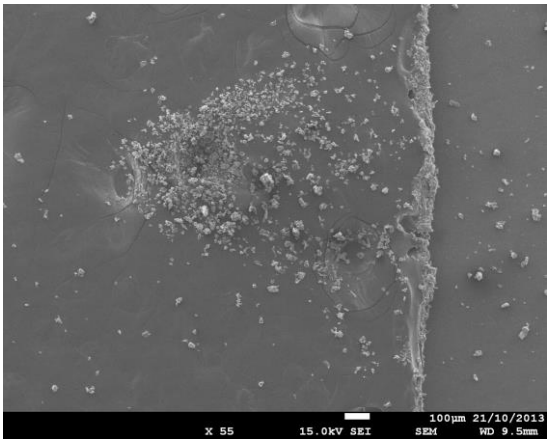

Figure 1. Volcanic aggregate collected during the eruption of Mt. Sakurajima (Japan) on the 3rd of August 2013.

References

[1] Ramkrishna D., "Population Balances:Theory and Applications to Particulate Systems in Engineering", Elsevier (2000)
[2] Kumar J., Peglow M., Warnecke G., Heinrich S., Morl L., "Improved accuracy and convergence of discretized population balance for aggregation: The cell average technique", Chemical Engineering Science (2006)
[3] Kumar J., Peglow M., Warnecke G., Heinrich S., "The cell average technique for solving multi-dimensional aggregation population balance equations", Computers & Chemical Engineering (2007)

cmg2016 - - Tuesday, June 7, 2016 - 11:45/12:30 (45min)

Experimental investigation of volcanic particles aggregation

S. Pollastri, C. Bonadonna

Université de Genève
Département des sciences de la terre, Geneva, Switzerland.

Key words: Volcanic particles aggregation; sticking efficiency; sticking velocity; restitution coefficient; bouncing glass spheres; impact angle; adhesion forces; viscous forces.

The large amount of fine ash released in the atmosphere by explosive volcanic eruptions constitutes a serious hazard to various economic and transport sectors (e.g. aviation), and potentially to both human and animal health. Since most of the fine ash sediments in the form of aggregates, which commonly fall considerably faster than single particles, a quantitative understanding of aggregation mechanisms is of primary importance for an accurate estimation of ash concentration over time and space. Nevertheless, a quantitative understanding of these processes has not been achieved yet. In fact, even though particle aggregation has already been investigated in astrophysics (aggregation of pre-planetary dust), meteorology (aggregation of water droplets), pharmaceutical chemistry (powder pills production), printing technology (aggregation of ink droplets), mechanical engineering (aggregation in particulate filters), the complex conditions in volcanic plumes and the particular chemical composition of volcanic particles require a dedicated investigation. The final goal of this work will be to estimate the sticking probability of volcanic particles by filming a large amount of binary collisions inside a vertical wind tunnel. However, due to the great number of variables involved (temperature, humidity, turbulence intensity, electrical charge of the particles, collision velocity, size of the particles, etc.) and the impossibility to simultaneously monitor all of them, some preliminary experiments have been performed inside a settling column releasing several particles (whose size was between 20 and 100 μm) towards a flat glass plate. After filming the collisions with a high speed camera, the restitution coefficient and the sticking velocity were computed for both volcanic particles and silica spheres, in order to investigate the effect of material and shape. The neutrality of the particles was checked making them fall through a condenser, which allowed to filter out the charged particles. As real collisions are generally oblique, several impact angles were tested tilting the plate. Furthermore, the experiment was repeated with a wet plate in order to see the effect of a water layer. Besides giving the dependence of the sticking velocity on particle size, the results gave some useful insight about the effect of collision angle, material and particle shape, and the presence of a water layer on the amount of energy dissipated during collisions.

.

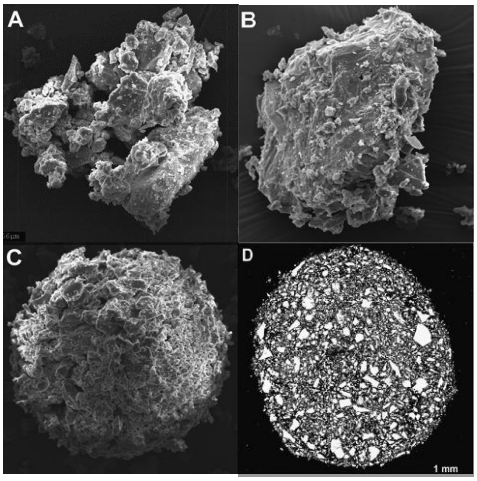

Figure 1. Different kinds of volcanic aggregates.

References

[1] A review of volcanic ash aggregation, Brown, Bonadonna, Durant, Physics and chemistry of the earth (2012)
[2] Fundamentals of atmospheric modeling, Jacobson, Chapter 15, Cambridge University press (2005)
[3] Ash aggregation in explosive volcanic eruptions, Telling et al., geophysical research letter (2013)
[4] Modeling volcanic processes, chapter 9: modelling tephra sedimentation from volcanic plumes, Bonadonna, Costa, Cambridge university press (2013).

cmg2016 - - Tuesday, June 7, 2016 - 11:45/12:30 (45min)

Experimental study of the influence of particle concentration in gas-particle mixtures

A. Weit[1], O. Roche[1]
[1]*Laboratoire Magmas et Volcans, Université Blaise Pascal-CNRS-IRD, Clermont-Ferrand, France*

Key words explosive volcanism, gas-particle mixture, turbulence, particle concentration

Gas-particle mixtures (PDC´s, plumes) are known to result from explosive volcanic eruptions, which can generally be differentiated into two end-members: dilute and dense gas particle mixtures [1]. In dilute flows the particles are carried by the turbulent gas and usually show concentrations around 1 %, whereas dense flows carry particle concentrations between 30 – 50 % [2]. Recent work by Cantero [3] suggests that the turbulence that is received in dilute flows is suppressed if the particle concentration is above a given threshold, because too much kinetic energy would be needed to maintain the particles in suspension. This issue was addressed through laboratory experiments on gas-particle mixtures. Therefore experiments were performed in a vertical tube (75 cm) with an underlying air flow system. Air runs in through a porous plate at the bottom and escapes through a grid at the top, whereas the particles are kept inside the tube (fig. 1). To simulate a gas-particle mixture glass beads of 75-80 µm were used as particles with varying concentrations from 0,5 vol.% to 20 vol.%. The particles were either injected incrementally during a run or stepwise between the runs. A high speed video camera was used to observe the experiments. To ensure that the flow conditions are turbulent, dimensionless numbers as the Reynolds number and the Stokes number were taken into account. The Reynolds number (*Re*) represents the ratio of inertial to viscous forces, the flow is turbulent when the inertial forces overcome the viscous forces, which is valid for $Re > 4000$. A turbulent flow typically produces circular currents which are known as eddies or vortices. The Stokes number (S_T) determines the coupling of the particles to the eddies formed by the gasphase and should yield values $S_T < 1$ to preserve turbulence [1]. The ratio U/Ut (terminal fall velocity) ~1 represents that the particles are maintained in suspension and indicates a stable gas-particle mixture for a certain flow velocity. In visual observations the addition of particles suggests that turbulence of the ascending air flow is significantly affected at particle concentrations larger than 5-10 %. This could implicate that volcanic gas-particle mixtures are not stable at intermediate conditions and that an entire range of particle concentration is not possible. A goal for further experiments is the investigation of larger particle concentrations as well as the finding of a precise particle concentration threshold for turbulent suppression. In later experiments this affection will also be investigated in lock-exchange experiments.

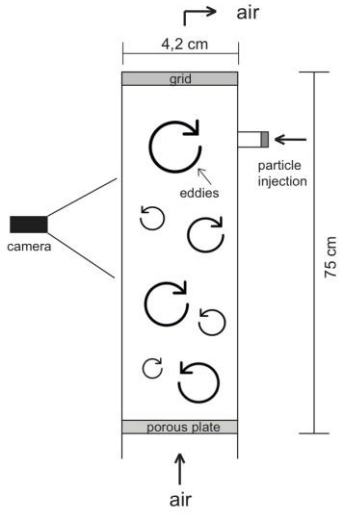

Figure 1 schematic sketch of experimental device

References

[1] A. Burgisser, W. Bergantz (2002), Reconciling pyroclastic flow and surge : the multiphase physics of pyroclastic density currents, *EPSL* (202) 405-418
[2] O. Roche (2015), Nature and velocity of pyroclastic density currents inferred from models of entrainment of substrate lithic clasts, *EPSL* (418) 115-125
[3] M.I. Cantero, M. Shringarpure, S. Balachandar (2012), Towards a universal criteria for turbulence suppression in dilute turbidity currents with non-cohesive sediments, *Geophys. Res. Lett.* (39) L14603

cmg2016 - - Tuesday, June 7, 2016 - 11:45/12:30 (45min)

ESTIMATION OF DEPTH TO THE BOTTOM OF MAGNETIC SOURCES AND RESULTING HEAT FLOW FROM HIGH RESOLUTION AEROMAGNETIC DATA OF THE ENTIRE BIDA BASIN, NIGERIA USING FOURIER TRANSFORM ANALYSIS

L. Nwankwo[1] & A. Sunday[2]
[1]*Department of Geophysics, University of Ilorin, Ilorin, Nigeria*
[2]*Department of Physics, Kwara State Polytechnic, Ilorin, Nigeria.*

Key words Aeromagnetic anomaly, spectral analysis, basal depth, heat flow, Bida basin, Nigeria.

Estimation of depths to the bottom of magnetic sources has been made in the entire Bida basin, north-central Nigeria. The regional estimates were made from a fractal source distribution of magnetic sources and Fourier transform analysis of the recently acquired high resolution aeromagnetic (HRAM) data of the basin. The HRAM data was divided into twenty seven (27) overlapping blocks of 200 x 200 km and each block analysed to obtain depths to the top, centroid and bottom of the magnetic sources. The depth values were subsequently used to evaluate the geothermal gradient and near-surface heat flow in the study area. The result shows that the depths to bottom of the magnetic sources varies between 13.67 and 28.22 km with an average of 21.73 km, the geothermal gradient varies between 19.59 and 42.43 ^{o}C/Km with an average of 27.71 ^{o}C/Km, while the resulting heat flow varies between 45.96 and 106.07 mWm^{-2} with an average of 69.27 mWm^{-2}. Thermal structure of the earth's crust is one of the main parameters controlling geodynamic processes; therefore, this study is crucial for quantitative understanding of the geo-processes and rheological/rock-physics parameters in the study area.

cmg2016 - - Tuesday, June 7, 2016 - 11:45/12:30 (45min)

Fluidization by collapse of fine particles into ambient air: a possible mechanism for sustained low interparticle friction in pyroclastic flows

C. Chédeville[1], O. Roche[1]
[1]*Laboratoire Magmas et Volcans, Université Blaise Pascal-CNRS-IRD, OPGC, Clermont-Ferrand, France*

Key words : pyroclastic flows, fluidization, experimental volcanology

Long runout distance of fines-rich pyroclastic flows is commonly attributed to their ability to generate and retain high pore pressure that reduces interparticle friction. This phenomenon, called fluidization, is caused by the relative vertical motion between a fluid (moving upward) and the particles (settling downward). Most of earlier works on fluidization have considered a constant vertical gas flux flowing through a static bed of particles. However, fluidization may also be caused by the collapse of particles into the (static) ambient air. Particle relative downward motion can occur during pyroclastic flow propagation, either when the flow bypasses a topographic break, propagates over a rough substrate (Chédeville and Roche 2014) or compacts itself. We carried out laboratory experiments which consisted of collapse of beds of particles (sub-spherical glass beads), in a static column of height of 1.4 m, triggered by rapid opening of a gate. Pressure sensors recorded the air pore pressure at different levels in the column. The collapse height was set at 20 or 90 cm, and bed properties such as bed thickness, particle size and bed temperature were systematically changed. The results showed three phases of pore pressure (Fig. 1): (1) An underpressure phase caused by the gate opening (t_1), rapidly followed by (2) a first overpressure phase in the reservoir (above the gate) when particles began to fall and forced the air to ascend through the bed (t_2), and (3) a second overpressure phase in the aggrading deposit at base of the column, during which pore pressure diffused slowly (t_4). Even at low collapse height of 20 cm, the maximum of the first overpressure phase showed that pore pressure compensated almost completely the bed lithostatic pressure, meaning that material was fluidized. This was true regardless the bed thickness and for particle sizes up to at least 400 µm. The second overpressure phase was strong when the particles were small enough (< 100-200 µm) but it was poorly developed or even absent when the particle size was increased. The duration of pressure diffusion in the deposit increased with the square of the bed thickness and decreased strongly with increasing particle size. Additional experiments with a natural ignimbritic material showed similar behavior but with a much longer diffusion duration (>30 s for a bed thickness of 28.5 cm), suggesting that such a fluidization mechanism can reduce internal friction for significant time in pyroclastic flows. At high temperature (up to 200 °C), overpressure during the first phase could overpass the bed lithostatic pressure. This suggested thermal pressurization of the cold air, which expanded rapidly when percolating through the hot material. We conclude that fluidization can be easily achieved for hot, fine-grained mixtures such as pyroclastic flows.

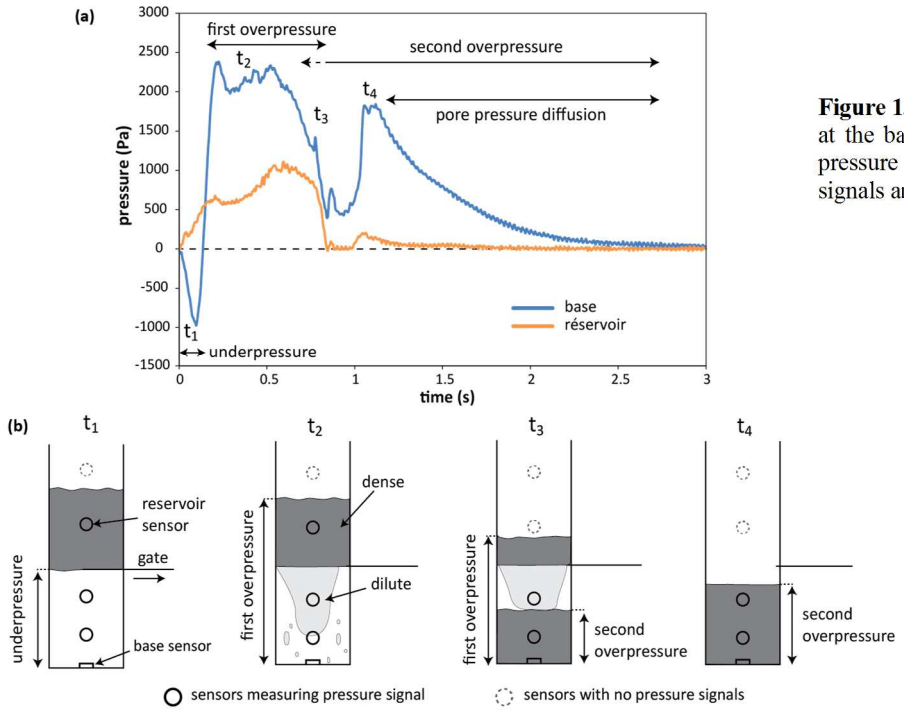

Figure 1. (a) Typical pressure signals measured at the base and in the reservoir, and principal pressure phases (b) Relation between pressure signals and position of particles in the column

Références

Chedeville, C., and O. Roche (2014), Autofluidization of pyroclastic flows propagating on rough substrates as shown by laboratory experiments, J. Geophys. Res. Solid Earth, 119, 1764–1776, doi:10.1002/2013JB010554

cmg2016 - - Tuesday, June 7, 2016 - 11:45/12:30 (45min)

COMBINED EFFECTS OF TOTAL GRAIN-SIZE DISTRIBUTION AND CROSSWIND ON THE RISE OF ERUPTIVE VOLCANIC COLUMNS

F. Girault[1], G. Carazzo[2], S. Tait[1] & E. Kaminski[1]
[1]*Institut de Physique du Globe, Paris, France*
[2]*Observatoire Volcanologique et Sismologique de Martinique, Fonds St Denis, Martinique*

Key words Plinian eruption; volcanic plume; atmospheric crosswind; turbulent entrainment; particle sedimentation

The maximum height of an explosive volcanic column, H, depends on the 1/4th power of the eruptive mass flux, Q, and on the 3/4th power of the stratification of the atmosphere, N. Expressed as scaling laws, this relationship has made H a widely used proxy to estimate Q. Two additional effects are usually included to produce more accurate and robust estimates of Q based on H: particle sedimentation from the volcanic column [1], which depends on the total grain-size distribution (TGSD) and the atmospheric crosswind [2]. Both coarse TGSD and strong crosswind have been shown to decrease strongly the maximum column height, and TGSD, which also controls the effective gas content in the column, influences the stability of the column. However, the impact of TGSD and of crosswind on the dynamics of the volcanic column are commonly considered independently. We propose here a steady-state 1D model of an explosive volcanic column rising in a windy atmosphere that explicitly accounts for particle sedimentation and wind together. We consider three typical wind profiles: uniform, linear, and complex, with the same maximum wind velocity of 15 $\mathrm{m\,s^{-1}}$. Subject to a uniform wind profile, the calculations show that the maximum height of the plume strongly decreases for any TGSD. The effect of TGSD on maximum height is smaller for uniform and complex wind profiles than for a linear profile or without wind. The largest differences of maximum heights arising from different wind profiles are observed for the largest source mass fluxes ($> 10^7$ $\mathrm{kg\,s^{-1}}$) for a given TGSD. Compared to no wind conditions, the field of column collapse is reduced for any wind profile and TGSD at the vent, an effect that is the strongest for small mass fluxes and coarse TGSD. Provided that the maximum plume height and the wind profile are known from real-time observations, the model predicts the mass discharge rate feeding the eruption for a given TGSD. We apply our model to a set of eight historical volcanic eruptions for which all the required information is known. Taking into account the measured wind profile and the actual TGSD at the vent substantially improves (by $\approx 30\%$) the agreement between the mass discharge rate calculated from the model based on plume height and the field observation of deposit mass divided by eruption duration, relative to a model taking into account TGSD only. This study contributes to the improvement of the characterization of volcanic source term required as input to larger scale models of ash and aerosol dispersion.

References

[1] F. Girault, G. Carazzo, S. Tait, F. Ferrucci & E. Kaminski, *The effect of total grain-size distribution on the dynamics of turbulent volcanic plumes*, Earth Planet. Sci. Lett. **394**, 124 (2014).
[2] F. Girault, G. Carazzo, S. Tait & E. Kaminski, *Combined effects of total grain-size distribution and crosswind on the rise of eruptive volcanic columns*, J. Volcanol. Geotherm. Res., http://dx.doi.org/10.1016/j.jvolgeores.2015.11.007 (2015).

cmg2016 - - Tuesday, June 7, 2016 - 11:45/12:30 (45min)

A NEW ANALYTICAL SCALING LAW FOR THE RISE OF BUOYANT JETS IN A CROSSFLOW AND IMPLICATION FOR WIND-BLOWN VOLCANIC PLUMES: COMPARISON WITH EXISTING SCALINGS

T. J. Aubry[1], A. M. Jellinek[1] & G. Carazzo[2]
[1]*University of British Columbia, Vancouver, BC, Canada*
[2]*Observatoire Volcanologique et Sismologique de Martinique, Fonds St Denis, Martinique*

Key words Explosive eruption; scaling; entrainment; plume height, wind

Various scaling relationships relate the height of volcanic plumes to key controls including eruptive source conditions, atmospheric density stratification, turbulent entrainment, and wind stresses (Fig. 1). Existing observational, analog, and numerical studies used to test these scalings capture only a narrow range of eruption source and atmospheric conditions, in particular wind. Accordingly, we develop a new analytical scaling for buoyant plume rising in density-stratified uniform crossflow. We compare this scaling to existing analytical [1, 2] and semi-empirical [3, 4, 5] scalings using an extensive experimental and eruption datasets [5, 6]. We show that our proposed scaling best predicts the height of experimental plumes. A key outcome of this scaling is an improvement over existing constraints on entrainment coefficients: in particular, we show that the ratio of the wind to radial entrainment coefficients is constant through a large span of dynamical regimes. Applied to natural eruptions, our scaling performs comparably well to published semi-empirical scalings typically applied in models. Furthermore, in a comparative analysis, we show that the performance success of tested existing scalings is restricted to the range of eruption magnitudes for which they are calibrated. For moderate to high wind stresses, plume shape evolves over the plume height, violating the self-similarity assumption on which all scalings and integral model results rely. Accordingly, we address why our and published scalings capture the effects of variable wind forcing nevertheless. We discuss consequences for relaxing the self-similarity hypothesis as well as potential improvements for standard integral plume models, in turn.

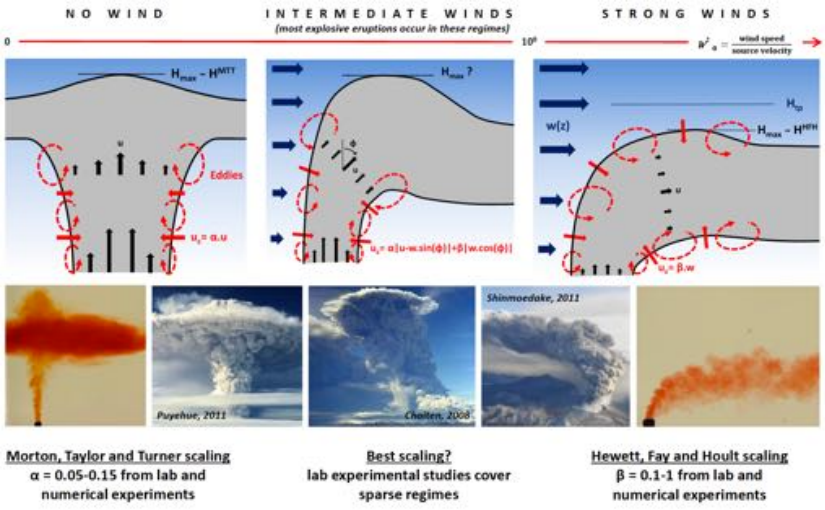

Figure 1. Entrainment hypothesis and scalings for plumes height across different wind regimes: quiescent atmosphere (left), intermediate winds (center), and high winds (right).

References

[1] B. R. Morton, G. I. Taylor, & J. S. Turner, *Turbulent gravitational convection from maintained and instantaneous source*, Proc. R. Soc. Lond. **234**, 1 (1956).
[2] T. A. Hewett, J. A. Fay & D. P. Hoult, *Laboratory experiments of smokestack plumes in a stable atmosphere*, Atmos. Environ. **5**, 767 (1971).
[3] W. Degruyter & C. Bonadonna, *Improving on mass flow rate estimates of volcanic eruptions*, Geophys. Res. Lett. **39**, L16308 (2012).
[4] M. J. Woodhouse, A.J. Hogg, J.C. Phillips & R. S. J. Sparks, *Interaction between volcanic plumes and wind during the 2010 Eyjafjallajokull eruption, Iceland*, J. Geophys. Res. Solid Earth **118**, 92 (2013).
[5] G. Carazzo, F. Girault, T. Aubry, H. Bouquerel & E. Kaminski, *Laboratory experiments of forced plumes in a density-stratified crossflow and implications for volcanic plumes*, Geophys. Res. Lett. **41**, 8759 (2014).
[6] L. G. Mastin, *Testing the accuracy of a 1-D volcanic plume model in estimating mass eruption rate*, J. Geophys. Res. Atmos. **119**, 2474 (2014).

cmg2016 - - Tuesday, June 7, 2016 - 11:45/12:30 (45min)

RHEOLOGICAL STICK-SLIP

A. Kurokawa[1], V. Vidal[2], T.Divoux[3], S. Manneville[2], & K. Kurita[1]
[1]*Earthquake Res.Inst.,Univ. of Tokyo, Japan*
[2]*Ecole Normale Supérieure, Lyon, France*
[3]*Universite de Bordeaux, Bordeaux, France*

Key words stick-slip,low frequency earthquake,solid-liquid transition,

In volcanic regions a peculiar type of earthquake activity is well known as the low frequency earthquake(LFE) [4]. The frequency content is completely different and shifted to be lower than that of similar sized tectonic earthquakes. Because of the low frequency nature involvement of liquid/gas phase is strongly suspected to generate LFE although the physical process is not specified yet. One of enigmatic points is why elastic wave radiation is restricted to low frequency though the wave form indicates a fracture like transient behavior. In this presentation we propose a possible mechanism to generate LFE.

In the earthquake generation process stick-slip phenomena in frictional sliding of solid material is a key process. Although the Amonton ' s law has been accepted as a basic law in the solid friction, deviations from the law are discussed such as lubrication in the presence of liquid phase at the interface. When the liquid is locally confined, however, it undergoes liquid-solid transition, which gives rise to the stick-slip behavior [1], [2]. Since similar transition is found to exist in flowing dense colloidal suspensions with aging [3], stick-slip behavior is strongly expected even in macroscopic flow system. Here we report this peculiar phenomena, rheological stick-slip.

[3] reported shear-induced fluidization for a dense colloidal suspension of fused silica. This fluid has a strong aging characteristic;viscosity and yield stress increase with time under rest. The rheological relation between shear rate and shear stress exhibits pronounced negative slope,hence the multiplicity relationship. When we apply constant shear rate on the aged sample in the Taylor-Couette geometry shear stress shows fluctuations after yielding(Figure A and B). Each fluctuation is characterized by saw-tooth type variation:gradual increase of stress followed by rapid decrease. By ultrasonic velocimetry to measure local velocity profiles, growth and destruction of shear banding are clearly demonstrated at this fluctuation. Figure C represents variation in the width of shear band. In the stress growth stage the solid region expands and in the subsequent stress drop stage it shrinks. This stress behavior is similar to what [1] reported. The essential difference is origin of solid-liquid transition; confinement to local nano space in the preceding researches and dense suspension with aging in this case.

At moment we do not have direct evidence of these characteristics for silicate magmas so that we can not evaluate a possibility of rheological stick-slip in the magmatic system. But several lines of collateral evidence indicate a strong similarity between this colloidal suspension and magmas;

1) in the magma composed of crystals and melt yield stress exists and solid-liquid transition is easily induced.
2) entanglement/aggregation of crystals is promoted by hydrodynamic effects. This should correspond aging.
3) formation/destruction of the aggregates is expected to produce yielding nature and rheological multiplicity.

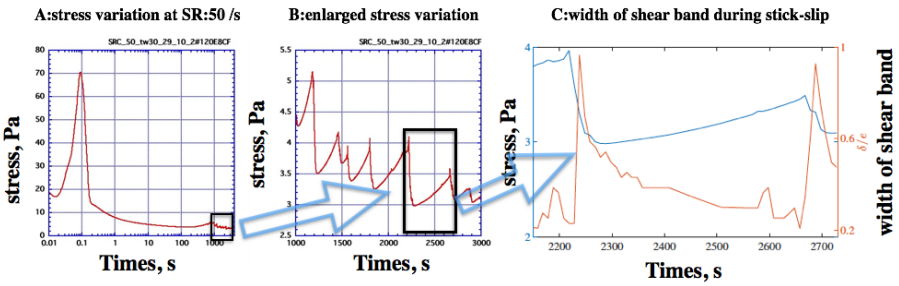

Figure 1. example of rheological stick-slip

References

[1] C.Drummond and J.Ishreelachivili, *Dynamic phase transitions in confined lubricant fluids under shear*, Phys. Rev.E., **63**,041506, (2001).
[2] S.Yamada, *Structural aging and stiction dynamics in confined fluid films*, J. Chem. Phys. **131**,184708,(2009).
[3] A.Kurokawa et al, *Avalanche-like fluidization of a non-Brownian particle gel*, Soft Matter, **11**,9026,(2015).
[4] H.Kawakastu and M.Yamamoto, *Volcano Seismology*, in Treatise in Geophysics, Elsevier **4**,389,(2015).

Cold Flows

cmg2016 - - Monday, June 6, 2016 - 18:45/19:00 (15min)

NUMERICAL MODELLING OF ICEBERG CALVING AND IMPLICATIONS IN SEISMIC WAVES GENERATED

A. Sergeant[1], V. Yastrebov[2], O. Castelnau[3], A. Mangeney[1], E. Stutzmann[1] & J.-P. Montagner[1]
[1]*Institut de Physique du Globe, Paris, France*
[2]*Centre des Matériaux, Mines ParisTech, Evry, France*
[3]*Procédés et Ingénierie en Mécanique et Matériaux, ENSAM, CNAM, Paris, France*

Key words Iceberg calving, Glacial earthquake, fluid-solid interaction.

Glacial earthquakes is a class of seismic events of magnitude up to 5, occurring primarily in Greenland, in the margins of large marine-terminated glaciers with near-grounded termini. They are caused by calving of cubic-kilometer scale unstable icebergs which penetrate the full-glacier thickness and, driven by the buoyancy forces, capsize against the calving front. These phenomena produce seismic energy including surface waves for $\sim$2 min, with dominant energy between 10-150 s of period whose seismogenic source is compatible with the contact force exerted on the terminus by the iceberg while it capsizes. During the capsize of the iceberg which can last typically for 5 min, the normal force applied to the calving front causes a reverse motion of the elastically compressed glacier terminus within a 500 m radius area. Once the contact is released, a terminus rebound is measured and the glacier terminus flows for few hours.
To simulate capsize events, we use a finite element model with special boundary conditions to model fluid-structure interaction (fluid pressure depending on depth, pressure and skin drags). A 2D plane strain formulation in linear elasticity is used. Contact and frictional forces are measured on the terminus and compared with laboratory experiments. We show the influence of geometric factors on the force history, amplitude and duration at the laboratory and field scales. Finally, the force inverted from seismic data is used to constrain the model and invert geometric and physical parameters as the iceberg dimensions, the local water depth, the calving front orientation or the ice-bedrock friction.

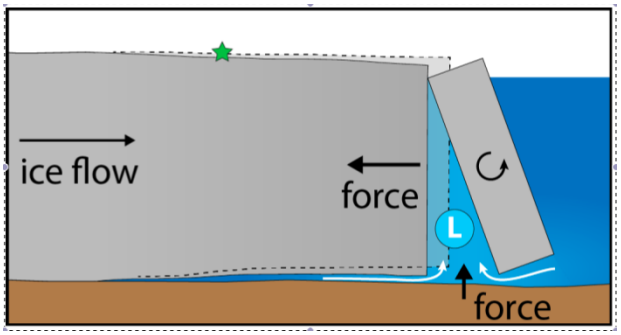

Figure 1. Cartoon of the calving sequence phenomena responsible for the generation of seismic waves. Glacier deflection caused by capsizing iceberg shown relative to initial position (dotted line). Acceleration of iceberg to right exerts a force in the upglacier direction (left), leading to reverse motion of the terminus. Reduced pressure behind the iceberg (âĂIJLâĂİ) draws water from beneath the glacier and from the proglacial fjord, pulling the floating portion of the glacier downward and exerting an upward force on the solid Earth. From Murray et al., 2015 [1].

References

[1] Murray, T., M. Nettles, N. Selmes, L. Cathles, J. Burton, T. James, S. Edwards, I. Martin, T. O'Farrell, R. Aspey, et al. (2015), *Reverse glacier motion during iceberg calving and the cause of glacial earthquakes*, Science, 349(6245), 305-308.S

cmg2016 - - Monday, June 6, 2016 - 18:00/18:30 (30min)

DISCRETE-ELEMENT MODELING OF SELECTED ASPECTS OF SEA ICE DYNAMICS AND FRACTURE

A. Herman[1]
[1]*Institute of Oceanography, University of Gdansk, Poland (oceagah@ug.edu.pl)*

Key words Sea ice, discrete-element models, sea ice dynamics, sea ice breaking, sea ice–waves interactions, floe-size distribution.

In terms of numerical modeling of sea ice dynamics, recent years have witnessed a certain revival of discrete-element methods, in which sea ice is represented as an assemblage of individual, interacting floes. Combined with new approaches to the analysis and interpretation of modeling results, inspired by methods of modern statistical physics and complex-network science, these tools provide new insights into the 'microscopic' (floe-level) and 'macroscopic' (large-scale, emergent) phenomena observed in sea ice. A crucial property of sea ice in this context is its extreme polydispersity. On the one hand, the floe-size distribution (FSD) results from sea ice deformation, breaking and healing (freezing) history. On the other hand, the FSD itself substantially influences the sea ice mechanical properties and thus its response to forcing and deformation. Both aspects of these relationships are only poorly understood at present.

In this talk, selected aspects of sea ice dynamics and fragmentation will be presented, based on results of simulations performed with a Discrete-Element bonded-particles Sea Ice model DESIgn [1]. The examples will include: force networks in deformed ice and their role in transmitting stress; wave-induced stress and floe breaking in the marginal ice zone, and the resulting floe-size distributions; and evolution of floe sizes and shapes due to 'grinding' of ice floes in shear zones (Fig. 1). In most examples, mutual interactions between the sea ice polydispersity and dynamics are responsible for complex, nontrivial behavior of the modeled system. Robust character of that behavior, occurring without any tuning within a very wide range of model parameters, hints at its universal character and suggests that similar mechanisms are at play in real-world sea ice as well.

The code and documentation of DESIgn are freely available at http://herman.ocean.ug.edu.pl/LIGGGHTSseaice.html. The model is implemented as a toolbox for the open-source numerical library LIGGGHTS (http://www.cfdem.com/).

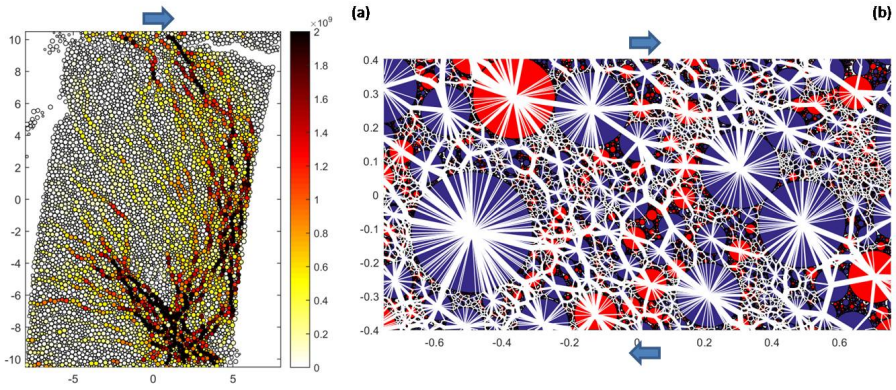

Figure 1. Example applications of the DESIgn model to the analysis of shear deformation of sea ice: grain–grain forces in a rectangular, bonded sample (a), and force networks in densely packed, unbonded ice pack composed of floes with a power-law size distribution (b). In (b), line thickness corresponds to the force strength, and grain colors show the direction of rotation of the grains.

References

[1] Herman, A., Discrete-Element bonded-particle Sea Ice model DESIgn, version 1.3 – model description and implementation. *Geosci. Model Dev. Discuss.*, **8**, 5481-5533, doi:10.5194/gmdd-8-5481-2015 (2015).

cmg2016 - - Monday, June 6, 2016 - 18:30/18:45 (15min)

DYNAMICS OF BLOWN-SNOW PARTICLES DEPENDING ON THE DIAMETER

H. Niiya[1] & K. Nishimura[1]

[1]*Graduate School of Environmental Studies, Nagoya University, Nagoya, 464-8601, Japan*

Key words Drifting snow, Numerical modeling, Suspension and Saltation, Splash process.

Splash process is the collision between a blown particle and deposited particles, and it is an important physical sub-process to characterize entrainments and dynamics of particle in aeolian transports such as blowing snows. However, it is difficult to analyze splash processes individually in the nature transport because the number of blown particles increases near the surface. As one of remarkable studies, Sugiura et al. [1] measured distribution functions for each splash in wind tunnel experiments with snow particles, which were carried out at low wind speeds. So far, we conduct numerical simulations of blowing snow by application these functions to higher wind speeds. Numerical results find some problems; the fine particle can hardly move to upper layer and the coarse particle mainly hop below $4\mathrm{cm}$. In this study, we modify the splash process of numerical model based on single splash experiments by Ammi et al. [2] to overcome problems in higher wind conditions, and we clearly study the blown particle dynamics depending on the diameter in the monodisperse system.

Our model is improved the random-flight model of blowing snow [3]. Key changes in the model are three: addition of fluid viscous stress, three-dimensional particle motion, and change of splash process. Distribution functions for the splash process are expressed using results of single splash experiments [2], in which dynamics of particles are divided into rebound and splash (i.e., new ejected particle). For the number of splashed particles, fitting parameters in the function are determined by the comparison with experiments [1] to address the snow particle.

In the setup of numerical simulations, particles are entrained from the snow surface with a constant roughness length, and the diameter d is assumed to be a constant. The domain size is a cuboid depending on d: $60d$ length, $30d$ width, and $1\mathrm{m}$ height. The vertical profile of wind speed is formed by the friction velocity u_t^* fixed at the top, whereas the lateral boundary condition for particles is set as the periodic boundary. Also, only two values (d and u_t^*) are independently varied in simulations.

Figure 1 shows particles located near the surface at $t = 1\mathrm{s}$, and blown particles are entrained by wind and splash. Each numerical simulation is carried out until the particle transport reaches the equilibrium state. As a result, the total mass flux Q below $1\mathrm{m}$ drastically changes depending on the diameter (Fig. 2). (i) $d = 10\mu\mathrm{m}$: Q is consistently maximized because particles are suspended up to the top. (ii) $d = 30\mu\mathrm{m}$: the height of suspension increases with increase in u_t^*. (iii) $d = 60, 100\mu\mathrm{m}$: the range of particle motion hardly expands despite the increase in u_t^*, thus the increasing rate of Q is low. (iv) $d = 300, 600\mu\mathrm{m}, 1\mathrm{mm}$: the increase in u_t^* activates the saltation, and the height of saltation exceeds $10\mathrm{cm}$ at $u_t^* = 0.6\mathrm{m/s}$.

In the talk, we focus on the splash process of model to clarify the difference in above particle dynamics.

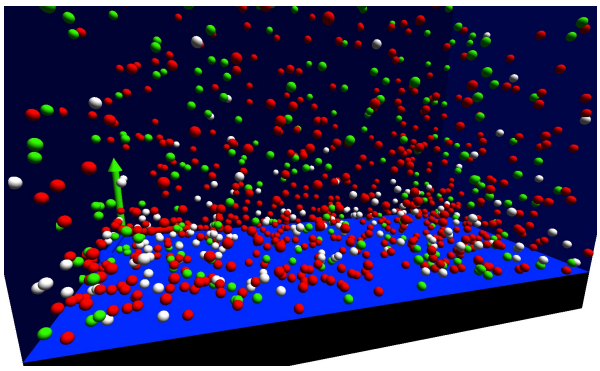

Figure 1. Simulation image at $t = 1\mathrm{s}$. (green: entrainment due to wind, white: splash, red: rebound)

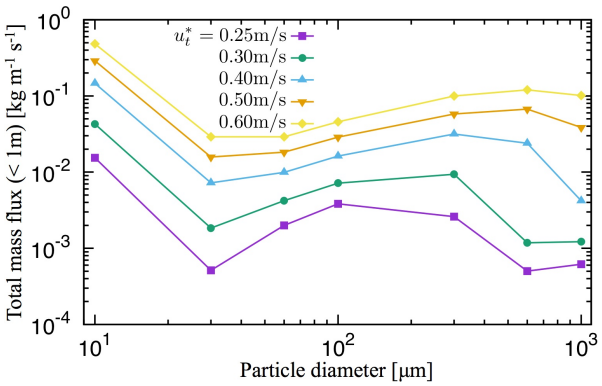

Figure 2. Diameter dependency of total mass flux at equilibrium state. Line colors indicate different top friction velocities.

References

[1] K. Sugiura and N. Maeno, *Wind-tunnel measurements of restitution coefficients and ejection number of snow particles in drifting snow: determination of splash functions*, Boundary-Layer Meteorol **95**, 123 (2000).

[2] M. Ammi, L. Oger, D. Beladjine, and A. Valance, *Three-dimensional analysis of the collision process of a bead on a granular packing*, Phys. Rev. E **79**, 021305 (2009).

[3] M. Nemoto and K. Nishimura, *Numerical simulation of snow saltation and suspension in a turbulent boundary layer*, J. Geophys. Res. **109**, D18206 (2004).

cmg2016 - - Monday, June 6, 2016 - 11:45/12:30 (45min)

A SIMPLE ANISOTROPIC FLOW LAW FOR POLAR ICE BASED ON ANISOTROPIC, SCALAR FLOW ENHANCEMENT

R. Greve[1], A. Treverrow[2] & R. C. Warner[2]
[1]*Institute of Low Temperature Science, Hokkaido University, Sapporo, Japan*
[2]*Antarctic Climate and Ecosystems Cooperative Research Centre, University of Tasmania, Hobart, Australia*

Key words Anisotropy; Flow law; Polar ice; Antarctic ice sheet; Modelling

The flow of polycrystalline polar ice is often described by Glen's flow law, in which ice is assumed to be an isotropic, non-linearly viscous fluid. This goes along with the assumption that the ice crystallites (grains) in the polycrystalline aggregate are essentially randomly oriented. However, observations show that under prolonged deformation, especially relevant to all but the uppermost parts of an ice sheet, different patterns of preferred c-axis orientations (crystal fabrics) and anisotropic flow properties develop which vary according to the flow regime. Based on earlier works by Wang and Warner [1] and Budd et al. [2], we describe a minimal anisotropic flow law (MAFL) that employs an anisotropic, scalar flow enhancement factor. The scalar character is similar to the flow law of the CAFFE model by Placidi et al. [3]. However, while the CAFFE model contains an evolution equation for the anisotropic fabric, here we assume that on a large scale the fabric (microstructure) evolves at a rate that remains compatible with the deformation regime. This approximation makes ice deformability a function of the current deformation regime, eliminating the requirement for a fabric evolution scheme. The parameters of the minimal anisotropic flow law are based on laboratory ice deformation experiments conducted in a range of combined stress configurations incorporating compression and simple shear (Li et al. [4], Budd et al. [2], Treverrow et al. [5]). These results show that ice is softer under simple shear than under compression. We have implemented MAFL in the three-dimensional ice sheet model SICOPOLIS (www.sicopolis.net), and we discuss some simulation results for a simple geometry (EISMINT; Payne et al. [6]) and for the Antarctic ice sheet.

References

[1] Wang, W. L. and R. C. Warner. 1999. Modelling of anisotropic ice flow in Law Dome, East Antarctica. *Ann. Glaciol.*, 29, 184–190.

[2] Budd, W. F., R. C. Warner, T. H. Jacka, J. Li and A. Treverrow. Ice flow relations for stress and strain rate components from combined shear and compression laboratory experiments. *J. Glaciol.* 59 (214), 374–392, 2013.

[3] Placidi, L., R. Greve, H. Seddik and S. H. Faria. 2010. Continuum-mechanical, Anisotropic Flow model for polar ice masses, based on an anisotropic Flow Enhancement factor. *Continuum Mech. Thermodyn.* 22 (3), 221–237.

[4] Li, J., T. H. Jacka and W. F. Budd. 1996. Deformation rates in combined compression and shear for ice which is initially isotropic and after the development of strong anisotropy. *Ann. Glaciol.* 23, 247–252.

[5] Treverrow, A., W. F. Budd, T. H. Jacka and R. C. Warner. 2012. The tertiary creep of polycrystalline ice: experimental evidence for stress-dependent levels of strain-rate enhancement, *J. Glaciol.* 58 (208), 301–314.

[6] Payne, A. J., P. Huybrechts, A. Abe-Ouchi, R. Calov, J. L. Fastook, R. Greve, S. J. Marshall, I. Marsiat, C. Ritz, L. Tarasov and M. P. A. Thomassen. 2000. Results from the EISMINT model intercomparison: the effects of thermomechanical coupling. *J. Glaciol.* 46 (153), 227–238.

cmg2016 - - Monday, June 6, 2016 - 11:45/12:30 (45min)

A MAXWELL-ELASTO-BRITTLE MODEL FOR THE DRIFT AND DEFORMATION OF SEA ICE

V. Dansereau[1], J. Weiss[2] & P. Saramito[3]

[1]*Laboratoire de Glaciologie et Géophysique de l'Environnement, CNRS UMR 5183, Université de Grenoble, Grenoble, France*

[2]*Institut des Sciences de la Terre, CNRS UMR 5275, Université de Grenoble, Grenoble, France*

[3]*Laboratoire Jean Kuntzmann, CNRS UMR 5224, Université de Grenoble, Grenoble, France*

Key words Sea ice deformation, Maxwell-elasto-brittle rheology, brittle mechanics, elastic interactions, viscous stress relaxation, heterogeneity, intermittency, anisotropy.

In recent years, analyses of available ice buoy and satellite data have revealed the strong heterogeneity and intermittency of the deformation of sea ice and have demonstrated that the viscous-plastic rheology widely used in current climate models and operational modelling platforms does not simulate adequately the mechanical behavior of the ice pack [1, 2, 3]. We developped a new mechanical model, named Maxwell-Elasto-Brittle, as an alternative to the standard viscous-plastic rheology in the view of accurately reproducing the drift and deformation of the ice cover in continuum sea ice models, at regional to global scales. The model builds on a damage mechanics framework used for ice and rocks (e.g., [4, 5]). A viscous-like relaxation term is added to the linear-elastic constitutive relationship together with an effective viscosity that evolves with the local level of damage of the material, like its elastic modulus. This framework allows the internal stress to dissipate in large, permanent deformations along the faults (or sea ice "leads") once the material is highly damaged, while reproducing the small deformations associated with the fracturing process and retaining the memory of elastic deformations over relatively low damage areas. A healing mechanism counterbalances the effects of damaging over large time scales. The numerics is based on finite elements and variational methods. The equations of motion are cast in the Eulerian frame and discontinuous Galerkin methods are implemented to handle advective processes.

Idealized simulations with mechanical parameters values consistent with sea ice on geophysical scales demonstrate that the Maxwell-EB rheological framework reproduces the main characteristics of sea ice mechanics: the anisotropy of the deformation, the strain localization and intermittency, as well as the associated scaling laws. Moreover, sensitivity analyses on the one model parameter setting the rate of viscous dissipation of the internal stress as a function of the increasing level of damage within the material show that the model, with few independent variables, can represent a large range of mechanical behaviours, from a regular, predictable stick-slip with a single damaging frequency corresponding to the prescribed rate of healing, to a marginally stable, unpredictable creep-like deformation with temporal correlations in the damaging activity at all time scales below the material's healing time. Over a range of values of this parameter, the model reproduces both the persistence of creeping faults/leads and the activation of new faults/leads with different shapes and orientations.

Idealized as well as realistic Maxwell-EB simulations of the flow of sea ice through a channel will be presented. These will demonstrate that the model reproduces the formation of stable ice bridges as well as the stoppage of the flow within the channel, a phenomenon observed in narrow straits of the Arctic [6] and common in granular materials [7, 8]. In agreement with observations, the propagation of damage along narrow arch-like features, defining ice floes moving like solid bodies, the discontinuities in the velocity field between the floes and the eventual opening of the channel are all represented.

References

[1] R. W. Lindsay, J. Zhang, D. A. Rothrock, *Sea-ice deformation rates from satellite measurements and in a model*, Atmosphere-Ocean **41**, 1 (2003).

[2] R. Kwok, E. C. Hunke, W. Maslowski, D. Menemenlis, J. Zhang, *Variability of sea ice simulations assessed with RGPS kinematics*, Journal of Geophysical Research: Oceans **113**, C11 (2008).

[3] L. Girard, J. Weiss, J. M. Molines, B. Barnier, S. Bouillon, *Evaluation of high-resolution sea ice models on the basis of statistical and scaling properties of Arctic sea ice drift and deformation*, Journal of Geophysical Research **114**, C08015 (2009).

[4] D. Amitrano, J.-R. Grasso, D. Hantz, *From diffuse to localised damage through elastic interaction*, Geophysical Research Letters **26** (1999).

[5] L. Girard, S. Bouillon, J. Weiss, D. Amitrano, T. Fichefet, V. Legat, *A new modeling framework for sea ice models based on elasto-brittle rheology*, Annals of Glaciology **52**, 57 (2011).

[6] R. Kwok, L. T. Pedersen, P. Gudmandsen, S. S. Pang, *Large sea ice outflow into the Nares Strait in 2007*, Geophysical Research Letters **37**, C08015 (2009).

[7] O. Richmond, G. C. Gardner, *Limiting spans for arching of bulk materials in vertical channels*, Chemical Engineering Science **17**, 12 (1962).

[8] D. M. Walker, *An approximate theory for pressures and arching in hoppers*, Chemical Engineering Science **21**, 11 (1966).

Imaging techniques

cmg2016 - - Friday, June 10, 2016 - 17:15/17:30 (15min)

IMAGING AN UNKNOWN OBJECT IN AN UNKNOWN MEDIUM

Roel Snieder[1] and Kees Wapenaar[2]
[1]*Center for Wave Phenomena, Colorado School of Mines*
[2]*Faculty of Civil Engineering and Geoscience, Delft University of Technology*

Key words imaging, inverse scattering

Imaging an unknown object in a medium that is known, such as a medium with constant velocity, is not difficult because one knows exactly where the waves are when they interact with the object. It is much more challenging to image an object in an unknown medium, because in that case one may know the waves that one sends into the medium, but one may does not know the waves that illuminate the object because the waves are distorted during their propagation to the object and back. Yet in many applications the medium is strongly scattering and the wavefield is strongly distorted as it propagates to the object. This is like imaging through frosted glass. How can one create an image in such media? And related to this, how can one focus a wavefield through a complicated medium that one does not know?

Inverse scattering methods, as developed in quantum mechanics[1, 2], make it possible to estimate the model or object at a prescribed location without knowing the medium between that location and the point where reflected waves are recorded. These inverse scattering methods are known as the Marchenko equation or Gel'Fand-Levitan equation. Recently, these inverse scattering methods have been generalized to applications in seismology[3, 4, 5, 6] where one seeks to image a target, such as a reservoir, under a complicated overburden, such as a salt body.

The main issue we will address is how it is possible that one can image the object at one location without knowing the medium between the observation point and the reconstruction point. The reason why inverse scattering make it possible to do this is that these methods involve an integral equation[7], and the function that one solves for is akin to the Green's function for the unknown medium. The function obtained by solving the Marchenko equation is, in fact, the incident wavefield that will focus the waves at a specified target location. In order to solve this integral equation one only needs to know a smooth estimate of he velocity model and the reflected waves recorded at the acquisition surface, but the details of the complexity of the medium need not be known. That means there exists a recipe to determine, given the reflected waves, the incident wavefield that focuses at a specified target point. Such focusing is exactly what is needed to determine the image at the target point.

There are many applications in geophysics where one seeks to create an image in strongly scattering media. These include hydrocarbon reservoirs under a complicated overburden, the interior of volcanoes, possibly the core mantle boundary, and crustal structure from high-frequency seismic waves.

References

[1] V.A. Marchenko. The construction of the potential energy from the phases of scattered waves. *Dokl. Akad. Nauk*, 104:695–698, 1955.
[2] Z.S. Agranovich and V.A. Marchenko. *The inverse problem of scattering theory*. Gordon and Breach, New York, 1963.
[3] F. Broggini and R. Snieder. Connection of scattering principles: a visual and mathematical tour. *Eur. J. Phys.*, 33:593–613, 2012.
[4] K. Wapenaar, P. Broggini, E. Slob, and R. Snieder. Three-dimensional single-sided Marchenko inverse scattering, data-driven focusing, Green's function retrieval, and their mutual relations. *Phys. Rev. Lett.*, 110:084301, 2013.
[5] F. Broggini, R. Snieder, and K. Wapenaar. Data-driven wavefield focusing and imaging with multidimensional deconvolution: Numerical examples from reflection data with internal multiples. *Geophysics*, 79:WA107–WA115, 2014.
[6] S. Singh, R. Snieder, J. Behura, J. van der Neut, K. Wapenaar, and E. Slob. Marchenko imaging: Imaging with primaries, internal multiples, and free-surface multiples. *Geophysics*, 80:S165–S174, 2015.
[7] R. Burridge. The Gel'Fand-Levitan, the Marchenko and the Gopinath-Sondi integral equations of inverse scattering theory, regarded in the context of the inverse impulse response problems. *Wave Motion*, 2:305–323, 1980.

cmg2016 - - Friday, June 10, 2016 - 16:45/17:00 (15min)

Including Short Period Information Into Full Waveform Tomographic Models

T. Bodin[1], M. Calo[2], B. Romanowicz[3,4]
[1]*CNRS – ENS Lyon, Univeristé Lyon1, France*
[2]*Instituto de Geofísica, UNAM, Mexico*
[3]*Institut de Physique du Globe, Paris, France.*
[4]*Berkeley Seismological Laboratory, UC Berkeley, USA*

Key words Full waveform Tomography, Homogeneization, Multiscale Imaging.

Thanks to the advent of the Spectral Element Method (SEM) in seismology, the resolution of regional and global tomographic models has improved in the last decade. However, due to computational costs, only relatively long period waveforms are considered, and therefore only long wavelength structure can be constrained. Thus, the resulting 3D models are smooth, and only represent a small volumetric perturbation around a smooth reference model that does not contain short scale information about upper-mantle discontinuities (e.g. MLD, LAB). A decrease in period, necessary for the resolution of smaller scale features is computationally challenging. In order to overcome these limitations and to account for layered structure in the upper mantle, we have developed a methodology that combines full waveform inversion and information provided by short period seismic observables (receiver functions and surface wave dispersion, sensitive to sharp boundaries and anisotropic structure respectively).

To combine short and long wavelength information, we use a procedure based on residual homogeneization (Capdeville et al. 2013). In a first step, receiver functions and dispersion curves are used as constraints to generate a number of 1D profiles beneath selected stations using a trans-dimensional Markov-chain Monte Carlo (McMC) algorithm. These 1D profiles, containing both isotropic and anisotropic discontinuities in the upper mantle, are then interpolated to build a 3D starting model for the full waveform tomographic inversion. This discontinuous starting model is homogenized to avoid meshing problems and heavy computations. The results of the tomographic inversion are volumetric velocity perturbations around the homogeneized starting model, which are then added to the discontinuous 3D starting model. We present here the first results of a multiscale model of the North American continent.

References

Capdeville, Yann, Éléonore Stutzmann, Nian Wang, and Jean-Paul Montagner. "Residual homogenization for seismic forward and inverse problems in layered media." Geophysical Journal International 194, no. 1 (2013): 470-487.

cmg2016 - - Friday, June 10, 2016 - 17:00/17:15 (15min)

DOES GRAVITY HELP TO IMPROVE SEISMIC INVERSION FOR DENSITY?

N.A. Blom[1], A. Fichtner[2], C. Böhm[2]
[1] *Universiteit Utrecht, Department of Earth Sciences, Utrecht, The Netherlands*
[2]*ETH Zürich, Department of Earth Sciences, Zurich, Switzerland*

Key words Seismic tomography; density; waveform inversion; joint inversion.

Density is one of the most important material properties that influence the dynamics of our planet's interior, yet its variations are poorly known. The travel times of seismic waves, the classical tool to probe the Earth's interior, are barely sensitive to density (with large tradeoffs) and gravity is so extremely non-unique that very little information can be extracted from it without placing very strong prior constraints. As a result, density has, up until now, usually only been regarded as a derived quantity, which may lead to erroneous interpretations.
Here, we aim to determine to what extent it is possible to image density as an independent parameter using modern geophysical techniques. The main technique is seismic (full) waveform inversion, which is more sensitive to density than travel-times alone, for the simple reason that more information of the seismogram is being used: in theory the amplitude and phase of every wiggle. We construct synthetic tests in 2-D where density is a completely independent parameter from S-wave velocity and P-wave velocity. This setup, while physically unrealistic, has the advantage that our ability to image density independently is assessed in an unbiased way.
We find that it is indeed possible to image density using waveform inversion. If prior information, such as constraints on S- and P-velocity structure, is included in the inversion, the results for density are markedly improved. The use of gravity data as an additional observable, however, deteriorates the inversion results. This is because of the significant non-uniqueness of potential field measurements, so that an unconstrained update based on gravity will only almost definitely work to push the inversion in the wrong direction.

cmg2016 - - Friday, June 10, 2016 - 16:00/16:15 (15min)

TRANS-DIMENSIONAL TREES FOR PARSIMONIOUS GEOPHYSICAL INVERSION

R. Hawkins[1], M. Sambridge[1], J. Dettmer[1], E. Saygin[1], J. Stipčević[1] & H. Tkalčić[1]
[1]*Research School of Earth Sciences, Australian National University, Canberra, Australia*

Key words Bayesian, Inverse methods, Seismic tomography

Geophysical inversion consists of choosing a model parameterization and a function that quantifies the fit of data predictions to observations. Within such framework, inferences of the Earth can be obtained from optimal parameter estimates and uncertainties[1]. In classical approaches, model parameterization is fixed at the outset and optimization is performed using a minimization of some combination of norms that attempt to balance the inherent trade off between model complexity and the spatial resolving power of the observations. Uncertainties are then estimated from linearized approximations from the optimization process. The initial choice of some fixed model parameterization has dramatic effects on the resulting inferences and equally on the estimated uncertainty.

In contrast, sampling based approaches using Markov chain Monte Carlo (McMC) techniques offer a way to obtain robust uncertainty estimates through numerically approximating the posterior probability density with large ensembles of solutions that are consistent with data and prior information. While computationally expensive, these approaches require no linearization assumptions. With advances in McMC techniques [2, 3] that allow the model parameterization to change, called reversible jump or trans-dimensional sampling in the literature, model parameterization can remain a variable whose complexity is data driven rather than subjectively fixed from the outset.

We have developed a novel Bayesian trans-dimensional approach which, at its core[4], uses an abstract tree to subdivide any space (e.g. 2D, 3D, spherical, Cartesian, temporal), allowing the model parameterization to vary spatially or temporally to better suit the problem at hand. Compared to previous work[5], our approach is more flexible in terms of the problem geometry and the ease with which various basis functions can be used. In our initial synthetic experiments with the new formalism, we have used simple functions such as box-car, triangle, and Lanczos functions, as well as many families of wavelets.

We present two recent applications of our new approach with wavelet parameterizations to geophysical inversion problems. First, we show the results of the inversion of ambient noise tomography data for the Iceland region. Second, we highlight the generality of the approach with a non-linear tsunami-source inversion to determine the spatio-temporal evolution of the sea surface displacement after the great 2011 Japan tsunami.

Recent experiments into truncated polynomial representations show great promise in the solution of geophysical imaging problems due to their greater utility. We demonstrate these through some early simulated and real data examples. These include large scale seismic tomography inversions using Finite Frequency kernels, and small scale inversions using full-waveform simulations. These may provide a template for Bayesian full waveform and joint inversions which will become more feasible as computational power increases.

References

[1] N. Rawlinson, A. Fichtner, M. Sambridge M. and M. Young, *Seismic tomography and the assessment of uncertainty*, Advances in Geophysics, **55**, Academic Press, 2014
[2] C. J. Geyer and J. Møller, *Simulation procedures and likelihood inference for spatial point processes*, Scandinavian Journal of Statistics, **21**, 1994,
[3] P. J. Green, *Reversible jump Markov chain Monte Carlo computation and Bayesian model determination*, Biometrika, **4**(82), 1995
[4] R. Hawkins and M. Sambridge, *Geophysical imaging using trans-dimensional trees*, Geophysical Journal International, **203** (2), 2015.
[5] T. Bodin and M. Sambridge *Seismic Tomography with the reversible jump algorithm*, Geophysical Journal International **178**, 2009

cmg2016 - - Friday, June 10, 2016 - 15:30/16:00 (30min)

DISCRETE SOLUTION OF THE SCATTERING PROBLEM APPLIED TO TARGET-ORIENTED TOMOGRAPHIC IMAGING

Y. Masson[1] & B. Romanowicz[1,2]
[1]*Institut de Physique du Globe, Paris, France*
[2]*University of California, Berkeley, CA, USA*

Key words Seismic Imaging, Wave Propagation, Scattering Problem, Inverse Problem

Target-oriented tomographic imaging aims to image localized regions of interest buried inside the Earth. Especially challenging is the situation where neither seismic sources nor seismic receivers are located in the vinicity of the region to be imaged. For example, for the study of a region in the deep mantle we must use remote data since all seismic stations as well as most earthquakes are located near the Earth's surface. In this case, we need to model wave propagation in the entire Earth in order to obtain the synthetic data (seismograms) needed to solve the inverse problem. Such global simulations are computationally heavy and have to be repeated thousands of times due to the non-linearity of the inverse problem. In order to lighten the computational burden, we developed a domain decomposition method that combines local wave propagation modeling with wavefield extrapolation techniques for fast and accurate imaging of remote targets. We first present a discrete solution to the direct scattering problem. We obtained a discrete formula for the exact boundary condition that is used to confine wave propagation modeling within a sub-volume of arbitrary shape, and, a discrete formula for the Helmholtz-Kirchhoff integral theorem that is used to extrapolate the numerical wavefield to remote seismic stations. Thanks to these formulas, we are able to compute synthetic seismograms that are exactly similar to thoses that would be obtained if we were modeling wave propagation in the entire Earth, but, at a reduced computational cost. Then, we investigate the tomographic imaging problem or inverse scattering problem where seismic records (full-waveforms) are inverted to deduce the visco-elastic structure of the propagating medium. Through numerical examples, we show that we are able to image remote targets in the deep Earth without having to model wave propagation in the entire Earth as illustrated in the figure. Further, we show that our method performs very well in the challenging situation where the propagating medium's structure is poorly constrained outside the region to be imaged.

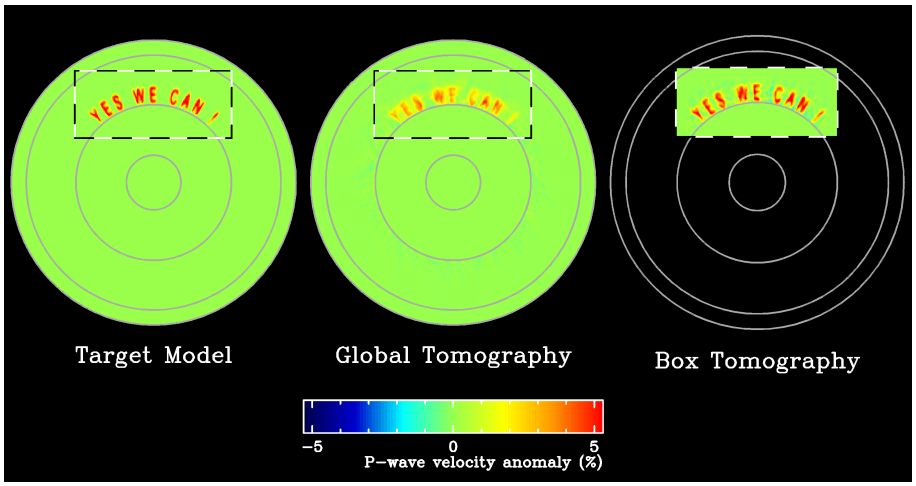

Figure 1. Tomographic images of the p-wave velocity structure within an idealized 2D planet. The left panel shows the actual structure of the planet that has a 1D axisymmetric structure similar to the one of the Earth (PREM) onto which we added some velocity anomalies at a depth corresponding to the base of the Earth's lower mantle. The middle panel shows the tomographic image obtained by doing global tomography that requiers to model wave propagation in the entire planet. The right panel shows the tomographic image obtained with the proposed domain decomposition method, here wave propagation modeling is confined within the imaged region.

References

[1] Masson, Yder, Paul Cupillard, Yann Capdeville, and Barbara Romanowicz. On the numerical implementation of time-reversal mirrors for tomographic imaging. *Geophysical Journal International*, 196(3):1580–1599, 2014.

cmg2016 - - Friday, June 10, 2016 - 11:45/12:30 (45min)

JOINT INVERSION OF NORMAL-MODE AND FINITE-FREQUENCY BODY-WAVE DATA USING AN IRREGULAR TOMOGRAPHIC GRID

Christophe Zaroli, Sophie Lambotte & Jean-Jacques Lévêque
Institut de Physique du Globe de Strasbourg, UMR 7516, EOST/CNRS, Strasbourg, France

Key words Inverse theory – Body waves – Surface waves and free oscillations – Seismic tomography

Global-scale tomographic models should aim at satisfying the full seismic spectrum. For this purpose, and to better constrain isotropic 3-D variations of shear velocities in the mantle, we tackle a joint inversion of spheroidal normal-mode structure coefficients and multiple-frequency *S*-wave delay-times.

In all previous studies for which normal modes were jointly inverted for, with body and/or surface waves, the mantle was laterally parametrized with uniform basis functions, such as spherical harmonics, equal-area blocks, and evenly spaced spherical splines. In particular, spherical harmonics naturally appear when considering the Earth's free oscillations. However, progress towards higher resolution joint tomography requires a movement away from such uniform parametrization, to overcome its computational inefficiency to adapt to local variations in resolution.

The main goal of this study is to include normal modes into a joint inversion based upon a non-uniform parametrization, that is adapted to the spatially varying smallest resolving-length of the data. Thus, we perform the first joint inversion of normal-mode and body-wave data using an irregular tomographic grid, optimized according to ray density (Fig. 1, right). We show how to compute the projection of 3-D sensitivity kernels for both data sets onto our parametrization made up of spherical layers spanned with irregular Delaunay triangulations. This approach, computationally efficient, allows us to map into the joint model multi-scale structural informations from data including periods in the 10–51 s range for body waves and 332–2134 s for normal modes.

Tomographic results are focussed on the 400–2110 km depth range, where our data coverage is the most relevant. We discuss the potential of a better resolution where the grid is fine, compared to spherical harmonics up to degree 40, as the number of model parameters is similar. Our joint model seems to contain coherent structural components beyond degree 40, such as those related to the Farallon subduction (Fig. 1, left). Assessing their robustness is postponed to a future work. A wider application of this tomographic workflow [1], holding promise to better understand mantle dynamics at various spatial scales, should primarily consist in adding surface-wave data and extending our sets of normal-mode and body-wave data.

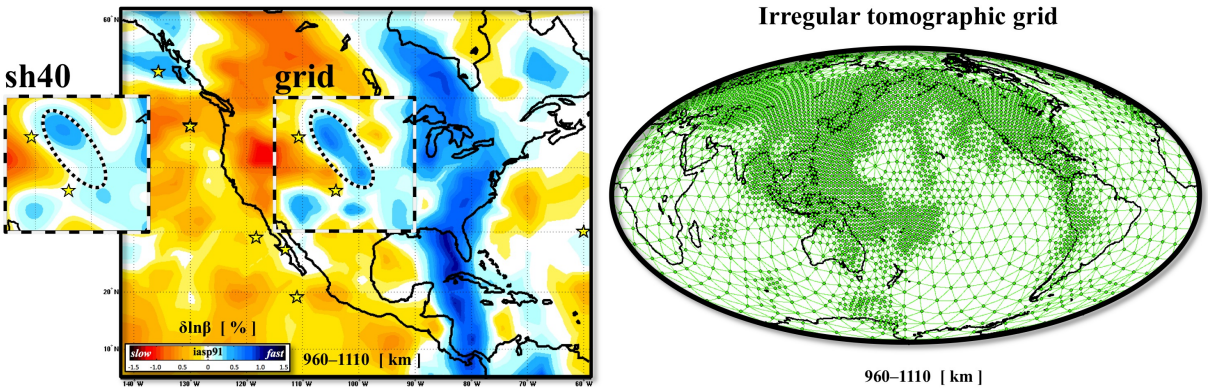

Figure 1. Zoom-in on the 3-D shear-velocity variations ($\delta \ln \beta$) related to the complex Farallon subduction system at 960–1110 km depth (left), as imaged in our joint model that was obtained using an irregular tomographic grid (right). Inset frame, on the left-hand side, shows the corresponding model from which all the spherical-harmonic components of degree greater than 40 have been filtered out. Note that our joint model seems to contain some coherent structural components well beyond degree 40.

References

[1] Zaroli, C., Lambotte, S., and Lévêque, J.-J., 2015. Joint inversion of normal-mode and finite-frequency *S*-wave data using an irregular tomographic grid, Geophysical Journal International, 203 (3): 1665-1681. doi: 10.1093/gji/ggv388

2D and 3D modeling of the Kef basin, gravity analysis of the Kef area and surrounding regions, Northwest Tunisia.

Nesrine FRIFITA [1]*, Kevin MICKUS[2], Fouad ZARGOUNI [1]

1. Unité de recherche : Géomatique, géologie structurale et appliquée, Faculté des Sciences de Tunis, 1060 Tunis, Tunisie.

2. Department of Geosciences, Missouri State University, Springfield, MO 65897, USA

* E-mail corresponding author: *frifitanesrine@yahoo.fr*

Abstract

The geology of the northern Atlas of Tunisia is characterized by NE-trending structures taking place as response to the NW compressive stress from Eocene to early Quaternary period. These structures were cutting by trough structures as evidenced by a series of grabens. These grabens were oriented orthogonally to the Atlasic deformation direction.

In order to characterize the subsurface structural makeup of this region and of the Kef basin in particular, we undertook a detailed gravity data analysis using publically available Bouguer gravity anomaly data and newly acquired 1 kilometer spaced data obtained by the National Office of Mines. The Bouguer gravity values show a gradual increase between almost -12 and 2 mGals within the Kef basin. The anomalies are represented by positive and negative responses separated by high gravity gradient interpreted as tectonic contacts shown in the derivatives gravity maps. The study area is dominated by two principal directions of faults NE-SW and NW-SE, the 2D modeling and the 3D inverse model indicate that the Kef basin contains at least 6-7 km of Cenozoic and Mesozoic sediments and this basin is bounded by set of faults oriented NE-SW, NW-SE and NS. A positive density region at 7.5 km situated northeast the basin is interpreted as NW-trending fault.

Key words: Gravity analysis, 2D and 3D modeling, Kef basin, northern Atlas foreland, Tunisia.

cmg2016 - - Friday, June 10, 2016 - 11:45/12:30 (45min)

TOWARDS A FULL WAVEFORM AMBIENT NOISE INVERSION

K. Sager[1], L. Ermert[1], C. Boehm[1] & A. Fichtner[1]
[1]*Swiss Federal Institute of Technology, Zürich, Switzerland*

Key words noise tomography, full waveform inversion, source imaging, adjoint techniques.

Noise tomography usually works under the assumption that the inter-station ambient noise correlation is equal to a scaled version of the Green function between the two receivers. This assumption, however, is only met under specific conditions, for instance, wavefield diffusivity and equipartitioning (e.g. [1], [2], [3]) or the isotropic distribution of both mono- and dipolar uncorrelated noise sources (e.g. [4], [5], [6]). These assumptions are typically not satisfied in the Earth. While attempts have been made to acknowledge heterogeneous noise source distributions (e.g. [7], [8]), the inconsistency between reality and theory inhibits the exploitation of the full waveform information contained in noise correlations regarding Earth structure and noise generation.
Realizing the need to go beyond the Green function principle and also its feasibility with current high-performance computing resources, we attempt to develop a method that consistently accounts for noise distribution, 3D heterogeneous Earth structure and the full seismic wave propagation physics. By this we intend to improve the current resolution of tomographic images of the Earth and to geographically map noise sources, thereby contributing to a better understanding of the generation of noise.

As an initial step towards a full waveform ambient noise inversion we develop a preliminary inversion scheme based on a 2D finite-difference code simulating correlation functions and on adjoint techniques. While the corresponding theory is mostly derived in the frequency domain (e.g. [9], [10]), time domain implementations of the seismic wave equation are widely used and further optimized in the seismology community. For future inversions using these codes, we present an efficient way to calculate kernels for the distribution of noise and for Earth structure in the time domain.
With respect to our final goal, a simultaneous inversion for noise distribution and Earth structure, we address the following two aspects:

1. The capabilities of different misfit functionals to image wave speed anomalies and source distribution.
2. Possible source-structure trade-offs, especially to what extent unresolvable structure could be mapped into the inverted noise source distribution and vice versa.

References

[1] O. I. Lobkis and R. L. Weaver, *On the emergence of the Green's function in the correlations of a diffuse field.*, J. Acoust. Soc. Am. **110**, 3011-3017, (2001).
[2] R. L. Weaver and O. I. Lobkis, *Diffuse fields in open systems and the emergence of Green's function.*, J. Acoust. Soc. Am. **116**, 2731-2734, (2004).
[3] F. J. Sánchez-Sesma and M. Campillo, *Retrieval of the Green's function from cross correlation: The canonical elastic problem.*, J. Acoust. Soc. Am. **96**, 1182-1191, (2006).
[4] K. Wapenaar, *Retrieving the elastodynamic Green's function of an arbitrary inhomogeneous medium by cross correlation.*, Phys. Rev. Lett. **93**, 254301, (2004).
[5] K. Wapenaar and J. Fokkema, *Green's function representations for seismic interferometry.*, Geophysics **71**, S133-S146, (2006).
[6] R. Snieder, *Extracting the Green's function of attenuating heterogeneous acoustic media from uncorrelated waves.*, Geophysics **121**, 2637-2643, (2007).
[7] H. Yao and R.D. van der Hilst, *Analysis of ambient noise energy distribution and phase velocity bias in ambient noise tomography, with application to SE Tibet.*, Geophys. J. Int. **179**, 1113-1132, (2009).
[8] N. Harmon, R. Catherine and P. Gerstoft, *Distribution of noise sources for seismic interferometry.*, Geophys. J. Int. **183**, 1470-1484, (2010).
[9] J. Tromp, Y. Luo, S. Hanasoge and D. Peter, *Noise cross-correlation sensitivity kernels.*, Geophys. J. Int. **183**, 791-819, (2010).
[10] A. Fichtner, *Source-structure trade-offs in ambient noise correlations.*, Geophys. J. Int. **202**, 678-694, (2015).

cmg2016 - - Friday, June 10, 2016 - 11:45/12:30 (45min)

Mantle structure of the North American continent inferred from transdimensional inversions of long and short period seismic data

M. Calo[1], T. Bodin[2] , and B. Romanowicz[3,4,5]

[1]*Instituto de Geofísica, Universidad Nacional Autónoma de México (UNAM), México D.F.*
[2]*CNRS-ENS Lyon, Université de Lyon 1, France*
[3] *Berkeley Seimological Laboratory, UC Berkeley, Berkeley, USA.*
[4] *Insitut de Physique du Globe de Paris (IPGP), France*
[5] *College de France, Paris, France*

Key words: Bayesian inversions, mantle structure, Mid-Lithosphere Discontinuity.

Different approaches have been used to image crust and lithospheric structure at continental scales, and in particular in North America (NA). At long periods (20-250 s), surface wave tomography provides resolution of volumetric heterogeneity of ~500 km laterally and ~50 km in depth, down to ~300 km. However, surface waves cannot uniquely resolve sharp interfaces, such as the Moho, the Lithosphere-Asthenosphere Boundary (LAB) or the possible presence of Mid-Lithospheric Discontinuities (MLD's). In order to image such discontinuities, methods based on the analysis of converted phases at crust and upper mantle interfaces (e.g. the receiver functions) have been developed. Since surface wave data and receiver functions provide complementary constraints on the Lithosphere, several studies showed the possibility to combine them to obtain more robust models of the crust and uppermost mantle.
Here we propose a trans-dimensional MCMC technique [1] that allows us to combine fundamental mode Love and Rayleigh wave dispersion curves and P-to-s converted phase data to retrieve 1D radially anisotropic layered models beneath a set of stations in NA.
Results at 30 stations deployed on the NA continent show that the tectonically active region west of the Rocky Mountain Front is marked by a Lithospheric Asthenosphere Boundary (LAB) and a Lehmann Discontinuity occurring at relatively shallow depths (60-150 km and 100-200 km, respectively), whereas further east, in the stable and old craton, these discontinuities are deeper (170-200 km and 200-250 km, respectively). In addition, in the stable part of the continent, at least two Mid Lithospheric Discontinuities (MLD's) are present at intermediate depths, suggesting the existence of strong lithospheric layering, and the possible presence of more layers, as lithospheric thickness increases with increasing cratonic age. The Moho across the continent as well as mid-crustal discontinuities in the craton are also imaged, and are generally in agreement with independent studies.

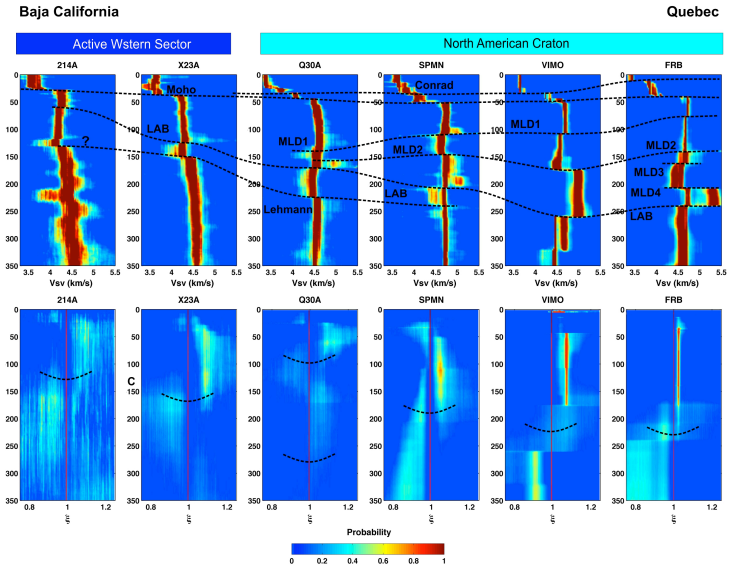

Figure 1. 1D Posterior Density Distributions of V_{sv} (top) and ξ (bottom) at stations aligned along a profile approximately oriented SW-NE. Dashed lines in V_{sv} connect the main variations in depth observed on the models and discussed in the text. Dashed lines in PPD of ξ roughly indicate the depth of change from ξ>1 to ξ<1.

References

[1] Green, P. *Reversible jump MCMC computation and Bayesian model selection*, Biometrika, 82, 711-732, (1995)

cmg2016 - - Friday, June 10, 2016 - 11:45/12:30 (45min)

GRADIENT-BASED SEISMIC INVERSION USING A FINITE FREQUENCY ASSUMPTION FOR IMAGING SUBSURFACE VELOCITY AND ATTENUATION FIELDS

G. Grandjean[1], & J. Gance[2]
[1]*BRGM, Orléans, France*
[2]*Iris Instrument, Orléans, France.*

Key words Seismic tomography, Subsurface, Gradient-based inversion.

Various studies operated seismic methods for imaging landslide structures. Among them, different approaches can be used to process the data, analyze and exploit the different kind of waves associated to particular propagation phenomena. Grandjean et al. [1] studied the first arrival traveltimes to recover P-wave velocity distribution across landslides. Finally, based on the work of Virieux and Operto [2], Romdhane et al. [3] showed the possibility to perform a full elastic waveform inversion (FWI) on a real dataset acquired over an earthflow. All those methods are more or less based on strong approximations and/or require complex data preprocessing. The issue of recovering the structural image of a landslide from the seismic velocity field estimated with an accurate, but not too unstable, method is thus posed. We propose here to revisit first arrival tomography approach which is a good compromise between the strong assumptions featuring simple refraction methods and the complexity of FWI approach when used in heterogeneous contexts. The Quasi-Newton (QN) method is based on the Tarantola's Gradient / Hessian formulation [4] ensuring an optimum convergence:

$$s(m) = \frac{1}{2}\left[(f(m) - d_{obs})^T C_D^{-1}(f(m) - d_{obs}) + \left(m - m_{prior}\right)^T C_M^{-1}(m - m_{prior})\right]$$

Where C_D and C_M are respectively the covariance operators on data and model, f represents the theoretical relationship between the model m and the data d, d_{obs} the observed data and m_{prior} the *a priori* information on the model. The QN method consists in minimizing the misfit function iteratively using its gradient and approximated Hessian functions, giving respectively the direction of steepest descent of the misfit function and a metric indicating its curvature, approximated locally by a paraboloid. The tomographic linear system in the case of no a priori information on the model can finally be written in its matrix form:

$$[(W^k)^T C_D^{-1}(W^k)]\,\delta m = [(W^k)^T \delta t] \quad \text{with} \quad W_{ij} = \frac{\omega_j}{l}$$

where k is iteration, ω represents the Fresnel volume, l is the length of the Fresnel surface along a direction perpendicular to the ray path i and for cell j. We only use here the first arrivals of the seismic signal due to direct or refracted waves. Nevertheless, we show that some regularization strategies allow detecting sharp velocity variations tending to reach FWI inversion performances (Fig.1).

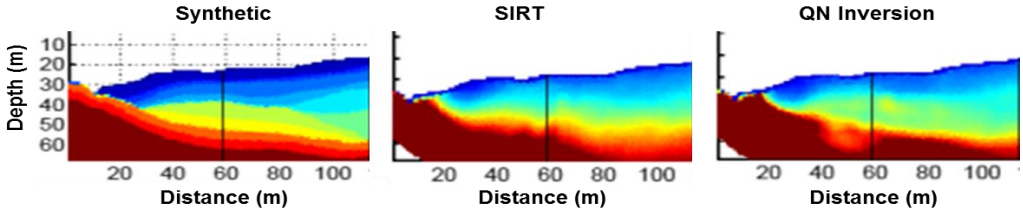

Figure 1. Initial (left), final velocity model inverted with SIRT (center) and with QN algorithm (right).

References

[1] Grandjean, G., Gourry, J.C., Sanchez, O., Bitri, A. and Garambois, S. 2011, Structural study of the Ballandaz landslide (French Alps) using geophysical imagery. *J. of App. Geophys*. 75, 531-542.
[2] Virieux, J. and Operto, S., 2009, An overview of full waveform inversion in exploration geophysics. *Geophysics*, 74(6), WCC1-WCC26.
[3] Romdhane, A., Grandjean, G., Brossier, RM, Réjiba, F., Operto, S. and Virieux, J., 2011, Shallow-structure characterization by 2D elastic full-waveform inversion. *Geophysics* 76, 81-93.
[4] Tarantola, A. 1987, Inverse Problem Theory. *Methods for data fitting and model parameters estimation*. Elsevier.

The free oscillations, or normal modes, of the Earth provide important constraints on the long-wavelength structure of our planet. Calculations using normal modes are also necessary if the effects of gravity are to be fully modeled in seismic waveforms, which becomes important at low frequencies, in particular if we wish to image density.

To implement these calculations in a 3D Earth, we typically initially compute the normal modes (eigenfunctions) of a spherically-symmetric model such as PREM. These form a complete set of basis functions, which may then be used to describe the seismic response of laterally heterogeneous models. This procedure is known as ‘mode coupling’. In order to implement the calculation, it is necessary to select a finite subset of modes (invariably defined by a frequency range) to be considered. This truncation of the infinite-dimensional equations necessarily introduces an error into the results. Here, we consider the fundamental question: if we wish to calculate synthetic spectra in a given frequency range, how many modes must we couple for the resulting spectra to be sufficiently accurate in a given 3D model?

To investigate this question, we compute spectra in the 3D model S20RTS up to 3mHz, but allowing coupling with all modes up to 6mHz. We then explore how the spectra change as we reduce the upper frequency used in the coupling. We compare this to the effects introduced by altering the 3D density structure of the model. Moreover, we repeat the calculations with a model composed of random numbers. We find that the coupling cutoff frequency depends on the power spectrum of heterogeneity. In this work we investigate the relation between power spectrum of the 3D model and the cutoff frequency in more detail. Clearly, if we wish to image Earth’s density structure accurately, it is important that the truncation error is small compared to the density signal.

cmg2016 - - Friday, June 10, 2016 - 11:45/12:30 (45min)

Time-reversal, cross-correlation and resolution of the focal spot: A novel seismological imaging approach based on properties of refocusing surface wavefields

G. Hillers[1], M. Campillo[1], Y. Ben-Zion[2] & P. Roux[1]
[1]*Institut des Sciences de la Terre, Université Joseph Fourier, Grenoble, France*
[2]*Department of Earth Sciences, University of Southern California, Los Angeles, USA*

Key words Seismic imaging, cross-correlation, time-reversal, near-field, fault zone structure, waveguide.

Modern dense seismological deployments allow the reconstruction of the seismic wavefield in the near-field from noise cross-correlations. The correlation approach makes it thus feasible to resolve the focus or focal spot, which is a characteristic feature of the cross-correlation wavefield at zero lag time t. The emergence of the focal spot is tied to the physics of a time-reversal process. Based on the equivalence of time-reversal and cross-correlation, the spatial correlation amplitude patterns at different lag times correspond to a converging (surface) wavefront at $t < 0$, the collapse or focal spot at $t = 0$ and the diverging wavefront at $t > 0$. We introduce a seismological imaging method based on high resolution reconstructions of the focal spot (Fig. 1a). This approach has been used in acoustics, nondestructive testing and medical imaging; we apply it here for the first time in a seismological context. The approach is based on the dependence of the spot shape on local properties of the propagation medium. We construct noise correlation functions from data collected by a highly-dense Nodal array centered on the San Jacinto fault zone south of Anza (southern California). The focal spot is obtained from the cross-correlation amplitude distributions at zero lag time (Fig. 1a). Strong body and fault zone waves that are associated with the complex fault zone structure prohibit the straightforward analysis of the spatially variable zero lag time distributions. We remove the body and fault zone wave components with a filter in the wavenumber domain. This yields improved reconstructions of the surface wave focal spot. The associated data of amplitude vs. distance are fitted with a damped Bessel function. The first zero-crossing of the function is directly proportional to a well-defined fraction of the seismic wavelength at the location of the correlation reference station. We repeat this analysis using each geophone location as the collapsing point to which the estimates of the wavelength or -speed (Fig. 1b) and of the damping-factor are related. Estimates of medium anisotropy can also be directly inferred from the non-circular spot shape (Fig. 1b). The overall consistency of the local wavespeed estimates from the focal spot properties and images obtained with a traditional travel time inversion using the same dataset validates the near-field approach. Both methods reveal a complex velocity structure that exhibits pronounced low-velocity zones whose location, extension and continuity depend strongly on frequency and hence depth.

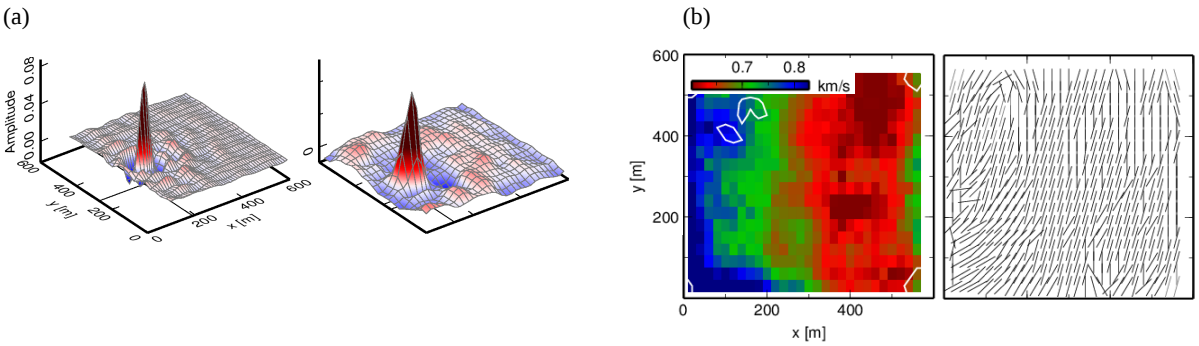

Figure 1. (a) Reconstruction of the refocusing surface wavefield in two frequency bands associated with a virtual source at the indicated locations. The focal spots are zero lapse time noise-correlation amplitude distributions obtained from correlation functions between the reference or source station and all other stations on the regular grid. (b) Measurements of the size and shape of the obtained focal spots yield, among other properties, spatial distributions of wavespeed estimates (left) and the directions of fast propagation (right). The spatial domain is defined by the array deployment.

cmg2016 - - Friday, June 10, 2016 - 11:45/12:30 (45min)

RESOLVABILITY OF REGIONAL DENSITY STRUCTURE

A. Plonka[1], A. Fichtner[2]
[1]*Utrecht University, Utrecht, the Netherlands*
[2]*ETH Zurich, Zurich, Switzerland*

Key words computational seismology, inverse theory, density heterogeneities, principal component analysis

Lateral density variations are the source of mass transport in the Earth at all scales, acting as drivers of convective motion. However, the density structure of the Earth remains largely unknown since classic seismic observables and gravity provide only weak constraints with strong trade-offs. Current density models are therefore often based on velocity scaling, making strong assumptions on the origin of structural heterogeneities, which may not necessarily be correct.

In order to assess if 3D density structure may be resolvable with emerging full-waveform inversion techniques, we proceed in two steps:

First, we quantify the impact of regional-scale crustal density structure on seismic waveforms. For this, we compare synthetic seismograms computed with and without realistic 3D density structure. For epicentral distances of around 1000 km, we detect time shifts reaching 2.5 s relative amplitude differences approaching 90 %. Our analyses indicate that reasonably sized density variations within the crust can leave a strong imprint on both travel times and amplitudes. While this can produce significant biases in velocity and Q estimates, the positive conclusion is that seismic waveform inversion for density may become feasible.

Second, we perform principal component analyses of sensitivity kernels for P velocity, S velocity, and density. This is intended to establish the extent to which these kernels are linearly independent, i.e. the extent to which the different parameters may be constrained independently. Since the density imprint we observe is not exclusively linked to travel times and amplitudes of specific phases, we consider waveform differences between complete seismograms, including the scattered wavefield.

cmg2016 - - Friday, June 10, 2016 - 11:45/12:30 (45min)

IMAGING THE SHALLOW INTERNAL STRUCTURE OF THE SAN JACINTO FAULT ZONE WITH HIGH FREQUENCY SEISMIC NOISE

D. Zigone[1,2], Y. Ben-Zion[1], M. Campillo[3], G. Hillers[3], P. Roux[3] & F. Vernon[4]

[1]*University of Southern California, Department of Earth Sciences, Zumberge Hall of Science (ZHS), 3651 Trousdale Pkwy, Los Angeles, CA 90089-0740, USA*

[2]*Present address: Institut de Physique du Globe de Strasbourg, Université de Strasbourg, EOST, CNRS, Strasbourg, France*

[3]*Institut des Sciences de la Terre, Université Grenoble Alpes, CNRS, IRD, BP 53, 38041, Grenoble, France*

[4]*Scripps Institute of Oceanography, University of California San Diego, La Jolla, CA 92093, USA*

Key words High frequency Noise-based imaging, high resolution fault structures, Rayleigh waves, San Jacinto fault zone region, low-velocity zones.

Recent tomography studies using local earthquakes and up to 3 s seismic noise provided detailed images of the region around the San Jacinto Fault Zone (SJFZ) in southern California, with nominal horizontal resolution of 1-2 km over the depth interval 0.5-15 km (Allam & Ben-Zion 2012 [1]; Allam et al. 2014 [2]; Zigone et al. 2015 [5]). To obtain high resolution information on local structures at the shallower crust, we cross correlate ambient seismic noise between 10 Hz and 70 Hz recorded by several linear arrays across the SJFZ with typical inter-station distances of 25-50 m. Following pre-processing involving earthquakes removal and whitening on 15 minutes time windows, we compute the 9-component correlation tensors for all station pairs. The obtained cross correlations exhibit coherent phase arrivals up to 30-40 Hz, which travel between the station pairs. Polarization and dispersion analyses show that both body and surface waves are reconstructed, with average Rayleigh group velocity around 450 m/s. The group velocity measurements on paths with sufficient signal to noise ratios are inverted with the Barmin et al. (2001) [3] approach using a 20 m grid size. The obtained maps reveal low velocity damage zones near the surface fault traces, with variations along strike reflecting various faulting behavior in different sections of the SJFZ. Three-dimensional images of shear wave speeds, derived with the inversion method of Herrmann (2013) [4], show local flower-shape damage structures in the top 200 m. The imaged Vs values at 30 m depths are around 250-300 m/s in agreement with available Vs30 results. These results demonstrate that close spacing between sensors allows imaging the subsurface material even at complex fault zone regions. The imaging method can be broadly utilized using the increasing number of dense deployments in various tectonic contexts.

References

[1] Allam, A. A. and Y. Ben-Zion (2012), *Seismic velocity structures in the Southern California plate- boundary environment from double-difference tomography*, Geophys. J. Int., **190**, 1181-1196, doi: 10.1111/j.1365-246X.2012.05544.x.

[2] Allam, A. A., Y. Ben-Zion, I. Kurzon, and F. L. Vernon (2014), *Seismic velocity structure in the Hot Springs and Trifurcation Seismicity Cluster Areas of the San Jacinto Fault Zone from double- difference tomography*, Geophys. J. Int., **171**, 2993-3011, doi: 10.1007/s00024-014-0784-0.

[3] Barmin, M., M. Ritzwoller, and A. Levshin (2001), *A fast and reliable method for surface wave tomography*, Pure Appl. Geophys., **158(8)**, 1351-1375.

[4] Herrmann, R. B. (2013), *Computer programs in seismology: An evolving tool for instruction and research*, Seism. Res. Lettr. **84**, 1081-1088, doi:10.1785/0220110096

[5] Zigone, D., Y. Ben-Zion, M. Campillo, and P. Roux, (2015), *Seismic tomography of the Southern California plate boundary region from noise-based Rayleigh and Love waves*, Pure Appl. Geophys., **172**, 1007-1032, doi: 10.1007/s00024-014-0872-1.

cmg2016 - - Friday, June 10, 2016 - 11:45/12:30 (45min)

WHAT DOES THE HESSIAN OPERATOR TELL US ABOUT UNCERTAINTIES AND OPTIMAL EXPERIMENTAL DESIGN?

Christian Boehm[1], Andreas Fichtner[1]
[1]*ETH Zurich, Switzerland*

Key words full-waveform inversion, low-rank approximation, uncertainty quantification, optimal experimental design

We discuss and apply methods for uncertainty quantification and optimal experimental design in time-domain full-waveform inversion based on a low-rank approximation of the Hessian operator. The fast decaying spectrum of the Hessian operator, which is a well-known property for problems in full-waveform inversion, motivates a parameterization using a small number of eigenvectors corresponding to the dominant eigenvalues of the Hessian. This only requires a few Hessian-vector products, which can be efficiently computed using adjoint methods at the cost of two additional simulations per vector. The resulting low-rank approximation of the Hessian has plenty of useful applications in the context of joint parameter inversion in elastic medium with multiple seismic sources. In particular, we focus on (i) steering the optimal experimental design of seismic events, (ii) providing information on uncertainties, and (iii) preconditioning the Newton system to speed up the solution of the deterministic inverse problem.

The separable structure of the multi-experiment inverse problem allows us to detect redundancies in the data and to gradually include more events. Furthermore, these techniques can be used to assess the quality of source-encoding strategies. In particular, we can extract information from the low-rank approximation of the Hessian to steer the selection of weights during the stacking of individual point sources.

In the context of uncertainty quantification, we utilize the low-rank approximation to construct an estimate of the covariance matrix. From this, we extract information on (i) spatial variance reduction, (ii) multi-parameter tradeoffs and (iii) spatial correlations. Furthermore, since the number of unknowns is reduced by several orders of magnitude compared to the usual nodal discretization, this method enables the use of sampling-based strategies like Markov Chain Monte Carlo methods.

We demonstrate the applicability of the approach as well as its limitations in numerical examples for 3D full-waveform inversion.

References

[1] Andreas Fichtner and Tristan van Leeuwen. Resolution analysis by random probing. *Journal of Geophysical Research: Solid Earth*, 120(8):5549–5573, 2015. 2015JB012106.

[2] Eldad Haber, Kees van den Doel, and Lior Horesh. Optimal design of simultaneous source encoding. *Inverse Problems in Science and Engineering*, 23(5):780–797, 2015.

[3] James Martin, Lucas C. Wilcox, Carsten Burstedde, and Omar Ghattas. A Stochastic Newton MCMC Method for Large-Scale Statistical Inverse Problems with Application to Seismic Inversion. *SIAM Journal on Scientific Computing*, 34(3):A1460–A1487, 2012.

[4] Noemi Petra, James Martin, Georg Stadler, and Omar Ghattas. A Computational Framework for Infinite-Dimensional Bayesian Inverse Problems, Part II: Stochastic Newton MCMC with Application to Ice Sheet Flow Inverse Problems. *SIAM Journal on Scientific Computing*, 36(4):A1525–A1555, 2014.

cmg2016 - - Friday, June 10, 2016 - 11:45/12:30 (45min)

NON-LINEAR INVERSION OF PROBABILITY DENSITY FUNCTIONS OF SURFACE WAVE DISPERSION

É. Beucler[1], I. Gaudot[1], M. Drilleau[2], A. Mocquet[1] & P. Lognonné[2]
[1]*Laboratoire de Planétologie et Géodynamique, Université de Nantes, Nantes, France*
[2]*Institut de Physique du Globe, Paris, France*

Key words Surface waves, Monte-Carlo Markov chain, Group velocity, Dispersion diagram, Seismic tomography.

A commonly used approach for inferring 3D shear wave velocity structure from surface wave measurements relies on regionalization of group (or phase) velocity curves at various frequencies as an intermediate step before 1D inversion at depth for each grid point. This choice relies on tracking the maximum energy in the dispersion diagram in order to get a unique dispersion curve and the estimate of associated measurement uncertainties usually depends on *ad hoc* user's criteria. We present an alternative by directly inverting the waveform, once it is converted into probability density functions of dispersion, in order to obtain a posterior probability of 1D shear wave structure integrated along the ray path. The dispersion diagram is sampled using a Markov-chain Monte Carlo algorithm and each trial model is parameterized by Bézier curves in order to ensure smooth variations and a fast forward problem. For each depth of the 1D shear wave posterior probabilities, path averaged velocities can be regionalized using classical least-squares criterion. We show inversion results of cross-correlations of ambient seismic noise in a regional context and at global scale of multiple orbit surface wave trains. This latter approach can be used for planetary purposes in the event of deployment of one seismic station on another planet.

cmg2016 - - Friday, June 10, 2016 - 11:45/12:30 (45min)

BAYESIAN SEISMIC TOMOGRAPHY BY INTERACTING MARKOV CHAINS

A. Bottero[12], A. Gesret[1], T. Romary[1], M. Noble[1], N. Desassis[1] & C. Maisons[3]
[1]*MINES ParisTech, PSL Research University, Centre de Geosciences, Fontainebleau, France.*
[2]*LMA, CNRS UPR 7051, Aix-Marseille University, Marseille, France.*
[3]*Magnitude SAS, Centre Regain, Saint-Tulle, France.*

Key words Seismic tomography, Bayesian approach, wavelet parameterization, seismic event location.

The velocity field estimated by first arrival traveltime tomography is commonly used as a starting point for further seismological, mineralogical, tectonic or similar analysis. In order to interpret quantitatively the results, the tomography uncertainty values as well as their spatial distribution are required.
The estimated velocity model is obtained through inverse modeling by minimizing an objective function that compares observed and computed traveltimes. This step is often performed by gradient-based optimization algorithms. The major drawback of such local optimization schemes, beyond the possibility of being trapped in a local minimum, is that they do not account for the multiple possible solutions of the inverse problem. They are therefore unable to assess the uncertainties linked to the solution. Within a Bayesian framework, solving the tomography inverse problem aims at estimating the posterior probability density function of velocity model using global sampling algorithms. Markov chains Monte-Carlo (MCMC) methods are known to produce samples of virtually any distribution. Nevertheless their use is problematic in high dimensional model spaces especially when the computational cost of the forward problem is consequent and/or the a posteriori distribution is multimodal. In the latter case the chain may even stay stuck in one of the modes and hence not provide an exhaustive sampling of the distribution of interest.
In order to improve the mixing properties of classical single MCMC, we propose to make interact several Markov chains at different temperatures (Romary [1]). This method can make efficient use of large CPU clusters, without increasing the global computational cost with respect to classical MCMC and is therefore particularly suited for Bayesian inversion. The exchanges between the chains (based on Importance Resampling) allow a precise sampling of the high probability zones of the model space while avoiding the chains to end stuck in a local probability maximum. This approach supplies thus a robust way to analyze the tomography imaging uncertainties.
The interacting MCMC approach is here first applied to a synthetic multimodal distribution in order to demonstrate its robustness and efficiency compared to a Simulated Annealing method. It is then applied to a first arrival time seismic tomography of calibration shots recorded in the context of hydraulic fracturing. We propose a wavelet based model parameterization. This allows to integrate the a priori information provided by sonic logs and to reduce optimally the dimension of the problem, making thus the algorithm efficient even for a complex velocity model. Our sampling algorithm allows us to generate velocity models distributed according to the posterior distribution and to estimate velocity model uncertainties for this real data case.
We then propagate these velocity model uncertainties to the seismic event location in a probabilistic framework (Gesret et. al. [2]). This Bayesian formulation that integrates properly the knowledge on the velocity model into the formulation of the probabilistic earthquake location enables us to obtain more reliable hypocentre locations as well as their associated uncertainties accounting for both picking and velocity model uncertainties.

References

[1] T. Romary, *Bayesian inversion by parallel interacting markov chains*, Inverse Problems in Science and Engineering, **18(1)**, 111–130 (2010).
[2] A. Gesret, N. Desassis, M. Noble, T. Romary & C. Maisons, *Propagation of the velocity model uncertainties to the seismic event location*, Geophys. J. Int., **200(1)**, 52–66 (2015).

cmg2016 - - Friday, June 10, 2016 - 11:45/12:30 (45min)

Anisotropic shear velocity models of the North American upper mantle based on waveform inversion and numerical wavefield computations.

P. Clouzet[1], Y. Masson[1], B. Romanowicz[1,2,3], S. W. French[2,4], H. Yuan[5]
[1] *Institut de Physique du Globe, Paris*
[2] *Berkeley Seismological Laboratory, Berkeley, CA*
[3] *Collège de France, Paris*
[4] *National Energy Research Scientific Computing Center, Berkeley, CA*
[5] *Macquarie University, Sydney, Australia*

Key words: Seismic Tomography, Upper Mantle, Anisotropy, Waveform modeling.

The Earthscope TA deployment across the continental US now has reached the eastern part of the US, providing the opportunity for high-resolution 3D seismic velocity imaging of both lithosphere and asthenosphere across the entire north-American continent (NA). Previously (Yuan et al., 2014), we presented a 3D radially anisotropic shear wave (Vs) model of North America (NA) lithospheric mantle based on full waveform tomography, combining teleseismic and regional distance data sampling the NA. Regional wavefield computations were performed numerically, using a regional Spectral Element code (RegSEM, Cupillard et al., 2012), while teleseismic computations were performed approximately, using non-linear asymptotic coupling theory (NACT, Li and Romanowicz, 1995). For both datasets, the inversion was performed iteratively; using a Gauss-Newton scheme, with kernels computed using either NACT or the surface wave, path average approximation (PAVA), depending on the source-station distance.

We here present a new radially anisotropic lithospheric/asthenospheric model of Vs for NA based entirely on SEM-based numerical waveforms from an augmented dataset of 155 regional events and 70 teleseismic events. The forward wavefield computations are performed using RegSEM down to 40s, starting from our most recent whole mantle 3D radially anisotropic Vs model (SEMUCB-wm1, French and Romanowicz, 2014). To model teleseismic wavefields within our regional computational domain, we developed a new modeling technique which allows us to replace a distant source by virtual sources at the boundary of the computational domain (Masson et al., 2014). Computing virtual sources requires one global simulation per teleseismic events.

We then compare two models obtained: one using NACT/PAVA kernels as in our previous work, and another using hybrid kernels, where the Hessian is computed using NACT/PAVA, but the gradient is computed numerically from the adjoint wavefield, providing more accurate kernels while preserving the fast convergence properties of the Gauss-Newton inversion scheme.

References

Cupillard P., Delavaud., Burgos G., Festa G., Vilotte J-P., Capdeville Y., Montagner J-P., *RegSEM: a versatile code based on the spectral element method to compute seismic wave propagation at the regional scale.,* Geophys. J. Int. (2012)

French S. W., Romoanowicz B., *Whole-mantle radially anisotropic shear velocity structure from spectral-element waveform tomography*, Geophys. J. Int. (2014)

Li, X-D and B. Romanowicz ,*Comparison of global waveform inversions with and without considering cross branch coupling,* Geophys. J. Int., 121, 695-709. (1995)

Masson Y., Cupillard P., Capdeville Y., Romanowicz B. *On the numerical implementation of time-reversal mirrors for tomographic imaging*., Geophys. J. Int. (2013)

cmg2016 - - Friday, June 10, 2016 - 11:45/12:30 (45min)

OPTIMAL TRANSPORT DISTANCE FOR SEISMIC TOMOGRAPHY: APPLICATION TO FULL WAVEFORM INVERSION

L. Métivier [1,2], R. Brossier[2], Q. Mérigot[3], E. Oudet[1], J. Virieux[2]
[1] *Laboratoire Jean Kuntzmann (LJK), Univ. Grenoble Alpes, CNRS, France*
[2] *Institut des sciences de la Terre (ISTerre), Univ. Grenoble Alpes, France*
[3] *Laboratoire CEREMADE, Univ. Paris-Dauphine, CNRS, France*

Key words Full waveform inversion, cycle skipping, optimal transport, proximal splitting.

Full waveform inversion (FWI) is a high resolution seismic imaging technique based on the minimization of the L^2 distance between observed and predicted seismic data. An initial estimation of the subsurface model is iteratively improved following local optimization techniques. When applied to the reconstruction of subsurface velocity parameters, the method is known to suffer from cycle skipping. Velocity models matching the observed data up to one or several phase shifts correspond to local minima of the L^2 misfit function. Avoiding to converge to these local minima requires a sufficiently accurate initial velocity model, and adequate data pre-processing: hierarchical approaches privileging the lowest components of the data and the transmitted energy are usually implemented for real data applications [Virieux and Operto, 2009].

In a recent study, we have propose to use an optimal transport distance for measuring the misfit between observed and predicted data [Métivier et al., 2016]. Optimal transport originates from the work of the French engineer Gaspard Monge (1790) in an attempt to devise the best strategy to move sand to a building site, in a prescribed configuration. In more modern mathematics language, the optimal transport distance between two mass distributions $\mu(x)$ and $\nu(y)$ is the solution of a minimization problem among the set of the mapping transporting $\mu(x)$ over $\nu(y)$, given a cost $c(x, y)$ measuring the effort for moving a unit mass from x to y [Santambrogio, 2015]. Such a distance has been successfully used in image processing for color histogram matching, pattern recognition, and shape identification [Lellmann et al., 2014]. The ability of this distance to detect shifted patterns in two distinct images is an interesting property for FWI. A better convexity of the associated misfit function with respect to time-shifts is expected, which should efficiently mitigate cycle skipping issues.

In its conventional formulation, optimal transport distance is dedicated to the comparison of positive signals with a strict mass conservation. Theses assumptions (positivity, mass conservation) are not satisfied by predicted and observed seismic data. For this reason, the use of a modified optimal transport distance, based on the Kantorovich-Rubinstein norm, is investigated. An efficient numerical strategy based on a proximal splitting method is implemented [Combettes and Pesquet, 2011], which offers the possibility to address large-scale problems associated with realistic 2D and 3D FWI applications. An example of application on the 2D Marmousi case study is provided in Figure 1. Starting from a crude initial model, conventional L^2 FWI fails in recovering the subsurface velocity. The strategy based on the optimal transport distance provides a significantly better subsurface velocity estimation. Future work will be dedicated to the application of this strategy on the 2D Nankai and the 3D Valhall data-sets.

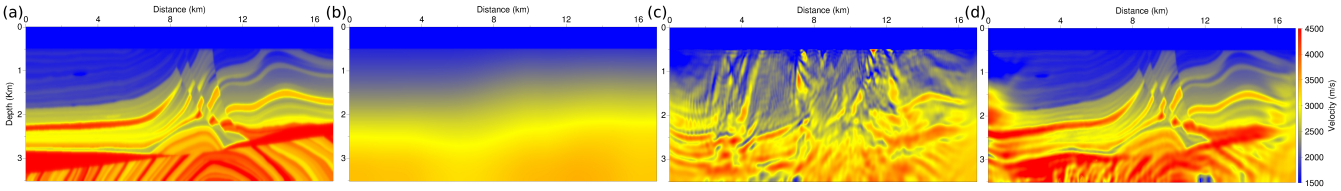

Figure 1. Marmousi model (a). Rough Initial model (b). FWI estimation using the L^2 distance (c). FWI estimation using the optimal transport distance (d).

References

[Combettes and Pesquet, 2011] Combettes, P. L. and Pesquet, J.-C. (2011). Proximal splitting methods in signal processing. In Bauschke, H. H., Burachik, R. S., Combettes, P. L., Elser, V., Luke, D. R., and Wolkowicz, H., editors, *Fixed-Point Algorithms for Inverse Problems in Science and Engineering*, volume 49 of *Springer Optimization and Its Applications*, pages 185–212. Springer New York.

[Lellmann et al., 2014] Lellmann, J., Lorenz, D., Schönlieb, C., and Valkonen, T. (2014). Imaging with kantorovich–rubinstein discrepancy. *SIAM Journal on Imaging Sciences*, 7(4):2833–2859.

[Métivier et al., 2016] Métivier, L., Brossier, R., Mérigot, Q., Oudet, E., and Virieux, J. (2016). Measuring the misfit between seismograms using an optimal transport distance: Application to full waveform inversion. *Geophysical Journal International*, in press.

[Santambrogio, 2015] Santambrogio, F. (2015). *Optimal Transport for Applied Mathematicians: Calculus of Variations, PDEs, and Modeling*. Progress in Nonlinear Differential Equations and Their Applications. Springer International Publishing.

[Virieux and Operto, 2009] Virieux, J. and Operto, S. (2009). An overview of full waveform inversion in exploration geophysics. *Geophysics*, 74(6):WCC1–WCC26.

Seismic waves

cmg2016 - - Friday, June 10, 2016 - 17:30/18:00 (30min)

ENVELOPE BROADENING AND SCATTERING ATTENUATION OF A WAVELET IN RANDOM MEDIA HAVING A POWER-LAW SPECTRA

Haruo Sato[1]
[1]*Tohoku University, Sendai, Japan*

Key words Random media, Scattering, Earthquakes, Seismograms, Envelope broadening, Lithospheric heterogeneity

Seismograms of small earthquakes show scattering effect of random heterogeneities in the lithosphere (e. g. Sato et al. 2012). As shown in Figure 1 (a), we see a delay of the maximum peak from the S-onset and a broadened envelope of S-wavelet larger than the source duration. Peak delay measurements offer fruitful information about lithospheric heterogeneities in relation with seismo-tectonic settings. In Japan arc, strong heterogeneities are found especially beneath Quaternary volcanoes (Takahashi et al. 2007). We also take notice of power-law spectra of velocity well log data, which suggests that random velocity fluctuations have power-law spectra even in seismic spectral range. Here, we study the mathematical aspect of the envelope of a scalar wavelet in von Kármán type random media. Figure 1 (b) shows an example of power spectral density function (PSDF) of random velocity fluctuation. When the center wavenumber of the wavelet is in the power-law spectral range, we propose to divide the random medium spectra into two parts taking the center wavenumber as a reference, and then, we study their scattering contribution to envelope broadening and amplitude attenuation [1]. For the wave propagation through the long-scale (low-wavenumber spectral) component of random media, we may apply the parabolic approximation to the wave equation, which well describes scattering in a narrow angle around the forward direction. Using the Markov approximation, which is a stochastic extension of the phase screen method, we can analytically synthesize the mean square (MS) wavelet envelope G_{M0} for an impulsive source radiation. The resultant envelope duration increases according to the second power of travel distance r; however, the time integral $\int 4\pi r^2 G_{M0} dt$ is conserved irrespective of r. Wide angle scattering caused by the short-scale (high-wavenumber spectral) component of random media contributes to the attenuation of wave amplitude. We use the total scattering coefficient of the short-scale component g_{S0} given by the Born approximation as a measure of scattering attenuation per distance. Multiplying the exponential scattering attenuation factor $\mathrm{Exp}(-g_{S0}V_0 t)$ by the MS envelope derived by the Markov approximation G_{M0}, we can synthesize the MS envelope G_{M0S} which reflects the scattering contribution of all the spectral components of random media. Figures 1 (c) and (d) show synthesized MS wavelet envelopes with geometrical correction for different center frequencies at a 100 km distance by way of example, where solid and dashed lines are with and without scattering attenuation correction. When the PSDF has a small role-off as $\kappa = 0.1$, the envelope broadening is large and increases with frequency, and the scattering attenuation is strong and increases with frequency. When the PSDF has a steep role-off as $\kappa = 1$, however, the envelope broadening is small and frequency independent, and scattering attenuation is weak. The proposed synthesis is fully analytic; therefore, it can be a theoretical basis for the evaluation of random heterogeneity of the earth medium from the envelope broadening of seismograms in short periods. In the above envelope synthesis, wide angle scattering is considered only for the amplitude attenuation effect. For explaining coda envelopes, it will be necessary to incorporate multiple wide-angle scattering process in the framework of the radiative transfer theory.

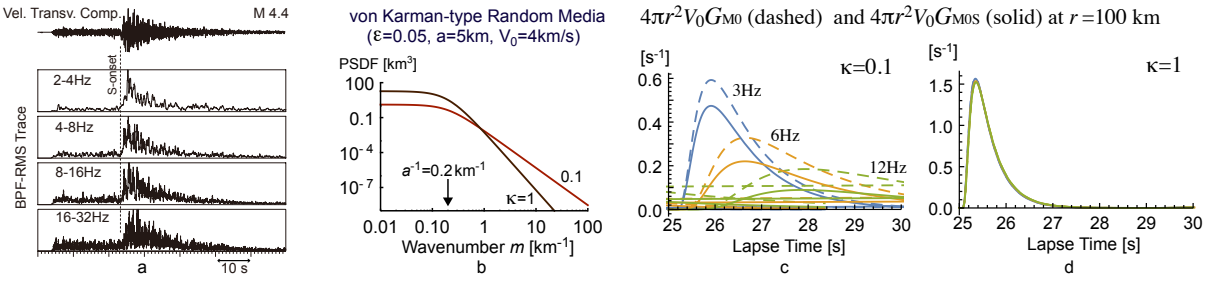

Figure 1. (a) RMS seismogram envelopes (Saito et al. 2002). (b) Example of PSDF of random velocity fluctuation. (c) and (d) synthesized MS envelopes with geometrical correction for an impulsive source radiation [1].

References

[1] Sato, H., *Envelope broadening and scattering attenuation of a scalar wavelet in random media having power-law spectra*, Geophys. J. Int., 204, 386–398 (2016).

cmg2016 - - Friday, June 10, 2016 - 18:00/18:30 (30min)

SOLVING SPATIAL INVERSION PROBLEMS USING EXACT SAMPLING

Andrew Curtis[1] and Matthew Walker[1,2]
[1]*University of Edinburgh, Edinburgh, United Kingdom*
[2]*Now at: BP, Building H, Chertsey Rd., Sunbury-on-Thames, United Kingdom*

Key words Bayesian, recursive, geology, geophysics, inversion, sampling, Monte Carlo, Markov chain, posterior, prior

Geoscientists often use spatially discretized cellular models of the Earth where data in each grid cell provide independent information about the model parameters of interest at that location, yet where parameters are spatially correlated. In Bayesian inference the data-derived information is given as a set of likelihoods describing the (unnormalized) probability of the parameters, given only the data in each cell. Pre-existing information about the model parameters' values and their spatial correlations may be described by a prior probability distribution. The prior, likelihoods, and Bayes' rule together specify a posterior probability distribution that describes the resultant state of information over all model parameters. However, due to the high dimensionality of typical models, the posterior is usually only known up to a multiplicative constant and only at specific, numerically evaluated points or samples in the model space (i.e., it is not known analytically). Markov chain Monte Carlo (McMC) methods are typically used to produce an ensemble of correlated samples which converges to the posterior as the number of samples tends to infinity. These ensembles are often slow to converge in distribution to the posterior; indeed, they may not converge in finite time, and detecting their state of convergence is often impossible in practice. Thus, estimates of the posterior obtained from such samples may be substantially biased.

We derive a recursive algorithm which samples the posterior exactly, providing independent (uncorrelated) posterior samples from the first sample onwards [1]. Thus the method avoids the above convergence issues completely. Its computational cost scales with the size of the parameters' sample space, the prior's spatial range of dependency, and the shortest edge dimension of the grid. We develop an approximation to the algorithm such that it may be used on large 2-D (and potentially 3-D) model grids.

We apply the algorithm to invert synthetic seismic attribute data (impedances) for subsurface structure, by combining the attribute data with Geological prior information that includes spatial correlations expected of real geological strata. We obtain results which compare favourably to the results of McMC (Gibbs) sampling – indeed the latter exhibits convergence problems and bias.

This method might be generalised to other types of problems as will be discussed, providing an alternative to McMC methods for a wider class of problems.

References

[1] M. Walker & A. Curtis, Spatial Bayesian inversion with localized likelihoods: An exact sampling alternative to McMC, J. Geophys. Res.. **119**, 5741-5761 (2014). Doi: 10.1002/2014JB011010

cmg2016 - - Friday, June 10, 2016 - 11:45/12:30 (45min)

CHARACTERIZING EARTHQUAKE SOURCE PHYSICS WITH SOURCE SCANNING ALGORITHMS

F. Massin[1], A. Malcom[1]
[1]*Memorial University of Newfoundland, St. John's, Canada.*

Key words Body-wave detection, hypocenter determination, earthquake parameter estimation, micro-earthquakes, earthquake swarms.

Earthquake swarms that lack a clear main-shock are particularly difficult to explain and characterize for hazard assessment. These events could be triggered in the vicinity of a local perturbation from many sources, natural or not, with implications for our understanding of the rupture characteristics of earthquakes. We tackle the problem of understanding perturbing mechanisms, by investigating the location, mechanism and extent of earthquake ruptures. Ultimately we are interested in estimating the stress field and pore pressure that control the mechanical instabilities of earthquakes and clustered seismicity sequences. In this preliminary study, we investigate the potential of shift and stack methodologies for the probabilistic analysis of focal mechanism determination and relative earthquake location.

Shift and stack methods for earthquake location, or source scanning algorithm (SSA), are based on three steps: 1) pre-calculation of travel time grids (also defining the hypocenter solution space), 2) calculating a characteristic function of the body-wave arrivals from continuous data, with signal processing methods, 3) the shifting and summation of the characteristic functions in each grid cell, with shifts defined by the pre-calculated travel times. Ideally, the power recovered by the entire network as a function of time can be used for simultaneous event detection and location. Although the SSA method shows promise for automatic detection and location of events, it is limited by the precision of the pre-defined grid.

We extend this approach to focal mechanism determination with slight modifications. We first pre-calculate the polarity distribution for all double couple orientations. Then polarity corrections are applied to the first motion wavelets (as extracted with SSA) from all possible mechanisms. For the optimal orientation, the wavelets with downward first motions are multiplied by negative polarities and thus all wavelets stack constructively. Finally, the probability of each double couple orientation is estimated by stacking the modified wavelets.

In the classic approach, the hypocenter position and double couple orientation are estimated by taking the maximum of gridded objective functions (i.e. the amplitude of the stacked characteristic functions and wavelets). To overcome the limitation in hypocenter precision mentioned above, we investigate inversion schemes and relative location procedures. We first study a simplified approach for relative location using reference events. To do so, we consider the classic relative location scheme of an event compared to several reference events in which the travel time differences of each event pair as a function of azimuth is a sinusoid.

References

cmg2016 - - Friday, June 10, 2016 - 11:45/12:30 (45min)

ACOUSTIC TIME REVERSAL IN GRANULAR MEDIA

M. Harazi, Y. Yang, M. Fink, A. Tourin, and X. Jia
ESPCI Paris, PSL Research University, CNRS, Institut Langevin, Paris, France

Key words: granular media, elastic wave propagation, time reversal focusing, multiple scattering of waves

In a non-dissipative medium, the wave equation is symmetric in time. Therefore for every wave diverging from a pulsed source, there exists in theory a wave, the time-reversed wave, that precisely retraces all its original paths in a reverse order and converges in synchrony at the original source as if time were going backwards. In the early nineties, M. Fink proposed an original method for generating such a time-reversed wave from a surface named a Time Reversal Mirror (TRM) [1]. This method was first tested with ultrasound and then successfully extended to other types of waves such as microwaves, water waves, and even in optics. It has led to numerous applications including seismic source imaging [2]. Several studies have shown that time reversal wave focusing is very robust to disorder [3], including situations where perturbations occur between forward and back propagation steps [4,5]. Here we investigate time reversal (TR) of elastic waves propagating in fragile granular media consisting of glass beads under static compression. Pulsed elastic waves transmitted from a compression or a shear wave source are measured by a TRM (Fig. 1.a and Fig. 1.b), time reversed and back-propagated. The ability of the time-reversed wave to focus at the initial source is checked as a function of the source amplitude. We find that TR of the ballistic coherent wave is very robust to perturbations but provides poor resolution. By contrast, the short-wavelength scattered waves offer a finer TR focusing but are sensitive to rearrangements induced by the forward propagation wave itself: at large source amplitudes, time reversal focusing is broken (Fig. 1.c). Experimental results are confronted with predictions from a numerical model in which the propagation medium is modelled by a percolating network of spherical balls interacting via linear springs.

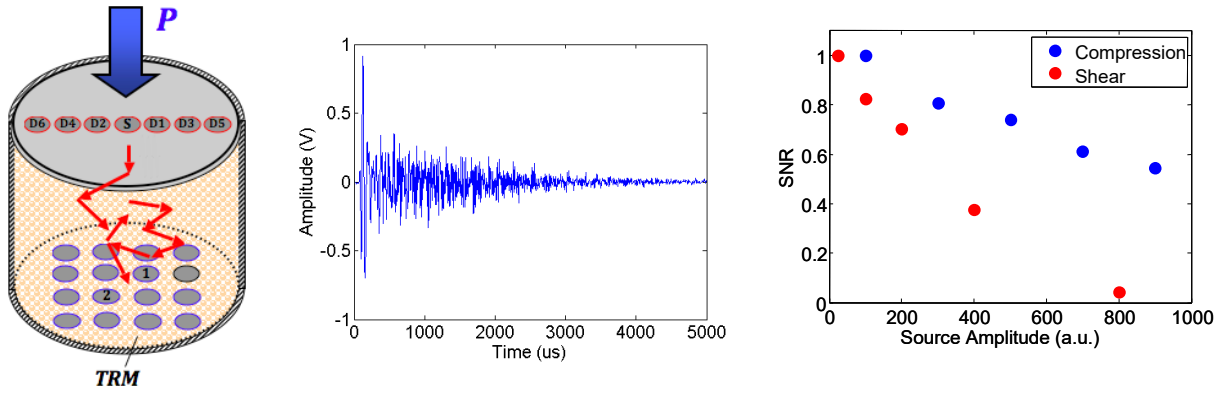

Figure 1. (a) Experimental setup: 1.5mm diameter glass beads are placed between the source S and the 16-element TRM. Detectors D1 to D6 allow for spatial focusing measurements. (b) A typical ultrasonic waveform transmitted through the glass bead packing consists of a low-frequency coherent wave followed by high-frequency scattered waves (c) Ratio of the time-reversed peak amplitude to the RMS of the side lobes as a function of the source amplitude for a compression (blue dots) and a shear wave source (red dots).

References

[1] M. Fink, Physics Today 50 (3), 34 (1997)
[2] C. Larmat, J. Montagner, M. Fink, Y. Capdeville, A. Tourin, E. Clévéde, Geophys. Res. Lett. 33, L19312 (2006)
[3] A. Derode, P. Roux, and M. Fink, Phys. Rev. Lett. 75, 4206 (1995)
[4] R.K. Snieder and J.A. Scales, Phys. Rev. E 58, 5668 (1998)
[5] A Tourin, A. Derode, and M. Fink, Phys. Rev. Lett. 87, 274301 (2001)

cmg2016 - - Friday, June 10, 2016 - 11:45/12:30 (45min)

LONG PERIOD SCATTERING OF SEISMIC WAVES IN SPHERICAL RANDOM MEDIA

Matthias Meschede[1], Barbara Romanowicz[123]
[1] *Institut de Physique du Globe de Paris, Paris 75005, France*
[2] *Collège de France, Paris 75005, France*
[3] *University of California, Berkeley, USA*

Key words seismology, random models, mantle structure, surface waves, scattering, coda, statistical approaches

We analyze scattering of seismic waves in the Earth due to structure that is beyond the resolution limit of current global tomographic mantle models. To this end, we use statistically defined models and examine scattered waves in the numerically computed wavefield.

We define the statistics of the small scale structure using a non-stationary covariance matrix that covers a range of distributions that are guided by the statistics of larger scale heterogeneities and the properties of regional high resolution models. A non-stationary second order model realisation can then be generated from the eigenbasis of the covariance matrix.

We find that scattering at the long periods (100s) is relatively small and has only limited influence on measurements of e.g. attenuation or travel times. However, it is noticeable in the simulations and data and can be used to constrain the amount of small scale variations of Earth's elastic structure.

Finally, we present a method to invert statistically for small random perturbations using standard Born (single scattering) waveform sensitivity kernels.

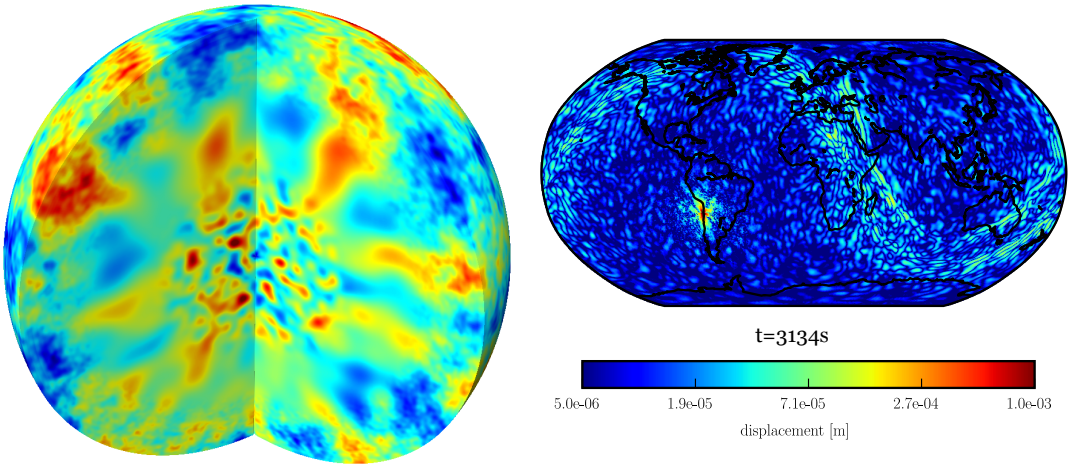

Figure 1.
Left: non-stationary spherical, second order (Gaussian) random model.
Right: long period ($T = 100s, \lambda_{\text{hor}} \approx 400km$) scattered wavefield generated in a tomographic model (resolution > 600km) that has been extended with different distributions of randomly located small scale structure.

cmg2016 - - Friday, June 10, 2016 - 11:45/12:30 (45min)

WAVE SOURCE LOCALIZATION: AN ENERGY BASED APPROACH

S. Turkaya[1], R. Toussaint[1], F. K. Eriksen[1, 2], O. Lengliné[1], G. Daniel[3], E. G. Flekkøy[2] & K. J. Måløy[2]
[1]*Institut de Physique du Globe, Strasbourg, France.*
[2]*Department of Physics, University of Oslo, P. 0. Box 1048, 0316 Oslo, Norway*
[3]*Magnitude, Route de Marseille 04220 Sainte Tulle, France*

Key words lamb waves, wave localization, thin plates

Noisy acoustic signal localization is a difficult problem having a wide range of applications. We propose a new localization method applicable for thin plates, based on energy amplitude attenuation and inversed source amplitude comparison. This inversion is tested on synthetic data using a direct model of Lamb wave propagation and on experimental dataset (recorded with 4 Brüel & Kjær Type 4374 miniature piezoelectric shock accelerometers, 1 - 26 kHz frequency range). We compare the performance of this technique with classical source localization algorithms, arrival time localization, time reversal localization, localization based on energy amplitude.

The experimental setup (Figure 1) consists of a glass / plexiglass plate of dimensions of 80 cm x 40 cm x 1 cm equipped with four accelerometers and an acquisition card. Signals are generated using a steel, glass or polyamide ball (of different sizes) hitting the plate quasi perpendicularly from a height of 2-3 cm. Signals are captured by sensors placed on the plate on different locations.

We measure and compare the accuracy of these techniques as function of sampling rate, dynamic range, array geometry, signal to noise ratio and computational time. We show that this new and very versatile technique works better than conventional techniques (arrival time delay localization, time reversal localization, and energy based localization) over a range of sampling rates 8 kHz – 1 MHz. It is possible to have a decent resolution (3cm mean error) using a very cheap equipment set. The numerical simulations allow us to track the contributions of different error sources in different methods. The effect of the reflections is also included in our simulation by using the imaginary sources outside the plate boundaries.
This proposed method can easily be extended for applications in three dimensional environments, to monitor industrial activities (e.g boreholes drilling/production activities) or natural systems (e.g earthquakes, volcanoes, avalanches).

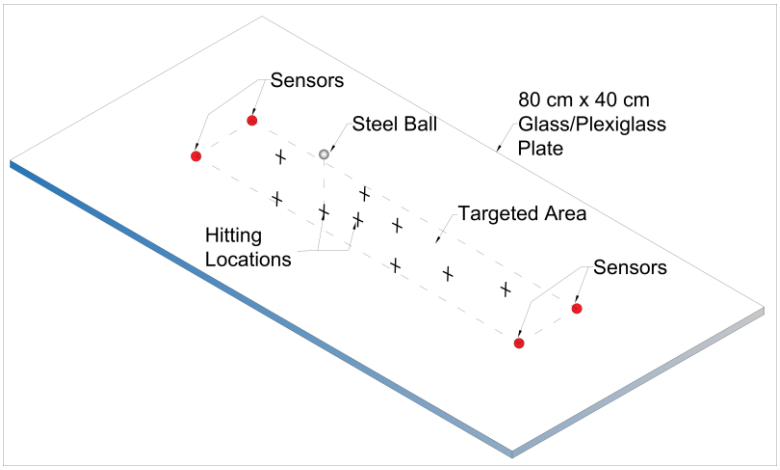

Figure 1. Experimental setup with steel ball hitting on thin plate (glass or plexiglass).

Mechanics of Faulting and Rocks

cmg2016 - - Wednesday, June 8, 2016 - 10:00/10:15 (15min)

THE STRUCTURE OF SLIP-PULSES AND SUPERSHEAR RUPTURES DRIVING SLIP IN BIMATERIAL FRICTION

H. Shlomai[1], J. Fineberg[1]
[1] *The Racah Institute of Physics, The Hebrew University of Jerusalem, Givat Ram, Jerusalem Israel*

Friction | bimaterial interface | rupture structure | slip-pulse | supershear ruptures

Frictional motion occurs when the contacts composing the interface connecting two bodies together detach via propagating rupture fronts. Most studies of frictional sliding have considered homogeneous systems, sliding bodies composed of the same material. The most common frictional motion in nature, however, involves *bimaterial* interfaces, when the contacting bodies possess different elastic properties. Important examples include natural faults that are bordered by different rock types [1]. The existence of a *bimaterial* interface can bring about qualitative differences in how contact points detach [2-3] as coupling between slip and normal stress variations, unique to bimaterial interfaces, has long been expected.

We study rupture dynamics in bimaterial system composed of PMMA (polymethylmethacrylate) and polycarbonate. Using high-speed simultaneous measurements of slip velocities, real contact area and near-interface stresses we will explicitly demonstrate the existence of both bimaterial coupling and its role in determining different classes of rupture modes, each with its accompanying structure. These include slip-pulses, highly localized slip (*pulse-like* rupture) accompanied by large local reductions of the normal stress near the rupture tip. These pulses only propagate near the softer material's shear wave speed and continuously evolve with their propagation distance. Slip pulses are the dominant mode when ruptures propagate in the direction of motion of the softer material, called the positive direction. In the opposite negative propagation direction, we find that bimaterial coupling drives dominant supershear fronts that are characterized by extended slip (*crack-like* rupture).

The robustness of these structures suggests that, despite the complexity of natural faults, distinct bimaterial effects should emerge in earthquakes along bimaterial faults. They might explain field observations as directionality of earthquake ruptures and asymmetry of rock damage along natural faults as well as contribute to understanding the "heat paradox", the relatively low amount of heat generated by earthquakes.

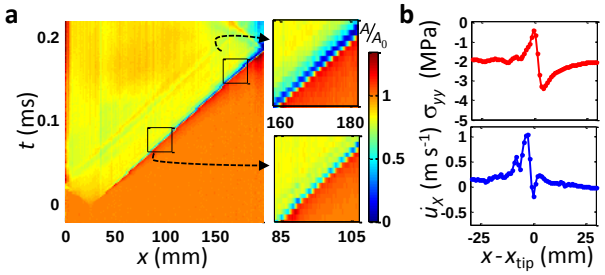

Figure 1. A slip-pulse rupture propagating in the positive direction in a bimaterial system. We reveal the structure of slip pulses using measurements of real contact area, $A(x,t)$ (**a**), normal stress, σ_{yy}, (**b**-top) and slip velocity, $\dot{u}_x$ (**b**-bottom). As the rupture tip approaches a measurement point, $A(x,t)/A_0(x)$ ($A_0(x) = A(x,t<0)$) is first compressed. With the tip passage, A drops dramatically to ~$0.1A_0$ (dark blue) for ~5mm and then heals to residual value of ~$0.8A_0$. σ_{yy} exhibits similar behavior. Initial compression is followed by a large release of normal stress for a short region of ~5mm. Then σ_{yy} is dynamically restored to its initial value. At the same time, the particle velocity adjacent to the interface, $\dot{u}_x$, is highly localized; non-zero values are only observed during the release in σ_{yy}. The correlation and synchronization of σ_{yy} and $\dot{u}_x$ provide clear evidence for slip-pulses (in the positive direction) driven by bimaterial coupling. Right panels (**a**) are close-ups of $A(x,t)$ in the denoted areas, showing both the continuous evolution of the slip pulse with propagation distance and highlighting the large reductions in real contact area surrounding the rupture tip.

References

[1] Dor, O., Rockwell, T. K. & Ben-Zion, Y. Geological observations of damage asymmetry in the structure of the San Jacinto, San Andreas and Punchbowl faults in Southern California: A possible indicator for preferred rupture propagation direction. *Pure and Applied Geophysics* **163**, 301-349 (2006).
[2] Weertman, J. Unstable slippage across a fault that separates elastic media of different elastic constants. *Journal of Geophysical Research* **85**, 1455-1461 (1980).
[3] Andrews, D. J. & Ben-Zion, Y. Wrinkle-like slip pulse on a fault between different materials. *Journal of Geophysical Research-Solid Earth* **102**, 553-571 (1997).

cmg2016 - - Wednesday, June 8, 2016 - 9:30/9:45 (15min)

THE ROLE OF THE INTERMEDIATE STRESS ON FAILURE DIRECTION

E. Shalev[1] & V. Lyakhovsky[1]
[1]*Geological Survey of Israel, Jerusalem, Israel*

Key words fault direction, damage.

The directions of faults are often suggested to correspond to the Coulomb failure criterion. In these analyses, only the maximum (σ_1) and least principle (σ_3) stresses control fault formation and their orientation. However, it has been demonstrated that the intermediate stress (σ_2) plays a major role in rock failure and that the Coulomb failure criterion is not accurate under true 3-D loading conditions. Alternative criteria for failure, as Drucker-Prager, Wiebols-Cook, Hoek-Brown, Lade, Mogi and others were suggested to include all stress components but did not attempt to predict the direction of failure with respect to the principle stress orientation. We numerically simulate rock failure using damage-rheology mechanical model that describes the accumulation of damage intensity as a function of the ongoing deformation that eventually leads to macroscopic brittle failure. Our criterion for the onset of damage accumulation is described as $\xi = I_1/\sqrt{I_1} > \xi_0$, where I_1 and I_2 are the first and second strain invariants, and ξ_0 is the critical strain invariants ratio which corresponds to the internal friction in the stress failure models. We run a set of simulations in which only σ_2 is varied between simulations while σ_1 and σ_3 remain the same. Nucleation and propagation of the faults were driven by fluid injection at the center of the simulated rock volume. Results show that the angle between the fault and σ_1 changes from oblique (~35^0) at σ_2=σ_3 to vertical (0^0) at σ_2=σ_1 (figure 1). Although all local failure where in shear mode of deformation and there was no tensile stress in the systems, the nearly vertical fault structure at σ_2=σ_1 is similar to tension regime or axial splitting. Keeping σ_1 and σ_3 constants and increasing the intermediate stress component from low values σ_2=σ_3 to σ_2=σ_1 significantly affects the proximity to failure. The mean stress (σ_m=(σ_1+σ_2+σ_3)/3) increases with σ_2, while the differential stress (σ_1−σ_3) remains the same. This stabilizes the rock and drives the state of stress farther from failure conditions. Therefore, stress shadowing that promotes only one conjugate direction is more significant at low intermediate stress values. At high intermediate stresses shadowing is weak and both conjugate directions are constantly active giving an average vertical fault direction. Interpreting fault patterns without considering the intermediate stress can lead to wrong conclusions regarding stress directions and failure mechanisms.

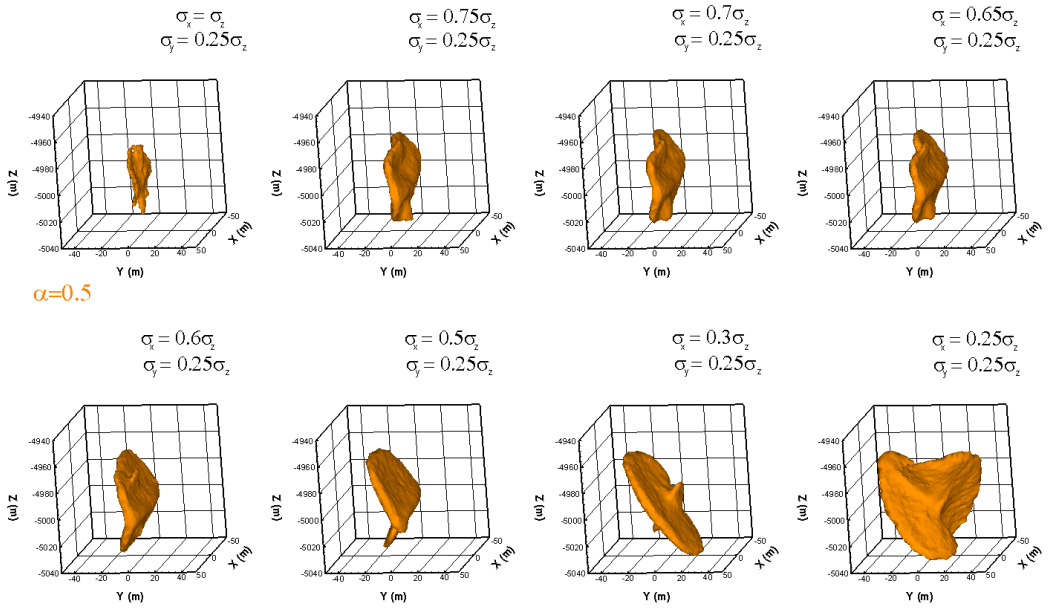

Figure 1. Iso-damage (a=0.5) surfaces for the simulated faults. σ_1 and σ_3 are the same for all cases. Direction of faults change with respect to σ_2.

cmg2016 - - Wednesday, June 8, 2016 - 9:15/9:30 (15min)

RUPTURE PROCESSES DURING LABOPRATORY EARTHQUAKES

A. Schubnel[1], F. Passelègue[2], H.S. Bhat[3], S. Latour[4], S.B. Nielsen[5] & R. Madariaga[1]
[1]*Laboratoire de Géologie, ENS, Paris, France*
[2]*School of Earth, Atmospheric and Environmental Sciences, Manchester University, UK*
[3]*Institut de Physique du Globe de Paris, France*
[4]*IRAP, Univesité Paul Sabatier, Toulouse, France*
[4] *Department of Earth Sciences, Durham University, UK*

Key words : Earthquake, damage, supershear, radiation efficiency, stress drop, fracture energy, nucleation, foreshocks, friction

Since the pioneering work of Brace and Byerlee (1966), the mechanism of stick-slip has been considered as a good analog to earthquake rupture propagation. Here, we report macroscopic stick-slip events in Westerly granite rock samples deformed under controlled upper crustal stress conditions in the laboratory. Experiments were conducted under triaxial loading using a high frequency acoustic monitoring array to record both particles acceleration during macroscopic stick-slip events and background microseismicity. For the first time, we also record the stress drop dynamically.

Prior to stick-slip instabilities, we observe a systematic exponential acceleration of precursory slip, but foreshocks are only observed when the normal stress becomes greater than ~ 50 *MPa*. This threshold corresponds to the normal stress above which the nucleation length becomes comparable to the size of typical fault asperities. Even in these conditions, most of precursory slip remains aseismic, but the total cumulative moment of the foreshock sequence also increases exponentially up to failure and the fault surface seem to evolve like a cascading asperity model. This exponential growth implies that the nucleation phase has a characteristic time, i.e. that both the foreshock sequence duration and precursory moment release scales with the size of the main asperity.

During the mainshock, we show that the dynamic stress drop, measured locally close to the fault plane, is almost total in the breakdown zone. The fault recovers strength within a few tens of microseconds. We demonstrate that the frictional behavior of stick-slip follows a slip-weakening law, well explained by flash heating theory, in agreement with our post-mortem microstructural analysis. Relationships between initial state of stress, rupture velocity, and stress drop demonstrate that supershear rupture is systematic at large normal stress. In these conditions, the ratio between fracture and radiated energies suggest that the rupture becomes more dispersive, meaning that the fracture energy eventually scales with both slip and stress drop. This result seems in agreement with linear elastic fracture mechanics theory and, possibly, with seismological observations.

References

[1] Brace, W. F., & Byerlee, J. D. (1966). *Stick-slip as a mechanism for earthquakes*. Science, *153*, 990-992.

cmg2016 - - Wednesday, June 8, 2016 - 9:45/10:00 (15min)

THE FAULT DAMAGE ZONE AS BARCODE OF EARTHQUAKES

C. Schrank[1,2], M. Veveakis[3,4], T. Poulet[4,3] & K. Regenauer-Lieb[4]
[1]*QUT, Brisbane, Australia;* [2]*UWA, Perth, Australia,* [3]*UNSW, Sydney, Australia;* [4]*CSIRO, Sydney, Australia*

Key words fault zone, damage zone, cnoidal waves, plastic P-waves.

The spatial footprint of a brittle fault is usually dominated by a wide halo of deformation bands and fractures surrounding a narrow, highly deformed fault core [1, Fig. 1]. This diffuse damage zone relates to the deformation history of a fault, including its seismicity, and has a significant impact on flow and mechanical properties of faulted rock [2, 3]. Here, we propose a new mechanical model for damage-zone formation. It is deduced from a novel mathematical theory postulating fundamental material instabilities in solids associated with volumetric deformation due to solitary elastoviscoplastic P-waves: cnoidal waves [4]. We show that transient cnoidal waves triggered by fault slip events can explain the typical distribution and extent of deformation bands and fractures within natural fault damage zones (Fig. 1). As a result, the damage zone can be considered as a barcode of earthquakes and inverted for earthquake overpressure and material properties of the host rock. Hence, cnoidal-wave theory may open a new chapter for predicting seismicity, material and geometrical properties as well as the location of brittle faults.

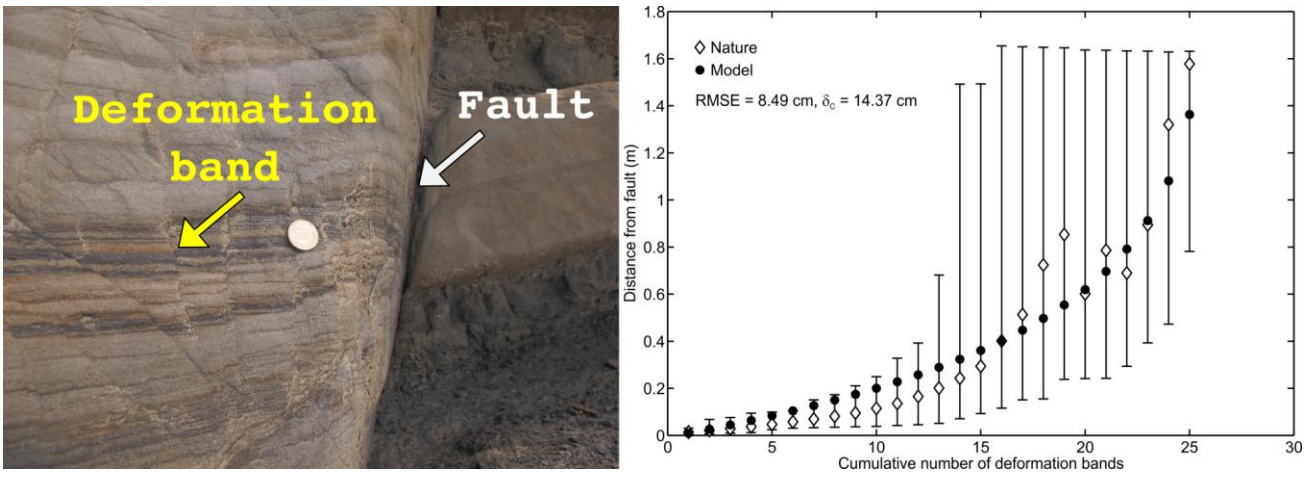

Figure 1. Left: Photograph of a normal fault (white arrow) cutting sand-, silt- and mudstones (Castlepoint, New Zealand). Its slip surface contains entrained mudstone and accommodated a vertical displacement of ~1.75 m. The fault exhibits a marked damage zone where deformation-band spacing increases non-linearly away from the core. Right: Plot of distance of deformation bands normal to the fault versus cumulative number of bands for the natural case and our best-fit model using transient cnoidal waves. The spatial statistics of the natural data were computed along 250 fault-normal scan lines. The diamonds indicate the mean distance of the nth band in nature. The vertical bars denote the lower and upper limit of the related distance distribution.

References

[1] Caine, J. S., Evans, J. P. & Forster, C. B. Fault zone architecture and permeability structure. *Geology* **24**, 1025- 1028 (1996).
[2] Okubo, C. H. & Schultz, R. A. Evolution of damage zone geometry and intensity in porous sandstone: insight gained from strain energy density. *Journal of the Geological Society* **162**, 939-949, doi:10.1144/0016-764904- 148 (2005).
[3] Xu, S. & Ben-Zion, Y. Numerical and theoretical analyses of in-plane dynamic rupture on a frictional interface and off-fault yielding patterns at different scales. *Geophysical Journal International* **193**, 304-320 (2013).
[4] Veveakis, E. & Regenauer-Lieb, K. Cnoidal waves in solids. *Journal of the Mechanics and Physics of Solids* **78**, 231-248, doi:http://dx.doi.org/10.1016/j.jmps.2015.02.010 (2015).

cmg2016 - - Wednesday, June 8, 2016 - 9:00/9:15 (15min)

DYNAMICS OF FRICTIONAL SLIP LOCALISATION

T. Putelat[1], J. Dawes[2] & A. Champneys[1]
[1]*Department of Engineering Mathematics, University of Bristol, Bristol BS8 1UB, UK.*
[2]*Department of Mathematical Sciences, University of Bath, Bath BA2 7AY, UK.*

Key words. rate-and-state friction, slip pulse, detachment front, global bifurcation.

An explanation is proposed of the origins of travelling waves of stick and slip that have been observed between frictional sliding surfaces [4, 1, 3]. Such waves, at very different lengthscales, are thought to underlie both earthquakes' source and the performance of mechanical brakes and dampers. An idealised situation is studied of a long thin elastic plate, subject to uniform shear stress $\bar{\mu}$ and frictional interaction with a rigid flat surface. Seeking deformation that is uniform in the transverse direction, a nonlinear wave equation is constructed under a long-wave assumption. Appearing from global homoclinic or heteroclinic bifurcations and under non-monotonic rate-and-state friction [9, 7, 8] a rich variety of solution types is discovered at intermediate shear stress between pure uniform stick and uniform slip, including: periodic stick-slip wave-trains, isolated pulses of stick or slip and detachment or attachment fronts. Careful consideration of the choice of the friction model and interfacial state kinetics is necessary to capture the full richness of wave types. See Fig. 1. This plethora of behaviours strongly depends on the analytical details of the friction model and may shed new light on the dynamics of earthquake ruptures, in particular with respect to the recent field evidence that suggests seismic slip localizes along a fault patch that is partially locked during the interseismic period [10]. Might a locked fault patch be a slow stick pulse? Finally we emphasise that this study shows that these slip patterns can exist over a wide range of speeds of travelling wave. This may explain the large variability of earthquake duration and frequency spectrum [6, 5]. Future work will study the stability of these localized slip structures and their physical selection.

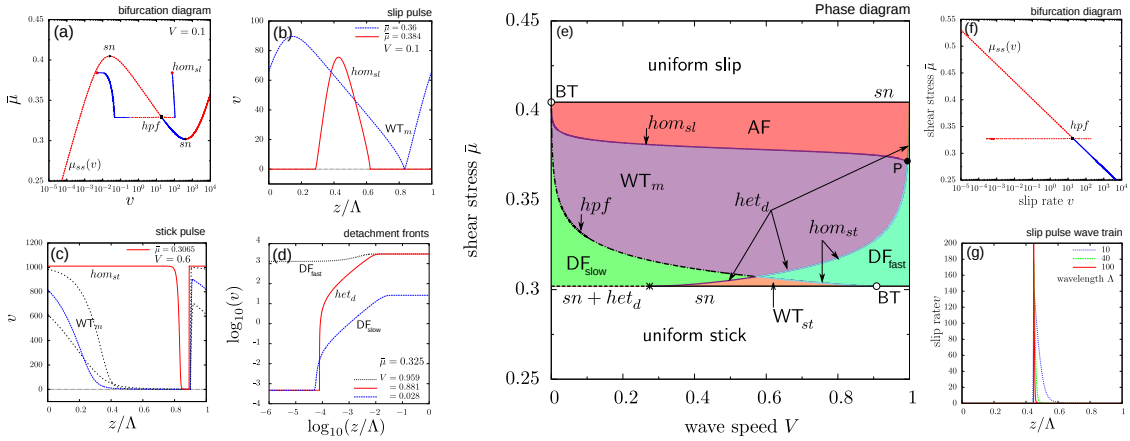

Figure 1: The diversity of travelling localised frictional slip patterns computed from a non-monotonic friction model [8]. (a) Bifurcation diagram showing the growth of wave-trains from a Hopf bifurcation (■), promoted by velocity-weakening friction, leading to the homoclinic orbit (●) of slip pulse (b) reminiscent of the pulses described by Heaton [4]. Such slip pulses are anchored at the equilibrium saddle point lying on the low-velocity-strengthening branch of the steady-state friction curve. (c) The existence of a high velocity strengthening branch of the friction curve $\mu_{ss}(v)$ also allows the existence of 'stick pulse' which corresponds to a narrow travelling 'stick' zone. (d) Heteroclinic orbits connecting the saddle equilibria lying on the low and high velocity-strengthening branches of μ_{ss} correspond to travelling 'detachment' (similar to [3, 2]) or 'attachment' fronts promoting the slab acceleration or deceleration. The location of attachment fronts, which is difficult to compute, is expected to follow very closely the slip pulse locus (hom_{sl}). (e) Phase diagram of travelling wave patterns: homoclinic (pulses) and heteroclinic (fronts) connections exist on lines within the $(V, \bar{\mu})$ parameter space that delineate domains of generic travelling fronts and wave-trains of different types. The precise topology of this bifurcation structure strongly depends on the mathematical details of the friction model, in particular the state evolution equation. Nomenclature: loci of slip pulses (hom_{sl}), stick pulses (hom_{st}), detachment fronts (het_d), Hopf bifurcation locus (hpf); saddle-node bifurcation loci at the local extrema of friction (sn); Stick-slip wave-trains (WT). Generic detachment (DF) and attachment (AF) fronts. Takens-Bogdanov bifurcation point (BT). By contrast the classic monotonic Dieterich-Ruina laws [9] only predict wave trains of slip-pulse solutions in a window of the applied shear stress $\bar{\mu}$ that is exponentially narrow, see (f-g). Note that the travelling waves are moving to the left in these examples. Similar solutions are expected for waves travelling to the right.

References

[1] Behrendt J. et al., J. Sound Vib., **330**:636–651, (2011).
[2] Bouchbinder E. et al., Phys. Rev. Lett., **107**:235501, (2011).
[3] Ben-David O. et al., Science, **330**:211–214 (2010).
[4] Heaton T.H., Phys. Earth Planet Int., **64**:1–20, (1990).
[5] Ide S., Proc Jpn Acad Ser B Phys Biol Sci. **90**:259–277, (2014).
[6] Peng Z. & Gomberg J., Nature Geosci., **3**:599–607, (2010).
[7] Putelat T. et al., J. Mech. Phys. Solids, **58**:27–53, (2010).
[8] Putelat T. & Dawes J., J. Mech. Phys. Solids, **78**:70–93, (2015).
[9] Ruina A.L., J. Geophys. Res., **88**:10,359–10,370, (1983).
[10] Thomas M.Y. et al., J. Geophys. Res., **119**: 5114–5139, (2014).

cmg2016 - - Wednesday, June 8, 2016 - 8:30/9:00 (30min)

Heating and Weakening of Shear Zones in Earthquake and Landslide Mechanics

James R. Rice
Harvard University, Cambridge, MA 02138, USA

Key words : earthquakes, landslides, thermal pressurization, mineral decomposition

Field and borehole observations of active earthquake fault zones show that shear is often highly localized to principal deforming zones of order 10s of microns to a few mm wide. Landslides in relatively homogeneous soils, especially clays, or in layered strata can likewise exhibit extremely narrow shear zones. Those two domains of study, landslide and earthquake mechanics, reached a stage of relative maturity with, it seems, very little communication of researchers in one field about developments in the other and vice versa, but with a great exception being the late Ioannis Vardoulakis who co-organized, with Y. Hatzor and J. Sulem, the unifying Batsheva de Rothschild conference of 2009 on "Shear Physics at the Meso-scale in Earthquake and Landslide Mechanics". The lecture will follow those pioneers to address narrow shear zone development as a thermo-hydro-mechanical localization process in wet granular media. In it, highly elevated pore pressure is a predicted and lab-verified consequence of rapid straining, which enables intense shear localization. That pressurization can develop in fluid which pre-exists in the gouge as groundwater, or in volatile phases emerging at high pressure from thermal decomposition reactions in hydrated silicates (clays, serpentines) or carbonates. The concepts show howshear zone materials with high static friction coefficients, ~0.6 to 0.8, can nevertheless undergo strongly localized shear at effective dynamic friction coefficients of order 0.1, thus fitting observational constraints, e.g., in the earthquake case, of producing negligible surface heat out-flow and rarely creating extensive melt. This is collaborative research with Nicolas Brantut (Univ. Col. Lond), John D. Platt (Smithsonian Inst. Sci.) and John W. Rudnicki (Northwestern Univ).

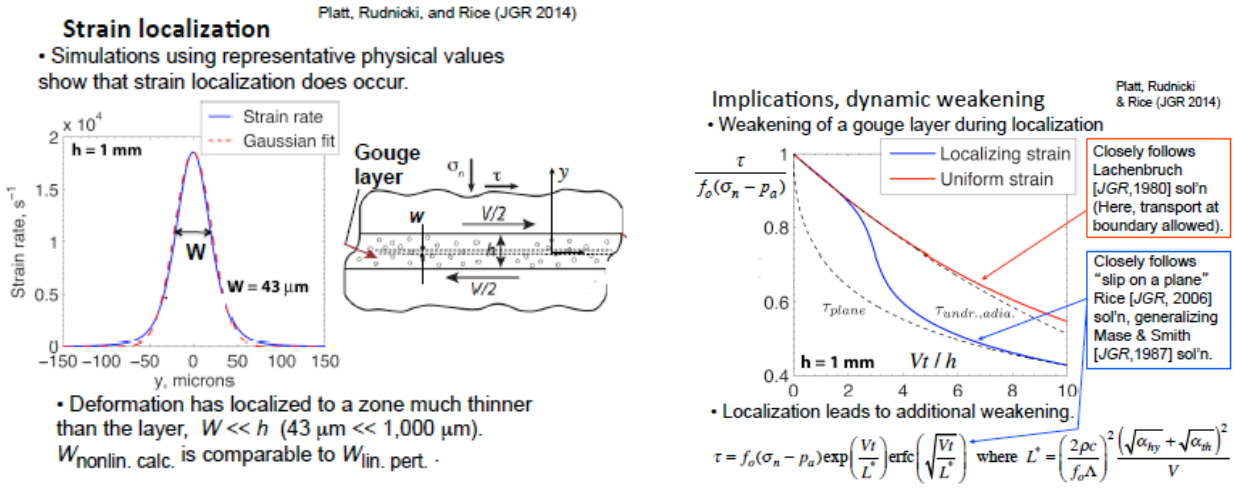

References

[1] J. R. Rice, *Heating and weakening of faults during earthquake slip*, J. Geophys. Res. B **111**, doi:10.1029/2005JB004006 (2006).

[2] J. R. Rice, J. W. Rudnicki, J. D. Platt, *Stability and localization of rapid shear in fluid-saturated fault gouge, 1. Linearized stability analysis*, J. Geophys. Res. B **119**, doi:10.1002/2013JB010710 (2014).

[3] J. D. Platt , J. W. Rudnicki, and J. R. Rice, *Stability and localization of rapid shear in fluid-saturated fault gouge, 2. Localized zone width and strength evolution*", J. Geophys. Res. B **119**, doi:10.1002/2013JB010711 (2014).

[4] J. D. Platt, N. Brantut, and J. R. Rice, *Strain localization driven by thermal decomposition during seismic shear*, J. Geophys. Res. B **120**, doi: 10.1002/2014JB011493, (2015).

cmg2016 - - Wednesday, June 8, 2016 - 12:00/12:45 (45min)

MODELING THE EFFECT OF ROUGHNESS ON THE NUCLEATION AND PROPAGATION OF SHEAR RUPTURE ON SMALL FAULTS

Y. Tal[1] & B.H. Hager[1]
[1]*Massachusetts Institute of Technology, Cambridge, MA, USA*

Key words Fault roughness, Mortar finite elements, shear rupture.

Faults are rough at all scales and can be described as self-affine fractals. This deviation from planarity results in geometric asperities and a locally heterogeneous stress field, which affect the nucleation and propagation of shear rupture. We study this effect numerically at the scale of small earthquakes, in which realistic geometry and friction law parameters can be incorporated in the model. We aim to understand the effect of roughness on faults with L ~ 10 – 200 m. At this scale we can choose the minimum roughness wavelength, λ_{min}, to be the size of lab samples (5 – 10 cm) and thus use the observed lab-scale slip or rate based friction laws without modifying the constitutive parameters, assuming that the experimental data already include the effects of smaller wavelengths of roughness. Moreover, using a variable time step size, we gradually increase the remote stress and let the rupture nucleate spontaneously, rather than introducing artificial procedures to nucleate a seismic event.

Numerically, maintaining λ_{min} and consequently the smallest element size, Δx, fixed while increasing the fault length poses two challenges. First, keeping Δx fixed is computationally expensive. Second, the slip increases with increasing fault length and the assumption of small slip relative to the size of the elements is not valid. To overcome the first challenge, we refine the mesh near the fault, using hanging nodes. To overcome the second challenge, we use the Mortar finite element method [Bernardi et al., 1994; Wohlmuth, 2000], in which non-matching meshes are allowed across the fault and the contacts are continuously updated. We introduce slip weakening and rate and state friction laws into the method and study both the nucleation and propagation of shear rupture, using variable time steps with a quasi-static scheme for the inter-seismic stage and a dynamic implicit Newmark scheme for the co-seismic stage.

For a static benchmark, we demonstrate that the method predicts accurately the stresses and displacements along a fault with a non-matching grid due to a uniform stress drop. We also design a benchmark problem to show that the method accurately models the behavior of the friction coefficient in response to a change in the slip rate on a fault governed by a rate and state friction law.

Simulations of a 10 meter long horizontal fault with different amplitude roughness and a slip-weakening friction law show the significant effect of roughness on: (1) Slip on the fault and consequently the seismic moment; (2) Stress drop; (3) Rupture properties, such as rupture velocity, breakdown zone, and the observed relation between shear stress and slip; and (4) Different stages in the nucleation processes. For example, with the adopted spontaneous nucleation procedure, the experiment-based nucleation model of Ohnaka [2000] is observed also in the simulations (Fig. 1), and important quantities regarding the nucleation and propagation of the rupture can be measured.

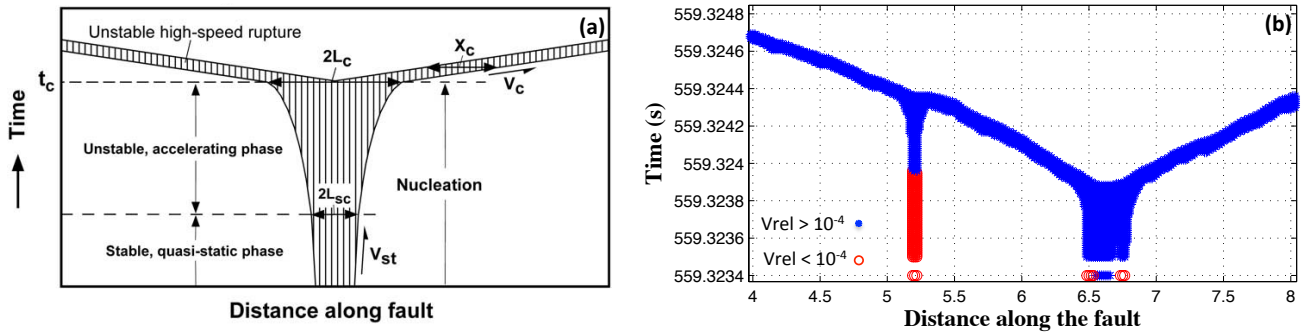

Figure 1. (a) A rupture nucleation model (after Ohnaka [2000]). (b) Observed nucleation and propagation of a shear rupture on a rough fault. The markers are shown only for nodes where the friction coefficient at a given time is $\mu_d < \mu < \mu_s$.

References

[1] Bernardi, C., Y. Maday, and A. T. Patera, A new nonconforming approach to domain decomposition: The mortar element method, in Nonlinear Partial Differential Equations and Their Applications, H. Brezis and J.-L. Lions, eds., Longman Scientific & Technical, Harlow, UK, pp. 13–51 (1994).
[2] Wohlmuth B. I., A mortar finite element method using dual spaces for the Lagrange Multiplier. SIAM J. Numer. Anal., 38(3), 989–1012 (2000).
[3] Ohnaka, M. A., physical scaling relation between the size of an earthquake and its nucleation zone size, Pure Appl. Geophys., 157, 2259–2282 (2000).

cmg2016 - - Wednesday, June 8, 2016 - 12:00/12:45 (45min)

ON THE EXTENSION OF THE JEFFREYS–LOMNITZ LAW FOR ROCK CREEP

F. Mainardi[1] & G. Spada[2]
[1]*Department of Physics and Astronomy, Bologna University, Bologna, Italy*
[2]*Department of Pure and Applied Sciences, Urbino University, Urbino, Italy*

Key words : linear viscoelasticity, rock creep, Jeffreys-Lomnitz law, glacial isostatic deformations .

In 1958 Jeffreys proposed a power law of creep, generalizing the logarithmic law earlier introduced by Lomnitz, to broaden the geophysical applications to fluid-like materials including igneous rocks. We revisit the Jeffreys-Lomnitz law of creep by allowing its power law exponent α, usually limited to the range $0 \le \alpha \le 1$ to all negative values so also solid-like viscoelastic materials are included in the extended law. This approach is consistent with the linear theory of viscoelasticity because the creep function still remains a Bernstein function, that is positive with a completely monotone derivative, with a related spectrum of retardation times. Indeed, in the extended Jeffrey-Lomnitz crrep law the complete range $\alpha \le 1$ (rather than $0 \le \alpha \le 1$) yields a continuous transition from a Hooke elastic solid with no creep $(\alpha \to -\infty)$ to a Maxwell fluid with linear creep $(\alpha = 1)$ passing through the Lomnitz viscoelastic body with logarithmic creep $(\alpha = 0)$, which separates solid-like from fluid-like behaviors. It is convenient to separately consider four cases:

$$t \ge 0\,, \quad \Psi(t) = \begin{cases} t/\tau_0\,, & \alpha = 1\,, \\ \dfrac{(1+t/\tau_0)^{\alpha}-1}{\alpha}\,, & 0 < \alpha < 1\,, \\ \log(1+t/\tau_0)\,, & \alpha = 0\,, \\ \dfrac{1-(1+t/\tau_0)^{-|\alpha|}}{|\alpha|} & \alpha < 0\,. \end{cases}$$

where we have considered the dimensionless creep function Ψ versus a dimensionless time t/τ_0. The behaviour of $\Psi(t)$ is illustrated in the Figures below, for some values of α in the range $-2 \le \alpha \le 1$, adopting a logarithmic time scale and a linear time scale. Here, geophysical applications of the extended Jeffreys-Lomnitz creep in the realm of global models of glacial isostatic deformations will be discussed.

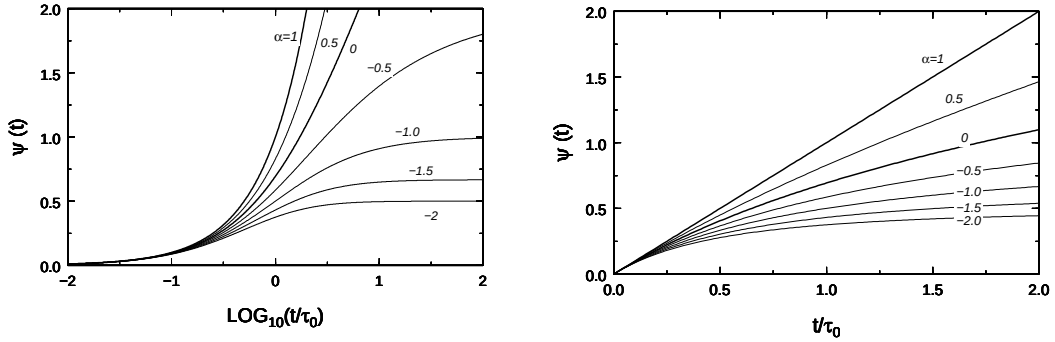

References

[1] H. Jeffreys, *A modification of Lomnitz's law of creep in rocks*, Geophys. J. R. Astron. Soc. **1**, 92–95 (1958).
[2] C. Lomnitz, *Creep measurements in igneous rocks*, J. Geol. **64**, 473–479 (1956).
[3] F. Mainardi & G. Spada, *On the viscoelastic characterization of the Jeffreys–Lomnitz law of creep*, Rheol. Acta **51**, 783–791 (2012). [E-print: `http://arxiv.org/abs/1112.5543`]
[4] E. Strick, *Implications of Jeffreys–Lomnitz transient creep*, J. Geophys. Res. **89**, 437–451 (1984).

cmg2016 - - Wednesday, June 8, 2016 - 12:00/12:45 (45min)

DYMANICRUPTUREINDAMAGE-BREAKAGERHEOLOGYMODEL

Vladimir Lyakhovsky[1], Yehuda Ben-Zion[2], Assen Ilchev[3], Aleksander Mendecki[3]

[1]Geological Survey of Israel, Jerusalem, Israel
[2]Department of Earth Sciences, University of Southern California, Los Angeles, USA
[3]Institute of Mine Seismology, Hobart, Australia

Key words fault zone rheology, phase transition, earthquake dynamics.

We present a thermodynamically-based formulation for modeling dynamic rupture processes in the brittle crust using a continuum damage-breakage rheology. The model combines aspects of a continuum viscoelastic damage framework for brittle solids with a continuum breakage mechanics for granular flow within dynamically generated slip zones. The formulation accounts for the density of distributed cracking and other internal flaws in damaged rocks with a scalar damage parameter, and address the grain size distribution of a granular phase in the slip zone with a breakage parameter. A dynamic brittle instability is associated with a critical level of damage in the solid, leading to loss of convexity of the solid strain energy, localization, and transition to a granular phase associated with lower energy level. The continuum damage-breakage rheology model treats the localization to a slip zone at the onset of dynamic rupture and post-failure recovery process as phase transitions between solid and granular states. The model generates sub- and super-shear rupture velocities and pulse-type ruptures seen also in frictional models, and additional important features such as strong dynamic changes of volumetric strain near the rupture front and diversity of nucleation mechanisms. The propagation of rupture front and slip accumulation at a point are correlated with sharp dynamic dilation followed by a gradual decay to a level associated with the final volumetric change associated with the granular phase transition in the slipping zone. The local brittle failure process associated with the solid-granular transition is expected to produce isotropic radiation in addition to the deviatoric terms. The framework significantly extends the ability to model brittle processes in complex geometrical structures and allows analyzing the roles of gouge thickness and other parameters on nucleation, rupture and radiation characteristics.

cmg2016 - - Wednesday, June 8, 2016 - 12:00/12:45 (45min)

EFFECT OF MELT SURFACE TENSION ON THE BEHAVIOUR AND MORPHOLOGY OF FAULT GOUGE

A. Kazzaz[1], I. Einav[1], G. Proust[1] & Y. Gan[1]
[1]*School of Civil Engineering, The University of Sydney, Sydney, NSW, Australia*

Key words fault gouge, frictional melt, surface tension, liquid bridge, particle morphology

Field evidence, laboratory experiments and theoretical predictions suggest that the formation of frictional melt within a layer of gouge separating fault surfaces is a regular occurrence during coseismic slip. The melt which may be localised or widespread, contributes to both slip-weakening and restrengthening processes through a range of physical phenomena. In particular we contend that melt surface tension and its interaction with other fault processes is a critical determinant of gouge coseismic mechanical response and morphology. We extend the model of Gan et al. [1] to include the effects of surface tension for a small segment of gouge by considering the formation of melt liquid bridges between partially molten particles at low melt volume fractions. We introduce additional inter-granular forces to account for this phenomenon based on the framework of Soulié et al [2] extended by Gan et al. [3]. We find that gouge apparent friction and particle size and shape are highly sensitive to changes in melt surface tension for a wide range of seismic shear regimes.

References

[1] Y. Gan, P. Rognon, I. Einav, *Phase transitions and cyclic pseudotachylyte formation in simulated faults*, Philos. Mag. 92, 1-13 (2012).
[2] F. Soulié, F. Cherblanc, M. El Youssoufi,C. Saix, *Influence of liquid bridges on the mechanical behaviour of polydisperse granular materials*, Int. J. Numer. Anal. Methods Geomech. 30, 213-228 (2006).
[3] Y. Gan, F. Maggi, G. Buscarnera, I. Einav, *A particle-water based model for water retention hysteresis*, Geotech. Lett. 3, 152-161 (2013).

cmg2016 - - Wednesday, June 8, 2016 - 12:00/12:45 (45min)

THE FRICTIONAL FREQUENCY RESPONSE AND MODEL IDENTIFICATION

A. Cabboi[1], T. Putelat[2] & J. Woodhouse[1]
[1]*Department of Engineering, University of Cambridge, Cambridge, UK.*
[2]*Department of Engineering Mathematics, University of Bristol, Bristol, UK.*

Key words. dynamic friction, vibration, rate-and-state, contact stiffness, pin-on-disc test, instability prediction.

The fields of earthquake mechanics and vibration engineering both provide problems in dynamics in which interfacial friction plays a key role. To make progress with modelling the phenomena in either field a reliable constitutive friction law is required in order to allow an accurate prediction of self-excited instability threshold and vibration levels. Although different friction laws have been proposed over the years, there is no consensus yet when it comes to problems involving relatively high frequency vibration; a frequency domain which may have been overlooked in experimental tribology and seismology. Recent advances [2, 3, 4] show that the concept of the *frictional frequency response* reveals new dynamic features of the frictional interface for a perturbed steady-sliding contact and is the required input for predicting friction-induced vibration by using linearised stability analysis.

The frequency response function $\beta(\omega) := F'/v'$ is constructed by measuring the perturbation in the frictional force F' divided by the perturbation of the sliding speed v' as a function of frequency. Such a measurement can be achieved by a pin-on-disc device (Fig. 1a) connected to a piezo actuator driven with band-limited random noise and used to superimpose a small fluctuation in sliding speed to the contact point. Both force and velocity fluctuation are measured in the frictional and normal directions by a package of sensors installed close to the contact region.

For different material combinations, it has been found [2, 4] that the measured frequency response is a frequency dependent complex number (Fig. 1d), which indicates that the friction force must also depend on variables with a dynamic evolution law. Up to mid-high frequencies, such measurements proved to be more repeatable than measurements of the steady-state friction curve (Fig. 1b-c). Previous efforts to explain such measurements from a theoretical model have failed. However, an enhanced rate-and-state model, that takes elastic deformations near the interface into account through a contact stiffness k_t [1, 4], is shown to match the measurements remarkably well over a parameter space that covers a range of normal forces, of sliding speeds and frequencies (Fig. 1b-d).

A systematic optimization methodology allows discriminating among possible variants of the model, and then identifying the model parameter values (Fig. 1d). The results suggest that the validity range of the enhanced rate-and-state model can be extended up to mid-high frequencies. It is worth underlining that the measurements done so far are mainly proofs of concept of this innovative experimental technique and the subsequent model-fitting process. Such a methodology could be extended to the characterisation of any frictional interface and the information gained could then be used for a linearised stability analysis for friction-induced vibration and stick-slip instability prediction. Future investigation could involve developing the proposed methodology from localised frictional contact to the case of extended contact, which would also relate to tests frequently performed in experimental seismology, by the use of an array of strain gauges and accelerometers placed near a sliding interface.

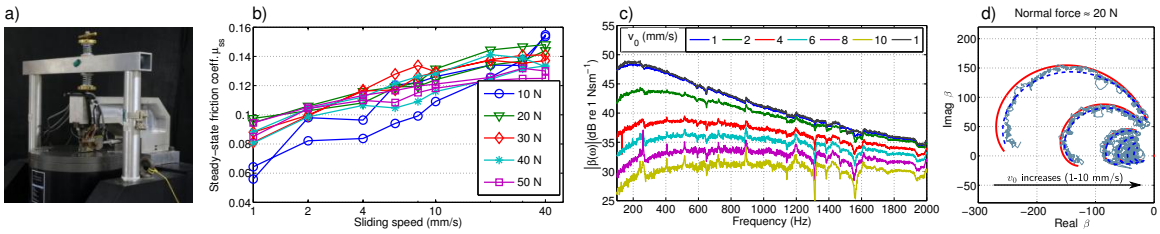

Figure 1. a) Pin-on-disc rig; b) Velocity-strengthening steady-state friction coefficient; c) Frictional frequency response $|\beta(\omega)|$ for different disc speed v_0 (Nylon pin - glass disc at $N = 20$ N): v_0 is increased stepwisely then decreased again showing a stricking repeatability of the measurement; d) Corresponding Nyquist plot: the red lines indicate the model prediction after fitting the whole data matrix (for various disc speeds and normal forces), the dashed lines indicate single curve fittings. In this experiment, the memory length L appears to be linearly dependent on v_0 regardless of the model, suggesting that a rather constant relaxation time-scale t_ϕ for the interficial state ϕ is more appropriate.
Identified rate-and-state parameters: $a = 0.0196$, $b = 0.0094$, $t_\phi = 0.00075$ s and $k_t = 0.27N^{0.349}$ in MN m.

References

[1] Bureau, L., Baumberger, T., Caroli, C., *Non-Amontons behavior of friction in single contacts.* EPJE **19**, 163 (2006).
[2] Wang S., Woodhouse J., *The frequency response of dynamic friction: A new view of sliding interfaces.* JMPS **59**, 1020 (2011).
[3] Butlin T., Woodhouse J., *Friction-induced vibration.* JSV **332**, 5302 (2013).
[4] Cabboi A., Putelat T., Woodhouse J., *The frequency response of dynamic friction: Enhanced rate-and-state models.* Sub judice (2016).

cmg2016 - - Wednesday, June 8, 2016 - 12:00/12:45 (45min)

THE MECHANICS AND PHYSICS OF CHEMICALLY ACTIVE FAULTS

M. Veveakis[1,2], T. Poulet[2,1] & S. Alevizos[1]
[1]*UNSW, Sydney, Australia*
[2]*CSIRO, Sydney, Australia*

Key words Rate and state friction, visco-plasticity, fluid-release reactions, chemo-mechanical oscillations.

Episodic Tremor and Slip (ETS) events display a rich behaviour of slow and accelerated slip with simple oscillatory to complicated chaotic time series. It commonly believed that the fast events that appear as non-volcanic tremors are signatures of deep fluid injection. The fluid source is suggested to be related to the breakdown of hydrous phyllosilicates, mainly the serpentinite group minerals such as antigorite or lizardite that are widespread in the top of the slab in subduction environments. Similar ETS sequences are recorded in different lithologies in exhumed crustal carbonate-rich thrusts. Here, the fluid source is suggested to be the more vigorous carbonate decomposition reaction. If indeed both events can be understood and modelled by the same generic fluid release reaction $AB_{(solid)} \rightleftharpoons A_{(solid)} + B_{(fluid)}$ the ETS sequences in subduction zones reveal a geophysical tractable temporal evolution with no access to the fault zone while conversely the exposed carbonate thrust offer direct access to the spatial manifestations without access to the temporal evolution. This work reviews recent advances in modelling ETS events considering the multiphysics instabilities triggered by the fluid release reaction and develops a thermal-hydraulic-mechanical-chemical oscillator THMC (spring) model for such mineral reactions (like dehydration and decomposition) in Megathrusts [1,2]. We describe advanced computational methods for THMC instabilities and discuss spectral and finite element solutions. We apply the presented numerical methods to field examples of this important mechanism and reproduce both the temporal signature of the Cascadia and Hikurangi trench (Fig. 1) with a serpentinite oscillator [3], as well as match the spatial manifestation of a canonical carbonate-driven crustal thrust, the Glarus thrust in the Swiss Alps [4].

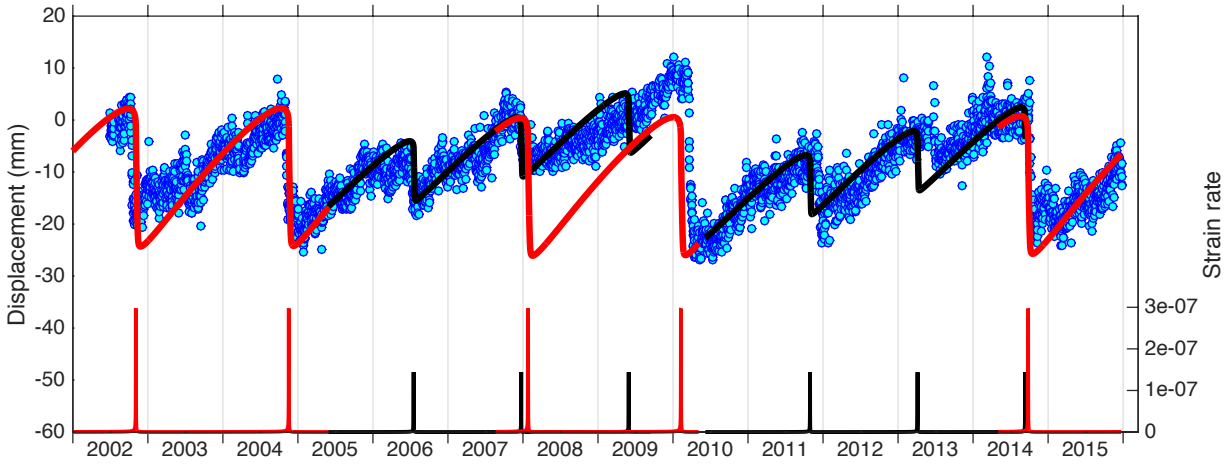

Figure 1. Irregular ETS sequence of Gisborne, New Zealand, station GISB (NASA, 2013). The GPS data (blue dots) represent raw displacement data with its linear trend removed. The signal is non-periodic and the suggested fit consists of 2 modes. The first mode (red line) has higher displacement and strain rates (shown at the bottom) per event and a period of 2 years, and the second one (black line) has a period of about 14 months. Figure last updated on the 31st of December 2015.

References

[1] Alevizos, S., Veveakis, M., Poulet, T., 2014. Thermo-poro-mechanics of chemically active creeping faults: 1. steady state. J. Geophys. Res. Solis Earth 119, 4558-4582.
[2] Veveakis, E., Poulet, T., Alevizos, S., 2014. Thermo-poro-mechanics of chemically active creeping faults: 2.transient considerations. J. Geophys. Res. Solis Earth 119, 4583–4605.
[3] Poulet, T., Veveakis, E., Regenauer-Lieb, K., Yuen, D., 2014a. Thermo-poro-mechanics of chemically active creeping faults: 3. the role of serpentinite in episodic tremor and slip sequences, and transition to chaos. J. Geophys. Res. Solis Earth 119, 4606-4625.
[4] Poulet, T., Veveakis, M., Herwegh, M., Buckingham, T., Regenauer-Lieb, K., 2014b. Modeling episodic fluid-release events in the ductile carbonates of the glarus thrust. Geophys. Res. Lett. 41, 7121–7128.

cmg2016 - - Wednesday, June 8, 2016 - 12:00/12:45 (45min)

ACOUSTIC MONITORING AND TRIGGERING OF SHEARING INSTABILITY IN GRANULAR MATERIALS

X. Jia[1], H.S. Bhat[2], J. Léopoldès[1] & A. Tourin[1]
[1] *ESPCI Paris, PSL Research University, CNRS, Institut Langevin, Paris, France*
[2]*Institut de Physique du Globe, CNRS, Paris, France.*

Key words: granular media, shear banding, acoustic monitoring, sound-induced fault slip

Laboratory studies of granular friction have emerged as a powerful tool for investigating dynamics of seismic faults [1], including dynamic triggering of earthquakes at remote distance [2]. However, the physical origin of dynamic triggering still remains a challenging issue due to small strain amplitude of impinging seismic waves (~ 10^{-6}) [3]. Advances in granular physics and acoustics have paved the way for better understanding of how seismic waves may trigger fault slips. Unlike ordinary solids and liquids, static and dynamic properties of dense granular media are determined by the inhomogeneous contact force network exhibiting multiple metastable configurations; they may undergo a transition from jammed solid to flowing liquid states when the external driving such as shearing or shaking is beyond a certain threshold [4]. The emerging view is that dynamic perturbation of sheared gouge materials causes a material failure and fault slip that can be characterized as unjamming transition induced by the acoustic fluidization [5].

Here we investigate the granular shear instability (earthquake nucleation) in *finite-thickness* granular media by acoustic *probing* (Fig. 1A). Decrease of the shear wave velocity decreases and development of the fabric anisotropy are observed prior to failure (Figs. 1B & 1C). We find that the correlation function of the multiply scattered Coda waves is very sensitive to the stick-slip like rearrangement of granular network during shear banding (Figs. 1B and 1D) [6]. Next, we study the causal effect of impinging elastic waves on their nucleation by nonlinear acoustic *pumping*. Two regimes of fast nonlinear dynamics can be identified with the material softening (Fig. 1E-a). In the irreversible regime of the sound-matter interaction, the wave velocity and correspondingly elastic modulus remains weakened after the wave transient and the force network is strongly modified even in the absence of visible grain motion (Fig. 1E-b) [5]. Finally, we show that the onset of sliding triggered far below the static threshold by nonlinear sound waves is due to the acoustic lubrication of the stuck contact area, which reduces the apparent coefficient of friction [7]. This scenario is confirmed by the instability triggering of granular layers on inclined plans in which the acoustic fluidization of *small vibration amplitude* affect basically the friction between solid particles rather than that arising from the dilatancy [1].

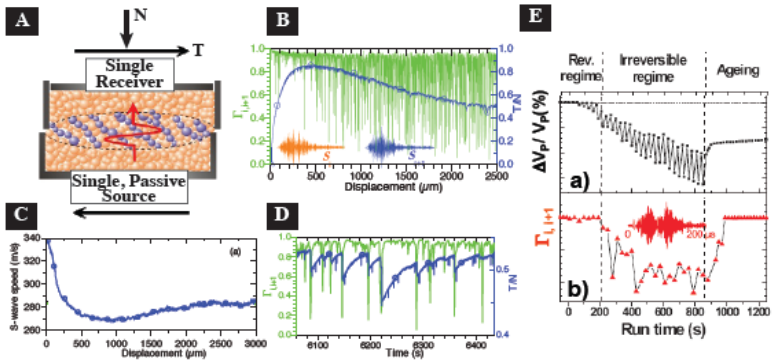

Figure 1. (A) Shear apparatus (B) Evolution of the shear with slip (in blue) and the cross-correlation of Coda waves shown inset (in green) (C) Monitoring the decrease of shear wave speed (D) Zoom into Fig. B. (E) Sound-induced fluidization in granular media.

References

[1] C. Marone, Ann. Revs. Earth & Plan. Sci. **26**, 643 (1998)
[2] P. Johnson and X. Jia, Nature **437**, 871 (2005)
[3] J. Gomberg et al, Nature **411**, 462 (2001)
[4] A.J. Liu and S. R. Nagel, Nature **396**, 21 (1998)
[5] X. Jia, T. Brunet and J. Laurent. Phys. Rev. E **84**, 020301(R) (2011)
[6] Y. Khidas and X Jia, Phys. Rev. E **85**, 051302 (2012)
[7] J. Léopoldès, G. Conrad and X. Jia, Phys. Rev. Lett. **110**, 248301 (2013)

cmg2016 - - Wednesday, June 8, 2016 - 12:00/12:45 (45min)

DISSOLUTION INDUCED STRAIN LOCALIZATION IN GEOMATERIALS

I. Stefanou & J. Sulem
Université Paris-Est, Laboratoire Navier, Ecole des Ponts ParisTech, Marne-la-Vallée, France

Key words Compaction bands, shear bands, bifurcation analysis, strain localization, chemical dissolution, instabilities.

Deformation bands play an important role in reservoir engineering, geological storage, underwater landslides and slow geological procedures. Various mechanisms can be involved at different scales and may be responsible for deformation bands. Mechanical and chemical degradation of the grain skeleton is a softening factor that can lead to compaction, shear or even dilation band formation [1,2]. The present study is twofold. On one hand it focuses on the mathematical modeling of chemically induced strain localization instabilities in porous rocks and on the other hand it explores the conditions for their creation [1,3]. The post localization regime is then studied by numerically integrating the governing equations of the system.

In a saturated porous rock, the progressive mechanical damage of the solid skeleton during deformation, results in the increase of the interface area of the reactants and consequently in the acceleration of the dissolution rate of the solid phase [4]. Under the presence of dissolving fluids the solid skeleton is degraded more rapidly (mass removal because of dissolution), the overall mechanical properties of the system diminish (contraction of the elastic domain – chemical softening), deformations increase and the solid skeleton is further damaged (intergranular fractures, debonding, breakage of the porous network etc.). By accounting for (a) the mass diffusion of the system, (b) a macroscopic failure criterion with dissolution softening and (c) the reaction kinetics at the micro level, a micromechanical model is proposed to account for the above positive feedback process. The conditions for deformation band triggering are investigated analytically through linear stability analysis by considering the strong chemo-poro-mechanical coupling due to chemical dissolution. The heterogeneity of the microstructure in terms of chemical reactivity of the constituents of the REV is taken into account resulting in a characteristic internal length of the system. The post bifurcation behavior is finally studied both analytically and numerically revealing the localization thickness. The effect of various parameters on the localization zone thickness is then explored.

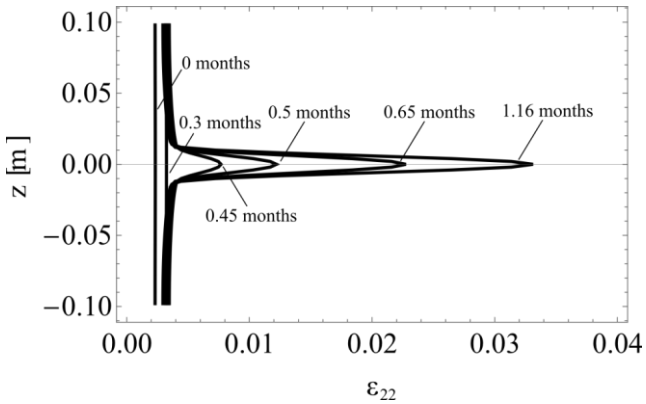

Figure 1. Profile of the vertical deformation at various times of a specimen under oedometric conditions. After a creep phase the deformation localizes into a narrow band, i.e. a compaction band.

References

[1] I. Stefanou and J. Sulem, "Chemically induced compaction bands: Triggering conditions and band thickness," Journal of Geophysical Research: Solid Earth, 2014, 119, no. 2, pp. 880–899, DOI: 10.1002/2013JB010342.
[2] M. Cha and J. C. Santamarina, "Dissolution of randomly distributed soluble grains : post-dissolution k 0 -loading and shear," Géotechnique, 2014, 64, no. 10, pp. 828–836, DOI: 10.1680/geot.14P.115.
[3] J. W. Rudnicki and J. R. Rice, "Conditions for the localization of deformation in pressure-sensitive dilatant materials," Journal of the Mechanics and Physics of Solids, 1975, 23, no. 6, pp. 371–394, DOI: 10.1016/0022-5096(75)90001-0.
[4] L.-B. Hu and T. Hueckel, "Coupled chemo-mechanics of intergranular contact: Toward a three-scale model," Computers and Geotechnics, 2007, 34, no. 4, pp. 306–327, DOI: 10.1016/j.compgeo.2007.02.009.

cmg2016 - - Wednesday, June 8, 2016 - 12:00/12:45 (45min)

REVISION OF THE BLOCK-SLIDER MODEL TO ACCOUNT FOR THE NORMAL ELASTIC DEFORMATION OF THE SURROUNDING ROCK: EFFECTS ON EARTHQUAKE NUCLEATION AND COSEISMIC SLIP

I. Stefanou[1], E. Veveakis[2] & J. Sulem[1]
[1]*Université Paris-Est, Laboratoire Navier, Ecole des Ponts ParisTech, Marne-la-Vallée, France*
[2]*University of New South Wales, Sydney, Australia*

Key words Reverse faults, earthquakes nucleation, coseismic slip, multiphysical couplings, block-slider model, bifurcation analysis, instabilities.

Three major types of faults exist in the earth crust, i.e. reverse faults, normal faults and strike slip faults. Faults accommodate large seismic slip during earthquakes. Multiphysical procedures such as thermal or chemical pressurization and chemical decomposition are nowadays quite well known mechanisms that control both earthquake nucleation and coseismic slip. The dissipated energy is strongly affected by these multiphysical procedures that occur and evolve at different scales, i.e. from the nano-metric to centi-metric scale [1-4].

The classical, conceptual model used for modeling faults is the block-slider system, depicted in Figure 1. The sliding of the block represents the co-seismic slip at the fault plane. A rate dependent constitutive friction law is usually adopted [5,6]. Even though simple, this model leads to very interesting conclusions regarding earthquake triggering, recurrence and energy dissipation at the fault plane. Nevertheless, this model has two important limitations. The first one is that in reality the co-seismic slip does not take place into a plane but to a zone of finite thickness. The second drawback is that it considers only the shear elastic deformation of the surrounding rock and not the normal elastic deformation. Therefore, this model is better adapted to strike-slip type of faults rather than normal or reverse faults, which can be quite devastating. Here we remove these two assumptions and we extent the existing approaches by considering that a) the energy is dissipated inside a layer of finite thickness (i.e. the fault gouge) and b) that the surrounding, healthy rock can accumulate elastic energy both due to progressive shearing and normal to the fault gouge compaction. This allows us to model properly the aforementioned multi-physical couplings and the orientation of the fault relative to the direction of the tectonic displacements.

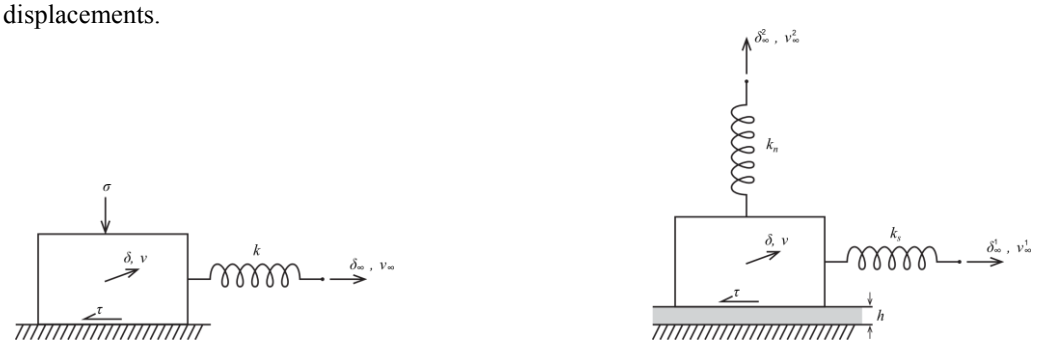

Figure 1. (a) Classical block-slider model; (b) Extended block-slider system. The thickness of the localization zone is h. The vertical spring repesents the normal elastic deformation of the surrounding rock.

References

[1] J. Sulem, I. Stefanou, and E. Veveakis, "Stability analysis of undrained adiabatic shearing of a rock layer with Cosserat microstructure," Granular Matter, 2011, 13, no. 3, pp. 261–268, DOI: 10.1007/s10035-010-0244-1.
[2] I. Stefanou and J. Sulem, "Chemically induced compaction bands: Triggering conditions and band thickness," Journal of Geophysical Research: Solid Earth, 2014, 119, no. 2, pp. 880–899, DOI: 10.1002/2013JB010342.
[3] E. Veveakis, S. Alevizos, and I. Vardoulakis, "Chemical reaction capping of thermal instabilities during shear of frictional faults," Journal of the Mechanics and Physics of Solids, 2010, 58, no. 9, pp. 1175–1194, DOI: 10.1016/j.jmps.2010.06.010.
[4] N. Brantut and J. Sulem, "Strain Localization and Slip Instability in a Strain-Rate Hardening, Chemically Weakening Material," Journal of Applied Mechanics, 2012, 79, no. 3, p. 031004, DOI: 10.1115/1.4005880.
[5] A. Ruina, "Slip instability and state variable friction laws," Journal of Geophysical Research, 1983, 88, no. B12, p. 10359, DOI: 10.1029/JB088iB12p10359.

cmg2016 - - Wednesday, June 8, 2016 - 12:00/12:45 (45min)

[6] J. R. Rice and A. Ruina, "Stability of Steady Frictional Slipping," Journal of Applied Mechanics, 1983, 50, no. 2, p. 343, DOI: 10.1115/1.3167042.

cmg2016 - - Wednesday, June 8, 2016 - 12:00/12:45 (45min)

THE GENERATION OF OVERPRESSURES BY COUPLED DEFORMATION AND DEHYDRATION IN SUBDUCTION ZONES

N. Brantut[1], I. Stefanou[2] & J. Sulem[2]
[1]*Rock and Ice physics Laboratory & Seismolab, Earth Sciences Department, University College London, UK*
[2]*Université Paris-Est, Laboratoire Navier, Ecole des Ponts ParisTech, Marne-la-Vallée, France*

Key words Subduction zones, earthquakes nucleation, dehydration, multiphysical couplings, instabilities.

We are here interested in the compacting behavior of dehydrating materials [1, 2]. During dehydration (for example, of serpentinites in subduction zones), a large volume of fluid is released, and a large porosity is generated. The generation of fluid induces pore pressure rises, while the generation of porosity induces a general weakening of the material. This latter aspect has been well demonstrated in experiments, which show that dehydrated and dehydrating serpentinites behave similarly to porous rocks, in the sense that they can yield in pure compaction (hydrostatic stress state). The yield caps of dehydrated serpentinites are hence “closed" at high mean stresses [3], which also implies negative friction coefficients and possibly negative dilatancy factors in the high stress regime.

How the evolution from a small porosity rock (or non-porous) to a porous one containing pressurized fluids, effects the strain localization within the material?
What is the role played by the feedbacks between reaction rate and pore fluid pressure rise?

Here we try to answer these questions by performing a stability analysis of a system composed of an initially homogeneous dehydrating rock, under nominally drained conditions. For simplicity we only consider the one dimensional case. We show that a positive feedback exists between inelastic compaction and reaction rate in the regime where the reaction produces a net decrease in total volume. This positive feedback tends to localize compaction, and generate shear instabilities, while reducing dramatically the effective pressure. This behavior is analogue to the "dehydration embrittlement" mechanism, but is shown here to occur even at very high pressure (and hence depths) in subduction zones.

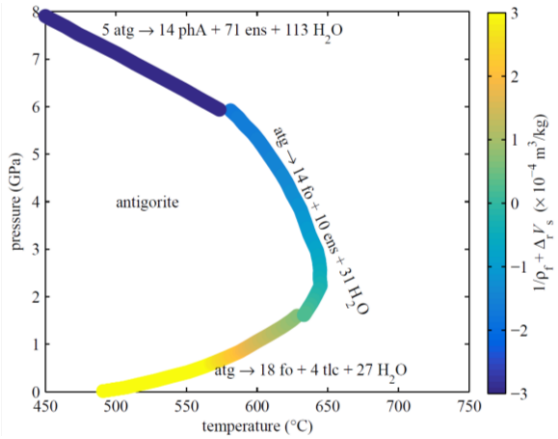

Figure 1. Net total volume change as a function of pressure and temperature, for various reactions (atg: antigorite; fo: forsterite; tlc: talc; ens: enstatite; phA: phase A).

References

[1] N. Brantut and J. Sulem, “Strain Localization and Slip Instability in a Strain-Rate Hardening, Chemically Weakening Material,” Journal of Applied Mechanics, 2012, 79, no. 3, p. 031004, DOI: 10.1115/1.4005880.
[2] E.H. Rutter, S. Llana-Fùnez and K. H. Brodie, “Dehydration and deformation of intact cylinders of serpentinite,” Journal of Structural Geology, 2009, 31, DOI:10.1016/j.jsg.2008.09.008.
[3] I. Stefanou and J. Sulem, “Chemically induced compaction bands: Triggering conditions and band thickness,” Journal of Geophysical Research: Solid Earth, 2014, 119, no. 2, pp. 880–899, DOI: 10.1002/2013JB010342.

cmg2016 - - Wednesday, June 8, 2016 - 12:00/12:45 (45min)

EARTHQUAKE NUCLEATION ON A HETEROGENEOUS RATE-AND-STATE INTERFACE

P. Dublanchet[1], J-P. Ampuero[2]
[1]*MINES ParisTech, PSL Research University, Centre de géosciences, Fontainebleau, France*
[2]*Seismological Laboratory, California Institute of Technology, Pasadena, USA*

Key words stable and unstable slip, average friction parameters, localization, foreshocks.

Earthquakes are often interpreted as frictional instabilities releasing tectonic stresses along crustal faults. These instabilities occur as a sudden acceleration of slip rate along the fault, which triggers the radiation of elastic waves. However, observations show that some instabilities do not fully develop, leading instead to aseismic transients. This could be possibly related to the frictional heterogeneity of fault zones. Here we investigate the very early stage (or nucleation) of such instabilities on heterogeneous faults, coupling stable and unstable frictional behavior. For that we consider a simple model of fault consisting in a planar interface between two elastic half-spaces representing the rock medium. The system is loaded at a constant rate, and slip along the interface is resisted by a heterogeneous friction, governed here by the laboratory-derived rate-and-state laws [2].

Our main results could be summarized as follows : (1) major instabilities occur if $a_0 - b_0 < 0$, a_0 and b_0 being the spatial averages of the a and b rate-and-state parameters, which extends the results by [4, 5]; (2) in the limiting case of a short wavelength heterogeneity we observe similar regimes of nucleation under heterogeneous and constant frictional conditions [3, 6, 1]; (3) the transition between the different regimes, the timescale of slip acceleration and the length-scale of slip localization are in this case controlled by the ratio a_0/b_0 (Fig. 1); (4) an increase in the wavelength of the heterogeneity results in an increase in complexity: the nucleation process involves a cascade of smaller seismic events (foreshocks) before the occurrence of the main instability. Such a model therefore provides insights into the way heterogeneity controls the transient acceleration of slip, and the occurrence of foreshocks preceding a major earthquake, which has strong implications for seismic hazard assessment.

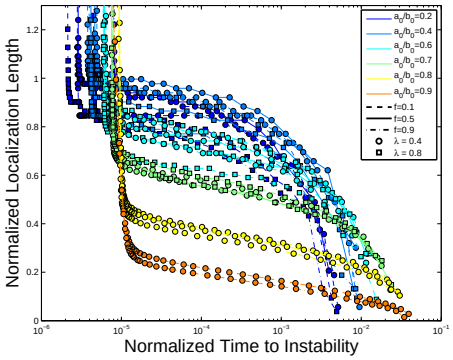

Figure 1. Localization of the slip acceleration zone on a planar fault with different levels of frictional heterogeneity. Colors indicate the ratio a_0/b_0. Heterogeneity is characterized by a small normalized typical wavelength $\lambda < 1$.

References

[1] Ampuero, J., and A. Rubin, *Earthquake nucleation on rate and state faults: Aging and slip laws* J. Geophys. Res, **113**, B01,302 (2008).
[2] Dieterich, J. H., *Modeling of rock friction-1. experimental results and constitutive equations.* J. Geophys. Res., **84** (1979).
[3] Dieterich, J. H., *Earthquake nucleation on faults with rate and state-dependent strength.* Tectonophysics, **211**, 115–134 (1992).
[4] Dublanchet, P., P. Bernard, and P. Favreau, *Interaction and triggering in a 3d rate-and-state asperity model* J. Geophys. Res. **118**, 005 (2013).
[5] Dublanchet, P., P. Bernard, and P. Favreau, *Creep modulation of Omori law generated by a Coulomb stress perturbation in a 3-D rate-and-state asperity model* J. Geophys. Res. **118**, 009 (2013).
[6] Rubin, A., and J. Ampuero, *Earthquake nucleation on (aging) rate and state faults* J. Geophys. Res. *110*, B11,312 (2005).

cmg2016 - - Wednesday, June 8, 2016 - 12:00/12:45 (45min)

DYNAMIC OFF-FAULT BRITTLE DAMAGE DUE TO EARTHQUAKE AND ASSOCIATED RADIATION

H. S. Bhat[1], & Marion Thomas[1]
[1]*Institut de Physique du Globe, Paris, France*

Key words Earthquake rupture,, brittle damage, micro-mechanics

Earthquakes occur on a fault where the earth is already weakened and deformation tends to localise. Typical faults consist of a narrow fault core of extremely granulated rock, where earthquake slip localises, surrounded by a fractured crust (off-fault damage zone or simply damage zone) whose fracture density decreases with distance away from the fault core[4]. This damage zone exhibits a unique mechanical and hydraulic behaviour which does affect earthquake ruptures [5]. The earthquake ruptures, in turn, impart a wide range of loading rates on the surrounding damage zone which affect the hydro-mechanical properties of the damage zone. A visual comparison of the microstructure around a fault zone and the same in new dynamic loading experiments, where the high strain rates expected around earthquakes can be reproduced in the lab, elucidates the fact that dynamic earthquake ruptures are an important source of the fracture damage around a fault. A consensus is now emerging among seismologists, geologists and rock mechanicians that there is an intimate hydro-mechanical interplay between the earthquake rupture and the damage zone around it. This results in a complex mechanical and hydraulic system that is dominated, and controlled, by fractures. The traditional earthquake cycle models, involving 100's of years of fault loading resulting in violent energy release via earthquakes that last for a few seconds to minutes, however, treat this off-fault damage zone passively making the resulting seismic hazard estimates unreliable. There is thus an urgent need to comprehensively understand, and quantify, the earthquake cycle that accounts for the coupling between an earthquake, on a fault, and the fracture damaged zone, around a fault, leading to reliable estimates of seismic risks and ground motion hazard.

To better model the dynamic off-fault damage, the micromechanical damage mechanics formulated by [1], and generalized by [3] has been extended to allow for a more generalised stress state and to incorporate an experimentally motivated new crack growth (damage evolution) law that is valid over a wide range of loading rates [2]. This law is sensitive to both the crack tip stress field and its time derivative. Incorporating this feature produces additional strain-rate sensitivity in the constitutive response. The model is also experimentally verified by predicting the failure strength of Dionysus-Pentelicon marble over wide range of strain rates. We then implement this constitutive response to understand the role of dynamic brittle off-fault damage on earthquake ruptures. We show that off-fault damage plays an important role in asymmetry of rupture propagation and is a source of high-frequency ground motion in the near source region [6].

References

[1] M. F. Ashby and C. G. Sammis. The damage mechanics of brittle solids in compression. *Pure Appl. Geophys.*, 133(3):489–521, 1990.

[2] H. S. Bhat, A. J. Rosakis, and C. G. Sammis. A micromechanics based constitutive model for brittle failure at high strain rates. *J. Appl. Mech.*, 79(3), 2012.

[3] V. S. Deshpande and A. G. Evans. Inelastic deformation and energy dissipation in ceramics: A mechanism-based constitutive model. *J. Mech. Phys. Solids*, 56(10):3077–3100, 2008.

[4] T. M. Mitchell and D. R. Faulkner. The nature and origin of off-fault damage surrounding strike-slip fault zones with a wide range of displacements: a field study from the Atacama fault system, northern Chile. *J. Struct. Geol.*, 31(8):802–816, 2009.

[5] Richard H. Sibson. Crustal stress, faulting and fluid flow. *Geol. Soc. Spec. Publ.*, 78(1):69–84, 1994.

[6] M. Y. Thomas and H. S. Bhat. *Dynamic off-fault damage and seismic radiation*. in prep., 2016.

cmg2016 - - Wednesday, June 8, 2016 - 12:00/12:45 (45min)

THERMO-CHEMO-MECHANICS IN ENHANCED GEOTHERMAL RESERVOIRS

M. Hu[1], M. Veveakis[1,2], T. Poulet[2,1] & K. Regenauer-Lieb[1]
[1]*School of Petroleum Engineering, UNSW, Sydney, Australia.*
[2]*CSIRO, Sydney, Australia.*

Key words Shear fracture, enhanced geothermal reservoir, fluid-rock interaction, thermo-chemo-plasticity, permeability.

Recently, the technique of Enhanced Geothermal System (EGS) has been employed to unlock thermal energy extraction from low permeability reservoirs. The key idea is to increase hydraulic connectivity between a pair of injection and production wells, in order to allow an economic flow rate (e.g. Desert-Peak geothermal field test, Nevada [1]). By pressurizing cold water into deep earth (1000~3000m beneath the ground), generation of new tensile (mode I) cracks as well as reactivation of pre-existing shear (mode II) fractures are achieved, which provides sufficient heat exchange surface area to extract energy from the hot environment. Being initially hot, the rock adjacent to the injection outlet is then subject to cooling-reheating cycles. Thermal shrinkage or expansion of the rock contributes to degradation of the medium and hence enhances crack propagation. A schematic of this process is shown in Figure 1. Meanwhile, increase in intrinsic permeability is achieved via acid injection (usually a mixture of HCl and HF), which dissolves filling mineral fines between grains. The effects of acids on mechanical properties of tensile fractures have been modelled [2] and tested [3], while the re-activation of shear fractures under thermal and chemical loads could be treated as an analogy to a transient slip of chemically active faults [4].

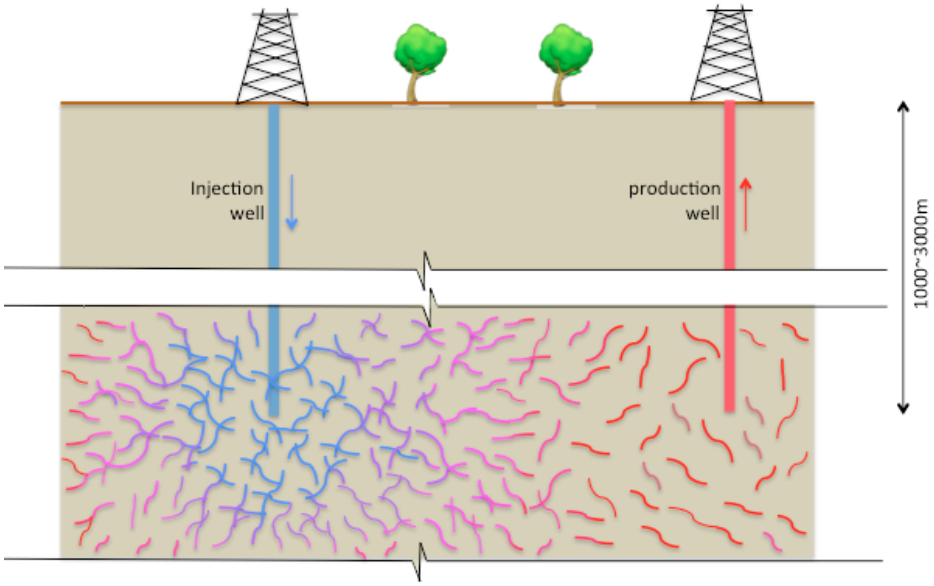

Figure 1. schematic of the stimulation process between a pair of geothermal wells.

References

[1] E. Chabora, et al., *Hydraulic stimulation of well 27-15, Desert Peak geothermal field, Nevada, USA*, Proceedings of thirty-seventh workshop on geothermal reservoir engineering, Stanford University, Stanford. **30**, (2012).
[2] M. Hu, and T. Hueckel, *Environmentally enhanced crack propagation in a chemically degrading isotropic shale*, Géotechnique **63** (4), 313-321 (2013).
[3] M. O. Ciantia, and T. Hueckel, *Weathering of submerged stressed calcarenites: chemo-mechanical coupling mechanisms*, Géotechnique **63** (9), 768-785 (2013).
[4] E. Veveakis, T. Poulet, S. Alevizos, *Thermo-poro-mechanics of chemically active creeping faults: 2.transient considerations*. J. Geophys. Res. Solis Earth **119**, 4583-4605 (2014).

cmg2016 - - Wednesday, June 8, 2016 - 12:00/12:45 (45min)

Towards a physics-based rock friction constitutive law

E. Aharonov[1] & C. Scholz[2]

[1]*Hebrew University of Jerusalem, Jerusalem, Israel*
[2]*Lamont Doherty Earth Observatory, NY, USA.*

friction, earthquakes

Experiments measuring friction at a variety of sliding velocities find that the value of the friction coefficient varies widely: friction is high and behaves according to the rate and state constitutive law during slow sliding, yet markedly weakens as the sliding velocity approaches seismic slip speeds. We introduce a physics-based theory to explain this behavior. Using conventional microphysics of creep, we calculate the velocity and temperature dependence of contact stresses during sliding, including the thermal effects of shear heating. Contacts are assumed to reach a coupled thermal and mechanical steady-state, and friction is calculated for steady sliding. Results from theory provide good fits to the reported experimental results for calcite and quartz friction at all velocity ranges and at varying ambient temperatures, see figure 1.

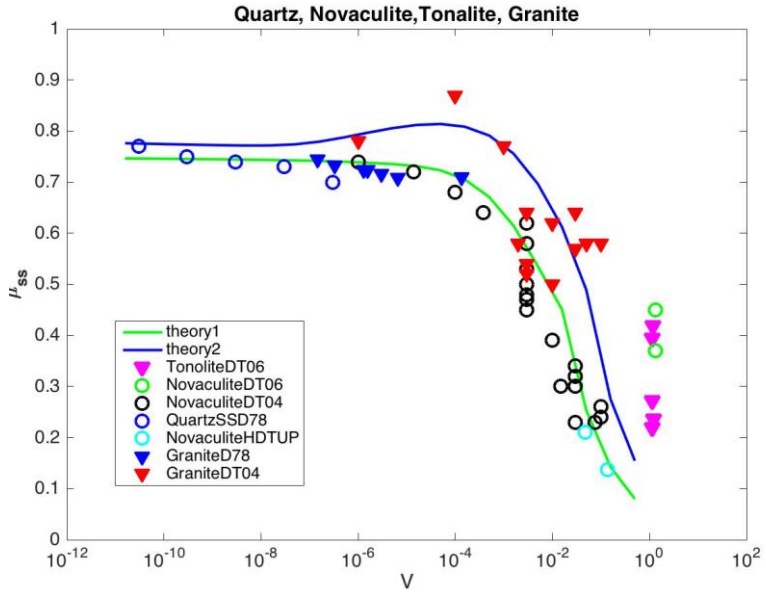

Figure 1. Experimental observations of steady-state friction from DiToro et al, 2006, 2004, and Dieterich 1978 (symbols) and our theory using 2 different parameter sets (lines), showing good fit across many orders of magnitude in velocity.

cmg2016 - - Wednesday, June 8, 2016 - 12:00/12:45 (45min)

AEROFRACTURES IN POROUS MEDIA: EXPLAINING MECHANICS WITH ACOUSTIC EMISSIONS

S. Turkaya[1], R. Toussaint[1], F. K. Eriksen[1, 2], M. Zecevic[3], G. Daniel[3], E. G. Flekkøy[2] & K. J. Måløy[2]
[1]*Institut de Physique du Globe, Strasbourg, France.*
[2]*Department of Physics, University of Oslo, P. 0. Box 1048, 0316 Oslo, Norway*
[3]*Magnitude, Route de Marseille 04220 Sainte Tulle, France*

Key words lamb waves, acoustic emissions, fracturing, porous medium.

Fluid induced brittle deformation of porous medium is an event commonly present in everyday life. From an espresso machine to volcanoes, from food industry to construction, it is possible to see traces of this phenomenon. In this work, analogue models are developed (similar to the previous work of Johnsen [1]) in a linear geometry, with confinement and at low porosity to study the instabilities that occur during fast motion of fluid in dense porous materials: fracturing, fingering, channeling (Figure 1a). We study these complex fluid/solid mechanical systems using two imaging techniques: optical imaging using a high speed camera (1000 fps), high frequency resolution accelerometers and piezoelectrical sensors. Additionally, we develop physical models rendering for the fluid mechanics (similar to the work of Niebling [2,3]) in the channels and the propagation of microseismic waves [4] around the fracture (Figure 2). We then compare a numerical resolution of this physical system with the observed experimental system.

The experimental setup [5] consists of a rectangular Hele-Shaw cell with three closed boundaries and one semi-permeable boundary which enables the flow of the fluid but not the solid particles. During the experiments, the fluid is injected into the system, with a constant injection pressure, from the point opposite to the semi-permeable boundary. At the large enough injection pressures, the fluid also displaces grains and creates channels, fractures towards the semi-permeable boundary.

In the analysis phase, we compute the power spectrum of the acoustic signal in time windows of 5 ms, recorded by shock accelerometers Brüel & Kjaer 4374 (Frq. Range 1 Hz – 26 kHz) with 1 MHz sampling rate. The evolution of the power spectrum is compared with the optical recordings. The power spectrum initially follows a power law trend and when the channel network is developed, stick-slip events generating peaks with characteristic frequencies at 10, 30, 60 and 180 kHz are seen. These peaks are strongly influenced by the size and branching of the channels, compaction of the medium, vibration of air in the pores and the fundamental frequency of the plate. Furthermore, the number of these stick-slip events, similar to the data obtained in hydraulic fracturing operations, follows a Modified Omori Law decay with an exponent p value around 0.5. An analytical model of overpressure diffusion predicting p = 0.5 and two other free parameters of the Omori Law (prefactor and origin time) is developed. The spatial density of the seismic events, and the time of end of formation of the channels can also be predicted using this developed model. Different sources of the signal (air vibration in the carved area, changes in the effective stress due to fluid-solid interactions) are separately analyzed and are investigated further using a far field approximation of Lamb waves presented by Goyder & White [6]. In the analysis phase, power spectrum of different timewindows (5 ms) obtained from the recorded signal are computed. We found that, in the synthetic dataset, the peaks in the low frequency range (f < 20 kHz) diminishes while the medium fractures as suggested in experimental work.

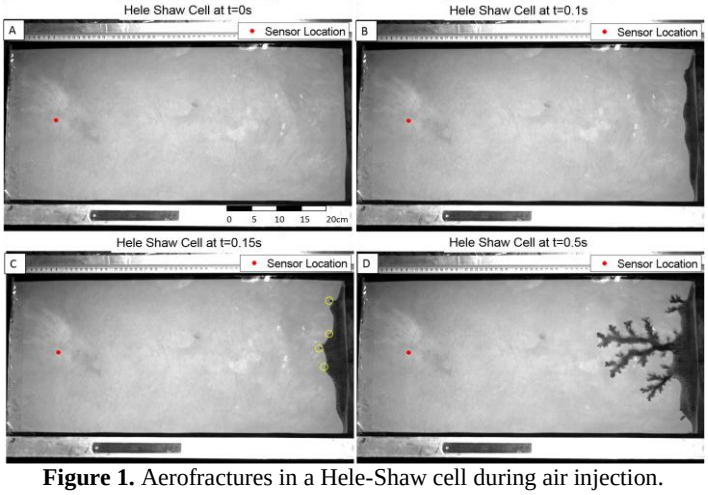

Figure 1. Aerofractures in a Hele-Shaw cell during air injection.

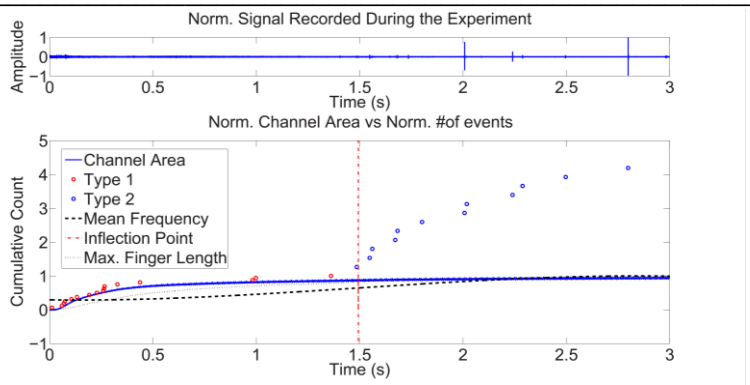

Figure 2. Top: Signal during air injection inside the cell. Bottom: Number of acoustic events compared with carved area, maximum finger length and mean frequency.

References

[1] Johnsen Ø, Toussaint R, Måløy KJ, Flekkøy EG. Pattern formation during air injection into granular materials confined in a circular hele-shaw cell. Phys Rev E (2006) **74**:011301. doi: 10.1103/physreve.74.011301

[2] Niebling MJ, Toussaint R, Flekkøy EG, Måløy KJ. Dynamic aerofracture of dense granular packings. Phys Rev E (2012) **86**:061315. doi: 10.1103/physreve.86.061315

[3] Niebling MJ, Toussaint R, Flekkøy EG, Måløy KJ. Numerical studies of aerofractures in porous media. Rev Cubana Fis. (2012) **29**:1E66–70. Available online at: http://www.fisica.uh.cu/biblioteca/revcubfis/files/Archivos/2012/Vol29-No1E/RCF-29-1E-66.pdf

[4] Farin, M, Mangeney A, Toussaint R, Rosny J, Shapiro N, Dewez T, Hibert C, Mathon C, Sedan O, and Berger F. Characterization of rockfalls from seismic signal: Insights from laboratory experiments. J. Geophys. Res. Solid Earth, (2015) **120**:7102–7137. doi:10.1002/2015JB012331

[5] Turkaya S, Toussaint R, Eriksen FK, Zecevic M, Daniel G, Flekkøy EG, Måløy KJ. Bridging aero-fracture evolution with the characteristics of the acoustic emissions in a porous medium. Front. Phys. (2015) **3**:70. doi: 10.3389/fphy.2015.00070

[6] Goyder, HGD, and White, RG. "Vibrational power flow from machines into built-up structures, part I: introduction and approximate analyses of beam and plate-like foundations." Journal of sound and vibration (1980). **68**:1, 59-75.

Tectonics and Solid Earth Geophysics

cmg2016 - - Thursday, June 9, 2016 - 17:30/18:00 (30min)

HETEROGENEOUS MANTLE CONVECTION IN A MICROWAVE OVEN

A. Limare[1], L. Fourel[1], E. Surducan[2], C. Neamtu[2], V. Surducan[2],
C. G. Farnetani[1], E. Kaminski[1] & C. Jaupart[1]
[1]*Institut de Physique du Globe, Paris, France*
[2]*INCDTIM, Cluj-Napoca, Romania*

Key words heterogeneous mantle convection, internal heating, radioactive elements, reservoir.

The pattern of convection in Earth′s mantle is still controversial because of conflicting evidence from geophysics and geochemistry: seismic tomography reveals slabs reaching the bottom of the mantle, arguments in favor of whole mantle convection and mixing while chemical composition of erupted magma requires distinct reservoirs with different isotopic composition. The origin and the dynamics of these reservoirs, as well as their contribution to the global thermo-chemical evolution of the Earth, are the objects of intense debates. The reservoirs can be pristine or due to the progressive accumulation of material subducted from the surface of the Earth. In the two cases, the question of the stability of the reservoirs at a geological time scale is central. To study the stability of such reservoirs in the context of vigorous mantle convection, we carry out two-layer experiments in which the bottom layer contains a higher amount of internal heating. For this purpose we have devised a new technology based on microwave heating, validated in previous studies [1]. A deeply modified microwave oven contains the experimental tank that accommodates the experimental fluids. A laser sheet scans the tank and two cameras acquire images in different spectral zones using adequate colour filters. The temperature is measured using laser-induced fluorescence while the 2D velocity field is measured using particle image velocimetry. The dimensionless numbers characterizing two-layer convection are: the depth layer ratio, d_1/d, the internal heating ratio, H_1/H_2, the viscosity ratio, γ, the buoyancy number, B_0 (the ratio of the stabilizing density anomaly to the destabilizing thermal anomaly), and the Rayleigh-Roberts number Ra_H describing the vigor of convection in each layer. Fig. 1 shows an example of a heterogeneous experiment with d_1/d=0.28, H_1/H_2=8, γ=0.7, B_0=0.9, Ra_{H1}=424 and Ra_{H2}=4500. Experiments are performed for a wide range of parameters to obtain stability diagrams giving the regime of convection as a function of dimensionless parameters. These diagrams indicate that even a highly stratified (B_0>1), low viscosity (γ<1) bottom layer ends up in piles. Piles eventually de-stabilize if the depth layer ratio exceeds a certain value. For high viscosity (γ>1) bottom layer we observed a stratified, two-layer convection with oscillating interface if the buoyancy number, B_0, exceeds a certain value.

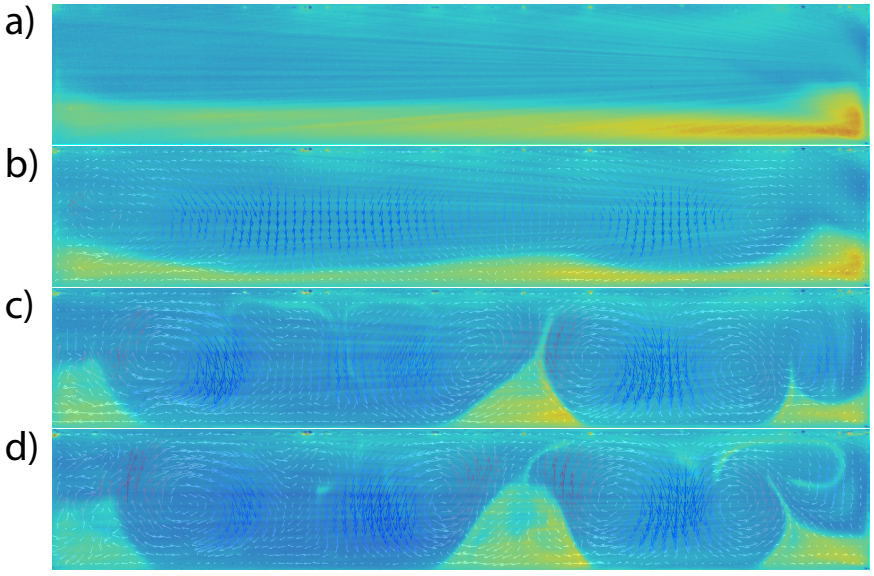

Figure 1. Cross-section of the experimental tank containing the optical image superposed on the 2D velocity field a) initial, stable condition, b) initiation of convection into the top layer, c,d) pile formation and tendril entrainment.

References

[1] A. Limare et al, *Microwave-heating laboratory experiments for planetary mantle convection*, J. Fluid. Mech. **777**, 50-67 (2015).

cmg2016 - - Thursday, June 9, 2016 - 18:30/18:45 (15min)

Tectonics Down Under: the mechanics of earthquakes and faulting driven by the ductile regime

K. Regenauer-Lieb[1],M. Veveakis[1,2], S. Alevizos[1], M. Hu[1], C. Schrank[3]and Thomas Poulet[2,1]
[1]*School of Petroleum Engineering, UNSW, Kensington, NSW 2052, Australia.*
[2]*CSIRO Mineral Resources Flagship, PO Box 1130, Bentley, WA 6102, Australia*
[3]*Science and Engineering Faculty, Queensland University of Technology, Brisbane, QLD 4001, Australia*

Keywords Continuum Mechanics, Fluid Dynamics, Instabilities, Elasto-Visco-Plastic Rheology, Multiphysics.

The classical model for the mechanics of earthquakes is based on the assumption that seismogenic faults are controlled by the brittle crust and diffuse into their ductile roots [*Scholz,* 1990]. However, field observations challenge this simple view:rocks in the ductile realm can localize in unusually narrow shear planes, as thin as millimetres. Well-known examples include the exposed Glarus, McConnell and Naukluftcarbonate thrusts, which display tens of kilometres of displacements on such ultra-thin layers. Geological observations infer repeated slippage events, similar to episodic tremors observed in subduction zones like Cascadia in Canada and Hikurangi in New Zealand. In all of the above cases, deep fluid release reactions were found to be an important trigger of slow earthquakes in the ductile realm [*Poulet et al.*, 2014a; *Poulet et al.*, 2014b]. In contrast to their brittle counterparts, the periodicity and slip magnitude of these ductile events is a result of a material instability and not of a random geometric stress concentration.Therefore, ductile events are predictable provided that the material properties can be inverted from geological and geophysical observations.

This finding opens a new way for understanding the mechanics of faulting and earthquakes based on fundamental multiphysics mechanisms underpinning the time-dependent instability. The approach converges in the long time scale (quasi-static) limit to the classical continuum mechanics failure envelopes of the classical fault mechanics approach. However, being time-dependent, it predicts that the long-term strength of faults is not governed by cracking of the brittle crust (geometrically controlled stress build up in the brittle crust) but rather by creeping flow (energy feedbacks) leading to slow slip instabilities that are driven by geodynamic processes. These instabilities propagate upwards from the ductile regime into the top and rupture the brittle crust. We explicitly identify the role of elastic P-waves and S-waves in triggering instability [*Veveakis and Regenauer-Lieb*, 2015] and show applications of the unified "wave mechanics" approach [*Regenauer-Lieb et al.*, 2016] as a quantitative link between rate-controlled elasto-dynamic instabilities in the brittle field and creeping flow instabilities of the deep earthquake generator.

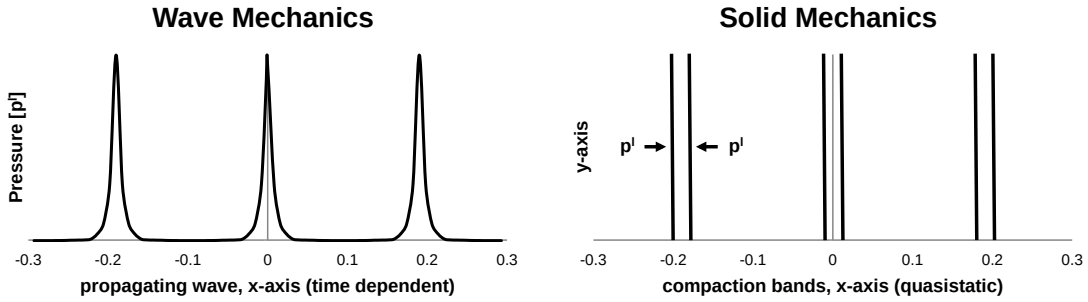

Figure 1 Duality of a *wave mechanics* (left panel) versus a *solid mechanics*(right panel) concept forelasto-visco-plastic P-wave instabilities. The time-dependent wave mechanics approach predicts material instabilities in the shape of a special form of propagating pressure (P)-waves that in the stationary limit are equivalent to compaction bands of solid mechanics.

References

[1] Poulet, T., E. Veveakis, M. Herwegh, T. Buckingham, and K. Regenauer-Lieb (2014a), Modeling episodic fluid-release events in the ductile carbonates of the Glarus thrust, Geophysical Research Letters, 41(20), 7121-7128.
[2] Poulet, T., E. Veveakis, K. Regenauer-Lieb, and D. A. Yuen (2014b), Thermo-Poro-Mechanics of chemically active creeping faults. 3: The role of Serpentinite in Episodic Tremor and Slip sequences, and transition to chaos, Journal of Geophysical Research: Solid Earth, 119(6), 4606–4625 doi:10.1002/2014JB011004.
[3] Regenauer-Lieb, K., T. Poulet, and E. Veveakis (2016), A novel wave-mechanics approach for fluid flow in unconventional resource, The Leading Edge, doi:10.1190/tle35010xxx.1.
[4] Scholz, C. H. (1990), The mechanics of earthquakes and faulting, 439 pp., Cambridge University Press.
[5] Veveakis, E., and Regenauer-Lieb (2015), Cnoidal Waves in Solids, Journal of Mechanics and Physics of Solids, 78, 231-248.

cmg2016 - - Thursday, June 9, 2016 - 17:15/17:30 (15min)

Recognising the patterns in mantle convection and what they can tell us about Earth

S. Atkins[1], A.P. Valentine[1], A.B. Rozel[2], P.J. Tackley[2] & J. Trampert[1]
[1]*Department of Earth Science, Universiteit Utrecht, Utrecht, The Netherlands*
[2]*Department of Earth Sciences, ETH Zurich, Switzerland.*

Key words Mantle dynamics, neural networks, probabilistic inversion, pattern recognitions

Inverting mantle flow for past configurations is one of the great outstanding problems in geodynamics. We demonstrate a new method for inverting present day Earth observations for mantle properties and history. Convection is a non-linear and chaotic, thwarting most standard inversion methods. Because of its chaotic and unpredictable nature, small errors in initial conditions, parameter selection, and computational precision can all significantly change the results produced by mantle convection simulations.

However, some patterns and statistics of convection contain the signature of the parameters used in the simulations over long time-scales. Geodynamical studies often vary these parameters to investigate their effects on the patterns produced. We show that with a large enough set of simulations, we can investigate the relationship between input parameters and convection patterns in a more rigorous way.

Probabilistic inversion is the only way to approach highly non-linear problems. We use neural networks to represent the probability density function linking convection simulation input parameters and the patterns they produce. This allows us to find input parameters, whilst taking into account all of the uncertainties that are inherent in the inversion of any Earth system: how well do we understand the physics of the process; what do we already know about that input parameter; and how certain are our observations?

We show that the mantle structures produced by 4.5 Gyr of convection simulations, considered at a single time frame, contain enough information on yield stress, viscosity coefficients, mantle heating rate, and the initial state of primordial material that we can infer them directly without requiring any other information, such as plate velocity.

cmg2016 - - Thursday, June 9, 2016 - 18:00/18:15 (15min)

Spontaneous episodic initiation of one-sided subduction using visco-elasto-plastic colloidal dispersions

A. Davaille[1] & E. Di Giuseppe[1,2]
[1]*Laboratoire FAST, CNRS / University Paris-Sud, Orsay, France*
[2]*Now at CEMEF, MINES ParisTech, CNRS UMR 7635, CS 10207, 06904 Sophia Antipolis, France.*

Key words Convection, Plate Tectonics, Subduction, Laboratory Experiments

One-sided subduction is a fundamental characteristics of the convective regime of plate tectonics on Earth, but its initiation and morphology are still not well-understood. We report new laboratory experiments using colloidal dispersions whose rheology varies from viscous to elasto-visco-plastic to brittle when their water content decreases (fig.1, [1]). So as an analogy to cooling from above, the fluid is dryed from above. Humidity, temperature, fluid thickness and solution concentration were systematically varied, which resulted in changing the intensity of convection and the magnitude of the rheological parameters of the fluid. As the fluid surface dries, a denser chemical boundary layer (CBL) develops, constituted of a thin brittle film on top of a more ductile layer; and convection develops under this stagnant lid. However, drying-induced stresses cause the skin to buckle, which then induces plastic failure, thereby initiating subduction of the gravitationally unstable skin (fig.2). Subduction is always one-sided and proceeds quickly by trench roll-back. Then the whole process starts again. Shear banding and a lubrication layer on the top of the subducting slab seem to be key ingredients to break the surface plate and initiate subduction episods.

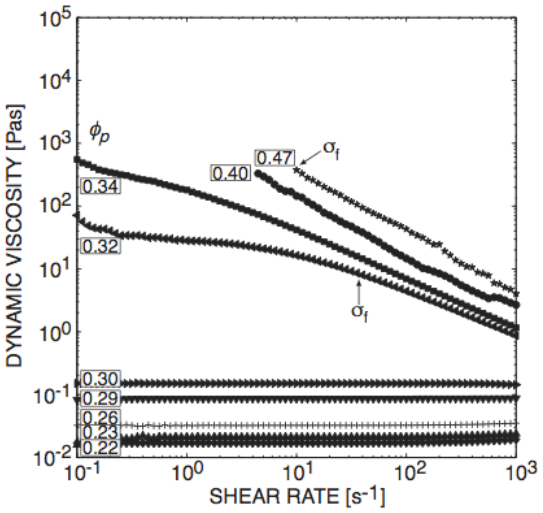

Figure 1. Rheology of Ludox HS40 for different particle volume fraction φ_p. Viscosity as a function of shear rate. σ_f corresponds to the stress above which the particle network is destroyed, the solution becomes shear-thinning and the viscosity can be described by a power law. [1].

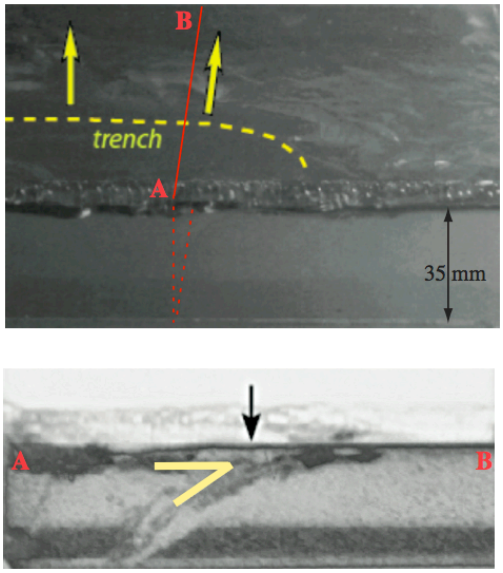

Figure 2. Spontaneous asymmetric subduction in a layer of colloids dried from above at constant temperature and humidity. a) view from above. The "trench" is outlined in yellow and the direction of trench rollback is indicated by the yellow arrows. b) view from the side. The contrast has been enhanced to better see the subducting plate. The trench position is marked with a black arrow.

References

[1] Di Giuseppe E., Davaille A., Mittlestaedt E., François M. (2012) *Rheol. Acta* 51(5), 451-465.

cmg2016 - - Thursday, June 9, 2016 - 18:15/18:30 (15min)

EXPLORING VISCOSITY VARIATIONS IN THE EARTH'S MANTLE

K. O'Farrell[1], C. Lithgow-Bertelloni[1]
[1]*University College London, London, United Kingdom*

Key words geodynamics, viscosity, geoid, mantle, tomographic models, dynamic topography

This is an extensive study which has gathered a set of over 50 tomographic models in order to explore viscosity variations in the Earth's mantle. This study looks at a range of different viscosity variations and their effect on the mantle flow, dynamics and ultimately the surface manifestation of the dynamics. We seek to constrain the value of the viscosity parameter which is so important to our further studies of dynamics of the Earth's interior and plate motions.

Seismic tomography can be used to investigate radial viscosity variations on instantaneous flow models by predicting the global geoid and comparing with the observed geoid. This method is one of many that has been used to constrain viscosity structure in the Earth's mantle in the last few decades. Examining over 50 tomographic models we found notable differences by comparing a synthetically produced geoid with the observed geoid. We compared S- and P-wave tomographic models and found the S-wave models provided a better fit to the observed geoid. Using this large suite of 50 tomographic models, we have been able to constrain the radial viscosity structure of the Earth. We found that two types of viscosity profiles yielded equally good fits. A viscosity profile with a low transition zone viscosity and a lower mantle viscosity equal to the upper mantle, or a profile with a large lower mantle viscosity and a transition zone viscosity similar to the upper mantle.

Following the recent study by Rudolph et al. [2], we further investigated the effect of a mid-mantle viscosity increase. Based on viscosity structures found by Rudolph et al. [2], we constructed three cases of viscosity profiles which all included a jump in viscosity starting at 660 km depth and a further change in viscosity at 1000km depth (either an increase or a decrease in viscosity compared with the jump at 660 km). Over 8000 different viscosity profiles were tested using our 50 tomographic models. Our results show that increases at 660 km or 1000km depth were able to produce a global geoid that matches closely with the observed geoid. We conclude that there must be an increase in viscosity by 1000 km depth, but the location (depth) of the increase can vary slightly.

Using the set of radial viscosity profiles that gave the best fit to the observed geoid, we can explore a range of lateral viscosity variations and see how they affect the different types of tomographic models. Improving on previous studies of lateral viscosity variations (e.g. [1]), we systematically explore a large range of tomographic models and density-velocity conversion factors. We explore which type of tomographic model (S- or P- wave) is more strongly affected by lateral viscosity variations, as well as the effect on isotropic and anisotropic models. We constrain the strength of lateral viscosity variations necessary to produce a high correlation between observed and predicted geoid anomalies. We discuss the wavelength of flow that is most affected by the lateral viscosity variations.

This suite of tomographic models and our constrained viscosity profiles can further be used to investigate the effect on dynamic topography generated at the Earth's surface. Dynamic topography is the residual topography of the Earth after removing the isostatic topography. This dynamic topography is generated by the flow of the mantle. Being able to constrain the dynamic topography on the surface requires good constraints on the internal structure and dynamics of the Earth. Here, we present the tomographic models which produce more realistic amplitudes for dynamic topography based on the range of viscosity profiles we have previously constrained.

By constraining the range of viscosity values in the mantle, we can constrain the types of dynamics we expect to observe, from the geoid to dynamic topography. These results will be of future use to other studies of the internal and surface dynamics.

References

[1] A. Ghosh, T. W. Becker, and S. J. Zhong, *Effects of lateral viscosity variations on the geoid*, Geophys. Res. Lett., **37**, L01301, doi:10.1029/2009GL040426 (2010).

[2] M. Rudolph, V. Lekic, C. Lithgow-Bertelloni, *Viscosity Jump in the Earth's Mid Mantle*, Science, **350**, (6266), 1349-1352 (2015).

cmg2016 - - Thursday, June 9, 2016 - 16:45/17:15 (30min)

GEODYNAMIC INVERSION TO CONSTRAIN THE RHEOLOGY OF THE LITHOSPHERE

T.S. Baumann[1] & B.J.P. Kaus[1]
[1]*Johannes Gutenberg-Universität, Mainz, Germany*

Key words Numerical modelling of lithosperic deformation – Geophysical inversion – Rheology of the lithosphere

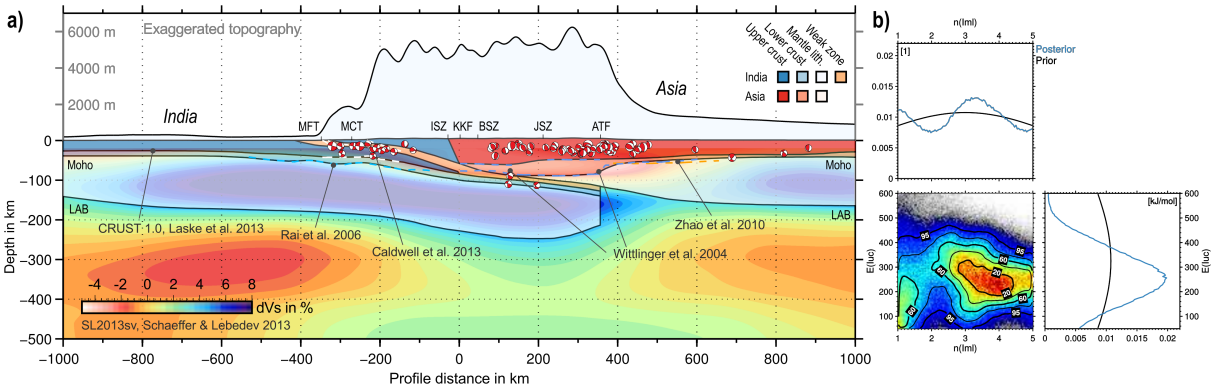

Figure 1. Geodynamic inversion applied to a SW-NE transect of the India-Asia collision [1]. **a)** 2D model geometry, constructed from multiple geophysical data. **b)** Example of the inversion results: marginal posterior distribution of two rheological parameters. Here, power-law exponent of the Indian mantle lithosphere and activation energy of the Indian upper crust.

A common method to determine the strength of the lithosphere is to estimate its effective elastic thickness (EET) from the coherence between gravity and topography. This method assumes a priori that the lithosphere is a thin elastic plate floating on a viscous mantle. Whereas this works well with oceanic plates, it has given controversial results in continental collision zones. Usually, continental collisions zones are well-studied areas for which additional geophysical datasets such as receiver functions and seismic tomography exist that constrain the geometry of the lithosphere and often show that it is rather complex. Yet, lithospheric geometry by itself is insufficient to understand the dynamics of the lithosphere, as this also requires knowledge of the rheology of the lithosphere. Experimental results show significant variability between various rock types and there are large uncertainties in extrapolating laboratory values to nature.

An independent approach is thus required to better understand the rheology and dynamics of the lithosphere in collision zones. Our method combines numerical thermo-mechanical forward models of the present-day lithosphere with a Bayesian inversion approach [1]. The geometry of the forward models is part of the a priori knowledge and is constructed from seismological data. We jointly invert topography, gravity, horizontal and vertical surface velocities to constrain the unknown rheological material parameters of the forward models in a probabilistic sense. The model rheology is described with experimentally determined viscous creep laws and other parameters describing the plastic behaviour. As viscosity is temperature dependent, the temperature structure of the forward models is parameterised as well.

We apply the method to a cross-section of the India-Asia collision system (Fig. 1a). In this case, we deal with 17 to 20 model parameters, which requires solving around 2×10^6 forward models (Fig. 1b). The resulting models fit the data within their respective uncertainty bounds, and show that the Indian mantle lithosphere must have a high viscosity. Results for the Asian part of the model are less clear, but a detailed appraisal of the model ensemble using a neural network technique enables us to identify four end-member models that fit the data nearly equally well. The striking differences between the end-member models can be reduced to the existence of three model characteristics: a weak lower Tibetan crust, a weak Asian lithospheric mantle and a strong dislocation creep character of the Indian mantle lithosphere. The classification results also suggest that reducing observational uncertainties of vertical velocities is crucial to reduce the model ambiguities.

References

[1] T.S. Baumann, B.J.P Kaus (2015), *Geodynamic inversion to constrain the non-linear rheology of the lithosphere*, Geophys. J. Int. **202(2)**, p. 1253–1270.

Physical Modeling of Tsunami Generation, Propagation and its disastrous effect

D. Shanker

Department of Earthquake Engineering, Indian Institute of Technology Roorkee, Roorkee-247667, Uttaranchal, India,

Email: dayasfeq@iitr.ernet.in

A tectonic earthquake when they occur beneath the sea, the water above the deformed area is displaced from its equilibrium position. Waves are formed as the displaced water mass, acting under the force of gravity, tries to regain equilibrium. When large areas of the sea floor elevate or subside, a tsunami can be created. The waves sweep across the open ocean at high speed and have caused severe damage to costal areas thousand of miles from the earthquake which generated them. An eye-witnesses of December 26, 2004 accounts in understanding tsunami effects. To understand the mechanism of tsunami propagation and the selection of certain section of coastline for waves of destructive amplitudes it is necessary to recognize the depth dependence of wave velocity which is the feature of shallow water wave. The velocity of this class of wave may be derived by assuming equipartition of the potential and kinetic energies of the wave motion. In the present article quantitative derivation of tsunami speed and its disastrous effect has been discussed. The tsunami's energy flux, being dependent on both its wave speed and wave height, remains nearly constant. As a result, the tsunami's speed decreases as it travels into shallower water and its height increases. In deep ocean it appears as low rise tidal waves But, when it reaches the coast, it may appear as a rapidly rising or a series of breaking waves. Being human inability to predict earthquakes and since earthquake magnitude does not determine tsunami impact,resulting tsunamis can be detected by seabed monitors and ocean buoys leaving adequate time for evacuation and information dissemination technologies though, is a minor part of the solution and a mechanism needs to be in place to interpret alerts, relay the warning to local communities through awareness and enable them to undertake quick action.

cmg2016 - - Thursday, June 9, 2016 - 11:45/12:30 (45min)

MODELING STRAIN LOCALIZATION, ZENER PINNING, AND PHASES NUCLEATION IN TWO-MINERALS AGGREGATES

B. Bevillard[1], G. Richard[1], R. Raimbourg[1] & L. Arbaret[1]
[1]*Institut des sciences de la Terre d'Orléans, Orléans, France*

Key words Ductile deformation, strain localization, Zener pinning, nucleation, phases mixture.

Strain localization involved in mylonites formation remains a widely discussed question. Indeed mylonitization requires both dynamic recrystallization to reduce grain-size and stress weakening through diffusion accommodated grain-boundary sliding [1], but these two creep processes do not occur in the same portion of the stress/grain-size space [2]. To address this problem at a lithospheric scale, Bercovici and Ricard [3] built a self-consistent model involving grain-damage in a two phases medium. Based on non equilibrium thermodynamics, their model produces rheological weakening synchronous with grain-size reduction through pinning of the interfaces between the two phases [4]. Deformation reduces pinning surfaces (increase interface roughness) which in turn facilitates grain damage. In order to adapt this model to Earth crust deformation at lower scales, this interpretation of the Zener pinning influence is discussed. Indeed, taking in account Zener pinning implies a limited range for initial interface roughness to ensure that the initial aggregate is energetically balanced. This necessary initial condition induces important differences in the model evolution, particularly concerning the importance and brevity of the stress drop (see figure 1). Furthermore, in mantle and crustal rocks, increasing phase mixture with increasing strain-rate is observed in mylonites in addition to grain-size reduction. To explain this phenomenon, a nucleation process occurring in the diffusion creep domain is proposed and its potential implications on the physical model and on strain localization are explored.

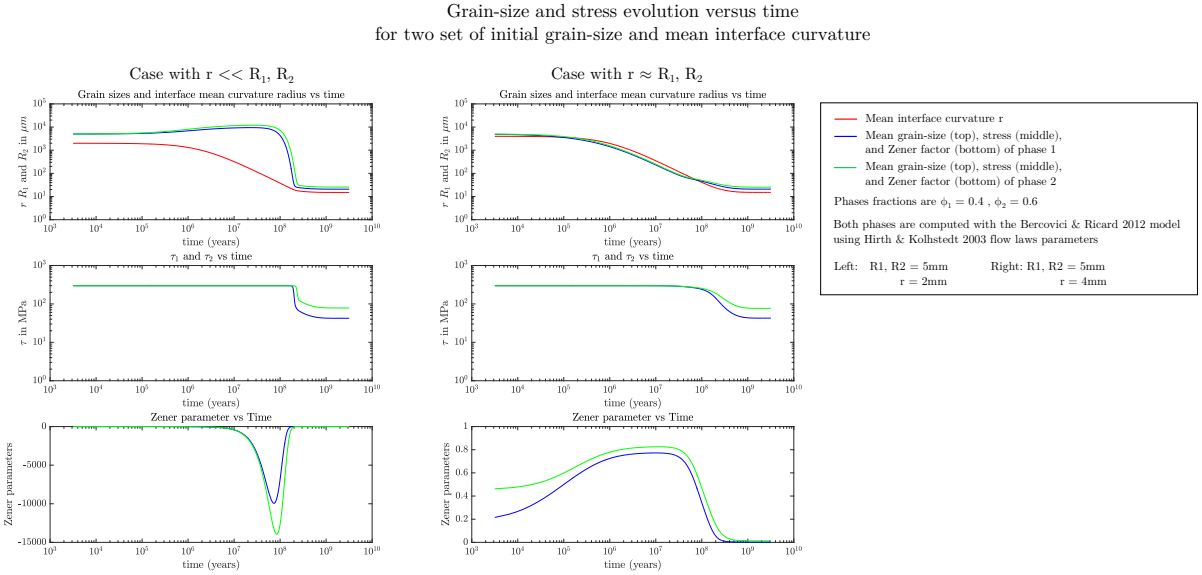

Figure 1. Grain-size, stress, and Zener factor evolutions versus time for two different set of initial grains parameters in ductile deformation conditions. *This figure illustrates the different model behaviors with respect to initial grain parameters. Grain-size of two mineral phases R_1 and R_2 are computed through competition of coarsening and damage. The Zener pinning factor models the impact of the interface pinning by small grains during grain coarsening, limiting it if $0 < Z < 1$ or supposedly promoting it if $Z < 0$. It depends on the two grain-sizes and on the mean interface curvature radius r representing the roughness of the interface between the phases. When the initial mean interface curvature radius r is fixed below a size limit given by the "pinned" state (where $Z = 0$), the Zener factor remains negative during the whole computation, therefore inducing strong grain-sizes and stresses drop. However, this case may not be relevant because it is the grain growth which leads small surrounding grains to pin the interface and slow down coarsening. Zener pinning can't induce grain-size evolution as it is a passive process. Thus, the case where r stay close to R_1, and R_2 demonstrates the expected behavior as the Zener pinning factor, stays between values of* 0 *("pinned" state no grain-growth) and* 1 *(no pinning effect). As a consequence, the softer grain-sizes and stress drops should be due to some nucleation process occurring in diffusion creep conditions.*

References

[1] J.P. Poirier *Shear localization and shear instability in materials in the ductile field.*, J. Struct. Geol. 2 **1/2**, 135-142 (1980).
[2] J.H.P. De Bresser, J.H. Ter Heege, C.J. Spiers *Grain-size reduction by dynamic recrystallisation: can it result in major rheological weakening* Int. J. Earth Sci. **90** 28-45 (2000).
[3] D.Bercovici, Y. Ricard *Mechanisms for the generation of plate tectonics by two phase grain damage and pinning*, Phys. Earth Planet. Int. **202-203**, 27-55 (2012).
[4] C.S. Smith *Grain, phases, and interfaces: an interpretation of microstructures* Trans A.I.M.E **175** 15-51 (1948).

cmg2016 - - Thursday, June 9, 2016 - 11:45/12:30 (45min)

Preliminary Results Of Gamma-Ray Measurements In Bodrum Peninsula; SW Turkey

E. Erbek[1], H. E. Tutunsatar[1], M. N. Dolmaz[1]
[1]*Department of Geophysical Engineering, Suleyman Demirel University, 32260, Isparta, Turkey*

Key words Radioactivity, Gamma – ray spectrometry, Aegean volcanic arc.

Since the beginning of the universe, natural radioactivity has existed. The most important sources of natural radioactivity are Uranium - ^{238}U, Thorium - ^{232}Th, Potassium - ^{40}K and their decay products. Gamma-ray spectrometry is one of the most practical methods that allows the measurement of concentrations of radionuclide elements. These elements have significant effect on internal heat source of the earth and contribute to terrestrial heat flux by producing heat. Bodrum Peninsula is located in Aegean Region, southwest of Turkey. This study field has a complex tectonic structure and it is affected by Aegean volcanic arc and the subduction zone between African oceanic lithosphere and the Aegean continental lithosphere. In this study, distribution maps of eU, eTh, K in the southwest of Anatolia where considered to be continuation of Aegean Volcanic arc have been constituted by using concentrations of radionuclide elements. Additionally, radioactive heat – producing map (RHP) of eU, eTh and K has been calculated and drawn as anomaly map. Obtained results have been compared with geological units (volcanic and non – volcanic units) located in the study field. Concentrations of eU, eTh and K reach up to maximum values (115.02 Bq/kg, 103.84 Bq/kg and 690.1 Bq/kg, respectively) in volcanic area (especially, in Bodrum Peninsula). According to interpretation results, obtained high RHP values in western part of the study field correspond with continuation in land of Aegean Volcanic arc.

cmg2016 - - Thursday, June 9, 2016 - 11:45/12:30 (45min)

GRAPH THEORY FOR ANALYZING PAIR-WISE DATA: APPLICATIONS TO INTERFEROMETRIC SYNTHETIC APERTURE RADAR DATA AT OKMOK VOLCANO, ALASKA

Elena C. Baluyut[1], Michael Cardiff[1] & Kurt L. Feigl[1]

[1] *University of Wisconsin - Madison, Madison, Wisconsin, USA*

Key words Remote Sensing of Volcanoes, Numerical Solutions, Transient Deformation, Inverse Theory

In this work, we apply techniques from graph theory in order to develop a novel technique for inferring time-dependent deformation from interferometric synthetic aperture radar (InSAR) data. Plotting acquisition dates (epochs) as vertices and pair-wise interferometric combinations as edges defines an incidence graph. The edge-vertex incidence matrix and the normalized edge Laplacian matrix are factors in the covariance matrix for the pair-wise data. Using empirical measures of residual scatter in the pair-wise observations, we estimate the variance at each epoch by inverting the covariance of the pair-wise data. We evaluate the rank deficiency of the corresponding least-squares problem via the edge-vertex incidence matrix. We implement our method in a MATLAB software package called GraphTreeTA available on GitHub (https://github.com/feigl/gipht). We apply temporal adjustment to the data set described by Lu, Masterlark, and Durizin (2005, Journal of Geophysical Research) at Okmok volcano, Alaska, which erupted most recently in 1997 and 2008. The data set contains 44 differential volumetric changes and uncertainties estimated from interferograms between 1997 and 2004. Using our method, we estimate that approximately half of the magma volume lost during the 1997 eruption was recovered by the summer of 2003. Our preferred model uses an exponential function followed by a secular interval and provides a reasonable fit that is compatible with viscoelastic relaxation in the five years following the 1997 eruption. Although we demonstrate the approach using volumetric rates of change, our formulation in terms of incidence graphs applies to any quantity derived from pair-wise differences, such as range changes, range gradients, or atmospheric effects.

cmg2016 - - Thursday, June 9, 2016 - 11:45/12:30 (45min)

INTERPRETATION OF MAGNETIC DATA OF THE BLACK SEA USING ANALYTIC SIGNAL METHODS

H. E. Tütünsatar[1], E. Erbek[1] M.N. Dolmaz[1]
[1]*Süleyman Demirel Üniversitesi, Isparta, Turkey*

Key words Black Sea, Magnetic, Analytic Signal.

The Black Sea formed as a result of the tectonic evolution of Alpine Himalayan Belt is an elliptical Basin and located among Caucasus and Crimean in the north and Pontides in the south. The Black Sea Basin is separated by the mid–Black Sea Ridge-a NW trending basement uplift that causes two deep expansion sub-basins (the West Black Sea Basin and the East Black Sea Basin).

Determination the depth and location of a magnetic source is a necessarily process in geophysical applications. One of these methods is Analytic Signal based on the horizontal and vertical derivatives of the potential field data to delineate the depths and boundaries of sources having magnetic properties. In recent years, Horizontal Gradient Analytic Signal method was developed from Analytic Signal method. In this study methods of Analytic Signal (AS) and Horizontal Gradient Analytic Signal (HGAS) were applied to magnetic data of the Black Sea. Reduced to pole (RTP) data was preferred for a better result. 2 km and 1 km downward continuation was applied to the RTP data and AS and HGAS was calculated respectively. We observed that noise affects the results at 2km. The high intensity of magnetic signature of major tectonic elements are observed on Odessa Shelf and Karkinit Trough, which are causative sources in the Precambrian basement of the East European Craton, in the northeast of the Black Sea. From the mid to northern westward of Black Sea, remarkable signs coincide with the Sorokin trough, Tuapse trough, and Shatsky Ridge respectively. Moreover Southern offshore consisting of late Eocence detachment with buried Sea Mount and Sinop trough are distinguished efficaciously in the south of the Black Sea. However, any magnetic signs are not detected in the deep East and West Black Sea Basins on account of thick sedimentary deposits.

cmg2016 - - Thursday, June 9, 2016 - 11:45/12:30 (45min)

FUNNELLING MELTS INTO MID-OCEAN RIDGES THROUGH MODIFIED COMPACTION THEORY

M. Veveakis[1,2] , T. Poulet[2,1] & K. Regenauer-Lieb[1]
[1]UNSW, Sydney, Australia; [2]CSIRO, Sydney, Australia

Key words mid-ocean ridge, melt segregation, cnoidal waves, thermal stress.

Mid-ocean ridges (MORs) are the longest mountain ranges on Earth [1]. Found along every ocean, they are one of the most obvious Earth surface expressions of life-sustaining plate tectonics, missing on all other terrestrial planets. They act as a heat valve releasing heat from the Earth's interior to the surface, thus stabilizing the internal temperature of the planet. This mechanism is found to be extremely efficient. Melt velocities under MORs, inferred both from observational [1] and experimental [2] evidence, are around 10-100 m/yr on average. Classical models [3] address melt focussing to MORs [4-6] but only obtain the lower limit of the observed extraction velocities (around 2 m/yr) as extreme end-members of the physical mechanisms assumed [7]. Here, we show that the formation of high velocity melt channels funnelling magma to the ridge can be the natural result of newly discovered channelling instabilities [8], which can develop in a nonlinear solid matrix with interstitial melts subject to a thermal stress field. A dendritic network of channels is found to accelerate melt towards the MOR, reaching observed velocities near the apex of the MOR (Fig. 1).

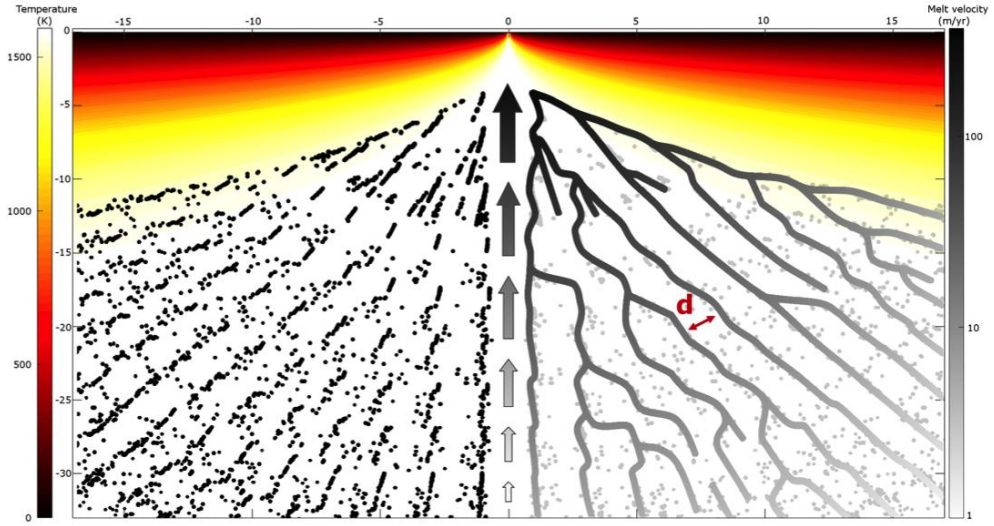

Figure 1. Schematic dendritic network of channels under MORs. The left-hand side shows the localised solution for melt fraction follows defining narrow areas where 100% melt fraction is reached. The locations of these melt pockets are shown enlarged by individual dots. These have been calculated using the above 1-D solution along the η-direction and they therefore do not consider 2-D interaction along η. A number of channels are defined by the alignment of dots. They are regularly spaced throughout the primary melting area with constant spacing. The right-hand side shows an interpretation of the connected dendritic network shaded by predicted melt velocity. Velocity magnitudes are given on the right-hand side of diagram, reaching velocities of 100's of m/yr at the apex. Arrows in the centre illustrate speed towards the surface.

References

[1] D. Forsyth *et al.*, Imaging the Deep Seismic Structure Beneath a Mid-Ocean Ridge: The MELT Experiment. *Science* **280**, 1215-1218 (1998).
[2] J. A. D. Connolly, M. Schmidt, G. Solferino, N. Bagdassarov, Permeability of asthenospheric mantle and melt extraction rates at mid-ocean ridges. *Nature* **462**, 209-2012 (2009).
[3] D. McKenzie, Some remarks on the movement of small melt fractions in the mantle. *Earth and Planetary Science Letters* **95**, 53-72 (1989).
[4] R. F. Katz, M. Spiegelman, B. Holtzman, The dynamics of melt and shear localization in partially molten aggregates. *Nature* **442**, 676-679 (2006).
[5] J. A. D. Connolly, Y. Y. Podladchikov, Decompaction weakening and channeling instability in ductile porous media: Implications for asthenospheric melt segregation. *Journal of Geophysical Research: Solid Earth* **112**, B10205 (2007).
[6] G. Suhr, Melt Migration under Oceanic Ridges: Inferences from Reactive Transport Modelling of Upper Mantle Hosted Dunites. *Journal of Petrology* **40**, 575-599 (1999).
[7] R. F. Katz, Magma dynamics with enthalpy method: Benchmark solutions and magmatic focusing at the Mid Ocean Ridge. *Journal of Petrology* **49**, 2099-2121 (2008).
[8] E. Veveakis, K. Regenauer-Lieb, R. F. Weinberg, Ductile compaction of partially molten rocks: the effect of non-linear viscous rheology on instability and segregation. *Geophysical Journal International* **200**, 519-523 (2015)

cmg2016 - - Thursday, June 9, 2016 - 11:45/12:30 (45min)

Postseismic and interseismic deformations associated with megaearthquakes: towards time-dependent lithospheric deformation

L. Fleitout[1], E. Klein[1], J.D. Garaud, O. Trubienko[1], C. Vigny[1]
[1]*Ecole Normale Supérieure, Paris, France*
[2] *ONERA, Chatillon, France.*

Key words viscoelastic asthenosphere, megaearthqiuakes, seismic cycle

Three megaearthquakes (Sumatra-Aceh(2004), Chili-Maule(2010) and Japan-Tohoku(2011)) struck the Earth during the last ten years. They are the first megaearthquakes since lithospheric deformations can be measured with a high precision (GPS, interferometry). What can we learn from the lithospheric deformations following these earthquakes concerning both the stress accumulation and release on the subduction plate interface, on the short-term mechanical properties of the mantle and on the interpretation of recent (decadal) intraplate deformation?

Velocity perturbations are clearly detected up to 2000km away from the epicenters. Subsidence is observed in the far-field while uplift is observed above the volcanic arc. The postseismic deformations are remarkably similar for the three megaearthquakes. They are modeled with the help of a finite element code (Zebulon-Zset), over a 3D mesh representing in a spherical shell a portion of the mantle more than 60° broad.
The coseismic displacements on the interface are inverted from the coseismic motions registered by GPS.
We show that the postseismic deformation can be explained only with the combination of viscoelastic relaxation in an asthenosphere 100 to 200km thick (newtonian viscosity of the order of 3.10^{18}Pas) and in a low viscosity serpentinized channel above the plate interface at depths larger than 45km (viscosity of some 10^{17}Pas). Slip on the plate interface at shallow depths is moreover required in the case of Aceh and Maule.

This mechanical model can be extended to predict deformations over the whole seismic cycle. We show that at distances over 1000km from zones of large earthquakes, the velocities and intraplate deformations vary significantly through the whole seismic cycle.

As a consequence, we suggest that the relative velocities of blocks or subplates measured by GPS during the last ten years near subduction zones (Sunda Block, Amurian plate) are in fact transient velocities. More generally, we question the geological significance of the 'stress-field' measured during the last decades.

Figure 1. Observed and modeled postseismic displacement in Japan

cmg2016 - - Thursday, June 9, 2016 - 11:45/12:30 (45min)

Comparison between observed and predicted velocities (jan to dec 2012)

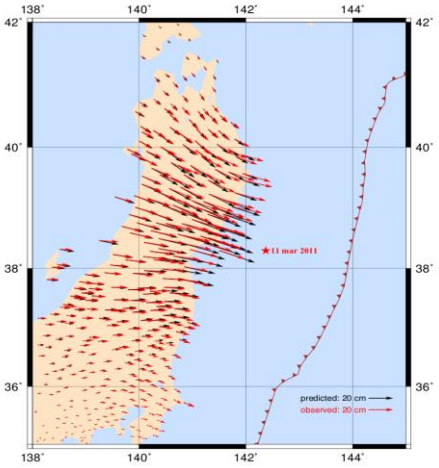

Horizontal velocities

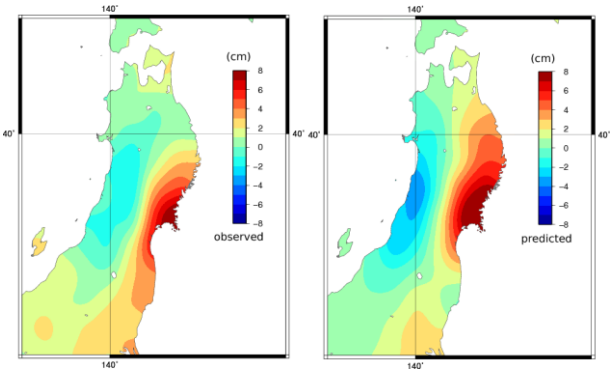

Vertical velocities

Fit to far-field stations time series

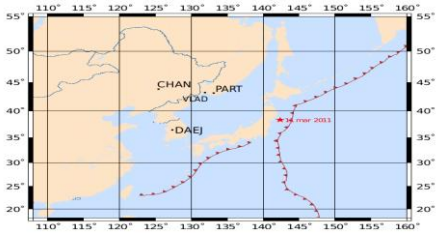

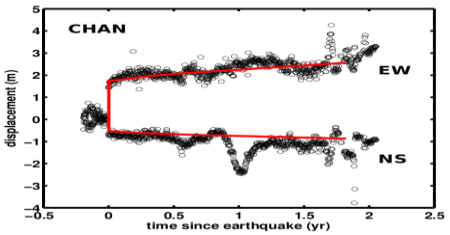

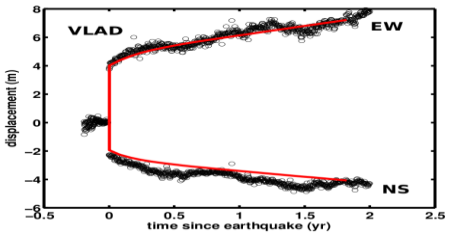

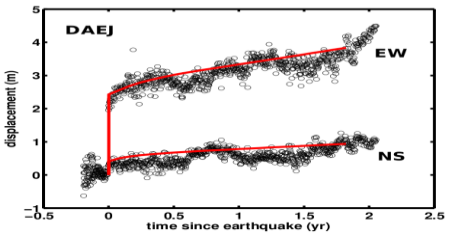

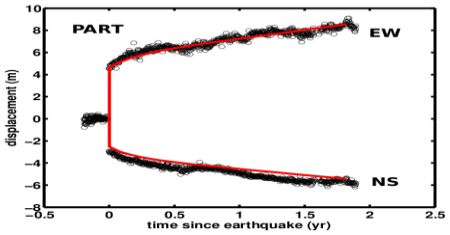

cmg2016 - - Thursday, June 9, 2016 - 11:45/12:30 (45min)

SCALING OF MIXING RATE IN MANTLE CONVECTION MODELS WITH SELF-CONSISTENT PLATE TECTONICS, MELTING AND CRUSTAL PRODUCTION

P. Tackley[1]
[1]*ETH Zurich, Zurich, Switzerland*

Key words Mantle convection, mixing, plate tectonics, magmatism.

It is generally thought that the early Earth's mantle was hotter than today, which using conventional convective scalings should have led to vigorous convection and mixing. Geochemical observations, however, suggest that mixing was not as rapid as would be expected, leading to the suggestion that early Earth had stagnant lid convection [1]. Additionally, the mantle's thermal evolution is difficult to explain using conventional scalings because early heat loss would have been too rapid, which has led to the hypothesis that plate tectonics convection does not follow the conventional convective scalings [2]. One physical process that could be important in this context is partial melting leading to crustal production, which has been shown to have the major effects of buffering mantle temperature and carrying a significant fraction of the heat from hot mantle [3], making plate tectonics easier [4], and causing compositional differentiation of the mantle that can buffer core heat loss [5]. Here, the influence of this process on mantle mixing is examined, using secular thermo-chemical models that simulate Earth's evolution over 4.5 billion years. Mixing is quantified both in terms of how rapidly stretching occurs, and in terms of dispersion: how rapidly initially close heterogeneities are dispersed horizontally and vertically through the mantle. These measures are quantified as a function of time through Earth's evolution. The results will then be related to geochemically-inferred mixing rates for different stages of Earth evolution.

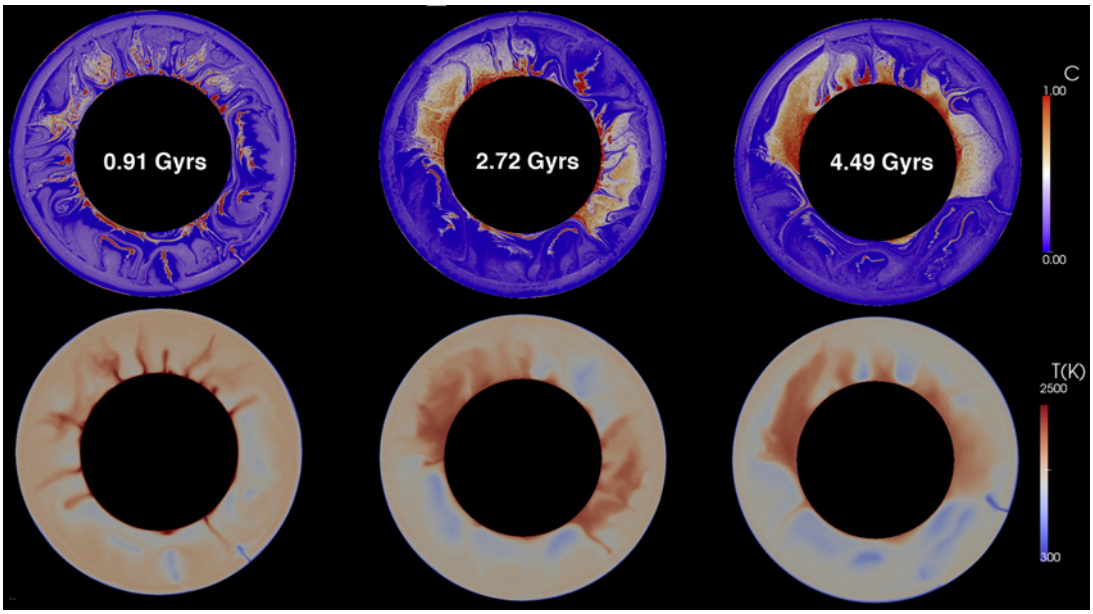

Figure 1. Time evolution of mantle composition and temperature in a simulation in [3].

References

[1] V. Debaille, C. O'Neill, A. D. Brandon, P. Haenecour, Q.-Z. Yin, N. Mattielli, & A. H. Treiman, *Stagnant-lid tectonics in early Earth revealed by 142Nd variations in late Archean rocks*, Earth Planet. Sci. Lett. **373**, 83-92 (2013).
[2] J. Korenaga, *Energetics of mantle convection and the fate of fossil heat*, Geophys. Res. Lett. **30**, 1437 (2003).
[3] T. Nakagawa, and P. J. Tackley, *Influence of magmatism on mantle cooling, surface heat flow and Urey ratio*, Earth Planet. Sci. Lett. **329-330**, 1-10 (2012).
[4] D. Lourenco, A. Rozel and P. J. Tackley, *Melting and crustal production helps plate tectonics on terrestrial planets*, Earth Planet. Sci. Lett., in press. (2016)
[5] T. Nakagawa, and P. J. Tackley, *Influence of initial CMB temperature and other parameters on the thermal evolution of Earth's core resulting from thermo-chemical spherical mantle convection*, Geophys. Geochem. Geosyst. **11** (Q06001) (2010).

cmg2016 - - Thursday, June 9, 2016 - 11:45/12:30 (45min)

CRYSTALLIZATION OF A MAGMA OCEAN

C-E Boukaré[1], Y. Ricard[2]
[1]*Laboratoire de Géologie, Université Lyon1, Villeurbanne, France*
[2]*Laboratoire de Géologie, Ecole Normale Supérieure, Lyon, France*

Key words Convection, magma ocean, crystallization.

The Earth mantle was significantly molten just after the accretion of our planet by the heat dissipation due to large impacts and by the segregation of the core. The mineralogical observations and thermodynamics models of solid-liquid equilibrium of silicates show that several type of crystallization may have happened at different depths in the mantle [1]. Solids were probably formed at the surface and in the middle of the lower mantle, leaving two possible magma oceans, a shallow one and an abyssal one. In the deep magma ocean, the liquid phase, richer in iron was likely gravitationally stable. In the shallow magma ocean, the solid phase formed near the surface was initially denser and sank through the magma to settle and compact at depth. However due to its enrichment in iron, the magma became eventually denser and at the end of crystallization the upper magma ocean might have undergone overturns (i.e. Rayleigh-Taylor instability) or a period were light solids were compacting under the lithosphere.
To understand these complex dynamics, we develop a two phase numerical code that can handle simultaneously the convection in each phase and in the slurry, and the compaction or decompaction of the two phases. The mathematical basis of the code akin to what we have used in [2-3] will be presented. Although our code can only run in a parameter range (Rayleigh number, viscosity contrast between phases, Prandlt number) very far from what would be realistic, we think it already provides a rich dynamics that illustrates what could have happened. We first study the simple situations of solidification where the melting curve is such that only a single magma ocean is expected (at depth or near the surface) but where the liquid phase can be either denser or lighter than the solid phase. We show situations in which the crystallization front is gravitationally stable and situations were the newly formed solid can "snow" across the magma in a regime that can be punctuated by large overturns. More complex cases where two magma oceans are present will also be presented and discussed.

References

[1] C.E. Boukaré, Y. Ricard and G. Fiquet, *Thermodynamics of the MgO–FeO–SiO2 system up to 140 GPa: Application to the crystallization of Earth's magma ocean*, J. Geophys. Res. **120**, 6085–6101, doi:10.1002/2015JB011929, 2015.
[2] Bercovici D. and Y. Ricard, *Energetics of a two phase model of lithospheric damage, shear localization and plate-boundary formation*, Geophys. J. Int., 152, 581-596, 2003.
[3] O. Sramek, Y. Ricard, and F. Dubuffet, *A multi-phase model of core formation*, Geophys. J. Inter., 181,198-220, 2010.

cmg2016 - - Thursday, June 9, 2016 - 11:45/12:30 (45min)

EVOLUTIONARY MODELS OF THE EARTH WITH A GRAIN SIZE-DEPENDENT RHEOLOGY: DIFFUSION VERSUS DISLOCATION CREEP

A. Rozel[1], G.J. Golabek[2], M. Thielmann[2] & P.J. Tackley[1]
[1]*ETH Zurich, Switzerland*
[2]*BGI Bayreuth, Germany*

Key words How to calibrate a numerical simulation of thermochemical convection with grain size evolution and composite rheology

We present a set of 2D numerical simulations of mantle convection considering grain size evolution and a composite visco-plastic rheology including diffusion and dislocation creep. A 1D parameterization allows us to anticipate the stress conditions for the present-day temperature profile in a convection cell. We are therefore able to obtain self-consistent 2D convecion models together with non-equilibrium grain size for present-day conditions, controlling the partitioning between diffusion and dislocation creep.

However, the internal temperature of the mantle is thought to have significantly evolved throughout the history of the Earth. Using a higher internal temperature is usually believed to decrease both viscosity and internal stresses. In our case, a high temperature potentially increases the grain size, which tends to increase the viscosity: the temperature and grain size-dependence of the viscosity are in competition.

We study the evolution of the diffusion-dislocation partitioning throughout the history of the Earth. We report the evolution of grain size and stress over time in our simulations.

Several complex processes are included in our models. Grain size evolution is a sum of grain growth and dynamic recrystallization. All our simulations consider thermochemical convection in a compressible mantle with melting producting basaltic crust and depleted mantle. Close to the surface, melting produces basaltic material which is erupted or intruded at the base of the crust. Phase transitions reset the grain size to a low value, which influences the whole dynamics of the mantle.

cmg2016 - - Thursday, June 9, 2016 - 11:45/12:30 (45min)

Temporal evolution of thermochemical plumes in the Earth's mantle

I. Kumagai[1], A. Davaille[2] & K. Kurita[3]
[1]*School of Science and Engineering, Meisei University, Tokyo, Japan*
[2]*Laboratoire FAST, CNRS / University Paris-Sud, Orsay, France*
[3]*Earthquake Research Institute, The University of Tokyo, Tokyo, Japan*

Key words Mantle plume, Convection, Thermochemical plume, Flow visualization.

Given the characteristics of the Earth's mantle, hot thermal plumes should be an important mean of heat and mass transfer in the planet, providing an explanation for the numerous « hot spots » on the surface, characterized by important volcanism. However, the bottom of the Earth's in also probably heterogeneous. In this case, Fluid Dynamics predicts that a variety of thermochemical plumes is generated from a thermal boundary layer which is stratified in composition [1, 2], with different morphologies reflecting the temporal and spatial variation of heat and mass transfers. The behaviors of thermochemical plumes depend on their initial buoyancy ratio B_0 (Fig.1), i.e. the ratio of the stabilizing chemical buoyancy to the destabilizing thermal buoyancy at the onset of convection, and also on time (Fig.2). Because a rising plume cools along the way by thermal diffusion, a chemically composite thermal plume eventually attains a level of neutral buoyancy (i.e. B=1), at which it begins to collapse. Separation within the plume then occurs, whereby the compositionally denser material sinks back while the heated surrounding fluid keeps rising. In order to find out the maximum height of the hot thermochemical plume head in the Earth's mantle, and the reccurence time of the plume generation, we carefully investigated the experimental results obtained by quantitative visualization techniques of temperature, composition, and velocity fields (TLCs-LIF method). Scaling analysis based on [1] shows that the maximum height increases with the Rayleigh number and decreases with B (Fig.3). This put tight constraints on the maximum compositional density contrast that a plume is able to pull to the surface (Fig.4) and gives a framework to interpret the increasing body of geochemical and seismological observations.

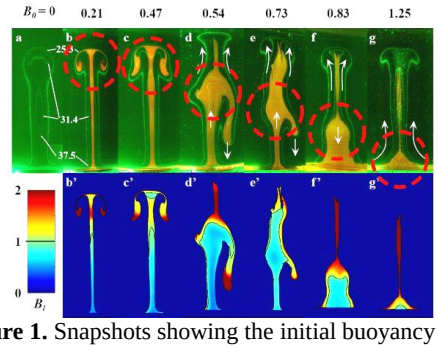

Figure 1. Snapshots showing the initial buoyancy ratio dependence (top) and the distribution of local buoyancy ratio obtained by TLCs-LIF method (modified [2]).

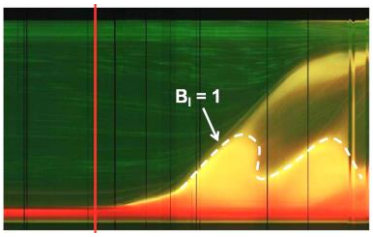

Figure 2. Spatio-temporal slice at the axis of a thermo-chemical plume (B_0=0.83). The oscillations reflect the reccurence time of the plume generation. The red line shows the onset of convection.

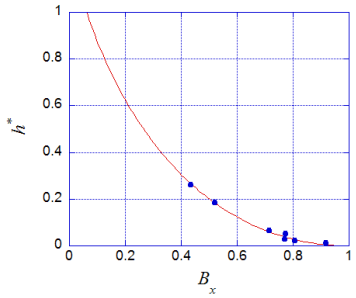

Figure 3. Maximum height h^* (= $h(t_{max})/\{\alpha g \Delta T d^4/\kappa\nu\}$) reached by a thermochemical instability as a function of B_x.

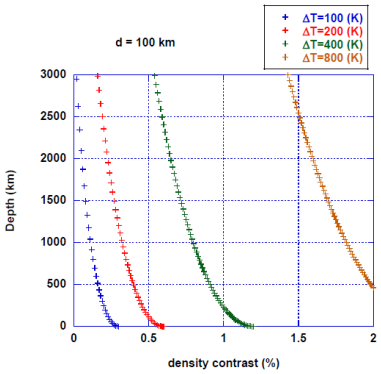

Figure 4. Maximum height reached by of a thermochemical instability in the Earth's mantle predicted by our scaling law.

References

[1] Le Bars, M., and Davaille, A., Whole layer convection in a heterogeneous planetary mantle, *Journal Geophysical Research*, 109, B03403, doi:10.1029 /2003JB002617 (2004).
[2] Kumagai, I., Davaille, A., Kurita, K., and Stutzmann E., Mantle plumes: Thin, fat, successful, or failing? Constraints to explain hot spot volcanism through time and space, *Geophysical Research Letters*, 35, L16301, doi:10.1029/2008GL035079 (2008).

cmg2016 - - Thursday, June 9, 2016 - 11:45/12:30 (45min)

ESTABLISHING MODELS OF SURFACE DEFORMATION FROM GEODETIC TIME SERIES GNSS IN THE SOUTHERN REGION OF THE IBERIAN PENINSULA AND NORTH AFRICA (SPINA)

B. Rosado[1], S. Plaza[2], R. Páez[124], J. Gárate[4], F. Fernández-Palacín[2], M. Berrocoso[134]

[1]*Laboratory of Astronomy, Geodesy and Cartography. University of Cadiz. Spain*
[2]*Department of Statistics and Operations Research. Science Faculty. University of Cadiz. Spain.*
[3]*Department of Mathematics. Science Faculty. University of Cadiz. Spain.*
[4]*Group of Geodesy and Geophysics Research, Government of Andalusia. Spain.*

Key words Deformation, geodynamic, tectonic, time series, wavelet analysis.

Global Positioning System (GPS) technology provides a powerful tool for studying geodynamic processes. It is particularly important in tectonic plate boundary areas when looking for subduction zone limits. In this work, our main interest is to focus on the time series analysis obtained from observations of GNSS-GPS satellites. Each GPS observation session provides topocentric geodetic coordinates (east, north, elevation) of the permanent stations that constitute the geodetic network established for this purpose. Horizontal components (east, north) use to show linear behaviors if there are no other effect affecting the site. Anyway the height component (elevation) uses to show periodical but not linear effects.

This work shows a detailed topocentric coordinates time series study for sites belonging to what we call the SPINA network, which stands for South of the Iberian Peninsula, North of Africa Region. The series under study are processed by techniques of relative positioning with respect to the IGS reference station located in Villafranca. Solutions are obtained from network approach with the Bernese software. Then, a designed methodology, using filter processes, harmonic adjustments and wavelets will be applied. Wavelet transform applied on the CGPS position time series is used to separate the noise of the signal, in order to provide useful information to further geodynamic interpretations. As final product we expect to get horizontal displacement model to describe the regional geodynamic main characteristics.

Dynamics of Seismicity

PLASTIC EVENTS IN SOFT-GLASSY MATERIALS FOLLOW EARTHQUAKE STATISTICS.

Roberto Benzi[1], Federico Toschi[2] & Jeannot Trampert[3]
[1]*Department of Physics, University of "Tor Vergata",*
Via della Ricerca Scientifica 1, 00133 Rome, Italy.
[2]*Department of Physics, Eindhoven University of Technology,*
PO Box 513, 5600 MB, Eindhoven, The Netherlands.
[3]*Department of Earth Sciences, Utrecht University,*
PO Box 80115, NL-3508 TC, Utrecht,The Netherlands.

Key words Earthquake statistics, earthquake catalogue, Lattice Bolzman approach, soft-glassy materials

It is commonly accepted that earthquakes are the result of some mechanical failure of earth materials. However, many details of the underlying physics, especially at the microscopic scale, are currently not understood. At the macroscopic scale, many aspects of earthquakes show a complex behaviour that can be addressed with tools of statistical physics. We propose a new approach for generating synthetic earthquake catalogues based on the physics of soft glasses. The continuum approach produces yield-stress materials based on Lattice-Boltzmann simulations [1]. We show that, if the material is stimulated below yield stress, plastic events occur, which have strong similarities with seismic events. Based on a suitable definition of displacement in the continuum, we show that the plastic events obey a Gutenberg-Richter law with exponents similar to those for real earthquakes. We further find that average acceleration, energy release, stress drop and recurrence times scale with the same exponent (Fig. 1). The approach is fully self-consistent and all quantities can be calculated at all scales without the need of ad hoc friction or statistical laws. We therefore suggest that our approach may lead to new insight into understanding of the physics connecting the micro and macro scale of earthquakes.

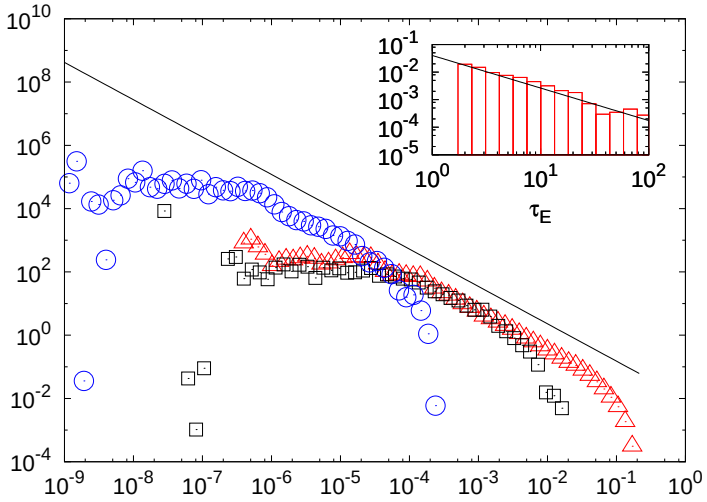

Figure 1. Probability density distribution for different quantities: red triangles correspond to the largest displacement in the medium, blue circles correspond to the average acceleration in the medium, black squares correspond to the energy release. In the insert we show the probability density function of the time between two consecutive events. The black line in the insert has the same slope as the black line in the main part of the figure.

References

[1] Benzi R., Sbragaglia M., Perlekar P., Bernaschi M., Succi S. and Toschi, F., *Direct evidence of plastic events and dynamic heterogeneities in soft-glasses*, Soft Matter, **10**, 4615-4624, (2014).

cmg2016 - - Wednesday, June 8, 2016 - 10:45/11:15 (30min)

Understanding Earthquake Clustering: A Nearest-Neighbor Approach

Ilya Zaliapin
Department of Mathematics and Statistics, University of Nevada Reno, Reno, NV, 89523, USA

Key words Earthquake clusters, induced seismicity, declustering

Clarifying whether earthquake clusters follow universal patterns or exhibit different forms related to physical properties of the lithosphere is among the main problems of statistical seismology. This talk reviews and discusses results obtained by nearest-neighbor analysis of earthquakes in space-time-magnitude domain. This approach connects every event in the catalog to its nearest neighbor, referred to as parent, thus creating a time-oriented spanning tree of events. Observational results show bimodality of nearest-neighbor earthquake distances, which allows partitioning catalogs into sub-trees corresponding to individual earthquake clusters. Application of this approach to a variety of problems validates its general utility and reveals the existence of several different robust types of earthquake clusters. We will discuss recent results on global earthquake clustering in relation to heat flow and plate boundary type, distinguishing between tectonic and human-induced seismicity, and catalog declustering. The presentation will also illustrate ramifications of the nearest-neighbor technique into multi-parent network-based cluster representation.

cmg2016 - - Wednesday, June 8, 2016 - 11:30/11:45 (15min)

EARTHQUAKE MULTIPLETS AND DYNAMIC TRIGGERING IN THE WESTERN CORINTH RIFT, GREECE

C. Duverger[1], P. Bernard[1], H. Lyon-Caen[2], M. Godano[3], S. Lambotte[4], A. Deschamps[5], A. Nercessian[1]
[1]*Institut de Physique du Globe, Paris, France*
[2]*École Normale Supérieure, Paris, France*
[3]*Mines ParisTech, Fontainebleau, France*
[4]*Institut de Physique du Globe, Strasbourg, France*
[5]*Géoazur, Sophia-Antipolis, France*

Key words Corinth rift, multiplets, swarms, transient processes, pore pressure, creep, dynamic triggering.

The Corinth rift (Greece) is one of the most active tectonic structures of the euro-mediterranean area. Its north-south opening rate of around 1.5 cm.yr^{-1} results into a high microseismicity level and a few destructive M>6 earthquakes per century. The seismic activity follows a swarm organization with alternation of intensive crisis and more quiescent periods. A large number of multiplets, which are a set of earthquakes with a similar waveform, are recorded in the western part of the rift. Multiplets are often assimilated as repeated ruptures of small asperities due to transient forcing such as silent creep or diffusion of a pore pressure front. Here, we present various analyses on microseismic multiplets occurring in the western Corinth rift from 2000 to 2014 to retrieve their spatio-temporal characteristics and their coupling with seismic-aseismic processes.

Firstly, we focus on slow transient forcings with evidence of (1) fluid pore pressure migrations within permeable corridors resulting from the intersection of the major faults with a brittle geological layer (Fig. 1) during the large 2003-2004 swarm [1], (2) creep through a repeater-like multiplet initiating the 2003-2004 seismic crisis and the specific clustering of a multiplet located at the border of the fault plane of the 1995 Aigion seismic rupture. We show that multiplets with a persistent activity through several years, suggesting some forcing by creep, are located close to the northern coast of the gulf, whereas short-lived (few days) multiplets, possibly related to fluid pressure instabilities, are located under the gulf [2]. Many of identified spatial clusters have been reactivated in the last 15 years, which provides some clues to better assess the local strain rate and the origin of the forcing.

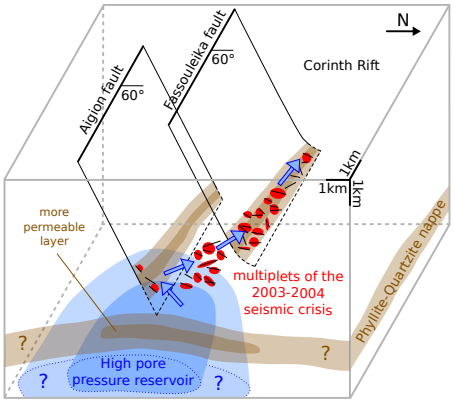

Figure 1. 3D view of the intersection of a Hellenic nappe with the Aigion-Fassouleika fault system. Permeable corridors allow the microseismicity diffusion forced by a deep capped high pore pressure reservoir.

Secondly, we analyze the dynamic triggering by moderate to large earthquakes of the microseismicity recorded in the western Corinth rift. We focus on three regional earthquakes: the 8 June 2008 M_w 6.4, the 22 January 2010 M_w 5.2, and the 7 November 2014 M_w 5.0. These events produced a global increase of the local microseismicity, and we attempt to characterize the differences in sensitivity of the various local clusters to the dynamic triggering.

References

[1] C. Duverger, M. Godano, P. Bernard, H. Lyon-Caen, S. Lambotte, The 2003–2004 seismic swarm in the western Corinth rift: Evidence for a multiscale pore pressure diffusion process along a permeable fault system, *Geophysical Research Letters*, **42**, 18, (2015)
[2] M. Godano, P. Bernard, P. Dublanchet, Bayesian inversion of seismic spectral ratio for source scaling: Application to a persistent multiplet in the western Corinth rift, *Journal of Geophysical Research*, **120**, 11, (2015)

cmg2016 - - Wednesday, June 8, 2016 - 11:15/11:30 (15min)

NON-LINEAR MAGMA-EDIFICE COUPLING AT GRIMSVÖTN VOLCANO (ICELAND)

J.-L. Got[1], A. Carrier[1], D. Marsan[1]
[1]*Institut des Sciences de la Terre, Chambéry, France*

Key words Seismicity, deformation, damage, volcano.

Continuous monitoring of seismicity and surface displacement on active volcanoes reveals important features of the eruptive cycle. In this work we analyzed high-quality GPS and earthquake data recorded at Grimsvötn volcano by the Icelandic Meteorological Office during its 2004-2011 inter-eruptive period. They show a characteristic pattern with an initial ~2 years exponential decay followed by a ~3 years constant inflation rate surface displacement, already observed on some other volcanoes. Such pattern was recently explained by a two-magma chamber model in a linear elastic edifice, with a constant magma inflow at the base of the conduit. Here we propose a one-magma chamber model, in a non-linear elastic damaging edifice, with incompressible magma and a constant pressure at the base of the magma conduit. We first modelled seismicity rate and damage as a function of time, and derived simple analytical expressions for the magma reservoir overpressure and the surface displacement as a function of time. We obtain a very good fit with the seismicity and surface displacement data, by adjusting only three phenomenological parameters. Reservoir overpressure was found to remain limited, quasi-constant during the constant inflation rate period, and to decrease during the pre-eruptive period. This decrease is controlled by the damage law. Magma flow was found to be constant during constant inflation rate period, and to increase during the pre-eruptive period. Magma flow variations are due to the non-linear variations of the reservoir volume, and not necessarily to variations of the pressure at the base of the magma conduit.

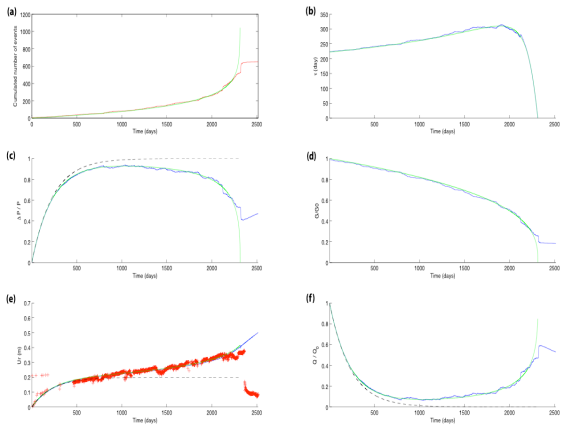

Figure 1. Model variables as a function of time from 1 December 2004 to 31 December 2011. Data are represented in red, Runge-Kutta (RK) numerical solution in blue, analytical solution in green, reference linear elastic solution in dashed black. a) Cumulated number of earthquakes (red: recorded by IMO seismic network; green: analytical model); b) characteristic time; c) dimensionless over-pressure in the réservoir ; d) normalized shear modulus; e) measured (at GPS station GFUM, red), modeled horizontal displacement, and reference linear elastic solution. f) magma flow rate (blue: from Poiseuille law and RK solution; green: from the analytical form).

Determination Site Effect of Zarqa City and Hashemite UniversityCampus Based on Microtremors Field Measurements: A microzonationStudy

WaleedEid Olimat
Jordan Seismological Observatory (JSO)
Ministry of Energy and Mineral Resources
Tel: 00962791444375
E-mail: w.olimat@gmail.com

Abstract

Zarqa governorate is one of the important governorates in Jordan. It is the second populated after the capital Amman, the location ofZarqa gives the city a great importance because it lies on the main high ways leading to Syria, Iraq and Saudi Arabia, most ofJordan's industries, power plants and strategic projects are located in Zarqa, which gives this city a special importance.
The Nakamura's technique is applied in this study for both areas; Zarqa city and Hashemite University Campus in order todetermine the resonance frequencies and amplification factors for each site then draw there maps which will be of a great use in thefield of civil and structural engineering by enriching the building codes.
The results of our study show that; values of resonance frequency F are not affected by the time of recording. While valuesof amplification factor A can vary accordingly. Results also show that the amplification factor A varies from 0.8 to 8.55 in Zarqa cityand varies from 0.4 to 9.36 in Hashemite University Campus, the resonance frequency (F) also varies between 0.37 Hz and 2.98 Hzin Zarqa city and varies from 0.59 Hz to 1.77 Hz in Hashemite University Campus, that means some constructions in the study area,in case of a major earthquake, may experience minor damages respectively.

Keywords: Site effect, Ambient Noise, Microtremors, Resonance Frequency, Amplification Factor, Dominant frequency

cmg2016 - - Wednesday, June 8, 2016 - 12:00/12:45 (45min)

Long term changes in seismic coupling revealed by seismicity dynamics

D. Marsan[1], T. Reverso[1], M. Bouchon[2], B. Gardonio[1], H. Perfettini[3]
[1]*ISTerre, Université de Savoie Mont Blanc, Le Bourget du Lac, France*
[2]*ISTerre, CNRS, Université Grenoble Alpes, France.*
[3]*ISTerre, IRD, Université Grenoble Alpes, France*

Key words seismic coupling, subduction, seismicity.

Seismic coupling is generally assumed to be constant in time, and to condition the maximum size that earthquakes can reach locally. Recent observations using GPS displacements of long term (> years) changes in 'interseismic' coupling of the Pacific and North American plates offshore Japan have however proved that coupling can change with time, and also that the inter-seismic phase is not stationary. We here describe a way to estimate changes in coupling using seismicity data rather than GPS displacements, allowing to explore even longer time fluctuations, i.e., lasting over at least 25 years. Several cases of decelerating or accelerating background seismicity occurring on or near the slip interface of the Pacific slab offshore Japan, prior to the 2011 Tohoku-Oki earthquake, are investigated, that suggest that non-stationary coupling is the norm rather than the exception. The cause for these time variations are still unknown, but clearly call for a reappraisal of our understanding of subduction dynamics.

cmg2016 - - Wednesday, June 8, 2016 - 12:00/12:45 (45min)

MAGNITUDE CORRELATION BETWEEN EARTHQUAKES IDENTIFIED IN AFTERSHOCK SEQUENCES

M. Stojanova[1], L. Vanel[1], O. Ramos[1]
[1]*Institut Lumière Matière, Université Lyon 1, Villeurbanne, France*

Key words Earthquakes, magnitude correlation, short-time aftershock incompleteness (STAI).

Although the time and space clustering of seismic occurrence is well established [1, 2], the existence of correlations between earthquake magnitudes is a rather controversial subject. They have historically been considered as non-existent, until recent works reporting magnitude correlations between earthquakes that are close in space and time [3, 4]. However, these results could be influenced by catalogue incompleteness, and their relevance is still being discussed [5, 6]. Here we present an original analysis that confirms the existence of magnitude clustering in aftershock sequences. We eliminate temporal correlations by converting the power law distribution of times (Omori's law) into a uniform distribution. In this new aftershock sequence, the number of low and medium magnitude earthquakes suffer from catalogue incompleteness at the beginning of the sequence, before getting a value that remains constant during the whole period of analysis. However, high magnitude earthquakes are abnormally more numerous at the beginning of the sequence, which reveals the existence of correlation between the mainshock's high magnitude and the aftershocks magnitudes. These results challenge the idea of randomly distributed magnitudes, indicating a need for updating the forecasting of high-energy events in aftershock sequences and opening new perspectives in the modelling and analysis of earthquake time series.

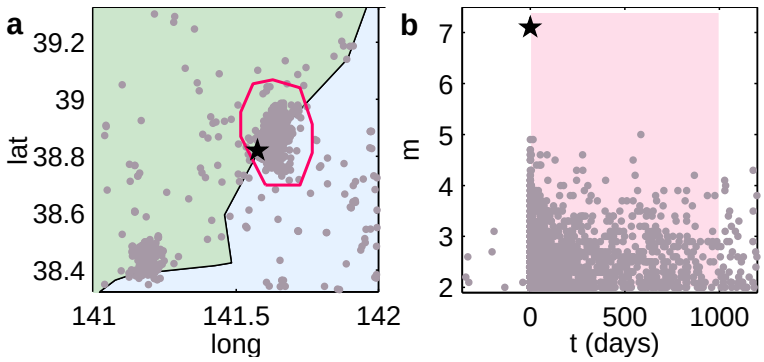

Figure 1. Example of data analyzed in the study. **a,** Part of the Japan map, near the east coast of Honshu, where earthquakes occurring from 26.05.2002 to 07.09.2006 are represented by gray dots. The star marks the earthquake of magnitude (JMA) 7.1 of May 26 2003. The delimiting polygon of the cluster is represented with the plain pink line. **b,** Time distribution of the events within the cluster on (a), for the same time period.

References

[1] Utsu, T., Ogata, Y., Matsu'ura, R.S., *J. Phys. Earth.* **43** 1 (1995)
[2] Kagan, Y. Y,. and Knopoff, L. *Geophys. J. Int.* **62** 303 (1980)
[3] Lippiello, E., de Arcangelis, L. & Godano, C. *Phys. Rev. Lett.*, **100** 038501 (2008).
[4] Lippiello, E., Godano, C., and de Arcangelis, L. *Geophys. Res. Lett.*, **39** L05309 (2012).
[5] Davidsen, J., Green, A. *Phys. Rev. Lett.*, **106** 108502 (2011).
[6] Davidsen, J., Kwiatek, D., and Dresen, G. *Phys. Rev. Lett.*, **108** 038501 (2012).

Non-linear Processes

cmg2016 - - Friday, June 10, 2016 - 15:15/15:30 (15min)

WHERE DO RIVERS GROW? PATH SELECTION AND GROWTH IN A HARMONIC FIELD.

Yossi Cohen[1], Olivier Devauchelle[2], Hansjörg F. Seybold[1], Robert S. Yi[1], Piotr Szymczak[3] and Daniel H. Rothman[1]

[1] *Lorenz Center, Department of Earth Atmospheric and Planetary Sciences, Massachusetts Institute of Technology, Cambridge, MA. 02139, USA.*

[2] *Institut de Physique du Globe, 4 place Jussieu, 75252 Paris cedex 05, France.*

[3] *Institute of Theoretical Physics, Faculty of Physics, University of Warsaw, 02-093, Warsaw, Poland*

Key words river channels | principle of local symmetry | harmonic growth | Loewner equation

The complex pattern of river networks has inspired decades of studies. However, the evolution and the dynamics of a growing channel remain elusive. Here we show that the principle of local symmetry, a concept originating in fracture mechanics, explains the path followed by growing streams fed by groundwater. Although path selection does not by itself imply a rate of growth, we additionally show how local symmetry may be used to infer how rates of growth scale with water flux. Our methods are applicable to other problems of unstable pattern formation, such as the growth of hierarchical crack patterns and geologic fault networks, where dynamics is not well understood.

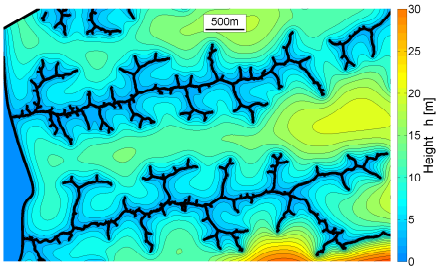

Figure 1. Numerical calculation of the height h of the water table above a seepage network (black) in Bristol, Florida [1].

References

[1] Cohen, Y., Devauchelle, O., Seybold, H. F., Yi R. S., Szymczak, P., & Rothman, D. H. (2015). Path selection in the growth of rivers. Proceedings of the National Academy of Sciences, 112(46), 14132-14137.

cmg2016 - - Friday, June 10, 2016 - 11:30/11:45 (15min)

EMPIRICAL RECONSTRUCTION OF COMPLEX SYSTEMS: PROGNOSTIC MODELS OF EVOLUTION OPERATOR, OPTIMAL PRE-PROCESSING OF HIGH-DIMENSIONAL DATA, APPLICATIONS TO CLIMATE

A. Feigin[1], A. Gavrilov[1], E. Loskutov[1] & D. Mukhin[1]
[1]*Institute of Applied Physics of the Russian Academy of Sciences, Nizhny Novgorod, Russia*

Key words empirical reconstruction, complex systems, critical transition prediction, data processing, principal dynamical modes

The report presents new empirical approach to predicting evolution of complex system including bifurcations (critical transitions) of their behavior. By complex system we mean high-dimensional, spatially distributed system possessing broad spectrum of temporal scales.

This approach relies on nonlinear stochastic modeling of the system's time-dependent evolution operator by the analysis of observed behavior. Empirical models that take the form of a discrete random dynamical system are constructed using artificial neural networks; these models include state-dependent stochastic components.

A key difficulty in applying this methodology to construct a model that helps simulate and predict the real climate system's behavior is the mismatch between the large number of variables by which one wishes to describe the system versus the shortness of the time series of available experimental data.

Efficient reduction of the system's dimensionality is thus essential in order to infer an evolution operator for a low-dimensional subsystem that determines the key properties of the observed dynamics. To solve this problem the suggested approach combines two procedures:

i. Optimal decomposition of the high-dimensional data produced by the system into (weakly) coupled space-time patterns ("modes"), which make the basic contribution to the observed variability;

ii. Construction of models of the separate modes in a form of low dimensional random dynamical systems.

The methods of solutions of these tasks are described in the report. The abilities of these methods are illustrated by dint of both really measured and generated numerically vector time series of climatic observables. Please upload the generated pdf on the abstract submission field in the New submission link, and provide a zipped version of the source text and figures as supplementary data.

cmg2016 - - Friday, June 10, 2016 - 14:15/14:45 (30min)

NON-LINEAR RELATIONSHIP BETWEEN VISCOUS DISSIPATION AND CONVECTIVE HEAT FLUX

T. Alboussière, J. Curbelo, L. Duarte, S. Labrosse, F. Dubuffet & Y. Ricard
Laboratoire de Géologie de Lyon, France

Key words Rayleigh-Bénard convection; Compressible convection; Equation of state.

The Boussinesq model of natural convection is a successful approximation that has been used extensively. This is a model containing two sources of non-linearities: heat convective transport and inertia. It follows that the solutions exhibit instabilities and chaotic behaviour at high Rayleigh numbers. However, a simple (time-averaged) linear relationship persists between the total viscous dissipation and the convective heat flux. This is due to the structure of the Boussinesq approximation [1] but becomes thermodynamically inconsistent when compressibility effects are significant [2]. This is the case for convection in the interior of planets where the effect of pressure differences on density is typically larger than the effect of temperature differences. This applies also to the atmosphere of the Earth, to giant gas planets and stars. When the Boussinesq model is abandoned, one does not replace it with the fundamental equations from mechanics and thermodynamics, because this model allows acoustic waves to develop. They can be very fast compared to the typical timescale of the convection and would make numerical solutions impossible to obtain. So-called anelastic models have been developed where acoustic waves are absent and which are supposed to be a fair representation of general convective phenomena. In our group, we have compared numerical solutions of the full set of equations to those of an anelastic model. We made our life easier by considering a "fluid" of infinite Prandtl number, an assumption well justified for the dynamics of the mantle of the Earth. With an infinite Prandtl number, acoustic waves do not develop and numerical calculations are not too time-consuming. In particular, we have looked at the relationship between dissipation and convective heat flux (see Fig. 1). There is indeed a departure from the linear Boussinesq relationship but that departure is only partially recovered by the anelastic model. I will discuss the possible reasons for this partial failure of the anelastic model and its implications.

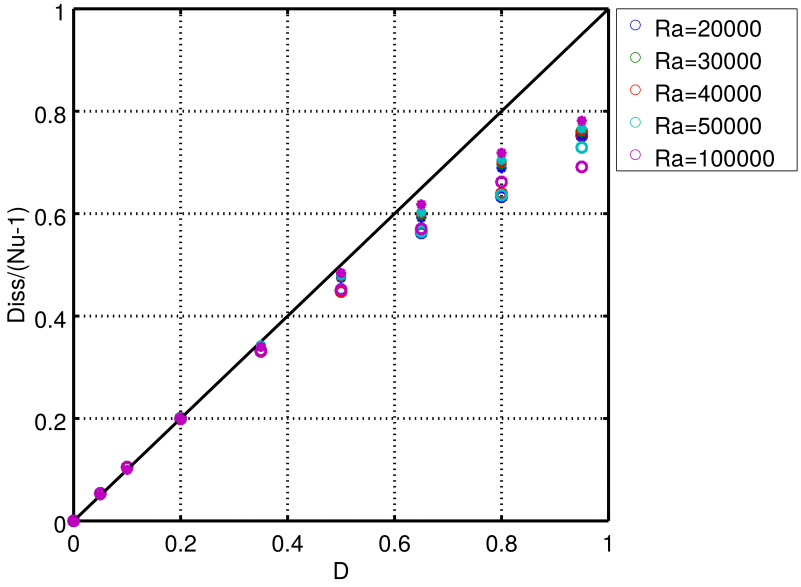

Figure 1. Ratio of viscous dissipation to convective heat flux, versus the dimensionless dissipation number $D = \alpha g L / c_p$. Full symbols correspond to the anelastic model while empty symbols correspond to the complete compressible equations.

References

[1] C.R. Doering and J.D. Gibbon, *Applied Analysis of the Navier-Stokes Equations*, Cambridge University Press, 1995
[2] T. Alboussière and Y. Ricard, *Reflections on dissipation associated with thermal convection*, Journal of Fluid Mechanics, **725**, 2013

cmg2016 - - Friday, June 10, 2016 - 11:15/11:30 (15min)

ON THE PREDICTABILITY OF EXTREMES: DOES THE BUTTERFLY EFFECT EVER DECREASE?

A.E. Sterk[1], D.B. Stephenson[2], M.P. Holland[2] & K.R. Mylne[3]
[1]*Johann Bernoulli Institute, University of Groningen, The Netherlands*
[2]*College of Engineering, Mathematics and Physical Sciences, University of Exeter, United Kingdom*
[3]*Met Office, United Kingdom*

Key words extreme events; predictability; mean squared error; ensemble forecasts

We have studied whether or not predictability always decreases for more extreme events. Predictability is measured by the Mean Squared Error (MSE), estimated here from the difference of pairs of ensemble forecasts, conditioned on one of the forecast variables (the "pseudo-observation") exceeding a threshold.

Using an exchangeable linear regression model for pairs of forecast variables, we show that the MSE can be decomposed into the sum of three terms: a threshold-independent constant, a mean term that always increases with threshold, and a variance term that can either increase, decrease, or stay constant with threshold. Using the Generalised Pareto Distribution to model wind speed excesses over a threshold, we show that MSE always increases with threshold at sufficiently high threshold. However, MSE can be a decreasing function of threshold at lower thresholds but only if the forecasts have finite upper bounds.

The methods are illustrated by application to daily wind speed forecasts for London made using the 24 member Met Office Global and Regional Ensemble Prediction System from 1 Jan 2009 to 31 May 2011. For this example, the mean term increases faster than the variance term decreases with increasing threshold, and so predictability decreases for more extreme events.

cmg2016 - - Friday, June 10, 2016 - 14:00/14:15 (15min)

HIERARCHICAL BRANCHING PROCESSES

Yevgeniy Kovchegov
Department of Mathematics, Oregon State University, USA

Key words Nonlinear processes; Horton self-similarity; Tokunaga self-similarity.

Nature produces many branching tree-like structures beyond the botanical trees. Despite their apparent diversity, a large number of rigorously studied natural branching structures exhibit simple two-parametric Tokunaga self-similarity and Horton scaling. The Horton scaling is a weaker property that addresses the principal branching in a tree; it is a counterpart of the power-law size distribution for system's elements. The stronger Tokunaga self-similarity addresses so-called side-branching; it ensures that different levels of a hierarchy have the same probabilistic structure (in a sense that can be rigorously defined). The solid empirical evidence motivates the search for a flexible and conveniently treatable class of models that exhibit Horton and Tokunaga self-similarity.

We introduce a class of stochastic processes that we call hierarchical branching processes. By construction, the processes satisfy the Tokunaga, and hence Horton, self-similarity constraints. Taking the limit of averaged stochastic dynamics, we obtain the deterministic system of differential equations that describe the temporal dynamics of a Tokunaga branching system. In particular, we study the averaged tree width function to establish a phase transition in the Tokunaga dynamics that separates fading and explosive branching. We then describe a class of critical Tokunaga processes (that happen at the phase transition boundary) that includes as a special case the celebrated critical Galton-Watson branching process. We illustrate efficiency of the critical Tukunaga processes in describing diverse observed dendritic structures, and discuss the related critical phenomena from the point of view of respective applications.

cmg2016 - - Friday, June 10, 2016 - 14:45/15:00 (15min)

DYNAMO BIFURCATIONS IN THE DIFFERENT DYNAMICAL REGIMES OBTAINED IN GEODYNAMO SIMULATIONS

L. Petitdemange[1]
[1]*Ecole Normale Supérieure, LRA/LERMA, Paris, France*

Key words Direct numerical simulations, systematic parameters study, magnetic field topology and dynamo action

We investigate the nature of the dynamo bifurcation in a configuration applicable to the Earth's liquid outer core i.e. in a rotating spherical shell with thermally driven motions with no-slip boundaries. The control parameters have been varied significantly in order to deduce systematic behaviours which could improve our understanding of planetary dynamos. A huge amount of models has been performed. To interpret our dynamo results, a hydrodynamical study and a kinematic one have been carried out. In other words, the action of the magnetic field on the flow is highlighted by comparing dynamo runs with non-magnetic models having the same parameters. In addition, the kinematic dynamo threshold is systematically determined.

Different dynamical regimes are explored in non-magnetic models by varying the different dimensionless parameters. Close to the onset of convection, only the critical mode develops as columnar vortices aligned with the rotation axis, in the form of alternating cyclones and anticyclones arranged around the solid inner core. Inertia does not play a major role in this regime which is then dominated by the global rotation and viscous effects. At higher convective driving, kinetic energy is distributed on many convection modes and inertia is one of the dominant forces. By lowering the viscosity, large-scale zonal flows can develop in this turbulent regime even with no-slip boundaries.

Previous studies highlighted a dichotomy between non-reversing dipole-dominated dynamos and the reversing non-dipole-dominated multipolar solutions. Because of its importance for geophysical applications, strong dipolar fields have been preferred as initial conditions. This field collapses if the ratio of inertia to the Coriolis force exceeds a critical value. A strong initial field prevents zonal flows. By considering weaker fields, we show the existence of a supercritical multipolar branch whereas stronger fields give rise to dipolar solutions. A bistable regime exists where the magnetic topology depends on the initial magnetic field strength. By lowering viscous effects, the importance of zonal flows becomes more and more important and the result is the larger extension of the bistable regime. Large-scale zonal flows are typical of multipolar dynamos and plays a role in the field generation. Far above the dynamo threshold, the Lorentz force reduces zonal flows and a transition from a multipolar dynamo to a dipolar one is observed.

The dipolar branch has a subcritical behaviour in any hydrodynamical regimes.In the laminar regime, convection cells do not develop in the whole spherical volume. Strong initial fields extend convection cells toward the outer boundary where toroidal fields are advected which allows to sustain dynamo action. In the turbulent regime, zonal flows and small-scale motions develop and perturb dynamo action. Strong dipolar fields prevent zonal flows and decrease the flow speed. Dipolar field are then maintained in time only if this field is initially strong-enough.

We argue on the existence of different physical regimes for dipolar models. In the vicinity of the dynamo threshold, the action of the magnetic field on the flow is highlighted by comparing hydrodynamical models and dynamo ones. Lorentz force modifies the energy of the convective flow at small-scales in the laminar regime. The Lorentz force is balanced mainly by a modification of viscous effects whereas the dominant terms in the equation of motion are the Coriolis force, pressure gradients, buoyancy and viscosity. In the turbulent regime, the dipolar field reduces the energy of the convective flow at large-scales which suggests that Lorentz force is balanced by a modification of inertia.

Far above the dynamo threshold, Lorentz force becomes dominant as it is expected in planets. In the turbulent regime, the magnetic field affects significantly the flow speed, the flow structure and the heat transfer efficiency. This physical regime seems to be relevant for studying geomagnetic processes. These arguments are in agreement with recent geodynamo studies.

References

cmg2016 - - Friday, June 10, 2016 - 15:00/15:15 (15min)

DESTABILISATION OF SHEAR FLOWS BY ALFVÉN WAVES AT LOCALISED MAGNETIC FIELDS

Stephen D. Griffiths
Department of Applied Maths, University of Leeds, Leeds, U.K.

Key words Instability, shear flows, magnetic fields, Alfvén waves, Rossby waves.

The instability of shear flows in the presence of magnetic fields is fundamental to understanding a wide range of geophysical and astrophysical phenomena. We investigate the simplest paradigm problem of interest, which is the instability of plane parallel shear flows with aligned field, to two-dimensional disturbances. It is well known that magnetic fields are stabilising in the sense that a sufficiently strong and widespread field always implies stability, even if the underlying shear flow is hydrodynamically unstable [1, 2]. We focus on cases where the shear flow has no inflexion points and is thus hydrodynamically stable, and show how such flows can nevertheless be destabilised by the addition of one or more thin regions of magnetic field.

The simplest such instability occurs when the basic flow has uniform shear (constant vorticity), and two thin regions of magnetic field are added. An explicit analytical solution for the linear instability is presented when the magnetic fields are idealised as having infinitesimal width, showing that there is always instability for some range of along-stream wavenumbers. The strength of the instability is reduced for the more realistic case of magnetic fields of finite width; the linear stage is investigated analytically using matched asymptotic expansions, and the nonlinear stage is investigated numerically using standard pseudospectral techniques. The instability can be unambiguously attributed to the mutual amplification of a pair of counter-propagating Alfvén waves, with one wave propagating along each thin region of magnetic field.

A distinct instability occurs when the basic flow has two regions of uniform shear separated by a thin vorticity gradient, and one thin region of magnetic field is added. An explicit analytical solution can be obtained for the linear instability when the vorticity gradient and magnetic field are both idealised as having infinitesimal width, which can be extended numerically to smooth profiles. This instability can be attributed to the mutual amplification of a Rossby wave (at the vorticity gradient) and an Alfvén wave (at the magnetic field).

Both of these instabilities are interesting extensions to magnetohydrodynamics of well-known shear instabilities in atmosphere-ocean fluid dynamics, involving interactions between various combinations of Rossby waves and internal gravity waves (e.g., [3, 4, 5]). Like their hydrodynamic counterparts, these magnetohydrodynamic instabilities can also be interpreted in terms of positive and negative energy waves (cf. [6]). For planetary flows, they could act as a primary instability of appropriately structured toroidal fields, or as a secondary instability on thin filaments of magnetic field drawn out by other processes.

References

[1] M.E. Stern, *Joint instability of hydromagnetic fields which are separately stable*, Phys. Fluids **6**, 636–642 (1963).
[2] D.W. Hughes & S.M. Tobias, *On the instability of magnetohydrodynamic shear flows*, Proc. Roy. Soc. Lond. **A 457**,1365–1384 (2001).
[3] B.J. Hoskins, M.E. McIntyre & A.W. Robertson, *On the use and significance of isentropic potential vorticity maps*, Quart. J. Roy. Meteor. Soc. **111**, 877–946 (1985).
[4] C.P. Caulfield. *Multiple linear instability of layered stratified shear flow*, J. Fluid Mech. **258**, 255–285 (1994).
[5] A. Rabinovich, O.M. Umurhan, N. Harnik, F. Lott & E. Heifetz, *Vorticity inversion and action-at-a-distance instability in stably stratified shear flow*, J. Fluid Mech. **670**, 301–325 (2011).
[6] Y.-Y. Hayashi & W.R. Young. *Stable and unstable shear modes of rotating parallel flows in shallow water*, J. Fluid Mech. **184**, 477–504 (1987).

cmg2016 - - Friday, June 10, 2016 - 11:45/12:30 (45min)

Lithofacies classification of the Barnett Shale gas reservoir using neural network.

S. Ouadfeul[1] & L.Aliouane[2]
[1]*Algerian Petroleum Institute, IAP, Algeria.*
[2]*LABOPHYT, FHC, UMBB, Algeria..*

Key words neural network, prediction, lithofacies, clay, Quartz, Barnett

Here, we show the power of the artificial intelligence such as neural network to predict the lithofacies in the lower Barnett shale gas reservoir. The Multilayer Perceptron (MLP) neural network with Hidden Weight Optimization Algorithm is used. The input is raw well-logs data recorded in a horizontal well drilled in the Lower Barnett shale formation, however the output is the concentration of the Clay and the Quartz calculated using the ELAN model and confirmed with the core rock measurement. After training of the MLP machine weights of connection are calculated, the raw well-logs data of two other horizontal wells drilled in the same reservoir are propagated though the neural machine and an output is calculated.
Comparison between the predicted and measured clay and Quartz concentrations in these two horizontal wells shows the ability of neural network to improve shale gas reservoirs characterization.

References

[1] C.Yu and M. T. Manry, "A modified hidden weight optimization algorithm for feed-forward neural networks," *Thirty-Sixth Asilomar Conference on Signals, Systems & Computers,* vol. 1, pp. 1034-1038, Nov. 2002.
[2]

cmg2016 - - Friday, June 10, 2016 - 11:45/12:30 (45min)

THE ENSEMBLE KALMAN PARTICLE FILTER FOR NON-GAUSSIAN SYSTEM WITH NONLINEAR MEASUREMENT FUNCTIONS

Zheqi Shen[1], Youmin Tang[1,2]

[1]*State Key Laboratory of Satellite Ocean Environment Dynamics, Second Institute of Oceanography, State Oceanic Administration, Hangzhou, China*

[2]*Environmental Science and Engineering, University of Northern British Columbia, Prince George, British Columbia, Canada*

Key words Data assimilation, Ensemble Kalman particle filter, nonlinear measurement function

The ensemble Kalman particle filter (EnKPF) is a combination of two Bayesian-based algorithms, namely, the ensemble Kalman filter (EnKF) and the sequential importance resampling particle filter (SIR-PF). It was recently introduced to address non-Gaussian features in data assimilation for highly nonlinear systems [*Frei and Künsch*(2013)], by providing a continuous interpolation between the EnKF and SIR-PF analysis schemes. In this paper, we first extend the EnKPF algorithm by modifying the formula for the computation of the covariance matrix, making it suitable for nonlinear measurement functions (we will call this extended algorithm nEnKPF). Further, a general form of the Kalman gain is introduced to the EnKPF to improve the performance of the nEnKPF when the measurement function is highly nonlinear (this improved algorithm is called mEnKPF).

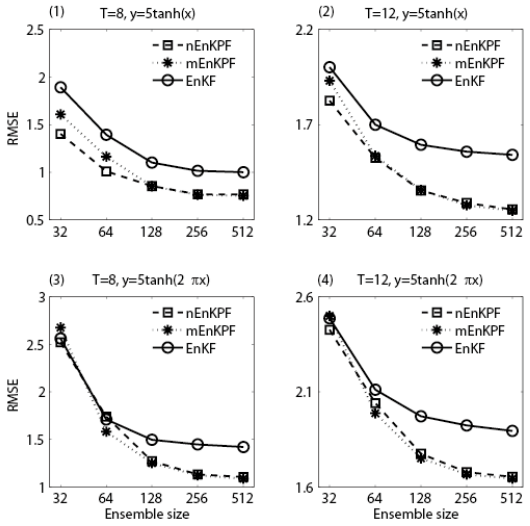

Figure 1. The performance of nEnKPF, mEnKPF and EnKF on Lorenz' 96 model, different data frequencies and nonlinear measurement functions are taken into consideration

The Lorenz '63 model and Lorenz '96 model are used to test the two modified EnKPF algorithms. The experiments show that the mEnKPF and nEnKPF, given an affordable ensemble size, can perform better than the EnKF for the nonlinear systems with nonlinear observations (see figure 1). These results suggest a promising opportunity to develop a non-Gaussian scheme for realistic numerical models.

References

[*Frei and Künsch*(2013)] Frei, M., and H. R. Künsch (2013), Bridging the ensemble kalman and particle filters, *Biometrika*, *100*(4), 781–800.

cmg2016 - - Friday, June 10, 2016 - 11:45/12:30 (45min)

IMPACT OF THE LITHOGRAPHIC DISCONTINUITIES ON THE KARST CONDUIT DEVELOPMENT - INSIGHTS FROM MODELLING

K. Petrus[1], P. Szymczak[1]
[1] *Faculty of Physics, University of Warsaw, Pasteura 5, 02-093 Warsaw, Poland*

Key words Reactive flow, reactive-infiltration instabilities, pattern formation, solution pipes, dissolution, porous medium, stratified medium, karst, inception horizon.

Karst formation is controlled by the processes of the fluid flow and reactant transport coupled to the chemical erosion of the limestone rock [1]. The coupling between these processes can lead to a number of different instabilities, resulting in the formation of dissolutional voids, caverns and conduits.

Arguably the simplest systems of this kind are solution pipes, in which gravitationally driven water movement carves vertical conduits in limestone rocks. In the homogeneous rocks these conduits are often cylindrical, with almost a constant diameter along their length. However, in a stratified medium, the morphology of the pipes changes. For example, if a number of less porous layers is introduced in an otherwise homogeneous medium, then the pipes are observed to narrow as they cross the layers and then widen up to form bulbous caverns as they emerge from the layer [1].

In this communication, we investigate these effects more closely, considering different kind of lithographic discontinuities to be present in the system: the layers of increased/decreased porosity and/or permeability as well as the solubility which is different from the rest of the system. Using a Darcy-scale numerical model we analyze the effects these layers have on the shape and growth of solution pipes and compare the results on the piping morphologies observed in nature. Finally we comment on the possible relevance of these results to the cave-formation phenomena and the inception horizon concept [3].

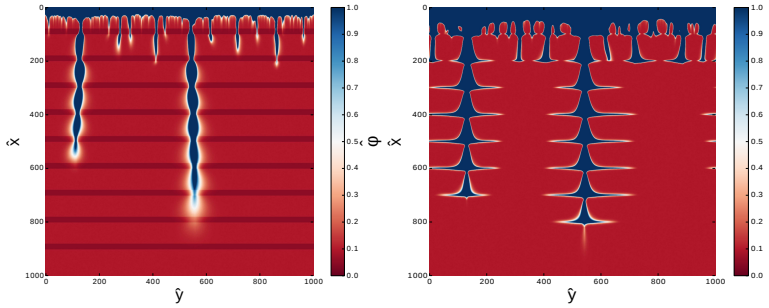

Figure 1. Effect of change of porosity (left) and permeability (right) on solution pipe shapes.

References:
1.Howard A. D., The development of karst features, Bull. Natl. Spel. Soc. **25***, 45-65 (1963)*
2.Petrus, K. and Szymczak, P., Influence of layering on the formation and growth of solution pipes. Front. Phys., **3***, 92, 2015*
3.Filipponi , M., Jeannin, P. and Tacher, L., Evidence of inception horizons in karst conduit networks, Geomorphology, **106***, 86-99 (2009)*

cmg2016 - - Friday, June 10, 2016 - 11:45/12:30 (45min)

MECHANICAL MEASUREMENTS REFLECT THE STRUCTURE OF A PARTICULATE MATERIALS

A.L.R. Sibrant[1,2] & L. Pauchard[2]
[1]*Department of Geological Sciences, University of Idaho, USA*
[2]*FAST, Univ Paris-Sud, CNRS UMR 7608 - F-91405, Orsay, France*

Key words Particulate material, Directional solidification, Mechanical properties, Drying.

Directional solidification of particulate materials takes place in many geological settings, at various scales, from millimeters in rocks to several kilometers on planetary surface (figure 1a). The mechanical properties of the resulting materials are strongly dependent on the solidification process. This process is investigated at the laboratory scale in modeled systems : the liquid-solid transition is caused by evaporation from a dispersion of silica colloidal particles in a volatile solvent. The transport of particles results in an aggregated, porous particle network. The mechanical behavior of this solid layer is investigated by indentation testing. Solid layers are found to exhibit non-homogeneous mechanical properties in depth (figure 1b) : The stiff is found to be larger at the drying surface (elastic modulus = 2 GPa) than at the bottom of the layer (elastic modulus = 0.75 GPa). We propose that the mechanical properties of the layer reflect the structure of the layer during the solidification. This particles distribution is well predicted by a numerical model based on the advection-diffusion process. This affects the crack formation and stability of crack propagation in the layer. As an evidence, we show that it is energetically less favorable for a crack generated inside a layer to propagate towards the stiffer region of the layer.

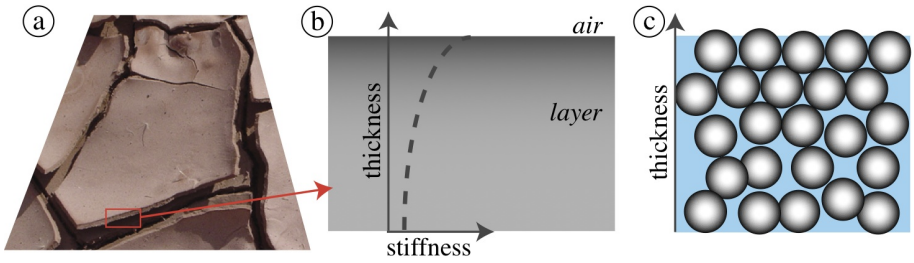

Figure 1. (a) Crack pattern in a drying mud (the polygons are approximately 30cm in length). (b) Non-uniform mechanical properties in the thickness of a layer. (c) The mechanical properties reflect the structure of a particulate material.

cmg2016 - - Friday, June 10, 2016 - 11:45/12:30 (45min)

EMPIRICAL FORECAST OF INTERANNUAL CLIMATE VARIABILITY

E. Loskutov[1], D. Mukhin[1], A. Gavrilov[1] & A. Feigin[1]
[1]*Institute of Applied Physics of Russian Academy of Sciences, Nizhny Novgorod, Russia*

Key words Empirical modeling, random dynamical systems, spatial-distributed data, climate variability.

In this work we suggest a method for empirical forecast of interannual climate variability from spatial-distributed time series. This method based on the reconstruction of reduced dynamical models in a form of random dynamical systems [1, 2] derived from observational time series. No doubt, the construction of proper embedding - the set of variables determining the phase space the model works in - is the most important step in such a modeling and this task is non-trivial due to huge dimension of time series of typical climatic fields. Actually, an appropriate expansion of observational time series is needed yielding the number of principal components considered as phase variables, which are to be efficient for the construction of low-dimensional evolution operator. We emphasize two main features the reduced models should have for capturing the main dynamical properties of the system: (i) taking into account time-lagged teleconnections in the atmosphere-ocean system and (ii) reflecting the nonlinear nature of these teleconnections. In accordance to these principles, in this report we present the methodology which includes the combination of a new way for the construction of an embedding by the spatio-temporal data expansion and nonlinear model construction on the basis of artificial neural networks. The methodology is applied to NCEP/NCAR reanalysis data including fields of sea level pressure, geopotential height, and wind speed, covering Northern Hemisphere. Its efficiency for the interannual forecast of various climate phenomena including ENSO, PDO, NAO and strong blocking event condition over the mid latitudes, is demonstrated. Also, we investigate the ability of the models to reproduce and predict the evolution of qualitative features of the dynamics, such as spectral peaks, critical transitions and statistics of extremes. This research was supported by the Government of the Russian Federation (Agreement No. 14.Z50.31.0033 with the Institute of Applied Physics RAS)

References

[1] Y.I. Molkov, E.M. Loskutov, D.N. Mukhin, and A.M. Feigin, *Random dynamical models from time series,*, Phys. Rev. E. **85**, p. 036216, (2012).

[2] D. Mukhin, D. Kondrashov, E. Loskutov, A. Gavrilov, A. Feigin, and M. Ghil *Predicting Critical Transitions in ENSO models. Part II: Spatially Dependent Models*, J. Clim., **8**, pp. 1962-1976, (2015).

UNIVERSALITIES IN THE CLUSTERING COEFFICIENT FOR SEISMIC COMPLEX NETWORK BUILT WITH REAL DATA AND WITH DATA FROM THE BURRIDGE-KNOPOFF MODEL

cmg2016 - - Friday, June 10, 2016 - 11:45/12:30 (45min)

D. Pastén[12], V. Muñoz[1], D. Comte[23] & B. Toledo[1]

[1]*Departamento de Física, Facultad de Ciencias, Universidad de Chile, Santiago, Chile*

[2]*AMTC, Facultad de Ciencias Físicas y Matemáticas, Universidad de Chile, Santiago, Chile*

[3]*Departamento de Geofísica, Facultad de Ciencias Físicas y Matemáticas, Universidad de Chile, Santiago, Chile*

Key words clustering coefficient, earthquakes, complex networks.

Complex networks using seismic data measured in three zones of Chile had been built [2]. Three undirected networks with seismic data sets that include an earthquake (1985, central zone of Chile, 1995 northern zone of Chile and 2010 southern zone of Chile) and one data set without an earthquake (central zone of Chile between years 2000 and 2007) had been constructed. This work has focused on the behavior of the clustering coefficient in these complex networks. A finite-size scaling was found [1] and the clustering coefficient shows an interesting behavior: this parameter converge to 0.8 for seismic data sets without a large seismic event and converge to 1 if the data set includes a large seismic event. This behavior was consistent for the data set measured in Chile and was compared with seismic complex networks built with data from other zones of the Earth [1], keeping the same behavior. This behavior was tested for data obtained from a classical Burridge-Knopoff model for earthquakes, two results were used: a BK model without a large event and a BK model with a large event and its aftershocks. The same results were obtained for the clustering coefficient with the data from de BK model. The results of the clustering coefficient, C, for the three seismic data sets measured in Chile that contain a large event are shown in Figs. 1, a), b) and c). The result for the data set measured in the central zone of Chile without a large event is shown in Fig. 1 d). Figs. 2 show the results for the clustering coefficient for the BK model.

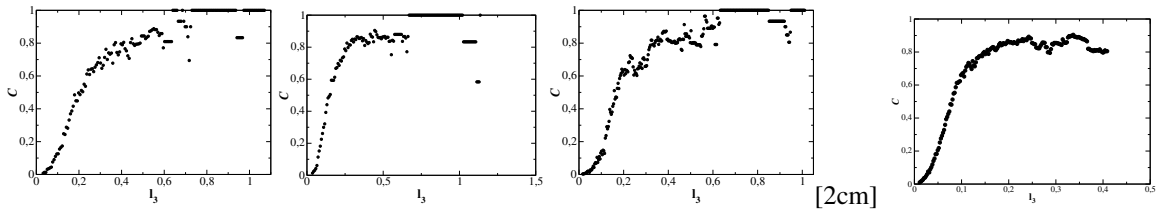

(a) Northern zone of Chile (1995).

(b) Central zone of Chile (1985).

(c) Southern zone of Chile (2010).

(d) Central zone of Chile without a large event, between years 2000 and 2007.

Figure 1: Clustering coefficient for the four complex networks built with sesimic events measured in Chile

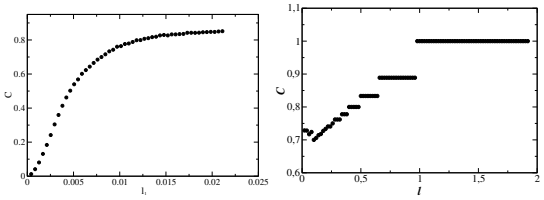

(a) BK model with 200 blocks, without a large event.

(b) BK model with 50 blocks, with a large event.

Figure 2: Clustering coefficient the complex networks built with the data obtained from a BK model.

References

[1] S. Abe and D. Pastén and N. Suzuki, *Finite data-size scaling of clustering in eartquake networks*, Physica A **390**, 7 (2010).

[2] S. Abe and D. Pastén and V. Muñoz and N. Suzuki, *Universalities of earthquake-network characteristics*, Chinese Science Bulletin **56**, 34 (2011)

cmg2016 - - Friday, June 10, 2016 - 11:45/12:30 (45min)

DECODING PHYSICS OF CONVECTIVE TURBULENCE

M. K. Verma[1], A. Kumar[1], A. Pandey[1]&A. G. Chatterjee[1]
[1]*Department of Physics, IIT Kanpur*

Key words Turbulent convection, Turbulence Modelling, Turbulent Spectrum, Rayleigh-Bénard convection

In this abstract we present the turbulence phenomenology of turbulent thermal convection (Rayleigh-Bénard convection). We performed numerical simulation of the flow for Rayleigh number Ra = 10^{10} and Prandtl number Pr = 1 on 2048^3 grid points. We observed that in the inertial range, the energy spectrum E(k) ~ $k^{-5/3}$ and energy flux Π(k) is a constant [1], consistent with he Kolmogorov's theory of fluid turbulence [see Fig. 1(a,b)]. We rule out the Bolgiano-Obukhov's spectrum E(k) ~ $k^{-11/5}$for convective turbulence due to the positive energy feed by the buoyancy; this is in contrast to the negative energy feed by the buoyancy in the stably stratified flows for which the Bolgiano-Obukhov theory is valid [1].

We also compute the rms values of various terms of the momentum equation of turbulent convection. As shown in Fig. 1(c), the acceleration of a fluid parcel is provided mainly by the pressure gradient $-\nabla p$, while the buoyancy $\alpha g\theta$and dissipation term $\nu\nabla^2\mathbf{u}$ are quite close to each other [2]. Here α, ν, θare the thermal expansion coefficient, kinematic viscosity, and temperature fluctuation of the fluid, and g is the acceleration due to gravity. The above force balance is also observed in the inertial range [1]. Thus, the effect of buoyancy is annulled in convective turbulence, leading to Kolmogorov's theory of turbulence. In addition, we observe that $0.5E_{\perp}(k)/E_{\parallel}(k) \approx 0.7$, where ∥ is the direction along the buoyancy. Thus the flow in convective turbulence is quite close to isotropy, consistent with the Kolmogorov's spectrum for the flow.

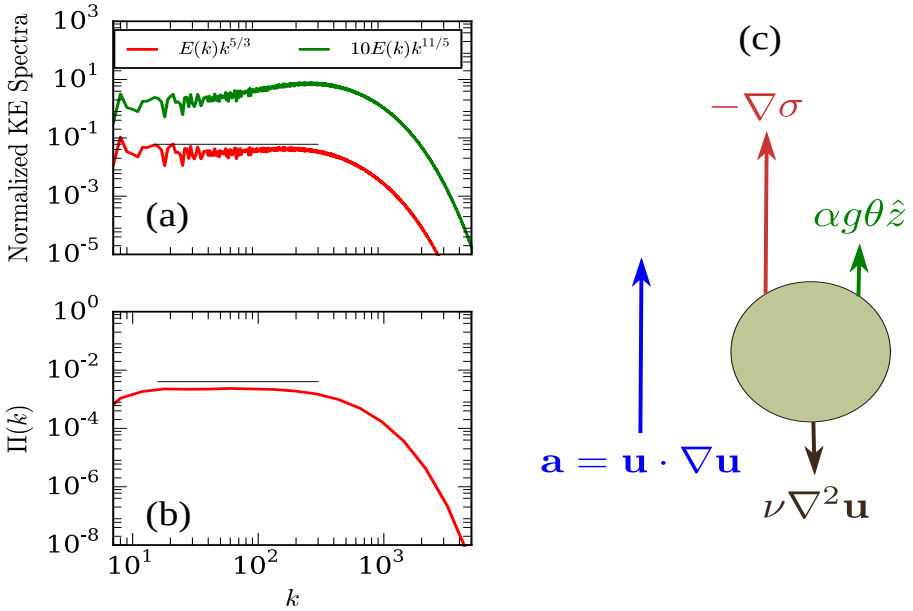

Figure 1.(a) The normalized energy spectrum E(k) ~ $k^{-5/3}$and (b) a constant energy flux, consistent with Kolmogorov's theory; (c) rms values of various terms of the momentum equation.

In summary, we show that the physics of convective turbulence is quite close to that of fluid turbulence. This result would enable us to model the convective flows in the interiors and atmospheres of planets and stars.

References

[1] A. Kumar, A. G. Chatterjee, and M. K. Verma, Energyspectrum of buoyancy-driven turbulence, Phys. Rev. E,**90**, 023016 (2014).
[2] A. Pandey, A. Kumar, A. G. Chatterjee, and M. K. Verma, Dynamics and scaling in Rayleigh-Bénard convection, Preprint.

cmg2016 - - Friday, June 10, 2016 - 11:45/12:30 (45min)

LATTICE BOLTZMANN MODELLING OF STREAMING POTENTIALS : INFLUENCE OF THE GAS-WATER INTERFACE DYNAMICS ON THE ELECTROKINETIC COUPLING

E.-A. Fiorentino, R. Toussaint & L. Jouniaux
Institut de Physique du Globe de Strasbourg, CNRS/UMR 7516, Strasbourg, France

Key words Hydrogeophysics - Streaming Potentials - Multiphase Flows - Lattice Boltzmann Method

The streaming potential phenomenon is an electrokinetic effect that occurs in porous media due to the presence of an electrical double layer at the fluid-rock interface. The electrical double layer generates an excess of positive charges at the immediate vicinity of the rock, which gives rise to an electric streaming current when the fluid flows in the porous medium. This streaming current is counterbalanced by a conduction current which leads to a measurable electrical voltage, characterized by an electrokinetic (EK) coefficient. In monophasic conditions, the EK coefficient is a function of four parameters that are the zeta potential (potential of the plane separating the moving ions from the ions adsorbed to the surface), the viscosity, the permittivity and the conductivity of the electrolyte. This phenomenon is at the origin of seismoelectric signals and self-potential signals, and is not well understood when the medium is partially saturated.

The lattice Boltzmann method allows to model the physical quantities involved in the streaming potential phenomenon (Fig. 1). The model presented in this study is a multiphase extension of the model described in [1]. This model allowed, in monophasic conditions, to assess the impact of the local variations of the electrolyte's viscosity, permittivity and conductivity on the EK coefficient. The local variations of the viscosity and permittivity remain negligible even at high salinity, but the local variations of conductivity can lead to a misinterpretation of the zeta potential in the low salinity domain, or in the presence of a polyvalent counterion. In multiphase conditions, the lattice Boltzmann method is a popular and powerful technique that allows to simulate the pore-scale multiphase dynamics without tracking the moving interface at each step of the calculation.

The aim of the current study is to model the streaming potential phenomenon in a capillary channel in the presence of two immiscible phases. This model does not aim at reproducing the complexity of natural systems, but aims at improving the understanding the electrokinetic mechanism in the presence of a multiphase flow. This study focuses on the behaviour of the electrokinetic coefficient as a function of the water saturation in the capillary, with a comparison to experimental analogs available in the literature.

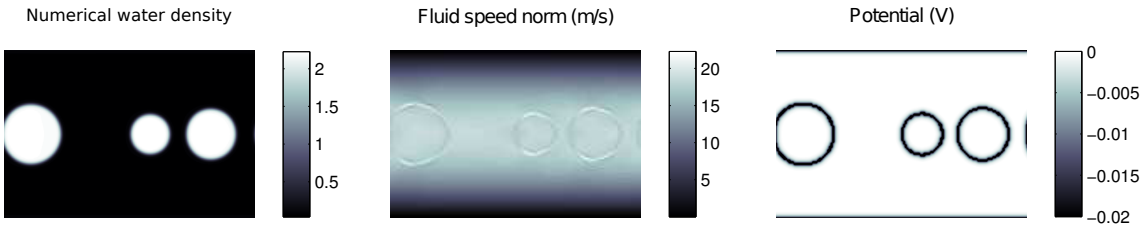

Figure 1. Numerical water density, flow velocity and electrical potential simulated using the lattice Boltzmann method [2, 3]

References

[1] E.-A. Fiorentino, R. Toussaint, L. Jouniaux, *Lattice Boltzmann modelling of streaming potentials : Variations with salinity in monophasic conditions*, Geophys. J. Int. (2016)
[2] X. Shan and H. Chen, *Lattice Boltzmann model for simulating flows with multiple phases and components*, Phys. Rev. E (1993)
[3] Z. Chai and B. Shi *A novel lattice Boltzmann model for the Poisson equation*, Applied Mathematical Modelling (2008)

cmg2016 - - Friday, June 10, 2016 - 11:45/12:30 (45min)

HOMOCLINIC BIFURCATION DRIVING CHEMICALLY ACTIVE CREEPING FAULTS

S. Alevizos[1], M. Veveakis[1], T. Poulet[1] & K. Regenauer-Lieb[1]
[1]*School of Petroleum Engineering, UNSW, Kensington, NSW, Australia.*

Keywords Homoclinic bifurcation, arc-length continuation, bifurcation diagrams, subduction zones.

This talk addresses the mathematical basis for the emerging topic of applying multi-physics frameworks to understand and study the governing mechanisms of complex phenomena at a geophysical scale. As suggested in Poulet et al. (2014a, b), a fundamental analysis of multiple steady-states, originally developed for combustion physics, can be used in fault mechanics to describe the temporal evolution of subduction zones and the spatial manifestation of exhumed thrusts (Alevizos et al. 2014). The main feature of this model is the coupling of a shear heating mechanism due to the material's internal friction, to an endothermic chemical reaction triggered by the temperature increase caused by prolonged shearing. In this study, we recapitulate the model's main features and use the arc-length continuation method proposed by Chan & Keller (1991) along with Spectral Element Method to produce bifurcation diagrams of its equilibrium solutions (Fig. 1). Furthermore, due to the appearance of complex eigenvalues in the upper branch of the solutions, we integrate the time-dependent system numerically in an effort to prove the existence of limit cycles. This leads to the discovery of a homoclinic bifurcation which defines the system's global behavior, since it self-organises around the homoclinic point B (Fig. 1).

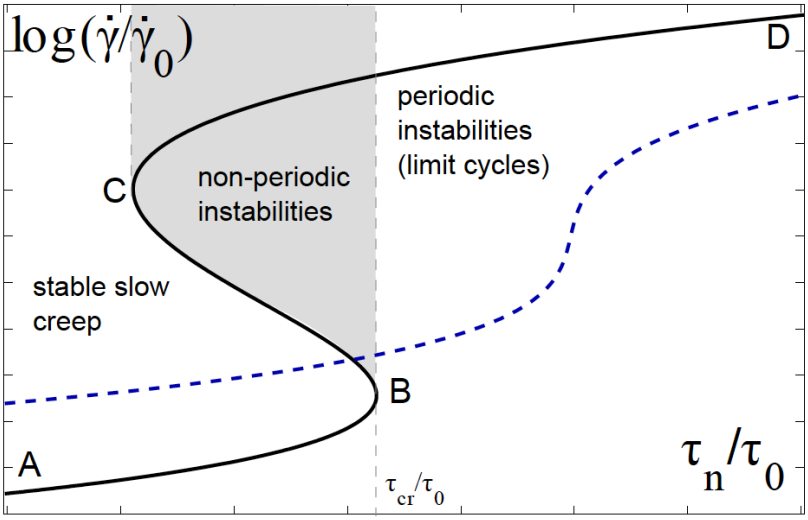

Figure 1. Bifurcation diagram of the model proposed by Alevizos et al. (2014). The system exhibits a folded S-curve response (solid black curve) or a stretched one (dashed blue curve) depending on the normal stress at the fault's boundary. As depicted by the highlighted areas of the diagram, depending on the normalized shear stress at the boundary (τ_n/τ_0), the system exhibits stable creep, periodic and non-periodic instabilities. The point B in this diagram is a homoclinic point.

References

[1] S. Alevizos, M. Veveakis, T. Poulet, *Thermo-poro-mechanics of chemically active creeping faults: 1. steady state*, J. Geophys. Res. Solid Earth **119**, 4558-4582 (2014).
[2] T. Chan, H. Keller, *Arc-length continuation and multi-grid techniques for nonlinear elliptic eigenvalue problems*, SIAM J. Sci. Stat. Comput., **3**(2), 173–194 (1991).
[3] T. Poulet, M. Veveakis, K. Regenauer-Lieb, D. Yuen, *Thermo-poro-mechanics of chemically active creeping faults: 3. the role of serpentinite in episodic tremor and slip sequences, and transition to chaos*, J. Geophys. Res. Solis Earth **119**, 4606-4625 (2014a).
[4] T. Poulet, M. Veveakis, M. Herwegh, T. Buckingham, K. Regenauer-Lieb, *Modeling episodic fluid-release events in the ductile carbonates of the Glarus thrust*, Geophys. Res. Lett. **41**, 7121-7128 (2014b).

cmg2016 - - Friday, June 10, 2016 - 11:45/12:30 (45min)

Analysis of the stability of geoelectric fluctuations, prior to a M6.3 earthquake, by means of non-extensive statistics and multifractal spectrum.

E. L. Flores-Márquez[1], A. Ramírez-Rojas[2] & L. Telesca[3]
[1]*Instituto de Geofísica, UNAM, C.U. Coyoacán, México.*
[2]*Area de Física de Procesos Irreversibles, Universidad Autónoma Metropolitana, México.*
[3]*Institute of Methodologies for Environmental Analysis, National Research Council, Tito Scalo, Potenza, Italy.*

Key words non-extensive, Tsallis' entropy, earthquake, geoelectric fluctuations.

The stability of geophysical systems is an important topic whose study can contribute to the knowledge of the dynamics underlying processes in the preparation of earthquakes. One of the mathematical tools that allows characterize the stability of complex systems is the non-extensive statistics based in the generalized Tsallis' entropy (S_q). As is known, the Tsallis' entropy [1] is characterized by means of a q-value and when $q \rightarrow 1$, $S_q \rightarrow S_{BG}$, the Boltzmann-Gibbs entropy, for equilibrium systems. In the Tsallis' non-extensive formulation of entropy all-length scale interactions are allowed.
On the other hand, the multifractal analysis has been able to describe many features of dynamical systems. The relationship $1/(1-q) = 1/\alpha_{min} - 1/\alpha_{max}$ allows to obtain the minimum and maximum values (α_{min}, α_{max}) of the multifractal distribution; moreover the q-value is associated with S_q. The q-value is a quantitative measure of the length scale of the spatial interactions. We link the Tsallis' entropy and the Generalized Pareto distribution (GPD) [2] through the scale and shape parameters of the distribution followed by the exceedances over thresholds in the analyzed values, by considering these values as point process.
The aim of this work is to analyze the geoelectric fluctuations along the time monitored a few days prior a M6.3 earthquake occurred in México and characterize their stability by calculating the q-values and obtain the (α_{min}, α_{max}) values associated with the studied geoelectric fluctuations by means of GPD.

References

[1] C. Tsallis, Journal of Statistical Physics 52 479 (1988)
[2] Cosma Rohilla Shalizi, Cornell University Library **arXiv:math/0701854 [math.ST]** (2007)
[3]R.L. Smith, Environmental Statistics, University of North Carolina www.stat.unc.edu/postscript/rs/semstatrls.ps (2003)

cmg2016 - - Friday, June 10, 2016 - 11:45/12:30 (45min)

STUDY OF TRANSITIONAL FLOWS IN ROUGH WALLS CHANNEL FLOWS

Anier Hernandez-Garcia, Rastin Matin, Marek Misztal & Joachim Mathiesen.
Niels Bohr Institute, University of Copenhagen, DK-2100 Copenhagen, Denmark.

Key words Channel flow, smooth/rough walls, hydrodynamic instability, transition mechanism, shear layer turbulence.

The laminar-turbulent transition in wall bounded shear flows exhibits a complex spatio-temporal scenario. Despite many efforts, a detailed understanding of the interaction among the scales excited at the onset of turbulence remains elusive. Here, we report direct numerical simulations of transitional three dimensional channel flows using the Entropic Lattice Boltzmann Method. We investigate the stability of localized turbulent patches (puffs) under noisy perturbations induced by wall irregular geometry. We study the effects of both amplitude and spatial distributions of wall roughness on the puff decaying-splitting processes.

cmg2016 - - Friday, June 10, 2016 - 11:45/12:30 (45min)

HORTON LAW IN SELF-SIMILAR TREES

Ilya Zaliapin
Department of Mathematics and Statistics, University of Nevada, Reno, USA

Key words Horton laws, Horton-Strahler orders, Tokunaga indices, Self-similar trees

Horton laws, which are akin to power-law distribution of the element sizes in a branching system, epitomize the scale invariance of natural dendritic structures. It is very intuitive that the existence of Horton laws should be related to the self-similar organization of branching, defined in suitable terms. Such relation, however, has escaped a rigorous explanation, remaining for long time a part of science literature folklore. This paper shows that a weak (mean) invariance under the operation of tree pruning is sufficient for the Horton law of branch numbers to hold in the strongest sense, hence explaining and unifying many earlier empirical observations and partial results in this direction. In particular, the existence of the Horton laws in Tokunaga self-similar trees is a special case of our general result.

Technically, self-similarity of random trees is related to the operation of pruning. Pruning $\mathcal{R}$ cuts the leaves and their parental edges and removes the resulting chains of degree-two nodes from a finite tree. A Horton-Strahler order of a vertex v and its parental edge is defined as the minimal number of prunings necessary to eliminate the subtree rooted at v. A branch is a group of neighboring vertices and edges of the same order. The Horton numbers $\mathcal{N}_k[K]$ and $\mathcal{N}_{ij}[K]$ are defined as the expected number of branches of order k, and the expected number of order-i branches that merged order-j branches, $j > i$, respectively, in a finite tree of order K. The Tokunaga coefficients are defined as $T_{ij}[K] = \mathcal{N}_{ij}[K]/\mathcal{N}_j[K]$. The pruning decreases the orders of tree vertices by unity. A rooted full binary tree is said to be mean-self-similar if its Tokunaga coefficients are invariant with respect to pruning: $T_k := T_{i,i+k}[K]$. We show that for self-similar trees, the condition $\limsup_{k\to\infty} T_k^{1/k} < \infty$ is necessary and sufficient for the existence of the strong Horton law: $\mathcal{N}_k[K]/\mathcal{N}_1[K] \to R^{1-k}$, as $K \to \infty$ for some $R > 0$ and every $k \geq 1$.

cmg2016 - - Friday, June 10, 2016 - 11:45/12:30 (45min)

HORTON LAW : EXACT FORMULAS AND ENTROPY RATES

E.V.Chunikhina[1]
[1]*EECS, Oregon State University, Corvallis, USA*

Key words Horton-Strahler indexing, entropy rate.

In this work we derive the closed form formula for the number of binary trees with particular Horton-Strahler numbers. We use these formulas to study the binary trees satisfying Horton law and obtain corresponding entropy rates.

Computational Geophysics

cmg2016 - - Friday, June 10, 2016 - 11:00/11:15 (15min)

DIMENSIONALITY REDUCTION AND UNCERTAINTY QUANTIFICATION FOR SEISMIC INVERSION

Tristan van Leeuwen
Mathematical Institute, Utrecht University, Utrecht, the Netherlands.

Key words full waveform inversion, uncertainty quantification, co-variance matrix, dimensionality reduction

In seismic waveform inversion, the goal is to estimate subsurface parameters, $\mathbf{m}$, from a collection of data $\{\mathbf{d}_i\}_{i=1}^k$ from various sources, indexed by i. Here, a single datum $\mathbf{d}_i \in \mathbb{R}^n$ represents a collection of n measurements, for example recorded by various stations or geophones. These recordings are modeled as noisy versions of the true signal, i.e.,

$$\mathbf{d}_i = F_i(\mathbf{m}) + \mathbf{n}_i,$$

where $F_i(\mathbf{m})$ is the (deterministic) forward operator, parametrized by $\mathbf{m}$ and $\mathbf{n}_i$ is a (stochastic) noise term. If these noise terms are Gaussian with mean zero and known covariance C (i.e., $\mathbf{n}_i \sim \mathcal{N}(\mathbf{0}, C)$) we arrive at the well-known non-linear least-squares formulation. The problem is that the covariance of the noise is typically not known a-priori. If there is enough data, i.e. $k > n$, we can formulate an extended problem that allows for estimation of both C and $\mathbf{m}$

$$\min_{\mathbf{m},C} \log\left(|C|\right) + \frac{1}{n}\sum_{i=1}^{k} \|F_i(\mathbf{m}) - \mathbf{d}_i\|^2_{C^{-1}}, \tag{1}$$

where $\|\mathbf{r}\|_A^2 = \mathbf{r}^T A \mathbf{r}$ is a weighted norm. The minimization over C has a closed-form solution

$$\widehat{C} = \frac{1}{n}\sum_{i=1}^{k} \mathbf{r}_i \mathbf{r}_i^T,$$

where $\mathbf{r}_i = F_i(\mathbf{m}) - \mathbf{d}_i$, allowing one to design an efficient alternating optimization algorithm for small-scale problems. Such an approach is based on a singular-value-decomposition (SVD) of the residual matrix $R = [\mathbf{r}_1, \mathbf{r}_2, \ldots, \mathbf{r}_k] = USV^T$, allowing one to express the covariance matrix as $C = n^{-1}RR^T = US^2U^T$. This, in turn, allows us to compute its inverse and determinant needed for the evaluation of the objective in (1) and its derivatives and apply a standard gradient-based method to solve for $\mathbf{m}$.

For large-scale problems, however, it is not feasible to compute a full SVD of the residual matrix. Instead, we propose to first reduce the dimensionality of the residual matrix by compressing it with a random (Gaussian) matrix $W \in \mathbb{R}^{k \times k'}$ with $k' \ll k$ to get $\widetilde{R} = RW$. Note that we can perform such a compression in practice at the cost of only k' applications of the forward model if the principle of superposition holds. If we normalize the random matrix we can approximate the covariance matrix as $\widehat{C} \approx n^{-1}\widetilde{R}\widetilde{R}^T$. This is an unbiased approximation, i.e., $\mathbb{E}(\widetilde{R}\widetilde{R}^T) = nC$, where $\mathbb{E}$ denotes expectation over W. The compressed residual matrix is much smaller, allowing us to compute a (truncated) SVD and proceed with the algorithm as stated above. Preliminary results are shown in figure 1.

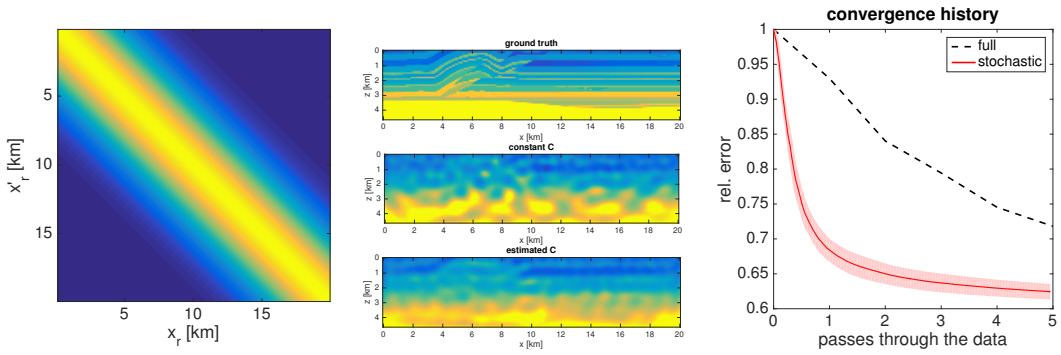

Figure 1. The Gaussian noise is generated according to the covariance matrix (left), inversion of the data for with constant covariance leads to a very poor reconstruction, while estimating the covariance on-the-fly gives a reasonable result (middle). The convergence plot (right) shows that the stochastic approach ($k' = 10$) converges much faster than the naive approach ($k = 200$), leading to an order of magnitude in computational savings.

cmg2016 - - Friday, June 10, 2016 - 10:30/10:45 (15min)

INVERSION AND INFORMATICS COMBINED: MAXIMISING BENEFIT FROM GEO- EXPERIMENT THROUGH COMPUTATION

A.M. Reading & M.J. Cracknell
School of Physical Sciences (Earth Sciences), Private Bag 79, University of Tasmania, Hobart, TAS 7001, Australia

Key words inversion, informatics, high-dimensional, solution space.

Many of the great and diverse challenges of understanding the natural, physical world use computational approaches to match a model to experimental data, through a process of geophysical inversion [1, 2]. Solving inverse problems has proven successful in geophysics with recent developments including thorough investigations of the solution space and uncertainty estimates [3]. This contribution explores complimentary, additional, approaches to learning from data through informatics approaches familiar to the information and communications technology (ICT) community. Such approaches work well with large volume and/or high-dimensional datasets, and include the possibility of combining categorical and numerical information. We show examples of how combining inversion and informatics, in computational geophysics, enables the benefit from experiments and resulting datasets to be maximised.

While approaches to solving inverse problems are familiar in the computational geophysics community, informatics approaches are less widely used. Learning from data in this frame may be accomplished through supervised or unsupervised learning, which corresponds respectively to a deductive or inductive underlying philosophy. In the former case, the predictive algorithm is developed through the use of a training dataset. Of the multiple algorithms [4] tested for this purpose, Random Forests [5] has proven a good first choice for geoscience datasets. Of the unsupervised algorithms, self-organising maps [6] has seen increasing use in the natural physical sciences. Key to the transfer of informatics approaches from ICT to geophysics is a robust process of prediction evaluation.

Combining inversion and informatics approaches is particularly valuable where data fusion across high-dimensional datasets is desired. This enables information from mixed-category data to be combined, thus making best use of data from field campaigns and/or remote sensing datasets. Using combined approaches provides not only a more complete approach to learning from hard earned data, but also a means of planning the next generation of field deployments or other experiments for maximum benefit. As we move from reconnaissance studies to the framing of first- and second-order experimental campaigns addressing particular hypotheses, the need to maximise the value of existing information and optimise ongoing data collection has never been greater.

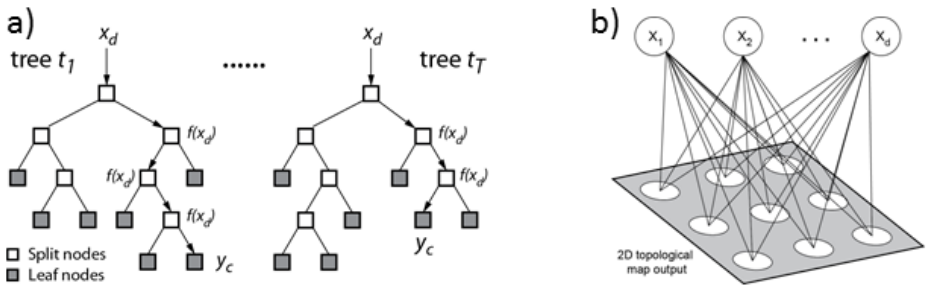

Figure 1. Representations of two informatics algorithms [5, 6] with potential wide application to geoscience data: a) Random Forests and b) self-organising maps.

References

[1] Aster, R.C., Borcher, B., and Thurber, C.H., 2013. *Parameter estimation and inverse problems*. – 2nd ed., Academic Press.
[2] Tarantola, A., 2005. *Inverse problem theory and methods for model parameter estimation*, Soceity of Industrial and Applied Mathematics.
[3] Bodin, T., Sambridge, M., Rawlinson, N., and Arroucau, P., 2012. Transdimensional tomography with unknown data noise. *Geophysical Journal International*, v. 189, 1536-1556.
[4] Cracknell, M.J., and Reading, A.M., 2014. Geological mapping using remote sensing data: A comparison of five machine learning algorithms, their response to variations in the spatial distribution of training data and the use of explicit spatial information. *Computers and Geosciences*, v. 63, 22-33.
[5] Breiman, L., 2001. Random Forests. *Machine Learning*, v. 45, 5-32.
[6] Kohonen, T., 2001. *Self-organising maps*, Springer-Verlang.

cmg2016 - - Friday, June 10, 2016 - 9:00/9:30 (30min)

RAPID, REPEATABLE PROBABILISTIC INVERSION: THE 'PRIOR SAMPLING' FRAMEWORK

A.P. Valentine, J. Trampert, S.E. Atkins, P.J. Käufl, & R.W.L. de Wit
Universiteit Utrecht, Utrecht, The Netherlands

Key words Inverse problems, learning algorithms.

Deterministic, linearised imaging techniques—such as those based on least-squares inversion—have contributed a huge amount to our understanding of the Earth. Nevertheless, they have their drawbacks: in particular, developing a proper understanding of model resolution and how uncertainties and systematic errors (such as approximations) propagate into solutions is challenging [1, 2, 3]. This creates a barrier to robust interpretation of results. Monte Carlo methods (based around 'sampling' the relationship between models and data) offer a route to circumventing many of these problems [4] and their use is increasingly widespread.

Typically, such methods rely on 'posterior sampling', where the sampling procedure is optimised towards explaining a given dataset. In many situations, this is sensible—but it brings two potential drawbacks. First, it imposes a fundamental restriction on the rate at which a solution can be obtained: no calculations can begin until observations have been collected. Second, samples cannot easily be 'recycled' in conjunction with a different dataset (perhaps obtained from a second location or point in time). These factors make it difficult to apply posterior sampling in real-time monitoring settings (such as for earthquake early warning), or to analyse local phenomena systematically around the globe (as in, say, receiver function inversion).

We therefore present a new approach, which we describe as 'prior sampling' [5]. Samples are distributed throughout the model space, according to any prior information that might be available. For each sample, the (potentially computationally-expensive) forward model is evaluated to obtain corresponding synthetic data. This data can be corrupted to mimic the effects of observational noise, and to account for any uncertainties due to any approximations or deficiencies in the forward code. The collection of (model, data) pairs obtained in this manner characterise a probability density function (pdf) in the joint data-model space. We assume that this pdf is smooth and continuous, and we fit a parametric representation to the samples. To do this, we employ a particular class of neural network called a 'mixture density network' (MDN) [6]. No observations of real data have been used in setting up this machinery. Once the MDN has been constructed, we are in a position to solve inverse problems repeatedly and rapidly: given a set of observations, the MDN outputs distributions on model parameters within milliseconds, and can be run on a standard desktop PC.

We demonstrate this framework in a range of applications, including earthquake early warning [7], analysis of Earth's radial structure [8], and as a tool for exploratory data mining, to investigate the parameters governing mantle convection [9]. Results are consistent with those obtained via posterior methods, although the less-targeted nature of sampling tends to result in more conservative uncertainty estimates. Nevertheless, we believe the approach is well-suited to inversion in circumstances where posterior approaches are infeasible.

References

[1] A. Valentine & J. Trampert, *Assessing the uncertainties on seismic source parameters: Towards realistic error estimates for centroid–moment-tensor determinations*, Phys. Earth Planet. Inter., **210–211**, 36–49 (2012).
[2] J. Trampert, A. Fichtner & J. Ritsema, *Resolution tests revisited: the power of random numbers*, Geophys. J. Int., **192**, 676–680 (2013).
[3] A. Valentine & J. Trampert, *The impact of approximations and arbitrary choices on geophysical images*, Geophys. J. Int., **204**, 59–73 (2016).
[4] M. Sambridge & K. Mosegaard, *Monte Carlo methods in geophysical inverse problems*, Rev. Geophys., **40**, 1–28 (2002).
[5] P. Käufl, A. Valentine, R. de Wit & J. Trampert, *Solving probabilistic inverse problems rapidly with prior samples*, Geophys. J. Int., in review.
[6] C. Bishop, *Neural networks for pattern recognition*, Oxford University Press (1995).
[7] P. Käufl, R. de Wit, A. Valentine & J. Trampert, *Robust and fast probabilistic source parameter estimation from near-field displacement waveforms using pattern recognition*, Bull. Seis. Soc. Am., **105**, 2299–2312 (2015).
[8] R. de Wit, P. Käufl, A. Valentine & J. Trampert, *Bayesian inversion of free oscillations for Earth's radial (an)elastic structure*, Phys. Earth. Planet. Inter., **237**, 1–17 (2014).
[9] S. Atkins, A. Valentine, P. Tackley & J. Trampert, *Inferring the initial conditions of mantle convection from the temperature structure using pattern recognition*, Phys. Earth. Planet. Inter., in review.

cmg2016 - - Friday, June 10, 2016 - 10:45/11:00 (15min)

GRADUAL WAVELET RECONSTRUCTION (GWR) FOR UNDERSTANDING THE NONLINEAR STRUCTURE OF TIME-SERIES DATA AND PLACING CONFIDENCE ON MODEL PARAMETERS

C. Keylock[1,2]
[1]*Sheffield Fluid Mechanics Group*
[2]*Department of Civil and Structural Engineering, University of Sheffield*

Key words Surrogate data; Time-series; Hypothesis testing; Wavelets; Nonlinear processes

Gradual wavelet reconstruction (GWR) is a data simulation method and this presentation will cover its formulation as well as geophysical applications. Surrogate data are extremely useful for testing hypotheses about data that are anticipated to be nonlinear, e.g. "is my time series chaotic?". Given an appropriate metric (e.g. maximal Lyapunov exponent), the value of the metric for the data is compared to the synthetic, linear, surrogate time series and a significant difference at the level α exists using a two-tailed test if the value for the original data is smaller or larger than that for $\left(\frac{2}{\alpha}\right) - 1$ surrogate series.
Fourier phase randomisation is the classic way to generate such linear surrogates. However, upon rejection of the null hypothesis (the data are nonlinear by the chosen metric) one cannot readily investigate how nonlinear a dataset is, or set up computational models with the appropriate degree of nonlinearity. GWR defines a continuum $0 \leq \rho \leq 1$ where the lower limit is the phase-randomised case, and the upper is the original data [1]. Using a wavelet transform to systematically preserve aspects of the phase in the original data, surrogates can be generated along this continuum. This permits a suite of new research possibilities:

- Generate synthetic river discharge data with the correct degree of asymmetry to the hydrograph (steep rising limb and gradual falling limb) to provide a new way to place confidence limits on extreme floods [2];
- Generate inlet boundary conditions for numerical simulations, and examining the sensitivity of the simulation to this perturbation [6];
- Show that the key nonlinearity driving differences in sediment entrainment by coherent flow structures is the frequency of occurrence of the structure, not the stress distribution [3];
- Show the the shape of gravel bed-forms in a channel increase in complexity with discharge and that the results are frame-of-reference dependent [4];
- Demonstrate that model parameters with small absolute values (in our case, a Fokker-Planck equation for the evolution of the velocity increments in turbulence) are significantly different to zero and are therefore dynamically relevant [5].

.

References

[1] Keylock, C.J. 2010. Characterizing the structure of nonlinear systems using gradual wavelet reconstruction, *Nonlinear Processes in Geophysics* **17**, 615-632.
[2] Keylock, C.J. 2012. A resampling method for generating synthetic hydrological time series with preservation of cross-correlative structure and higher order properties, *Water Resources Research* **48**, W12521, doi:10.1029/2012WR011923.
[3] Keylock, C.J., Lane, S.N., Richards, K.S. 2014. Quadrant/octant sequencing and the role of coherent structures in bed load sediment entrainment, *Journal of Geophysical Research* **119**, 264-286, doi: 10.1002/2012JF002698.
[4] Keylock, C.J., Singh, A., Foufoula-Georgiou, E. 2014. The complexity of gravel-bed river topography examined with gradual wavelet reconstruction, *Journal of Geophysical Research* **119**, 682-700.
[5] Keylock, C.J., Stresing, R. and Peinke, J. 2015. Gradual wavelet reconstruction of the velocity increments for turbulent wakes, *Physics of Fluids* **27**, 025104.
[6] Keylock, C.J., Tokyay, T.E., Constantinescu, G. 2011. A method for characterising the sensitivity of turbulent flow fields to the structure of inlet turbulence. *Journal of Turbulence* **12**, N45, doi: 10.1080/14685248.2011.636047.

cmg2016 - - Friday, June 10, 2016 - 9:45/10:00 (15min)

Improving Particle-in-Cell advection modeling using deforming particle kernels

H. Samuel[1,2]
[1]*CNRS ; IRAP, 14 avenue Edouard Belin, 31400 Toulouse, France*
[2]*Université de Toulouse ; UPS-OMP, Toulouse, France.*

Key words Advection, Particle-in-Cell method, Particle Kernel, Interface Tracking.

The particle-in-cell (PIC) method [1] is a flexible hybrid approach well suited for the modeling of multi-phase/multi-component flows. It uses a network of Lagrangian particles superimposed on a Eulerian grid (see Fig. 1). The grid represents the discretization of the physical domain and is used to determine the velocity field and the quantities affected by motionless processes (diffusion, radiation, source, reactions...). The particles carry information about several quantities (composition, temperature, momentum...). Their position is determined individually, usually by advecting them along their characteristics, via the interpolation of the Eulerian velocity field. The physical quantities are continuously transferred back and forth between the particles and the grid, through averaging. The latter involve particles kernels and grid shape functions. The method heavily relies on the choice of the particle kernels and on their meaning, which varies depending on the applications. The original PIC method [1] has been adapted to a variety of research domains. Despite a spatial accuracy often confined to first-order in practice it remains popular for many applications (dispersion of atmospheric and oceanic pollutants, geodynamics, computer graphics, MHD, astrophysics...) because the advection of Lagrangian particles significantly reduces numerical dissipation compared to purely Eulerian methods.

Unfortunately, PIC methods suffer from the clustering and the rarefaction of the number of particles in regions characterized by intense deformation. This phenomenon also concerns incompressible flows for which several grid cells can become completely empty of particles while others are over-represented (Fig. 1). Typical remedies involve: (1) the use of a large number of particles, often generating a prohibitive extra computational cost; (2) the redistribution of the particles in order to maintain a homogeneous sampling of the domain, which induces numerical dissipation that progressively degrades the accuracy of the solution.

I will present an evolution of the PIC method based on a new formulation of the particle kernels that takes into account the strain history in the vicinity of the particles. This new method, named DPIC, allows for a considerably more uniform spatial sampling by the particles with a reasonable computational extra cost (~ 50% relative to the PIC approach using the same number of particles). The DPIC method with only 4 particles per cell (in 2D) generates a solution whose accuracy is comparable to the standard PIC approach with more than 64 particles per cell. Therefore, at comparable precision this new approach allows reducing the computational cost by more than one order of magnitude. This gain is even more important for cases requiring the knowledge of the Lagrangian deformation (as common for applications in geodynamics [2], and more generally to characterize mixing and dispersion in a given flow). The DPIC approach could also be adapted to purely Lagrangian methods (SPH, vortex method), which are also prone to spatial sampling problems.

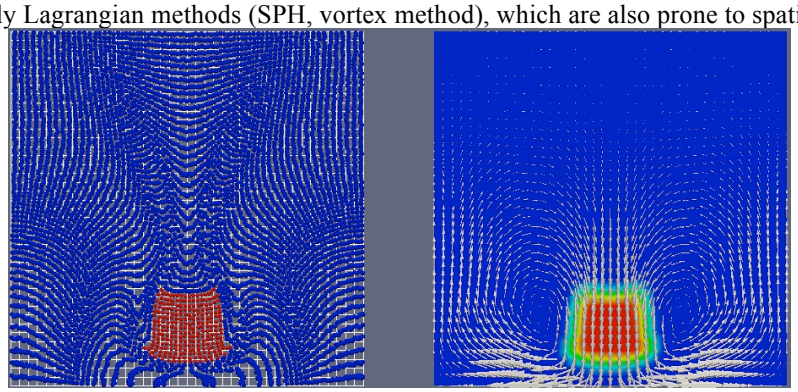

Figure 1. Example of the application of the PIC method, as proposed in [2]. Gravitational flow resulting from the presence of a more viscous and denser, initially square, body (red) relative to the surrounding fluid (blue). Left: Position of Lagrangian particles superimposed on the Eulerian grid. Right: Eulerian velocity field (calculated on the grid) and compositional field (obtained by averaging over the particles' population).

References

[1] F. H. Harlow, *Hydrodynamics problem involving large flow distorsion*, J. Assoc. Compos. Mach.,**4**, 137, (1957)

[2] T. Gerya, D. Yuen, *Characteristics-based marker-in-cell method with conservative finite-differences schemes for modeling geological flows with strongly variable transport properties,* Phys. Earth Planet. Int. **140**, 293-318 (2003).

cmg2016 - - Friday, June 10, 2016 - 9:30/9:45 (15min)

A SIMULATION-BASED STUDY OF MICRON SCALE, BINARY FLOWS IN POROUS ROCKS

R. Matin[1], M.K. Misztal[1], A. Hernandez-Garcia[1] & J. Mathiesen[1]
[1]*Niels Bohr Institute, University of Copenhagen, Copenhagen, Denmark*

Key words Porous flows, binary flows, relative permeability.

The microscopic properties of the multiphase flows in the pore networks of reservoir rocks have important implications for the large-scale flow properties. However, detailed empirical studies of porous flows at the micron scale are difficult. Numerical fluid simulations can provide additional insight. In the recent years, the lattice Boltzmann method has become a standard tool in simulating microscopic porous flows [1]. By solving the lattice Boltzmann equation on three-dimensional unstructured meshes, we have efficiently modelled single-phase fluid flow in real rock samples and used the resulting fields to numerically estimate the single-phase permeability and the particle dispersion in the samples [2]. By extending our model with a free-energy based method, we are now able to simulate binary fluid systems with moderate density ratios in a thermodynamically consistent way. This allows us to investigate binary flows in complex geometries when principal control parameters, such as the surface tension and the contact angle, can be adjusted. In this talk, we present the results of a numerical study of multiphase flows in the pore networks of both artificial and real rock samples. The goal of this study is to determine the behavior and fluctuations of relative permeabilities for an oil and water system, in response to varying water saturation, surface tension and wettability properties, and to compare the simulation results to the existing, experimental measurements.

References

[1] H. Liu, Q. Kang, C.R. Leonardi, S. Schmieschek, A. Narváez, B.D. Jones, J.R. Williams, A.J. Valocchi, J. Harting. *Multiphase lattice Boltzmann simulations for porous media applications: A review*, Comp. Geosciences, pp 1-29 (2015).

[2] M.K. Misztal, A. Hernandez-Garcia, R. Matin, D. Müter, D. Jha, H.O. Sørensen, J. Mathiesen. *Simulating anomalous dispersion in porous media using the unstructured lattice Boltzmann method*, Front. Phys. **3**, 50 (2015).

cmg2016 - - Friday, June 10, 2016 - 8:45/9:00 (15min)

THE SOURCE OF NUMERICAL ERRORS IN SYMPLECTIC INTEGRATION AND PERSPECTIVES IN MULTISYMPLECTIC INTEGRATION FOR THE ELASTIC WAVE EQUATION

H. Jiménez-Pérez[1], J.-P. Vilotte[1] & B. Romanowicz[1,2,3]
[1]*Institut de Physique du Globe, Paris, France*
[2]*Berkeley University of california (UC Berkeley), USA*
[3]*Collège de France, Paris, France*

Key words Symplectic integrators, Numerical error, Multisymplectic integrators, Elastic wave equation.

The idea of using geometric integration for long time wave propagation computations in seismology has been proposed for several authors, but no consistent (intrinsically defined) theory has been developed for elastic dynamics, in particular for the elastic wave equation. Some extensions of the multisymplectic formalism from Bridges and Reich [1] and Marsden, Patrick and Skoller [2] have been proposed by some authors, in particular by Jing-Bo [4, 3], and his collaborators. Unfortunatelly, almost all the numerical algorithms in the literature are based on the discretization proposed in [1] and/or [2].

Instead of using the Moser-Veselov discretization for variational integrators [2] or the method of multiple-symplectic forms [1], we started a systematic study of symplectic integration in order to base the construction of intrinsic symplectic algorithms only with the Hamiltonian formalism and symplectic geometry.

In this talk we present a new method for constructing symplectic integrators [5], which enables us to manipulate the numerical Hamiltonian error around a fixed energy level (see Figure 1) [6]. We present the mechanism which produces this error and some conditions for constructing exact symplectic algorithms. We will present our advances in the translation of the method of Liouvillian forms [5] to the multisymplectic formalism and the role the elastic tensor will play for obtaining very accurate methods for solving the elastic wave equation.

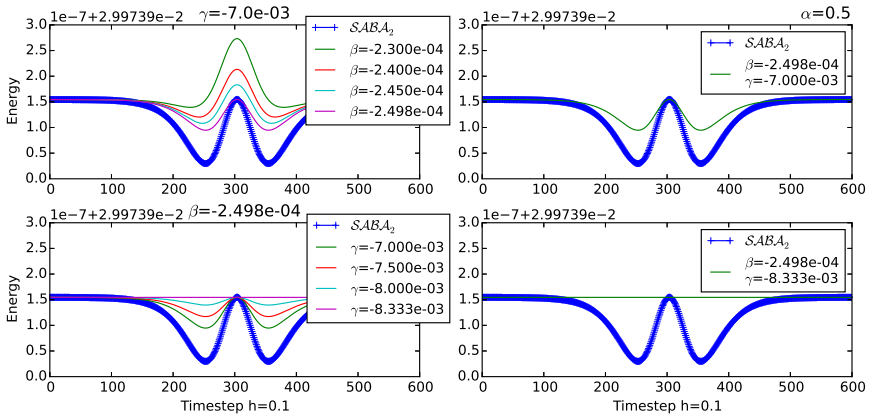

Figure 1. Some plots showing the manipulation of the numerical oscillations around a fixed energy value for the Hamiltonian pendulum. The fixed oscillating orbit corresponds to the numerical solution of the SABA2 integrator from Laskar and Robutel (2001). The oscillations of the flat line in the last plot have order 10^{-12}. All plots have initial condition (q0, p0) = (3.1, 0.0) and stepsize h = 0.1.

References

[1] Thomas J. Bridges , Sebastian Reich, *Multi-symplectic integrators: numerical schemes for Hamiltonian PDEs that conserve symplecticity*, Physics Letters A **284** (2001), 184-193.
[2] E. Marsden, George W. Patrick, Steve Shkoller *Multisymplectic Geometry, Variational Integrators, and Nonlinear PDEs*, Commun. Math. Phys. **199** (1998), 351-395.
[3] Jing-Bo, Chen, *A Multisymplectic Variational Framework for the Nonlinear Elastic Wave Equation*, Chin. Phys. Lett. **Vol 23**, No. 2 (2006) 320.
[4] Jing-Bo Chen, *Multisymplectic geometry for the seismic wave equation*, Commun. Theor. Phys., **41**, (2004) 561-566.
[5] H. Jiménez-Pérez, *Symplectic maps: from generating functions to Liouvillian forms*, preprint (arxiv:1508.03250), (2015).
[6] H. Jiménez-Pérez, J-P. Vilotte, and B. Romanowicz, *New insights on numerical error in symplectic integration*, submitted (arXiv:1508.03303), (2015).

cmg2016 - - Friday, June 10, 2016 - 11:45/12:30 (45min)

DIRECT IMPLICIT ALGORITHM FOR THE SOLUTION OF ADVECTION-DIFFUSION EQUATION ON A SPHERE

Yuri N. Skiba
Centro de Ciencias de la Atmósfera, Universidad Nacional Autónoma de México, Mexico City, Mexico

Key words Finite volume method, splitting method, bordering method.

A numerical algorithm for the solution of advection-diffusion equation on the surface of a sphere is suggested. The velocity field on a sphere is assumed to be known and non-divergent. The discretization of advection-diffusion equation in space is carried out with the help of the finite volume method, and the Gauss theorem is applied to each grid cell. For the discretization in time, the symmetrized double-cycle componentwise splitting method and the Crank-Nicolson scheme are used. The numerical scheme is of second order approximation in space and time, correctly describes the balance of mass of substance in the forced and dissipative discrete system, and is unconditionally stable. In the absence of external forcing and dissipation, the total mass and L_2-norm of solution of discrete system is conserved in time. The one-dimensional periodic problems arising at splitting in the longitudinal direction are solved with Sherman-Morrison's formula and Thomas's algorithm. The one-dimensional problems arising at splitting in the latitudinal direction are solved by the bordering method that requires a prior determination of the solution at the poles. The resulting linear systems have tridiagonal matrices and are solved by Thomas's algorithm. The suggested method is direct (without iterations) and rapid in realization. It can also be applied to linear and nonlinear diffusion problems, and some elliptic problems on a sphere.

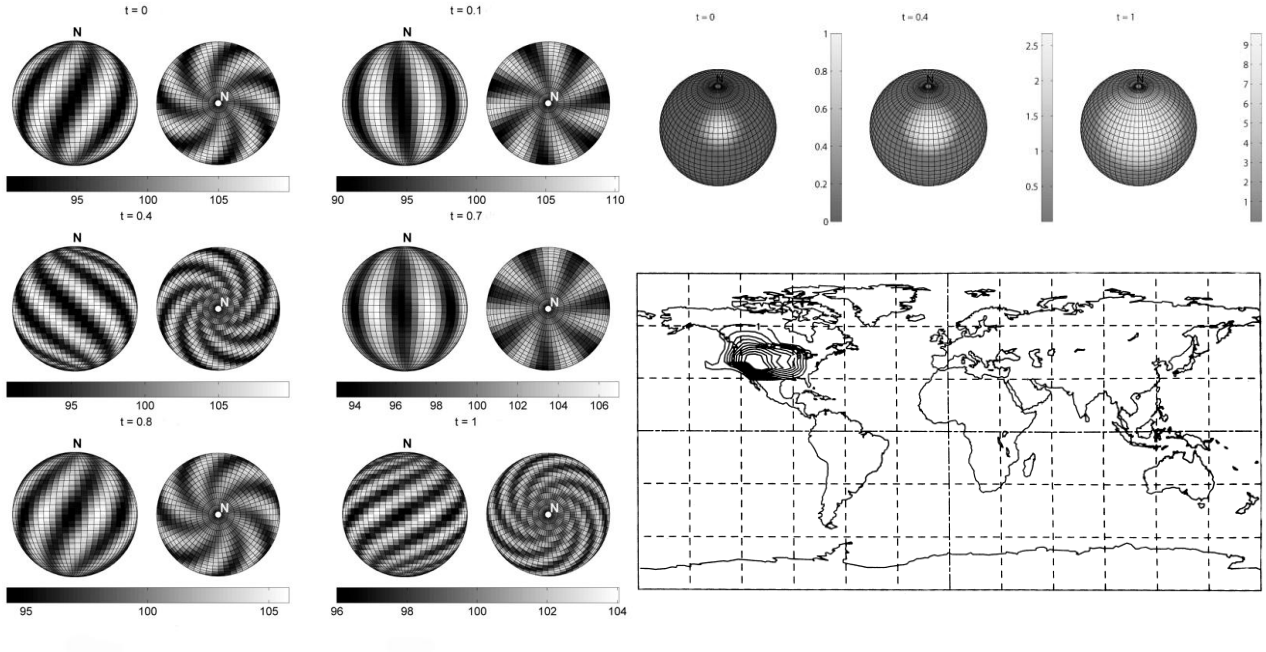

Figure 1. Nonlinear spiral waves, side and top view (a); The HS-regime of nonlinear combustion, t=0, 0.4, 1.0 (b); Solution of adjoint advection-diffusion problem for USA territory, $t = T - \tau / 2$ (T = 60 days, τ = 10 days) (c).

References

[1] Yuri N. Skiba. A non-iterative implicit algorithm for the solution of advection-diffusion equation on a sphere, *Intern. J. Numer. Methods in Fluids*. **78** (5), 257 (2015).

cmg2016 - - Friday, June 10, 2016 - 11:45/12:30 (45min)

COHERENT SEISMIC NOISE ATTENUATION USING THE WAVE ATOMS TRANSFORM.

S. Ouadfeul[1] & L.Aliouane[2]
[1]*Algerian Petroleum Institute, IAP, Algeria.*
[2]*LABOPHYT, FHC, UMBB, Algeria..*

Key words wave atoms, coherent noise, attenuation, directional, multiscale.

The wave atoms has becoming a very useful tool in image processing in the last decade, it has demonstrated its power to detected any directional phenomenon with considering its scaling properties (Demanet and Ying, 2007). Here we suggest the use of this technique to attenuate the ground roll from Seismic data recorded in the Algeria. The wave atoms transform is applied to the seismic data, then the ground roll characterized by low frequency and high energy in a given direction are identified and attenuated, after that the origin seismic data are reconstructed using the wave atoms inverse transform. Obtained results demonstrate the power of this technique to attenuate complex coherent noises such as the dispersive ground roll.

References

[1] L.Demanet and L. Ying, 2007, Wave Atoms and Sparsity of Oscillatory Patterns, Appl. Comput. Harmon. Anal., vol. 23(3) pp.368 387.

cmg2016 - - Friday, June 10, 2016 - 11:45/12:30 (45min)

UNCONVENTIONAL LIKELIHOOD FUNCTIONS IN GEOPHYSICAL INFERENCE

M. Sambridge[1],
[1]*Research School of Earth Sciences, Australian National University, Canberra, ACT 2601, Australia*

Key words Likelihoods, Seismic Waveforms, Regression problems

Likelihood functions are at the basis of all modern inference. They play a pivotal role in statistical inference, are a key part of popular Bayesian Inference methods and when recast as data misfit functions form the central component of nonlinear optimization methods of inversion. In both Maximum Likelihood and Bayesian Inference approaches the definition of the Likelihood has a major influence on the solution of an inverse problem and yet in many studies its form receives relatively little attention. The role of the Likelihood function is to measure the *probability of the data given the model*, which requires the statistics of the noise to be known. However in many cases data noise characteristics are not well known, and guesses have to be made. A particularly common Likelihood crime is to choose its form for convenience e.g. by ignoring correlations in the noise between successive data measurements in a time series, or by assuming quantities that are measured, and hence have associated noise, are error free auxiliary variables. A common situation in regression problems witihin the geosciences. Each of these crimes are committed to simplify the Likelihood often in the hope that the solution with Maximum Likelihood or Maximum *a posteriori* PDF is not too affected by the approximations introduced. Even when this is true, however, estimates of uncertainty and also goodness of fit can be drastically influenced by such approximations.

In this paper we look at two unconventional approaches to building Likelihood functions. In the first we derive and justify a Likelihood function for time series fitting problems with arbitrary data errors, i.e. where both parameters y and t (or x) are measured and contain error which may be correlated between components of a single datum or correlated between data, and may be multi-dimensional Gaussian or otherwise. We illustrate use of the Likelihood function in a 1-D changepoint problem. [**?**]. A comparison is made between results of Maximum Likelihood and Bayesian Partition modelling. We also apply the latter to reconstruction of relative sea-level over the past five glacial cycles, 500, 000 years before present based on published $\delta^{18}O$ measurements [**?**]. We show that using the unconventional Likelihood here provides robust uncertainty measurements on both relative sea level height and its gradient.

The second unconventional Likelihood involves utilizing concepts from Compressive Sensing. Here we build Likelihoods from random sub-samples in time of a seismic waveform time series and examine the constraint that may be placed on an Earth model. The results suggest that large portions of a seismic waveform may be discarded without significant loss in the constraint provided by the Likelihood. This may suggest new ways to approach full seismic waveform inversion.

References

[1] Gallagher, K., T. Bodin, M. Sambridge, D. Weiss, M. Kylander, and D. Large (2011), Inference of abrupt changes in noisy geochemical records using transdimensional changepoint models, *Earth Planet. Sci. Lett.*, *311*, 182–194.

[2] Rohling, E. J., K. Grant, M. Bolshaw, A. P. Roberts, M. Siddall, C. Hemleben, and M. Kucera (2009), Antarctic temperature and global sea level closely coupled over the past five glacial cycles, *Nature Geoscience*, *2*, 500–504.

cmg2016 - - Friday, June 10, 2016 - 11:45/12:30 (45min)

TRANSDIMENSIONAL MODELLING OF ARCHEOMAGNETIC DATA

A. Fournier[1], P. W. Livermore[2], Y. Gallet [1] & T. Bodin[3]
[1]*Institut de Physique du Globe, Paris, France*
[2]*University of Leeds, UK*
[3]*Ecole Normale Supérieure, Lyon, France*

Key words Archeomagnetism – Geomagnetic secular variation – Monte Carlo methods

One of the main goals of archeomagnetism is to document the secular changes of Earth's magnetic field by laboratory analysis of the magnetization carried by archeological artefacts [1]. A few studies [e.g. 2] have highlighted possible extremely rapid changes in the archeomagnetic field, which do not seem to stand on a very solid physical footing, given our current understanding of Earth's core dynamics and the geodynamo [3]. In addition, strong temporal damping used in the associated models (due to the sparsity of data) makes them difficult to detect robustly. Key to proper modelling (and physical understanding) is a method that places a minimum level of regularisation on any fit to the data.

Here we investigate how transdimensional modelling [e.g. 4], whereby the degree of complexity of the model is not set a priori, can be used for that purpose. We first illustrate how this technique can be implemented for regional curves of archeointensity, assuming that the ages of the artefacts are perfectly known. To that end, we implement a Reversible Jump Monte Carlo Markov Chain (RJ-MCMC) technique based on a variable number of changepoints, akin to that developed by Gallagher et al. [5] in a geochemical context. Figure 1 below shows an application to French measurements spanning the past three thousand years [6, 7]. Next, we consider the more realistic case of uncertain ages, which prompts us to add another Monte Carlo layer in order to draw an ensemble of age realizations for the data at hand, each realization being subsequently treated with the RJ-MCMC approach. We finally discuss the generalization of this approach to global models of the archeomagnetic field.

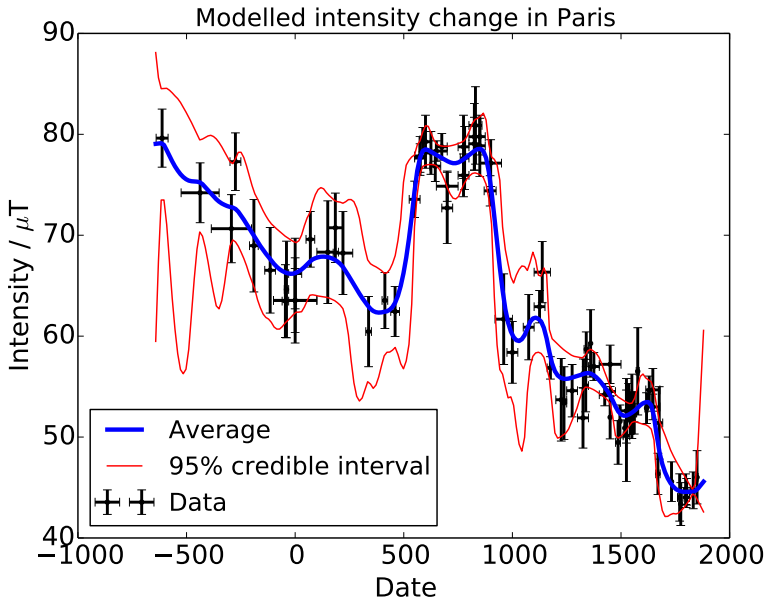

Figure 1. Transdimensional modelling of the geomagnetic intensity in Paris since 700 BC.

References

[1] Y. Gallet, A. Genevey, M. Le Goff, N. Warmé, J. Gran-Aymerich, and A. Lefèvre. On the use of archeology in geomagnetism, and vice-versa: Recent developments in archeomagnetism. *Comptes Rendus Physique*, 10(7):630 – 648, 2009.

[2] R. Shaar, E. Ben-Yosef, H. Ron, L. Tauxe, A. Agnon, and R. Kessel. Geomagnetic field intensity: How high can it get? How fast can it change? Constraints from Iron Age copper slag. *Earth and Planetary Science Letters*, 301(1):297–306, 2011.

[3] P. W. Livermore, A. Fournier, and Y. Gallet. Core-flow constraints on extreme archeomagnetic intensity changes. *Earth and Planetary Science Letters*, 387:145–156, 2014.

[4] M. Sambridge, T. Bodin, K. Gallagher, and H. Tkalčić. Transdimensional inference in the geosciences. *Philosophical Transactions of the Royal Society of London A: Mathematical, Physical and Engineering Sciences*, 371(1984):20110547, 2013.

[5] K. Gallagher, T. Bodin, M. Sambridge, D. Weiss, M. Kylander, and D. Large. Inference of abrupt changes in noisy geochemical records using transdimensional changepoint models. *Earth and Planetary Science Letters*, 311(1):182–194, 2011.

[6] A. Genevey, Y. Gallet, E. Thébault, S. Jesset, and M. Le Goff. Geomagnetic field intensity variations in Western Europe over the past 1100 years. *Geochemistry, Geophysics, Geosystems*, 14(8):2858–2872, 2013.

[7] A Genevey, Y. Gallet, S. Jesset, E. Thébault, J. Bouillon, A. Lefèvre, and M. Le Goff. Geomagnetic intensity variations during the early middle ages in Western Europe: New constraints from French medieval ceramic production. In preparation for submission to Physics of the Earth and Planetary Interiors.

cmg2016 - - Friday, June 10, 2016 - 11:45/12:30 (45min)

COMBINING DATA ASSIMILATION AND MOVING MESHES FOR MOVING BOUNDARY PROCESSES: APPLICATION TO ICE SHEET MODELLING

B. Bonan[1], M. J. Baines[1] & N. K. Nichols[1]
[1]*School of Mathematical and Physical Sciences, University of Reading, Reading, United Kingdom*

Key words Data assimilation, moving meshes, ensemble methods, moving boundary problems, ice sheets.

Numerous processes in geosciences (for example glacier melting or flooding) are governed by nonlinear time-dependent partial differential equations on domains with finite moving boundaries whose position depends on the solution of the problem itself. Predicting their evolution including tracking the trajectory of their moving boundaries can be challenging. Here we propose to combine a particular moving mesh method and data assimilation to overcome the issue. The moving mesh method based on the preservation of mass fractions is well-suited to tracking moving phenomena accurately [1]. In order to initialise our model, we apply advanced data assimilation techniques to the system. We develop particularly an Ensemble Kalman Filter approach in this context. The data assimilation procedure treats both the mesh node positions and physical variables at these locations as unknown state variables and updates both of these at each assimilation step. The advantage of the ensemble approach is that it enables the sensitivity of the system to be understood and, more importantly, provides information on the correlations between the state variables, in particular between the grid and the physical variables. We demonstrate the success of the technique, especially for estimating the position of the boundaries in the context of ice sheet modelling.

References

[1] M. J. Baines, M. E. Hubbard and P. K. Jimack, *Velocity-based moving mesh methods for nonlinear partial differential equations*, Commun. Comput. Phys., **10**, 509-576 (2011).

cmg2016 - - Friday, June 10, 2016 - 11:45/12:30 (45min)

NOVEL APPROACH FOR THE DETERMINATION OF THE CORE-MANTLE BOUNDARY BASED ON "NATIVE" WAVELET TRANSFORM OF THE GRAVITY DATA

N. Matveeva, E. Utemov, D. Nourgaliev
Kazan Federal University, Institute of Geology and Petroleum Technologies, Kazan, Russia

Key words Wavelet transforms, Gravity data, Core-mantle boundary, Spherical surface.

The hypothesis about uneven structure of the core-mantle boundary was offered in 1957 by Garland [1]. Hide made the assumption [2] that large-scale gravitational anomalies could be linked with irregularities on the core-mantle boundary. Details of topography of the core-mantle boundary based on the seismological data were described in [3], [4], [5].

In this study we propose a novel approach to determine topography of the core-mantle boundary. Our approach is based on continuous wavelet transform of gravity data with the so-called "native" basis. This method was developed specially for analysis data acquired on a spherical surface. The obtained model of core-mantle boundary is in a good agreement with ones from the seismological approach [3] and another gravity approach [6].

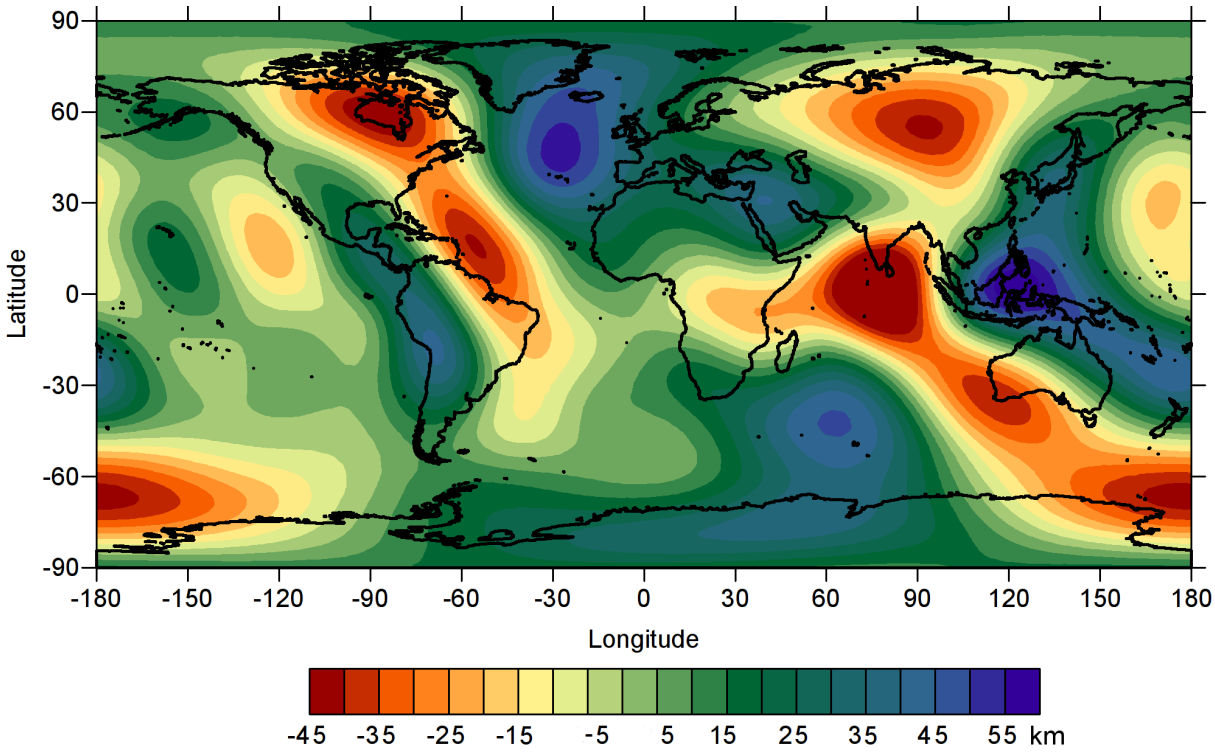

Figure 1. The topography of deviations of the core-mantle boundary from the spheroid obtained by using continuous "native" wavelet transform of gravity data. Harmonic coefficients of gravity field were received by model eigen-6s2 (ICGEM, http://icgem.gfz-potsdam.de/ICGEM).

References

[1] G. D. Garland, The figure of the Earth's core and the non-dipole field, J. Geophys. Res., 62(3), 486–487, 1957
[2] R. Hide, S.R.C. Malin, Novel correlation between global features of Earth's gravitational and magnetic fields. Nature 225, 605–609, 1970
[3] O. Gudmundsson, R.W. Clayton, D.L. Anderson, Core mantle boundary topography inferred from ISC PcP travel times. Trans. Am. Geophys. Union 67 (44), 1100, 1986
[4] A. Morelli, A.M. Dziewonski, Topography of the core-mantle boundary and lateral homogeneity of the liquid core. Nature 325, 678–683, 1987
[5] D.J. Doornbos, T. Hilton, Models of the core-mantle boundary and the travel times of internally reflected core phases. J. Geophys Res., 1989
[6] I.L. Prutkin, Nonlinear inverse potential problems and construction of two-layer models of Earth and Moon. Izvestiya. Phys. Solid Earth 25 (11), 913–918,1989

cmg2016 - - Friday, June 10, 2016 - 11:45/12:30 (45min)

HIGH-PERFORMANCE PARALLEL SOLVER FOR INTEGRAL EQUATIONS OF ELECTROMAGNETICS BASED ON GALERKIN METHOD

M. Kruglyakov[1] & L. Bloshanskaya[2]
[1]*Lomonosov Moscow University, Moscow, Russia*
[2]*SUNY New Paltz, USA*

Key words Electromagnetic sounding; Forward modeling; Integral equations; Galerkin method; High-performance computing

A new parallel solver for the volumetric integral equations (IE) of electrodynamics is presented. The solver is based on the Galerkin method which ensures the convergent numerical solution. The main features include:

1. the reduction of the memory usage in 8 times, compared to analogous IE based algorithms, without additional restriction on the background media;
2. accurate and stable method to compute matrix coefficients corresponding to the IE;
3. high degree of parallelism.

The solver's computational efficiency is shown on a problem of magnetotelluric sounding of the high conductivity contrast media. A good agreement with the results obtained with the second order finite element method by [1] is demonstrated (Fig 1). Due to effective approach to parallelization and distributed data storage the program exhibits perfect scalability on different hardware platforms.

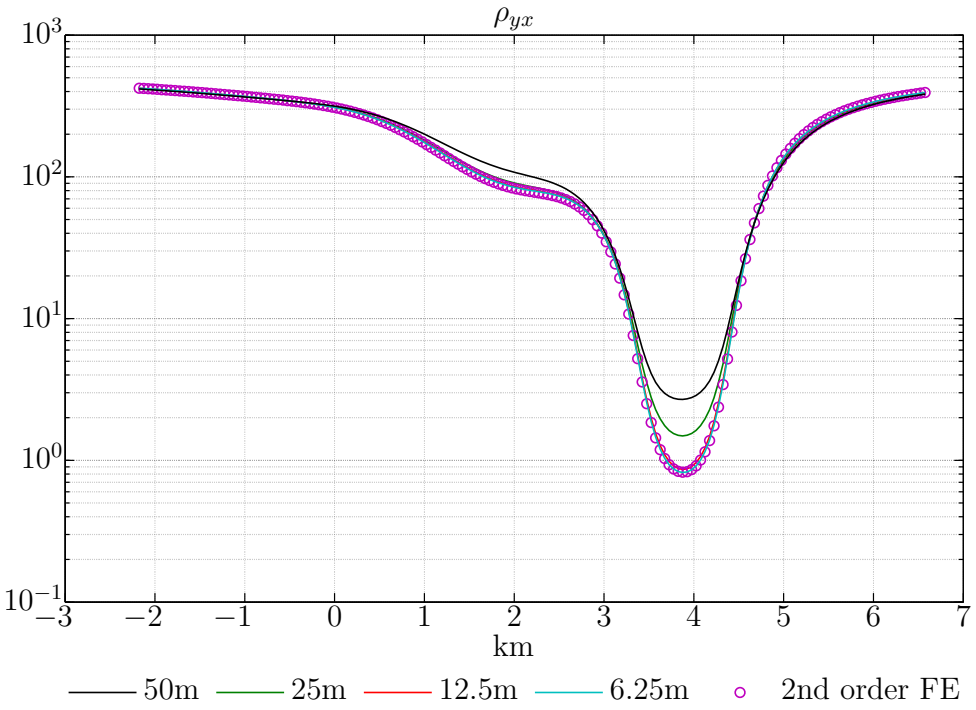

Figure 1. Apparent resistivity ρ_{yx} at period 1 s along profile $y = 1$ km for different subdomain sizes, for COMMEMI3D-3 model from [2].

References

[1] Grayver A, Kolev T (2015) Large-scale 3d geo-electromagnetic modeling using parallel adaptive high-order finite element method. Geophysics 80(6):277–291
[2] Hursan G, Zhdanov MS (2002) Contraction integral equation method in three-dimensional electromagnetic modeling. Radio Science 37(6):1–13

An enhanced-automated-array method for earthquake detection and location and its application on the Preparatory Phase of the Mw 8.2 Iquique Earthquake, Chile 2014

Florent Aden-Antoniow, Claudio Satriano, Natalia Poiata, Pascal Bernard, Jean-Pierre Vilotte, El-Madani Aissaoui

Automated methods for detection and location are more and more used in seismology, given the size of arrays and the quantity of data-set to process. Among these methods, some compute the statistical distribution of a signal trough time in order to emphasize the seismic onsets [Saragiotis 2002; Baillard et al. 2014]. The Multi-Band Backprojection method [Poiata et al. 2016] use high-order statistics to build seismic arrival characteristic functions for each station of a given network. These functions are cross-correlated between stations, and the resulting correlation function is back-projected on a 3-D time-lag grid according to a given velocity model, and stacked for all pair of station. A coherent source will make the stacked time-lag grid focus at the source location.

This method already proved its efficiency for building large catalogues [Aden-Antoniow et al. AGU 2015]. However the resolution of the location of a coherent source is very sensitive to outliers onsets in the same time window, in particular those due to other earthquakes. Here we further develop our method in order to improve event picking and location , in particular for events clustered in time. We filter each time-lag grid by the stacked time-lag grid computed during a first round, which allows to keep only the most coherent source across the network on each correlation function. Then we back-project it onto the 3-D hypocenter space, transform it into to probability density functions (pdf), and combine these pdfs for each stations pair on the 3-D hypocentral grid. This processing improves the location of seismic sources and better quantifies its uncertainties, as well as the picking of the seismic onsets themselves.

We apply this improved processing methodology to the data set provided by the IPOC and ILN seismic networks, covering the 3 months of the preparatory phase of the 2014, M=8.2, Iquique earthquake (Chile). We then compare the resulting hypocenter catalogue to the one which we generated with the first, simpler version of the method, to qualify the efficiency of this new step in the methodology.

Experimental Geophysics

cmg2016 - - Tuesday, June 7, 2016 - 18:15/18:30 (15min)

LARGE-SCALE REALISTIC LABORATORY MODELING OF INTERNAL TIDE GENERATION AT THE LUZON STRAIT

M. J. Mercier[a 1], L. Gostiaux[b], K. Helfrich[c], J. Sommeria[d], S. Viboud[d], H. Didelle[d], S. J. Ghaemsaidi[a], T. Dauxois[e], T. Peacock[a]

[a] *Department of Mechanical Engineering, Massachusetts Institute of Technology, Cambridge, MA, USA.*
[b] *Laboratoire de Mécanique des Fluides et d'Acoustique, UMR 5509, CNRS, École Centrale de Lyon, Écully, France.*
[c] *Woods Hole Oceanographic Institution, Woods Hole, Massachusetts, USA.*
[d] *LEGI, CNRS UMR5519, University of Grenoble Alpes, Grenoble, France.*
[e] *Université de Lyon, Laboratoire de Physique, École Normale Supérieure de Lyon, CNRS, Lyon, France.*

Key words experimental geophysics, stratified flows, rotating flows, internal waves.

The Luzon Strait, located between Taiwan and the Philippines, is a fine example of internal tide generation by complex bathymetry. Strong internal tides propagate away from this double-ridge system resulting in some of the largest internal solitary waves observed worldwide with vertical displacements up to 200 m and velocity of the order of 1 m/s. In recent years, this setting has been the focus of extensive field studies, remote observations and numerical simulations.

To complement the aforementioned studies, we performed an internal tide laboratory experiment on an unprecedented scale. The experiment was conducted at the Coriolis facility at LEGI (Grenoble, France), site of the world largest rotating table (13 m in diameter). We modeled the generation of internal tides using realistic three-dimensional topography, density stratification and barotropic tidal forcing; the latter was achieved through the use of prismatic tide generators. Particular care was taken to achieve dynamical similarity with the ocean problem, with the values of dimensionless groups such as criticality, Froude number and tidal excursion being closely matched to established values for the Luzon Strait.

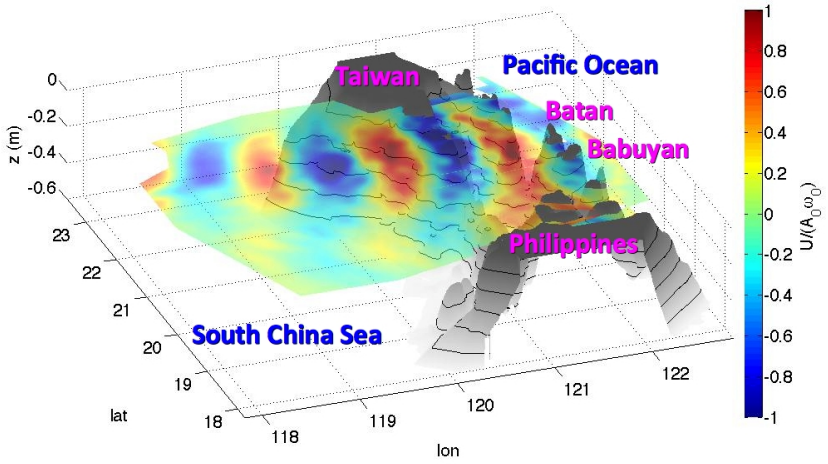

Figure 1. Experimental observations of the radiated internal tide for a semidiurnal case. The bathymetry is in gray, the colormap indicates the horizontal (east-west) velocity U in a plane near the pycnocline, normalized by the amplitude of the barotropic flow $A_0\omega_0$.

The experimental results [1] advocate that a broad and coherent weakly nonlinear, three-dimensional, semidiurnal internal tide that is shaped by the overall geometry of the double-ridge system is radiated into the South China Sea (cf. Fig. 1) and subsequently steepens, as opposed to being generated by a particular feature or localized region within the ridge system. On the contrary, the radiated diurnal internal tide is less sensitive to the Luzon bathymetry and is unlikely to evolve in a nonlinear manner.

References

[1] M. J. Mercier, L. Gostiaux, S. Ghaemsaidi, J. Sommeria, H. Didelle, S. Viboud, K. R. Helfrich, T. Dauxois, T. Peacock. *Large-scale, realistic laboratory modeling of M_2 internal tide generation at the Luzon Strait*, Geophys. Res. Lett., **40**, 5704–5709 (2013).

[1] now at INPT, UPS, CNRS, IMFT (Institut de Mécanique des Fluides de Toulouse), Université de Toulouse, F-31400 Toulouse, France.

cmg2016 - - Tuesday, June 7, 2016 - 18:30/18:45 (15min)

GENERATING JOVIAN-LIKE ZONAL JETS IN A RAPIDLY ROTATING FLUID EXPERIMENT

S. Cabanes[1], J. Aurnou[2], B. Favier[1] & M. Le Bars[1]
[1]*CNRS, Aix-Marseille Université, École Centrale Marseille, IRPHE UMR 7342, Marseille, France.*
[2]*Department of Earth, Planetary, and Space Sciences, University of California - Los Angeles, USA.*

Key words Zonal jets, zonostrophic turbulence.

Abstract

Using a large-scale rotating fluid experiment, we report the formation of strong zonal jets due to topographical effects in rotating turbulence. For the first time, we reach the so-called "zonostrophic" regime, thought to be relevant to Jupiter atmosphere for example. The jets dominate the small-scale turbulent fluctuations in amplitude and appear very stable and long-lived. Although their size is consistent with the so-called Rhines scale, we observe interesting dynamics over very long time-scales such as merging events where the number of jets decreases and their amplitude increases. These first results open new perspectives in the study of large-scale zonal flows in the laboratory.

For our experimental set up (see figure 1(c)), we use a cylindrical container 1.4 meter high with an internal radius of 0.5 meter filled with up to 400 liters of water and mounted on a rotating table. The depth of the fluid layer at rest is $h_0 = 50$cm and the rotation rate of the table is 75 RPM. This leads to a very large deformation of the fluid layer (topographic β-effect), with a minimum depth after the spin-up phase of $h = 20$cm at the center of the container and a maximum depth of on the side boundary of $h = 88cm$. A turbulent small-scale flow is driven via a basal injection/suction system made of a square tiled set of 64 inlet/outlet ports, generating velocities in the range $U \approx 1 - 5$ cm/s (corresponding to a Reynolds number $2.5 \times 10^3 < Re < 1.3 \times 10^4$ and a Rossby number $3.3 \times 10^{-3} < Ro < 1.6 \times 10^{-2}$). Lagrangian surface velocities are measured using a Particle Tracking method using small floating particles with a typical diameter of 5 mm.

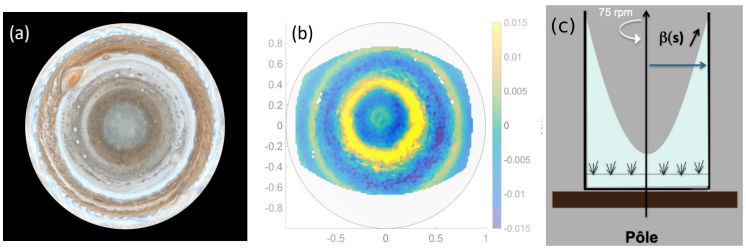

Figure 1. zonal jets visualization and experimental set-up. (a) Polar view of Jupiter atmosphere (Credit: NASA/JPL/Space Science Institute). (b) Time averaged zonal velocity map obtained by particles tracking in our experiment: blue/yellow values are retrograde/prograde jets (velocity non-dimensionalized by the rotation rate times the tank radius). (c) Sketch of our experimental model reproducing the suitable zonostrophic planetary conditions in a cylindrical geometry, i.e. fast rotation, topographic β-effect and small scale turbulent energy injection.

After the spin-up is complete, we start the pumping system forcing quasi-homogeneous small-scale turbulence at the base of the domain. Due to the very low Rossby numbers, the basal forcing very quickly drives a nearly depth-invariant turbulent flow. The dominantly geostrophic flow is confirmed by the numerical simulations and shows that Lagrangian surface measurements are sufficient to characterize the system in a first approach. After several tens of rotation times, alternating zonal jets start to grow as shown figure 1. The initial number of jets is consistent with the so-called Rhines scale, derived from a balance between the turbulent turn-over time scale and the typical frequency of Rossby waves [3]. Contrary to previous experiments, where the zonal jets are mainly observed after time averaging, our jets reach the so-called "zonostrophic" regime, where the instantaneous amplitude of the jets is greater than that of the small-scale fluctuations.

We obtained for the first time strong zonal jets in the so-called zonostrophic regime. These jets are extremely stable and live over many rotation timescales, but we nevertheless observe interesting merging events. Our systematic study allows to understand this dynamics, as well as what fixes the size and the amplitude of the jets. In the near future, implementations of our system will allow tacking many interesting questions in the laboratory, like the formation of large-scales vortices in the presence of a top stratified layer [4] and the existence of inertial wave turbulence [5] .

References

[1] P. L. Read, et al.: An experimental study of multiple zonal jet formation in rotating, thermally driven convective flows on a topographic beta-plane. Phys. Fluids 27, 085111, 2015.
[2] P. F. Fischer, et al.: Simulation of high-Reynolds number vascular flows. Comp. Meth. App. Mech. and Eng. 196 (31), 3049–3060, 2007.
[3] G. K. Vallis & M. E. Maltrud: Generation of mean flows and jets on a beta plane and over topography. Journal of Physical Oceanography 23, no. 7, 1346–1362, 1993.
[4] M. Heimpel, T. Gastine & J. Wicht: Simulation of deep-seated zonal jets and shallow vortices in gas giant atmospheres. Nature Geoscience 9, 19–23, 2016.
[5] E. Yarom & E. Sharon: Experimental observation of steady inertial wave turbulence in deep rotating flows. Nature Physics 10, 510–514, 2014.

cmg2016 - - Tuesday, June 7, 2016 - 17:30/17:45 (15min)

MEMORY OF PASTE : VISUALIZATION AS CRACK PATTERN AND NON-DESTRUCTIVE STRUCTURAL ANALYSIS

A. Nakahara[1], Y. Matsuo[1], K. Uchida[2], H. Izui[2], S. Kitsunezaki[3] & F. Kun[4]
[1]*Laboratory of Physics, College of Science and Technology, Nihon University, Funabashi, Japan*
[1]*Department of Aerospace Engineering, College of Science and Technology, Nihon University, Funabashi, Japan*
[3]*Research Group of Physics, Division of Natural Sciences, Faculty of Nara Women's University, Nara, Japan*
[4]*Department of Theoretical Physics, University of Debrecen, Debrecen, Hungary*

Key words Memory effect, crack pattern, plasticity, rheology, paste, colloidal suspension, vibration, flow, magnetic field

A densely packed colloidal suspension, called a paste, remembers the direction of external forces, such as vibration, flow and magnetic field, even after the external field is removed, and these memories in paste can be visualized as morphology of desiccation crack patterns [1]. When a paste remembers the direction of vibration, desiccation cracks run in the direction perpendicular to the initial vibration, while desiccation cracks run along the direction of initial flow and magnetic field when the paste remembers the direction of flow and magnetic field [1-4]. The memory of vibration can be explained by residual tension theories [4-6]. However the mechanism of memory of flow is still under investigation.

Recent X-ray CT scan has been performed to dried magnetic pastes and it is revealed that the memory of magnetic field is stored as chain formation of magnetic particles along the magnetic field. The chain formation of magnetic particles along the magnetic field is confirmed by our numerical simulations.

There are many applications of the memory effect of paste. For example, the morphology of desiccation cracks can be controlled by imprinting the memory of external field into paste, and various desiccation crack patterns are produced, such as lamellar, radial, ring, spiral, lattice and so on. Examination of the memory in paste reveals what happend when the paste was in a plastic state. It would be a useful tool to know the history of ancient lithospheric phenomenon.

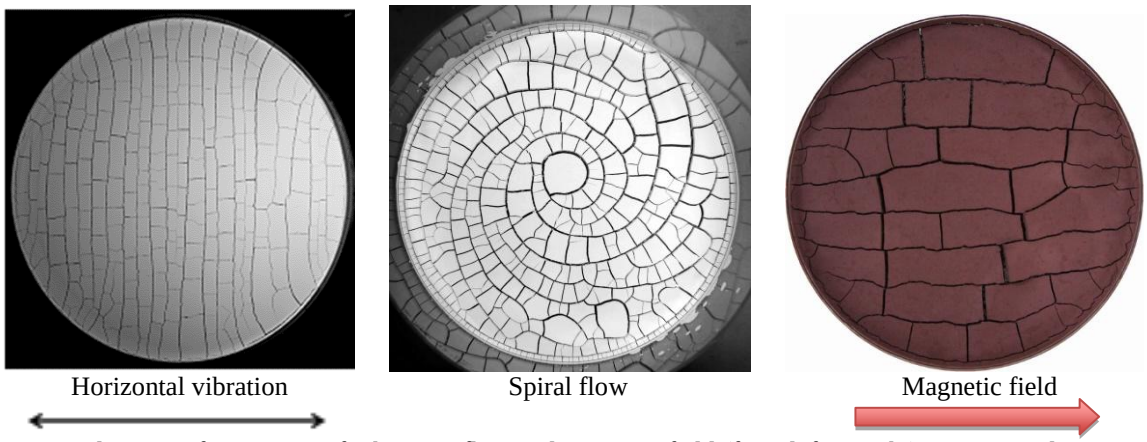

Figure 1. Visualization of memories of vibration, flow and magnetic field (from left to right) in paste as desiccation crack patterns

References

[1] A. Nakahara and Y. Matsuo, *Imprinting Memory Into Paste and Its Visualization as Crack Patterns in Drying Process*, J. Phys. Soc. Jpn. **74**, 1362 (2005).
[2] A. Nakahara and Y. Matsuo, *Transition in the pattern of cracks resulting from memory effects in paste*, Phys. Rev. E **74**, 045102(R) (2006).
[3] H. Nakayama, Y. Matsuo, Ooshida T. and A. Nakahara, *Position control of desiccation cracks by memory effect and Faraday waves*, Eur. Phys. J. E **36**, 1 (2013).
[4] L. Goehring, A. Nakahara, T. Dutta, S. Kitsunezaki and S. Tarafdar, *Desiccation cracks and their patterns: Formation and Modelling in Science and Nature* (*Statistical Physics of Fracture and Breakdown*), WILEY-VCH, Weinheim, Germany (2015).
[5] M. Otsuki, *Memory effect on the formation of drying cracks*, Phys. Rev. E **72**, 046115 (2005).
[6] Ooshida T., Three-Dimensional Residual Tension Theory of Nakahara Effect in Pastes, J. Phys. Soc. Jpn. **78**, 104801 (2009).

cmg2016 - - Tuesday, June 7, 2016 - 17:45/18:00 (15min)

COOLING CARAMEL ANALOG EXPERIMENTS DESIGNED TO STUDY CRACK SPACING IN LAYERED ROCKS

S. Paillat[1], V. Lazarus[1]
[1]Laboratoire FAST, Univ. Paris-Sud, CNRS, Université Paris-Saclay, Orsay, France

Key words layered rocks, crack spacing, analog experiments

Crack patterns are very frequent in nature, for example during the drying of mud or the cooling of a lava flow. They are present on Earth but also on other planets [1]. We can also observe cracks in layered materials, for instance in sedimentary rocks [2]. The understanding of these fractures is important notably because of its impact on the flow of groundwater or hydrocarbons or for the safety of the mines. To study the patterns observed when a layer is cooled or dried on a rigid surface, we propose analog experiments with caramel. The caramel is made by the dissolution of sugar in distilled water. This mixture is heated to 180 °C and poured in a mould placed on a glass surface. The caramel is then cooled down in a chamber where we control the humidity and impose a temperature gradient. During the cooling, crack pattern appears and we can measure the characteristic length between two fractures for a given thickness of the layer, temperature gradient in the chamber or adhesion of the surface. We then can compare these observations with results of a model which minimizes the elastic energy and the fracture energy in a thin layer [3] [4]. These results may be applied to make hypotheses on the origins of fractures observed in rocks.

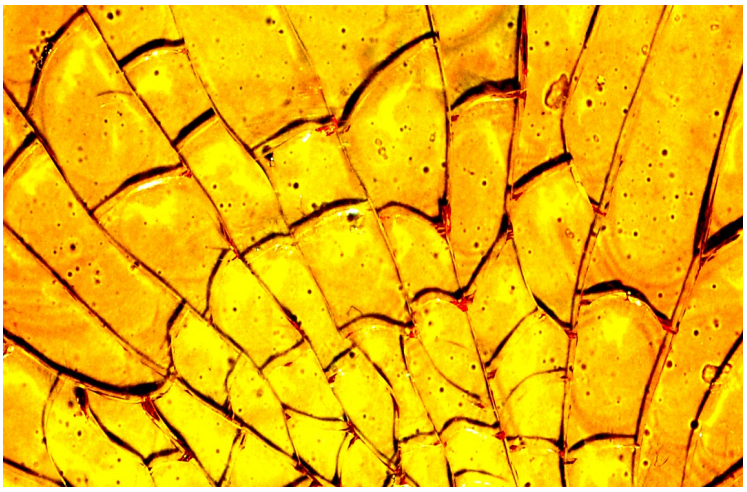

Figure 1*:* Fissures in a thin layer of caramel

References

[1] L. Goehring and S.W. Morris,Cracking mud, freezing dirt, and breaking rocks, *Physics Today*, **67**, 39-44 (2014)/
[2] W. Narr, J. Suppe, Joint spacing in sedimentary rocks, *Journal of Structural Geology*, **13** (9), 1037-1048 (1991)
[3] G. Gauthier, V. Lazarus, & L. Pauchard, Shrinkage star-shaped cracks: Explaining the transition from 90 degrees to 120 degrees. *EPL (Europhysics Letters)*, **89** (2), 26002 (2010)
[4] B. Bourdin, J.J. Marigo, C. Maurini, & P. Sicsic, Morphogenesis and propagation of complex cracks induced by thermal shocks. *Physical review letters*, **112** (1), 014301 (2014)

cmg2016 - - Tuesday, June 7, 2016 - 16:45/17:15 (30min)

KINNEYIA: A FOSSIL HYDRODYNAMIC INSTABILITY

L. Goehring[1], K. Thomas[1], S. Aliaskarisohi[1] , H. Porada[2] & S. Herminghaus[1]
[1]*Max Planck Institute for Dynamics and Self-Organization, Göttingen, Germany*
[2]*University of Göttingen, Geowissenschaftliches Zentrum, Göttingen, Germany*

Key words Kinneyia; Hydrodynamics; Kelvin-Helmholtz instability; Microbial mats; Linear stability analysis

Microbial mats are complex colonies of single-celled organisms, existing in a mass of extracellular polymeric substances (EPS, or, slime). Usually, these mats are roughly flat, but fossils can sometimes be found with intriguing ripple patterns covering them, featuring regular wrinkles a few millimetres wide, as in Fig. 1(a). These trace fossils (microbially mediated sedimentary fossils) are known as Kinneyia, and have been found from around the globe, at sites covering billions of years. Their appearance, however, gradually declined with the rise of multicellular life, and they finally disappeared from the fossil record during the Jurassic.

Characterized by clearly defined ripple structures, Kinneyia are generally found in areas that were formally littoral habitats (near shorlines) and covered by microbial mats. To date, there has been no conclusive explanation of the processes involved in the formation of these fossils, but the fossil evidence shows that they formed immediately after major storm events. Composed mainly of EPS, microbial mats behave like viscoelastic fluids. We have proposed [1,2] that the key mechanism involved in the formation of Kinneyia is a Kelvin–Helmholtz-type instability of the surface in a viscoelastic film under flowing water [Fig. 1(b,c)]. A ripple corrugation is spontaneously induced in the film and grows in amplitude over time. Theoretical predictions show that the ripple instability has a wavelength proportional to the thickness of the film. Experiments carried out using viscoelastic films confirm this prediction: the ripple pattern that forms has a wavelength roughly three times the thickness of the film. This behaviour is independent of the viscosity of the film and the flow conditions. Laboratory-analogue Kinneyia were also formed via the sedimentation of glass beads, which preferentially deposit in the troughs of the ripples. Well-ordered patterns form, with both honeycomb-like and parallel ridges being observed, depending on the flow speed. These patterns, and their scaling, correspond well with those found in Precambrian Kinneyia samples collected from Namibia, with similar morphologies, wavelengths and amplitudes being observed.

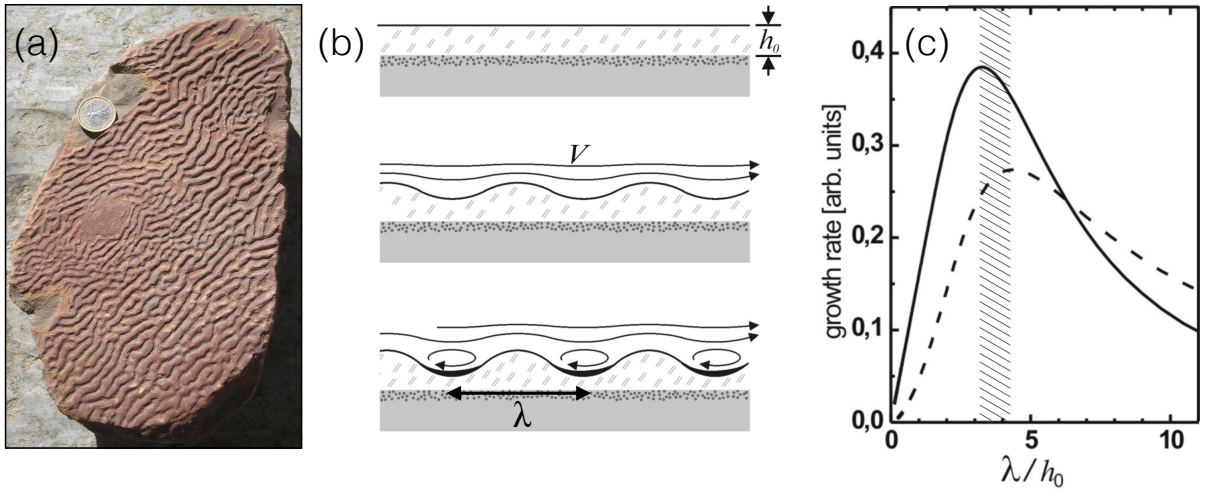

Figure 1. (a) Kinneyia fossil from Namibia. (b) We model the conditions of Kinneyia formation by a biomat of thickness h_0 under a superficial flow V. The surface is unstable to wrinkles, with a most unstable wavelength λ that (c) is proportional to h. This model is tested rigorously against analogue experiments and field data, and appears to also match the wavelength of the saturated pattern.

References

[1] K. Thomas, S. Herminghaus, H. Porada, and L. Goehring, *Formation of Kinneyia via shear-induced instabilities in microbial mats*, Phil. Trans. R. Soc. A **371**, 20120362 (2013).

[2] S. Herminghaus, K. Thomas, S. Aliaskarisohi, H. Porada and L. Goehring, *Kinneyia: a flow-induced anisotropic fossil pattern from ancient microbial mats*, Submitted to Front. Mater. (2015).

cmg2016 - - Tuesday, June 7, 2016 - 18:00/18:15 (15min)

TRANSPORT OF PARTICLES BY INTERNAL WAVES

E. Horne[1,2], D. Micard[1,2], P. Odier[1] & S. Joubaud[1]

[1]*Laboratoire de Physique, École Normale Supérieure de Lyon, Université de Lyon, CNRS, Lyon, France*
[2]*Laboratoire de Mécanique des Fluides et d'Acoustique, UMR 5509, CNRS, École Centrale de Lyon, Université de Lyon, Écully, France*

Key words Stratified flows, internal waves, transport of particles.

The settling of organic particles from the upper layers of the ocean to the deep sea (known as oceanic snow) has an intense effect on global ocean properties. It is substantial for the development of diversified life in the benthic layer and it also sequesters large quantities of CO_2 from the atmosphere. The dispersion and concentration of these particles will be strongly attached to the dynamics of the ocean via its carrying fluid. Internal waves, omnipresent in the ocean, can act as a mechanism producing resuspension of particles lying in the boundary layers and generate net transport of the oceanic snow that could play a role in the behavior of marine habitat [1]

Experimental and numerical efforts have been performed to understand the dynamics of a single body settling in a stratified environment [2], as well as the collective dynamics of particles settling in a stratified fluid [3]. In our work, we include an additional degree of complexity, by trying to study experimentally the main effects of an internal plane wave propagating through a column of slowly settling particles, in a stratified fluid.

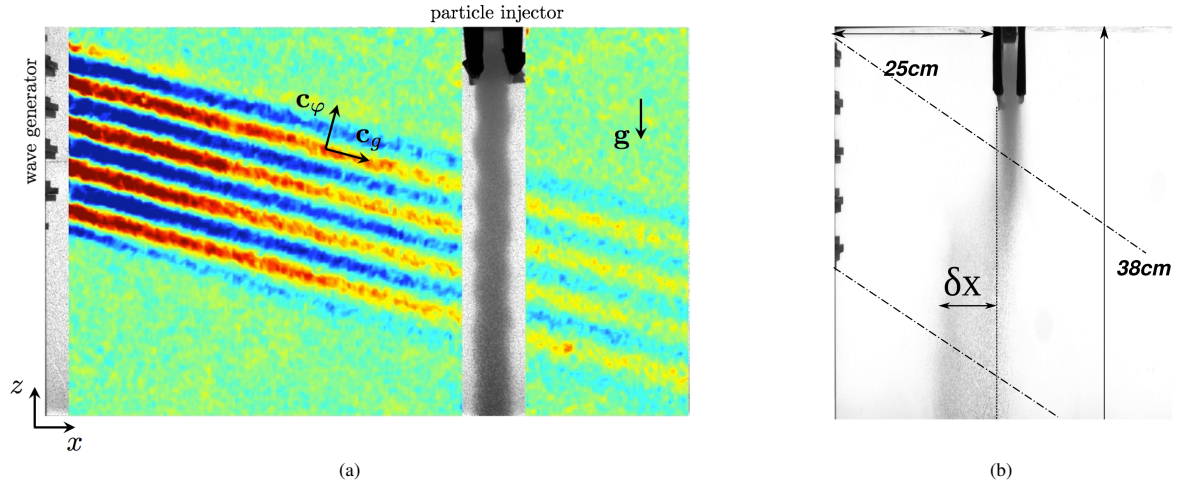

Figure 1. (a) Snapshot of an internal wave beam passing through a column of settling particles. The column oscillates following the group velocity of the wave. The colormap indicates the intensity of the horizontal gradient of density measured using Synthetic Schlieren technique [4]. (b) Column displacement obtained for a particular set of control parameters. The value of the displacement after a given time is denoted δx. In both figures, the wave field is generated in the upper-left corner and propagates to the lower-right corner.

The granular column formed by the particles oscillates around an equilibrium position due to the presence of the internal gravity waves (figure 1a). Depending on the frequency and the amplitude of the internal waves, the column can even be displaced as a whole (figure 1b). Surprisingly, this displacement is directed towards the source of the waves. A resonant behavior of this displacement with the frequency of the internal waves is observed. A theoretical approach based on the drift induced by internal waves is developed.

References

[1] J. PINEDA, V. STARCZAK, J.C.B. DA SILVA, K. HELFRICH, M. THOMPSON AND D. WILEY, Whales and waves: Humpback whale foraging response and the shoaling of internal waves at Stellwagen Bank, *Journal of Geophysical Research: Oceans*, **120**(4), 2555–2570 (2015).

[2] Yick K. Y., Torres C. R., Peacock T., Stocker R.: Enhanced drag of a sphere settling in a stratified fluid at small Reynolds number. J. Fluid Mech., 632:49ÃŘ68, 2009.

[3] Bush J. W. M., Thurber B. A., Blanchette F.: Particle clouds in homogeneous and stratified environments. J. Fluid Mech., 489, pp 29-54. 2003.

[4] S.B. DALZIEL AND G.O. HUGHES AND B.R. SUTHERLAND Whole-field density measurements by synthetic schlieren *Experiments in Fluids*, **28**, 322–335 (2000).

cmg2016 - - Tuesday, June 7, 2016 - 17:15/17:30 (15min)

Experimental investigation of dissolution patterns created by a free-surface runoff flow

M. Berhanu [1], C. Cohen[1], J. Derr[1] & S. Courrech du Pont[1]
[1] *Matiéres et systèmes complexes, Université Paris Diderot, CNRS, Paris, France*

Key words : Geomorphology, dissolution, fluids mechanics

Erosion by dissolution is in addition of mechanical erosion, an important process shaping small-scale landscape morphology **[1]**. On the surface of soluble rocks like gypsum, salt (halite) or limestone, characteristic patterns known as Rillenkarren can be observed, when the dissolving surface is inclined and subjected to a thin run-off flow usually fed by rain. On different natural examples, rock surface is incised by nearly parallel channels (rills) directed along the main slope like the runoff flow. These channels present also a regular wavelength in the transverse direction. This common shape with different materials, suggests a physical mechanism at play. Nevertheless appearance of this pattern remains incompletely understood to our knowledge **[2]**. Only one experimental simulation has been reported by Glew and Ford in 1980 **[3]**, presenting few experiments with gypsum under rain, without hydrodynamics flow characterization or dynamic measurement of the eroded solid surface. A modelling approach was carried out by Perne in 2009 **[2]**, but simulations of the model fail to produce Rillenkarren patterns.
We perform new experiments on dissolution patterns produced by a runoff water flow on an inclined solid and soluble surface. This flow can be generated by a homogeneous artificial rain or by a water flowing film of controlled flow rate. As we expect that a general physical mechanism can explain the observed shapes, we use materials whose dissolution speed with water is large. 3D shape of the eroded surface will be quantitatively reconstructed a different steps during the dissolution process. Finally, we will discuss if the characteristic length scale can be predicted by a simple linear stability analysis.

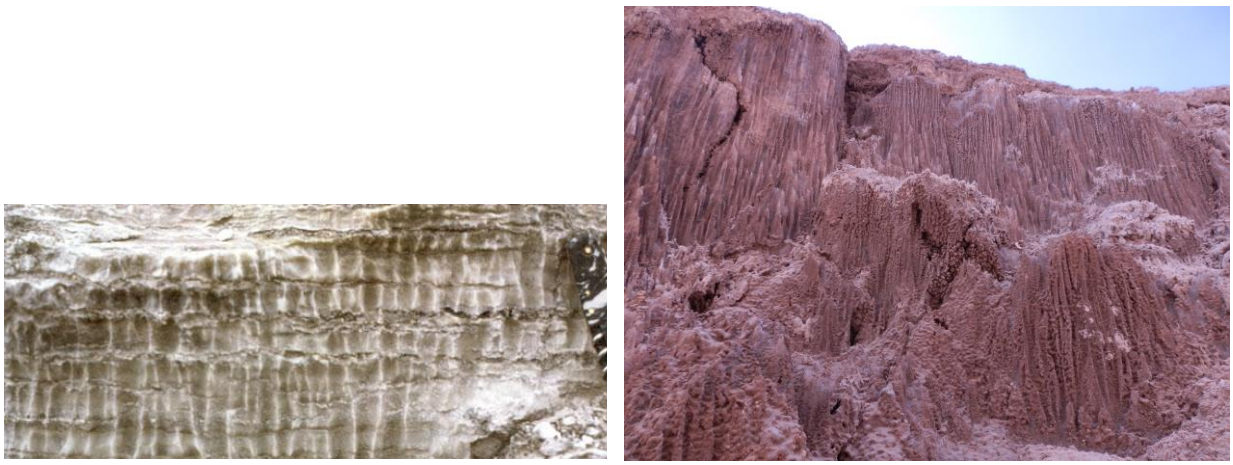

Figure 1. (left) Rillenkarren on gypsum in Vaucluse, France. (Credits http://planet-terre.ens-lyon.fr/).

(right) Rillenkarren on halite in Valle de la Luna, San Pedro de Atacama, Chile.

References :

[1] **P. Meakin and B. Jamtveit**, *Geological pattern formation by growth and dissolution in aqueous systems,* Proc. R. Soc. A **466** 659-694 (2010)

[2] **M. Perne**, *Modelling of Rillenkarren formation,* in Proc. "Sustainability of the Karst environment" HP-VII/2010/GW-2, UNESCO p163-170 (2010)

[3] **J.R. Glew and D.C. Ford**, *A simulation study of the development of Rillenkarren,* Earth surf. Proc. **5**, 25-36 (1980).

cmg2016 - - Tuesday, June 7, 2016 - 11:45/12:30 (45min)

AN EXPERIMENTAL VIEW ON EARTHQUAKE MAGNITUDE CORRELATIONS

K. Stavrianaki [1], P. Sammonds[1], & G. J. Ross[1,2]
[1]*Institute for Risk and Disaster Reduction, University College London, UK*
[2]*Department of Statistics, University College London, UK*

Key words earthquake statistics, acoustic emissions, magnitude correlations

The clustering of earthquakes in time and space is widely accepted, however the existence of correlations in earthquake magnitudes is more questionable [1]. In standard models of seismic activity, it is usually assumed that magnitudes are independent and therefore in principle unpredictable. Our work seeks to test this assumption by analysing magnitude correlation between earthquakes and their aftershocks. In other words, does an increase in the seismic activity mean an increase in the magnitude?

Fracturing is the most prevalent deformation mechanism in rocks deformed in the laboratory under simulated upper crustal conditions. Fracturing produces acoustic emissions (AE) at the laboratory scale and earthquakes on a crustal scale The AE technique provides a means to analyse microcracking activity inside the rock volume and since experiments can be performed under confining pressure to simulate depth of burial, AE can be used as a proxy for natural processes such as earthquakes.
Experimental rock deformation provides us with several ways to investigate time-dependent brittle deformation. Two main types of experiments can be distinguished: (1) constant strain rate experiments in which stress varies as a result of deformation, and (2) creep experiments in which deformation and deformation rate vary over time as a result of an imposed constant stress [2]. We conducted constant strain rate and creep experiments on air-dried Darley Dale sandstone samples in a variety of confining pressures in water saturated samples with 20 MPa initial pore fluid pressure.

Firstly the magnitude of each AE event was calculated and then we search the relationship between the conditional intensity estimates of the Epidemic Type Aftershock Sequence (ETAS) model in which magnitude correlations are absent by construction and the AE events magnitudes. The ETAS model characterizes a sequence of earthquakes and aftershocks over space and time via a conditional intensity. The conditional intensity function is a convenient and intuitive way of specifying how the present depends on the past in an evolutionary point process. A positive relation would suggest the existence of magnitude correlations. Applying the ETAS model to experimental data will allow us to validate our results from earthquake catalog data and provide for the first time a holistic view on the correlation of earthquake magnitudes.

References

[1] E. Lippiello, L. de Arcangelis and C. Godano, *Influence of Time and Space Correlations on Earthquake Magnitude*, Physical review letters. **3**, 100 (038501).
[2] N. Brantut, MJ Heap, P. Baud and PG Meredith, *Rate-and strain-dependent brittle deformation of rocks*, Journal of Geophysical Research: Solid Earth **3**, 119 (1818–1836).

cmg2016 - - Tuesday, June 7, 2016 - 11:45/12:30 (45min)

SELF SIMILAR EVOLUTION OF AN ANTICYCLONE IN A ROTATING STRATIFIED FLOW - APPLICATION TO MEDDIES

G. Facchini[1], M. Le Bars[1]
[1]*Institut de Recherche sur les Phénomènes Hors Équilibre, UMR 7342, Marseille, France*

Key words Meddies, Self Similar, Rotating Stratified flows

We present a theoretical model for the time evolution of an isolated vortex in a rotating stratified flow. We support our study with both laboratory experiments and numerical simulations. This work is motivated by the existence of huge coherent vortical structures [1] observed to form at the exit of the Gibraltar straits. These anticyclonic vortices, known as Meddies, show a strikely long lifetime of the order of years.
We consider the axisymmetric Navier-Stokes equations in the Boussinesq approximation. We initialize the system with a vortex whose density and velocity anomalies fulfill the quasi-geostrophic equilibrium solution derived by Hassanzadeh et al [3] and verified in experiments by Aubert et al [2]. In the limit of small Rossby and Ekman numbers the velocity and density equations can then be linearised and reduced to a single equation for the pressure. In the region of the parameter space explored by experiments the pressure equation further simplifies to a radial diffusion equation which admits a self similar solution. Depending on the initial velocity and density profiles (e.g. an isolated Gaussian vortex), the time evolution of the velocity and density anomalies can be explicitly predicted.

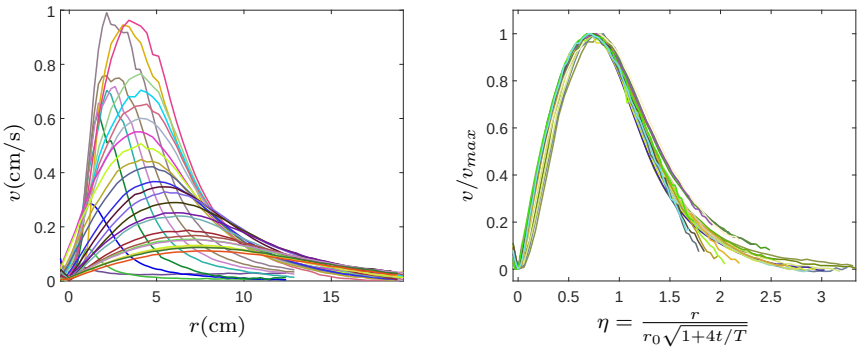

Figure 1. On the left: the radial profile of the tangential velocity at different times during one hour of experiment. Here the control parameters are $f = 2\,\mathrm{rad/s}$ and $N = 1.23\,\mathrm{rad/s}$. On the right: rescaled version of the left diagram. The velocity is divided by its max. The radius is rescaled according to a diffusive law.

We perform laboratory experiments with the same apparatus as [2]. We generate anticyclones injecting a small amount of neutrally buoyant fluid at the center of a rotating tank filled with salty water linearly stratified in density. The fluid motion is investigated using PIV techniques, providing the velocity field in a plane orthogonal to the vorticity vector. We also perform numerical experiments with initial conditions similar to experiments using a finite elements code. Our two control parameters are the background Coriolis parameter f and Brunt-Väisälä frequency N. We consider the radial profile of the tangential velocity and observe that it evolves in a diffusive self-similar way (see figure 1). This result which is common to experiments and simulations is predicted by the model with no adjustable parameter. We remark that, according to the model, a radial diffusion occurs irrespective of the initial aspect ratio (e.g. even for an initial vortex elongated in the radial direction). We claim that this is a consequence of the critical role played by the recirculation inside the vortex, which in general should not be neglected.
Real Meddies occupy a region of the parameter space which is difficult to reach with laboratory experiments but according to the model their evolution should follow the same mechanism. Using an effective value for the deep ocean viscosity we can roughly estimate the lifetime of a Meddy with the right order of magnitude.

References

[1] L. Armi, D. Hebert, N. Oakey, J. Prices, P.L. Richardson, T. Rossby, and P. Ruddick. The history and decay of a Mediterranean salt lens. *Nature*, **333**, 649-651 (1988).
[2] O. Aubert, M. Le Bars, P. Le Gal, and P.S. Marcus. The universal aspect ratio of vortices in rotating stratified flows: experiments and observations. *Journal of Fluid Mechanics*, **706**, 34-45 (2012).
[3] P. Hassanzadeh, P.S. Marcus, and P. Le Gal. The universal aspect ratio of vortices in rotating stratified flows: theory and simulation. *Journal of Fluid Mechanics*, **706**, 46–57 (2012).

cmg2016 - - Tuesday, June 7, 2016 - 11:45/12:30 (45min)

GENERATION AND STABILITY OF GRAVITO-INERTIAL WAVES

P. Maurer[1], S. Joubaud[1] & P. Odier[1]
[1]*Laboratoire de Physique, École Normale Supérieure de Lyon, France*

Key words Stratification, rotation, gravito-inertial waves, parametric subharmonic instability.

In the ocean, stratification and rotation allow for the existence of gravito-inertial waves. Instabilities of these waves, such as parametric subharmonic instability (PSI), may play a key role in the mixing process of the deep ocean. In an experimental setup, we generate gravito-inertial waves which undergo instabilities that match the spatial and temporal resonance conditions of PSI, stipulated by the theory. In order to take into account the effect of rotation on the growth of the PSI, we introduce the Coriolis force in a preexisting model, which predicts the growth rate of the PSI instability in the case of an infinite plane wave. In this case, we show that rotation stabilizes the primary waves. However, experimentally, we see that increasing the rotation does in fact destabilize the primary wave (see figure 1, left panel). This phenomenon is explained by adding a finite size effect to the theoretical growth rate for infinite plane waves similar to what is done in [1] for purely internal waves (no rotation). We find that this effect is in agreement with the enhanced parametric subharmonic instability observed at the "critical latitude" in the ocean [2].

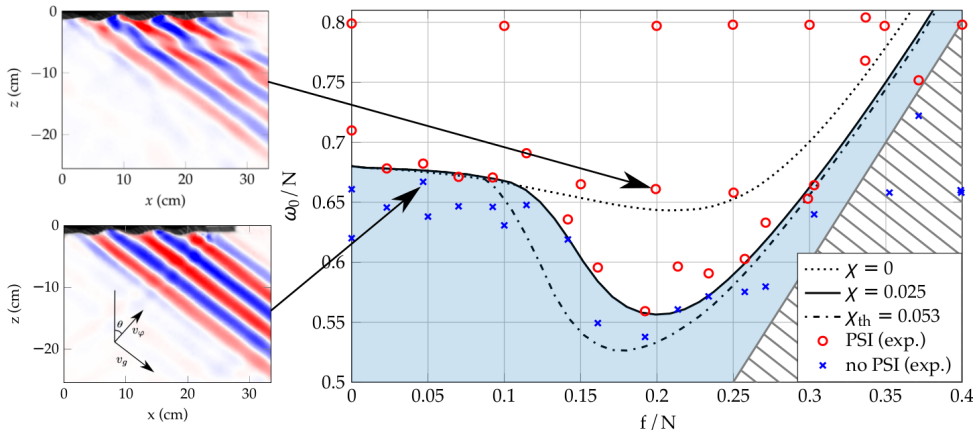

Figure 1. Left panels: vertical density gradient field, associated to two waves generated for the same characteristics of the wave generator and same stratification (buoyancy frequency $N \approx 1$ rad.s^{-1}) but two different Coriolis parameters ($f = 2\Omega$, where Ω is the angular rotation velocity): $f/N = 0.05$ and $f/N = 0.2$. Only the wave at the highest rotation speed undergoes an instability (top left panel). Right panel: evolution of the PSI threshold with rotation. Circles (crosses) mark experimental observation where PSI was (not) observed. The arrows show the corresponding experiments in the left panel. Different theoretical predictions are shown for various values of χ, which corresponds to the relative strength of the finite size effect. The best agreement was found for $\chi = 0.025$.

Estimation of the theoretical growth rate of the instability allows us to find the threshold of the instability in terms of primary wave frequency. As shown in figure 1, the theoretical predictions ($\chi = 0.025$) are in very good agreement with experimental observations. These results confirm our approach in the modeling of the finite size of the primary wave beam.

Finally, at constant primary wave frequency, we analyze the evolution of the secondary wave characteristics with rotation. We find that rotation has a complex role: it shifts the frequency of the secondary waves but may also foster the appearance of multiple triads. For the largest values of rotation rate, unexpected sub-inertial waves appear, whose existence we try to interpret.

References

[1] B. Bourget, H. Scolan, T. Dauxois, M. LeBars, P. Odier, and S. Joubaud. Finite-size effets in parametric subharmonic instability. *Journal of Fluid Mechanics*, 759:739–750, 2014.
[2] J. A. MacKinnon. Subtropical catastrophe: Significant loss of low-mode tidal energy at 28.9°. *Geophysical Research Letters*, 32(15):L15605, 2005.

cmg2016 - - Tuesday, June 7, 2016 - 11:45/12:30 (45min)

Effect of the surface roughness on the seismic signal generated by a single rock impact: insight from laboratory experiments

V. Bachelet[1], A. Mangeney[1,2], J. deRosny[3] & R. Toussaint[4]
[1]*Institut de Physique du Globe, Paris, France*
[2]*ANGE team, INRIA, CEREMA, Lab. J.-Louis Lions, Paris, France*
[3]*Institut Langevin, ESPCI, CNRS, Paris Sciences et Lettre, Paris, France*
[4]*Institut de Physique du Globe, Strasbourg, France*

Key words: rockfalls, seismic signal, scaling laws, statistics

The seismic signal generated by rockfalls, landslides or avalanches is a unique tool to detect, characterize and monitor gravitational flow activity, with strong implication in terms of natural hazard monitoring. Indeed, as natural flows travel down the slope, they apply stresses on the ground, generating seismic waves in a wide frequency band. Our ultimate objective is to relate the granular flow properties to the generated signals that result from the different physical processes involved. We investigate here the more simple process: the impact of a single bead on a rough surface.

Farin et al. [1] have already shown theoretically and experimentally the existence of a link between the properties of an impacting bead (mass and velocity) on smooth surfaces, and the emitted signal (radiated elastic energy and mean frequency). This demonstrates that the single impactor properties can be deduced from the form of the emitted signal. We extend this work here by investigating the impact of single beads and gravels on rough and erodible surfaces.

Experimentally, we drop glass and steel beads of diameters from 2 mm to 10 mm on a PMMA plate. The roughness of this last is obtained by gluing 3mm-diameter glass beads on one of its face. Free beads have been also added to get erodible beds. We track the dropped impactor motion, times between impacts and the generated acoustic waves using two fast cameras and 8 accelerometers. Cameras are used in addition to estimate the impactor rotation. We investigate the energy balance during the impact process, especially how the energy restitution varies as a function of the energy lost through acoustic waves. From these experiments, we clearly observe (see fig. 1) that even if more dissipative processes are involved (friction, grain reorganization, etc.), the single bead scaling laws obtained on smooth surfaces remain valid. A main result of this work is to quantify the fluctuations of the characteristic quantities such as the bounce angle, the seismic energy and frequency induced by the plate roughness.

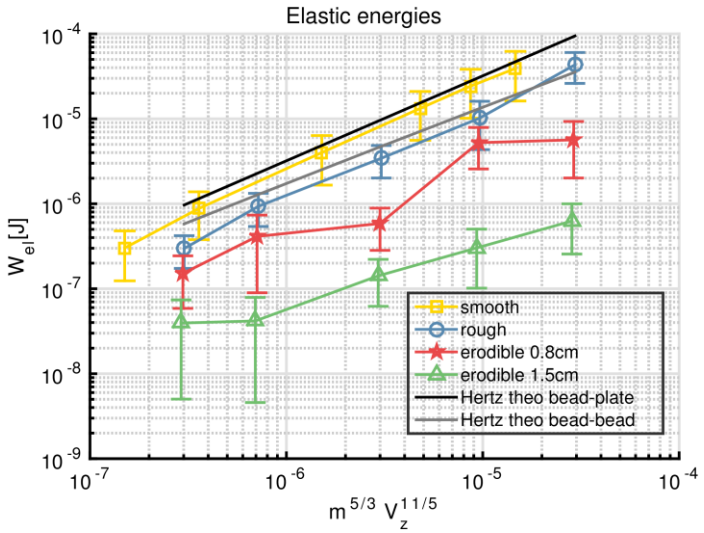

Figure 1. Scaling laws for different diameters of steel bead dropped on different surfaces

References

[1] M. Farin et al., *Characterization of rockfalls from seismic signal: Insights from laboratory experiments*, J. Geophys. Res.-sol ea, **120** (10), 7102–7137 (2015).

cmg2016 - - Tuesday, June 7, 2016 - 11:45/12:30 (45min)

STRESS ANISOTROPY INDUCED BY THE MEMORY EFFECT OF DRYING PASTE

S. Kitsunezaki[1], A. Nakahara[2] & Y. Matsuo[2]
[1]*Research Group of Physics, Division of Natural Sciences, Faculty of Nara Women's University, Nara, Japan*
[2]*Laboratory of Physics, College of Science and Technology, Nihon University, Funabashi, Japan*

Key words memory effect of paste, desiccation cracks, stress anisotropy, yield stress, plasticity

Mud crack patterns familiar in everyday life have isotropic cell structures, but applying horizontal oscillation for a short time before drying makes laminar crack patterns perpendicular to the shaking direction after dying in a uniform layer of paste-like mixture of fine granular materials and liquid, such as clay paste. This *memory effect of shaking* is known to occur in paste with plasticity when stresses larger than the yield stress are applied initially[1, 2]. A few phenomenological continuum theories propose mechanisms of initial shaking to make anisotropic residual stresses[3, 4]. However it had been difficult to detect the anisotropy experimentally before emergence of a crack pattern. Recently we used a soft container with a thin sheet of elastic bottom for drying experiments of paste and found that the elastic sheet bended along the direction of initial oscillation as the paste layer shrank with drying. Horizontal stresses in the bending direction can be estimated from the curvature of the elastic sheet. In this research, stresses developing in a uniform layer of drying paste were measured in this method.

We made a special container which has 4 flat stainless springs as parts of the flat bottom and measured the vertical displacements with 4 laser sensors. As each spring is allowed to bend only in one direction, stresses parallel and perpendicular to the initial oscillation direction can be estimated from the displacements of the two springs labeled A and the other two springs labeled B in the photograph of Fig. 1, respectively. We investigated development of stresses in a drying process of a mixture of Calcium carbonate ($CaCO_3$) powder and water while monitoring its solid volume fraction, which was determined from the weight of paste.

The experimental results confirmed that stresses in $CaCO_3$ paste develop up to the order of $20 - 40$kPa for cracking and a little anisotropy between A and B was found before cracking. The stress difference A-B is positive before cracking, that is, stresses parallel to the initial oscillation is larger than stresses perpendicular to the initial oscillation. Although A-B is at most several kPa, the magnitude increases significantly with drying in comparison with the yield stress of initial paste, which is known to be less than 10Pa [1]. Mechanical responses of paste were also investigated with bending tests in the middle stage of a drying process. The results indicate that $CaCO_3$ paste layers behave as a typical plastic material even just before cracking and suggest that drying process develops initial weak anisotropy significantly with accompanying plastic deformation to make a preferential crack direction.

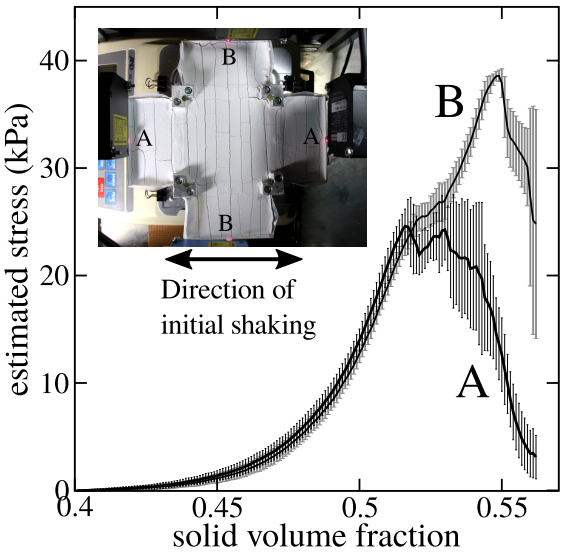

Figure 1. Stresses in a paste layer increase as the solid volume fraction increases with drying. A and B indicate the average stresses in the direction parallel and perpendicular to initial shaking. Their maximum values correspond to the first appearances of perpendicular and parallel cracks, respectively.

References

[1] A.Nakahara and Y.Matsuo, J. Phys. Soc. Jpn. **74**(2005) 1362.
[2] *Desiccation Cracks and their Patterns: Formation and Modelling in Science and Nature*, L. Goehring, and A. Nakahara, and T. Dutta, and S. Kitsunezaki, and S. Tarafdar (Wiley, 2015)
[3] M.Otsuki, Phys. Rev. E **72**(2005) 046115.
[4] Ooshida Takeshi, J. Phys. Soc. Jpn. **78**(2009) 104801.

cmg2016 - - Tuesday, June 7, 2016 - 11:45/12:30 (45min)

WAVE EXCITATION UNDER DOUBLE PLASMA RESONANCE CONDITION IN A MIRROR-CONFINED PLASMA

S. Golubev[1], D. Mansfeld[1], M. Viktorov[1] & V. Zaitsev[1]
[1]*Institute of Applied Physics RAS, Nizhny Novgorod, Russian Federation*

Key words laboratory experiments for geophysics, wave excitation, kinetic instabilities, double plasma resonance.

Study of kinetic instabilities of non-equilibrium plasma produced in an open magnetic trap by powerful microwave radiation under electron cyclotron resonance (ECR) conditions is of fundamental interest including prospects to simulate physical processes in the magnetospheres of the Earth and other planets, in the solar corona. Heating under the ECR conditions allows to create two component plasma which is typical for the inner magnetosphere of the Earth. Plasma contains cold dense component with an isotropic velocity distribution, and less dense component of hot electrons with anisotropic distribution function (with a predominance of the transversal to the magnetic field momentum as compared to the longitudinal one). In such plasma different types of kinetic instabilities may occur as a result of resonant interaction of hot electrons and plasma waves. For example, plasma instabilities in magnetic traps are the sources of powerful broadband radio emission which is interpreted as the excitation of plasma waves by fast electrons in the upper hybrid resonance frequency followed by transformation in electromagnetic waves. In the case of double plasma resonance condition when the frequency of the upper hybrid resonance coincides with one of the electron gyrofrequency harmonics the instability increment of plasma waves is greatly increased. This leads to the appearance of bright narrow-band radio emission near the harmonics of the electron gyrofrequency – the so-called zebra patterns. It should be noted that the possible manifestations of double plasma resonance effect are not rare in astrophysical plasmas. The phenomenon of zebra pattern is observed in kilometric radiation of the Earth, in electromagnetic emission of the Sun, in the decametric radiation of the Jupiter and even in the radio emissions of pulsars. In connection with the above, verification of theoretical and numerical models of instabilities under double plasma resonance in a laboratory plasma experiments is a very relevant task.

With the use of non-equilibrium mirror-confined plasma produced by the ECR discharge we provide the possibility to study plasma instabilities under double plasma resonance condition in the laboratory [1]. In the experiment such conditions are fulfilled just after ECR heating switch-off, i.e. in the very beginning of a dense plasma decay phase. The observed instability is accompanied by a pulse-periodic generation of a powerful electromagnetic radiation at a frequency close to the upper hybrid resonance frequency and a second harmonic of the electron gyrofrequency, and synchronous precipitations of fast electrons from the trap ends. It is shown that the observed instability is due to the excitation of plasma waves at a double plasma resonance in decaying plasma of the ECR discharge [2]. Also a pulse-periodic regime of the observed instability is discussed.

References

[1] M. Viktorov, D. Mansfeld and S. Golubev // EPL. 2015. V.109, No.6. P.65002.
[2] M.E. Viktorov et al. // Radiophysics and Quantum Electronics. 2015. V.57, No.12. P.849.

cmg2016 - - Tuesday, June 7, 2016 - 11:45/12:30 (45min)

SAWTOOTH WAVE-LIKE PRESSURE CHANGES APPEARED IN A SLUG FLOW EXPERIMENT: TOWARD UNDERSTANDING OF VOLCANIC OSCILLATION SYSTEMS

Y. Kanno[1] & M. Ichihara[1]
[1]*Earthquake Research Institute, The University of Tokyo, Tokyo, Japan*

Key words Volcano, Sawtooth wave, Cyclic behavior, Gas-liquid flow, Slug flow, Annular flow, Laboratory experiment, Mathematical model

We are developing a laboratory eruption experiment system to investigate multi physics of volcano eruptions. In this study, we focus on a sawtooth wave-like pressure change (STW) observed in a preliminary system that is a syrup eruption experiment. The STW is cyclic pressure changes of which a cycle consists of a gradual pressure increasing stage and an abrupt pressure drop stage. STWs have been observed at many active volcanoes as geodetical signals including tilt, displacement (*Genco and Ripepe*, 2010; *Ohminato et al.*, 1998).

An apparatus for a slug-flow experiment was designed based on the syrup eruption experiment. This apparatus was equipped with a gas chamber (volume, V_c) and a vertical pipe for a slug flow. Initially the pipe was partially filled with the syrup to the height of H_s from the end. Then, gas was injected at a constant mass flux (Q_{in}) to the chamber to flow into the pipe pushing up the syrup in the pipe. Two representative flow patterns were observed in the pipe. One was characterized by alternate layers of syrup slugs and gas slugs ascending in the pipe, which we called a slug flow. The other was characterized by repetitive transitions between the slug flow and an annular flow, which we called a slug-annular flow oscillation. The STW was observed during the slug-annular flow oscillation.

Pressure change in the chamber and acoustic waves at the vent of the pipe were measured. These measurements were assumed to correspond to geodetic and infrasonic observations at actual active volcanoes. In the experiment, the flow patterns were also constrained by image analyses. The occurrences and features of the STW in the chamber pressure were investigated with taking V_c, Q_{in}, and H_s as the experimental parameters. The results showed that the STWs were observed if there were sufficiently large V_c and Q_{in}, and that the STW changed from periodic to non-periodic cycles with increasing Q_{in}.

A mathematical model was constructed based on the experimental results of the pressure changes and the flow behaviors in the pipe. The model took account of the compressibility of the gas in the chamber, and the nonlinearity of the pressure loss in the pipe flow due to the interaction between the ascending liquid slugs and falling liquid film along the pipe wall. The dependence of the occurrence, the period, and the amplitude of the periodic STW on the experimental parameters were well explained by the model. The model has a mathematically similar aspect compared to existing models for the volcanic oscillation, .

Moreover, not only the periodic STW but also the non-periodic STW was observed in this experiment. The non-periodic STW behavior has not been captured by the present model. According to the image analyses, we inferred that the non-periodic behaviors were caused by the interaction between the ascending liquid slugs and surface disturbances of the falling liquid film. From these results, we obtain an insight that irregularity of actual eruptions can be caused not only by fluctuations in ascending flow but also by influences of descending flow such as a fall back, a drain back and a magma convection of magma in the conduit.

References

Genco, R., and M. Ripepe (2010), Inflation-deflation cycles revealed by tilt and seismic records at Stromboli volcano, *Geophysical Research Letters*, *37*(12), L12,302, doi:10.1029/2010GL042925.

Ohminato, T., B. a. Chouet, P. Dawson, and S. Kedar (1998), Waveform inversion of very long period impulsive signals associated with magmatic injection beneath Kilauea volcano, Hawaii, *Journal of Geophysical Research*, *103*, 23,839–23,862, doi:10.1029/98JB01122.

cmg2016 - - Tuesday, June 7, 2016 - 11:45/12:30 (45min)

DYNAMICS OF AN UNCONFINED AQUIFER

A. Guérin[1], O.Devauchelle[1] & E. Lajeunesse[1]
[1]*Institut de Physique du Globe, Paris, France*

Key words groundwater, flood hydrograph

During a rain event, water infiltrates into the ground where it flows slowly towards rivers. We use a tank filled with glass beads to simulate this process in a simplified laboratory experiment. A sprinkler pipe generates rain, which infiltrates into the porous material. Groundwater exits this laboratory aquifer through one side of the tank. The resulting water discharge increases rapidly during rainfall, and decays slowly after the rain has stopped. A theoretical analysis based on Darcy's law and the shallow-water approximation reveals two asymptotic regimes. At the beginning of a rain event, the water discharge increases linearly with time, with a slope proportional to the rainfall rate at the power of 3/2. Long after the rain has stopped, it decreases as the inverse time squared, as predicted by [1]. These predictions compare well against our experimental data. Field measurements from two distinct catchments exhibit the same asymptotic behaviors as our experiment. This observation suggests that river floods are primarily controlled by the dynamics of groundwater flow.

References

[1] P.Y. Polubarinova-Kochina. *Theory of ground water movement*, Princeton University Press. *Princeton, NJ*, (1962).

cmg2016 - - Tuesday, June 7, 2016 - 11:45/12:30 (45min)

PNEUMATIC FRACTURES IN CONFINED GRANULAR MEDIA

F. K. Eriksen[1,2], S. Turkaya[1], R. Toussaint[1], K. J. Måløy[2] & E. G. Flekkøy[2]
[1]*Institut de Physique du Globe de Strasbourg, Université de Strasbourg/EOST, CNRS, 5 rue René Descartes 67084 Strasbourg Cedex, France*
[2]*Department of Physics, University of Oslo, P.O. Box 1048 Blindern, 0316 Oslo, Norway*

Key words Porous media, Air invasion, Fracturing, Pattern formation, Granular flow, Compaction

We will present our ongoing study of the patterns formed when air flows into a dry, non-cohesive porous medium confined in a horizontal Hele-Shaw cell. This is an optically transparent system consisting of two glass plates separated by 0.5 to 1 mm, containing a packing of dry 80 micron beads in between. The cell is rectangular and has an air-permeable boundary (blocking beads) at one short edge, while the other three edges are completely sealed. The granular medium is loosely packed against the semi-permeable boundary and fills about 80 % of the cell volume. This leaves an empty region at the sealed side, where an inlet allows us to set and maintain the air at a constant overpressure (0.1 - 2 bar). For the air trapped inside the cell to relax its overpressure it has to move through the deformable granular medium. Depending on the applied overpressure and initial density of the medium, we observe a range of different behaviors such as seepage through the pore-network with or without an initial compaction of the solid, formation of low density bubbles with rearrangement of particles, granular fingering/fracturing, and erosion inside formed channels/fractures. The experiments are recorded with a high-speed camera at a framerate of 1000 images/s and a resolution of 1024×1024 pixels. We use various image processing techniques to characterize the evolution of the air invasion patterns and the deformations in the surrounding material. The experiments are similar to deformation processes in porous media which are driven by pore fluid overpressure, such as mud volcanoes and hydraulic or pneumatic (gas-induced) fracturing, and the motivation is to increase the understanding of such processes by optical observations. In addition, this setup is an experimental version of the numerical models analyzed by Niebling et al. [1, 2], and is useful for comparison with their results. In a directly related project [3], acoustic emissions from the cell plate are recorded during experiments, where we aim to localize acoustic events and correlate them with the optical observations.

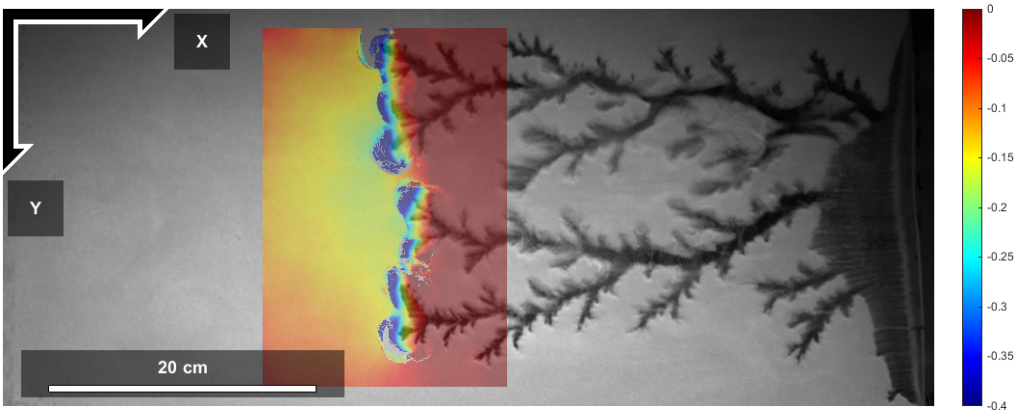

Figure 1. Air invades the granular medium from right to left forming granular fingering channels. One of the techniques we use is digital image correlation to analyze particle displacements. In this example, the color map shows x-component displacements in cm, outside fingers on a 100 ms interval

References

[1] Niebling M.J., Toussaint R., Flekkøy E.G. and Måløy K.J. (2012), *Dynamic aerofracture of dense granular packings*, Phys. Rev. **E**86, 061315. doi:10.1103/PhysRevE.86.061315
[2] Niebling M.J., Toussaint R., Flekkøy E.G. and Måløy K.J. (2012), *Numerical studies of aerofractures in porous media*, Rev. Cub. Fis. 29, 1E66
[3] Turkaya S., Toussaint R., Eriksen F.K., Zecevic M., Daniel G., Flekkøy E.G. and Måløy K.J. (2015), *Bridging aero-fracture evolution with the characteristics of the acoustic emissions in a porous medium*, Front. Phys. 3:70. doi: 10.3389/fphy.2015.00070

cmg2016 - - Tuesday, June 7, 2016 - 11:45/12:30 (45min)

INVASION PATTERNS DURING TWO-PHASE FLOW IN DEFORMABLE POROUS MEDIA

F. K. Eriksen[1,2], R. Toussaint[1], K. J. Måløy[2] & E. G. Flekkøy[2]
[1]*Institut de Physique du Globe de Strasbourg, Université de Strasbourg/EOST, CNRS, 5 rue René Descartes 67084 Strasbourg Cedex, France*
[2]*Department of Physics, University of Oslo, P.O. Box 1048 Blindern, 0316 Oslo, Norway*

Key words Porous media, Two-phase flow, Fracturing, Viscous fingering, Deformation

We will present our experimental study of the viscous fingering and fracturing patterns that occur when air at constant overpressure invades a circular Hele-Shaw cell containing a liquid-saturated deformable porous medium [1] – i.e. during the flow of two non-miscible fluids in a confined granular medium at high enough rate to deform it. The resulting patterns are characterized in terms of growth rate, average finger thickness as function of radius and time, and fractal properties. Based on experiments with various injection pressures, we identify and compare typical pattern characteristics when there is no deformation, compaction, and/or decompaction of the porous medium. This is achieved by preparing monolayers of glass beads in cells with various boundary conditions, ranging from a rigid disordered porous medium to a deformable granular medium with either a semi-permeable or a free outer boundary. We show that the patterns formed have characteristic features depending on the boundary conditions. For example, the average finger thickness is found to be constant with radius in the non-deformable system, while in the deformable ones there is a larger initial thickness decreasing to the non-deformable value. Then, depending on whether the outer boundary is semi-permeable or free there is a further decrease or increase in the average finger thickness. When estimated from the flow patterns, the box-counting fractal dimensions $D_b = 1.59 \pm 0.06$ are not found to change significantly with boundary conditions, but by using a method to locally estimate fractal dimensions, we see a transition in behavior with radius for patterns in deformable systems; In the deformable system with a free boundary, it seems to be a transition in universality class as the local fractal dimensions decrease towards the outer rim, where fingers are opening up like fractures in a paste. In addition, we show a collapse of mass N plotted as function of radius r for the patterns at different snapshots, when normalized by obtained power laws with time $N(t) \propto t^{\alpha}$ and $r(t) \propto t^{\beta}$.

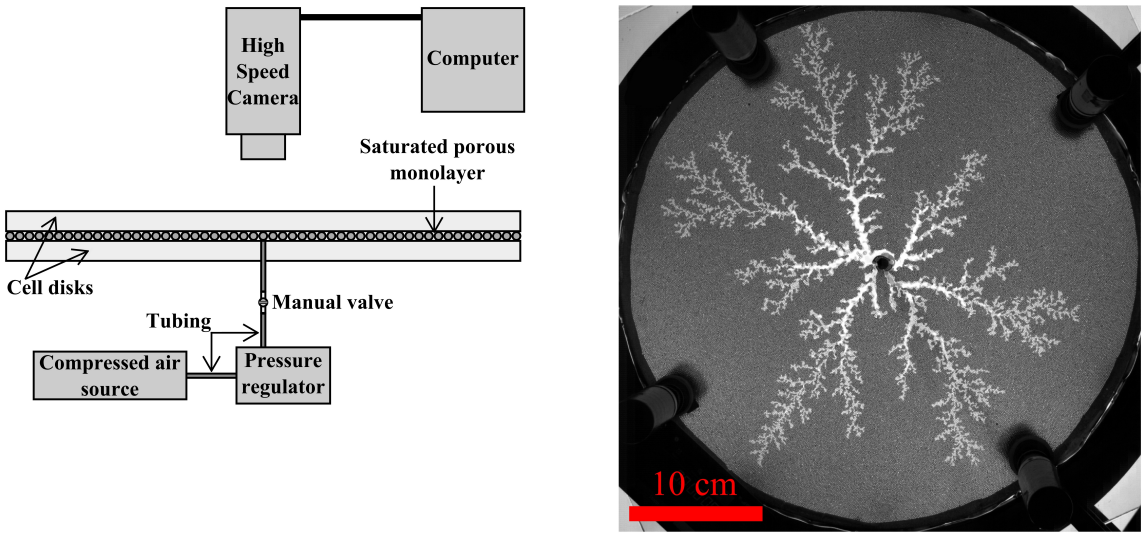

Figure 1. Sketch of our experimental setup seen from the side (left), and a top-down image at the breakthrough time of an experiment (right). During the experiment, air invades the saturated porous medium from the center, forms viscous fingers and induces deformations in the surrounding medium.

References

[1] Eriksen F.K., Toussaint R., Måløy K.J. and Flekkøy E.G. (2015), *Invasion patterns during two-phase flowin deformable porous media*, Front. Phys. 3:81. doi: 10.3389/fphy.2015.00081

cmg2016 - - Tuesday, June 7, 2016 - 11:45/12:30 (45min)

PORE SCALE DYNAMICS DURING TWO-PHASE FLOW IN POROUS MEDIA

M. Ayaz[1,2], R. Toussaint[1], G. Schäfer[3], K.J Måløy[2] & E. Flekkøy[2]
[1]*Institut de Physique du Globe, University of Strasbourg, France*
[2]*Department of Physics, University of Oslo,Norway*
[3]*Laboratoire d'Hydrologie et de Geochimie de Strasbourg, University of Strasbourg, France*

We study experimentally the interface dynamics between two immiscible fluid during drainage, as the nonwetting phase displaces the wetting phase in an initially fully saturated porous medium. The goal is to develop methods of fluid displacement monitoring in soils and porous media, as e.g. for problems of pollution remediation. The system is confined by a vertically oriented Hele-Shaw cell, with piezoelectric type acoustic sensors mounted along the centerline. During drainage potential surface energy is stored at the interface up to a given threshold in pressure, at which an instability occurs as new pores are invaded and the radius of curvature of the interface increases locally, the energy gets released, and part of this energy is detectable as acoustic emission. By detecting pore-scale events emanating from the interface at various points, we look to develop techniques for localizing the displacement front. To assess the quality, optical monitoring is done using a high speed camera.

In our study we also aim to gain further insight into the interface dynamics by varying parameters such as the effective gravity, the invasion speed and probing the system by means of active tomography.

cmg2016 - - Tuesday, June 7, 2016 - 11:45/12:30 (45min)

APPROACHING EARTHQUAKES THROUGH A GRANULAR EXPERIMENT

S. Lherminier[1], R. Planet[1], G. Simon[1], K. J. Måløy[2], L. Vanel[1], O. Ramos[1]
[1]*Institut Lumière Matière, Université Lyon 1, Villeurbanne, France*
[2]*Department of Physics, University of Oslo, Oslo, Norway*

Key words Earthquakes, Scale-Invariant avalanches, Granular dynamics.

In order to analyze different questions related to earthquakes (and scale-invariant phenomena in general) we will present an original experimental setup that mimics the dynamics of a tectonic fault by studying a two-dimensional granular layer that is sheared continuously while submitted to a controlled confining pressure. As the ?(tectonic) plates? move in relation to each other at a controlled and very low speed, shear stresses build up on the packed grains, and eventually they are liberated through sudden avalanches (reorganization of the pack). Acoustic measurements will be the main source of information. However, both the position of all the grains and the force networks in the structure will be monitored. I will present the first preliminary results obtained in this experiment, which show a very good resemblance with real earthquakes: The size of the events are distributed following a power law, similar to the Gutenberg-Richter (G-R) law. The distribution of waiting time between avalanches also follows the same law as real earthquakes, showing a gamma distribution for all the events, and a poissonian process when only large events are considered [1].

The increase of the force between the plates results in larger avalanche sizes, however, the G-R distribution is robust. Currently the analysis focuses on the acoustic [2], with the main goals of understanding the relations between the different measurement (dynamics of force networks, structural disorder, global force and acoustics) and finding precursors of large events.

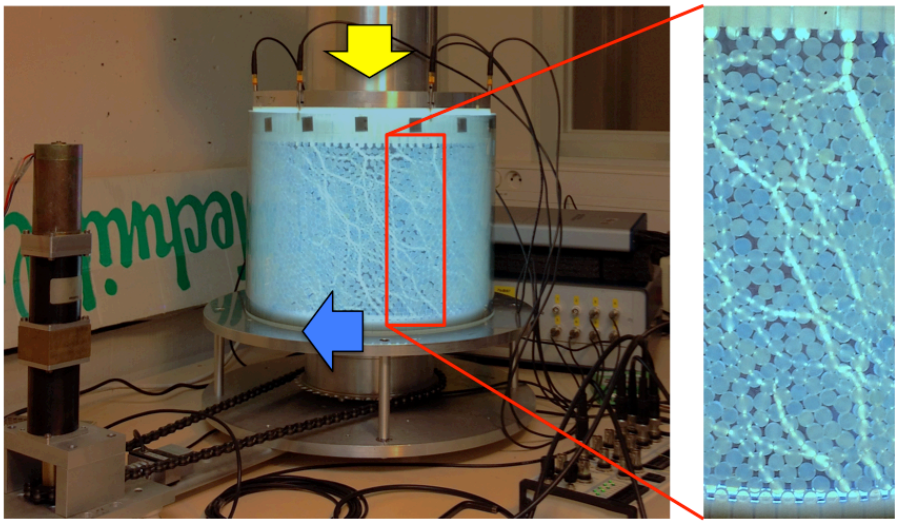

Figure 1. experimental setup.

References

[1] Planet, R., Lherminier, S., Simon, G., Måløy, K. J., Vanel, L., and Ramos, O., *Proceedings CFM 2015, Lyon, France* (August 2015).
[2] Lherminier, S., Planet, R., Simon, G., Vanel, L., and Ramos, O., *Phys. Rev. Lett.*, **113** 098001 (2014).

Author Index